

A-1

JOINT VENTURE TEAM

**COMPARISON REPORT
SECOND DRAFT**

**COMPARISON STUDIES TO IDENTIFY MODEL TO PROTOTYPE
AGREEMENT**

A Joint Venture Evaluation

For:

The US Army Corps of Engineers:

Mississippi Valley Division

Memphis District

St. Louis District

Engineer Research and Development Center

By:

Roger A. Gaines, CEMVM

David Gordon, CEMVS

Stephen T. Maynard, ERDC

September 2002

TABLE OF CONTENTS

	Page
1. ANALYSIS OF AVAILABLE LOOSE BED PHYSICAL MODEL AND PROTOTYPE DATA.....	1-1
1.1. Purpose.....	1-1
1.2. Comparison Concept (what parameters to compare?).....	1-4
2. COMPARISONS.....	2-1
2.1. Methodology.....	2-1
2.1.1. Model Selection.....	2-2
2.1.2. Data.....	2-4
2.1.3. Processing.....	2-6
2.1.4. Comparisons.....	2-11
2.1.5. Analysis of Data.....	2-12
2.1.5.1 Analysis of Range data.....	2-13
2.1.5.2 Weighted reach values.....	2-14
2.2. Data Interpretation.....	2-16
2.2.1. Difference and Mean Squared Error Values.....	2-16
2.2.2. Prototype Variability.....	2-17
2.2.3. Selection of Key Water Surface Elevations.....	2-22
2.2.4. Use of Truncated Cross-Section Data.....	2-27
3. KATE-AUBREY CASE STUDY.....	3-1
3.1. Case Studies.....	3-1
3.1.1. History of Kate-Aubrey Reach.....	3-1
3.1.2. Large-Scale Models.....	3-2
3.1.3. Small-Scale Models.....	3-12
3.1.4. Predictive Comparisons.....	3-26
3.1.5. Summary of Kate-Aubrey Model Analysis.....	3-36
3.2. Bathymetric Repeatability.....	3-38
3.2.1. Kate-Aubrey 1:16,000 Micromodel.....	3-39
3.2.2. Jefferson Barracks Micromodel.....	3-44
3.2.3. Dogtooth Bend Micromodel.....	3-49
3.2.4. Future Work.....	3-50
4. RESULTS.....	4-1
4.1. General.....	4-1

TABLE OF CONTENTS

APPENDICES

- A. IMPACT OF USING TRUNCATED CROSS-SECTION DATA
- B. PREVIOUS LARGE SCALE MODEL STUDIES
- C. PREVIOUS MICROMODEL STUDIES

BIBLIOGRAPHY

LIST OF FIGURES

FIGURE	Page
2-1 Cross-section Parameter Locations (Flow is into Page).....	2-1
2-2 Plan View of Typical River Reach Showing Range Locations.....	2-7
2-3 Microstation® MDL Channel.ma Interface Dialog Display.....	2-9
2-4 Schematic of Real and Effective Termini.....	2-10
2-6 Hypothetical Model and Prototype Data.....	2-18
2-7 Model/Prototype Differences versus LWRP Elevation - Kate-Aubrey Reach.....	2-25
3-1 Model Extent and Range Locations for 1:8,000 and 1:16,000 Micromodels.....	3-3
3-2 Model Extent and Range Locations for 1:300 Model.....	3-3
3-3 Kate-Aubrey Large-Scale Physical Sediment Model.....	3-4
3-4 1975 Prototype Bathymetry, Kate-Aubrey Reach.....	3-5
3-5 1976 Prototype Bathymetry, Kate-Aubrey Reach.....	3-6
3-6 Model Verification Bathymetry, Kate-Aubrey Reach.....	3-8
3-7 Thalweg Position, 1:300 Kate-Aubrey Model.....	3-9
3-8 Hydraulic Depth, 1:300 Kate Aubrey Model.....	3-9
3-9 Width, 1:300 Kate Aubrey Model.....	3-10
3-10 Area, 1:300 Kate Aubrey Model.....	3-10
3-11 Width to Depth Ratio, 1:300 Kate Aubrey Model.....	3-11
3-12 Kate-Aubrey Small-Scale Physical Sediment Model.....	3-12
3-13 1973 Prototype Bathymetry, Kate-Aubrey Reach Small-Scale Models.....	3-14
3-14 1975 Prototype Bathymetry, Kate-Aubrey Reach Small-Scale Models.....	3-15
3-15 1976 Prototype Bathymetry, Kate-Aubrey Reach Small-Scale Models.....	3-16
3-16 Calibrated Bathymetry, Kate-Aubrey Reach 1:8,000 Model.....	3-18
3-17 Calibrated Bathymetry, Kate-Aubrey Reach 1:16,000 Model.....	3-19
3-18 Thalweg Position, 1:8000 Kate-Aubrey Micromodel.....	3-20
3-19 Hydraulic Depth, 1:8000 Kate-Aubrey Micromodel.....	3-20
3-20 Width, 1:8000 Kate-Aubrey Micromodel.....	3-21
3-21 Width to Depth Ratio, 1:8000 Kate-Aubrey Micromodel.....	3-21
3-22 Area, 1:8000 Kate-Aubrey Micromodel.....	3-22
3-23 Thalweg Position, 1:16,000 Kate-Aubrey Micromodel.....	3-22
3-24 Hydraulic Depth, 1:16,000 Kate-Aubrey Micromodel.....	3-23
3-25 Width, 1:16,000 Kate-Aubrey Micromodel.....	3-23

LIST OF FIGURES

3-26 Width to Depth Ratio, 1:16,000 Kate-Aubrey Micromodel.....	3-24
3-27 Area, 1:16,000 Kate-Aubrey Micromodel.....	3-24
3-28 Dike Locations, Kate Aubrey Reach.....	3-28
3-29 Kate Aubrey Dredging Amounts and Costs.....	3-29
3-30 Kate Aubrey Dredge Locations by Year.....	3-29
3-31 1998 Prototype Bathymetry, Kate-Aubrey Reach.....	3-30
3-32 Predictive Model Bathymetry, Kate-Aubrey 1:8,000 Micromodel.....	3-31
3-33 Predictive Model Bathymetry, Kate-Aubrey 1:16,000 Micromodel.....	3-32
3-34 Thalweg Position Predictive Kate-Aubrey Model Case.....	3-33
3-35 Hydraulic Depth Predictive Kate-Aubrey Model Case.....	3-33
3-36 Width Predictive Kate-Aubrey Model Case.....	3-34
3-37 Width/Depth Ratio Predictive Kate-Aubrey Model Case.....	3-34
3-38 Area Predictive Kate-Aubrey Model Case.....	3-35
3-39 Repeatability of Model Bathymetry, Kate-Aubrey Range 10.....	3-40
3-40 Repeatability of Model Bathymetry, Kate-Aubrey Range 20.....	3-40
3-41 Repeatability of Model Bathymetry, Kate-Aubrey Range 30.....	3-41
3-42 Repeatability of Model Bathymetry, Kate-Aubrey Range 40.....	3-41
3-43 Repeatability of Model Bathymetry, Kate-Aubrey Range 50.....	3-42
3-44 Repeatability of Model Bathymetry, Kate-Aubrey Range 60.....	3-42
3-45 Repeatability of Model Bathymetry, Kate-Aubrey Range 70.....	3-43
3-46 Repeatability of Hydraulic Depth in Model Reach, Kate-Aubrey 1:16,000 Model	3-43
3-47 Repeatability of Model Bathymetry, Jefferson Barracks Section 1.....	3-45
3-48 Repeatability of Model Bathymetry, Jefferson Barracks Section 2.....	3-46
3-49 Repeatability of Model Bathymetry, Jefferson Barracks Section 3.....	3-46
3-50 Repeatability of Model Bathymetry, Jefferson Barracks Section 4.....	3-47
3-51 Repeatability of Model Bathymetry, Jefferson Barracks Section 5.....	3-47
3-52 Repeatability of Model Bathymetry, Jefferson Barracks Section 6.....	3-48
3-53 Repeatability of Model Bathymetry, Jefferson Barracks Section 7.....	3-48
4-1 Thalweg Differences and MSE.....	4-7
4-2 Area at 0.0 LWRP Differences and MSE.....	4-8
4-3 Width at 0.0 LWRP Differences and MSE.....	4-9
4-4 Hydraulic Depth at 0.0 LWRP Differences and MSE.....	4-10

LIST OF FIGURES

4-5 Width/Depth Ratio at 0.0 LWRP Differences and MSE 4-11

LIST OF TABLES

TABLE	Page
2-1 Previous Large-Scale Model Investigations	2-3
2-2 Previous Small-Scale Model Investigations	2-4
2-3 Hypothetical Model Difference and MSE Values	2-20
2-4 Prototype and Model Variability: Kate-Aubrey Case Study	2-21
2-4 Elevation Sensitivity of Morphologic Parameter Values	2-26
3-1 Morphologic Parameter Assessment, Kate-Aubrey Model	3-11
3-2 Morphologic Parameter Assessment, Kate-Aubrey 1:8,000 Micromodel	3-25
3-3 Morphologic Parameter Assessment, Kate-Aubrey 1:16,000 Micromodel	3-26
3-4 Morphologic Parameter Assessment, 1:8,000 Kate-Aubrey Predictive Micromodel	3-35
3-5 Morphologic Parameter Assessment, 1:16,000 Kate-Aubrey Predictive Micromodel	3-36
3-6 Reach Morphologic Parameter Values by Two Methods.....	3-37
3-7 Differences Between Model and Prototype, Case Study Examples.....	3-38
3-8 Number of Hydrograph Cycles Between Surveys.....	3-39
4-2. Area Comparisons for Thirty Previous Model Study Results	4-3
4-3. Width Comparisons for Thirty Previous Model Study Results	4-4
4-4. Hydraulic Depth Comparisons for Thirty Previous Model Study Results	4-5
4-5. Width/Depth Ratio Comparisons for Thirty Previous Model Study Results	4-6

1. ANALYSIS OF AVAILABLE LOOSE BED PHYSICAL MODEL AND PROTOTYPE DATA

1.1. Purpose

The original use of the term model concerned representation of something larger. The stated definition is "Something that accurately resembles something else" or "A simplified or idealized description or conception of a particular system, situation, or process ... that is put forward as a basis for calculations, predictions, or further investigation." The physical processes in a model must replicate those processes observed in the prototype. Successful extension of model results to the prototype requires adherence to certain model "rules" or criteria. These rules are referred to as similitude or similarity criteria. Similitude principles provide a means for maintaining constant proportions between physical phenomenon in a model and its prototype.

Strict adherence to similitude relationships requires that all governing parameters provide consistent relationships between model and prototype. In order to achieve similar behavior between model and prototype, all geometric, kinematic and dynamic processes should be the same. Similitude relationships and dimensional analysis provide a mechanism to help identify important engineering variables that describe the physical relationships necessary to provide geometric, kinematic, and dynamic similarity. Froude, Reynolds, and Weber numbers, derived from dimensional analysis, are of primary concern for models with a free surface. Derivations and definitions of Froude, Reynolds and Weber numbers as well as other dimensionless parameters appear in most basic hydraulics texts as well as in many other publications (ASCE 1942, Janna 1981, Vennard 1981, French 1985, and ASCE 2000).

Physical sediment modeling techniques generally rely heavily (or exclusively) on a calibration/verification process to establish an empirical model-to-prototype similarity. This similarity refers to overall agreement between observations in the model and observations in the prototype and does not imply the use of similarity criteria.

The empirical approach to similitude employed in the development of physical sediment models was not easily defined because the degree of similarity depended on the particular problem being analyzed, on the available resources, and on the desired accuracy of a solution. A fundamental question in this regard was: In what way(s) does

the model have to match the prototype to be considered valid? In other words, what measures provided the expected degree of accuracy/similarity and just what was “good enough” (Gaines and Maynard, 2001). Therefore, evaluating criteria for the application of small-distorted scale physical sediment models required an understanding of two concepts: 1) how much variability occurred in the prototype conditions that were used to define similarity, and 2) how well various models reproduced their respective prototype’s bathymetry. Developing such an understanding entailed consideration of various parameters in a quantitative way. A method to define the level of empirical similitude was developed using a series of bathymetric comparisons. These comparisons targeted the identification of a quantitative relationship useful in assessing morphological similarity.

Model-to-prototype similarity must be based on a relationship of designated parameters between a model and its prototype. Consequently, the degree of variability in the prototype, spatially and temporally, has a direct influence on similarity, yet this does not imply that large distortions or exxageration in similarity criteria are permissible. If a prototype morphologic parameter such as width or hydraulic depth varies over a considerable range, then model reproduction of that morphologic parameter should be expected to vary in a comparable manner. Alternately, if a prototype morphologic parameter varies only slightly, then model reproduction of that morphologic parameter should be expected to more closely match prototype values.

Establishing the degree of geometric, kinematic, and dynamic similitude also depends on the amount of change observed in the prototype. Consideration of similitude as a uniquely valued function does little to describe the unsteady nature of many river modeling problems. The unsteady characteristics often significantly impact (and severely complicate) similitude considerations -- which condition at what location should be used for establishing model similarity criteria? In addition, prototype and model data vary in accuracy and spatial density. Data collection procedures employed in the prototype also differ substantially from those used for acquiring model data.

Point depth data collected for prototype surveys vary in accuracy depending on the technique used in acquiring the data. For example, prior to the early 1990’s point hydrographic survey depth data were collected with acoustic equipment that utilized

transponders mounted to the hull of a survey boat. Data collected by this equipment had a maximum accuracy of ± 2 to 3 feet primarily because of fluctuations in the water surface and the continually adjusting bed surface. Horizontal position data obtained for point depth measurements also had inaccuracies that depended on the method used for locating the survey vessel. Procedures for locating northing and easting coordinates for survey points varied considerably over time as newer technologies replaced older, more labor intensive methods. Recent advances in survey capabilities (e.g., mid-1990's to present) have significantly improved collection of accurate horizontal position data and the rate at which point data can be collected. However, only marginal improvements in the accuracy of depth measurements have occurred.

The inaccuracies in depth measurements are largely a function of fluctuations in the bed levels as sediment is continuously being transported through the survey reach. An extreme example of bed level fluctuation is apparent when considering the movement of large-scale bed forms (e.g., dunes) that may have heights of 30 feet or more in the Mississippi River. Movement of such large bed forms through a prototype reach while a survey is being conducted introduces a high degree of variability in bed elevations. The length of time required to acquire prototype data directly impacts the final bathymetric surface. The time required to collect prototype data for a 15-to-20-mile hydrographic survey in the 1980's has been reduced from as much as three or more weeks to three or four days¹ by advances in technology. However, even the relatively short duration of three days permits significant changes in water levels and bed levels to occur during the course of data collection. Older surveys, obtained over much longer time periods, exhibit a higher degree of variability due to changing bed conditions.

Prototype survey conditions are significantly different from those found in either large-scale or small-scale models. While bed levels are continuously changing in the models during simulation periods (as observed in the prototype), model surveys are most often conducted with no flow present. This results in a static bed condition throughout collection of model bed elevations. Data collected in the model, therefore, represent a

¹ The actual length of time required to conduct a hydrographic survey of the Mississippi River depends on the amount of spatial coverage required. Low-water surveys (surveys conducted when river stages are at +10LWRP or lower) can require less than one-half the time required to conduct surveys for high-water conditions (stages at +30 or higher).

true “snap-shot” in time of the model bed. No such representation of prototype bed conditions is available, or indeed possible for most alluvial rivers/streams. This disparity makes it difficult to compare ~~and~~ model and prototype.

Deviation from similarity criteria are often expressed in terms of parameter relaxation based on a particular modeling objective, on other modeling constraints (such as time or space), and on modeling technique. However, variability of prototype parameter values has received little or no attention in the literature. The present work investigated the influence of prototype variability on model-to-prototype agreement in an effort to gain an understanding of morphologic similarity. Examination of scale and scale distortion effects on model similitude also required an evaluation of how selected similarity criteria differed between model and prototype.

1.2. Comparison Concept (what parameters to compare?)

Movable bed physical model studies recorded in the literature provided little detail regarding assessment of model and prototype agreement. Most reported a qualitative comparison of cross-sectional area or shape as the primary means for verifying model-to-prototype agreement. This qualitative comparison generally consisted of a visual comparison of model and prototype bathymetric contours and, on occasion, plots of reference cross-sections with model data superpositioned over prototype data. Even the detailed descriptions of model procedures in USBR (1980) and more particularly Franco (1978) yielded little detail of the exact methodology used to assess model verification with the prototype.

Review of various report drawings indicated that model and prototype bathymetric contour maps were shaded (e.g., color coded) to facilitate ready visual comparisons. This technique is virtually the same as utilized by the micromodel approach described by Davinroy (1994) and in Gaines (1999). Based on published literature, on discussions with various modelers and on previous experience, the real comparisons of whether a model was considered calibrated/verified depended on a visual interpretation of model and prototype bathymetry by the respective modeler(s) as opposed to any rigorous technique. The current research identified a need for

quantitative comparison data to facilitate evaluation of the morphologic similarity criteria.

Following Vernon-Harcourt's description of measures demonstrating a successful model, two areas became the focus for measuring model and prototype similarity. These areas were: 1) model reproduction of original existing conditions in the prototype, and 2) model reproduction of future response of the prototype to a constructed training feature. Because of the temporal variability of prototype bathymetry, attempts to reproduce the exact bed configuration in the model are usually an exercise in futility. Therefore, a judgement of model success must also account in some way for the natural variability in the prototype. In the research reported herein, this was taken as a third area of focus in judging success of a model.

These three areas were targeted to develop a quantitative assessment of variability among the various bathymetric surfaces, between successive prototype surveys and between model and prototype surveys. Parameters describing the channel morphology seemed most useful for this assessment (Rosgen, 1996, and Leopold, et al. 1964). Initially, several morphologic parameters were considered for the analysis. These parameters were:

1. Discharge
2. Channel Sinuosity,
3. Width,
4. Depth, and
5. Cross-sectional area.

Because the dependence of channel shape and planform on discharge has been clearly established by geomorphologists and engineers alike, discharge was a primary characteristic. Yet, various model approaches treated discharge in different ways. Extreme examples of this are illustrated by the fact that some model approaches utilized a continuous flow hydrograph cycle (e.g., Franco, 1978), while others utilized a single constant discharge (e.g., Struikisma, 1980). Both Franco and Struikisma acknowledged that correct model bathymetric response necessitated a variable model discharge for cases

where the prototype discharge hydrograph varied. The influence of using a continuous flow hydrograph as opposed to using a single constant discharge in defining channel morphology has been studied for years as mentioned by Khan (1970), Schumm and Khan (1972) and more recently by Garcia (2000). The influence, often debated between geomorphologists and engineers, remains an unresolved issue. In spite of its significance, discharge data were not available for all model studies considered in this investigation.

micromodel
discharge did not
el design and
range was not
reaction most
new micromodel studies

The lack of model discharge data, particularly for the small-scale models, precluded the consideration of discharge in the analysis of previous model results.

Sinuosity was also widely used by both geomorphologists and engineers in defining channel morphology. Channel sinuosity provided a means for considering the longitudinal aspect of individual cross-section parameters. Schumm and Khan (1972) defined two measures of sinuosity. One measure, channel sinuosity, depended on the high-flow channel length to valley length ratio. The predominant velocity pathline at bankfull discharge provided a measure of channel length. A second measure, thalweg sinuosity, resulted from measuring the low-flow channel length and relating it to the valley length. Actual thalweg length defined the low-flow channel length. Thalweg sinuosity most often described a more sinuous flow path than suggested by the channel sinuosity.

Direct calculation of thalweg length for each model case provided little contribution toward evaluating morphological similarity on a cross-sectional basis. Therefore, a slightly different use of thalweg sinuosity was considered in the present research. Position of the thalweg laterally across the cross-section was adopted to address similarity between prototype and model sinuosity. Exact similarity in the thalweg position occurs when the distance between a common reference point for the cross-section (e.g., referenced to the left descending bank) and the thalweg for both model and prototype are the same. Variation in thalweg position between two bathymetric surveys was expressed through a relative comparison of the respective thalweg positional lengths (between the thalweg and the reference baseline) for each survey.

Analysis of channel morphology also utilized channel width and depth to describe the hydraulic geometry of a Range. Channel width described the horizontal linear

distance between points on the left and right banks of the stream at a common elevation. Width influenced the lateral distribution of flow and sediment across the channel and provided some indication of the type of flow (e.g., 2-dimensional or 3-dimensional patterns) anticipated in the reach. Similarity considerations also indicated a relationship between width and bed roughness (Ettema, 2000). The cross-section depth for the current investigation was represented by the hydraulic depth (area divided by top width). Hydraulic depth (H) provided an indication of channel depth and influenced both the relative roughness and the vertical distribution of velocity. The ratio of width to hydraulic depth, W/H, also helps to describe the channel geometry. The width/depth ratio aids in determining the two-dimensional character of flow patterns.

Channel cross-sectional area values were a function of water surface elevation used in the area computation. Initial comparison work considered the use of area versus elevation curves to assess prototype and model variability. While the area-elevation data provided insight into parameter sensitivity, this approach resulted in a large volume of data that produced no useful summary relationships. The data contributed little toward understanding overall model-to-prototype similarity. The cross-sectional area-elevation approach was subsequently modified to limit calculations to specific key elevations. The key elevations were selected to coincide with elevations typically associated with defining actual prototype conditions and with assessing a model's ability to reproduce prototype conditions. Channel width and hydraulic depth at these key elevations provided an additional means to evaluate cross-section shape.

Considering the previous parameter descriptions, discharge was not included in the present investigation because of its unavailability (neither prototype nor model discharge data were available for the small-scale models). Additionally, the sinuosity was represented by thalweg position in each cross-section as referenced to a common point on the section. Cross-section area, width, depth and width/depth ratio describe the hydraulic geometry and offer insight into the two-dimensional character of the flow. Therefore, the morphologic parameters selected for the present analysis are:

1. Thalweg position within the active channel (as a surrogate for sinuosity),
2. Cross-section area,

3. Channel width,
4. Hydraulic depth, and
5. Width/depth ratio (from cross-section width and hydraulic depth).

Using these parameters, a framework was established to evaluate: 1) prototype variability, 2) model-to-prototype differences, and 3) model predictive capability.

The first area requiring a quantitative description is the bed surface variability (e.g., natural aggradation/degradation over time) found between prototype surveys that are used in the calibration or verification of the individual models. ^{to match} ~~Because~~ model-to-prototype agreement is exemplified by how well a model reproduces prototype bathymetry, the magnitude of differences between the prototype surveys ^{may influence} ~~is a direct~~ indicator of how well the model could be expected to match the prototype. Prototype reaches exhibiting a high degree of variability indicate reaches that are difficult to model, while prototype reaches exhibiting a lesser degree of variability are generally easier to model.

The second area pertained to identifying how closely a particular model matched prototype conditions used for model calibration. Comparison of the five selected parameters (listed previously) for this analysis was intended to serve as a measure of model-to-prototype morphologic similarity.

Predictive capability of models was the third area requiring definitive data. Quantitative comparisons of predicted model response to observed prototype response is intended to substantiate (or refute) the degree of similarity between the two. These data coupled with comparison of calibrated model conditions were also intended to aid in identifying possible scale effects and distortion effects.

2. COMPARISONS

2.1. Methodology

Elevations in all models analyzed were based on an ~~arbitrary~~ reference plane that was developed to support maintenance of navigation on the subject rivers. The prototype reference plane equated a zero elevation with the most likely minimum water level anticipated on the specific river reach. An example of this reference plane was the Low Water Reference Plan (LWRP) used for the Mississippi River. The Mississippi River LWRP corresponded to the water surface elevation equaled or exceeded 97 percent of the time. ~~Therefore~~, bottom elevations reported in terms of LWRP elevation indicated navigable depths below an expected low water level. ~~The advantage of using such a~~ ^{Although prototype LWRP represents} reference plane manifested itself through a ready discernment of areas with inadequate navigation depths, thus aiding maintenance activities. The reference elevation selected for the present comparisons was the zero elevation of this reference plane. This elevation represented a focal elevation for the various model studies considered and therefore provided useful indications of model-to-prototype bathymetry agreement. An LWRP elevation of +30 represents a typical bankfull prototype stage. ~~Although~~

has variability in slopes based upon LWRP in the micro model approximate with a small unit slope through the model reach

Evaluating variability between various bathymetric surfaces was accomplished by considering five particular cross-sectional characteristics determined for both model and prototype surveys. Each of these characteristics described a particular morphological or hydraulic aspect of the bathymetry being analyzed. Selected characteristics included cross-sectional area at 0.0 LWRP (A_0), channel width at 0.0 LWRP (W_0), hydraulic depth at 0.0 LWRP (H_0), and the thalweg position (TP). Thalweg position was referenced to the left descending bank as depicted in Figure 2-1. ~~The location of the thalweg within the channel was determined by an interpretation of cross-section data~~ ^{The location of the thalweg within the channel was determined by an interpretation of cross-section data} ~~and~~ ^{and} ~~depended somewhat on the analyst.~~

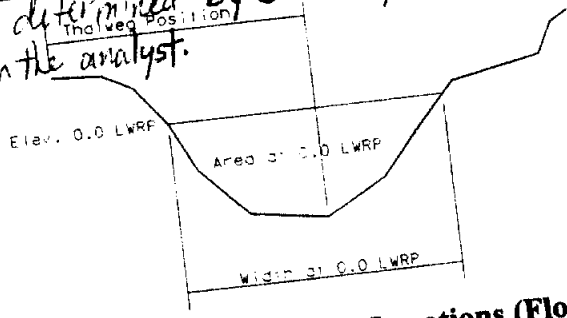


Figure 2-1 Cross-section Parameter Locations (Flow is into Page).

2.1.1. Model Selection. Evaluating prototype variability and model/prototype similarity necessitated finding as many physical sediment model study cases that fit specified criteria. Criteria used for determining if a model study could be included in the present analysis were simple. Inclusion of a model required that at least one prototype hydrographic survey was used to calibrate the model and that both calibrated model bathymetry and all prototype bathymetry used in model calibration were available either in hard copy map, tabular coordinate listing, or digital terrain model form. Regardless of these simple requirements, very few model studies outside the US Army Corps of Engineers were found to have the requisite information. A data call to the engineering public at large (Gaines and Maynard, 2001) resulted in no new information to supplement the present study.

Relatively few model studies were included in the present research; however, the thirty models analyzed provided a sufficiently large data set to gain an understanding of the relationship between model/prototype similarity and prototype variability. Models were grouped into two categories, large-scale models (horizontal scale less than 1:600) and small-scale models (horizontal scale greater than 1:3600). Case study examples of each type of model (e.g., large-scale and small-scale) are included in later sections (3.1.2 and 3.1.3, respectively). The case studies include details of the project along with pictures, maps, and data for both the models and prototype river reach. No attempt was made to differentiate between the type of models (crushed coal, sand, or plastic bed material) or operational constraints such as time and/or data limitations. Rather, models were grouped in a manner that best facilitated analysis.

Sixteen large-scale physical models were identified for inclusion in the present study. Horizontal scales of these models ranged from 72:1 to 600:1 with vertical distortion ranging from 1.0 to 10. Large-scale model studies included in the present investigation are shown in Table 2-1. Appendix B provides general descriptions of these models. Most of these model studies were completed prior to 1990 at the Engineering Research and Development Center (ERDC) formerly the Waterways Experiment Station (WES). Model data were available through report plates depicting both model and prototype bathymetry. Fourteen micromodels were also identified for inclusion in the present study. These models had horizontal scales ranging from 3,600:1 to 20,000:1 with

vertical distortions ranging from 6 to 20. Appendix C provides general descriptions of these models. Models were completed primarily by the St. Louis District Corps of Engineers Applied River Engineering Center, with two models completed by the Memphis District Corps of Engineers Applied River Engineering Center.

Table 2-1 Previous Large-Scale Model Investigations

Name (River)	Prototype Data Used in Model Verification	Horizontal Scale ^a	Distortion (Horiz:Vert.)
Baleshed-Ajax Bar (Mississippi)	1967, 1968	600:1	10:1
Blountstown (Apalachicola)	1977, 1978	120:1	1.5:1
Buck Island (Mississippi)	1976, 1977, 1978, 1979	300:1	3:1
Chipola Cutoff (Apalachicola)	1978, 1979	120:1	1.5:1
Devil's Island (Mississippi)	1973	400:1	4:1
Dogtooth Bend, (Mississippi)	1977, 1983	400:1	4:1
Kate Aubrey (Mississippi)	1975, 1976	300:1	3:1
Lake Dardanelle (Arkansas)	1971, 1973	120:1	1.5:1
Lock & Dam #2 (Red River)	1978, 1981	120:1	1.5:1
Lock and Dam #4 (Red River)	1978, 1981	120:1	1.5:1
Loosahatchie-Memphis (MS)	Jan 1986, Nov 1986	300:1	3:1
New Madrid Bar (Mississippi)	1976, 1977	480:1	8:1
Redeye Crossing (Mississippi)	1982, 1983	240:1	1.2:1
Smithland Locks & Dam (Ohio)	1983	150:1	1:1
West Access (Atchafalaya)	1989	120:1	1.5:1
Willamette River	1977, 1980	100:1	2:1
*Scale is prototype/model ratio.			

The two micromodels completed by the Memphis District specifically targeted scale studies for the present investigation. These models of the Kate Aubrey reach of the Mississippi River were designed with horizontal scales of 1:16,000 and 1:8,000 (one was exactly twice the size of the other in the horizontal dimension). Selection of these horizontal scales resulted from consideration of scales previously used in micromodels of the Mississippi River. The smaller Kate Aubrey micromodel, 1:16,000, was near the lower extreme of micromodel scale while the larger micromodel, 1:8,000, was near the

upper extreme of micromodel scale. Both of the Kate-Aubrey micromodels were also used to assess the predictive capability of the micromodel technique as subsequently described. Small-scale model studies included in the present investigation are shown in Table 2-2. Chapter three provides summary descriptions of the Kate-Aubrey models included in the comparative analysis.

Table 2-2 Previous Small-Scale Model Investigations

Name (River)	Prototype Data Used in Model Calibration	Horizontal Scale ^a	Distortion (Horz.: Vert.)
Mouth of White River (Mississippi)	1994, 1997	12000:1	10:1
Clarendon, AR (White)	1999	4200:1	14:1
Augusta, AR (White)	1999	3600:1	20:1
Vicksburg Front (Mississippi)	1994, 1997	14400:1	12:1
Wolf Island (Mississippi)	1997, 1998	7200:1	12:1
Memphis Harbor (Mississippi)	1996, 1997	4800:1	8:1
Lock & Dam 24 (Mississippi)	1993, 1995	9600:1	16:1
Savanna Bay (Mississippi)	1996	4800:1	8:1
Copeland Bend (Missouri)	1991, 1996	3600:1	15:1
Salt Lake (Mississippi)	1993, 1995, 1996, 1998	9600:1	16:1
Morgan City/Berwick Bay (Atchafalaya)	1999	7200:1	6:1
New Madrid (Mississippi)	1994	20000:1	16.7:1
Kate Aubrey (Mississippi) ¹	1973, 1975, 1976	16000:1	17.8:1
Kate Aubrey (Mississippi) ¹	1973, 1975, 1976	8000:1	13.3:1
^a Scale is prototype/model ratio.			
¹ Models conducted as part of present research for studying scale effects.			

2.1.2. Data. Recent model/prototype study data (1994 or after) were available in a digital format that was conducive to computer manipulation. Older study data, both prototype and model, were generally in paper map form. The large number of surfaces to be analyzed and the existence of more recent data in the digital format strongly supported the need to convert the older data to the digital format. Conversion of all data to a

common format was further supported by the need for consistent analysis. Data were subsequently converted to a digital format.

Conversion of older survey data to a digital form was accomplished by the following steps:

1. Scan original hard copy hydrographic surveys
2. Georegister scanned images to current prototype coordinate system
3. Digitize contours from scanned images
4. Digitize point elevations from scanned images
5. Build ASCII surface point file
6. Triangulate terrain model from point file and verify computer generated bathymetric map against original survey maps.

Transformation of older hydrographic survey data required great care to ensure that both point and contour elevation data were included in the digital terrain model. While computer contours could be generated from point data alone, the contour elevation data from older surveys included hand drawn curves that reflected the additional knowledge about the river supplied by the technician. The skill and knowledge possessed by the technician greatly affected the quality and accuracy of those older hydrographic surveys. Regardless of their sophistication, computer algorithms currently used in creating contour lines have no intrinsic knowledge about river processes and only represent a mathematical interpolation of the bathymetric surface. Often, the contours obtained by hand methods and those generated by computer are markedly different. In fact, different computer algorithms can produce significantly different contour lines. As a result, prototype variability depends partly on the method used in analyzing point and associated contour elevation data. To minimize the potential for introducing additional variability, analysis focused on the use of point elevation data supplemented by original² contour elevation data. This was accomplished by aligning Ranges at standard prototype

² Original contour elevations were digitized from historic hydrographic survey maps and were included in the triangulated terrain surface developed by computer software.

hydrographic survey Ranges used for periodically monitoring river conditions. By using locations where actual prototype data were acquired, the influence of interpolated data was reduced. This also applied to the WES models because model survey were also typically collected at these locations.

The resulting terrain model served as the basis for the remaining analysis. Data were managed by both AutoCAD® and Microstation® software and associated add-in packages. These software packages also generated supplemental data as required in the analysis. Supplemental data were location and position of range lines (cross-sections) and lines indicating thalweg position. The analysis was also restricted to just the active channel: defined as the area located between natural bank and the riverward end of training structures³. All model data were in the form of prototype units. Model data prior to being converted to prototype units were not available.

2.1.3. Processing. Comparison of morphologic parameters as described in Chapter three required the analysis of cross-sectional data for each bathymetric surface included in the present research. Calculation of cross-section areas, widths, hydraulic depth and thalweg position began by establishing cross-section locations (also referred to as Ranges) for each model-prototype reach. A plan view of a river reach depicting Range and thalweg locations is shown in Figure 2-2. The figure depicts the Kate-Aubrey reach of the Mississippi River located north of Memphis, Tennessee.

Placement of the Ranges at the same location for all model and prototype surveys provided a direct physical connection between the data. Stated more explicitly, parameter values calculated at a Range for each bathymetric survey could be used to assess changes in prototype values and/or to approximate the degree of model and prototype agreement.

³ Only the active channel was considered in the analysis because typical prototype hydrographic survey data were restricted to this area. Specific, localized bathymetric features were not well defined for prototype surveys near training structures. This was particularly so for older hydrographic surveys where manual interpretation of survey data points were the only distinguishable features in the vicinity of training structures. The potential for bias resulting from varying availability of localized survey data around structures indicated that such areas should be excluded from the analysis.

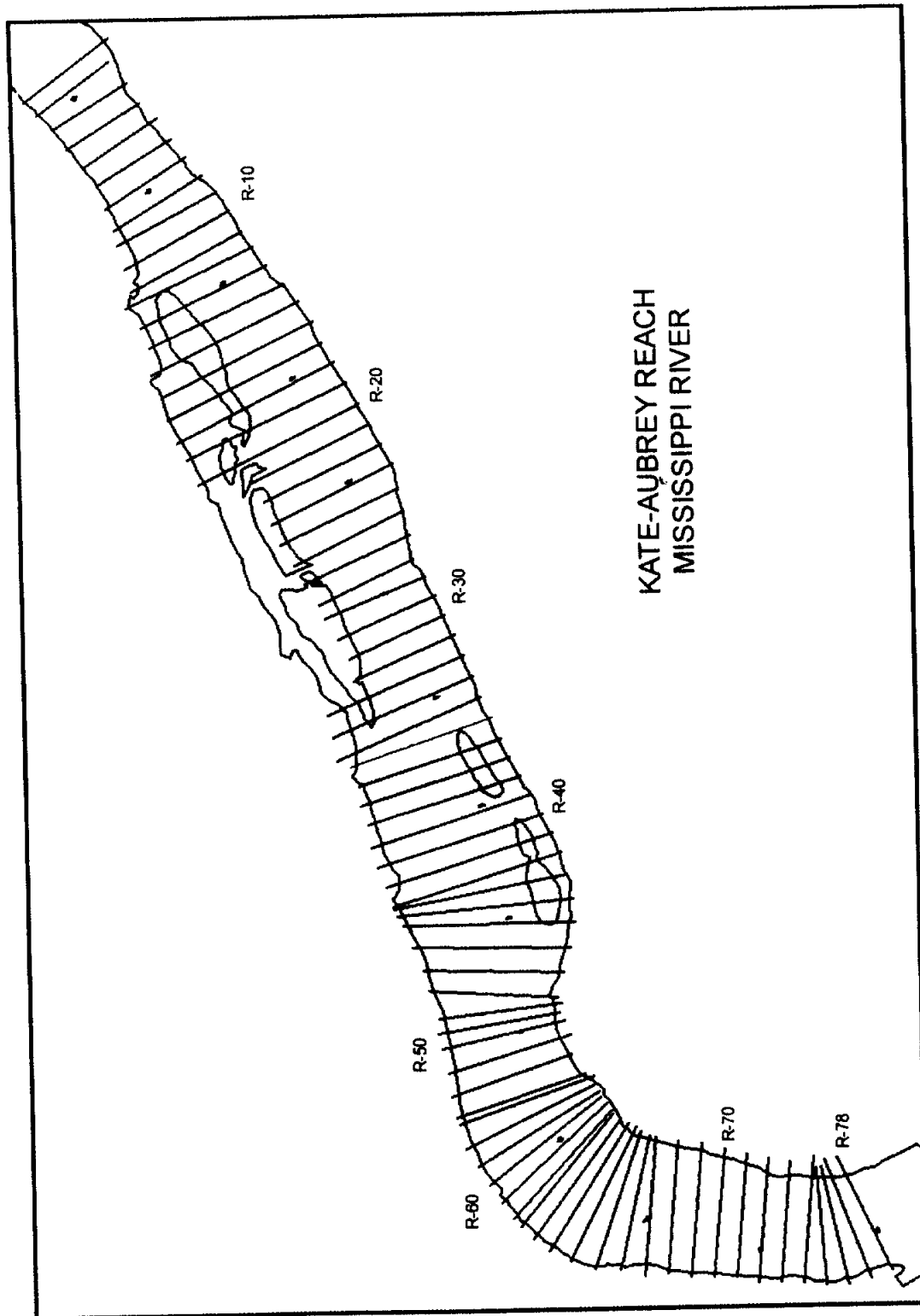


Figure 2-2 Plan View of Typical River Reach Showing Range Locations.

Range lines were located for each model reach at the approximate locations where actual survey data existed. These locations were selected to provide the most accurate depiction of Range elevations. A sufficient number of ranges were used to encompass the full extent of available model data. Coordinate points (x, y, z) for each range line were then derived from the surface using AutoCAD® and Microstation® for the large-scale and small-scale models, respectively. Each Range in a particular model reach produced a separate ASCII text file containing the coordinate point information for individual surfaces analyzed.

Calculation of selected parameter values was accomplished through several computer applications developed specifically for this study. One program was developed as a Microstation® Development Language (MDL) application named Channel.ma. Channel.ma provided an original capability to work directly with triangulated network surfaces to develop cross-section plots, to calculate cross-sectional area-elevation data, to calculate cross-section wetted perimeter data, and to locate the thalweg position within the cross-section. Cross-sectional area was computed by stepwise summation of incremental trapezoidal areas between the triangulated bathymetric surface and the target water levels. Wetted perimeter was determined by calculating the linear distance across the triangulated network surface along each Range. Where the water surface did not intersect the bathymetric surface (e.g., where the water was against the model wall or where prototype data were limited), a vertical line was extended between the surface edge and the water surface. Channel.ma placed the thalweg position at the lowest point in the cross-section. Because the thalweg position sought for the present research entailed the depiction of a continuous line through the lowest possible elevations, consideration of elevations upstream and downstream of a Range was necessary. Channel.ma had no intrinsic logic to account for a continuous line of minimal elevations. For this reason, manual review and adjustment of the thalweg line was necessary.

Single or multi-surface analysis was possible using Channel.ma. Beacon Resources, Madison, AL developed Channel.ma under contract with the US Army Corps of Engineers, Memphis. Figure 2-3 illustrates the Channel.ma dialog interface as

displayed in Microstation®. Later requirements included adding a component to Channel.ma for exporting cross-section coordinate point values to an ASCII format.

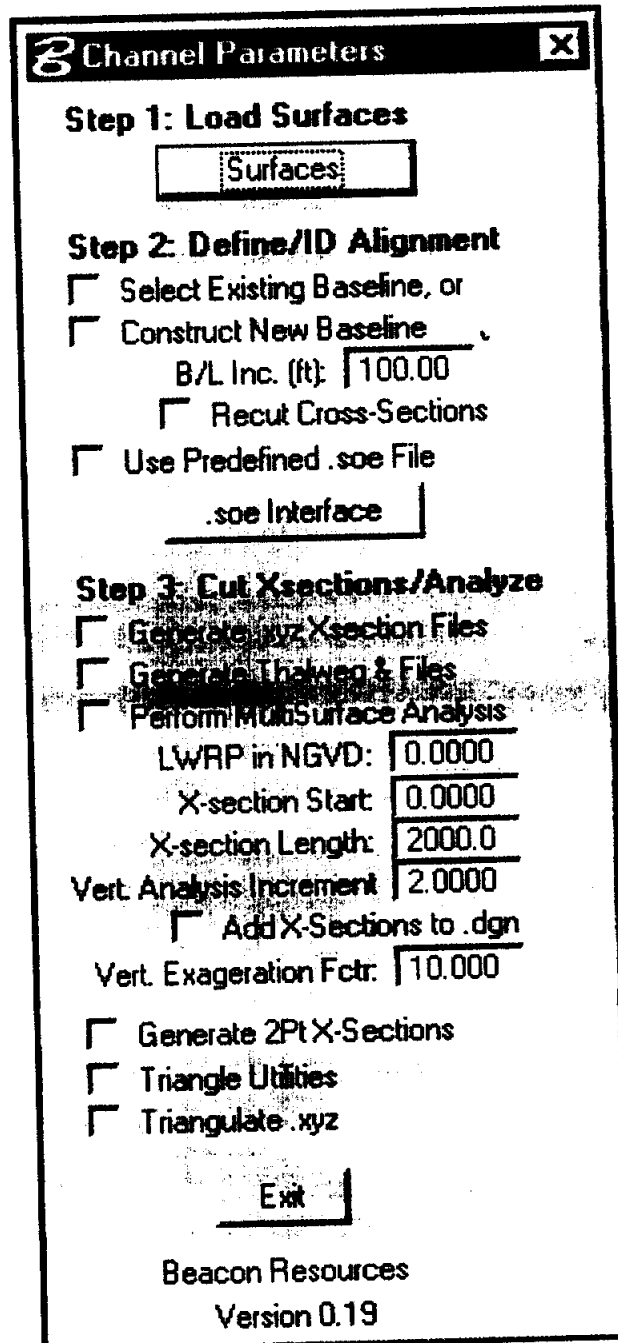


Figure 2-3 Microstation® MDL Channel.ma Interface Dialog Display

Thalweg position was also exported as an ASCII x, y, z file for subsequent analysis. Delineation of the active channel required digitizing the location of real or effective structure termini at each Range line. Real termini occurred where a Range intersected the physical end of constructed training structures. Effective termini occurred at Ranges that did not intersect a physical structure, but where training structures affected the active channel width (See Figure 2-4). Effective termini were defined by an imaginary line connecting the riverward end of training structures. The resulting line, or Dike Line, defined the lateral extent of the active channel within an area affected by training structures. The effective termini was the location where Ranges intersected the Dike Line.

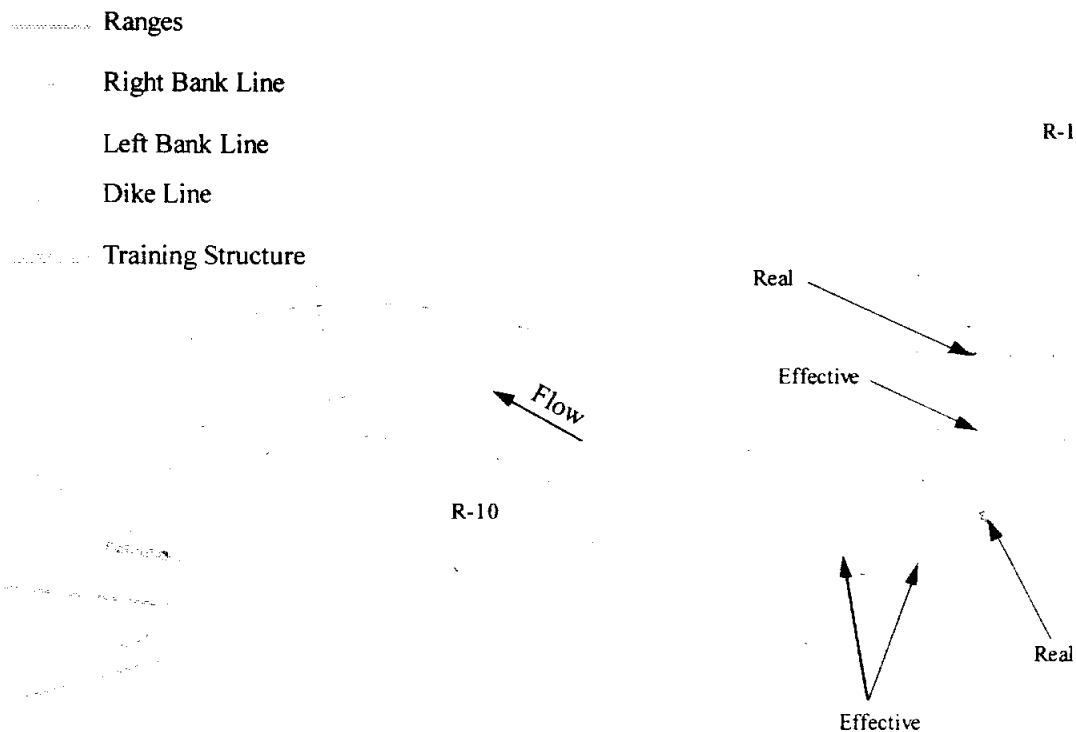


Figure 2-4 Schematic of Real and Effective Termini

Errors detected during routine use of the CHANNEL.MA program required extensive checking of previous results. Therefore,, most of the micromodel analysis was repeated using InRoads™ software which revealed that CHANNEL.MA had random errors in generating x,y,z cross-section files. For this reason the experimental version of CHANNEL.MA cannot be used for routine model analysis in its current form. Correction of the CHANNEL.MA program code is recommend to aid in the analysis and processing of model calibration data.

An additional program, MBANAL.FOR, was written in the FORTRAN language by Dr. Steve Maynard, WES. MBANAL calculated the area, hydraulic depth, and the channel widths as previously described. Inputs to MBANAL were range line x, y, z coordinate point files, the thalweg position coordinates (x, y, z), and dike location coordinates for each cross-section being analyzed. MBANAL required that coordinate point data be extracted from the digital terrain model into a separate ASCII file for each range line. Outputs from MBANAL were in the form of ASCII files. These files were imported into Microsoft Excel® and further manipulated to produce the desired tables, charts, and difference comparisons.

2.1.4. Comparisons. Conditions in alluvial streams are continuously changing and are affected by variations in hydrologic conditions, channel geometry, and sediment movement. The channel morphology and man-made features are additional factors influencing this change. Because of the complex spatial and temporal interaction of these and other factors, it is not possible to distinguish the cause effect relationship for each individual factor (Biedenham, 1995). While it is not the intent of the present study to relate channel response to these factors, each of these factors has a direct influence on variations found in the prototype. This variability in turn affects model-to-prototype similarity.

Although extensive data were available for study of prototype variability, accomplishment of present study goals required that only data associated with available model studies be analyzed. Not all model studies incorporated in the analysis utilized multiple prototype surveys for model verification/calibration. In particular, the verification process employed by the Waterways Experiment Station (WES) generally

utilized only one prototype survey to assess model reproduction of prototype conditions (The WES models are hereafter generally referred to as the large-scale models). Their verification began with a specified prototype condition which was molded into the model bed. The model was then operated (and adjusted) to reproduce prototype discharges and sediment loads necessary to reproduce a second, later prototype bathymetry. Verification was assessed through a visual qualitative interpretation of model and prototype bathymetry. Franco (1978) provides further details of the WES verification procedure.

Contrasting this method of verification, micromodels (subsequently referred to as small-scale models) employed an equilibrium sediment recycling approach, which utilized a number of prototype surveys in a calibration process. This process involved operating a model through a series of hydrograph cycles with adjustments to slope, discharge, and boundary conditions until prototype conditions were reproduced in the model. Where available, multiple prototype surveys were visually and qualitatively compared to model bathymetry in a manner similar to that used for the WES models to assess the state of model calibration. Where only one prototype survey was available, the comparison technique involved only the model and the single prototype bathymetric survey. Gaines (1999) described the micromodel procedure more extensively. Gaines et.al. (in progress) further explain the micromodel procedure used in this study.

2.1.5. Analysis of Data. Analysis of individual bathymetric surfaces to obtain the five morphologic parameters began by considering individual Range values. Consideration of individual Range values revealed a high degree of variability throughout a model or prototype reach. Though expected, this variability caused difficulty in assessing similarity conditions for model application. Therefore, two approaches were required to ascertain the degree of model and prototype agreement. The first approach included individual Range values in the calculation of model-to-prototype differences. The second approach involved the use of weighted reach values for the five morphologic parameters to explore similarity relationships for the previous model studies.

2.1.5.1 Analysis of Range data. Analysis of individual Range values involved a large number of values for a particular model reach. Inspection of tabulated range values of TP, H₀, W₀, A₀, and W₀/H₀ revealed little about the prototype or about model's ability to reproduce prototype conditions. Statistical parameters (e.g., mean, standard deviation, and variance) could not be reliably calculated for individual ranges because only two to five data values were available. Various difference calculations (such as direct calculation of a percent difference from actual data values) revealed no significant trends in the data.

Differences between the model and expected prototype values are calculated using the Expected Model Value (taken as the computed parameter value for the model) and the Expected Prototype Value (taken as the analogous parameter value for the prototype data). A representative reach difference value is calculated by averaging the individual Reach differences for the reach. The difference calculation (in percent) for individual ranges becomes:

$$DIFF_i = \left(\frac{\text{Expected Model Value} - \text{Expected Prototype Value}}{\text{Expected Prototype Value}} \right) 100$$

And the representative reach difference calculation is the average of the individual Range differences:

$$DIFF = \frac{\sum_{i=1}^n DIFF_i}{n}$$

Variability between model and prototype was also expressed by a Sum of Squares Error (SSE_i) term based upon individual range data. SSE_i values were calculated at each Range using the following equation

$$SSE_i = \left(\frac{\text{Model Value} - \text{Prototype Value}}{\text{Prototype Value}} \right)^2$$

where i is the Range number, Model Value represents any model morphological parameter value, and Prototype Value represents the corresponding prototype morphological parameter value for any individual prototype bathymetry. A graphic representation of Range versus SSE_i can be used in conjunction with plots of individual Range parameter values to assess the amount of variability between model and prototype values by location. While the plotted parameter values illustrate the variability, values of SSE provide a quantitative measure of this variability. An additional measure of overall agreement for the entire reach can be obtained by the Mean Squared Error (MSE)

$$MSE = \frac{1}{n} \sum_{i=1}^n SSE_i$$

Larger values of MSE indicate less agreement between the model and prototype, and smaller values indicate better agreement.

2.1.5.2 Weighted reach values. One aspect of the present investigation involved assessing individual model similarity to gain insights into the important aspect of developing criteria for use in applying small-scale models. To achieve a measure of morphological similarity, individual Range values of H_0 , W_0 , A_0 , and W_0/H_0 had to be combined in a way that reach conditions were adequately expressed. One possibility for developing representative reach values consisted of calculating a direct arithmetic average of all Range values. Such an averaging technique treated each Range value equally irrespective of the interval between successive ranges, the alignment of the ranges, or the length of the reach. The present investigation initially utilized a simple average of parameter values. However, a weighting procedure that involved the reach characteristics was favored over a straight average for final analysis.

Although it is an important parameter in assessing model and prototype agreement, thalweg position was not expressed in any similitude relationships considered in the present study. The arbitrary reference point used in determining the thalweg position provided no consistent definition of this parameter throughout the model reach. Therefore, no reach value for thalweg position was calculated.

Thalweg length between individual ranges was estimated from map coordinates defined by the thalweg position. This thalweg length provided a means to calculate reach volumes and to calculate reach weighted values for the remaining morphologic parameters. A volume based weighting technique was used in calculating reach values for width, area, and hydraulic depth. Calculation of reach average conditions involved the following four step process.

1. Calculate the weighted width for the reach by

$$T_{WR} = \frac{1}{L} \sum_{i=1}^{n-1} \left[\frac{T_{W_i} + T_{W_{i+1}}}{2} \right] L_i$$

where L is the total reach length measured along the thalweg, L_i is the thalweg length between consecutive Ranges, T_{WR} is the reach weighted width, T_{W_i} is the individual Range width, i is a counter, and n is the number of ranges.

2. Calculate the total reach volume by using average end area methods,

$$V_{WR} = \frac{1}{L} \sum_{i=1}^{n-1} \left[\frac{A_{W_i} + A_{W_{i+1}}}{2} \right] L_i$$

where V_{WR} is the total reach water volume and A_{W_i} is the individual Range cross section area at i and $i+1$ Ranges,

3. Calculate the weighted area for the reach by

$$A_{WR} = \frac{V_{WR}}{L}$$

where A_{WR} is the weighted area for the reach., and

4. Calculate the weighted hydraulic depth for the reach using T_{WR} and A_{WR} ,

$$D_R = \frac{A_{WR}}{T_{WR}}$$

where D_R is the weighted hydraulic depth for the reach. Use of interval volumes (between consecutive Ranges) in the weighting included basic channel characteristics of cross section area, thalweg length, and channel width. Calculation of the reach width to depth ratio using T_{WR} and D_R precluded the need for an weighting procedure for the width to depth ratio (e.g. the results are the same).

Analysis of the thirty previous model studies required the synthesis of a large body of data through cumulative frequencies and by reach averages. The methodology is best presented by example. The Kate-Aubrey reach described in the following section illustrates the procedures employed in the present investigation.

2.2. Data Interpretation

The evaluation of previous model study results involved a large volume of data. The methods employed by the present investigation attempted to utilize relatively straight forward methods that provided a quantitative expression of model and prototype agreement. Although more complex methods may exist, their usefulness in every day model applications is limited. The methods presented provide a means for including a quantitative description of the morphologic similarity with each micromodel study.

As with any assessment technique, there are special considerations that must be identified. The following sections describe factors that must be considered when interpreting the results of this investigation and/or when applying the recommended methodology.

2.2.1. Difference and Mean Squared Error Values. Evaluation of individual ~~of individual~~ morphologic parameter values begins by calculation of ~~of~~ differences between average prototype parameter values ~~in~~ the model. Differences describe the relative magnitude of model parameter values relative to the average prototype. Relative

magnitude includes both the numerical value of the difference and the sign. Larger difference values indicate a greater deviation from the prototype, and smaller difference values have less deviation from the prototype. Negative differences represent model values less than found in the prototype. Positive differences represent model values greater than found in the prototype. Calculated differences at each Range provide a representation of how the model relates to the prototype at the separate locations. To assess the overall reach, difference values must be averaged over the entire model.

Mean squared error (MSE) provides an estimate of goodness of fit between model values and prototype values. As with the differences, larger MSE values indicate greater departure from the prototype while smaller MSE values indicate less departure from the prototype. The MSE represents the entire model reach.

Averaged values over the entire model provide only part of the information necessary for comparing model and prototype data. Consideration of individual Range parameter values (or differences) plays an indispensable role in determining model and prototype agreement. Average difference values and/or MSE values may be misleading depending on the relationship between model results and the prototype. For example, consider the hypothetical situation depicted in Figure 2-6. Figure 2-6 describes how three model results relate to the prototype. Visual interpretation of this figure quickly leads to the conclusion that Model 1 provides the best representation of the prototype. However, differences calculated for each of the three models are the same as shown in Table 2-3.

The variation of model parameter values above and below the prototype results in an average difference that does not represent the true relationship between the model and the prototype. The cancellation of differences with alternate signs (positive and/or negative) requires an additional factor. The addition of MSE values (also shown in Table 2-3) provides the remainder of the picture. The lowest MSE value between Models 1, 2, and 3 comes from Model 1 -- in agreement with the original assessment from Figure 2-6.

2.2.2. Prototype Variability. There are two types of prototype variability, spatial and temporal. Reach averages and statistics (minimum, maximum, and standard deviation) provide a description of spatial variability within a single survey. Analysis of average morphologic parameter values and their associated statistics at a single range for multiple

surveys describes the temporal variability. In models, the temporal variability relates to uncertainty – no two simulation periods produce exactly the same bed configuration. While this is consistent with observed prototype behavior, the temporal changes are not fully understood. The lack of understanding comes largely from an inability to collect the necessary data in the prototype. ~~Therefore, only the spatial variability can be considered.~~

Some rivers have a greater degree of spatial variability than others. Reaches having higher variability are generally more difficult to model than less variable reaches.

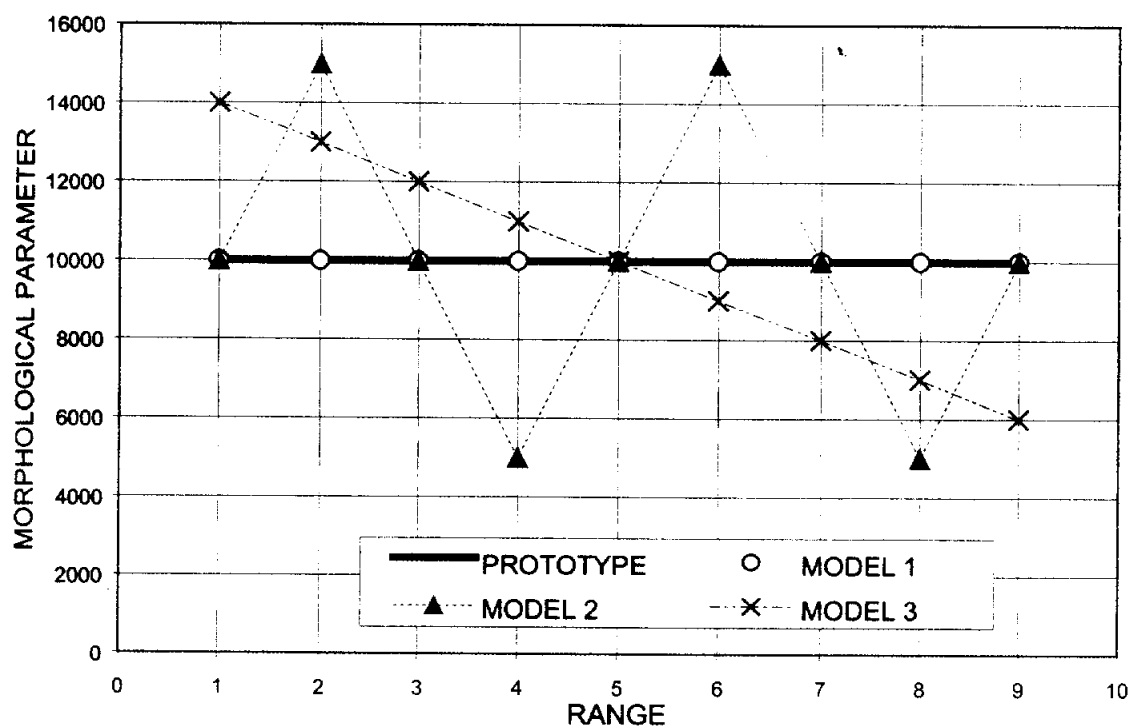


Figure 2-6 Hypothetical Model and Prototype Data

Table 2-4 lists mean, minimum, maximum, and standard deviation for cross section area, hydraulic depth, width, and the width/depth ratio at an elevation of 0.0 LWRP for the Kate-Aubrey reach.

Values shown in Table 2-4 for the 1:300 model reflect a different reach length than for the 1:8000 and 1:16,000 models. ^{location and} The number of ranges used in calculating the mean, minimum, maximum, and standard deviation also had an impact on computed values.

The 1:300 model utilized 28 ranges between River miles 789 to 794.

The number of ranges for the 1:8000 and 1:16,000 models differed depending on available model survey data. Typically, the parameter standard deviation was 30 percent of the mean for the reach. The relatively high standard deviation indicates a large variability of each morphologic parameter through the reach. Additionally, the difference between maximum and minimum values can be large (on the order of the mean value). Although the data in Table 2-4 represent only a single prototype reach, three models are included in the comparison. All three models exhibit similar variability in calculated parameter values as found in the prototype.

Identifying the conditions used for specifying model similitude requirements becomes difficult when prototype conditions involve a high degree of spatial and temporal variability. This leads to the conclusion that similitude in open rivers is not an absolute.

The micromodels utilized more than 70 ranges between River miles 785 to 798.

Table 2-3 Hypothetical Model Difference and MSE Values

Range	Prototype Area	Area Model 1	Area Model 2	Area Model 3	Difference 1	SSE 1	Difference 2	SSE 2	Difference 3	SSE 3
1	10000	10000	10000	14000	0	0	0.0000	0.0000	0.4000	0.1600
2	10000	10000	15000	13000	0	0	0.5000	0.2500	0.3000	0.0900
3	10000	10000	10000	12000	0	0	0.0000	0.0000	0.2000	0.0400
4	10000	10000	5000	11000	0	0	-0.5000	0.2500	0.1000	0.0100
5	10000	10000	10000	10000	0	0	0.0000	0.0000	0.0000	0.0000
6	10000	10000	15000	9000	0	0	0.5000	0.2500	-0.1000	0.0100
7	10000	10000	10000	8000	0	0	0.0000	0.0000	-0.2000	0.0400
8	10000	10000	5000	7000	0	0	-0.5000	0.2500	-0.3000	0.0900
9	10000	10000	10000	6000	0	0	0.0000	0.0000	-0.4000	0.1600
Mean	10000	10000	10000	10000	0		0.0000		0.0000	
Maximum	10000	10000	15000	14000	0		0.5000		0.4000	
Minimum	10000	10000	5000	6000	0		-0.5000		-0.4000	
Std.Dev.	0	0	3535	2738	0		0.3536		0.2739	
MSE						0		0.1111		0.0667

Table 2-4 Prototype and Model Variability: Kate-Aubrey Case Study

Reach Weighted Morphologic Parameter Values and Variability - Kate Aubrey Reach, Mississippi River																			
Survey	Description	Number of Ranges	Area (sq. ft.)				Hydraulic Depth (ft.)				Width (ft.)				Width/Depth				
			Mean	Minimum	Maximum	Std. Dev.	Mean	Minimum	Maximum	Std. Dev.	Mean	Minimum	Maximum	Std. Dev.	Mean	Minimum	Maximum	Std. Dev.	
1:300 Model	Verification	28	26501	8197	64391	13420	13.6	5.3	30.9	7.4	2107	788	3895	751	211	44	480	136	
1975 Prototype		28	33394	18527	58653	11591	13.7	6.3	27.8	6.0	2696	1241	5240	1056	252	57	629	164	
1976 Prototype		28	38064	18803	56403	10644	16.6	5.6	44.6	8.5	2644	1264	5889	1060	227	28	892	199	
1:8,000 Micromodel	Calibration	71	35540	7560	11467	17817	15.6	6.9	39.5	6.3	2385	921	4906	989	182	42	526	115	
1973 Prototype		71	45839	26256	76794	12856	16.3	8.6	29.4	4.8	2983	1343	5274	984	209	46	545	111	
1975 Prototype		71	42688	20014	71793	10576	18.4	7.4	29.8	5.2	2488	1145	4736	869	159	48	456	99	
1976 Prototype		71	46372	22637	67926	9846	19.8	8.3	44.2	6.1	2509	859	4821	796	148	22	584	91	
1:16,000 Micromodel	Calibration	75	51034	14953	12963	21176	17.5	6.6	35.3	7.4	3030	1496	5376	851	213	43	675	126	
1973 Prototype		75	45054	24824	76794	12995	16.1	7.5	29.4	4.9	2973	1343	5274	986	213	46	545	116	
1975 Prototype		75	42323	20014	71793	10623	18.1	7.4	29.8	5.3	2508	1145	4736	853	164	48	456	100	
1976 Prototype		75	46065	22637	67926	9794	19.5	7.0	44.2	6.2	2552	859	4821	831	157	22	617	110	
1:8,000 Micromodel	Predictive	78	36836	13904	92159	13439	16.1	6.4	37.5	6.7	2366	1556	4393	572	173	49	423	80	
1998 Prototype		78	48761	32205	66695	7332	21.9	13.4	33.7	4.8	2326	1262	3988	570	117	37	273	53	
2001 Prototype		78	47942	32901	71781	7840	21.2	14.2	31.7	4.3	2326	1515	3850	475	117	56	239	43	
1:16,000 Micromodel	Predictive	78	49825	24812	11729	19822	19.3	10.1	39.1	6.6	2604	932	4488	580	150	31	298	56	
1998 Prototype		78	48761	32205	66695	7332	21.9	13.4	33.7	4.8	2326	1262	3988	570	117	37	273	53	
2001 Prototype		78	47942	32901	71781	7840	21.2	14.2	31.7	4.3	2326	1515	3850	475	117	56	239	43	

Thalweg Position was not included in Mean, Minimum, Maximum, or Standard Deviation calculations.

2.2.3. Selection of Key Water Surface Elevations. The geomorphologic approach to analyzing stream systems considers a number of basin and channel characteristics. Basin characteristics include channel slope, valley slope, and channel sinuosity. Morphologic channel characteristics typically consist of the cross-section area, the channel width, the channel depth, and the ratio of the width divided by the depth (the width to depth ratio) at the bankfull stage (Leopold. et al., 1964, Rosgen, 1996). Parameters describing the basin and channel characteristics of one stream serve as the basis to analyze another stream system. For the purposes of analyzing stream stability, a stable stream system (i.e. a reference reach) provides desirable parameter conditions useful in stabilizing a second stream having similar basin characteristics (drainage area, valley slope, topography, and climatic conditions) (Rosgen, 1996). In other words, the morphologic approach utilizes similarity between stream systems to assess stream stability or to design stabilizing measures. Morphologic similarity, then, provides a mechanism for comparing two stream systems or for comparing a model and prototype stream.

While determining model and prototype similarity differs from the typical application of geomorphologic principles, the use of channel characteristics to assess model and prototype similarity provides a means to consider similarity of bathymetry between model and prototype. This similarity (referred to as morphologic similarity) uses hydraulic geometry in the model and in the prototype to describe the level of agreement between the respective channels.

One primary difference between the geomorphologist's use of morphologic characteristics and the micromodeler's use of morphologic similarity derives from the fact that ~~many loose bed models~~ ^{micro models} do not simulate the bankfull channel stage. More specifically, micromodels generally simulate flow conditions up to approximately stage +20 LWRP. Bankfull conditions in the prototype typically occur at a stage of +30 LWRP. Therefore, evaluation of morphologic similarity using cross-section area, top width, hydraulic depth, and the width to depth ratio requires the selection of a water surface elevation for each series of calculations.

The water surface elevation selected for the basis of calculations directly influences the calculated values of cross-section area, top width, hydraulic depth and width to depth ratio. Differences in cross-section area, top width, hydraulic depth, and

width to depth ratio calculated at the true bankfull stage provide a holistic representation of the river channel. The same difference calculation made using morphologic parameter values at an elevation lower than bankfull describes less than the full channel. Therefore, different aggradational and/or depositional patterns found in the lowest portion of the channel (where most change in the channel boundary occurs) have a greater impact on the calculated differences. Figure 2-7 illustrates the relationship of selected water surface elevation (in LWRP elevations) ^{and cross-section area} to the difference calculation for Ranges 25 through 59 in the Kate-Aubrey reach of the Mississippi River. Prototype conditions are from a 2001 hydrographic survey. Model data are from the 1:8,000 micromodel.

Figure 2-7 indicates that larger differences result when the selected water surface elevation is lowest. As the water surface elevation used for calculating cross-section area increases, the difference between model and prototype reduces until approximately the ± 20 percent level of difference. This is consistent with observations of the physical response of both the model and prototype channels where the greatest changes occur in the low flow channel.

Prototype variability between successive surveys is generally greater in the lowest elevations of the cross-section than found at higher cross-section elevations. The channel boundary in the lowest region of the cross-section experiences more change than observed in the higher depositional features. The variable flow rates and associated stages observed in the prototype (and used in the model) contribute to the greater change at lower elevations because sediment transport continues through most of the hydrograph cycle⁴. At the higher elevations, where depositional features experience periods of no (zero) flow and no sediment transport during part of the hydrograph, changes in the bathymetric surface are smaller. Table 2-~~5~~⁵ presents the percent differences (averaged over the model reach specified by the indicated Ranges) calculated for twelve micromodels. Table 2-~~5~~⁵ includes only cross-section area below +20 LWRP and 0 LWRP for illustration. ₅ α

⁴ Sediment transport continues through the entire hydrograph cycle in the Mississippi and Missouri Rivers. Sediment transport in smaller tributary streams may occur only when discharges exceed a threshold value. When tributary discharge is below the threshold value, the bed is immobile.

Calculated differences shown in Table 2-4⁵ indicate that ~~there is more agreement~~ ^{the differences are smaller} ~~there is less difference~~ ^{there is more agreement} between the model and the prototype surveys using an elevation of +20 LWRP than when using elevation 0 LWRP. Clearly, there is greater variability between successive prototype surveys and between model and prototype surveys at lower elevations than exists at higher elevations. For these reasons, interpretation of the degree of similarity between model and prototype using difference calculations requires caution. The perceived level of model and prototype agreement must be tempered with an understanding of the basis used in calculating morphologic parameter values. The availability of bathymetric data at the higher elevations must also be considered.

Parameter values used in assessing morphologic similarity should be sensitive enough to reveal differences between the model and prototype. Yet, parameter values should not be overly sensitive (thereby giving a false representation that there is no similarity between the two). Selected methods for calculation of parameter values should facilitate an adequate description of both variations between available prototype bathymetric surveys and between the model and prototype.

Because most prototype surveys used in micromodeling have only partial coverage of the prototype bathymetry⁵, the calculation of morphologic parameter values above 0 LWRP can be problematic. Sometimes, only a limited amount of data exists for elevations above 0 LWRP. On the other hand, calculation of morphologic parameter values at lower elevations tends to exaggerate calculated difference values. In light of the sensitivity of morphologic parameters to elevation, an elevation of 0 LWRP provides the basis for supporting principal study findings. This elevation, equivalent to the water

⁵ Prototype surveys of the Mississippi River primarily focus on navigation requirements. Typical bathymetry obtained for assessing navigation requirements extend only over the navigable portion of the channel and are generally obtained for low water conditions (i.e. less than +10 LWRP). Bathymetric data are rarely obtained over the entire prototype channel width. Although limited bathymetric data for elevations of +10 LWRP or higher may be available, few reaches have elevation data that consistently describes the bathymetry for elevations at or above +10 LWRP.

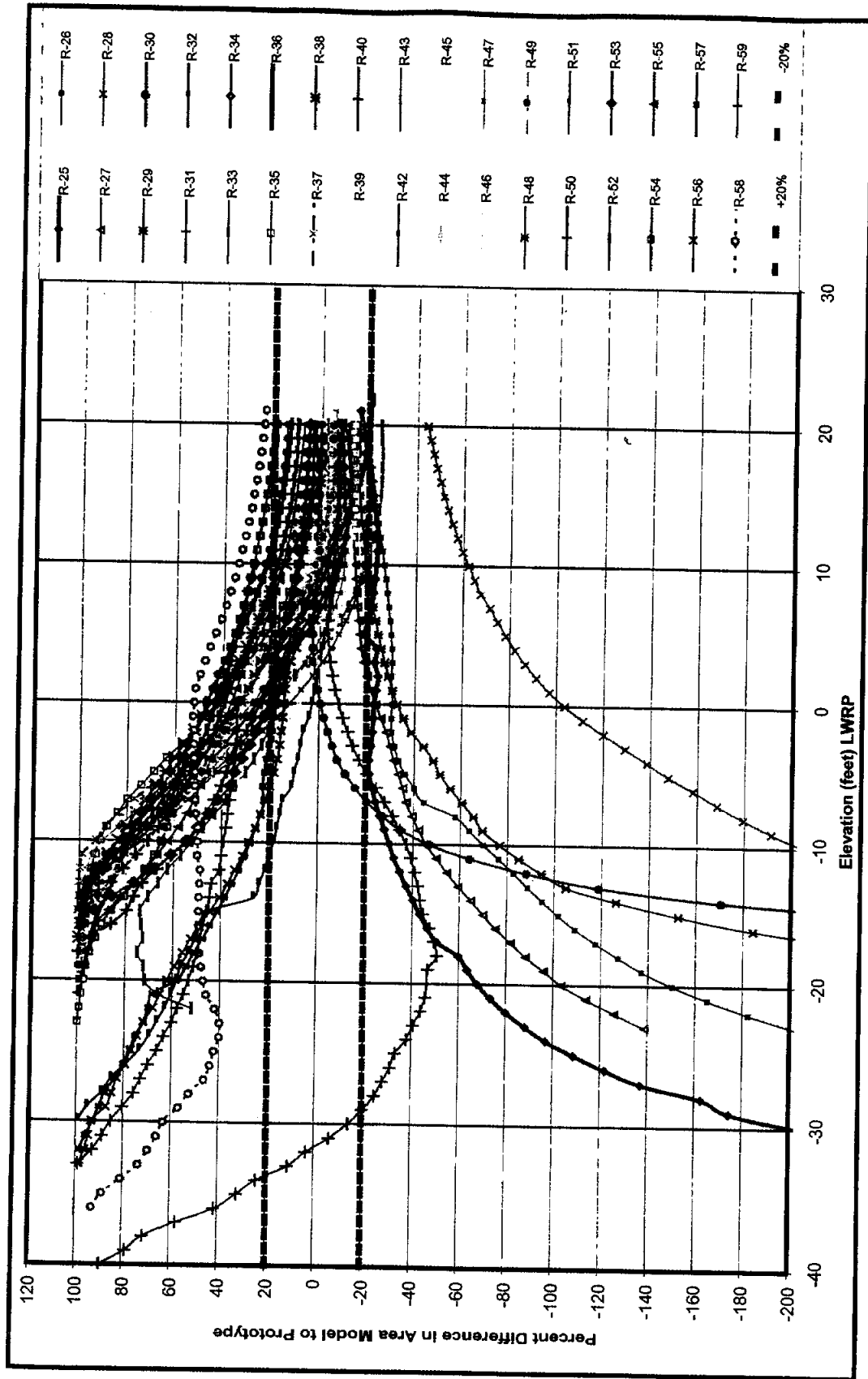


Figure 2-7 Model/Prototype Differences versus LWRP Elevation - Kate-Aubrey Reach

5
Table 2-4 Elevation Sensitivity of Morphologic Parameter Values

Micromodel	CROSS-SECTION AREA @ 0 LWRP		CROSS-SECTION AREA @ +20 LWRP	
	<i>Avg DIFF Difference</i>	MSE	<i>Avg DIFF Difference</i>	MSE
Augusta	0.1899	0.1040	0.0973	0.0151
Clarendon	0.4020	0.3740	0.2144	0.0932
Copeland	0.1096	0.0235	-0.0139	0.0038
Kate-Aubrey 1:8000 Base	0.0685	0.2164	0.1942	0.1170
Kate-Aubrey 1:8000 Predictive	-0.1426	0.1050	0.0855	0.0351
Kate-Aubrey 1:16,000 Base	0.2841	0.3186	0.2744	0.1709
Kate-Aubrey 1:16000 Predictive	0.1109	0.1842	0.2059	0.0874
Lock & Dam 24	0.1277	0.0634	0.0324	0.0104
Memphis Harbor	-0.2127	0.0911	-0.0695	0.0238
Morgan City	0.0403	0.0477	0.0520	0.0311
New Madrid	-0.2613	0.1577	-0.2253	0.0871
Salt Lake	0.2048	0.0566	0.0878	0.0119
Savanna Bay	-0.1710	0.0567	-0.0509	0.0082
Vicksburg	0.0221	0.1136	0.0182	0.0256
White River	-0.3507	0.1559	-0.2139	0.0662
Wolf Island	0.3868	0.4559	0.1756	0.0978

surface elevation equaled or exceeded 97 percent of the time, represents an important elevation used in navigation work. However, the percentage of time that flow exceeds this elevation suggests that morphologic parameters calculated at this level may be overly sensitive -- the channel boundary may change disproportionately in response to the amount of sediment transport resulting from flow at higher stages. Data for other elevations (i.e. -10 LWRP, +10 LWRP, and/or +20 LWRP) are presented, where feasible, to provide additional insight regarding model and prototype agreement.

Interpretation of percent difference values requires consideration of several factors. The following list describes these factors.

1. Thalweg position does not depend on any particular elevation used for calculation of hydraulic geometry components (unless such elevations physically restrict the model in a way that limits the active width of the channel). Therefore, this study assumes that thalweg position is independent of the elevation used in calculating the cross-section area, the channel width, the hydraulic depth, and the width to depth ratio.
2. Cross-section area, channel width, hydraulic depth, and width to depth ratio are a function of the elevation used for computations. Percent differences between model and prototype are highly sensitive to the elevation used in calculating these morphologic parameter values.
3. Cross-section area and channel width are independent parameters. These parameters are calculated directly from cross-section geometry.
4. Hydraulic depth and width to depth ratio are dependent parameters; they are derived parameters. These parameters depend on cross-section area and width parameter values, which are calculated from cross-section geometry.
5. The greatest change in the bathymetric surface occurs at lower cross-section elevations.
6. As a minimum, morphologic similarity is assessed at an elevation of 0 LWRP.
7. Morphologic similarity includes a consideration of morphologic parameter values at a variety of elevations (i.e. -10 LWRP, +10 LWRP, and/or +20 LWRP) where bathymetric data are available.

2.2.4. Use of Truncated Cross-Section Data. Truncation of range data results when the survey does not extend across the entire channel width. The amount of truncation depends on the coverage obtained during survey efforts and may be different for model and prototype. A simplistic approach to evaluate truncation effects on the morphologic parameters is described in Appendix A. Several previous model study results were omitted from the comparison analysis in order to eliminate bias introduced by truncation and more specifically effects from random truncation. The micromodels included in the scale ratio analysis were determined to have no truncation effects up to an elevation of zero LWRP. Truncation effects above elevation zero LWRP were considered to be none or minimal because the fourteen micromodels had prototype data extending to (or very near to) the bankline. Any vertical extension of the cross-section at the bankline would therefore involve no truncation.

3. KATE-AUBREY CASE STUDY

3.1. Case Studies

The Kate-Aubrey reach of the Mississippi River was selected for detailed study in the present investigation because a large amount of data existed for the prototype. Additionally, a large-scale coal-bed model had previously been constructed and utilized for channel improvements between approximately River Miles 785 and 800. Although earlier model studies of the Kate-Aubrey reach aided in design of navigation improvements, problems persist in the area as of 2001. The need for additional model studies of this reach provided an opportunity to explore model similarity requirements. For this reason, the current investigation included construction of two micro-scale models (micromodels) of the Kate-Aubrey reach to aid in assessing and validating the micro-scale methodology. Construction of the micromodels for Kate-Aubrey also provided the tools needed to assess further improvements for navigation. Alternative analysis related to these improvements are not included in the present investigation.

3.1.1. History of Kate-Aubrey Reach. Franco (1978) describes the Kate-Aubrey reach beginning just prior to 1968 and continuing through 1975. Franco (1978) also provides a description of the prototype and model study results obtained with an earlier sand-bed physical model. The reach had considerable variability in the thalweg location from year to year even with training structures constructed to restrict adjustment of the navigation channel alignment. This variability resulted in several shallow crossings, most notably in the vicinity of River Mile 790. Following a major flood event in 1973, the navigation channel exhibited an almost ninety-degree crossing from the left descending bank to the right descending bank at River mile 793.4. Significant dredging was required on at least an annual basis to maintain a navigable channel in this area. For example, dredging at Kate-Aubrey for the four year period between 1976 and 1979 averaged 4,000,000 cubic yards annually. The high annual cost of maintenance prompted the use of a physical model to study alternative plans for improving the reach.

A coal-bed physical model was designed and constructed by WES in the late-1970's to mid-1980's to assist river engineers in developing an improvement plan for the reach. The coal-bed model was calibrated to 1975 and 1976 prototype conditions. Prototype hydrographic surveys existed for each year beginning in 1968 through 1979 with some years having only partial coverage of the entire reach. Hydrographic surveys in years following 1980 were at one to three year intervals. Hydrographic surveys for 1973, 1975, and 1976 were selected for calibration of the micromodels to coincide with the period used in large-model verification. Use of this prior time period as the basis for calibration permitted use of the three model scales in assessing scale effects on similarity. A further benefit of using the prior time period for calibration was that a more recent prototype condition could be placed in the model to assess the predictive capability of the micromodels. The predictive analysis is described in subsequent sections.

The Kate Aubrey micromodels were designed to encompass the range of horizontal scales typically used in micromodeling. Horizontal scales of 8,000:1 and 16,000:1 were selected. The same bank lines, upstream and downstream limits, and physical boundary conditions were used for both micromodels. Ranges utilized for analysis of the two micromodels were the same (shown in Figure 3-1). However, these Range locations were different than those used in analyzing the large-scale model. Figure 3-2 shows the Ranges used for the large-scale Kate-Aubrey model. The model reach length was also different. The 1:300 model extended over river miles 785.5 to 797.0 and the two micromodels extended between river miles 784.0 to 803.0.

3.1.2. Large-Scale Models. An example of large-scale model is the Kate-Aubrey model of the Mississippi River conducted by WES. A photograph of the large-scale Kate-Aubrey physical sediment model is shown in Figure 3-3. The Kate-Aubrey reach is

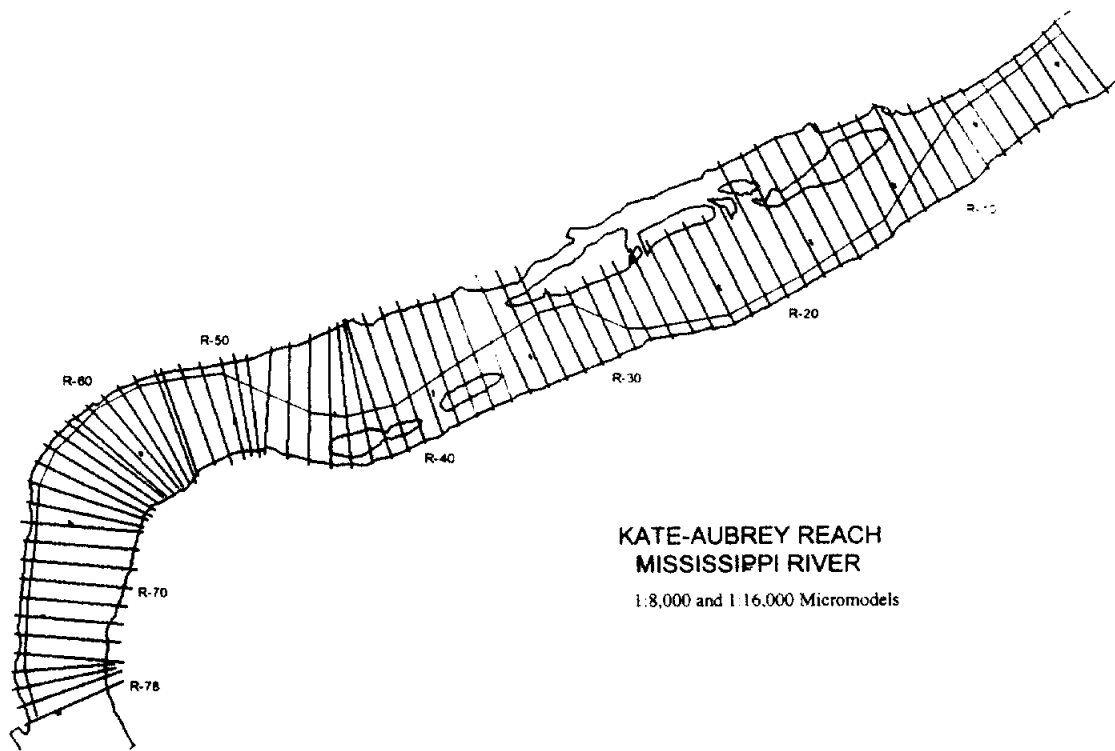


**Figure 3-1 Model Extent and Range Locations for 1:8,000 and 1:16,000
Micromodels**

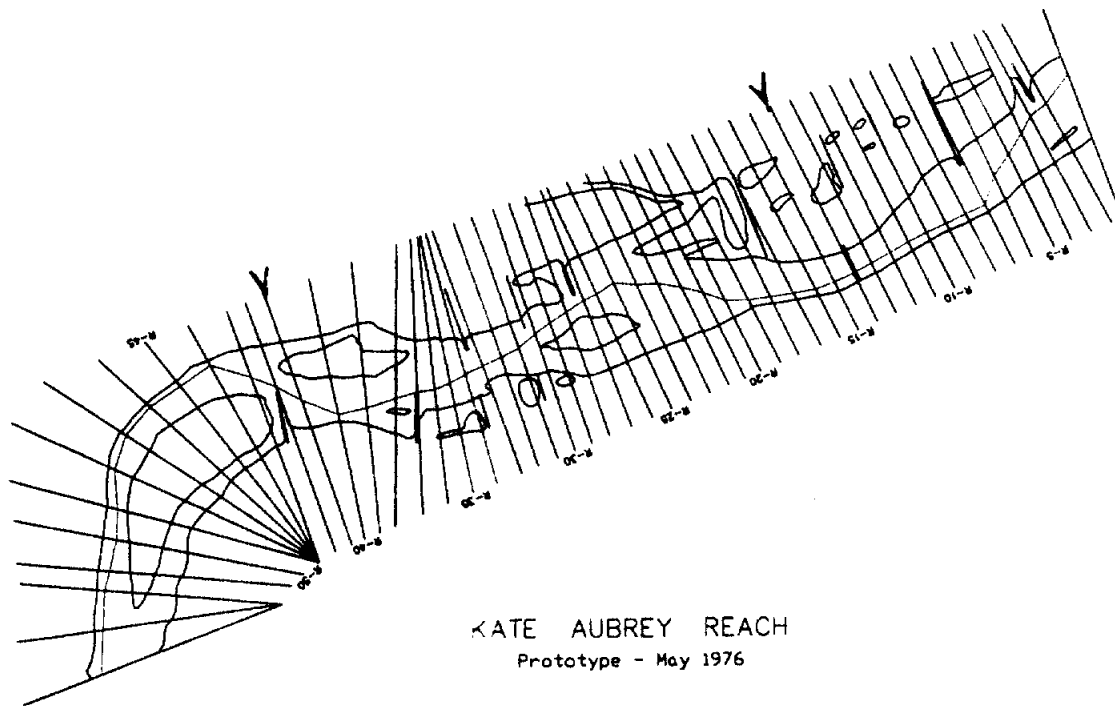


Figure 3-2 Model Extent and Range Locations for 1:300 Model

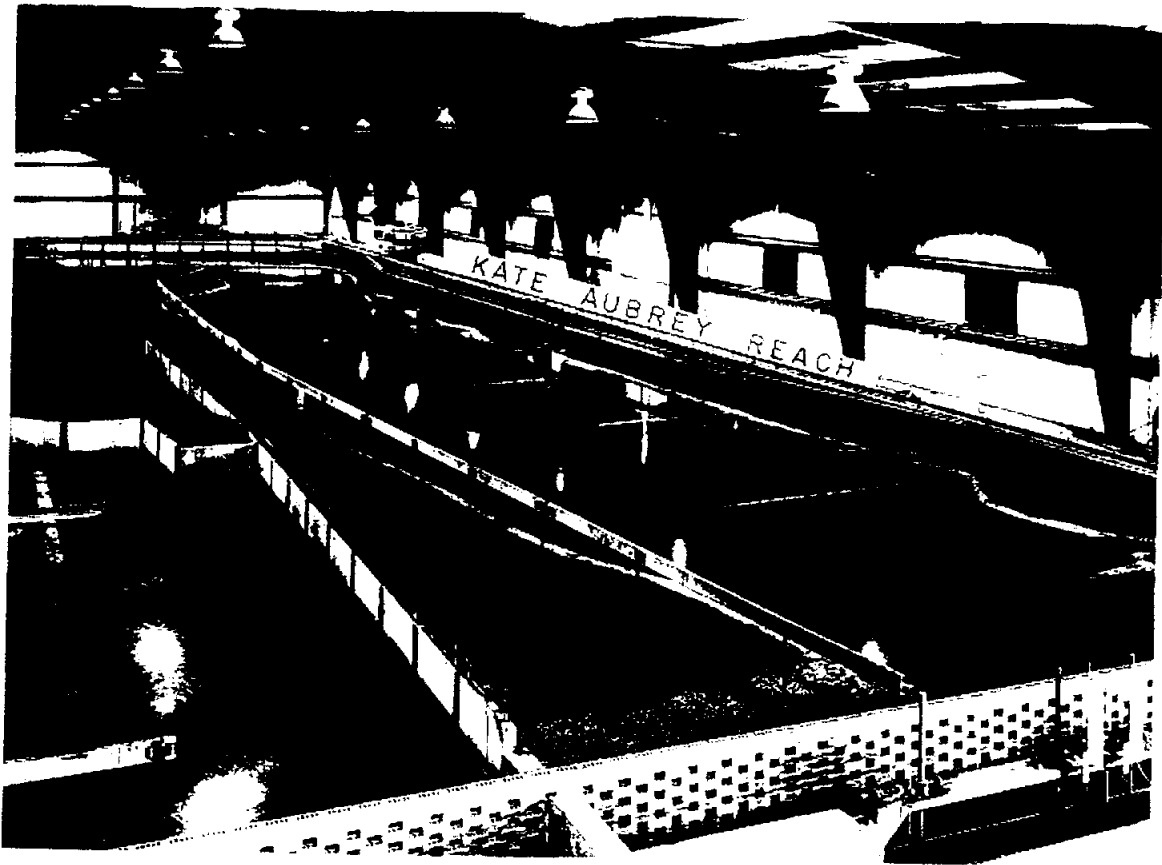


Figure 3-3 Kate-Aubrey Large-Scale Physical Sediment Model

located north of Memphis, Tennessee between river miles 785 and 797. The purpose of the study was to determine the extent of shoaling between river miles 788 and 792.5. The model used for the study was a loose-bed model with crushed coal sediment material constructed to scales of 1:300 horizontal and 1:100 vertical (model to prototype, respectively). The coal had a median diameter of 4 mm and a specific gravity of 1.30. Prototype data used in this study were bathymetric surveys for May 1975 and May 1976. Prototype bathymetry for 1975 and 1976 are shown in Figures 3-4 and 3-5, respectively. The model was initially formed (or molded) to the 1975 prototype bathymetry. A model discharge hydrograph was developed from historical stage and discharge records for the prototype. The resulting hydrograph (also referred to as the verification hydrograph) was used to simulate the period between May 1975 and May 1976 in the model. Sediment material was added to the upstream end of the model (a sediment feed system was used)

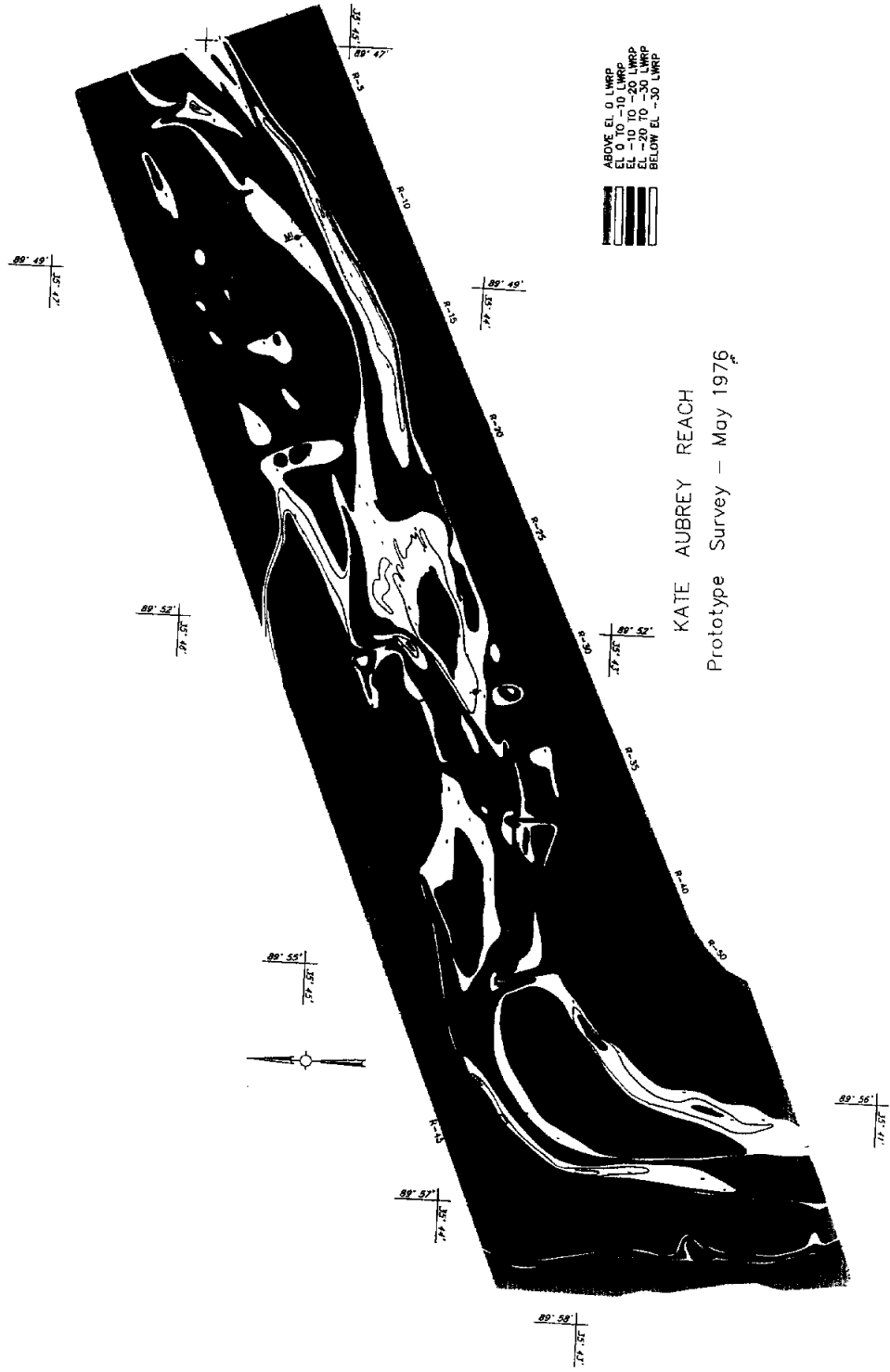


Figure 3-5 1976 Prototype Bathymetry, Kate-Aubrey Reach

during simulations to maintain a desired rate of sediment load relative to water discharge for the reach. This produced a model sediment rating curve. The model slope, rate of sediment load and water discharge, and boundary conditions (e.g. tailgate setting and bank roughness) were adjusted over the course of several repetitions until the final model bathymetry reproduced the May 1976 prototype conditions. Each repetition began with the May 1975 prototype condition formed in the model. The model was then used to simulate the verification hydrograph (including the corresponding sediment rating curve) to obtain model bathymetry to compare with the May 1976 prototype survey. The large-scale models employed a verification process to establish basic model operating parameters. The verification procedure relied on a visual comparison of model and prototype bathymetry as described in Gaines (2002). Once the May 1976 prototype condition was reproduced in the model, the model was considered verified. Model bathymetry after verification is shown in Figure 3-6.

Analysis of morphologic parameters described in Section 2.1.5 provides a quantitative means for assessing model and prototype agreement. A graphic comparison of individual Range values for each parameter provides a first view of model and prototype agreement. Thalweg position at each range for the large-scale Kate-Aubrey model is shown in Figure 3-7. Hydraulic depth, water surface width, cross-section area, and width to depth ratio at an elevation of 0.0 LWRP are shown in Figures 3-8, 3-9, 3-10, and 3-11, respectively. These graphs illustrate the variability inherent in the prototype as the channel boundary continually adjusts to changes in discharges and sedimentation processes over time. The model results (scaled to prototype coordinates) provide a ready comparison of how well model trends reproduce prototype trends.

Examination of the bathymetric data (Figures 3-4 to 3-6) and individual parameter graphs (Figures 3-7 to 3-11) provides a general assessment of prototype variability and model similarity as shown in Table 3-1. However, a quantifiable expression of model similarity is not expressed by individual parameter graphs or by visual assessment of the bathymetric data.

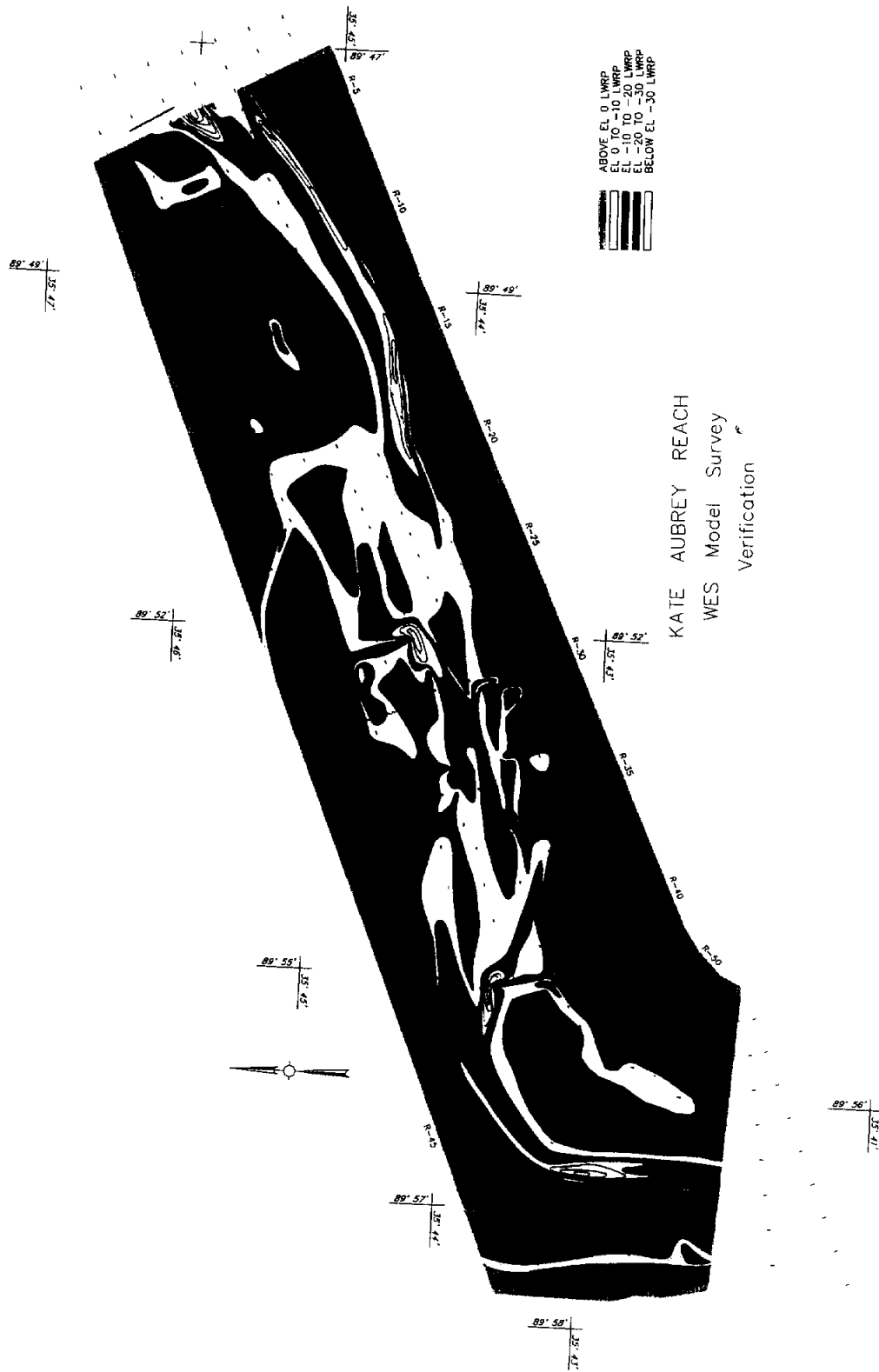


Figure 3-6 Model Verification Bathymetry, Kate-Aubrey Reach

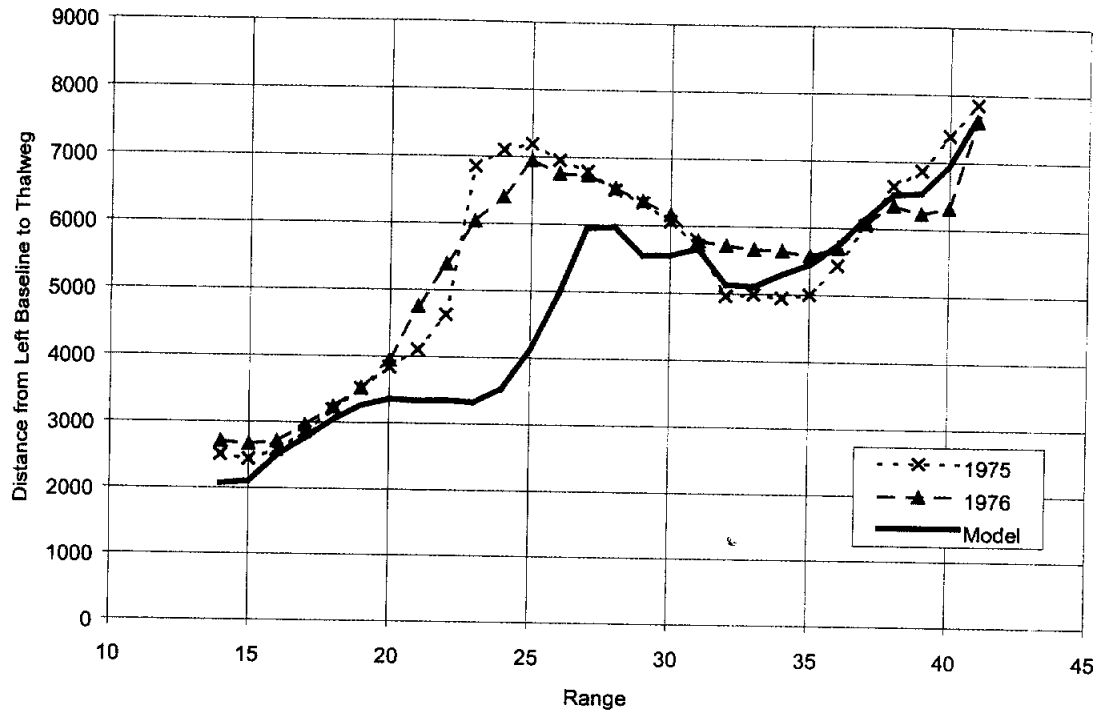


Figure 3-7 Thalweg Position, 1:300 Kate-Aubrey Model

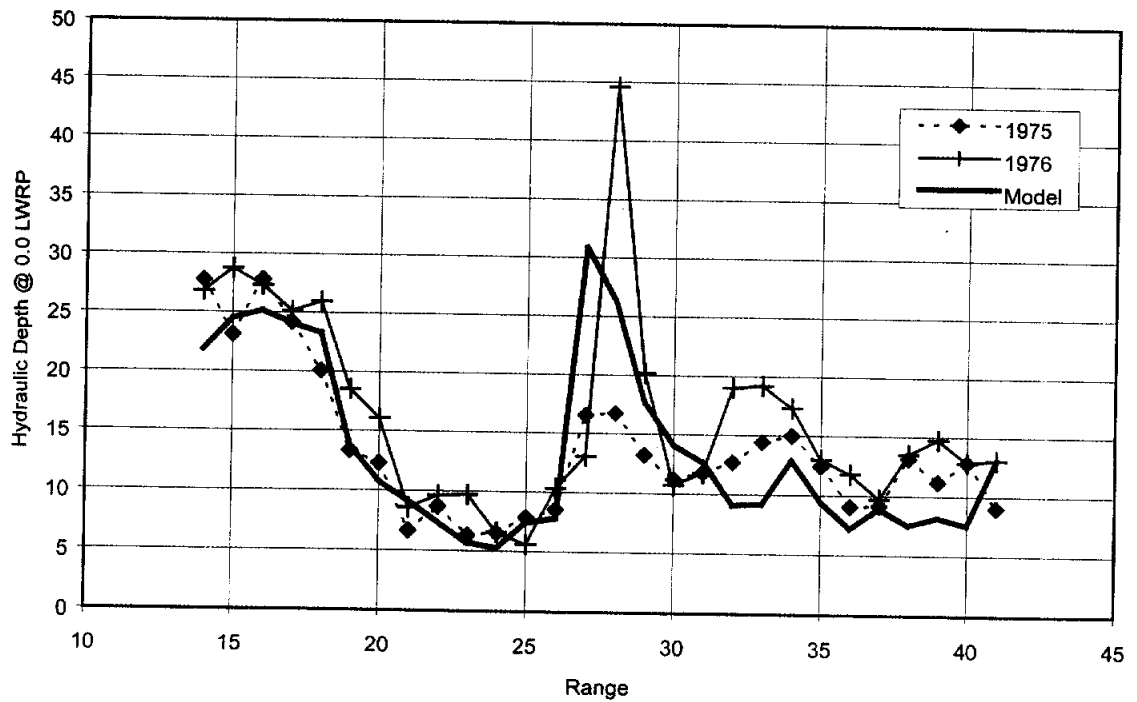


Figure 3-8 Hydraulic Depth, 1:300 Kate Aubrey Model

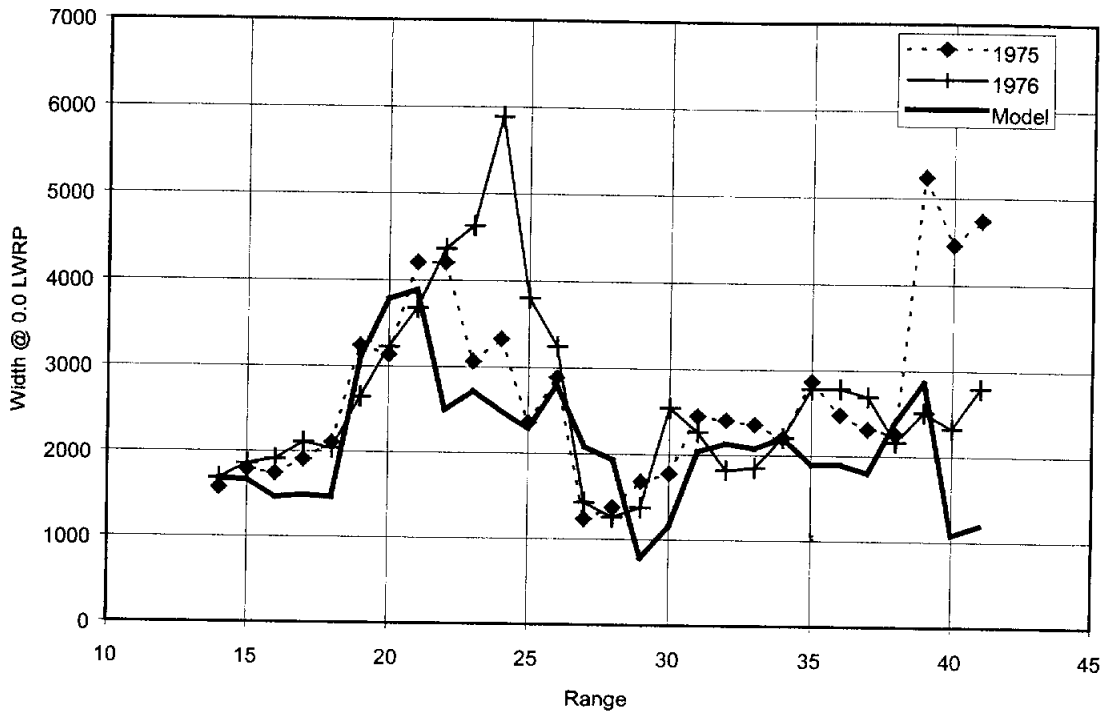


Figure 3-9 Width, 1:300 Kate Aubrey Model

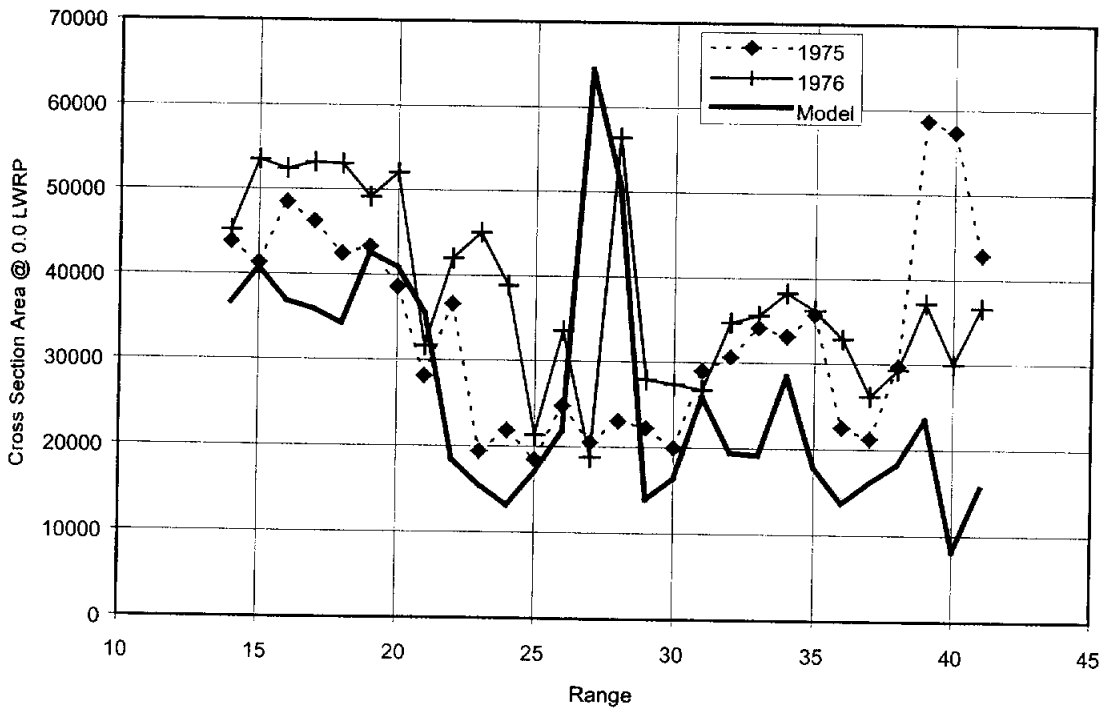


Figure 3-10 Area, 1:300 Kate Aubrey Model

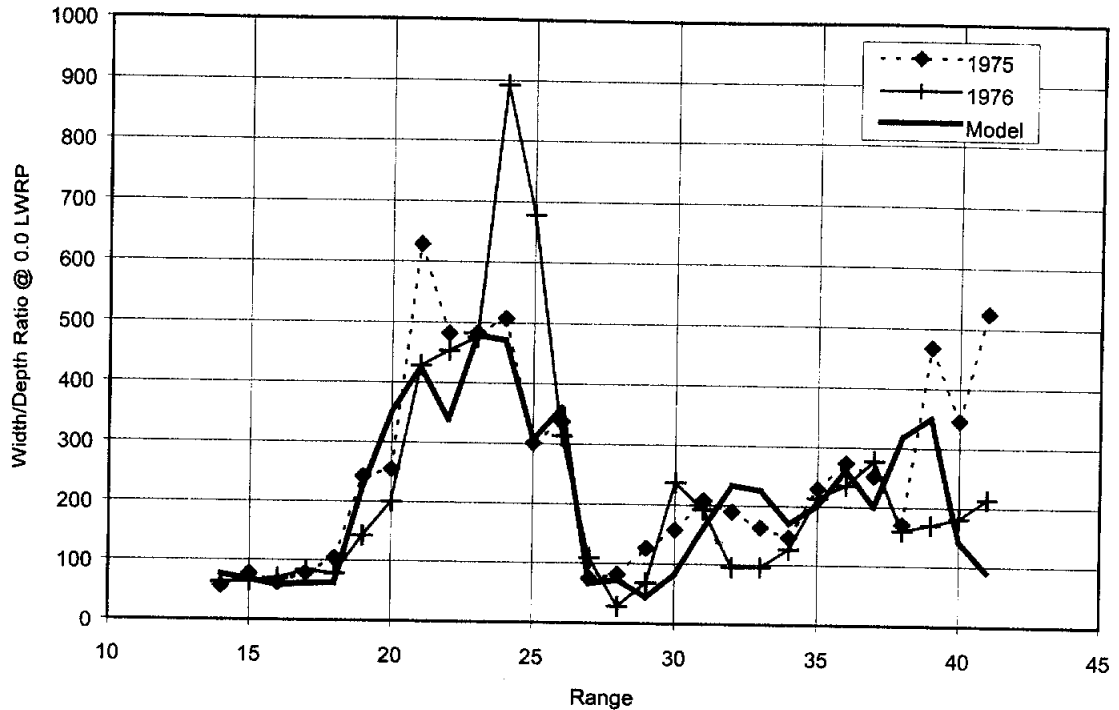


Figure 3-11 Width to Depth Ratio, 1:300 Kate Aubrey Model

Table 3-1 Morphologic Parameter Assessment, Kate-Aubrey Model

Morphologic Parameter	Model	Prototype
Thalweg Position	Thalweg not reproduced between R20 and R28	Thalweg more variable in areas, particularly R20 to R28, or R32-35.
Hydraulic Depth at 0.0 LWRP	Appears to match prototype trends overall, model depth too low R30-R40	High degree of variability between 1975 and 1976 surveys
Width at 0.0 LWRP	Overall width too low particularly R21-R26	High degree of variability between 1975 and 1976 surveys especially R21-R26, and R39-41
Area at 0.0 LWRP	Appears to match prototype trends exhibited in 1975 survey	Variability of 5000 to 10000 square feet overall but much higher R23-R29
Width/Depth Ratio at 0.0 LWRP	Matches 1975 survey best (the molded case), but area low throughout reach, except where area is high	Large variability R24-R26 and R39-41

3.1.3. Small-Scale Models. Two small-scale models (micromodels) of the Kate-Aubrey reach were also developed as part of the present investigation. The Kate-Aubrey micromodels extended between river miles 783 and 803. A photograph of the small-scale Kate-Aubrey physical sediment model is shown in Figure 3-12. The purpose of the micromodel studies was to determine the effect of scale on model results and to evaluate the model's predictive capability by comparing a predicted result to actual prototype response. The models used for the study were loose-bed models with Urea PlastiGrit sediment having a specific gravity of 1.48. Scales for these models were 1:16,000 horizontal and 1:900 vertical for the smaller model and 1:8,000 horizontal and 1:600 vertical for the larger model. Median particle sizes were 0.73mm and 0.62mm for the smaller and larger micromodels, respectively. Prototype data used in this study were



Figure 3-12 Kate-Aubrey Small-Scale Physical Sediment Model

bathymetric surveys for June 1973, May/June 1975 and May/June 1976. Prototype bathymetry is shown in Figures 3-13, 3-14, 3-15 for the 1973, 1975, and 1976 surveys respectively. Both models were designed with rigid, vertical banks at the location of prototype top bank. Both small-scale models utilized a synthetic discharge hydrograph that approximated a sine wave function between maximum and minimum discharge settings. Sediment was recirculated in the small-scale models (no external sediment feed system was used). To achieve a state of calibration in the small-scale models (termed calibration as opposed to verification as used for the large-scale models) the model was operated through several hydrograph cycles to achieve a state of equilibrium.

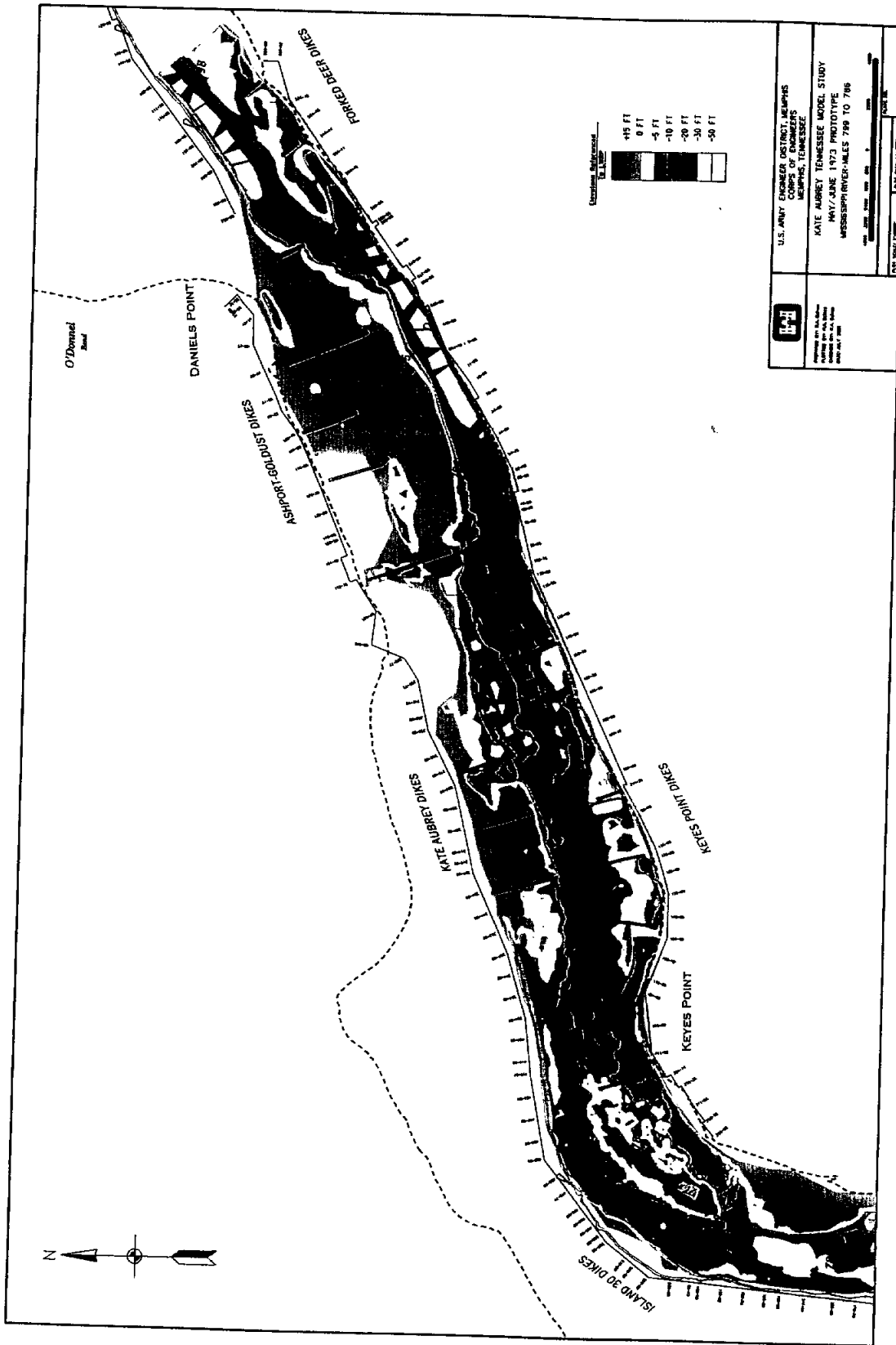


Figure 3-13 1973 Prototype Bathymetry, Kate-Aubrey Reach Small-Scale Models

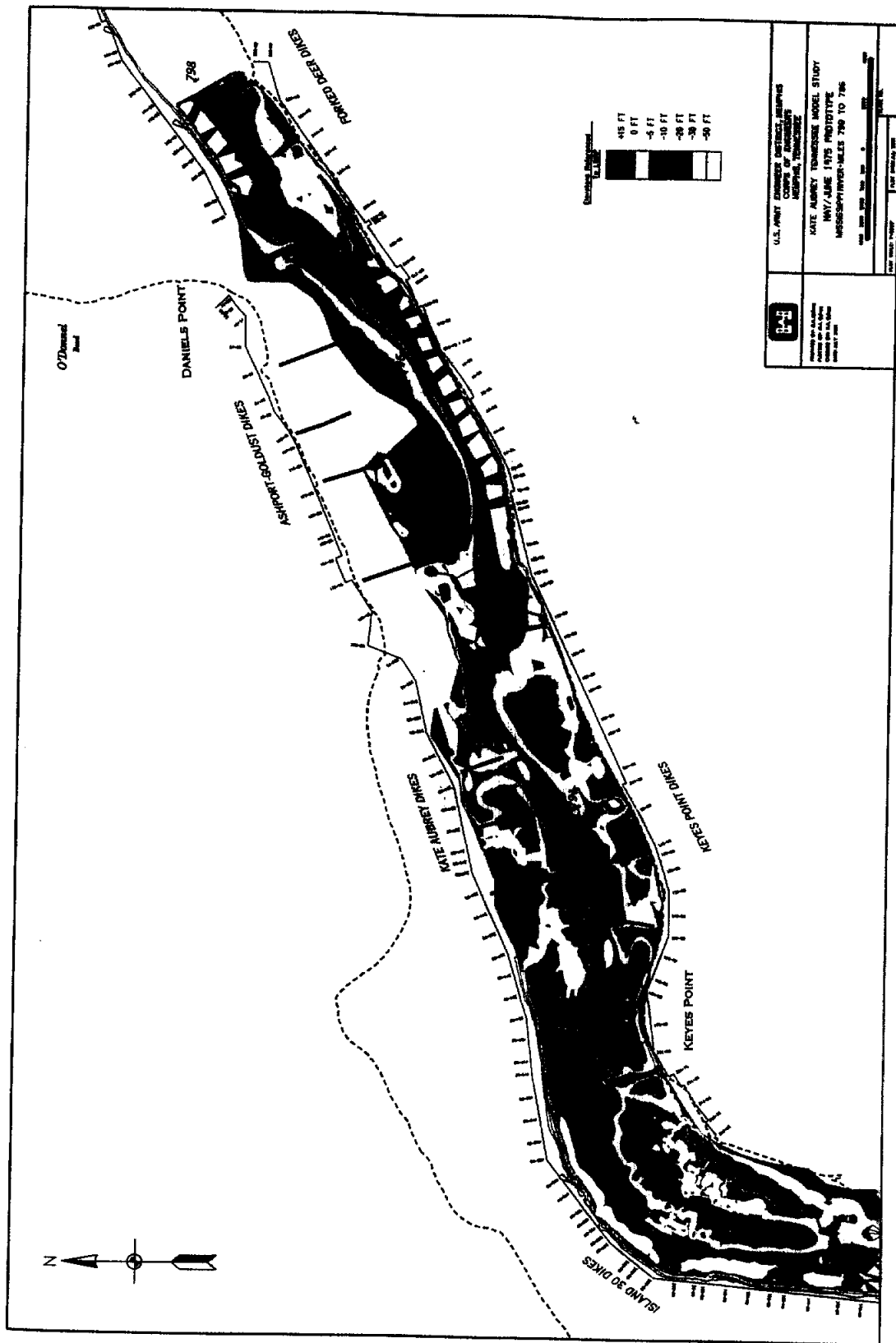


Figure 3-14 1975 Prototype Bathymetry, Kate-Aubrey Reach Small-Scale Models

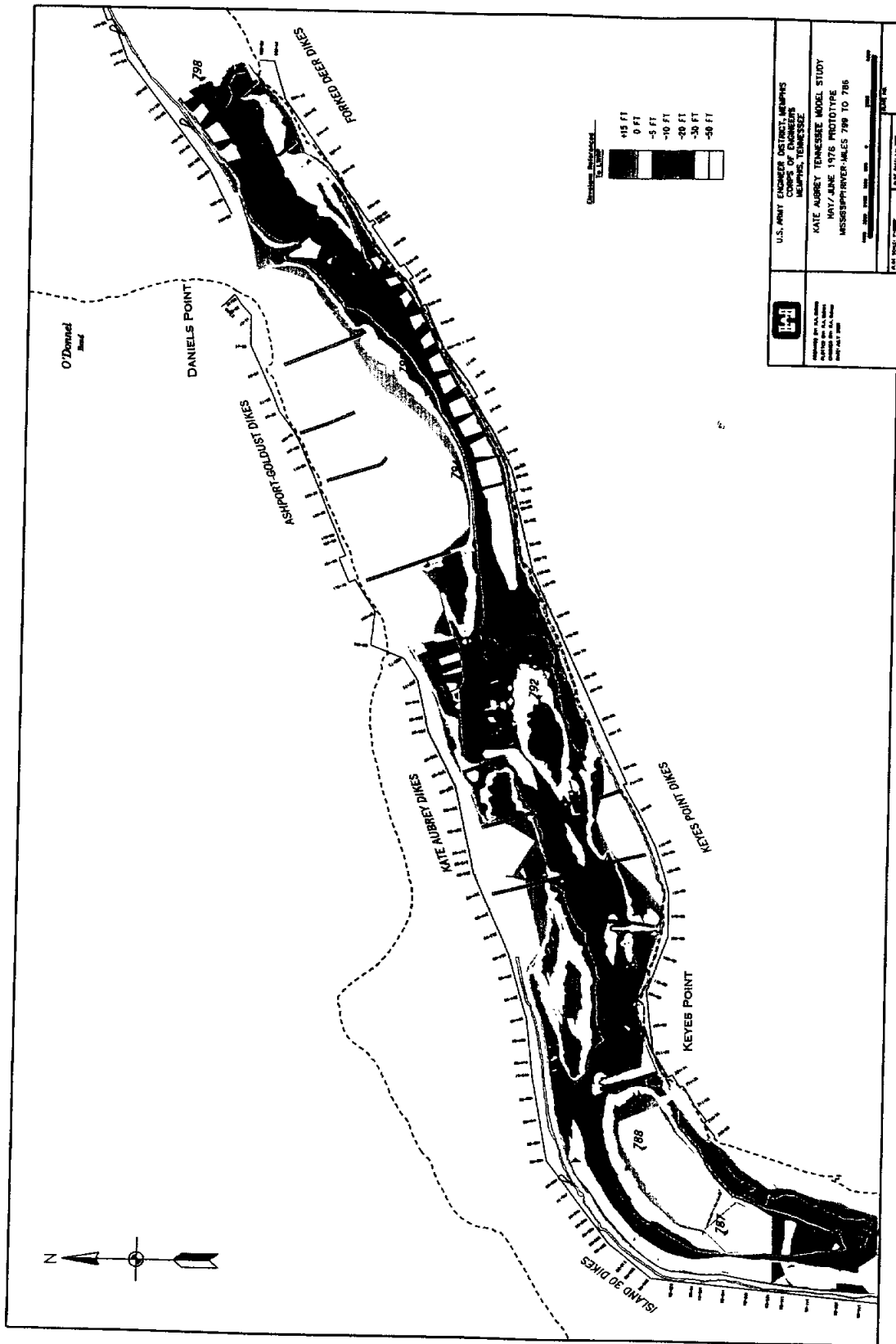


Figure 3-15 1976 Prototype Bathymetry, Kate-Aubrey Reach Small-Scale Models

Equilibrium in the small-scale models represented the condition where net sediment transport and bed bathymetry remained consistent for successive cycles (there was no net aggradation or degradation over time observed in the model). Once equilibrium was obtained, the resulting model bathymetry was visually compared to the three prototype surveys to assess whether the model had reproduced prototype conditions. The model slope, discharge, and boundary conditions (e.g. downstream weir elevation and bank roughness) were adjusted over the course of several simulation periods until the final model bathymetry reproduced the observed prototype conditions. Visual comparison of model bathymetry to prototype bathymetry generally focused on trends in color coded contour elevations and thalweg position through the reach. Bathymetry for the calibrated 1:8,000 micromodel is shown in Figure 3-16. Bathymetry for the calibrated 1:16,000 micromodel is shown in Figure 3-17. All micromodel bathymetry was obtained after a consistent procedure of shutting down the models. This method involved closing the tailgate to flow and stopping the inflow at the end of the hydrograph peak. The model was then allowed to slowly drain thereby preventing disruption of the bed as flow exited the model.

Analysis of the five morphologic parameters described in Section 1.2 was performed for the small-scale models. Comparison of individual Range values for each morphologic parameter was performed graphically by plotting parameter values by Range just as done for the large-scale model. The 1:8000 micromodel parameter values for thalweg position, hydraulic depth, width, width to depth ratio, and area are shown in Figure 3-18, Figure 3-19, Figure 3-20, Figure 3-21, and Figure 3-22, respectively.

Thalweg position, hydraulic depth, width, width to depth ratio, and area for the 1:16,000 micromodel are shown in Figure 3-23, Figure 3-24, Figure 3-25, Figure 3-26, and Figure 3-27, respectively.

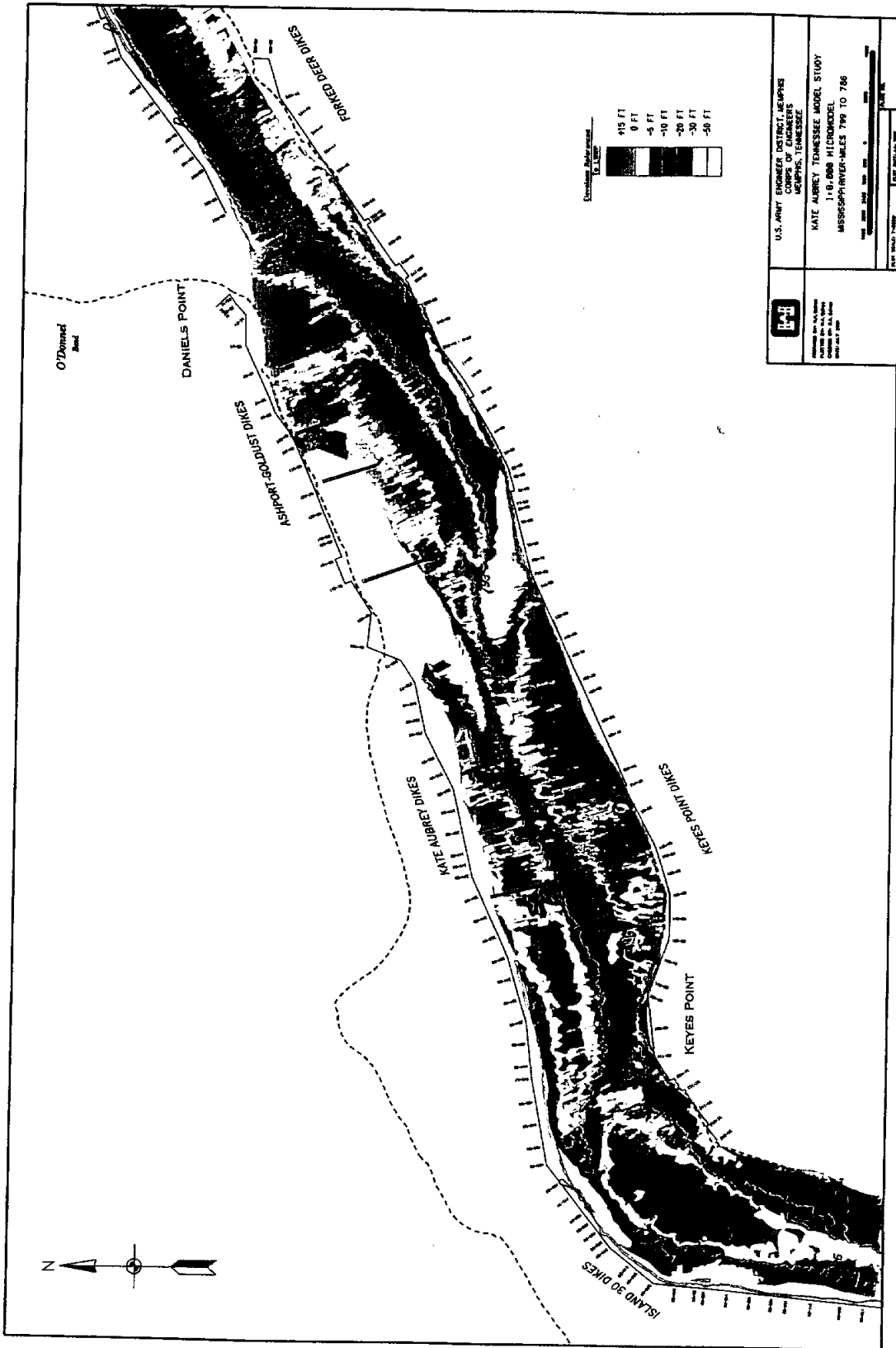


Figure 3-16 Calibrated Bathymetry, Kate-Aubrey Reach 1:8,000 Model

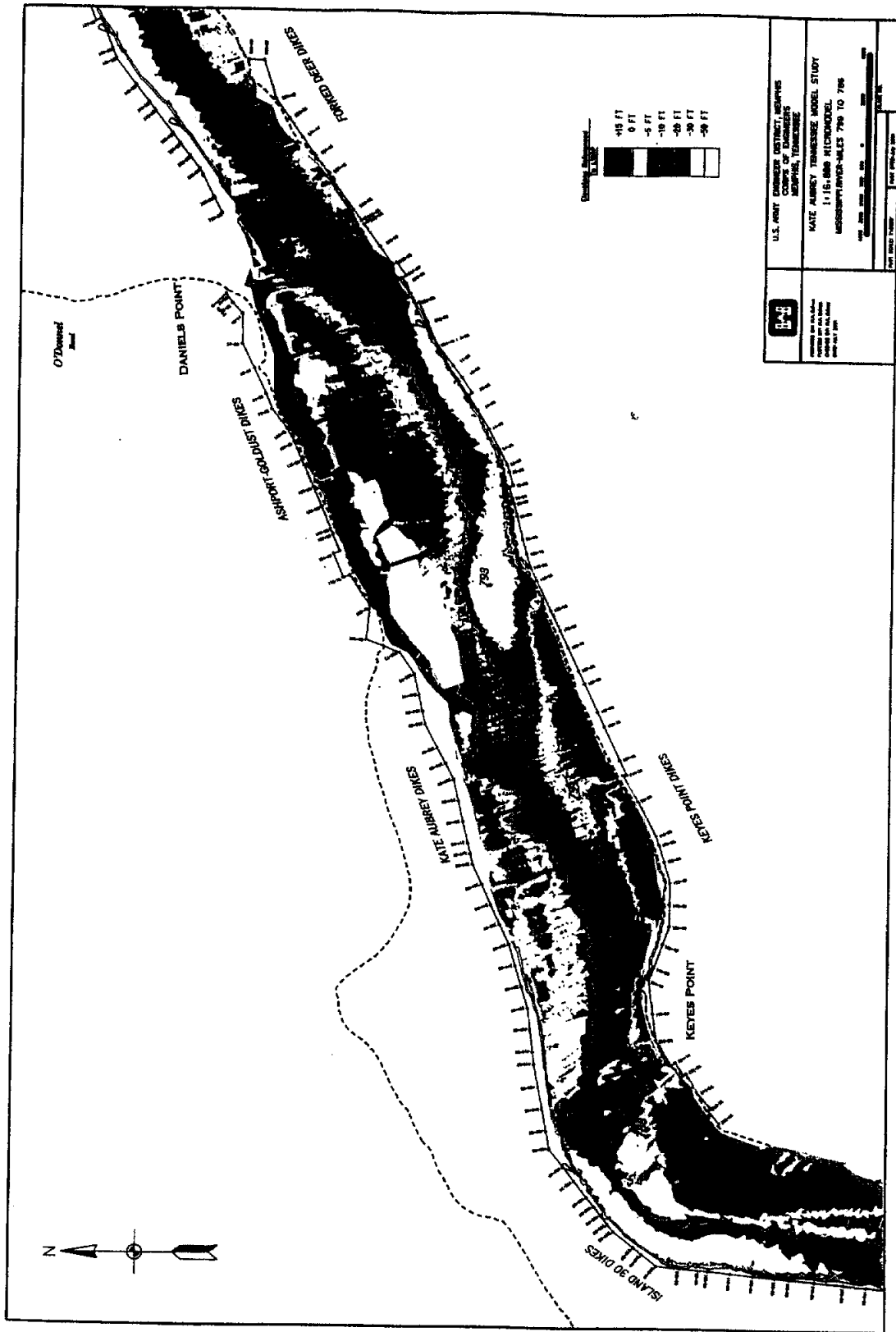


Figure 3-17 Calibrated Bathymetry, Kate-Aubrey Reach 1:16,000 Model

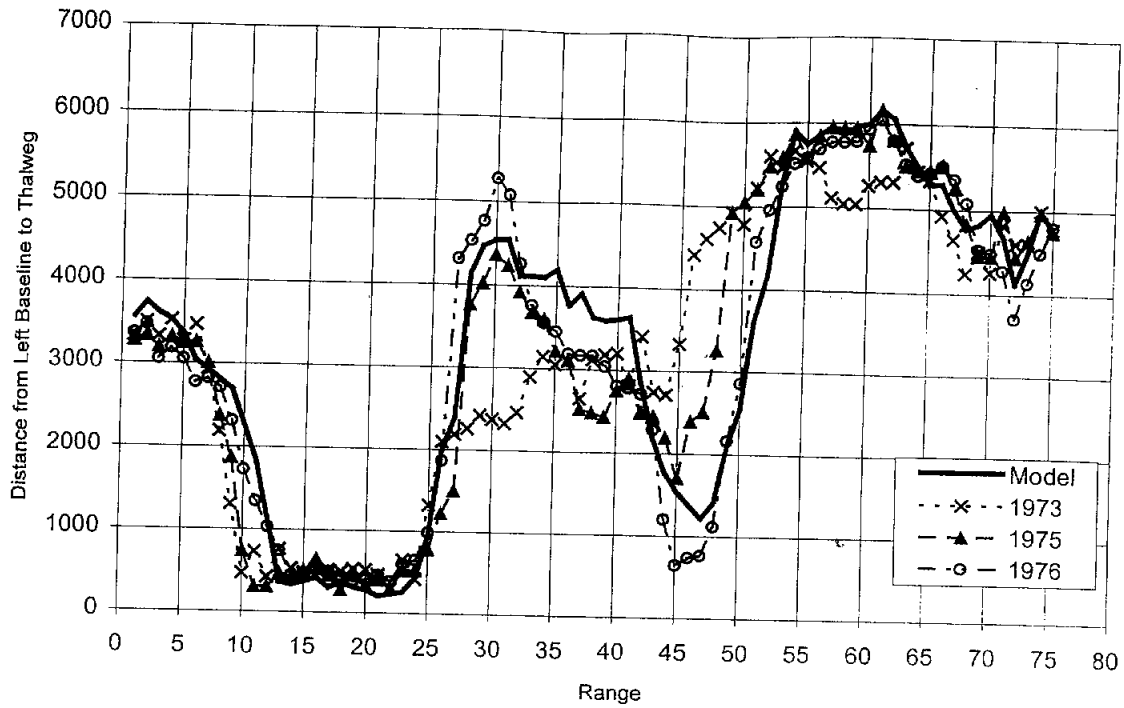


Figure 3-18 Thalweg Position, 1:8000 Kate-Aubrey Micromodel

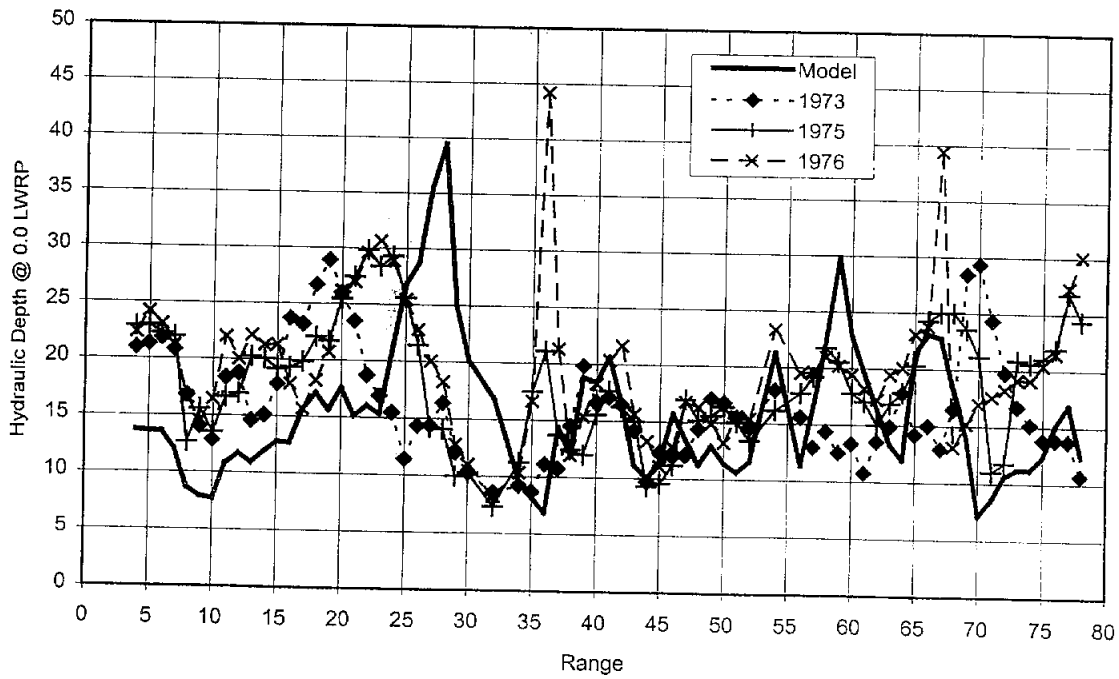


Figure 3-19 Hydraulic Depth, 1:8000 Kate-Aubrey Micromodel

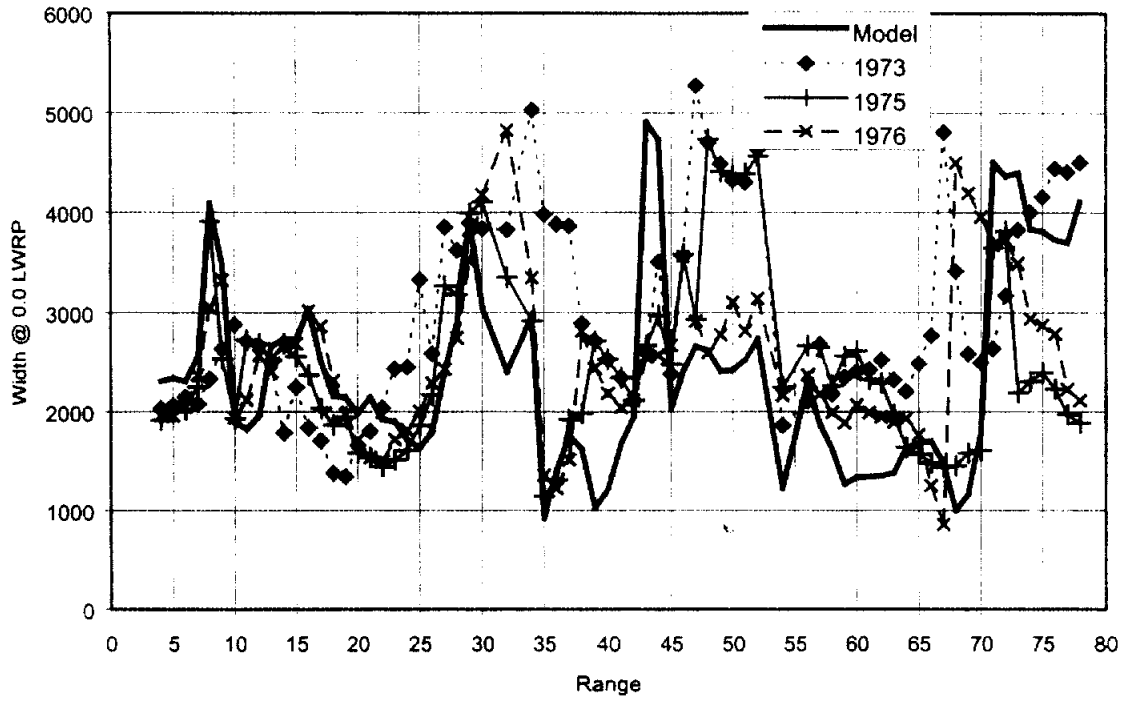


Figure 3-20 Width, 1:8000 Kate-Aubrey Micromodel

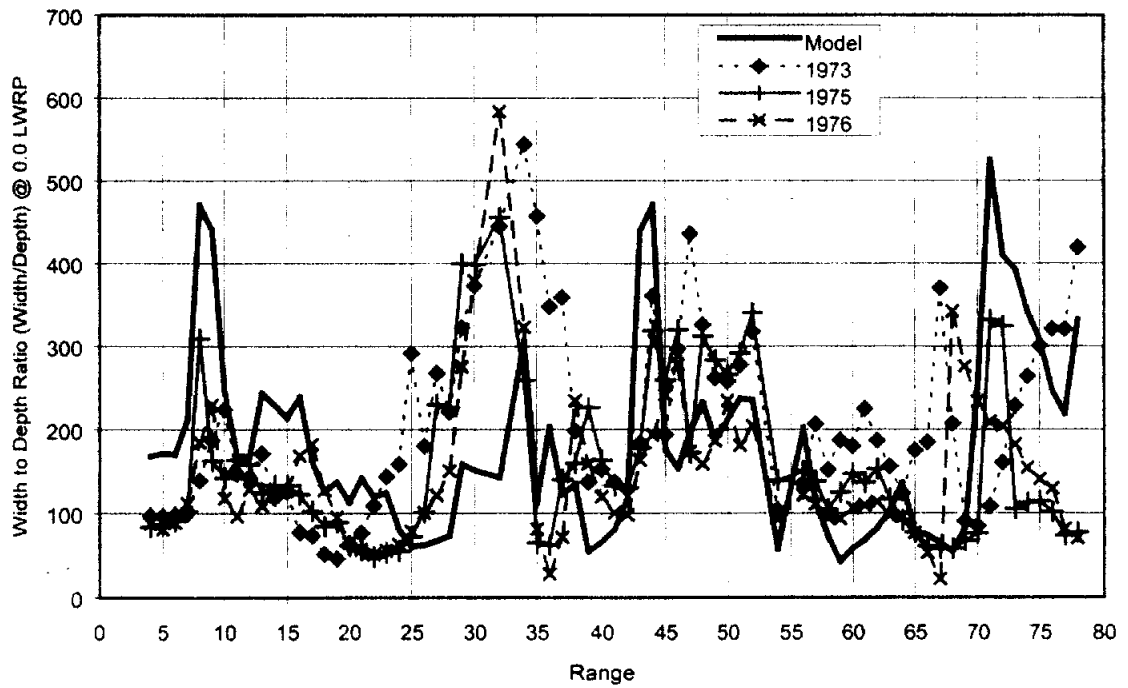


Figure 3-21 Width to Depth Ratio, 1:8000 Kate-Aubrey Micromodel

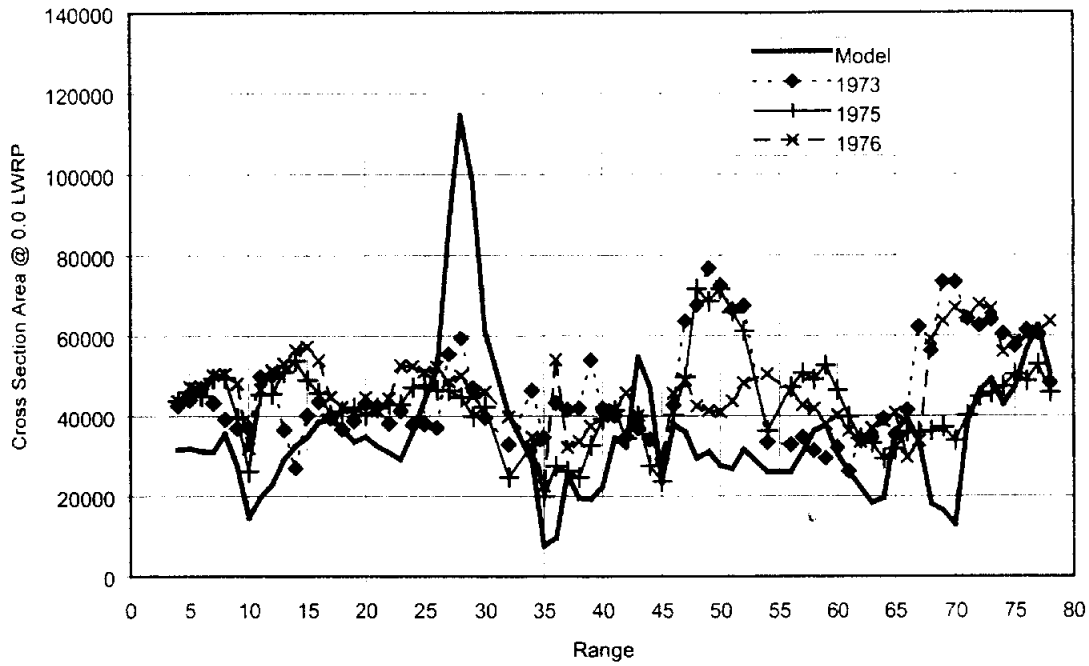


Figure 3-22 Area, 1:8000 Kate-Aubrey Micromodel

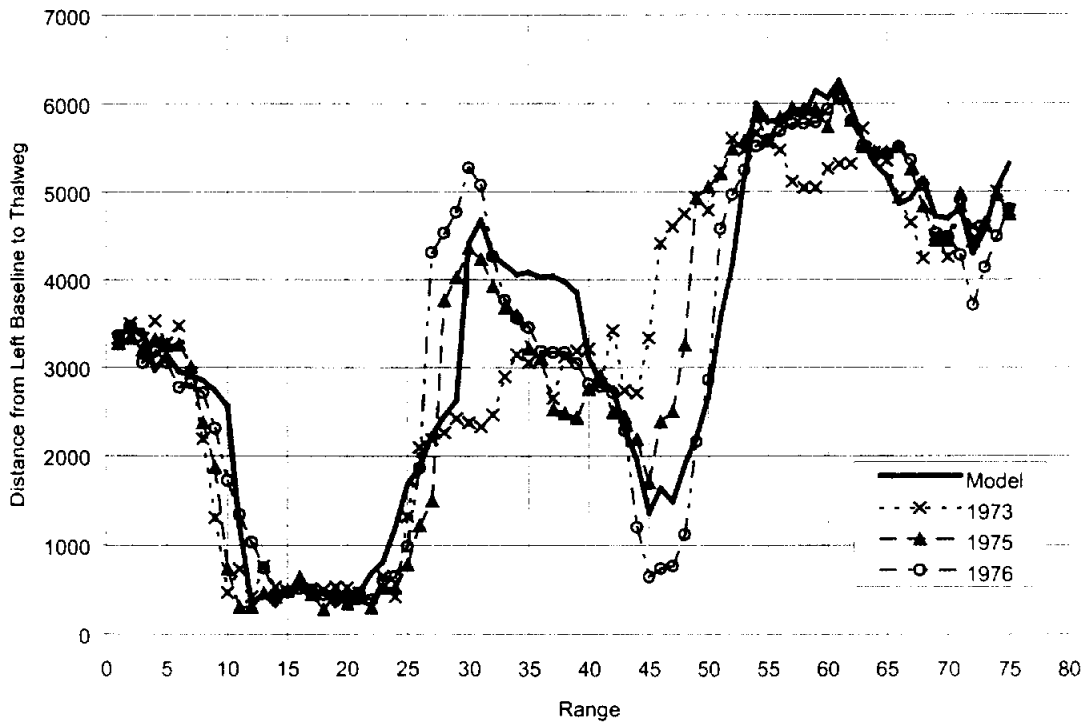


Figure 3-23 Thalweg Position, 1:16,000 Kate-Aubrey Micromodel

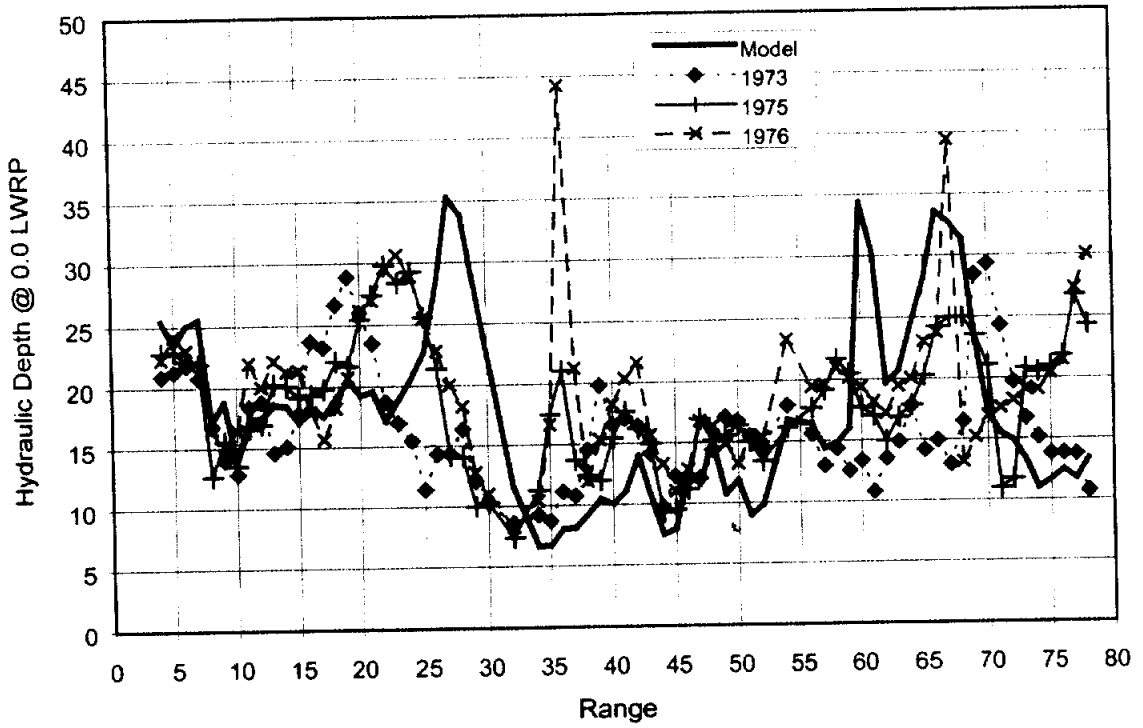


Figure 3-24 Hydraulic Depth, 1:16,000 Kate-Aubrey Micromodel

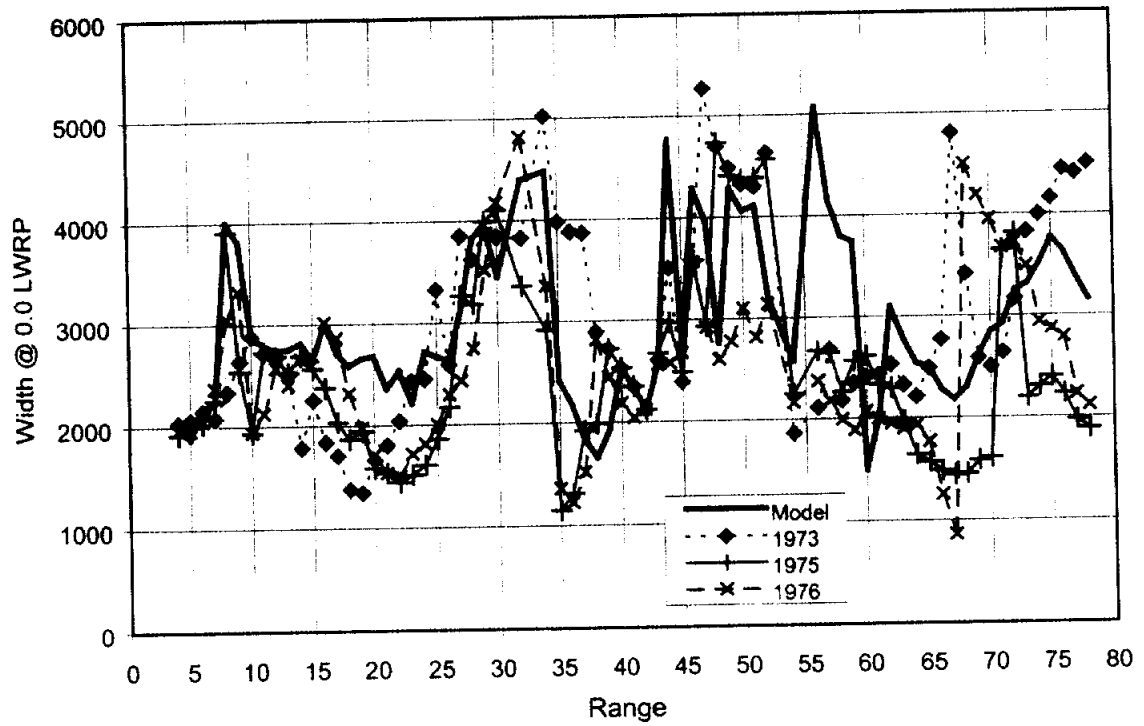


Figure 3-25 Width, 1:16,000 Kate-Aubrey Micromodel

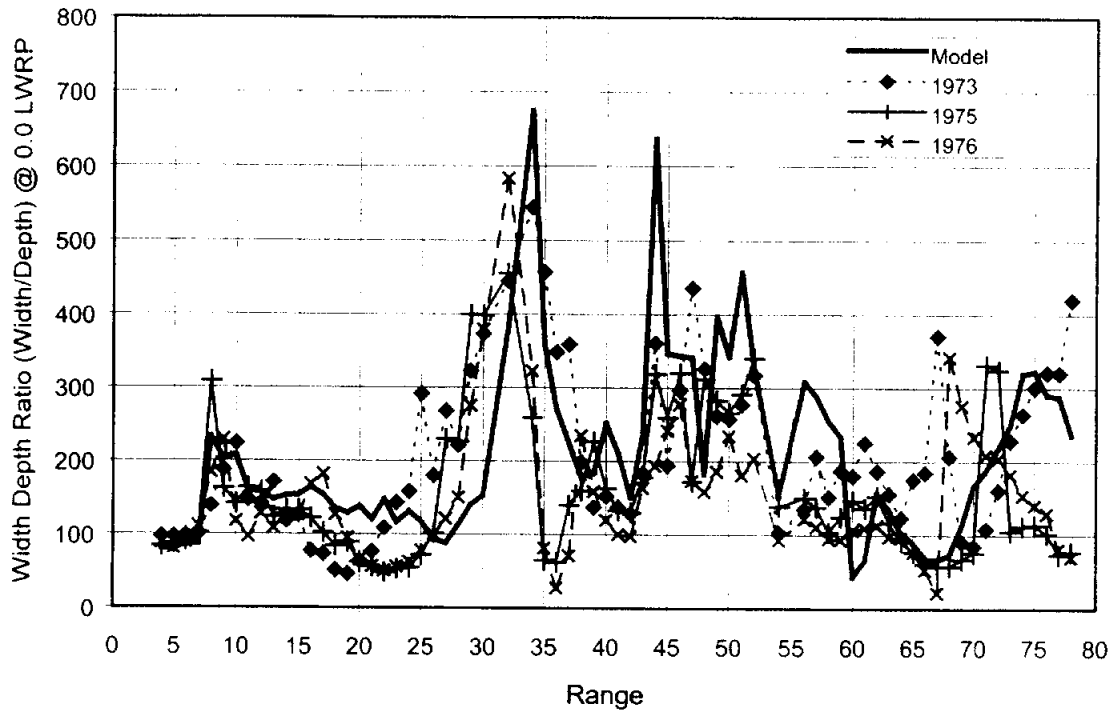


Figure 3-26 Width to Depth Ratio, 1:16,000 Kate-Aubrey Micromodel

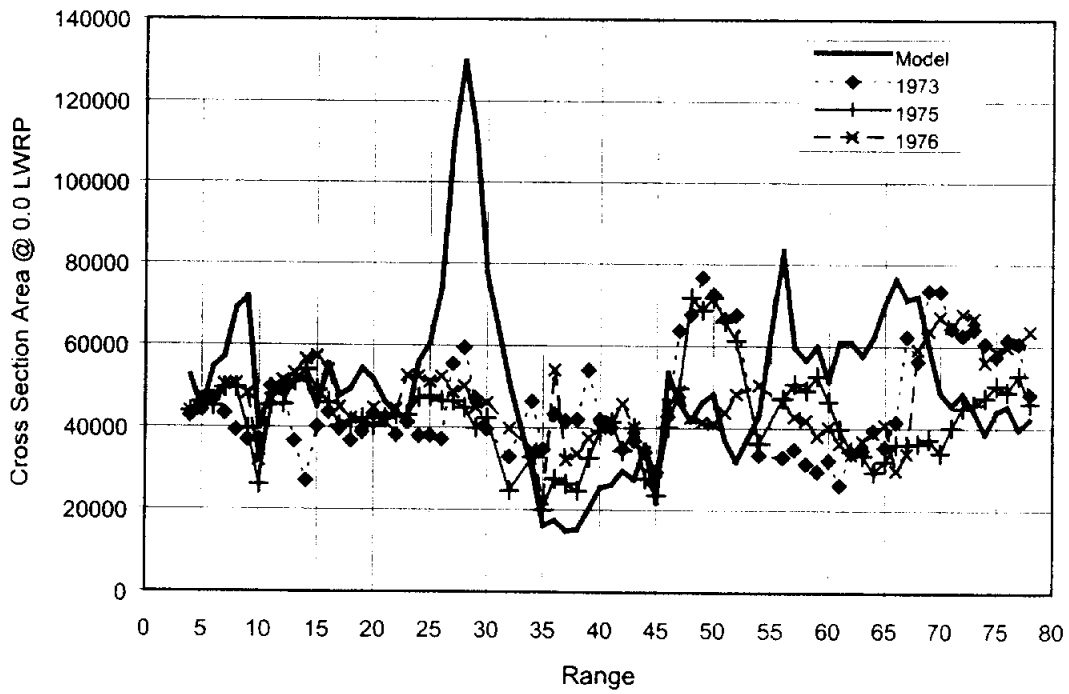


Figure 3-27 Area, 1:16,000 Kate-Aubrey Micromodel

The prototype bathymetry used in micromodel calibration was consistent with that used for the large-scale models except an additional survey, 1973, was included. Observations noted in Table 3-1 for the prototype are similar for the three hydrographic surveys (1973, 1975, and 1976) except that variability is dramatically higher because of the 1973 data. One explanation for the higher variability exhibited by the 1973 data is that a major flood occurred in 1973. This extreme flood event had a significant impact on channel sedimentation features as the bathymetry shows. An assessment of bathymetric data (Figures 3-13 to 3-17) and individual morphologic parameter graphs (Figures 3-18 to 3-22) for the 1:8,000 micromodel is shown in Table 3-2.

Table 3-2 Morphologic Parameter Assessment, Kate-Aubrey 1:8,000 Micromodel

Morphologic Parameter	Model	Prototype
Thalweg Position	Thalweg not reproduced well between R33 and R41	Thalweg more variable in areas, particularly R26 to R40 and R44 to 54.
Hydraulic Depth at 0.0 LWRP	Appears to match prototype trends overall, model depth too high R25-R34	Degree of variability between 1975 and 1976 surveys low compared to 1973 survey
Width at 0.0 LWRP	Overall width too low particularly R29-R34 and R47-R64.	High degree of variability between 1973, 1975 and 1976 surveys especially R29-R54
Area at 0.0 LWRP	Matches 1976 survey best, but area low through reach except R26-R31 where approx. twice prototype	Variability of 5000 to 10000 square feet overall but much higher R46-R54, R66-74
Width/Depth Ratio at 0.0 LWRP	Appears to match prototype trends exhibited in 1976 survey, low R25-R38	Large variability, especially R20-R40

An assessment of bathymetric data (Figures 3-13 to 3-17) and individual morphologic parameter graphs (Figures 3-23 to 3-27) for the 1:16,000 micromodel is shown in Table 3-3.

Table 3-3 Morphologic Parameter Assessment, Kate-Aubrey 1:16,000 Micromodel

Morphologic Parameter	Model	Prototype
Thalweg Position	Thalweg not reproduced well between R33 and R41	Thalweg more variable in areas, particularly R26 to R40 and R44 to R54.
Hydraulic Depth at 0.0 LWRP	Appears to match prototype trends overall, model depth too high R25-R34 and R60-R61.	Degree of variability between 1975 and 1976 surveys low compared to 1973 survey
Width at 0.0 LWRP	Overall width matches prototype trends, too high R17-R23 and R55-R59.	High degree of variability between 1973, 1975 and 1976 surveys especially R29-R54
Area at 0.0 LWRP	Matches general trends but high R24-R34 and R55-R67, low R46-R54	Variability of 5000 to 10000 square feet overall but much higher R46-R54, R66-74
Width/Depth Ratio at 0.0 LWRP	Appears to match prototype trends exhibited in 1973	Large variability, especially R20-R40

3.1.4. Predictive Comparisons. Given that the physical sediment models included in this investigation relied on a calibration/verification phase to achieve a form of empirical similarity, the ability of a model to reproduce prototype response to a specific modification became a direct measure of the actual similarity between the model and the prototype. In other words, if the model actually reproduced a future response observed in the prototype, then the model behaved in a similar fashion to the prototype. The degree to which a model did (or did not) reproduce detailed features that occurred a prototype was considered as a quantitative measure of the model and prototype agreement (or lack thereof). Additionally, consideration of models at different scales provided a means to assess scale effects on the predictive capability of models and the associated similarity.

Unfortunately, very few cases were found where model recommendations were actually constructed in the prototype. Most cases had only a limited portion of the recommendations implemented. Construction in the Kate-Aubrey reach of the Mississippi River had implemented structural measures very close to model large-scale model recommendations. The improvements for this reach were not built in complete

accordance with model recommendations primarily because of adaptations required to fit actual prototype conditions and to accommodate minimal changes for environmental considerations. Modifications required to fit prototype conditions included adjustments in structure lengths and heights to fit changed river bathymetry (from the model condition) at initial construction and a phased construction sequence over a period of years (as opposed to placing all structures in the prototype at once as done in the models). Environmental adaptations involved minor adjustments whereby structure length was adjusted over a very limited range of 90 to 200 feet or notched, 3 to 6 feet vertical and 90 to 200 feet in length, to provide opportunities for side channel development. Figure 3-28 shows prototype training structure locations for 1975 (base test) and 1998 (predictive case).

The 1:300 large-scale model study conducted at WES (see Section 3.1.2) had the intended purpose of solving a complex navigation alignment problem. However, a phased construction approach in the prototype resulted in a slightly different structure arrangement than recommended by the WES study. For this reason the WES study was not utilized in assessing model predictive similarities.

Calibration of the two Kate Aubrey micromodels was discussed in the previous section. Predicted response was based on model results obtained for training structures completed in the prototype through 1999 (1999 was the last construction in the reach). Prototype data obtained in 1998 provided the basis for describing prototype conditions for the comparisons. Prototype data for years following 1998 were influenced by a large dredge cut made in 1999 (Figure 3-29 and Figure 3-30). However, the large quantity of dredging that occurred during the late 1980's must also be considered in assessing prototype response between the calibration period, mid-1970's, and current prototype conditions.

Although construction in the reach ended in 1999, modifications following 1998 had an insignificant effect on the overall reach configuration. Therefore, 1998 survey data were used in the evaluation of model predictive capability. Prototype bathymetry in the Kate-Aubrey reach for 1998 is shown in Figure 3-31. Predicted model bathymetric maps for the 1:8,000 and 1:16,000 micromodels are shown in Figure 3-32 and Figure 3-33, respectively.

Plots of thalweg position, hydraulic depth, width, width to depth ratio, and cross-section area are shown in Figure 3-34, Figure 3-35, Figure 3-36, Figure 3-37 and 3-38, respectively, for the 1998 prototype, for the 1:8,000 micromodel, and the 1:16,000 micromodel surveys. Hydraulic depth, width, width to depth ratio, and cross-section area values for the morphologic parameter graphs were calculated using a water surface elevation of 0.0 low water reference plane.

Table 3-4 provides a summary of observations made from plotted morphologic parameters in the 1:8,000 micromodel analysis. Table 3-5 provides summary descriptions of morphologic parameter plots for the 1:16,000 micromodel.

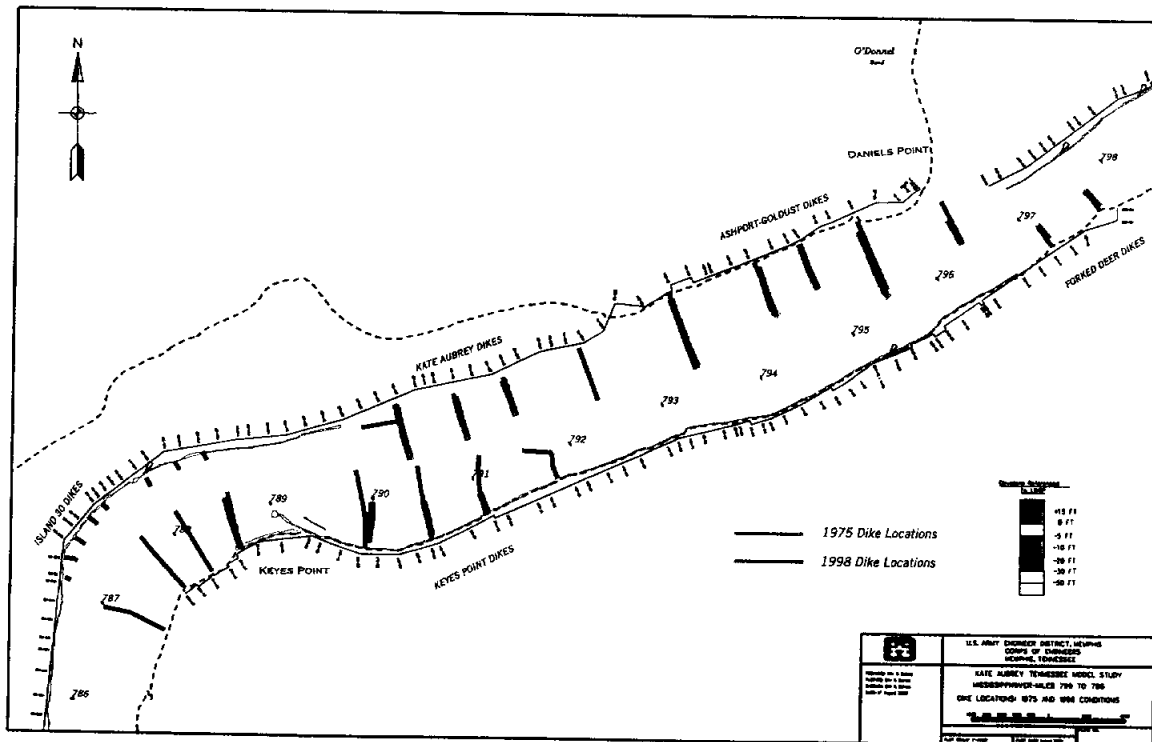


Figure 3-28 Dike Locations, Kate Aubrey Reach

KEYES POINT(KATE AUBREY) DREDGING
MILES 787-793

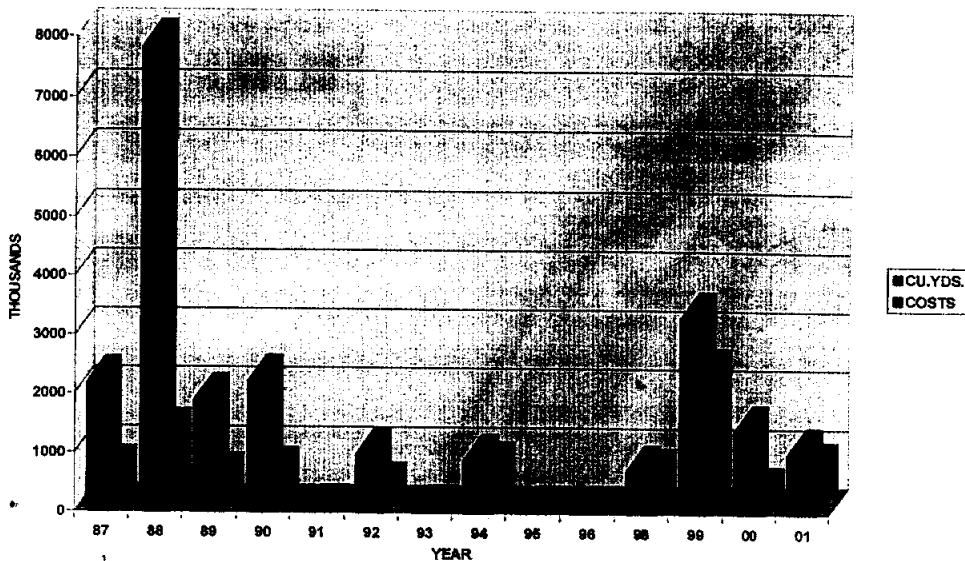


Figure 3-29 Kate Aubrey Dredging Amounts and Costs

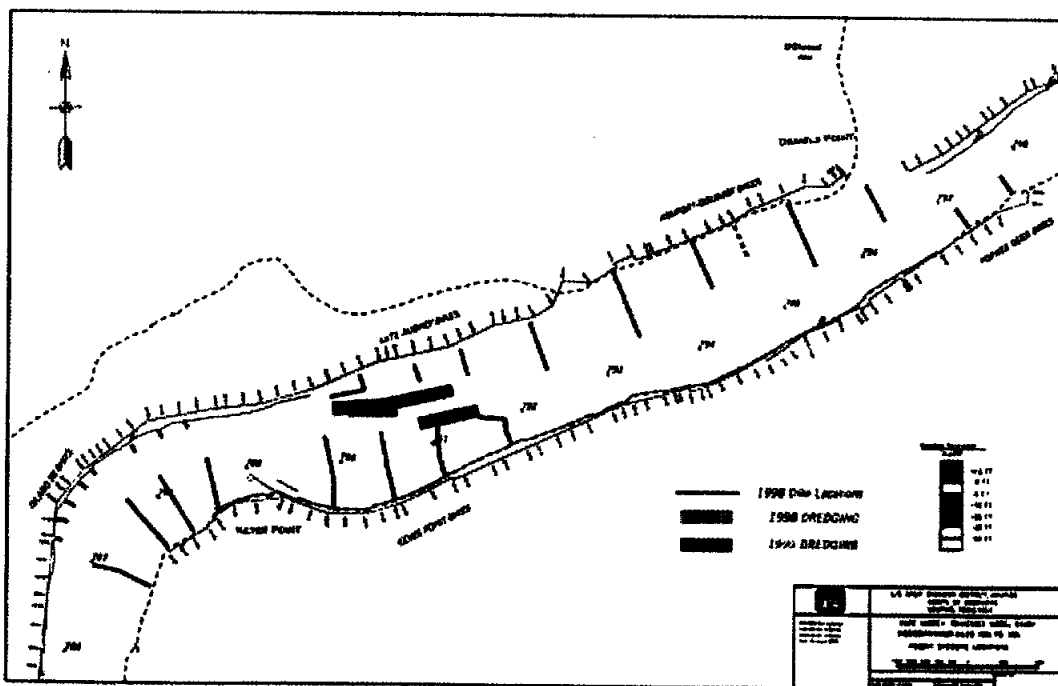


Figure 3-30 Kate Aubrey Dredge Locations by Year

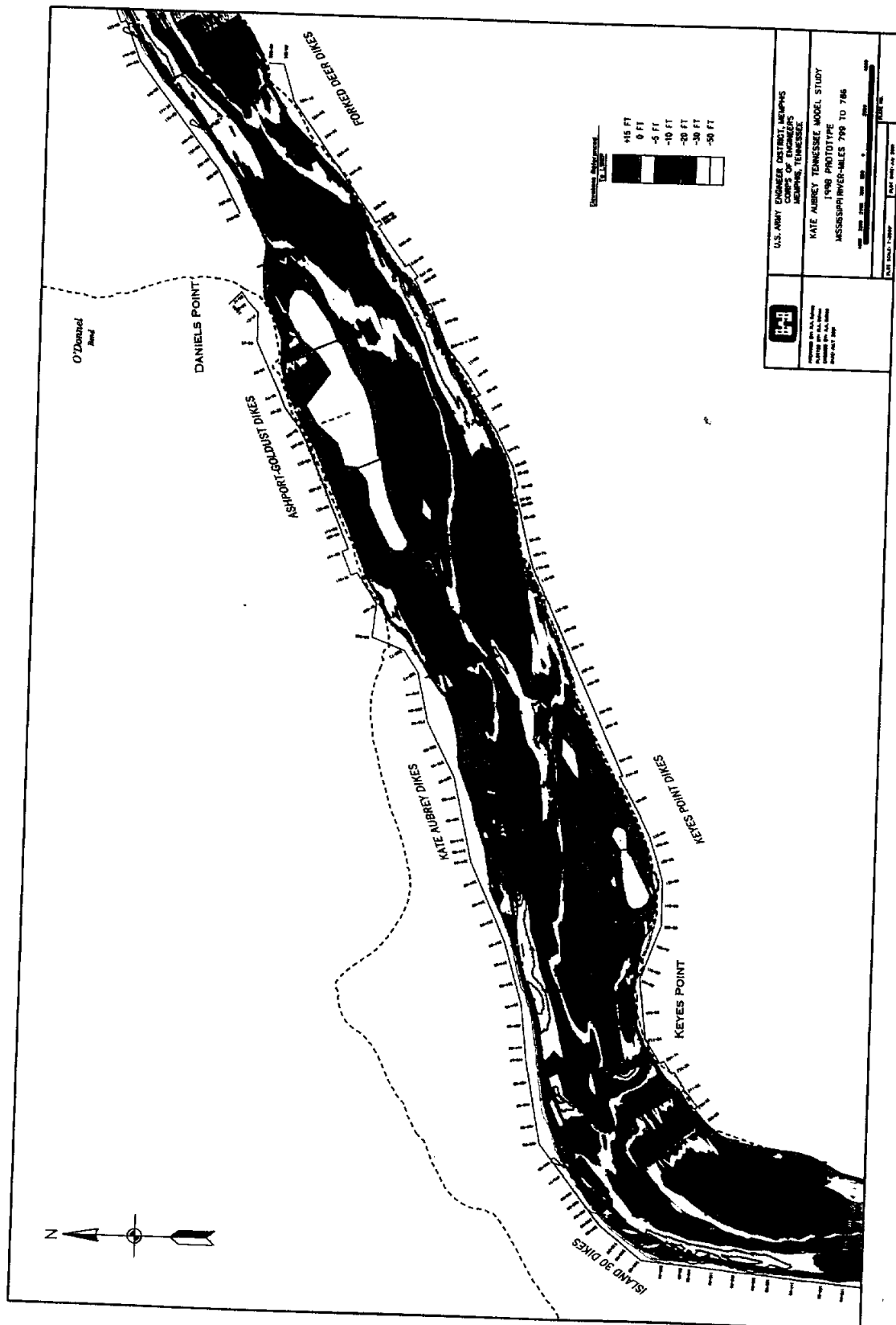


Figure 3-31 1998 Prototype Bathymetry, Kate-Aubrey Reach

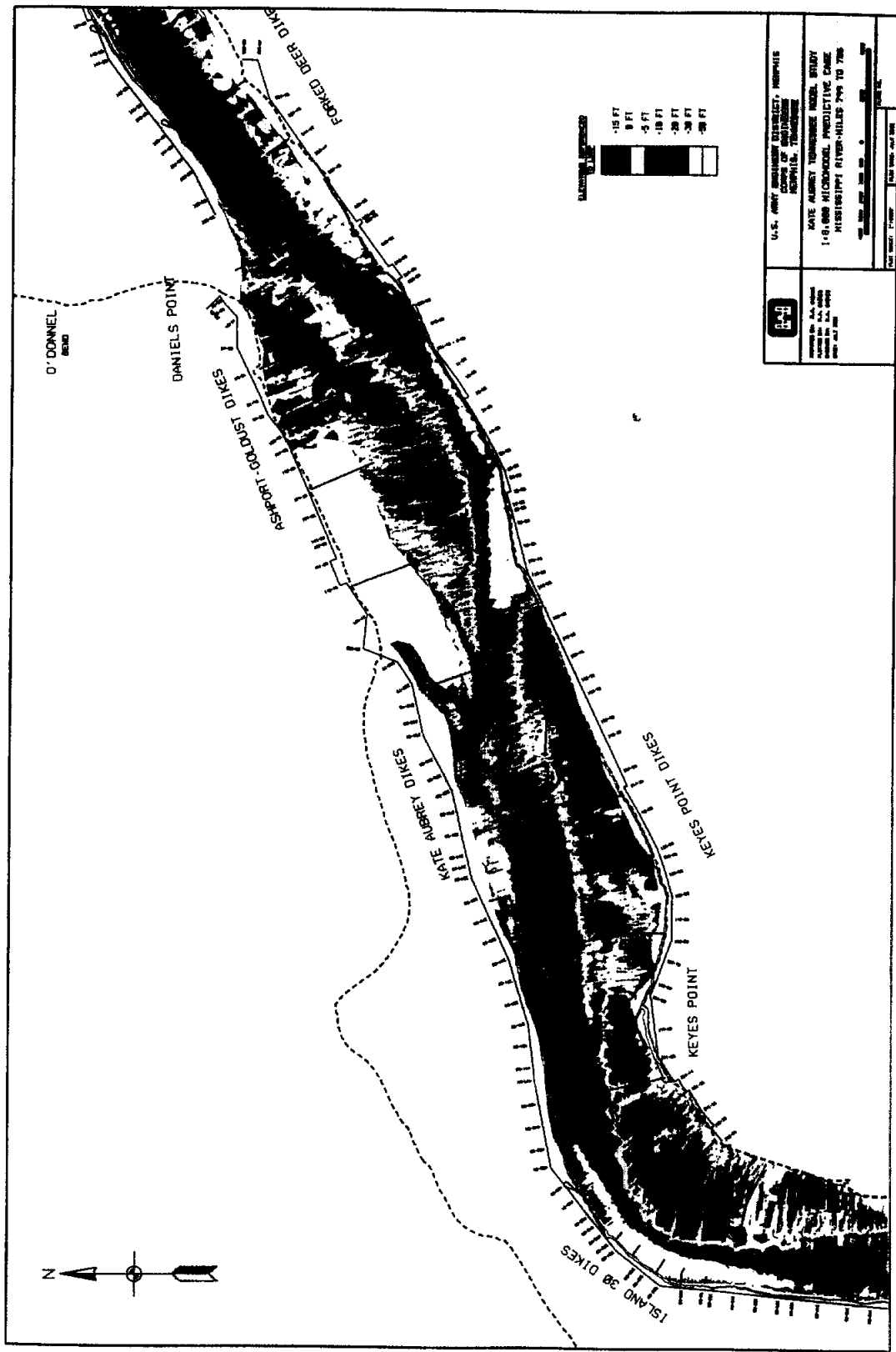


Figure 3-32 Predictive Model Bathymetry, Kate-Aubrey 1:8,000 Micromodel

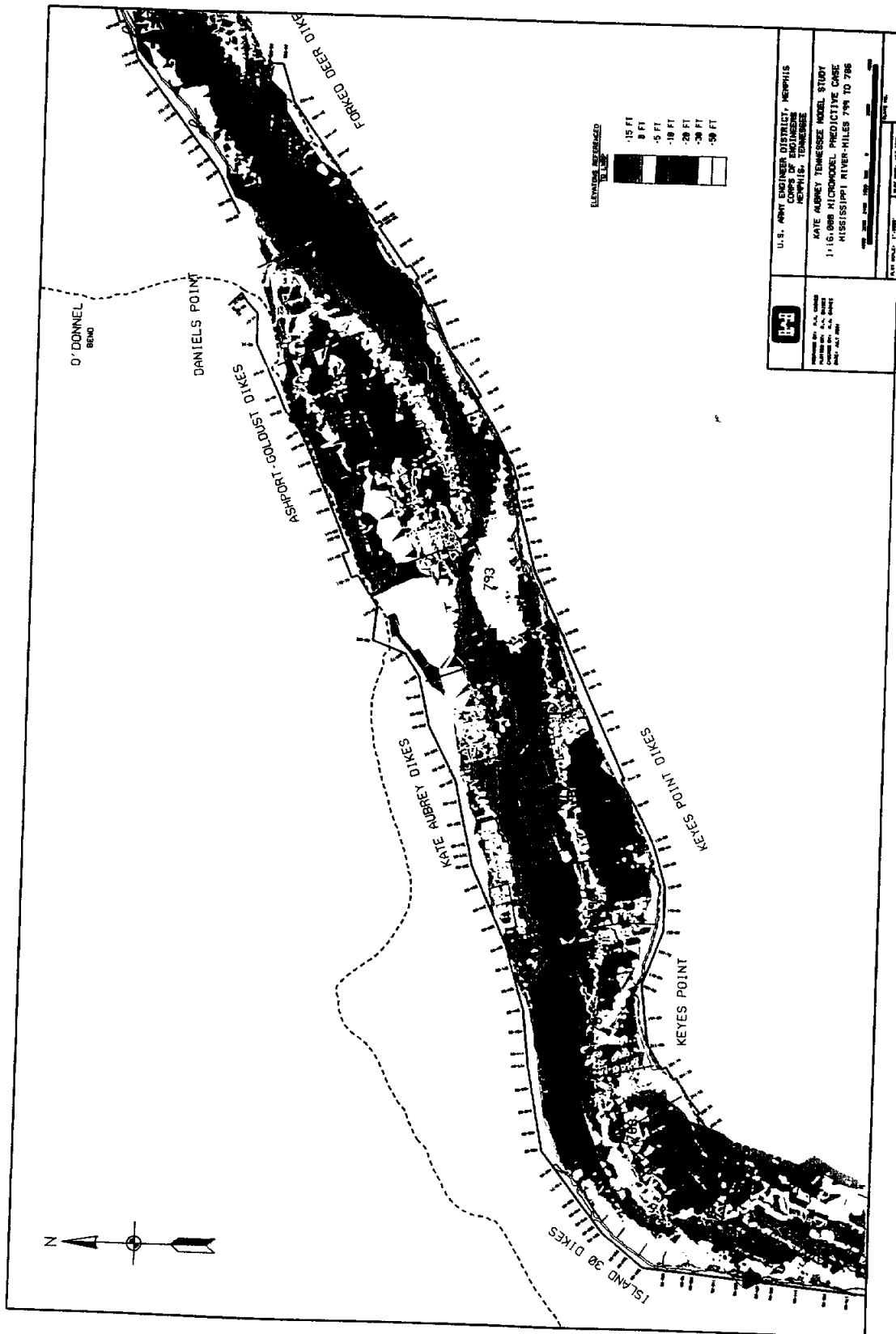


Figure 3-33 Predictive Model Bathymetry, Kate-Aubrey 1:16,000 Micromodel

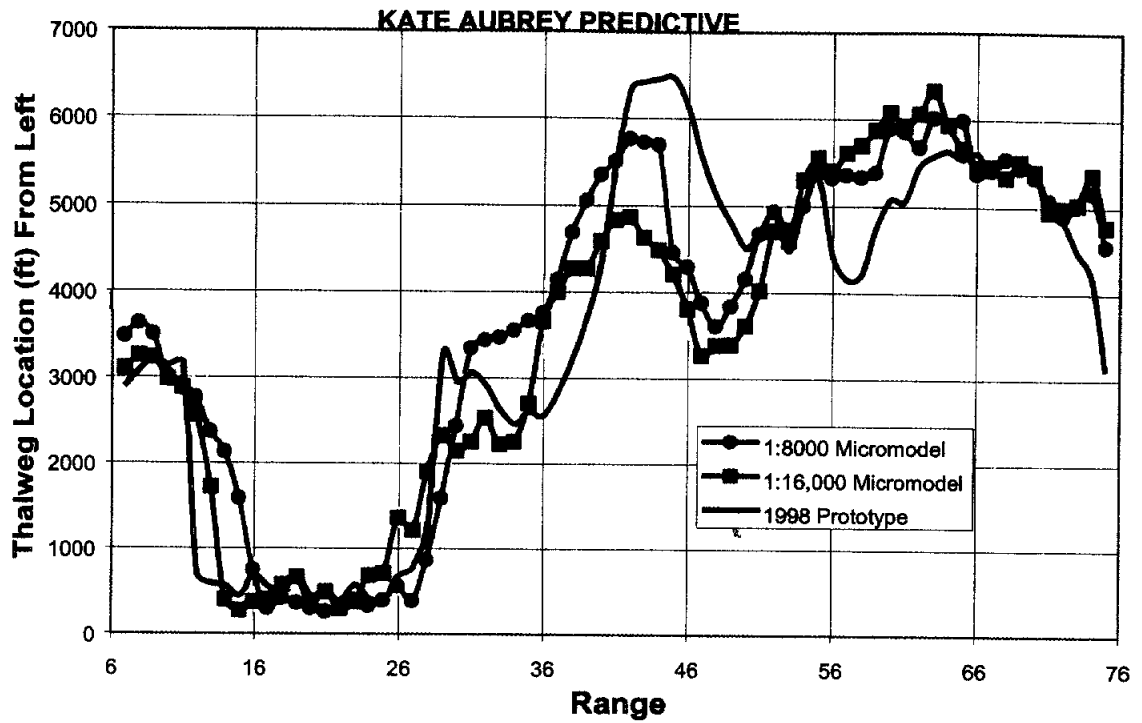


Figure 3-34 Thalweg Position Predictive Kate-Aubrey Model Case

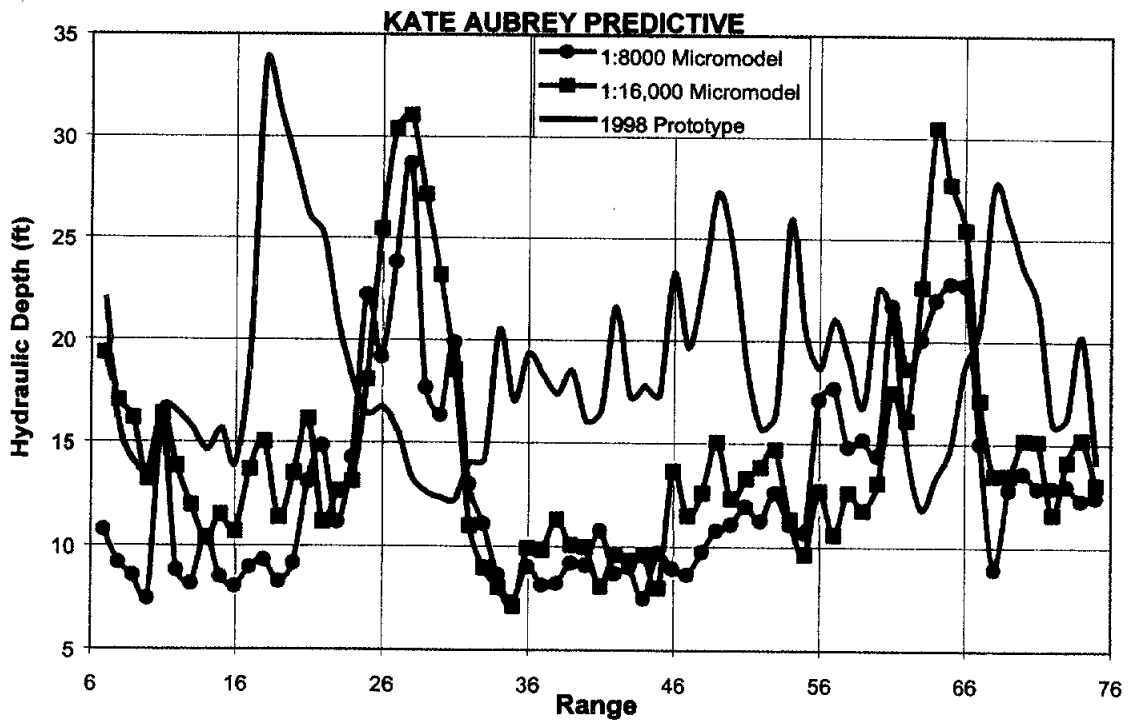


Figure 3-35 Hydraulic Depth Predictive Kate-Aubrey Model Case

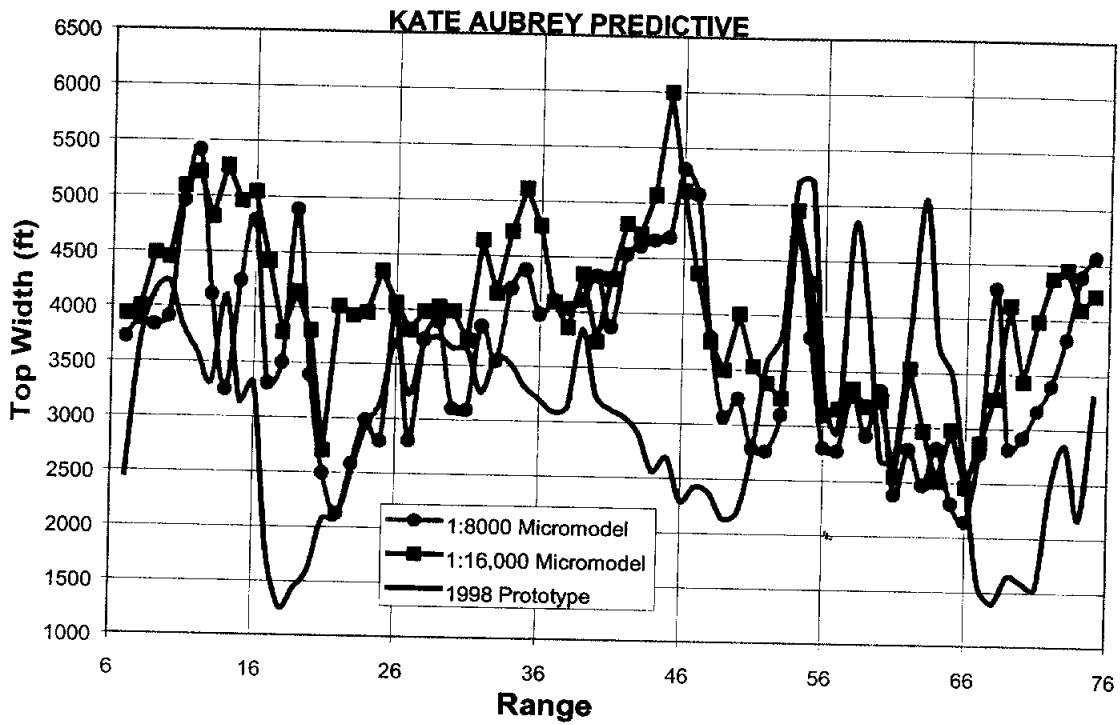


Figure 3-36 Width Predictive Kate-Aubrey Model Case

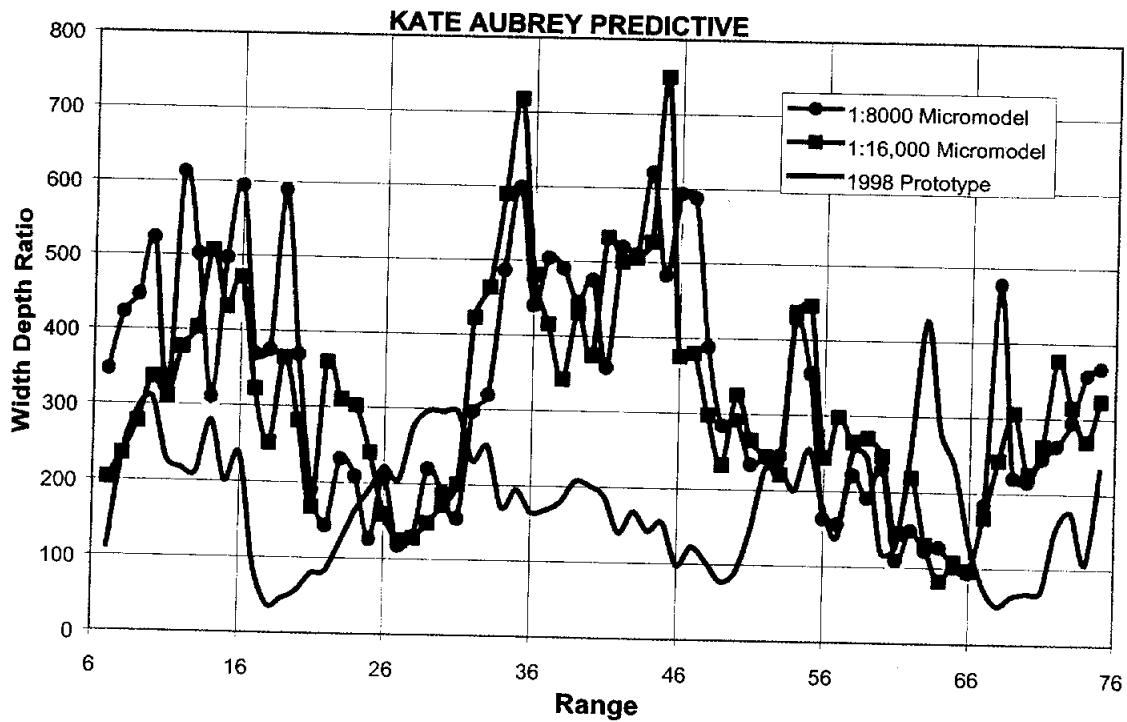


Figure 3-37 Width/Depth Ratio Predictive Kate-Aubrey Model Case

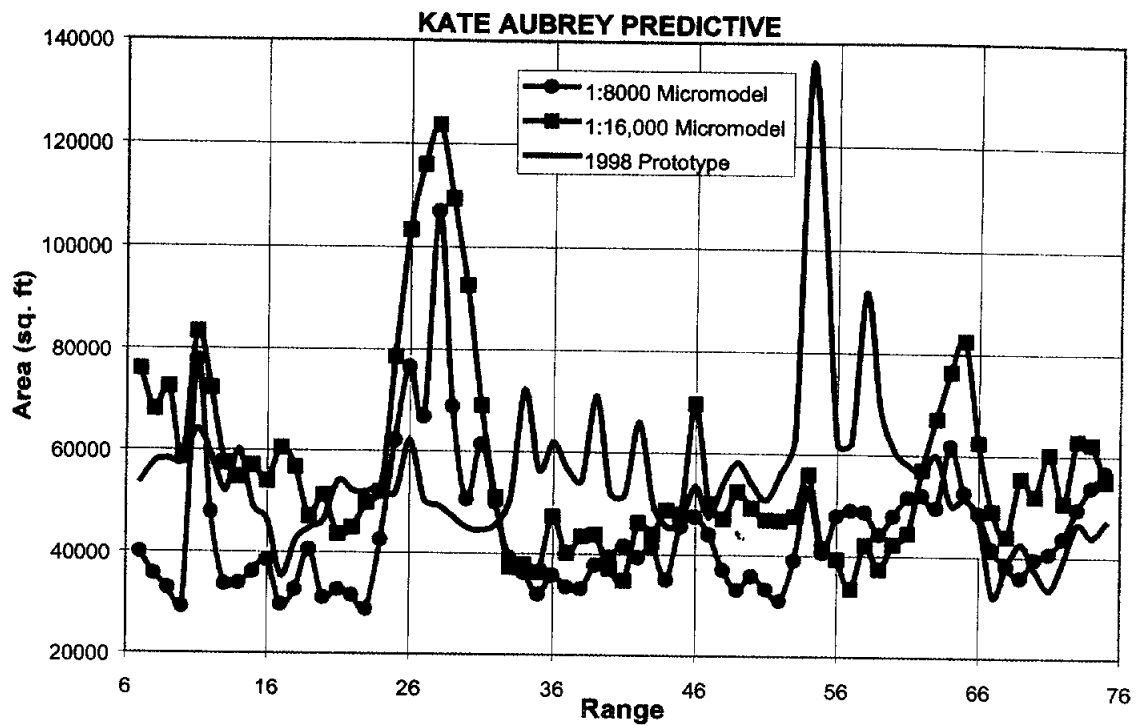


Figure 3-38 Area Predictive Kate-Aubrey Model Case

Table 3-4 Morphologic Parameter Assessment, 1:8,000 Kate-Aubrey Predictive Micromodel

Morphologic Parameter	Notes
Thalweg Position	Agreement between model and prototype fair except R44-50 and R55-65
Hydraulic Depth at 0.0 LWRP	model under predicts depth by approximately 5.0 feet
Width at 0.0 LWRP	Model over predicts width
Width/Depth Ratio at 0.0 LWRP	Ratio over predicted
Area at 0.0 LWRP	Area under predicted by model, esp. R52-63; Area over predicted R28-30

Table 3-5 Morphologic Parameter Assessment, 1:16,000 Kate-Aubrey Predictive Micromodel

Morphologic Parameter	Notes
Thalweg Position	Agreement between model and prototype fair except R40-50 and R55-65.
Hydraulic Depth at 0.0 LWRP	Model under predicts depth
Width at 0.0 LWRP	Model over predicts width
Width/Depth Ratio at 0.0 LWRP	Ratio over predicted
Area at 0.0 LWRP	Area under predicted by model, esp. R52-62; area over predicted R25-32

3.1.5. Summary of Kate-Aubrey Model Analysis. Basic interpretation of model results in previous sections was based on visual inspection of bathymetry and parameter plots. Parameter values obtained by averaging and weighting techniques are shown in Table 3-6. Table 3-6 presents reach morphologic parameter values calculated by two methods: arithmetic average and reach weighted. Table 3-7 lists percent differences between model and prototype values by each calculation method for each of the Kate Aubrey examples.

Although construction of training structures in the reach were similar to the recommended model alternative, dredging within the reach (Figure 3-29) was not simulated by the model. The locations of dredge cuts made prior to about 1990 are unknown.

3.2. Bathymetric Repeatability

An important aspect of loose-bed physical sediment models pertains to the ability of a model to reproduce consistent, or nearly so, bathymetry between successive runs. Ideally, if model boundary conditions (input hydrograph, slopes, sediment loadings, etc.) remain constant between successive runs, then the expectation would be to produce the same bathymetry for each run, there would be a unique model solution. Although the micromodel operates with an equilibrium bed concept where sediment is recirculated, the stochastic nature of sediment transport produces non-unique model bathymetry for a consistent hydrographic input. The prototype exhibits variable bathymetry primarily in

Table 3-6 Reach Morphologic Parameter Values by Two Methods

Reach Morphologic Parameter Values - Kate Aubrey Reach, Mississippi River								
Survey	Case	Method for Determining Reach Value	Number of Ranges	Area (sq. ft.)	Hydraulic Depth (ft.)	Width (ft.)	Width/Depth	Thalweg Position ¹
1:300 Model	Verification	Arithmetic	28	26501	13.6	2107	211	na
		Reach Weighted		26195	12.4	2108	170	na
1975 Prototype		Arithmetic	28	33394	13.7	2696	252	na
		Reach Weighted		34116	12.1	2823	234	na
1976 Prototype		Arithmetic	28	38064	16.6	2644	227	na
		Reach Weighted		38058	14.2	2687	190	na
1:8,000 Micromodel	Calibration	Arithmetic	71	35540	15.6	2385	182	na
		Reach Weighted		35993	15.2	2375	157	na
1973 Prototype		Arithmetic	71	45839	16.3	2983	209	na
		Reach Weighted		45937	15.3	3010	197	na
1975 Prototype		Arithmetic	71	42688	18.4	2488	159	na
		Reach Weighted		42333	16.6	2556	154	na
1976 Prototype		Arithmetic	71	46372	19.8	2509	148	na
		Reach Weighted		46493	17.9	2603	146	na
1:16,000 Micromodel	Calibration	Arithmetic	75	51034	17.5	3030	213	na
		Reach Weighted		51490	16.9	3041	180	na
1973 Prototype		Arithmetic	75	45054	16.1	2973	213	na
		Reach Weighted		45482	15.3	2981	195	na
1975 Prototype		Arithmetic	75	42323	18.1	2508	164	na
		Reach Weighted		42199	16.6	2540	153	na
1976 Prototype		Arithmetic	75	46065	19.5	2552	157	na
		Reach Weighted		46206	17.8	2596	146	na
1:8,000 Micromodel	Predictive	Arithmetic	78	36836	16.1	2366	173	na
		Reach Weighted		36689	15.5	2364	152	na
1998 Prototype		Arithmetic	78	48761	21.9	2326	117	na
		Reach Weighted		48539	20.6	2352	114	na
2001 Prototype		Arithmetic	78	47942	21.2	2326	117	na
		Reach Weighted		47927	20.4	2353	116	na
1:16,000 Micromodel	Predictive	Arithmetic	78	49825	19.3	2604	150	na
		Reach Weighted		50248	19.2	2616	136	na
1998 Prototype		Arithmetic	78	48761	21.9	2326	117	na
		Reach Weighted		48539	20.6	2352	114	na
2001 Prototype		Arithmetic	78	47942	21.2	2326	117	na
		Reach Weighted		47927	20.4	2353	116	na

¹ Thalweg position is measured relative to an arbitrary point at each Range. Values of average or reach weighted Thalweg Position, therefore, provide no meaningful description of thalweg behavior in the reach.

Table 3-7 Differences Between Model and Prototype, Case Study Examples

Summary of Differences ¹ in Morphologic Parameter Values by Various Methods Kate Aubrey Reach, Mississippi River							
Survey	Method for Determining Reach Value	Number of Ranges	Percent Difference between Model Value and Individual Survey				
			Area (sq. ft.)	Hydraulic Depth (ft.)	Width (ft.)	Width/Depth	Thalweg Position ²
1:300 Model - Verification							
1975 Prototype	Arithmetic	28	-20.6	-0.3	-21.9	-16.0	na
	Reach Wtd.		-23.2	2.8	-25.3	-27.4	na
1976 Prototype	Arithmetic	28	-30.4	-17.9	-20.3	-6.9	na
	Reach Wtd.		-31.2	-12.3	-21.5	-10.5	na
1:8,000 Micromodel - Base Calibration							
1973 Prototype	Arithmetic	71	-22.5	-3.9	-20.1	-12.8	na
	Reach Wtd.		-21.6	-0.7	-21.1	-20.6	na
1975 Prototype	Arithmetic	71	-16.7	-14.8	-4.2	14.6	na
	Reach Wtd.		-15.0	-8.5	-7.1	1.5	na
1976 Prototype	Arithmetic	71	-23.4	-21.1	-5.0	23.4	na
	Reach Wtd.		-22.6	-15.2	-8.8	7.5	na
1:16,000 Micromodel - Base Calibration							
1973 Prototype	Arithmetic	75	13.3	8.8	1.9	0.1	na
	Reach Wtd.		13.2	11.0	2.0	-8.1	na
1975 Prototype	Arithmetic	75	20.6	-3.2	20.8	30.1	na
	Reach Wtd.		22.0	1.9	19.7	17.5	na
1976 Prototype	Arithmetic	75	10.8	-10.4	18.7	35.4	na
	Reach Wtd.		11.4	-4.9	17.2	23.2	na
1:8,000 Micromodel Predictive Case							
1998 Prototype	Arithmetic	78	-24.5	-26.3	1.7	48.1	na
	Reach Wtd.		-24.4	-24.8	0.5	33.6	na
2001 Prototype	Arithmetic	78	-23.2	-23.8	1.7	47.1	na
	Reach Wtd.		-23.4	-23.8	0.5	31.9	na
1:16,000 Micromodel - Predictive Case							
1998 Prototype	Arithmetic	78	2.2	-11.8	11.9	28.7	na
	Reach Wtd.		3.5	-6.9	11.2	19.4	na
2001 Prototype	Arithmetic	78	3.9	-8.8	11.9	27.8	na
	Reach Wtd.		4.8	-5.7	11.2	17.8	na

¹ Differences calculated between Model and prototype parameter values expressed as a percent and are not indicative of model accuracy.

² Thalweg differences provide only a relative expression of agreement, model to prototype, for measurements taken from a common baseline. Therefore, differences for Thalweg Position were not computed.

na = Average and Weighted Thalweg Position not considered representative of Reach conditions.

response to variable inputs of discharge and sediment inflow, but even consistent flow conditions⁶ result in an ever changing bed configuration in the prototype.

Repetition of model bathymetry is considered by evaluating multiple bed surveys obtained after operating the calibrated model through the same series of inflow hydrographs.

3.2.1. Kate-Aubrey 1:16,000 Micromodel. The Kate-Aubrey 1:16,000 micromodel was subjected to several repetitive hydrograph cycles in order to assess the ability of the model to reproduce consistent bathymetric data. In all, five repetitions were completed. The surveys of the 1:16,000 micromodel were taken after model calibration. Each repetition included operating the model for a number of hydrograph cycles, stopping the model at the peak of the hydrograph cycle, allowing the model to slowly drain, and then surveying the bathymetry. The number of cycles between repetitions varied as shown in Table 3-8.

Table 3-8 Number of Hydrograph Cycles Between Surveys

Survey	Number of Hydrograph Cycles Between Surveys ⁷
022301d	Calibration - Base Test
022701a	3
022701b	5
022701c	21
022801a	5

Variability between successive model runs is presented by cross-section comparison plots (Figures 3-39 to 3-45) and by a plot of hydraulic depth at 0.0 LWRP

⁶ Consistent boundary conditions in the prototype may be approximated for short time-intervals during extended low flow periods.

⁷ Cycle length in the 1:16,000 micromodel was 1.8 minutes per cycle.

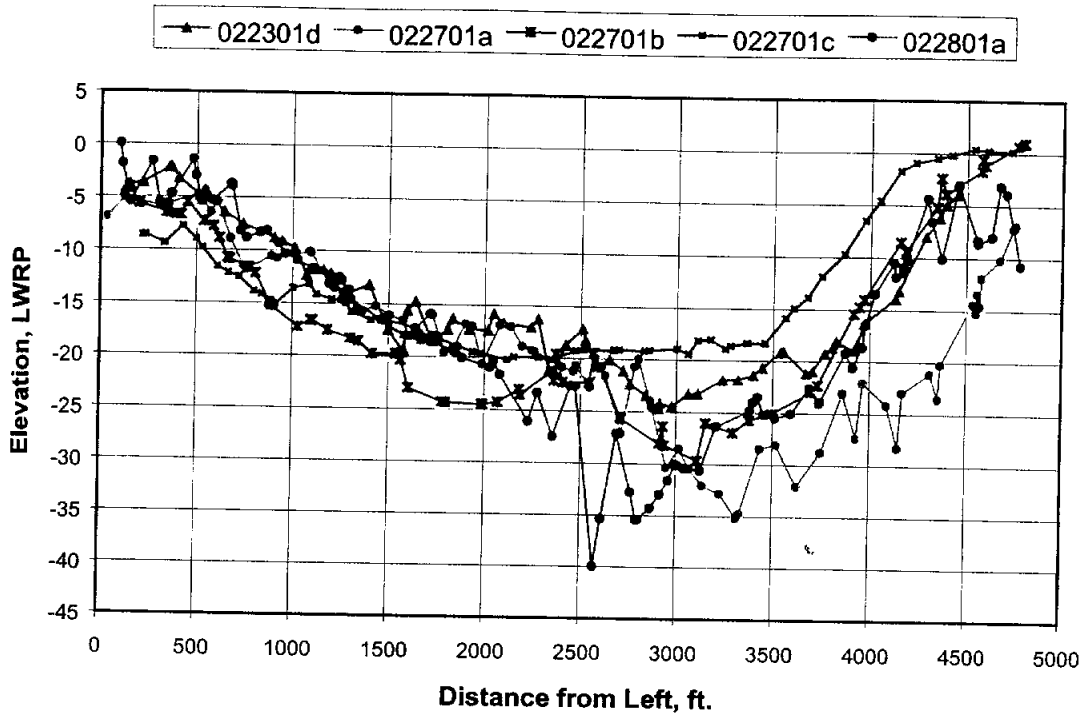


Figure 3-39 Repeatability of Model Bathymetry, Kate-Aubrey Range 10

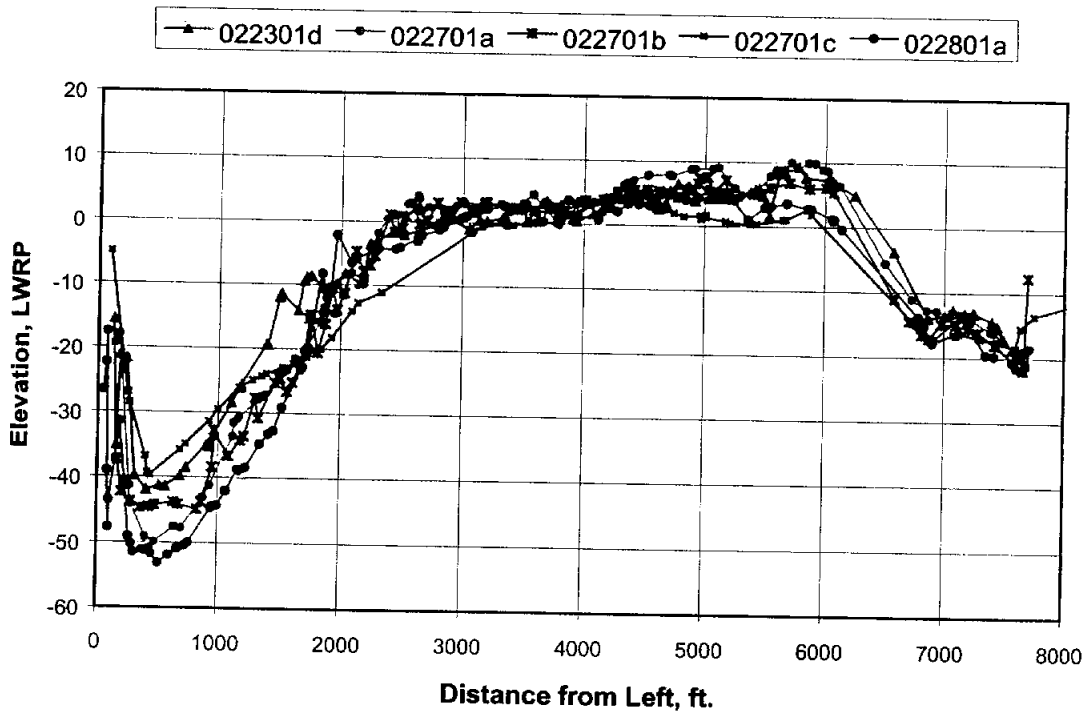


Figure 3-40 Repeatability of Model Bathymetry, Kate-Aubrey Range 20

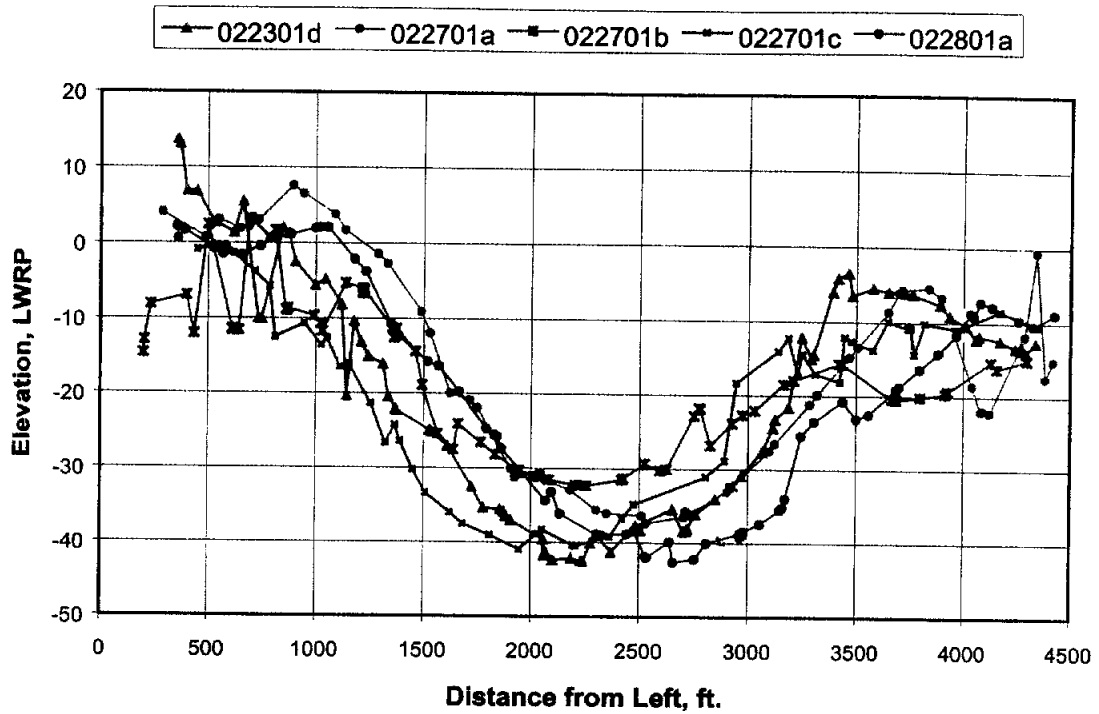


Figure 3-41 Repeatability of Model Bathymetry, Kate-Aubrey Range 30

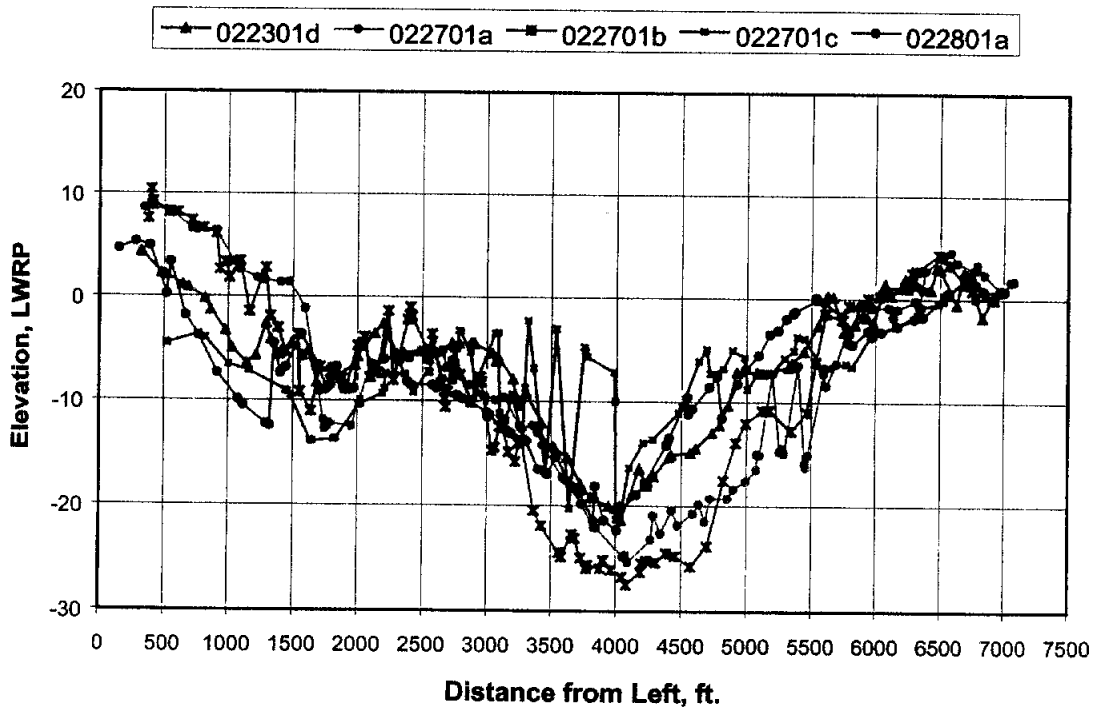


Figure 3-42 Repeatability of Model Bathymetry, Kate-Aubrey Range 40

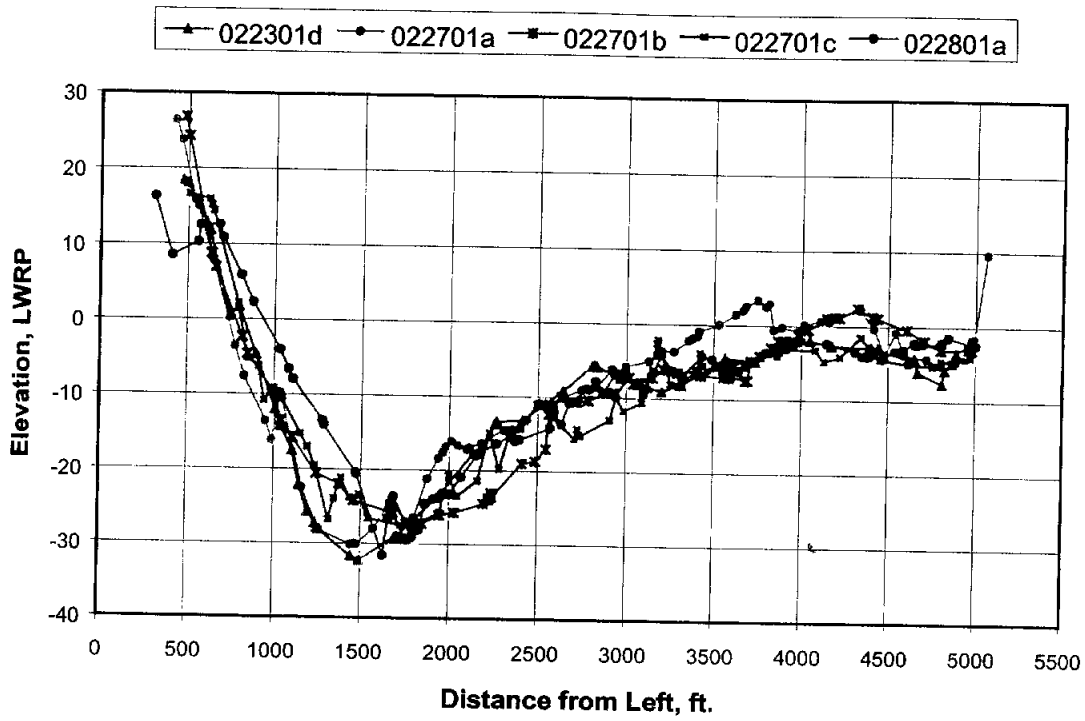


Figure 3-43 Repeatability of Model Bathymetry, Kate-Aubrey Range 50

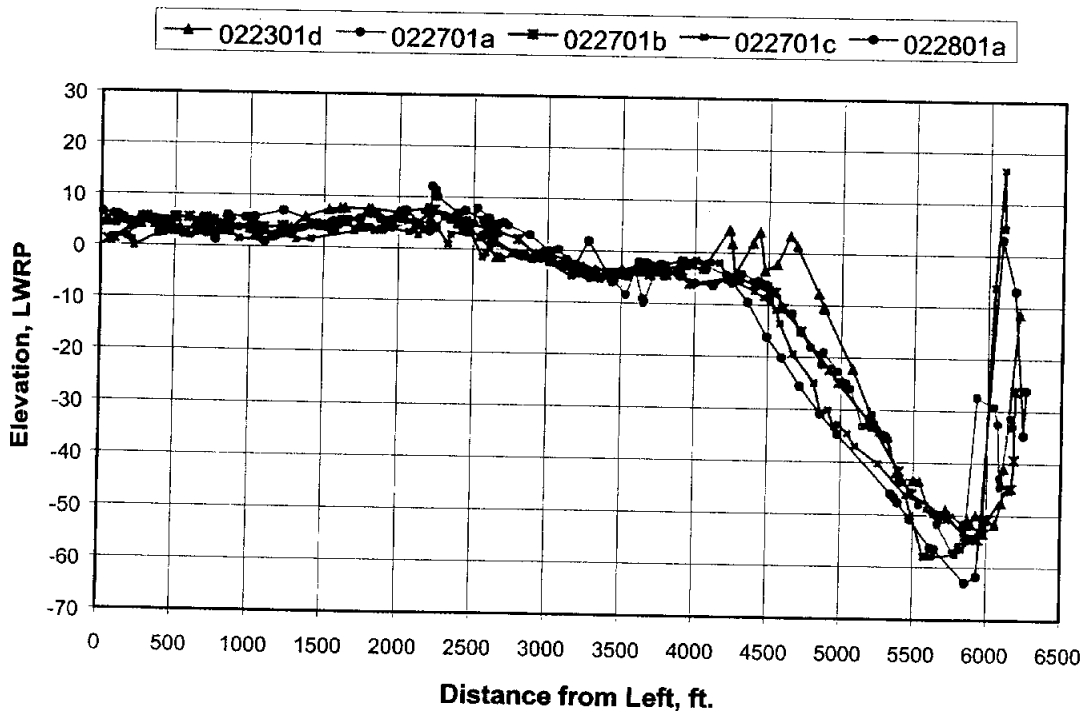


Figure 3-44 Repeatability of Model Bathymetry, Kate-Aubrey Range 60

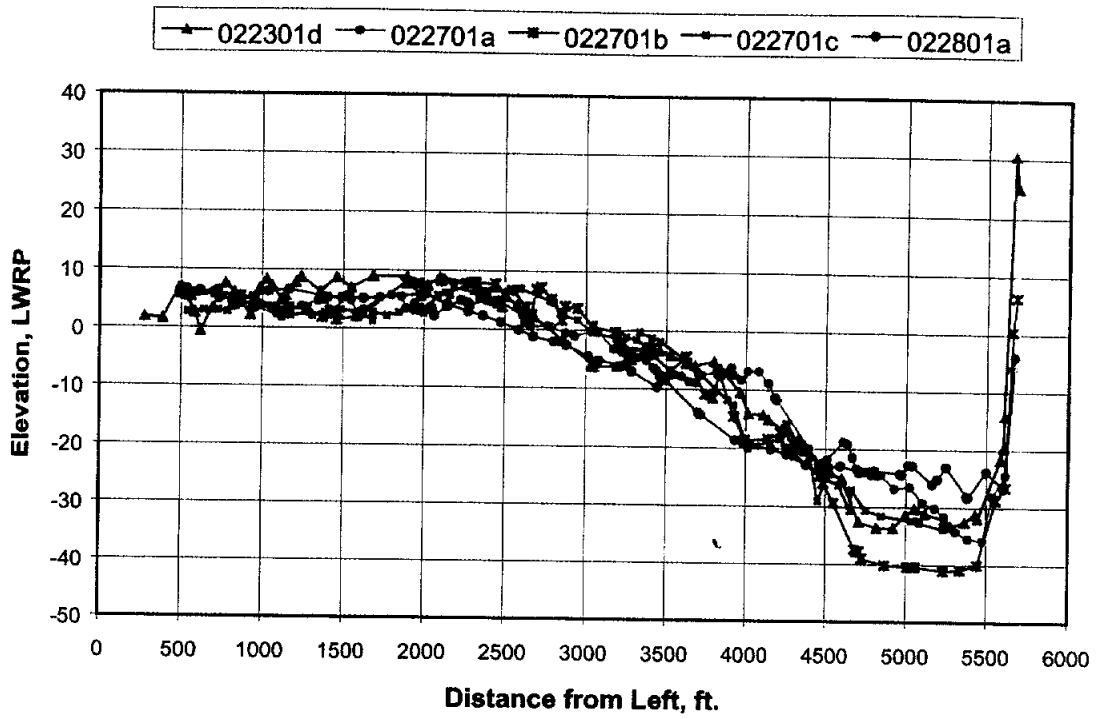


Figure 3-45 Repeatability of Model Bathymetry, Kate-Aubrey Range 70

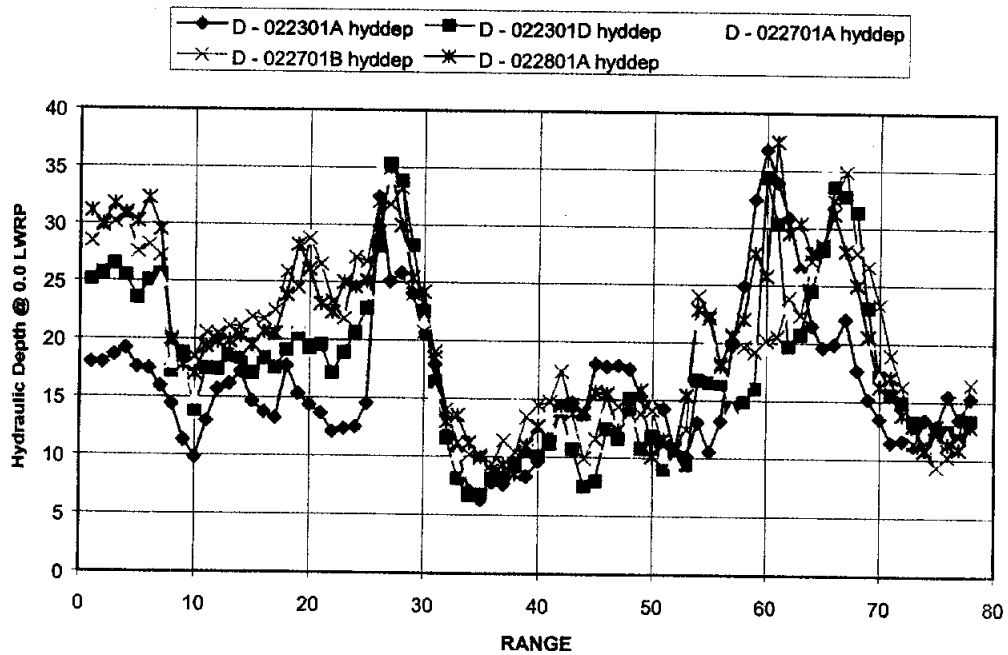


Figure 3-46 Repeatability of Hydraulic Depth in Model Reach, Kate-Aubrey 1:16,000 Model

over the model length (Figure 3-46). Cross-section plots provide a description of how the channel geometry is replicated when the model is operated with consistent, variable hydrographs for each run. Plots of hydraulic depth for all ranges in the model provide a description of how depth varies over the length of the model for each bathymetric survey.

The repeatability for the five Kate-Aubrey 1:16,000 micromodel surveys was expressed by statistical variance for seven ranges. Variance was calculated at equal intervals of 100 feet across each range. Therefore, bed elevations were interpolated at each position for the analysis. Figures 3-39 to 3-45 show the model cross-section elevations. Computed values of variance for the seven Kate-Aubrey ranges follow.

Range 10 Average Variance:	20.7 feet ²
Range 20 Average Variance:	14.0 feet ²
Range 30 Average Variance:	37.0 feet ²
Range 40 Average Variance:	16.7 feet ²
Range 50 Average Variance:	9.6 feet ²
Range 60 Average Variance:	30.6 feet ²
Range 70 Average Variance:	11.8 feet ²
Overall Average Variance:	20.0 feet ²

Because variance is a function of the spread in elevations being analyzed, minimum to maximum within the cross-section, variance values cannot be used in comparing cross-sections or reaches having dissimilar characteristics. Variance, therefore, only provides a relative comparison between individual locations.

3.2.2. Jefferson Barracks Micromodel. The ability of the Jefferson Barracks model to repeatedly produce similar resultant bed configurations between identical experimental runs was also analyzed using statistical variance. The Jefferson Barracks Micromodel (Mississippi River Miles 176 to 166) was used to study the change or variance in relative elevations of the bed for the base test condition after numerous identical flows were run in the model. The scales of this model were 1:9600 horizontal and 1:1200 vertical, for a

distortion of 8. For each run, a constant flow of 0.9 gallons per minute was subjected to the model bed for a variable period of time (1/2 hour average). The Jefferson Barracks micromodel was calibrated and alternatives were tested using a constant discharge of 0.9 gallons per minute.

A total of eighteen experimental runs were conducted. At the end of each run the flow was shut off, the water was allowed to drain, and the resultant bed configuration was surveyed with a three-dimensional laser scanner. The survey data was then processed and converted to prototype coordinates with all elevations being referenced to the Low Water Reference Plane (LWRP). Cross-section plots were then generated at seven locations over a representative four-mile reach of the model. The variances in elevations produced by the 18 runs were analyzed using statistical variance at each of the sections. Cross sectional plots of the model data are shown in Figures 3-47 through 3-53.

Statistical variance was computed for cross-section elevations using the Microsoft Excel™ VAR function. Elevations were interpolated at intervals of 100 feet across the

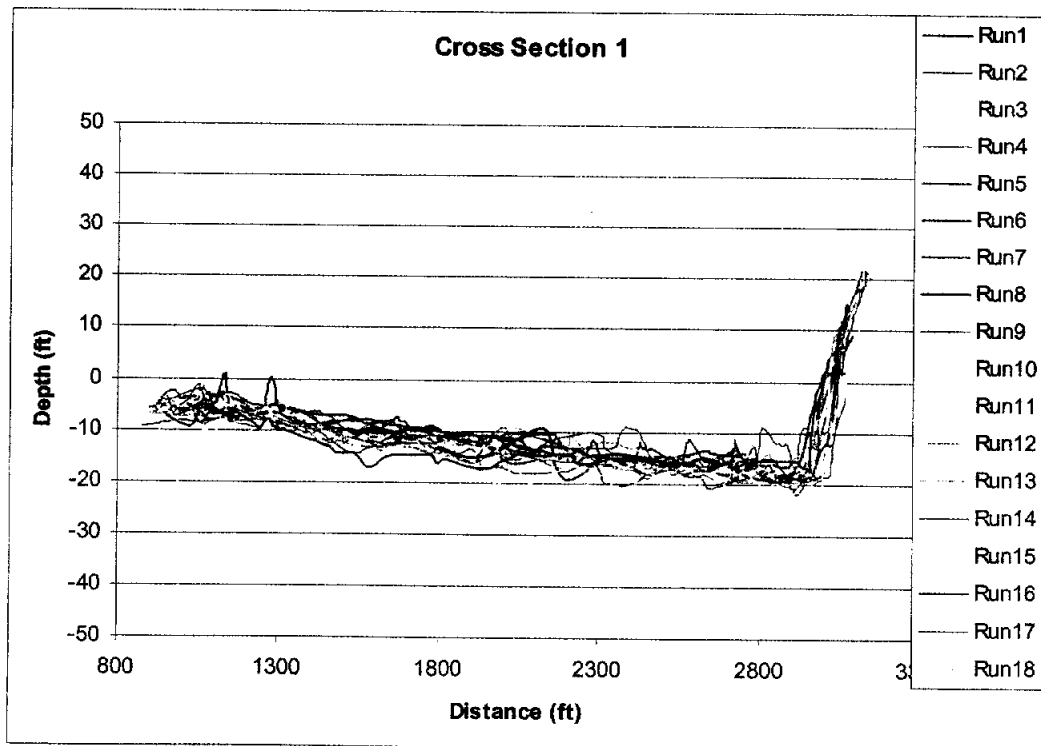


Figure 3-47 Repeatability of Model Bathymetry, Jefferson Barracks Section 1

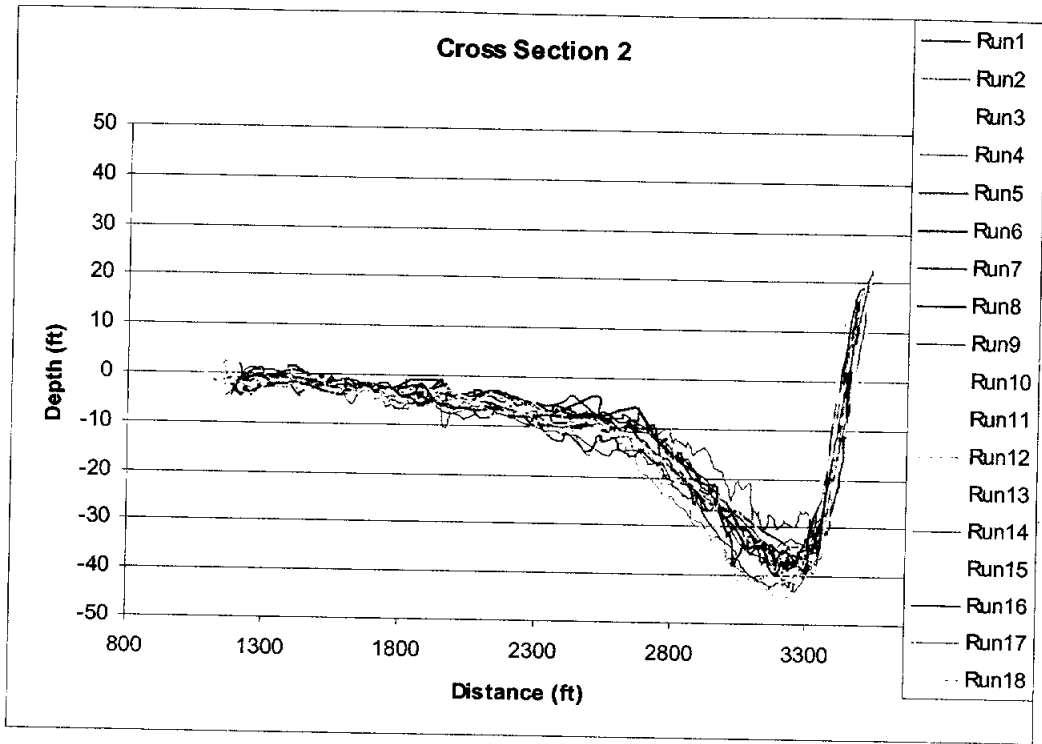


Figure 3-48 Repeatability of Model Bathymetry, Jefferson Barracks Section 2

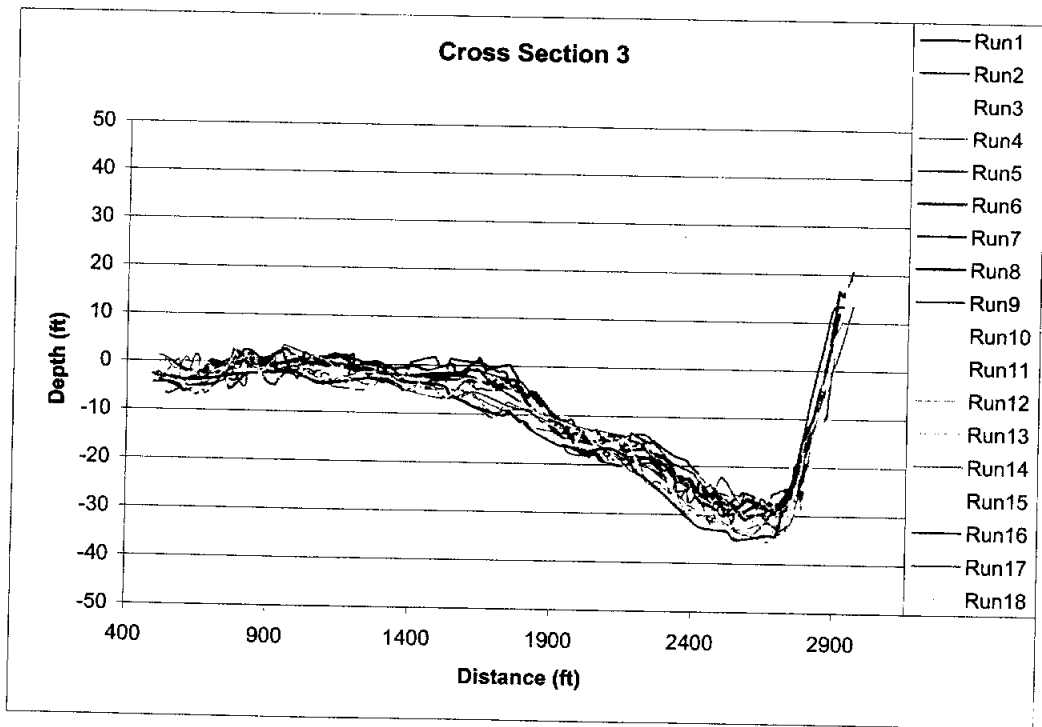


Figure 3-49 Repeatability of Model Bathymetry, Jefferson Barracks Section 3

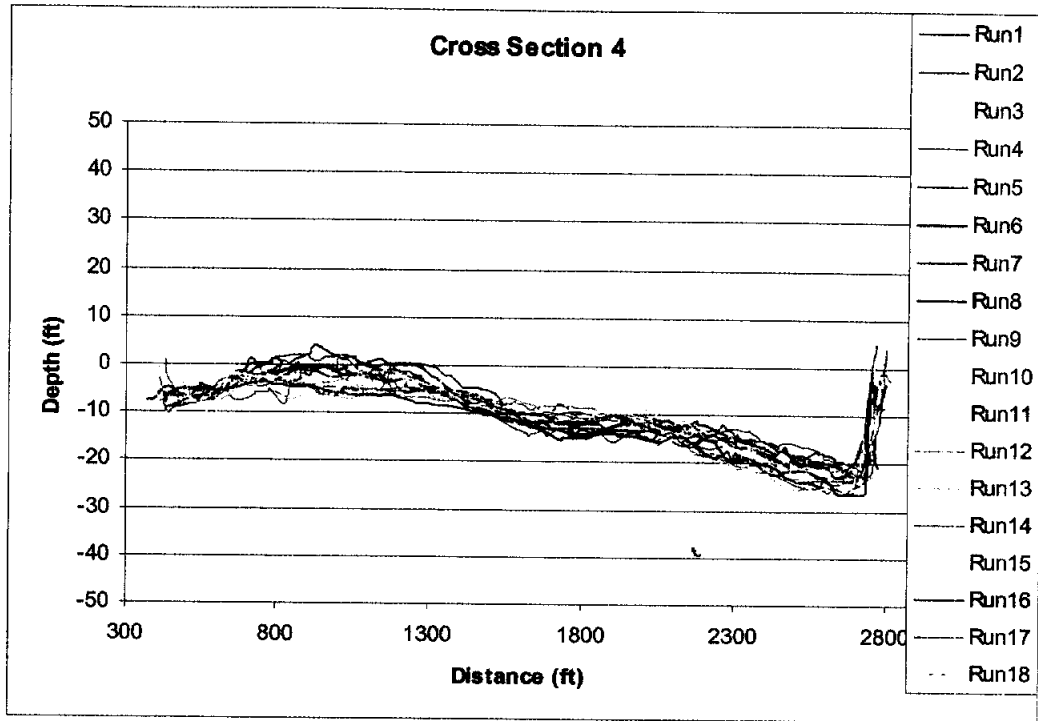


Figure 3-50 Repeatability of Model Bathymetry, Jefferson Barracks Section 4

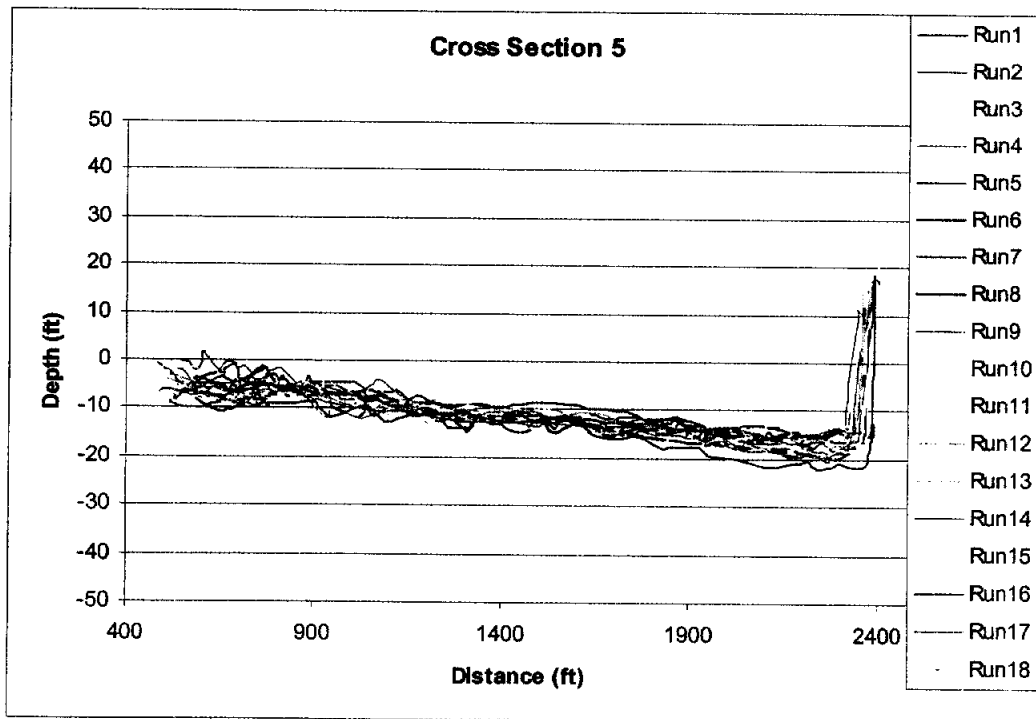


Figure 3-51 Repeatability of Model Bathymetry, Jefferson Barracks Section 5

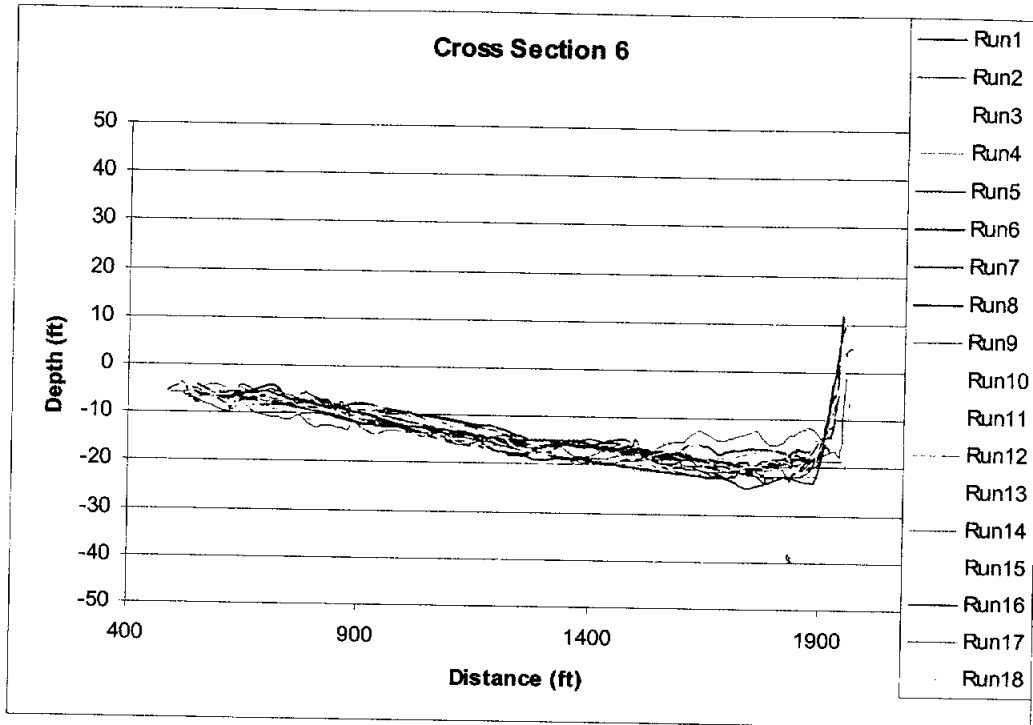


Figure 3-52 Repeatability of Model Bathymetry, Jefferson Barracks Section 6

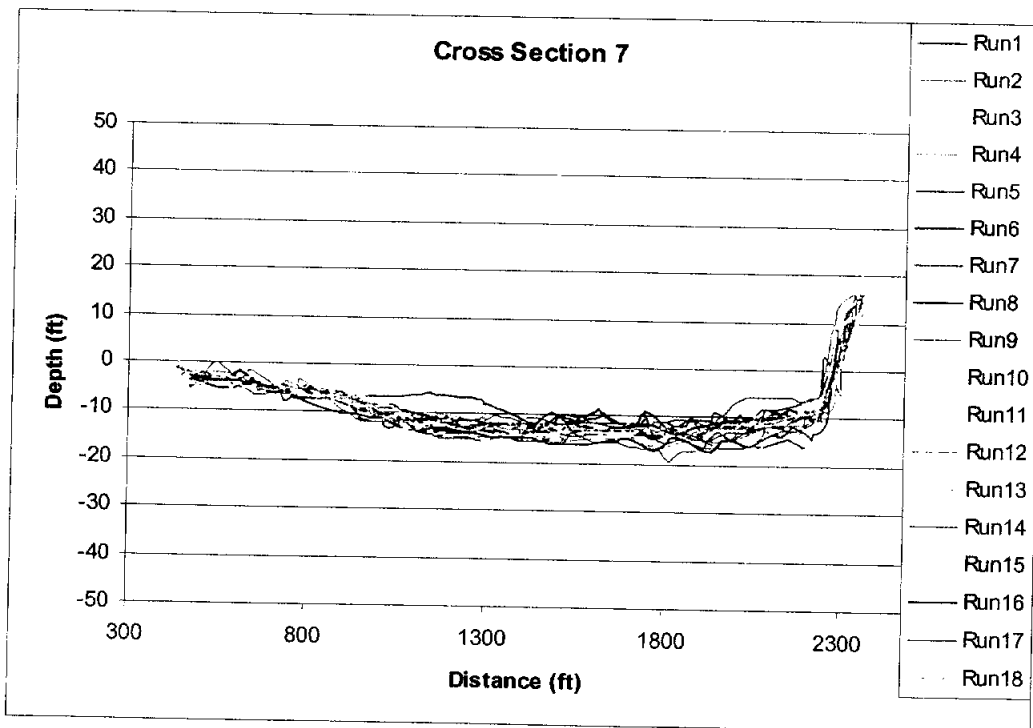


Figure 3-53 Repeatability of Model Bathymetry, Jefferson Barracks Section 7

cross-sections. Therefore, elevation points analyzed for each survey were essentially located at the same x,y coordinates. A limited amount of manual smoothing in the raw cross-section data was performed to eliminate spurious spikes in the data. These spikes were suspected to be a result of errors resulting from the laser-scanner as opposed to actual fluctuations in the bed.

Average values of variance at each cross-section in the Jefferson Barracks micromodel were as follows:

Cross section 1: Average Variance:	3.69 feet ²
Cross section 2: Average Variance:	5.78 feet ²
Cross section 3: Average Variance:	5.76 feet ²
Cross section 4: Average Variance:	3.91 feet ²
Cross section 5: Average Variance:	2.71 feet ²
Cross section 6: Average Variance:	2.69 feet ²
Cross section 7: Average Variance:	2.71 feet ²
Overall Average Variance:	3.89 feet ²

There are a number of other factors that could contribute to the amount of variance experienced in the reach. These are reach specific factors such as channel alignment, width/depth ratio, influence of river training structures, overall reach stability, and sediment size and load. For example, a shallow straight reach may experience less variability than a highly sinuous reach.

3.2.3. Dogtooth Bend Micromodel. Davinroy (1994) conducted a similar variance analysis comparing the repeatability of a micromodel with a WES model (Dogtooth Bend Model, Mississippi River, Miles 38 to 20). Unlike the Kate-Auibrey and Jefferson Barracks variance analysis, the Dogtooth Bend micromodel required no interpolation because the survey points were collected at the same exact location after each run. Davinroy (1994) indicates that data used in calculating variance from the WES Dogtooth Bend model were derived from numerous base test runs. The multiple base test runs

were made during initial development of the base test bed configuration (Davinroy, 1994).

Davinroy (1994) describes the operation of the Dogtooth Bend micromodel as substantially different than the model operation currently used. Flow was controlled manually and sediment was introduced at the upper end of the Dogtooth Bend model by hand. Current operational procedures utilize a computerized control system to regulate discharge and sediment is automatically re-circulated through the model.

The experimental runs in the Dogtooth Bend model were the result of continuous, variable hydrographs applied to the model. This is similar to the operation utilized in the Kate-Aubrey micromodel described previously but dissimilar to the constant discharge technique used in the Jefferson Barracks micromodel.

The average variance computed by Davinroy (1994) for the Dogtooth Bend reach was 10.46 feet² for the micromodel and 8.34 feet² for the WES model. These values of variance provide a relative comparison of the variability between each model because they represent the same reach of river.

Variance depends on the relative magnitude of differences between individual data values. Because channel geometry has a significant influence on the value of variance, variance cannot be used to evaluate one reach of river to another reach. Variance as used herein only provides a relative expression of agreement (or difference) for a single reach of river.

3.2.4. Future Work. The data analyzed for the three micromodels can only be used as a general indication of model repeatability. Further experimental runs with additional model studies would be required to obtain more specific results.

4. RESULTS

4.1. General

The thirty previous model study results were considered adequate for developing solutions to the particular problems under investigation. Therefore, these model studies help establish an acceptable standard for morphologic similarity requirements that can be associated with the types of problems and control measures investigated. These problems primarily consist of channel control measures implemented by the US Army Corps of Engineers.

Morphologic similarity is quantified in this study using difference calculations and associated graphs and mean square error (MSE) values for each of the thirty previous model studies. ~~A case study example also presented the use of cumulative frequency graphs in assessing morphologic similarity for three Kate-Aubrey models.~~ Average difference and MSE values between individual data sets provide a quantitative expression of overall parameter similarity. The magnitude of differences, calculated for the five morphologic parameters in the micromodels, are similar to those calculated for the large-scale models. ~~For example, differences in area are -25 percent, -22 percent, and +13 for the Kate-Aubrey large-scale model, the 1:8000 micromodel and the 1:16000 micromodel, respectively. The MSE values for these models were 0.331, 0.216, 0.319.~~

Difference and MSE values for each model included in this study are shown in Tables 4-1, 4-2, 4-3, 4-4, and 4-5. Graphs of the average difference and MSE values provide a visual comparison the results obtained for each model (Figures 4-1, 4-2, 4-3, 4-4, and 4-5).

Conclusions derived from these model to prototype comparisons are reported in a separate report by Gaines, Gordon, and Maynard (in progress).

Table 4-1. Thalweg Comparisons for Thirty Previous Model Study Results

Large-Scale Model NAME	MODEL		Micromodel NAME	MODEL	
	DIFF	MSE		DIFF	MSE
Baleshed-Ajax	0.211	0.109	Augusta	-0.017	0.049
Blountstown	-0.074	0.031	Clarendon	0.035	0.032
Buck Island	-0.034	0.088	Copeland	0.029	0.002
Chipola Cutoff	0.278	0.247	KA 1:8000 Base	0.032	0.221
Devil's Island	-0.040	0.149	KA 1:8000 Predictive	0.071	0.064
Dogtooth Bend	-0.0474	0.0159	KA 1:16,000 Base	0.022	0.192
Kate-Aubrey	-0.270	0.224	KA 1:16000 Predictive	-0.006	0.091
Lake Dardanelle	0.404	0.470	Lock & Dam 24	0.003	0.023
Lock & Dam #2	-0.095	0.086	Memphis Harbor	0.023	0.051
Lock & Dam #4	-0.054	0.054	Morgan City	0.035	0.004
Loosahatchie- Memphis	-0.153	0.049	New Madrid	-0.031	0.027
New Madrid Bar	0.093	0.049	Salt Lake	-0.118	0.025
Redeye Crossing	0.013	0.008	Savanna Bay	0.009	0.009
Smithland Lock & Dam	0.042	0.074	Vicksburg	-0.057	0.010
West Access	-0.026	0.031	White River	0.064	0.011
Willamette River	-0.047	0.024	Wolf Island	0.001	0.009

Table 4-2. Area Comparisons for Thirty Previous Model Study Results

Large-Scale Model NAME	MODEL		Micromodel NAME	MODEL	
	DIFF	MSE		DIFF	MSE
Baleshed-Ajax	-0.406	0.213	Augusta	0.190	0.104
Blountstown	0.074	0.174	Clarendon	0.402	0.374
Buck Island	-0.248	0.149	Copeland	0.110	0.024
Chipola Cutoff	0.026	0.046	KA 1:8000 Base	0.0685	0.216
Devil's Island	-0.048	0.063	KA 1:8000 Predictive	-0.143	0.105
Dogtooth Bend	-0.011	0.179	KA 1:16,000 Base	0.284	0.319
Kate-Aubrey 1:300	-0.218	0.331	KA 1:16000 Predictive	0.111	0.184
Lake Dardanelle	0.058	0.248	Lock & Dam 24	0.128	0.063
Lock & Dam #2	-0.061	0.042	Memphis Harbor	-0.213	0.0911
Lock & Dam #4	0.257	0.156	Morgan City	0.040	0.048
Loosahatchie- Memphis	-0.003	0.023	New Madrid	-0.261	0.158
New Madrid Bar	-0.069	0.122	Salt Lake	0.205	0.0566
Redeye Crossing	-0.280	0.112	Savanna Bay	-0.171	0.0567
Smithland Lock & Dam	-0.098	0.073	Vicksburg	0.0221	0.114
West Access	0.037	0.014	White River	-0.351	0.156
Willamette River	0.028	0.028	Wolf Island	0.387	0.456

Table 4-3. Width Comparisons for Thirty Previous Model Study Results

Large-Scale Model NAME	MODEL		Micromodel NAME	MODEL	
	DIFF	MSE		DIFF	MSE
Baleshed-Ajax	-.0125	0.1091	Augusta	0.1317	0.0253
Blountstown	-.0710	0.0731	Clarendon	0.1648	0.0695
Buck Island	-.1719	0.0743	Copeland	0.0791	0.0147
Chipola Cutoff	-.0187	0.0405	KA 1:8000 Base	0.1799	0.2292
Devil's Island	-.0322	0.0169	KA 1:8000 Predictive	0.2601	0.2543
Dogtooth Bend	0.0897	0.0498	KA 1:16,000 Base	0.1938	0.1910
Kate-Aubrey	-.1636	0.1090	KA 1:16000 Predictive	0.4067	0.3484
Lake Dardanelle	-.0845	0.1788	Lock & Dam 24	-0.0361	0.0043
Lock & Dam #2	-.0349	0.0186	Memphis Harbor	0.0713	0.0268
Lock & Dam #4	0.1129	0.0393	Morgan City	0.0524	0.0233
Loosahatchie- Memphis	0.0873	0.0346	New Madrid	-0.1803	0.0714
New Madrid Bar	-.0091	0.0702	Salt Lake	0.0230	0.0045
Redeye Crossing	-.1472	0.0618	Savanna Bay	-0.00804	0.0220
Smithland Lock & Dam	-.0027	0.0007	Vicksburg	0.1140	0.0399
West Access	0.0334	0.0024	White River	0.0892	0.0426
Willamette River	-.0041	0.0132	Wolf Island	0.1000	0.0383

Table 4-4. Hydraulic Depth Comparisons for Thirty Previous Model Study Results

Large-Scale Model NAME	MODEL		Micromodel NAME	MODEL	
	DIFF	MSE		DIFF	MSE
Baleshed-Ajax	-0.394	0.177	Augusta	0.056	0.062
Blountstown	0.150	0.165	Clarendon	0.208	0.155
Buck Island	-0.080	0.141	Copeland	0.031	0.011
Chipola Cutoff	0.077	0.079	KA 1:8000 Base	-0.007	0.275
Devil's Island	-0.012	0.047	KA 1:8000 Predictive	-0.257	0.198
Dogtooth Bend	-0.094	0.127	KA 1:16,000 Base	0.156	0.395
Kate-Aubrey	-0.095	0.099	KA 1:16000 Predictive	-0.155	0.218
Lake Dardanelle	0.162	0.093	Lock & Dam 24	0.174	0.090
Lock & Dam #2	-0.019	0.043	Memphis Harbor	-0.267	0.103
Lock & Dam #4	0.137	0.095	Morgan City	-0.003	0.049
Loosahatchie- Memphis	-0.072	0.028	New Madrid	-0.059	0.171
New Madrid Bar	-0.079	0.093	Salt Lake	0.178	0.043
Redeye Crossing	-0.090	0.084	Savanna Bay	-0.134	0.093
Smithland Lock & Dam	-0.100	0.070	Vicksburg	-0.094	0.059
West Access	0.003	0.009	White River	-0.380	0.206
Willamette River	0.031	0.014	Wolf Island	0.261	0.263

Table 4-5. Width/Depth Ratio Comparisons for Thirty Previous Model Study Results

Large-Scale Model NAME	MODEL		Micromodel NAME	MODEL	
	DIFF	MSE		DIFF	MSE
Baleshed-Ajax	0.729	1.107	Augusta	-0.010	0.154
Blountstown	-0.113	0.142	Clarendon	0.045	0.131
Buck Island	0.008	0.176	Copeland	0.054	0.028
Chipola Cutoff	-0.038	0.092	KA 1:8000 Base	0.585	2.099
Devil's Island	0.024	0.053	KA 1:8000 Predictive	1.137	3.446
Dogtooth Bend	0.348	0.422	KA 1:16,000 Base	0.264	0.662
Kate-Aubrey	-0.033	0.162	KA 1:16000 Predictive	1.031	2.277
Lake Dardanelle	-0.199	0.196	Lock & Dam 24	-0.145	0.053
Lock & Dam #2	0.036	0.095	Memphis Harbor	0.532	0.461
Lock & Dam #4	0.019	0.114	Morgan City	0.102	0.077
Loosahatchie- Memphis	0.207	0.181	New Madrid	0.177	0.964
New Madrid Bar	0.112	0.203	Salt Lake	-0.129	0.028
Redeye Crossing	0.018	0.130	Savanna Bay	0.288	0.302
Smithland Lock & Dam	0.249	0.366	Vicksburg	0.284	0.225
West Access	0.040	0.012	White River	0.996	1.457
Willamette River	-0.028	0.022	Wolf Island	0.011	0.285

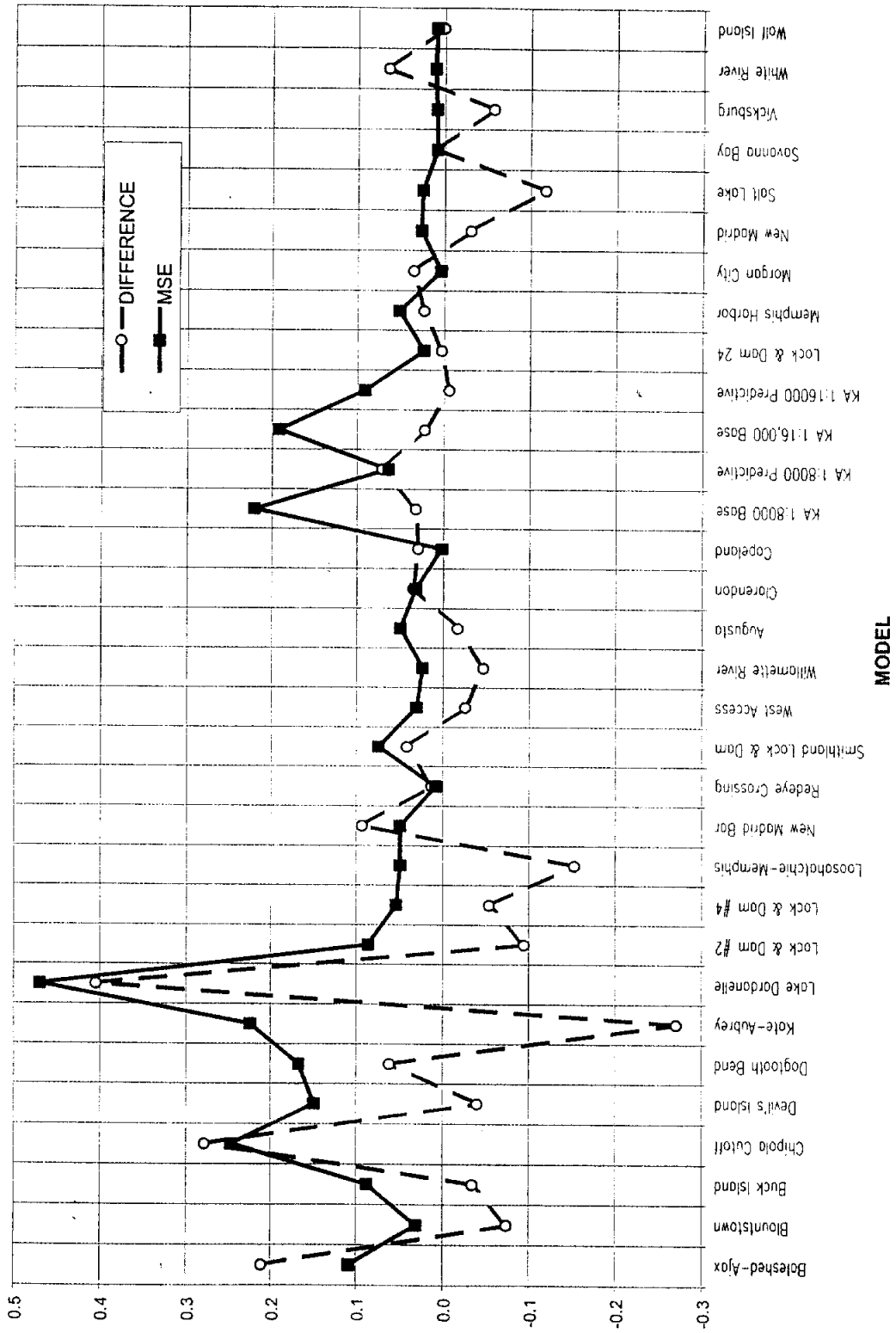


Figure 4-1 Thalweg Differences and MSE

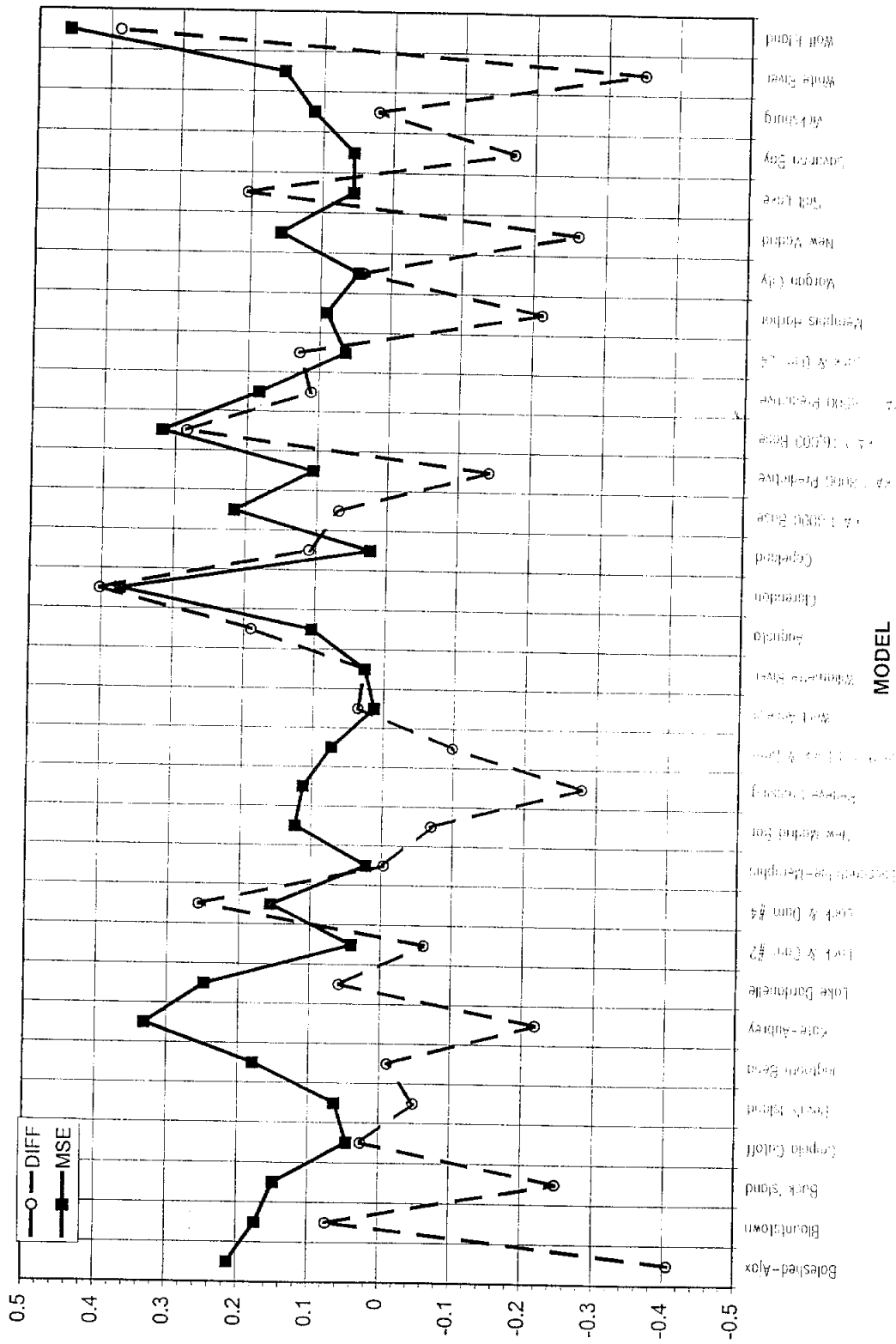


Figure 4-2 Area at 0.0 LWRP Differences and MSE

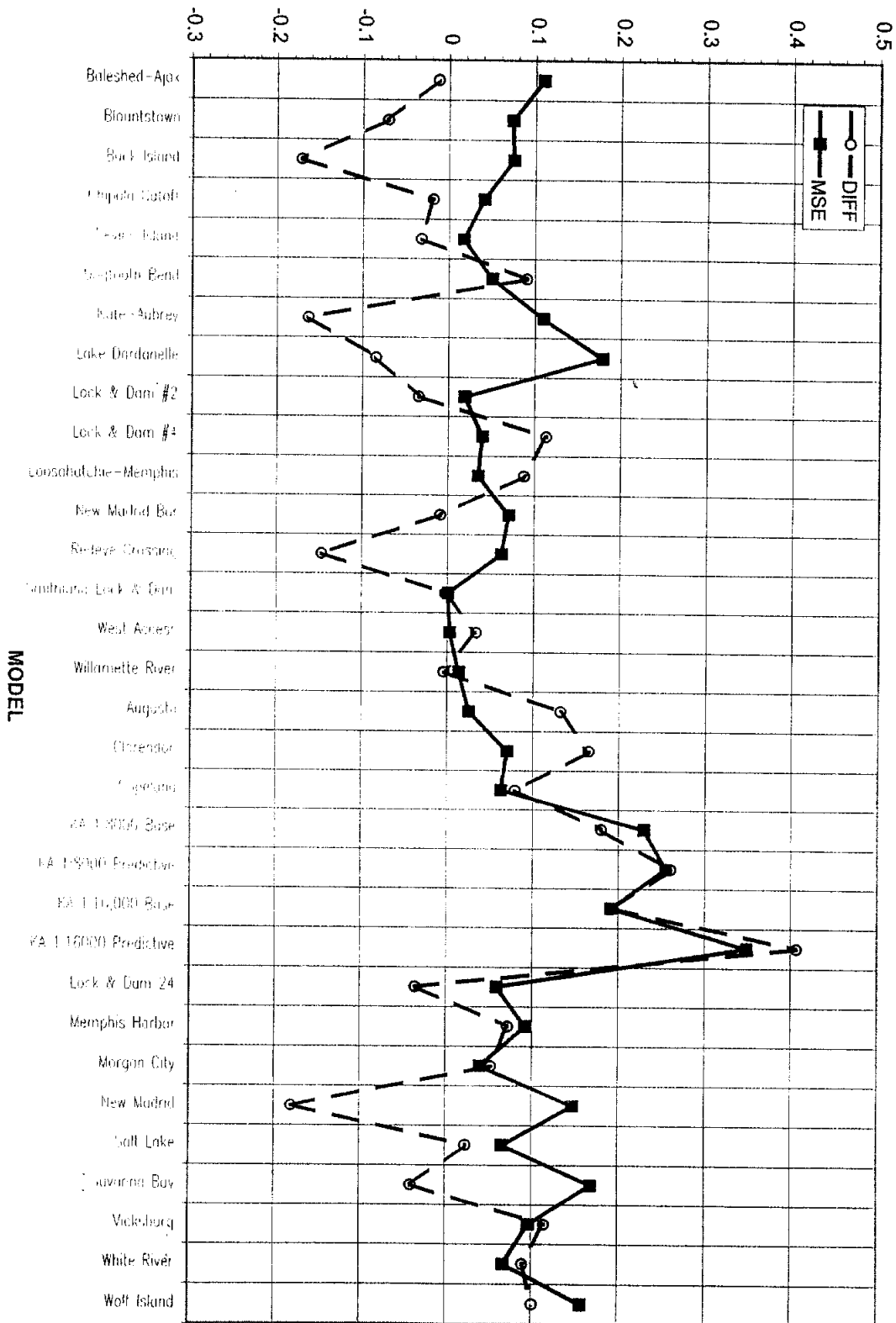
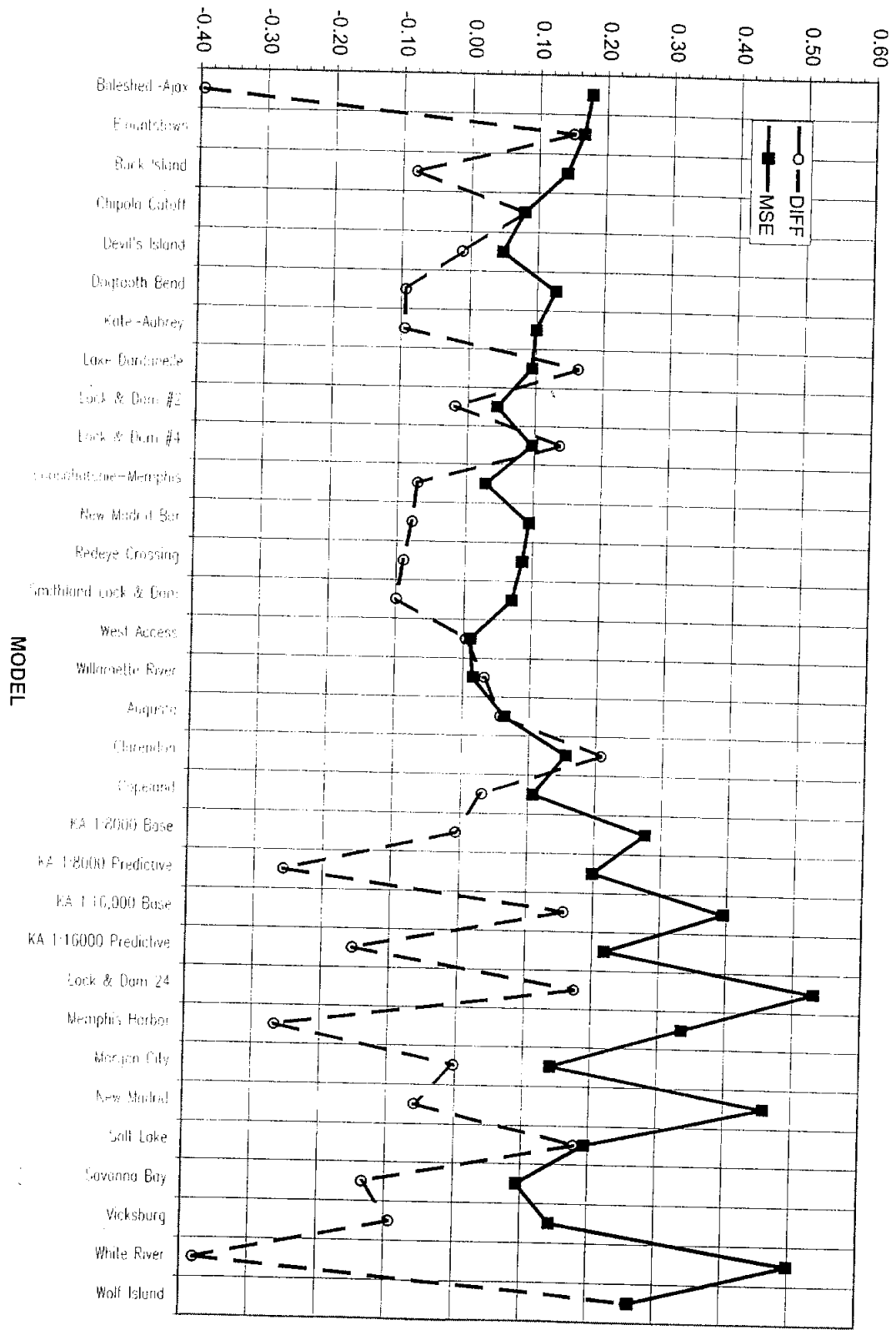


Figure 4-3 Width at 0.0 LW/RP Differences and MSE

Figure 4-4 Hydraulic Depth at 0.0 LWRP Differences and MSE



BIBLIOGRAPHY

- Biedenharn, D.S., (1995). *Lower Mississippi River Channel Response Past, Present, and Future*, Doctoral Thesis, Colorado State University, Fort Collins, CO.
- Davinroy, R.D., (1994). *Physical Sediment Modeling of the Mississippi River on a Micro Scale*, Masters Thesis, University of Missouri-Rolla, Rolla, Missouri.
- Ettema, R., (2000). "A Framework for Evaluating Micro-Models," *IHR Limited Distribution Report 295*, Iowa Institute of Hydraulic Research, The University of Iowa, Iowa City, IA.
- Franco, J.J., (1978). "Guidelines for the Design, Adjustment, and Operation of Models for the Study of River Sedimentation Problems," Instruction Report H-78-1, US Army Engineer Waterways Experiment Station, Vicksburg, Mississippi.
- Gaines, R.A., (2002). *Micro-Scale Moveable Bed Physical Sediment Models*, Doctoral Thesis, University of Missouri-Rolla, Rolla, MO.
- Gaines, R.A., (1999). "Micromodel Procedures," Report to UMR Graduate Committee, Unpublished.
- Gaines, R.A. and Maynard, S.T., (2001). "Microscale Loose-Bed Hydraulic Models," *Journal of Hydraulic Engineering*, Vol. 127, No.5, ASCE, New York.
- Gaines, R.A., Gordon, D., and Maynard, S.T., (in progress). "Micromodel Capabilities and Limitations," Technical Report to Mississippi Valley Division, US Army Corps of Engineers, Memphis, TN.
- García, M., (2000). "Discussion: The Legend of A.F. Shields," *Journal of Hydraulic Engineering*, ASCE, New York, pp 718-720.
- Haan, C. T., (1977). *Statistical Methods in Hydrology*, The Iowa State University Press, Ames, IA.
- Leopold, L.B., Wolman, M.G., and Miller, J.P. (1964). *Fluvial Processes in Geomorphology*, Freeman, San Francisco, CA 522 pp.
- Rosgen, D., (1996). *Applied River Morphology*, Wildland Hydrology, Colorado.
- Schuum, S.A. and Khan, H.R. (1972). "Experimental Study of Channel Patterns," *Geological Society of America Bulletin*, V. 83, pp1755-1770.
- Struiksmá, N., (1980). "Recent Developments in Design of River Scale Models with Mobile Bed," IAHR Symposium, Belgrad and Delft Hydraulics Laboratory, Publication No. 236.
- USBR, (1980). *Hydraulic Laboratory Techniques*, Water Resources Technical Publication, Denver, Colorado.
- Vining, G. Geoffrey, (1998). *Statistical Methods for Engineers*, Duxbury Press, New York.

APPENDIX A

IMPACT OF USING TRUNCATED CROSS SECTION DATA

LIST OF TABLES

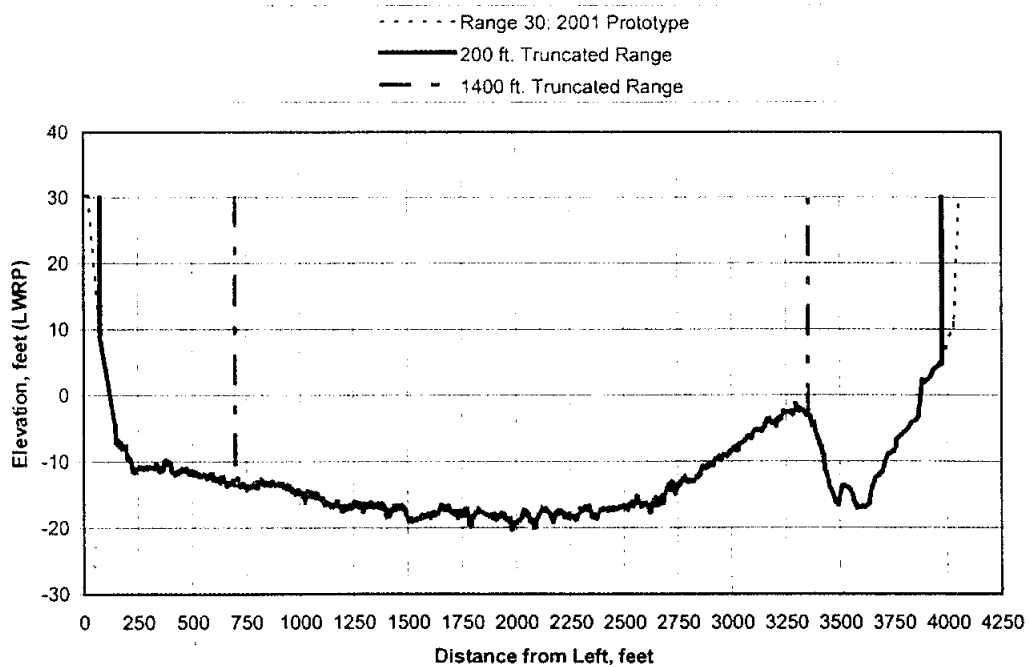
Table	Page
A-1a Effects of Truncation Range 30 Kate-Aubrey Reach	5
A-1b Effects of Truncation Range 30 Kate-Aubrey Reach (Continued).....	6
A-2a Effects of Truncation Range 30 Kate-Aubrey Reach	7
A-2b Effects of Truncation Range 30 Kate-Aubrey Reach (Continued).....	8
A-3a Effects of Truncation Range 50 Kate-Aubrey Reach	9
A-3b Effects of Truncation Range 50 Kate-Aubrey Reach (Continued).....	10

LIST OF FIGURES

Figure	Page
A-1 Example Truncation Range 30 Kate-Aubrey Reach	1
A-2 Location of Truncated Ranges, Kate-Aubrey Reach.....	3
A-3 Kate-Aubrey Channel Geometry Range 10.....	3
A-4 Kate-Aubrey Channel Geometry Range 30.....	4
A-5 Kate-Aubrey Channel Geometry Range 50.....	4
A-5 Truncation Effects on Area.....	12
A-6 Truncation Effects on Width	12
A-7 Truncation Effects on Wetted Perimeter	13
A-9 Truncation Effects on Hydraulic Depth.....	13
A-10 Truncation Effects on Hydraulic Radius	14

APPENDIX A: IMPACT OF USING TRUNCATED CROSS-SECTION DATA

Truncation of range data results when the survey does not extend across the entire channel width. The amount of truncation depends on the coverage obtained during survey efforts and may be different for model and prototype. A simplistic approach to evaluate truncation effects on the morphologic parameters uses range data for the entire section width as a baseline and then compares successively narrower portions of the channel to represent truncation of data. The method used in analyzing three ranges (Range 10, Range 30 and Range 50) of the Kate-Aubrey 2001 prototype survey reduces the channel cross-section data by eliminating data from a specified width from the full channel cross-section. The widths specified in the evaluation are 200, 400, 600, 800, 1000, 1200, and 1400 feet. Each of these widths is divided equally between the left and right banks. For example, the reduction of 200 feet in section width removes 100 feet of survey data from the left bank side of the channel and 100 feet of survey data from the right bank side of the channel. A-1 illustrates how the truncation applies to the cross-section for this analysis.

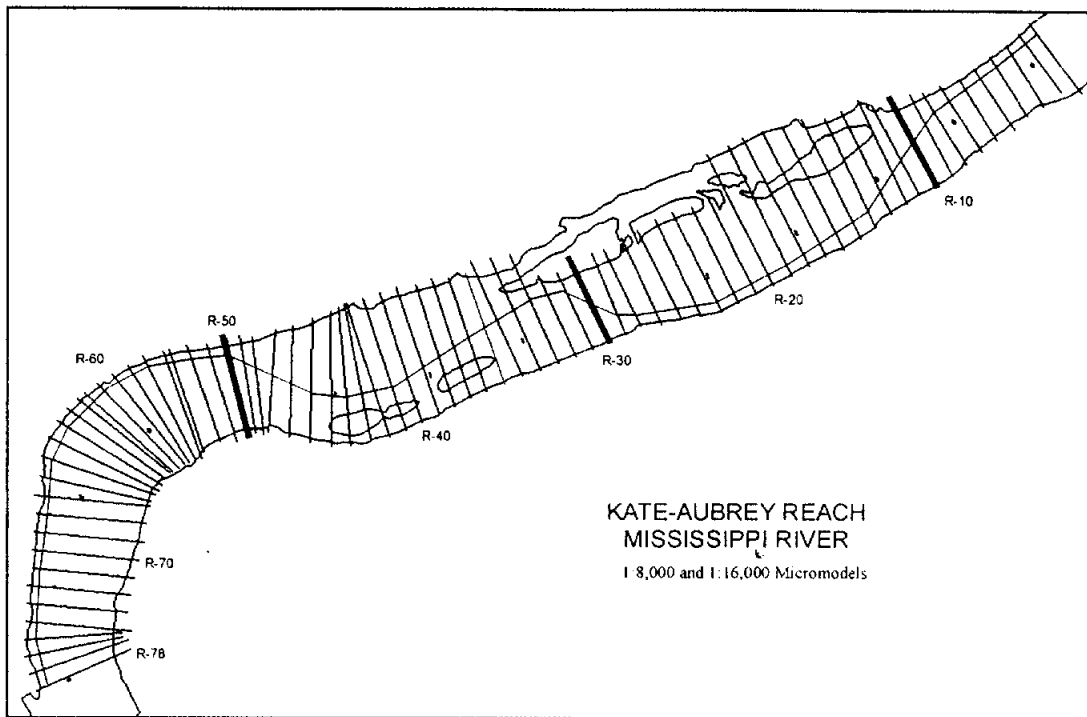


A-1 Example Truncation Range 30 Kate-Aubrey Reach

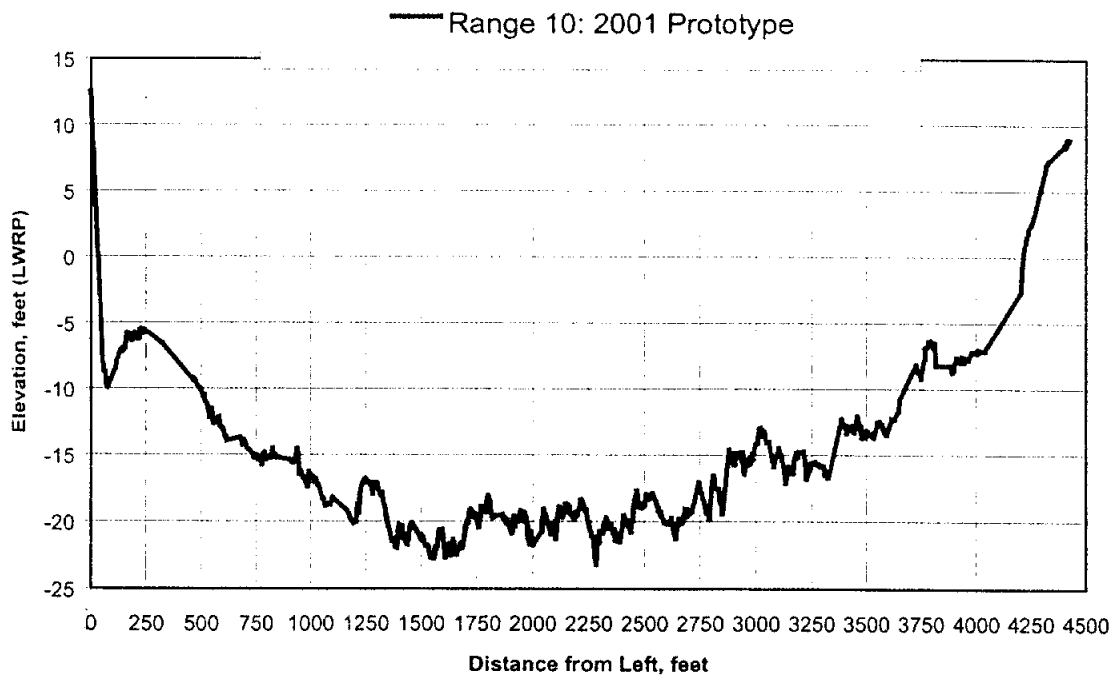
The simplified approach of equally dividing the truncated width between the left and right sides of the channel differs from reality because rarely would truncation be the same on both sides of the channel. For example, in bendway reaches little if any truncation occurs in the deep, outer part of the cross-section. However, a large amount of truncation typically occurs on the inner part of the bendway cross-section due to point-bar deposition. Truncation in channel crossings tends to mimic the simplified approach described herein because hydrographic surveys often omit areas of the channel adjacent to the bankline due to insufficient water depth. An inconsistent amount of truncation exists in the prototype data because limits imposed by hydrographic surveys produce a random degree of truncation (i.e. individual survey Ranges have differing amounts of truncation). Although the random truncation found in actual survey bathymetry is not reproduced by the simplified analysis utilized in this section, the effects of truncation are reproduced in a manner that helps quantify these effects. The following paragraphs describe the truncation effects on cross-section area. While the values shown are for a specific location and time, the relative magnitude of the results between the various truncation widths represent the overall effects of truncation.

The three ranges analyzed in the Kate-Aubrey reach represent typical cross-sections at two crossings and at one bendway. Range 10 is in a crossing. Range 30, also a crossing, is located within the problem area of this reach. Range 50 is in a bend with the deep channel along the right descending bank. Locations of the Ranges used for this analysis are shown in A-2. Figures A-3, A-4, and A-5 show cross-section geometry for Ranges 10, 30, and 50, respectively.

Calculated morphologic parameter values of area, top width, wetted perimeter, hydraulic radius, and hydraulic depth are shown in Table A-1 Table A-2 and Table A-3. Morphologic parameter values were calculated at four water surface elevations, -10 LWRP, 0 LWRP, +10 LWRP, and +20 LWRP. Data shown in these tables demonstrate the effects of truncation on the morphologic parameter values. Percent differences between the baseline condition (range with no truncation) and successively larger amounts of truncation help to quantify the truncation effects.



A-2 Location of Truncated Ranges, Kate-Aubrey Reach



A-3 Kate-Aubrey Channel Geometry Range 10

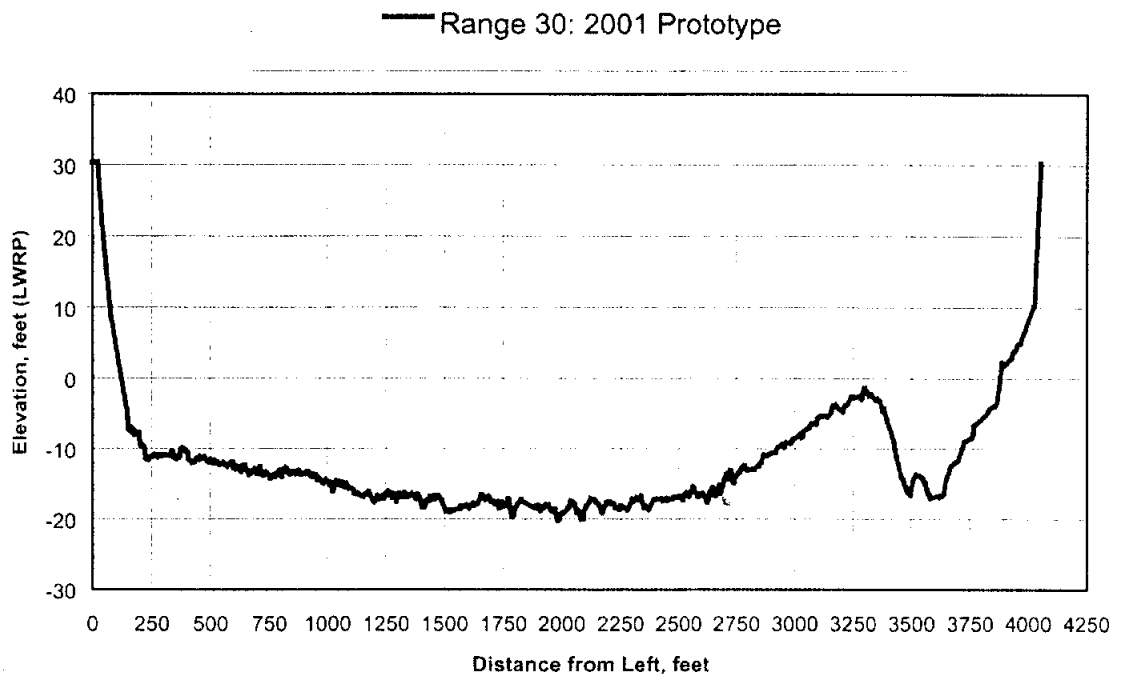


Figure A-4 Kate-Aubrey Channel Geometry Range 30

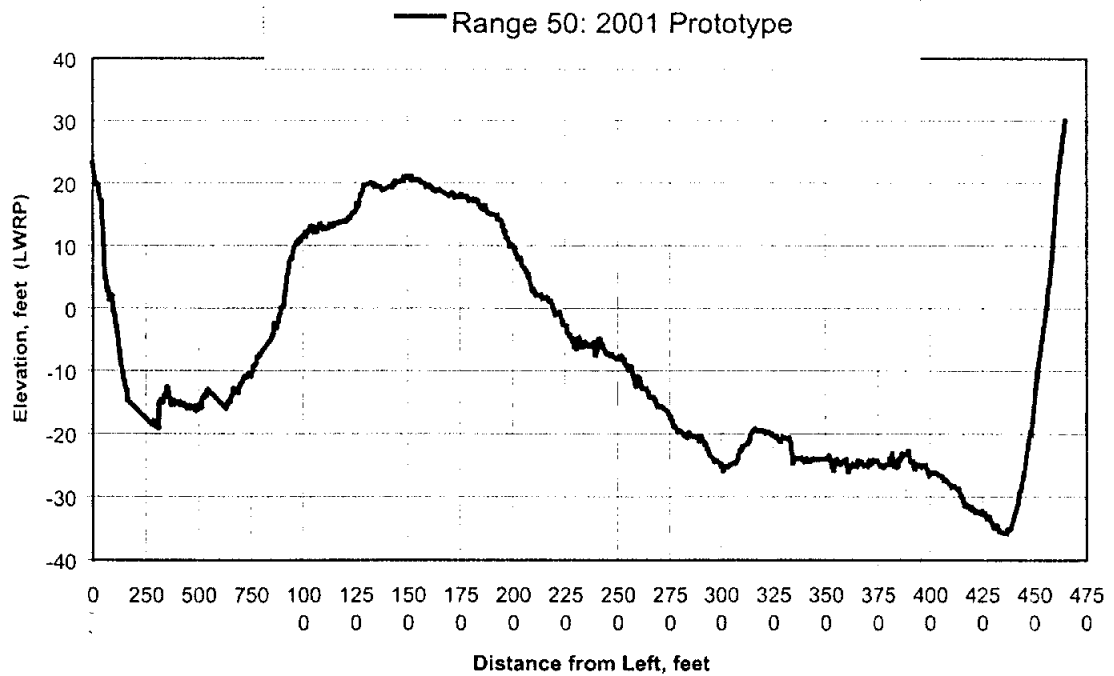


Figure A-5 Kate-Aubrey Channel Geometry Range 50

Table A-1a Effects of Truncation Range 30 Kate-Aubrey Reach

RANGE 10 - KATE AUBREY 2001 SURVEY									
NO TRUNCATION									
LWRP ELEV.	-10.0	0.0	10.0	20.0					
AREA	23702	62599	105055	149624					
WIDTH	3186	4195	4377	4423					
WETTED PERIMETER	3196	4206	4402	4456					
HYDRAULIC RADIUS	7.4	14.9	23.9	33.6					
HYDRAULIC DEPTH	7.4	14.9	24.0	33.8					
100' TRUNCATION ON EACH SIDE (LEFT & RIGHT) [TOTAL 200' TRUNCATED]					PERCENT DIFFERENCE FROM NO TRUNCATION				
LWRP ELEV.	-10.0	0.0	10.0	20.0	-10.0	0.0	10.0	20.0	
AREA	23702	62036	103879	146103	0.0	-0.9	-1.1	-2.4	
WIDTH	3186	4115	4222	4222	0.0	-1.9	-3.5	-4.5	
WETTED PERIMETER	3196	4135	4275	4315	0.0	-1.7	-2.9	-3.2	
HYDRAULIC RADIUS	7.4	15.0	24.3	33.9	0.0	0.8	1.8	0.8	
HYDRAULIC DEPTH	7.4	15.1	24.6	34.6	0.0	1.0	2.5	2.3	
200' TRUNCATION ON EACH SIDE (LEFT & RIGHT) [TOTAL 400' TRUNCATED]					PERCENT DIFFERENCE FROM NO TRUNCATION				
LWRP ELEV.	-10.0	0.0	10.0	20.0	-10.0	0.0	10.0	20.0	
AREA	23702	61304	101388	141472	0.0	-2.1	-3.5	-5.4	
WIDTH	3186	4008	4008	4008	0.0	-4.4	-8.4	-13.2	
WETTED PERIMETER	3196	4025	4065	4105	0.0	-4.3	-7.7	-7.9	
HYDRAULIC RADIUS	7.4	15.2	24.9	34.5	0.0	2.3	4.5	2.6	
HYDRAULIC DEPTH	7.4	15.3	25.3	35.3	0.0	2.5	5.4	4.3	
300' TRUNCATION ON EACH SIDE (LEFT & RIGHT) [TOTAL 600' TRUNCATED]					PERCENT DIFFERENCE FROM NO TRUNCATION				
LWRP ELEV.	-10.0	0.0	10.0	20.0	-10.0	0.0	10.0	20.0	
AREA	23702	60628	99496	138363	0.0	-3.1	-5.3	-7.5	
WIDTH	3186	3887	3887	3887	0.0	-7.3	-11.2	-12.1	
WETTED PERIMETER	3196	3906	3946	3986	0.0	-7.1	-10.4	-10.6	
HYDRAULIC RADIUS	7.4	15.5	25.2	34.7	0.0	4.3	5.6	3.4	
HYDRAULIC DEPTH	7.4	15.6	25.6	35.6	0.0	4.5	6.7	5.2	

Table A-1b Effects of Truncation Range 30 Kate-Aubrey Reach (Continued)

	400' TRUNCATION ON EACH SIDE (LEFT & RIGHT) [TOTAL 800' TRUNCATED]				PERCENT DIFFERENCE FROM NO TRUNCATION			
LWRP ELEV.	-10.0	0.0	10.0	20.0	-10.0	0.0	10.0	20.0
AREA	23702	58684	94447	130211	0.0	-6.3	-10.1	-13.0
WIDTH	3186	3576	3576	3576	0.0	-14.7	-18.3	-19.1
WETTED PERIMETER	3196	3603	3623	3643	0.0	-14.4	-17.7	-18.3
HYDRAULIC RADIUS	7.4	16.3	26.1	35.7	0.0	9.5	9.2	6.5
HYDRAULIC DEPTH	7.4	16.4	26.4	36.4	0.0	10.0	10.0	7.6
	500' TRUNCATION ON EACH SIDE (LEFT & RIGHT) [TOTAL 1000' TRUNCATED]				PERCENT DIFFERENCE FROM NO TRUNCATION			
LWRP ELEV.	-10.0	0.0	10.0	20.0	-10.0	0.0	10.0	20.0
AREA	23599	56765	90424	124083	-0.4	-9.3	-13.9	-17.1
WIDTH	3106	3366	3366	3366	-2.5	-19.8	-23.1	-23.9
WETTED PERIMETER	3118	3396	3436	3476	-2.4	-19.3	-21.9	-22.0
HYDRAULIC RADIUS	7.6	16.7	26.3	35.7	2.1	12.3	10.3	6.3
HYDRAULIC DEPTH	7.6	16.9	26.9	36.9	2.1	13.0	11.9	9.0
	600' TRUNCATION ON EACH SIDE (LEFT & RIGHT) [TOTAL 1200' TRUNCATED]				PERCENT DIFFERENCE FROM NO TRUNCATION			
LWRP ELEV.	-10.0	0.0	10.0	20.0	-10.0	0.0	10.0	20.0
AREA	23236	54385	85810	117235	-2.0	-13.1	-18.3	-21.6
WIDTH	2999	3142	3142	3142	-5.9	-25.1	-28.2	-28.9
WETTED PERIMETER	3012	3174	3214	3254	-5.7	-24.5	-27.0	-27.0
HYDRAULIC RADIUS	7.7	17.1	26.7	36.0	4.0	15.1	11.9	7.3
HYDRAULIC DEPTH	7.7	17.3	27.3	37.3	4.1	16.0	13.8	10.3
	700' TRUNCATION ON EACH SIDE (LEFT & RIGHT) [TOTAL 1400' TRUNCATED]				PERCENT DIFFERENCE FROM NO TRUNCATION			
LWRP ELEV.	-10.0	0.0	10.0	20.0	-10.0	0.0	10.0	20.0
AREA	22758	52215	81720	111225	-4.0	-16.6	-22.2	-25.7
WIDTH	2898	2950	2950	2950	-9.1	-29.7	-32.6	-33.3
WETTED PERIMETER	2913	2984	3024	3064	-8.9	-29.1	-31.3	-31.3
HYDRAULIC RADIUS	7.8	17.5	27.0	36.3	5.3	17.6	13.2	8.1
HYDRAULIC DEPTH	7.9	17.7	27.7	37.7	5.6	18.6	15.4	11.4

Table A-2a Effects of Truncation Range 30 Kate-Aubrey Reach

RANGE 30 - KATE AUBREY 2001 SURVEY								
	NO TRUNCATION							
LWRP ELEV.	-10.0	0.0	10.0	20.0				
AREA	16137	50463	88992	128710				
WIDTH	2984	3779	3959	3988				
WETTED PERIMETER	2991	3789	3971	4006				
HYDRAULIC RADIUS	5.4	13.3	22.4	32.1				
HYDRAULIC DEPTH	5.4	13.4	22.5	32.3				
100' TRUNCATION ON EACH SIDE (LEFT & RIGHT) [TOTAL 200' TRUNCATED]					PERCENT DIFFERENCE FROM NO TRUNCATION			
LWRP ELEV.	-10.0	0.0	10.0	20.0	-10.0	0.0	10.0	20.0
AREA	1613	50487	88408	127118	0.0	0.0	-0.7	-1.2
WIDTH	2984	3789	3832	3879	0.0	0.3	-3.2	-2.8
WETTED PERIMETER	2991	3799	3869	3942	0.0	0.3	-2.6	-1.6
HYDRAULIC RADIUS	5.4	13.3	22.8	32.2	0.0	-0.2	2.0	0.4
HYDRAULIC DEPTH	5.4	13.3	23.1	32.8	0.0	-0.2	2.6	1.6
200' TRUNCATION ON EACH SIDE (LEFT & RIGHT) [TOTAL 400' TRUNCATED]					PERCENT DIFFERENCE FROM NO TRUNCATION			
LWRP ELEV.	-10.0	0.0	10.0	20.0	-10.0	0.0	10.0	20.0
AREA	16137	49887	86432	123029	0.0	-1.1	-2.9	-4.4
WIDTH	2984	3658	3656	3659	0.0	-3.2	-7.7	-11.5
WETTED PERIMETER	2991	3677	3716	3756	0.0	-3.0	-6.4	-6.2
HYDRAULIC RADIUS	5.4	13.6	23.3	32.7	0.0	1.9	3.8	1.9
HYDRAULIC DEPTH	5.4	13.6	23.6	33.6	0.0	2.1	5.2	4.2
300' TRUNCATION ON EACH SIDE (LEFT & RIGHT) [TOTAL 600' TRUNCATED]					PERCENT DIFFERENCE FROM NO TRUNCATION			
LWRP ELEV.	-10.0	0.0	10.0	20.0	-10.0	0.0	10.0	20.0
AREA	16054	48279	82851	117544	-0.5	-4.3	-6.9	-8.7
WIDTH	2906	3460	3461	3469	-2.6	-8.4	-12.6	-13.0
WETTED PERIMETER	2913	3489	3521	3562	-2.6	-8.1	-11.3	-11.1
HYDRAULIC RADIUS	5.5	13.9	23.5	33.0	2.1	4.1	5.0	2.7
HYDRAULIC DEPTH	5.5	14.0	23.9	33.9	2.1	4.5	6.5	5.0

Table A-2b Effects of Truncation Range 30 Kate-Aubrey Reach (Continued)

	400' TRUNCATION ON EACH SIDE (LEFT & RIGHT) [TOTAL 800' TRUNCATED]				PERCENT DIFFERENCE FROM NO TRUNCATION			
LWRP ELEV.	-10.0	0.0	10.0	20.0	-10.0	0.0	10.0	20.0
AREA	15847	46086	78650	11136	-1.8	-8.7	-11.6	-13.5
WIDTH	2749	3258.7	3262	3273	-7.9	-13.8	-17.6	-18.0
WETTED PERIMETER	2758	3281	3322	3364	-7.8	-13.4	-16.3	-16.0
HYDRAULIC RADIUS	5.7	14.0	23.7	33.1	6.5	5.4	5.6	3.0
HYDRAULIC DEPTH	5.8	14.1	24.1	34.0	6.6	5.9	7.3	5.5
	500' TRUNCATION ON EACH SIDE (LEFT & RIGHT) [TOTAL 1000' TRUNCATED]				PERCENT DIFFERENCE FROM NO TRUNCATION			
LWRP ELEV.	-10.0	0.0	10.0	20.0	-10.0	0.0	10.0	20.0
AREA	15111	43353	73872	104468	-6.4	-14.1	-17.0	-18.8
WIDTH	2551	3056	3054.0	3058	-14.5	-19.1	-22.9	-23.3
WETTED PERIMETER	2562	3086	3126	3166	-14.3	-18.5	-21.3	-21.0
HYDRAULIC RADIUS	5.9	14.0	23.6	33.0	9.3	5.5	5.4	2.7
HYDRAULIC DEPTH	5.9	14.2	24.2	34.2	9.5	6.2	7.6	5.9
	600' TRUNCATION ON EACH SIDE (LEFT & RIGHT) [TOTAL 1200' TRUNCATED]				PERCENT DIFFERENCE FROM NO TRUNCATION			
LWRP ELEV.	-10.0	0.0	10.0	20.0	-10.0	0.0	10.0	20.0
AREA	14433	40690	69236	97804	-10.6	-19.4	-22.2	-24.0
WIDTH	2350	2856	2855	2856	-21.3	-24.4	-27.9	-28.4
WETTED PERIMETER	2361	2887	2927	2967	-21.1	-23.8	-26.3	-25.9
HYDRAULIC RADIUS	6.1	14.1	23.7	33.0	13.3	5.8	5.5	2.6
HYDRAULIC DEPTH	6.1	14.2	24.2	34.2	13.6	6.7	7.9	6.1
	700' TRUNCATION ON EACH SIDE (LEFT & RIGHT) [TOTAL 1400' TRUNCATED]				PERCENT DIFFERENCE FROM NO TRUNCATION			
LWRP ELEV.	-10.0	0.0	10.0	20.0	-10.0	0.0	10.0	20.0
AREA	14071	38550	64953	91504	-12.8	-23.6	-27.0	-28.9
WIDTH	2222	2643	2645	2654	-25.5	-30.0	-33.2	-33.4
WETTED PERIMETER	2228	2661	2701	2742	-25.5	-29.8	-32.0	-31.5
HYDRAULIC RADIUS	6.3	14.5	24.1	33.4	17.1	8.8	7.3	3.9
HYDRAULIC DEPTH	6.3	14.6	24.6	34.5	17.1	9.2	9.3	6.8

Table A-3a Effects of Truncation Range 50 Kate-Aubrey Reach

RANGE 50 - KATE AUBREY 2001 SURVEY									
NO TRUNCATION									
LWRP ELEV.	-10.0	0.0	10.0	20.0					
AREA	30082	59092	92632	131435					
WIDTH	2578	3175	3520	4446					
WETTED PERIMETER	2589	3190	3541	4473					
HYDRAULIC RADIUS	11.6	18.5	26.2	29.4					
HYDRAULIC DEPTH	11.7	18.6	26.3	29.6					
100' TRUNCATION ON EACH SIDE (LEFT & RIGHT) [TOTAL 200' TRUNCATED]					PERCENT DIFFERENCE FROM NO TRUNCATION				
LWRP ELEV.	-10.0	0.0	10.0	20.0	-10.0	0.0	10.0	20.0	
AREA	30082	59088	92099	129899	0.0	0.0	-0.6	-1.2	
WIDTH	2578	3162	3438	4306	0.0	-0.4	-2.4	-3.1	
WETTED PERIMETER	2589	3178	3455	4325	0.0	-0.4	-2.4	-3.3	
HYDRAULIC RADIUS	11.6	18.6	26.7	30.0	0.0	0.4	1.9	2.2	
HYDRAULIC DEPTH	11.7	18.7	26.8	30.2	0.0	0.4	1.8	2.0	
200' TRUNCATION ON EACH SIDE (LEFT & RIGHT) [TOTAL 400' TRUNCATED]					PERCENT DIFFERENCE FROM NO TRUNCATION				
LWRP ELEV.	-10.0	0.0	10.0	20.0	-10.0	0.0	10.0	20.0	
AREA	28684	55251	85459	120456	-4.6	-6.5	-7.7	-8.4	
WIDTH	2369	2881	3157	4026	-8.1	-9.2	-10.3	-12.9	
WETTED PERIMETER	2401	2936	3213	4083	-7.2	-8.0	-9.3	-8.7	
HYDRAULIC RADIUS	11.9	18.8	26.6	29.5	2.8	1.6	1.7	0.4	
HYDRAULIC DEPTH	12.1	19.2	27.1	29.9	3.8	3.0	2.9	1.2	
300' TRUNCATION ON EACH SIDE (LEFT & RIGHT) [TOTAL 600' TRUNCATED]					PERCENT DIFFERENCE FROM NO TRUNCATION				
LWRP ELEV.	-10.0	0.0	10.0	20.0	-10.0	0.0	10.0	20.0	
AREA	26063	51300	80179	113847	-13.4	-13.2	-13.4	-13.4	
WIDTH	2236	2749	3024	3893	-13.3	-13.4	-14.1	-12.4	
WETTED PERIMETER	2277	2812	3089	3959	-12.0	-11.9	-12.8	-11.5	
HYDRAULIC RADIUS	11.4	18.2	26.0	28.8	-1.5	-1.5	-0.8	-2.1	
HYDRAULIC DEPTH	11.7	18.7	26.5	29.2	-0.1	0.3	0.8	-1.1	

Table A-3b Effects of Truncation Range 50 Kate-Aubrey Reach (Continued)

400' TRUNCATION ON EACH SIDE (LEFT & RIGHT) [TOTAL 800' TRUNCATED]					PERCENT DIFFERENCE FROM NO TRUNCATION			
LWRP ELEV.	-10.0	0.0	10.0	20.0	-10.0	0.0	10.0	20.0
AREA	23186	46403	73261	104909	-22.9	-21.5	-20.9	-20.2
WIDTH	2034	2547	2822	3691	-21.1	-19.8	-19.8	-17.0
WETTED PERIMETER	2066	2601	2878	3748	-20.2	-18.5	-18.7	-16.2
HYDRAULIC RADIUS	11.2	17.8	25.5	28.0	-3.4	-3.7	-2.7	-4.7
HYDRAULIC DEPTH	11.4	18.2	26.0	28.4	-2.3	-2.1	-1.3	-3.9
500' TRUNCATION ON EACH SIDE (LEFT & RIGHT) [TOTAL 1000' TRUNCATED]					PERCENT DIFFERENCE FROM NO TRUNCATION			
LWRP ELEV.	-10.0	0.0	10.0	20.0	-10.0	0.0	10.0	20.0
AREA	20468	41688	66550	96201	-32.0	-29.5	-28.2	-26.8
WIDTH	1834	2346	2623	3491	-28.9	-26.1	-25.5	-21.5
WETTED PERIMETER	1864	2399	2676	3546	-28.0	-24.8	-24.4	-20.7
HYDRAULIC RADIUS	11.0	17.4	24.9	27.1	-5.5	-6.2	-4.9	-7.7
HYDRAULIC DEPTH	11.2	17.8	25.4	27.6	-4.4	-4.6	-3.6	-6.8
600' TRUNCATION ON EACH SIDE (LEFT & RIGHT) [TOTAL 1200' TRUNCATED]					PERCENT DIFFERENCE FROM NO TRUNCATION			
LWRP ELEV.	-10.0	0.0	10.0	20.0	-10.0	0.0	10.0	20.0
AREA	18050	36992	59576	86948	-40.0	-37.4	-35.7	-33.8
WIDTH	1607	2119	2395	3263	-37.7	-33.3	-32.0	-26.6
WETTED PERIMETER	1633	2168	2445	3315	-36.9	-32.0	-31.0	-25.9
HYDRAULIC RADIUS	11.1	17.1	24.4	26.2	-4.9	-7.9	-6.9	-10.7
HYDRAULIC DEPTH	11.2	17.5	24.9	26.6	-3.7	-6.2	-5.5	-9.9
700' TRUNCATION ON EACH SIDE (LEFT & RIGHT) [TOTAL 1400' TRUNCATED]					PERCENT DIFFERENCE FROM NO TRUNCATION			
LWRP ELEV.	-10.0	0.0	10.0	20.0	-10.0	0.0	10.0	20.0
AREA	16275	33553	54472	80180	-45.9	-43.2	-41.2	-39.0
WIDTH	1440	1953	2228	3097	-44.1	-38.5	-36.7	-30.3
WETTED PERIMETER	1461	1995	2273	3143	-43.6	-37.4	-35.8	-29.7
HYDRAULIC RADIUS	11.1	16.8	24.0	25.5	-4.1	-9.2	-8.4	-13.2
HYDRAULIC DEPTH	11.3	17.2	24.4	25.9	-3.1	-7.7	-7.1	-12.4

The effects of truncation have a direct influence on the interpretation of morphologic similarity particularly if two surveys have different amounts of truncation. The percent differences shown for the example Range calculations show that area (A), width (W), and wetted perimeter (P) are decreased with increasing truncation. Hydraulic depth (H) and hydraulic radius (R_h) can be increased or decreased with truncation because these variables are ratios of A and W or A and P. The magnitude, positive or negative, for H or R_h differences, therefore, depends on the relative difference in A and P or A and R_h . For example, if truncation decreases A by a larger percentage than P, then the ratio of A/P increases. Calculated differences for higher water surface elevations compound the truncation effects. Truncation effects are shown in Figure 2-13 for area, Figure 2-14 for width, Figure 2-15 for wetted perimeter, Figure 2-16 for hydraulic depth, and Figure 2-17 for hydraulic radius.

Truncated data in the prototype results when hydrographic survey data do not cover the entire channel width. Historical data sets cannot be extended. A variety of reasons may limit prototype hydrographic survey coverage. Possible reasons for limited hydrographic survey data are:

1. Shallow water (restricted boat access)
2. Obstructions such as barges
3. Low water surveys
4. Funding

Generally, model data collected using the laser scanner covers the entire model channel. Therefore, truncation effects are minimal when comparing multiple model surveys (secondary channels may not be surveyed if not part of the model study). Because model calibration considers depositional features across the width of the channel (i.e. sand deposits within dike fields), prototype data should adequately define these features. Calibration of models using a maximum stage of +20 LWRP requires that prototype depositional features be defined to at least +20 LWRP. Future surveys obtained for modeling purposes should cover the full channel width where feasible. Model calibration efforts should include at least one full width channel survey.

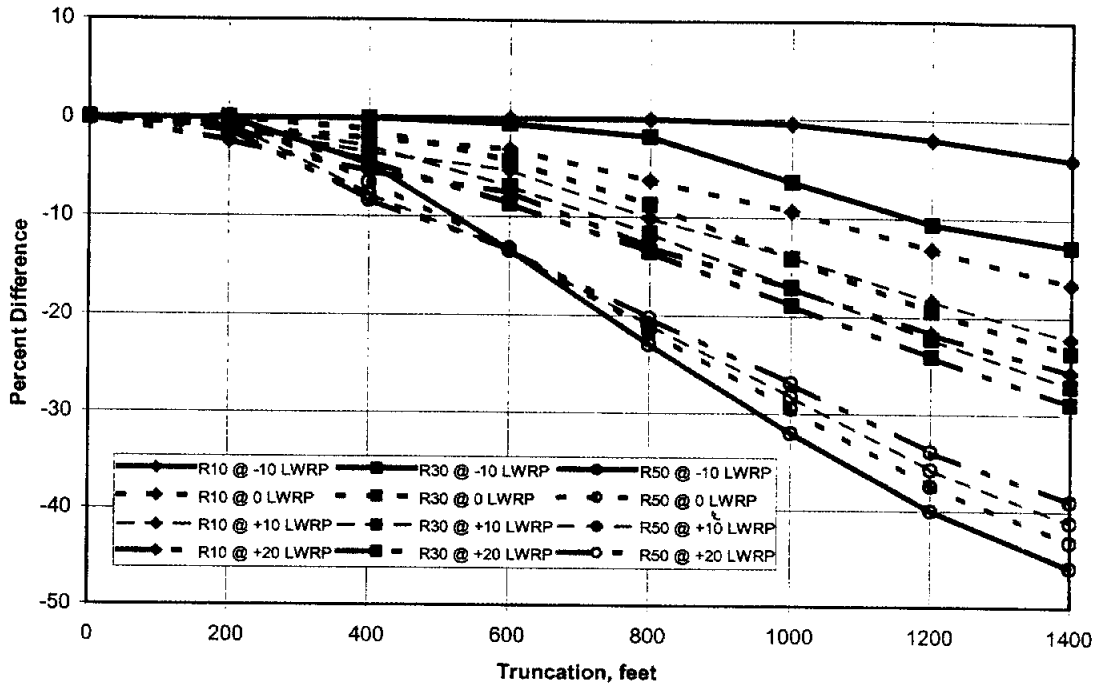


Figure A-5 Truncation Effects on Area

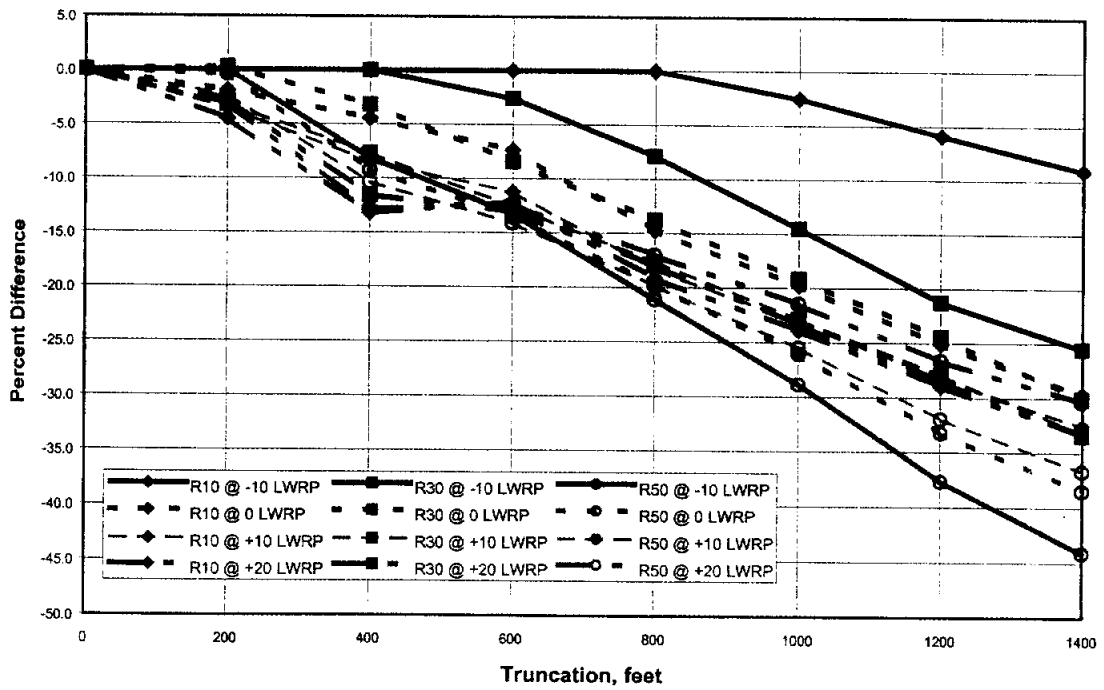


Figure A-6 Truncation Effects on Width

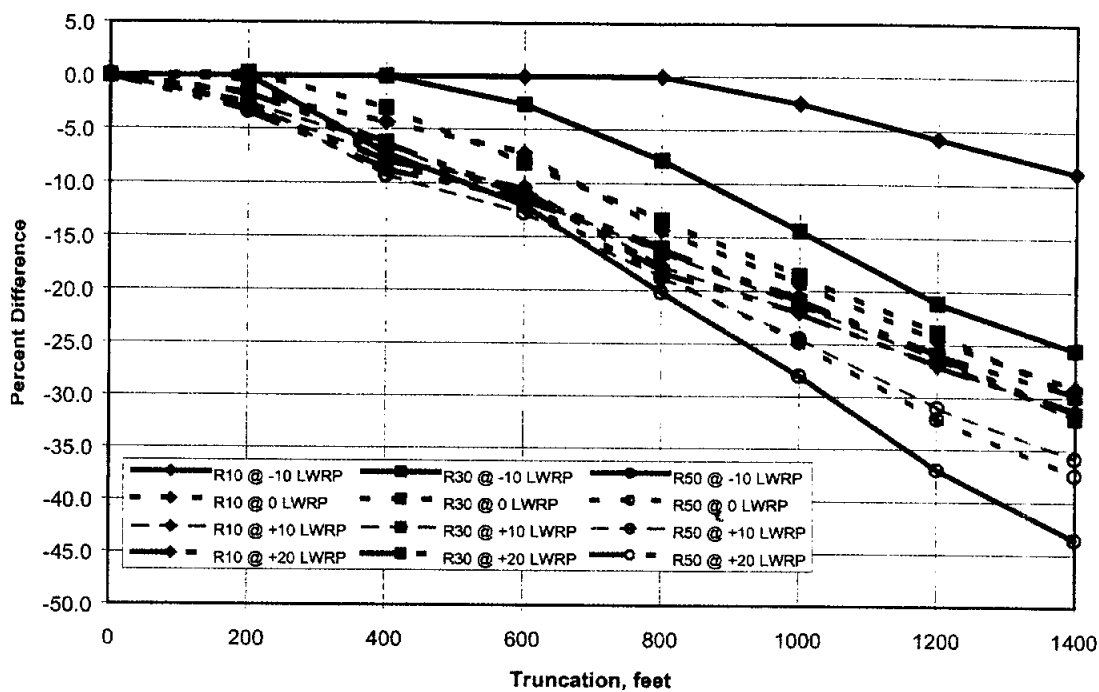


Figure A-7 Truncation Effects on Wetted Perimeter

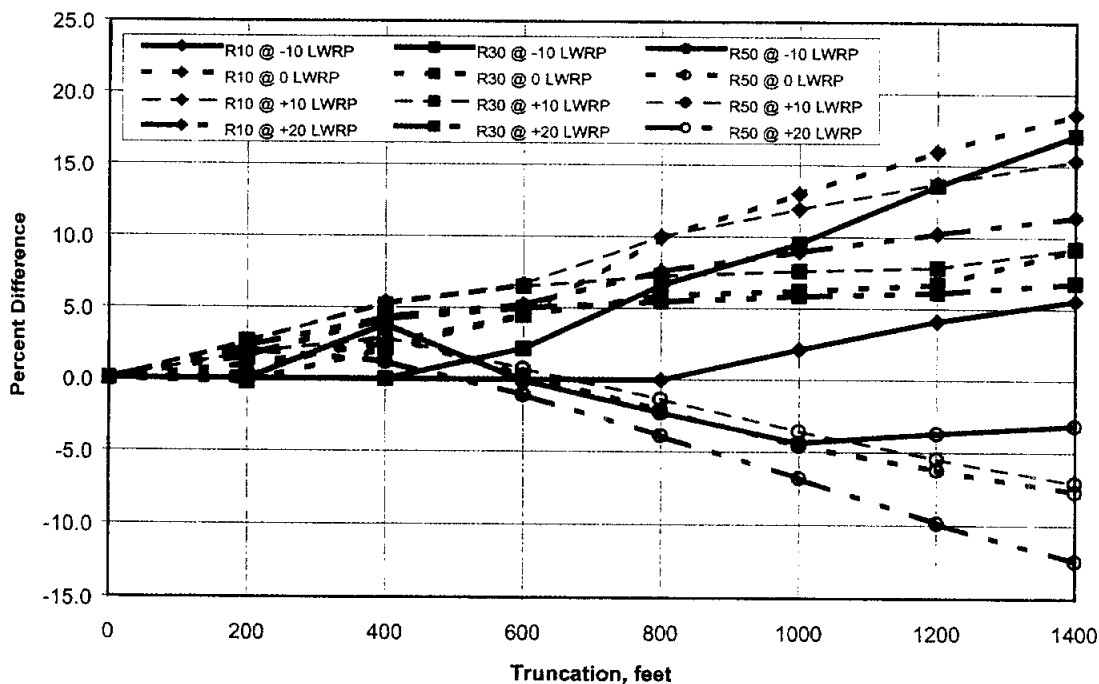


Figure A-9 Truncation Effects on Hydraulic Depth

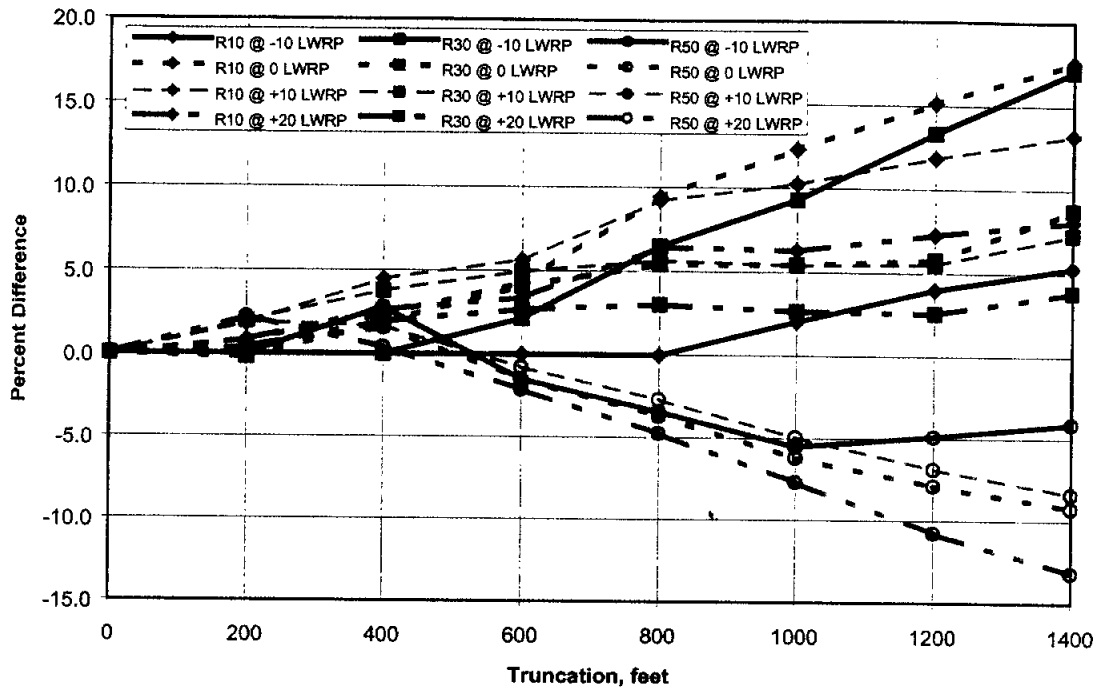


Figure A-10 Truncation Effects on Hydraulic Radius

Inadequate prototype survey data is a limitation in applying the micromodel methodology. Although this limitation may not preclude the use of a micromodel (where sources of survey data are sparse), the best micromodel results can be achieved when the prototype is well defined.

Comparisons of previous model study results utilized available information for the prototype surveys. Prototype bathymetric data for a particular model reach had no specific coverage and some models had surveys covering only the low water channel. Limited prototype channel coverage, particularly in some micromodel study reaches, introduced the potential for random truncation effects. Random truncation effects occur when individual Ranges have varying degrees of truncation (i.e. each Range has more or less truncation than adjacent Ranges).

Several previous model study results were omitted from the comparison analysis (Gaines, 2000) in order to eliminate bias introduced by truncation and more specifically effects from random truncation. The micromodels included in the scale ratio analysis were determined to have no truncation effects up to an elevation of zero LWRP.

Truncation effects above elevation zero LWRP were considered to be none or minimal because the fourteen micromodels had prototype data extending to (or very near to) the bankline. Any vertical extension of the cross-section at the bankline would therefore involve no truncation.

APPENDIX B

PREVIOUS LARGE-SCALE LOOSE-BED MODEL STUDIES



Appendix B: Previous Large-Scale Model Investigations

Name (River)	Prototype Data Used in Model Verification	Horizontal Scale ^a	Distortion (Horiz:Vert.)
Baleshed-Ajax Bar (Mississippi)	1967, 1968	600:1	10:1
Blountstown (Apalachicola)	1977, 1978	120:1	1.5:1
Buck Island (Mississippi)	1976, 1977, 1978, 1979	300:1	3:1
Chipola Cutoff (Apalachicola)	1978, 1979	120:1	1.5:1
Devil's Island (Mississippi)	1973	400:1	4:1
Dogtooth Bend, (Mississippi)	1977, 1983	400:1	4:1
Kate Aubrey (Mississippi)	1975, 1976	300:1	3:1
Lake Dardanelle (Arkansas)	1971, 1973	120:1	1.5:1
Lock & Dam #2 (Red River)	1978, 1981	120:1	1.5:1
Lock and Dam #4 (Red River)	1978, 1981	120:1	1.5:1
Loosahatchie-Memphis (MS)	Jan 1986, Nov 1986	300:1	3:1
New Madrid Bar (Mississippi)	1976, 1977	480:1	8:1
Redeye Crossing (Mississippi)	1982, 1983	240:1	1.2:1
Smithland Locks & Dam (Ohio)	1983	150:1	1:1
West Access (Atchafalaya)	1989	120:1	1.5:1
Willamette River	1977, 1980	100:1	2:1
^a Scale is prototype/model ratio.			

TABLE OF CONTENTS

Model	Page
1.1. Baleshed-Ajax Bar Reach, Mississippi River	1
1.2. Blountstown Reach, Apalachicola River	1
1.3. Buck Island Reach, Mississippi River	2
1.4. Chipola Cutoff Reach, Apalachicola River	3
1.5. Devil's Island Reach, Mississippi River	3
1.6. Dogtooth Bend Reach, Mississippi River	4
1.7. Kate Aubrey Reach, Mississippi River	5
1.8. Lake Dardanelle, Arkansas River	5
1.9. Lock and Dam #2, Red River	6
1.10. Lock and Dam #4, Red River	7
1.11. Loosahatchie-Memphis Reach, Mississippi River	8
1.12. New Madrid Bar Reach, Mississippi River	8
1.13. Redeye Crossing Reach, Lower Mississippi River	9
1.14. Smithland Locks and Dam, Ohio River	10
1.15. West Access Channel, Atchafalaya River	11
1.16. Bass Location, Willamette River	12

TABLE OF CONTENTS

LIST OF FIGURES

Figure	Page
B-1.1a Baleshed-Ajax Bar Model Plan View	13
B-1.1b Baleshed-Ajax Bar April 1967 Prototype Survey.....	14
B-1.1c Baleshed-Ajax Bar October 1968 Prototype Survey.....	15
B-1.1d Baleshed-Ajax Verification Test Survey	16
B-1.2a Thalweg Position From Left, Baleshed-Ajax.....	17
B-1.2b Cross-Section Area by Range, Baleshed-Ajax	18
B-1.2c Top Width by Range, Baleshed-Ajax	19
B-1.2d Hydraulic Depth by Range, Baleshed Ajax	20
B-1.2e Width/Depth Ratio by Range, Baleshed-Ajax	21
B-2.1a Blountstown Model Plan View	22
B-2.1b Blountstown June 1977 Prototype Survey	23
B-2.1c Blountstown June 1978 Prototype Survey	24
B-2.1d Blountstown Verification Test Survey.....	25
B-2.2a Thalweg Position From Left by Range, Blountstown Reach.....	26
B-2.2b Cross-Section Area by Range, Blountstown Reach.....	27
B-2.2c Top Width by Range, Blountstown Reach.....	28
B-2.2d Hydraulic Depth by Range, Blountstown Reach	29
B-2.2e Width/Depth Ratio by Range, Blountstown Reach.....	30
B-3.1a Buck Island Model Plan View	31
B-3.1b Buck Island June 1976 Prototype Survey	32
B-3.1c Buck Island May 1977 Prototype Survey	33
B-3.1d Buck Island May 1978 Prototype Survey	34
B-3.1e Buck Island February 1979 Prototype Survey	35
B-3.1f Buck Island Verification Test Survey.....	36
B-3.2a Thalweg Position From Left by Range, Buck Island	37
B-3.2b Cross-Section Area by Range, Buck Island	38
B-3.2c Top Width by Range, Buck Island.....	39
B-3.2d Hydraulic Depth by Range, Buck Island	40
B-3.2e Width/Depth Ratio by Range, Buck Island.....	41

LIST OF FIGURES

B-4.1a Chipola-Cutoff Model Plan View	42
B-4.1b Chipola-Cutoff January 1978 Prototype Survey.....	43
B-4.1c Chipola-Cutoff June 1979 Prototype Survey	44
B-4.1d Chipola-Cutoff Verification Test Survey.....	45
B-4.2a Thalweg Position From Left by Range, Chipola Cutoff.....	46
B-4.2b Cross-Section Area by Range, Chipola Cutoff.....	47
B-4.2c Top Width by Range, Chipola Cutoff.....	48
B-4.2d Hydraulic Depth by Range, Chipola Cutoff	49
B-4.2e Width/Depth Ratio by Range, Chipola Cutoff.....	50
B-5.1a Devil's Island Model Plan View	51
B-5.1b Devil's Island November 1969 Prototype Survey	52
B-5.1c Devil's Island Verification Test Survey.....	53
B-5.2a Thalweg Position From Left by Range, Devil's Island.....	54
B-5.2b Cross-Section Area by Range, Devil's Island.....	55
B-5.2c Top Width by Range, Devil's Island.....	56
B-5.2d Hydraulic Depth by Range, Devil's Island	57
B-5.2e Width/Depth Ratio by Range, Devil's Island	58
B-6.1a Dogtooth Bend Model Plan View	59
B-6.1b Dogtooth Bend March 1977 Prototype Survey.....	60
B-6.1c Dogtooth Bend April 1983 Prototype Survey	61
B-6.1d Dogtooth Bend Verification Test Survey	62
B-6.1e Dogtooth Bend Verification Test Survey (with 1983 flood hydrograph).....	63
B-6.2a Thalweg Position From Left by Range, Dogtooth	64
B-6.2b Cross-Section Area by Range, Dogtooth.....	65
B-6.2c Top Width Area by Range, Dogtooth	66
B-6.2d Hydraulic Depth by Range, Dogtooth	67
B-6.2e Width/Depth Ratio by Range, Dogtooth.....	68
B-7.1a Kate Aubrey Model Plan View	69
B-7.1b Kate Aubrey May 1975 Prototype Survey.....	70
B-7.1c Kate Aubrey May 1976 Prototype Survey.....	70

LIST OF FIGURES

B-7.1d Kate Aubrey Verification Test Survey.....	71
B-7.2a Thalweg Position From Left by Range, Kate Aubrey.....	72
B-7.2b Cross-Section Area by Range, Kate Aubrey.....	73
B-7.2c Top Width by Range, Kate Aubrey.....	74
B-7.2d Hydraulic Depth by Range, Kate Aubrey.....	75
B-7.2e Width/Depth Ratio by Range, Kate Aubrey.....	76
B-8.1a Lake Dardanelle Model Plan View.....	77
B-8.1b Lake Dardanelle November 1971 Prototype Survey.....	78
B-8.1c Lake Dardanelle October 1973 Prototype Survey.....	79
B-8.1d Lake Dardanelle Verification Test Survey.....	80
B-8.2a Thalweg Position From Left by Range, Lake Dardanelle.....	81
B-8.2b Cross-Section Area by Range, Lake Dardanelle.....	82
B-8.2c Top Width by Range, Lake Dardanelle.....	83
B-8.2d Hydraulic Depth by Range, Lake Dardanelle.....	84
B-8.2e Width/Depth Ratio by Range, Lake Dardanelle.....	85
B-9.1a Lock and Dam No. 2, Red River Model Plan View.....	86
B-9.1b L &D No. 2 1968 Prototype Survey.....	87
B-9.1c L &D No. 2 Verification Test Survey.....	88
B-9.2a Thalweg Location From Left by Range, Lock and Dam 2.....	89
B-9.2b Cross-Section Area by Range, Lock and Dam 2.....	90
B-9.2c Top Width by Range, Lock and Dam 2.....	91
B-9.2d Hydraulic Depth by Range, Lock and Dam 2.....	92
B-9.2e Width/Depth Ratio by Range, Lock and Dam 2.....	93
B-10.1a Lock and Dam No. 4 Model Plan View.....	94
B-10.1b L &D No. 4 1978 Prototype Survey.....	95
B-10.1c L &D No. 4 1981 Prototype Survey.....	96
B-10.1d L &D No. 4 Verification Test Survey.....	97
B-10.2a Thalweg Location From Left by Range, Lock and Dam 4.....	98
B-10.2b Cross-Section Area by Range, Lock and Dam 4.....	99
B-10.2c Top Width by Range, Lock and Dam 4.....	100

LIST OF FIGURES

B-10.2d Hydraulic Depth by Range, Lock and Dam 4	101
B-10.2e Width/Depth Ratio by Range, Lock and Dam 4	102
B-11.1a Loosahatchie-Memphis Model Plan View	103
B-11.1b January 1986 Prototype Survey, Loosahatchie-Memphis	104
B-11.1c November 1986 Prototype Survey, Loosahatchie-Memphis	105
B-11.1d April 1990 Prototype Survey, Loosahatchie-Memphis	106
B-11.1e Verification Survey, Loosahatchie-Memphis	107
B-11.2a Thalweg Location From Left by Range, Loosahatchie Memphis.....	108
B-11.2b Cross-Section Area by Range, Loosahatchie Memphis.....	109
B-11.2c Top Width by Range, Loosahatchie Memphis.....	110
B-11.2d Hydraulic Depth by Range, Loosahatchie Memphis	111
B-11.2e Width/Depth Ratio by Range, Loosahatchie Memphis.....	112
B-12.1a New Madrid Model Plan View	113
B-12.1b New Madrid May 1976 Prototype Survey	114
B-12.1c New Madrid May 1977 Prototype Survey	115
B-12.1d New Madrid April 1978 Prototype Survey	116
B-12.1e New Madrid Verification Test Survey	117
B-12.2a Thalweg Position From Left by Range, New Madrid.....	118
B-12.2b Cross-Section Area by Range, New Madrid.....	119
B-12.2c Top Width by Range, New Madrid.....	120
B-12.2d Hydraulic Depth by Range, New Madrid	121
B-12.2e Width/Depth Ratio by Range, New Madrid.....	122
B-13.1a Redeye Crossing Model Plan View	123
B-13.1b 1982 Prototype Survey, Redeye Crossing	124
B-13.1c 1983 Prototype Survey, Redeye Crossing.....	125
B-13.2a Thalweg Location From Left by Range, Redeye Crossing.....	127
B-13.2b Cross-Section Area by Range, Redeye Crossing.....	128
B-13.2c Top Width by Range, Redeye Crossing.....	129
B-13.2d Hydraulic Depth by Range, Redeye Crossing	130
B-13.2e Width/Depth Ratio by Range, Redeye Crossing.....	131

LIST OF FIGURES

B-14.1a Smithland Lock Model Plan View.....	132
B-14.1b Smithland Lock October 1966 Prototype Survey.....	133
B-14.1c Smithland Lock Verification Test Survey.....	134
B-14.2a Thalweg Location From Left by Range, Smithland Lock and Dam.....	135
B-14.2b Cross-Section Area by Range, Smithland Lock and Dam.....	136
B-14.2c Top Width by Range, Smithland Lock and Dam.....	137
B-14.2d Hydraulic Depth by Range, Smithland Lock and Dam.....	138
B-14.2e Width/Depth Ratio by Range, Smithland Lock and Dam.....	139
B-15.1a West Access Channel Model Plan View.....	140
B-15.1b West Access Channel 1975 Prototype Survey.....	141
B-15.1c West Access Channel Verification Test Survey.....	142
B-15.2a Thalweg Location From Left by Range, West Access.....	143
B-15.2b Cross-Section Area by Range, West Access Channel.....	144
B-15.2c Top Width by Range, West Access Channel.....	145
B-15.2d Hydraulic Depth by Range, West Access Channel.....	146
B-15.2e Width/Depth Ratio by Range, West Access Channel.....	147
B-16.1a Willamette River Model Plan View.....	148
B-16.1b 1977 Willamette River Prototype Survey.....	149
B-16.1c 1980 Willamette River Prototype Survey.....	150
B-16.1d Willamette River Verification Test Survey.....	151
B-16.2a Thalweg Location From Left by Range, Willamette River.....	152
B-16.2b Cross-Section Area by Range, Willamette River.....	153
B-16.2c Top Width by Range, Willamette River.....	154
B-16.2d Hydraulic Depth by Range, Willamette River.....	155
B-16.2e Width/Depth Ratio by Range, Willamette River.....	156

Waterways Experiment Station Individual Study Results

1.1. Baleshed-Ajax Bar Reach, Mississippi River

Location: Baleshed-Ajax Bar reach is located about 485 river miles about Head of Passes (AHP) on the Mississippi River.

Purpose of Study: The purpose of the Baleshed-Ajax Bar reach study was to determine the effectiveness of a proposed dike system and the effectiveness of alternate systems using vane dikes and combination of vane and spur dikes of troublesome reaches on the Mississippi River.

Problem Area:

Data: Data used in this study was as follows: (1) Prototype survey April 1967 (2) Prototype survey October 1968 and, (3) Verification Test survey.

Scale: The movable-bed model used for this study reproduced to a horizontal scale of 1:600 and a vertical scale of 1:60 reproducing approximately 18 miles of the Mississippi River between river miles 478.6 and 496.4

Thalweg Index: Thalweg index was calculated using an Index width of 2500 feet. The index width defined the active channel width for this reach.

Type of Model: Sand bed.

Reference: J. J. Franco, J. E. Glover, and T. J. Pokrefke. (1970). "Investigation of Proposed Dike Systems on the Mississippi River, Report 1, Baleshed-Ajax Bar Reach, Hydraulic Model Investigation," Miscellaneous Paper H-70-1, U. S. Army Engineer Waterways Experiment Station, Vicksburg, MS. 39180.

1.2. Blountstown Reach, Apalachicola River

Location: The location of Blountstown Reach is between navigation miles 81 and 76 on the Apalachicola River.

Purpose of Study: The model study was considered essential to determine the effects of proposed methods of dredged material disposal and develop a contraction works plan to improve the navigation channel.

Problem Area:

Data: Data used in this study was as follows: (1) Prototype survey June 1977, (2) Prototype survey June 1978, (3) Base Test survey, and (4) Verification Test survey.

Scale: The Blountstown Reach model was of the movable-bed type built to a horizontal scale of 1:120 and a vertical scale of 1:80.

Thalweg Index: Thalweg index was calculated using an Index width of 300 feet. The index width defined the active channel width for this reach.

Type of Model: The overbank and bed were molded in crushed coal having a median grain diameter of 4 mm and a specific gravity of 1.3. The fixed bank line and nonerodible bed material were molded in crushed stone. Stone-filled dikes were reproduced with crushed stone, and pile dikes were simulated by rows of metal rods.

Reference: R. A. McCollum. (1988). "Blountstown Reach, Apalachicola River, Movable-Bed Model Study," Technical Report HL-88-17, U. S. Army Engineer Waterways Experiment Station, Vicksburg, MS. 39180.

1.3. Buck Island Reach, Mississippi River

Location: The Buck Island reach of the Mississippi River is a straight reach of river where dike fields have been constructed to form a sinuous navigation channel. The reach is located approximately halfway between Memphis, Tennessee, and Helena, Arkansas at about 700 river miles AHP.

Purpose of Study: The purpose of the study was to obtain some indication of the effectiveness of the proposed dike systems to maintain the existing alignment and the feasibility of channel realignment, and to development any modifications that might be required.

Problem Area:

Data: Data used in this study was as follows: (1) Prototype survey June 1976, (2) Prototype survey May 1977, (3) Prototype survey May 1978, (4) Prototype survey February 1979, (5) Base Test survey, and (6) Verification Test survey.

Scale: The movable-bed model reproducing approximately 12.5 miles of the Mississippi River between miles 690.5 and 703.0 AHP was used for this study reproduced to a horizontal scale of 1: 300 and a vertical scale of 1:100.

Thalweg Index: Thalweg index was calculated using an Index width of 2500 feet. The index width defined the active channel width for this reach.

Type of Model: Crushed coal of specific gravity of 1.30 and a medial grain size of about 4 mm was used for the bed material.

Reference: Charles R. Nickles, Thomas J. Pokrefke, Jr., and J. Edwin Glover. (1985). "Buck Island Reach, Mississippi River, Hydraulic Model Investigation," Technical Report HL-85-2, U. S. Army Engineer Waterways Experiment Station, Vicksburg, MS. 39180.

1.4. Chipola Cutoff Reach, Apalachicola River

Location: The model reproduced the reach of the Apalachicola River from navigation mile 42.7 to 39.5 and approximately one mile of the Chipola Cutoff.

Purpose of Study: This reach is one of which there is difficulty in maintaining an authorized navigation depth of 9-ft. The purpose of the study was due to the continuing decline in suitable sites for disposal of dredge material, various alternative methods of dealing with dredge material and construction of channel contraction works.

Problem Area:

Data: Data used in this study was as follows: (1) Prototype survey January 1978, (2) Prototype survey June 1979, (3) Base Test survey, and (4) Verification Test survey.

Scale: The model was constructed to scales of 1:120 horizontally and 1:80 vertically.

Thalweg Index: Thalweg index was calculated using an Index width of 300 feet. The index width defined the active channel width for this reach.

Type of Model: The overbank and bed were molded in crushed coal having a median grain diameter of 4 mm and a specific gravity of 1.3. Fixed-bank line and bed rock were molded in crushed stone.

Reference: Randy A. McCollum, (1994), "Chipola Cutoff Reach, Apalachicola River, Movable-Bed Model Study," Technical Report HL-94-8, U. S. Army Engineer Waterways Experiment Station, Vicksburg, MS. 39180.

1.5. Devil's Island Reach, Mississippi River

Location: Devil's Island Reach of the Mississippi River is located about 5 miles upstream of Cape Girardeau, Missouri between miles 55.0 and 68.0 above the mouth of the Ohio River.

Purpose of Study: The purpose of the study was to evaluate the effectiveness of a proposed plan of improvement and to develop modifications considered necessary to provide a satisfactory channel for navigation.

Problem Area:

Data: Data used in this study was as follows: (1) Prototype survey November 1969, and (2) Verification Test survey.

Scale: A movable-bed model with scale ratios of 1:400 horizontal and 1:100 vertical, reproducing approximately 13.0 miles of the Mississippi River was used in this study.

Thalweg Index: Thalweg index was calculated using an Index width of 1500 feet. The index width defined the active channel width for this reach.

Type of Model: The movable-bed model bed material was coal which a medial grain size of about 4 mm and a specific gravity of 1.30.

Reference: J. J. Franco and C. D. McKellar, Jr. (1973). "Channel Conditions, Devil's Island Reach, Mississippi River, Missouri and Illinois," Technical Report H-73-1, U. S. Army Engineer Waterways Experiment Station, Vicksburg, MS. 39180.

1.6. Dogtooth Bend Reach, Mississippi River

Location: The Dogtooth Beach reach of the middle Mississippi River extends from mile 39.6, Thebes Gap to mile 20.2, Thompson Landing (river miles above mile zero, which is located at the confluence of the Ohio and Mississippi Rivers near Cairo, IL).

Purpose of Study: This hydraulic model study was undertaken to obtain some indication of the effectiveness of the various proposed river training structure plans.

Problem Area:

Data: Data used in this study was as follows: (1) Prototype survey March 1977, (2) Prototype survey April 1983, (3) Base Test survey, and (4) Verification Test survey.

Scale: The movable-bed model used for this study reproduced to a horizontal scale of 1:400 and a vertical scale of 1:100.

Thalweg Index: Thalweg index was calculated using an Index width of 1500 feet. The index width defined the active channel width for this reach.

Type of Model: The movable-bed model consisted of crushed, granulated coal with a specific gravity of 1.30 and median grain size of approximately 4 mm as the movable bed material.

Reference: David L. Derrick, Thomas J. Pokrefke, Jr., Marden B. Boyd, James P. Crutchfield, and Raymond R. Henderson. (1994). "Design and Development of Bendway Weirs for the Dogtooth Bend Reach, Mississippi River, Hydraulic Model Investigation," Technical Report HL-94-10, U. S. Army Engineer Waterways Experiment Station, Vicksburg, MS. 39180.

1.7. Kate Aubrey Reach, Mississippi River

Location: Kate Aubrey Reach is located approximately 60 miles north of Memphis, TN between river miles 785.5 and 797.0.

Purpose of Study: The purpose of this study was to determine the extent of the shoaling in between Keyes Point dikes and Kate Aubrey dikes (river miles 788.5 and 792.5).

Problem Area: The problem area was in between Keyes Point dikes and Kate Aubrey dikes (river miles 788.5 and 792.5).

Data: Data used in this study was as follows: (1) Prototype survey May 1975, (2) Prototype survey May 1976, (3) Base Test survey, and (4) Verification Test survey.

Scale: The vertical scale was 1:100 and the horizontal scale was 1:300.

Thalweg Index: Thalweg index was calculated using an Index width of 2500 feet. The index width defined the active channel width for this reach.

Type of Model: The model used for this study was a movable-bed model with crushed coal of median diameter 4 mm and a specific gravity of 1.30.

Reference: Charles R. Nickles. (2000). Unpublished report, U. S. Army Engineer Waterways Experiment Station, Vicksburg, MS. 39180.

1.8. Lake Dardanelle, Arkansas River

Location: Lake Dardanelle is a 51-mile-long reservoir formed by Dardanelle Lock and Dam, one of the four high-lift structures in the system. Dardanelle Dam is located on the Arkansas River at mile 205.5, 2 miles upstream from Dardanelle and 3 miles southwest of Russellville.

Purpose of Study: The purpose of the study was to determine the type and location of control structures needed to develop a stable navigation channel with a satisfactory alignment in the vicinity of the proposed bridge by the Arkansas Highway Department and to make Lake Dardanelle an efficient sediment trap.

Problem Area:

Data: Data used in this study was as follows: (1) Prototype survey November 1971, (2) Prototype survey October 1973, (3) Base Test survey, and (4) Verification Test survey.

Scale: The model of Lake Dardanelle, which reproduced the reach of the Arkansas River from mile 231.3 to 238.5 was built to linear scale ratios of 1:120 horizontally and 1:80 vertically.

Thalweg Index: Thalweg index was calculated using an Index width of 1500 feet. The index width defined the active channel width for this reach.

Type of Model: The model was of the movable-bed type with fixed-banks and overbanks molded in sand-cement mortar. The bed material was coal having a median grain diameter of about 4 mm and a specific gravity of 1.30.

Reference: James E. Foster and John J. Franco. (1977) "Lake Dardanelle, Arkansas River, Hydraulic Model Investigation," Technical Report H-77-4, U. S. Army Engineer Waterways Experiment Station, Vicksburg, MS. 39180.

1.9. Lock and Dam #2, Red River

Location: The John H. Overton Lock and Dam is located in a cutoff channel between 1967 river miles 89.0 and 86.5 on the Red River.

Purpose of Study: The purposes of the model study were (1) to study tendency for scour fill in the approaches to the lock and dam, and (2) determine training structures that would improve navigation conditions and minimize dredging requirements and scour problems.

Problem Area:

Data: Data used in this study was as follows: (1) Prototype survey 1978, (2) Prototype survey 1981, (3) Base Test survey, and (4) Verification Test survey.

Scale: A model reproducing a reach of the Red River from 1967 river miles 90.0 to 85.0 was designed for movable-bed operations and built to linear scale ratios of 1:120 horizontally and 1:80 vertically.

Thalweg Index: Thalweg index was calculated using an Index width of 400 feet. The index width defined the active channel width for this reach.

Type of Model: A movable-bed model was used with crushed coal that had a median diameter of 4 mm and a specific gravity of 1.30.

Reference: Randy A. McCollum. (1997) "Red River Waterway, John H. Overton Lock and Dam, Report 3, Sedimentation Conditions, Hydraulic Model Investigation" Technical Report HL-98-16, U. S. Army Engineer Waterways Experiment Station, Vicksburg, MS. 39180.

1.10. Lock and Dam #4, Red River

Location: Lock and Dam No. 4 is the fourth lock and dam on the Mississippi River to Shreveport reach of the Red River waterway. The proposed lock and dam will be located in a cutoff between 1967 river miles 205 and 210.

Purpose of Study: The purpose of the study was to investigate and solve potential channel development and maintenance problems associated with Lock and Dam No.4 on the Red River in Louisiana.

Problem Area:

Data: Data used in this study was as follows: (1) Prototype survey 1978, (2) Prototype survey 1981, (3) Base Test survey, and (4) Verification Test survey.

Scale: The model reproduced the Red River 1967 river mile 213.1 to 204.7 using a distorted scale of 1:120 horizontally and 1:80 vertically.

Thalweg Index: Thalweg index was calculated using an Index width of 550 feet. The index width defined the active channel width for this reach.

Type of Model: The bed of the model was molded in crushed coal having the following properties: $d_{84} = 5.5$ mm, $d_{50} = 2.9$ mm, $d_{16} = 1.5$ mm, and a specific gravity of 1.30.

Reference: D. S. Mueller, D. M. Maggio, and T. J. Pokrefke. (1992) "Red River Waterway, Lock and Dam No. 4, Report 3, Sedimentation Conditions, Hydraulic Model Study," Technical Report HL-90-2, U. S. Army Engineer Waterways Experiment Station, Vicksburg, MS. 39180.

1.11. Loosahatchie-Memphis Reach, Mississippi River

Location: The Loosahatchie-Memphis reach is the portion of the lower Mississippi River that lies adjacent to Memphis, TN. The reach includes the entrance to the Memphis Harbor, the confluence with the Wolf and Loosahatchie Rivers and Mud Island and is crossed by four bridges.

Purpose of Study: The purpose of the study was (1) to investigate the increasing shoaling upstream of the I-40 Highway bridge and the increased dredging requirements to maintain a channel through the I-40 bridge during low-water periods, and (2) to investigate the instability of the left riverbank immediately downstream of the entrance to the harbor.

Problem Area:

Data: Data used in this study was as follows: (1) Prototype survey January 1986, (2) Prototype survey November 1986, (3) Prototype survey April 1990, (4) Base Test survey, and (5) Verification Test survey.

Scale: The movable-bed model use for this study reproduced to a horizontal scale of 1:300 and a vertical scale of 1:100 the reach of the Mississippi River between miles 738.8 and 743.5 AHP including the overbank area between the main-line levees.

Thalweg Index: Thalweg index was calculated using an Index width of 2500 feet. The index width defined the active channel width for this reach.

Type of Model: The model was a movable-bed type and was constructed with the banks fixed about el +10 and the overbank areas molded in sand-cement mortar. The steep portions of the banks below el +10 and all dikes were molded using 19-mm (3/4-in.) crushed stone. The remaining river channel was molded in crushed coal having a median diameter of 2 mm and a specific gravity of 1.30.

Reference: Charles R. Nickles. (1996). "Loosahatchie-Memphis Reach, Lower Mississippi River, Hydraulic Model Investigation," Technical Report HL-96-4, U. S. Army Engineer Waterways Experiment Station, Vicksburg, MS. 39180.

1.12. New Madrid Bar Reach, Mississippi River

Location: The location of this study is a reach of the Mississippi River between miles 882.5 and 893.5 AHP, in the vicinity of New Madrid, MO.

Purpose of Study: The model study was undertaken to obtain some general indications as to the effectiveness of the proposed plan of a system of dikes designed to improve the alignment of the navigation channel and eliminate the need for maintenance dredging.

Problem Area:

Data: Data used in this study was as follows: (1) Prototype survey May 1976, (2) Prototype survey May 1977, (3) Prototype survey April 1978, (4) Base Test survey, and (5) Verification Test survey.

Scale: The movable-bed model used for this study reproduced to a horizontal scale of 1:480 and a vertical scale of 1:60 the reach of the Mississippi River between miles 882.5 and 893.5 AHP.

Thalweg Index: Thalweg index was calculated using an Index width of 2500 feet. The index width defined the active channel width for this reach.

Type of Model: The bed material used was sand having a median grain diameter of about 0.2 mm and specific gravity of 2.65.

Reference: Thomas J. Pokrefke, Jr., and John J. Franco. (1981) "Investigation of Proposed Dike System on the Mississippi River, Report 2, New Madrid Bar Reach, Hydraulic Model Investigation," Miscellaneous Paper H-70-1, U. S. Army Engineer Waterways Experiment Station, Vicksburg, MS. 39180.

1.13. Redeye Crossing Reach, Lower Mississippi River

Location: Redeye Crossing is located on the lower Mississippi River between river miles 223 and 225, Above Head of Passes (AHP), about 3 miles downstream of the I-10 Highway Bridge at Baton Rouge, LA.

Purpose of Study: The purpose of the Redeye Crossing Reach study was to evaluate the effectiveness of proposed constricting dikes at Redeye Crossing in reducing maintenance dredging requirements while maintaining safe navigation conditions through the reach.

Problem Area:

Data: Data used in this study was as follows: (1) Prototype survey September 1982 (2) Prototype survey August 1983 (3) Verification Test survey, and (4) Base Test survey.

Scale: The movable-bed model used for this study reproduced to a horizontal scale of 1:240 and a vertical scale of 1:200 the reach of the Mississippi River between miles 219.0 to 228.0 AHP.

Thalweg Index: Thalweg index was calculated using an Index width of 2500 feet. The index width defined the active channel width for this reach.

Type of Model: This model used crushed coal having a medial diameter of 2 mm and a specific gravity of 1.30.

Reference: T. J. Pokrefke, Jr., C. R. Nickles, N. K. Raphelt, M. J. Trawle, and M. B. Boyd. (1995). "Redeye Crossing Reach, Lower Mississippi River, Report 1, Sediment Investigation," Technical Report HL-95-13, U. S. Army Engineer Waterways Experiment Station, Vicksburg, MS. 39180.

1.14. Smithland Locks and Dam, Ohio River

Location: Smithland Locks and Dam is located on the Ohio River at mile 918.5 below Pittsburgh, Pennsylvania. The site is about 2 miles upstream from Smithland, Kentucky, and about 16 miles upstream from Paducah, Kentucky.

Purpose of Study: The purpose of the model investigation was to determine the following:

- a. Optimum location and location and alignment of the locks and arrangement of the lock auxiliary walls.
- b. Navigation conditions in the lock approaches and over the fixed weir with the various plans considered.
- c. Shoaling and erosion tendencies.
- d. Effects of various amounts of rock excavations.
- e. Optimum alignment for the lock lower approach channel and training structures required to eliminate or reduce the need for maintenance dredging.
- f. Effects of various dam modifications.
- g. Conditions that can be expected during construction with various phase cofferdams.
- h. Modification required to eliminate any undesirable conditions or to improve the efficiency of the project.

Problem Area:

Data: Data used in this study was as follows: (1) Prototype survey October 1965, and (2) Verification Test survey.

Scale: The model was constructed to an undistorted scale ratio of 1:150.

Thalweg Index: Thalweg index was calculated using an Index width of 1000 feet. The index width defined the active channel width for this reach.

Type of Model: The model was constructed initially as a fixed-bed type with provisions for converting a portion of the channel bed upstream and downstream of the proposed damsite to a movable bed. Except for the reach between miles 917.5 and 925.0, the channel bed and overbank area were molded in sand-cement mortar to sheet metal templates. The section of the model to be converted to movable bed was molded initially with pea gravel that was later replaced with crushed coal. The reach of the model between miles 917.5 and 925.0, without the locks and dam, was converted to a movable bed reproduced with crushed coal and molded to the conditions indicated by the prototype survey of October 1966.

Reference: John J. Franco and Thomas J. Pokrefke, Jr. (1983). "Smithland Locks and Dam, Ohio River, Hydraulic Model Investigation," Technical Report HL-83-19, U. S. Army Engineer Waterways Experiment Station, Vicksburg, MS. 39180.

1.15. West Access Channel, Atchafalaya River

Location: The location of this study is a reach of the Atchafalaya River between miles 72.9 and 77.4, including the entrance and approximately 2.9 miles of the upstream end of the West Access Channel. This entrance is located at Atchafalaya River mile 76.8, which is approximately 37 river miles downstream of Krotz Springs, LA, and 40 miles upstream of Morgan City, LA.

Purpose of Study: The purpose of the study was to investigate the relocation of the entrance of the West Access Channel approximately 3 miles upstream of its present site and realign the upper portion of the channel. The model study was undertaken to obtain some indication of the effectiveness of the proposed relocation and realignment to reduce the sediment entering the channel and the effects on the Atchafalaya River Channel.

Problem Area:

Data: Data used in this study was as follows: (1) Prototype survey 1975, and (2) Verification Test survey.

Scale: The movable-bed model used for this study reproduced to a horizontal scale of 1:120 and a vertical scale of 1:80 the reach of the Atchafalaya River between miles 72.9 and 77.4.

Thalweg Index: Thalweg index was calculated using an Index width of 1100 feet. The index width defined the active channel width for this reach.

Type of Model: The model was constructed with the banks fixed above el 0.0 and the overbank area molded in sand-cement mortar. The Atchafalaya River Channel below el 0.0 feet referred to the National Geodetic Vertical Datum (NGVD) from mile 72.9 to mile

75.8 was reproduced using ¾-in. crushed stone. This area was fixed after a study of geological survey and prior hydrographic surveys of the channel indicated that the river channel was entrenched in a layer of back-swamp clay, which is highly resistant to erosion. The remaining river channel from mile 75.8 to mile 77.4 and the West Access Channel were molded in crushed coal having a medial diameter of 2 mm and a specific gravity of 1.30.

Reference: D. M. Maggio and C. R. Nickles. (1989) "West Access Channel Realignment Atchafalaya River, Hydraulic Model Investigation," Technical Report HL-89-2, U. S. Army Engineer Waterways Experiment Station, Vicksburg, MS. 39180.

1.16. Bass Location, Willamette River

Location: The Bass Location, Willamette River, is located between river miles 137 and 135, just southeast of Corvallis, Oregon.

Purpose of Study: The model study was conducted to look at the alternative of using stone groins as a method of bank protection instead of blanket stone revetment.

Problem Area:

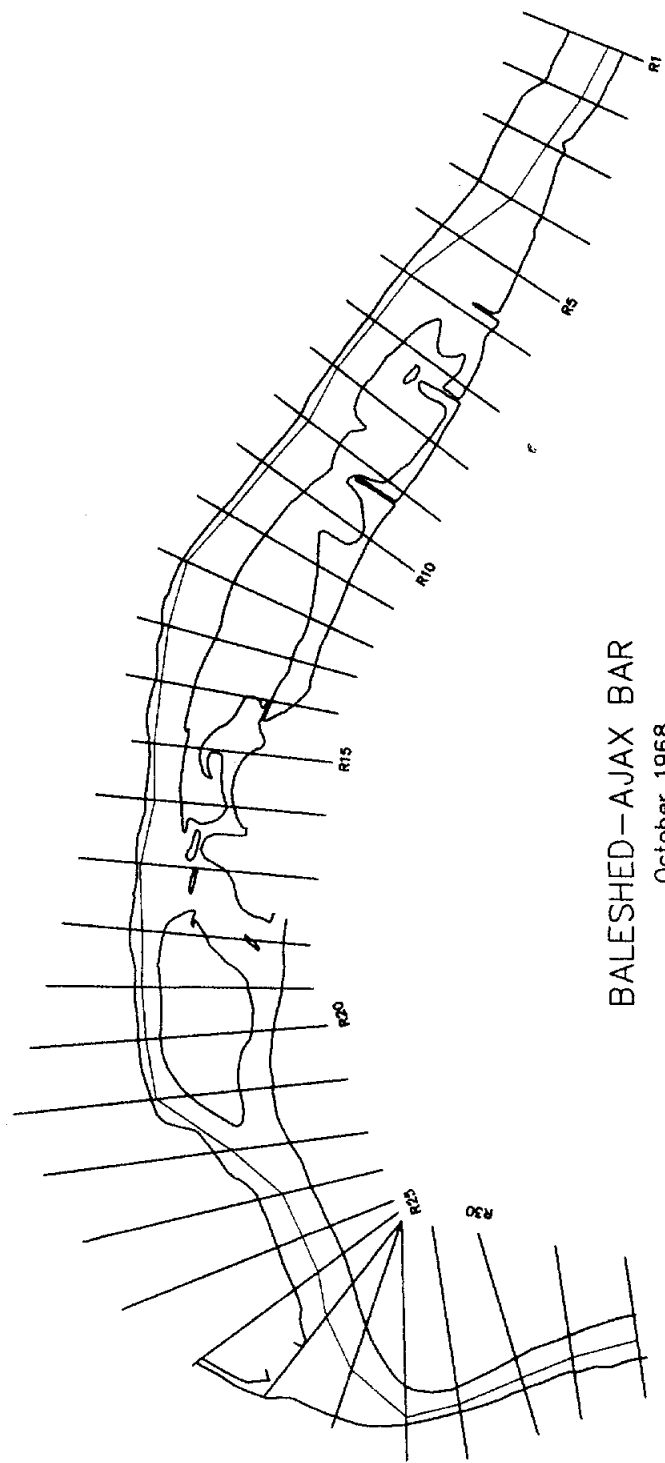
Data: Data used in this study was as follows: (1) Prototype survey 1977, (2) Prototype survey 1980, (3) Base Test survey 25-year flood, (4) Base Test survey 2-year flood, and (5) Verification Test survey.

Scale: The model was built to a horizontal scale of 1:100 and a vertical scale of 1:50.

Thalweg Index: Thalweg index was calculated using an Index width of 500 feet. The index width defined the active channel width for this reach.

Type of Model: Portions of the right overbank and all the left overbank were molded in concrete. The difference in the bed and bank material was simulated by using different grain size material in the channel and the erodible section of bank line. The right bank in the area of concern was molded in crushed coal having a medial grain diameter of 4 mm, and the bed of the model was molded in crushed coal having a median grain diameter of about 10 mm. The specific gravity of the coal was 1.30.

Reference: Randy A. McCollum, C. Wayne O'Neal, and J. Edwin Glover. (1987) "Bank Protection, Bass Location, Willamette River, Oregon," Technical Report HL-87-7, U. S. Army Engineer Waterways Experiment Station, Vicksburg, MS. 39180.



BALESHED-AJAX BAR
October 1968

Figure B-1.1a Baleshed-Ajax Bar Model Plan View

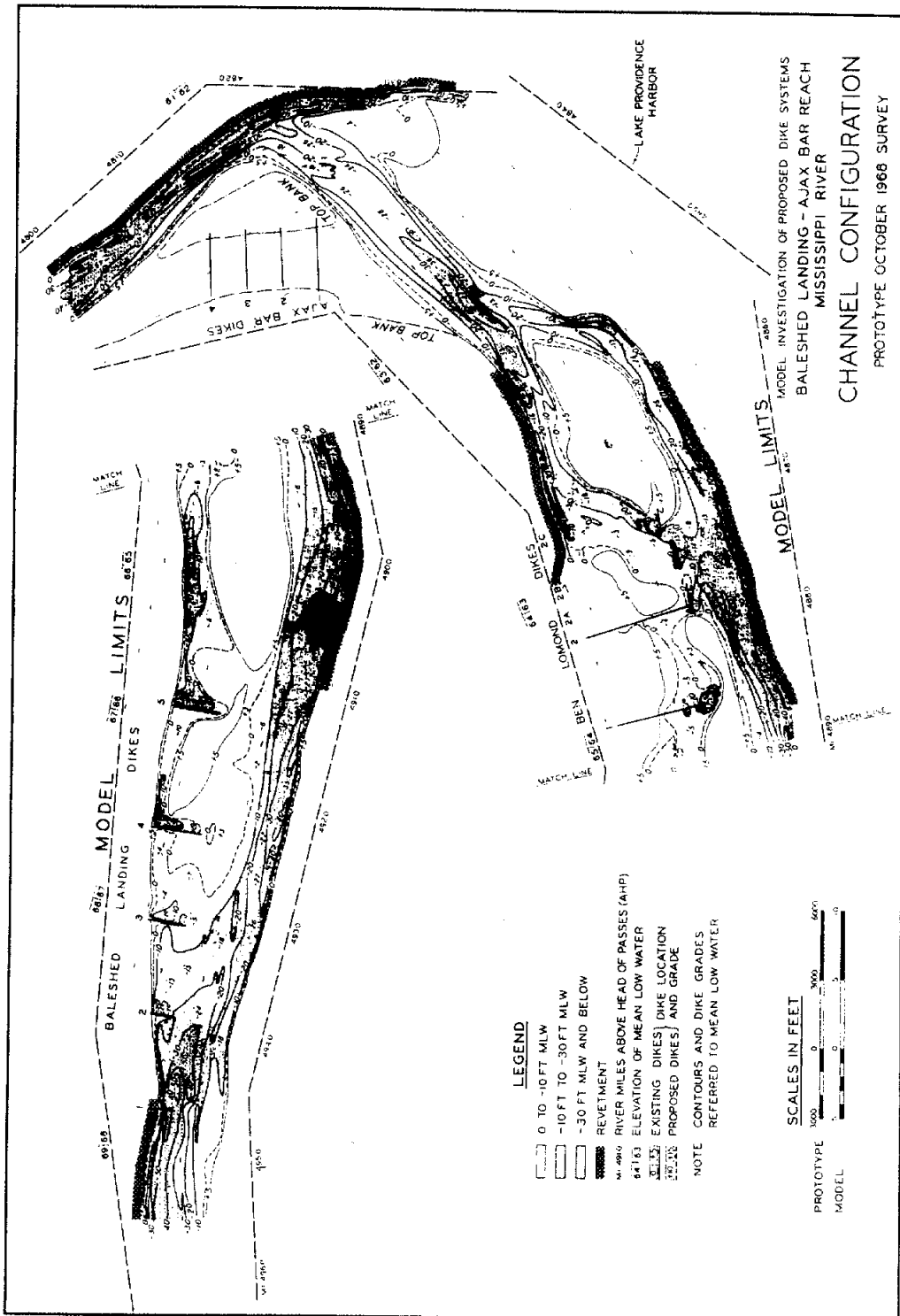


Figure B-1.1c Baleshed-Ajax Bar October 1968 Prototype Survey

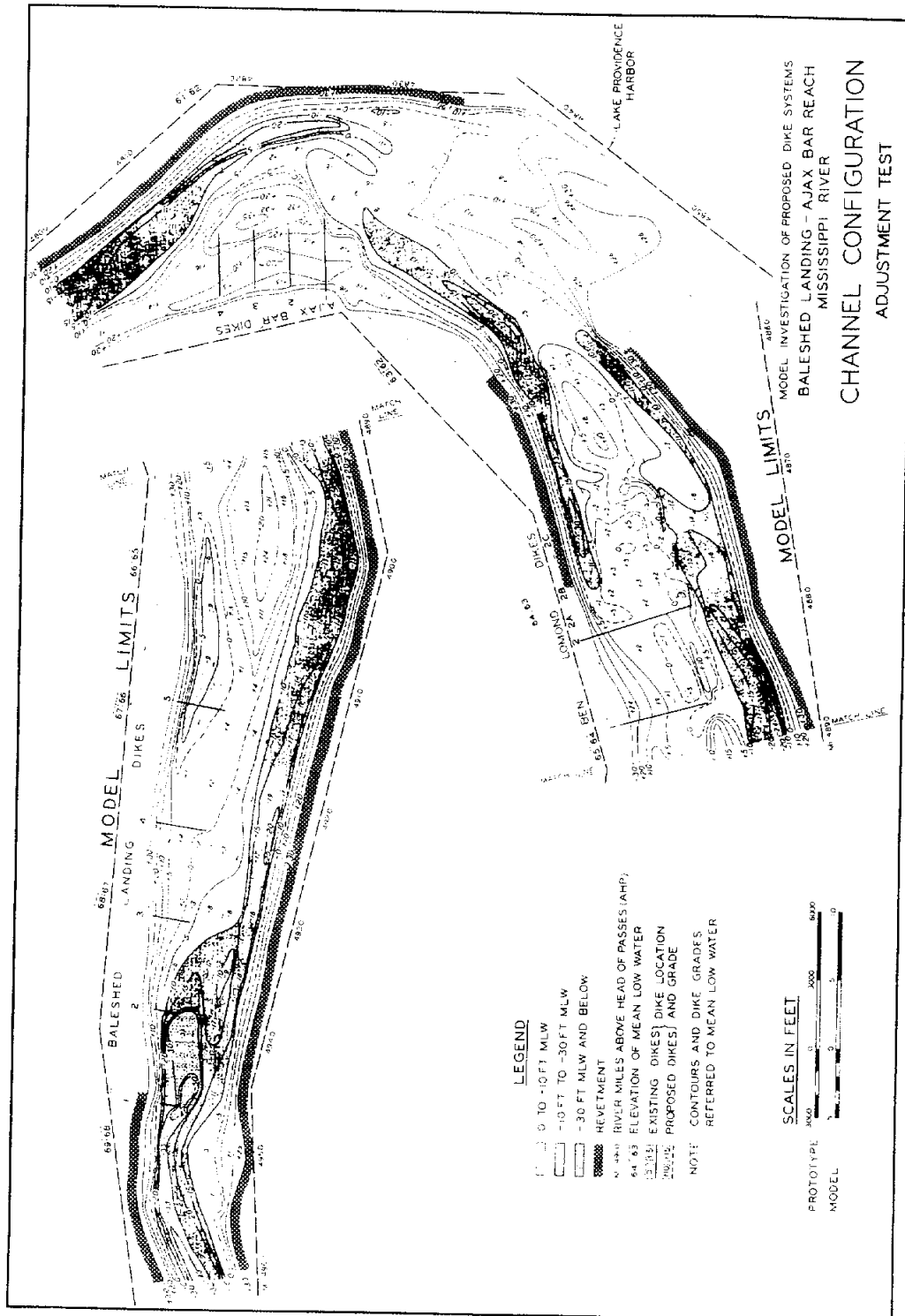


Figure B-1.1d Baleshed-Ajax Verification Test Survey

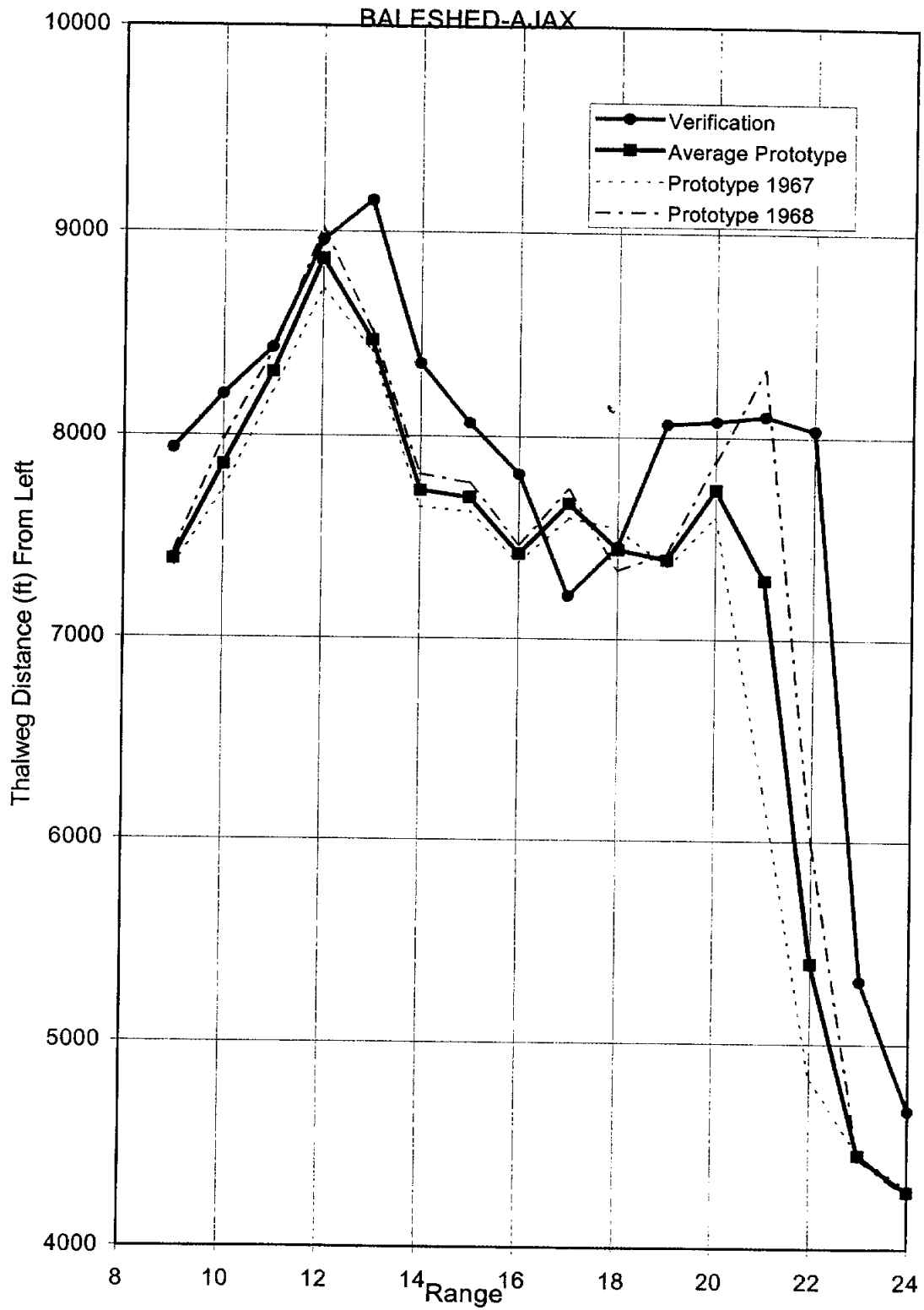


Figure B-1.2a Thalweg Position From Left, Baleshed-Ajax

BALESHED AJAX

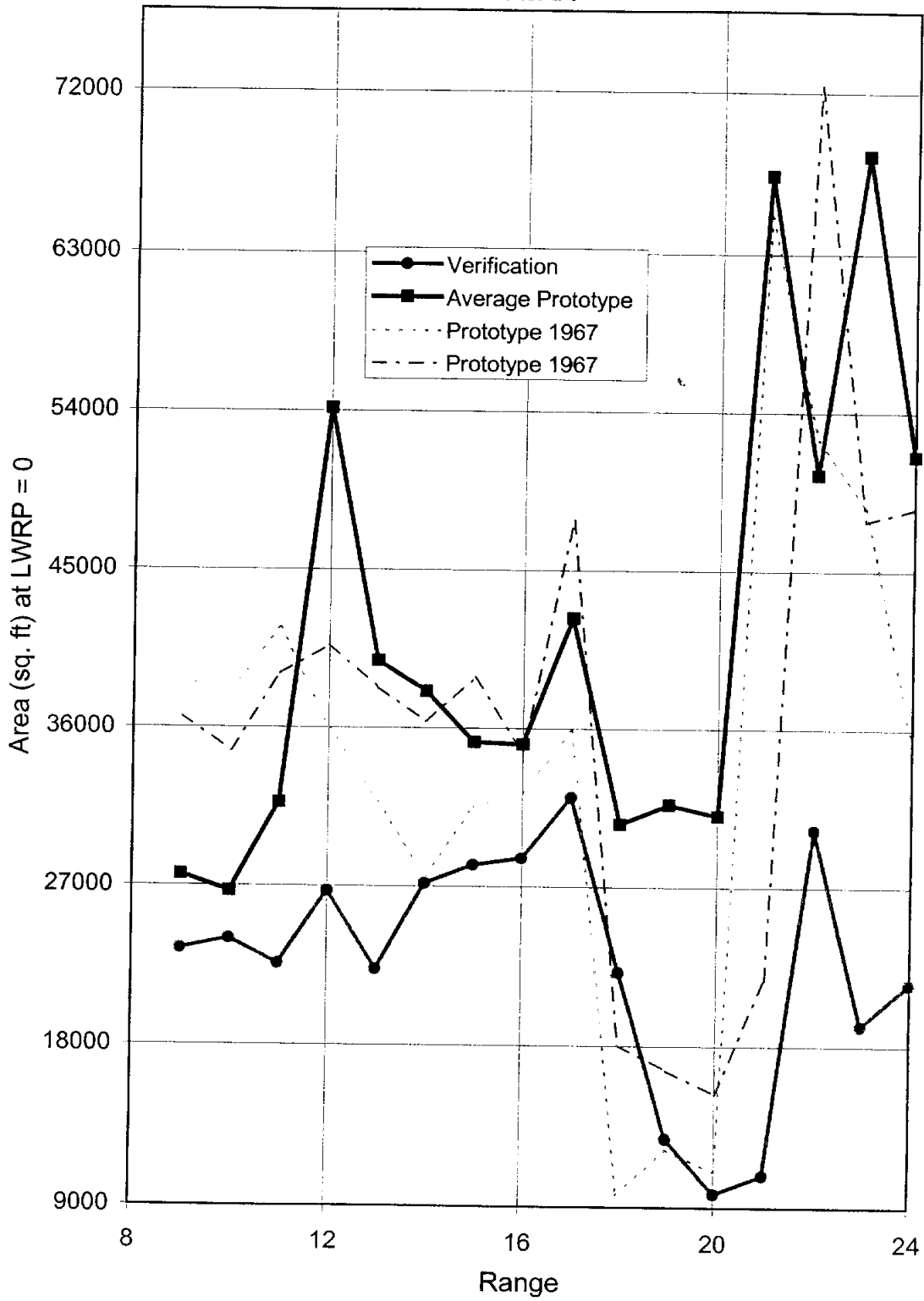


Figure B-1.2b Cross-Section Area by Range, Baleshed-Ajax

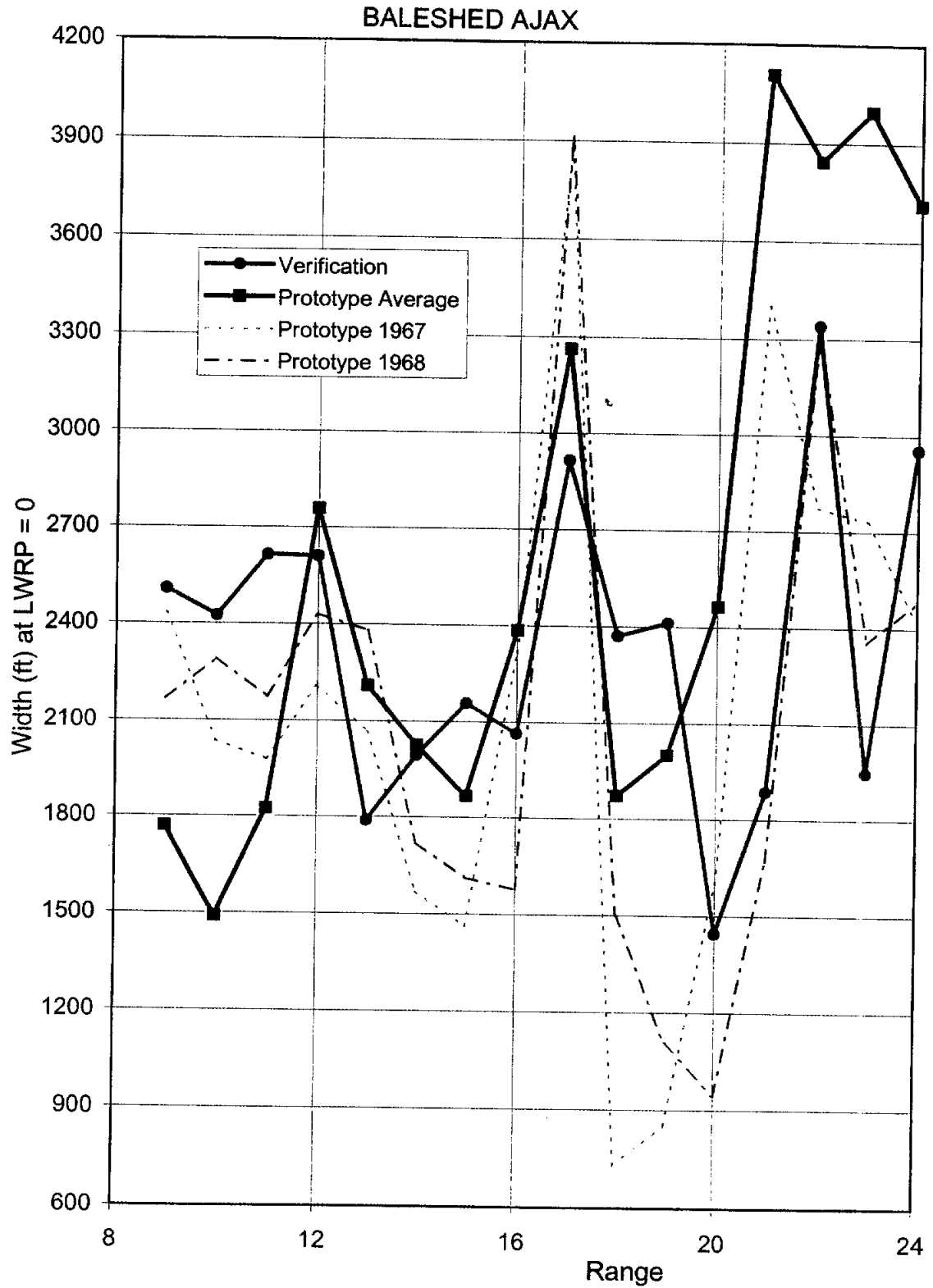


Figure B-1.2c Top Width by Range, Baleshed-Ajax

BALESHED AJAX

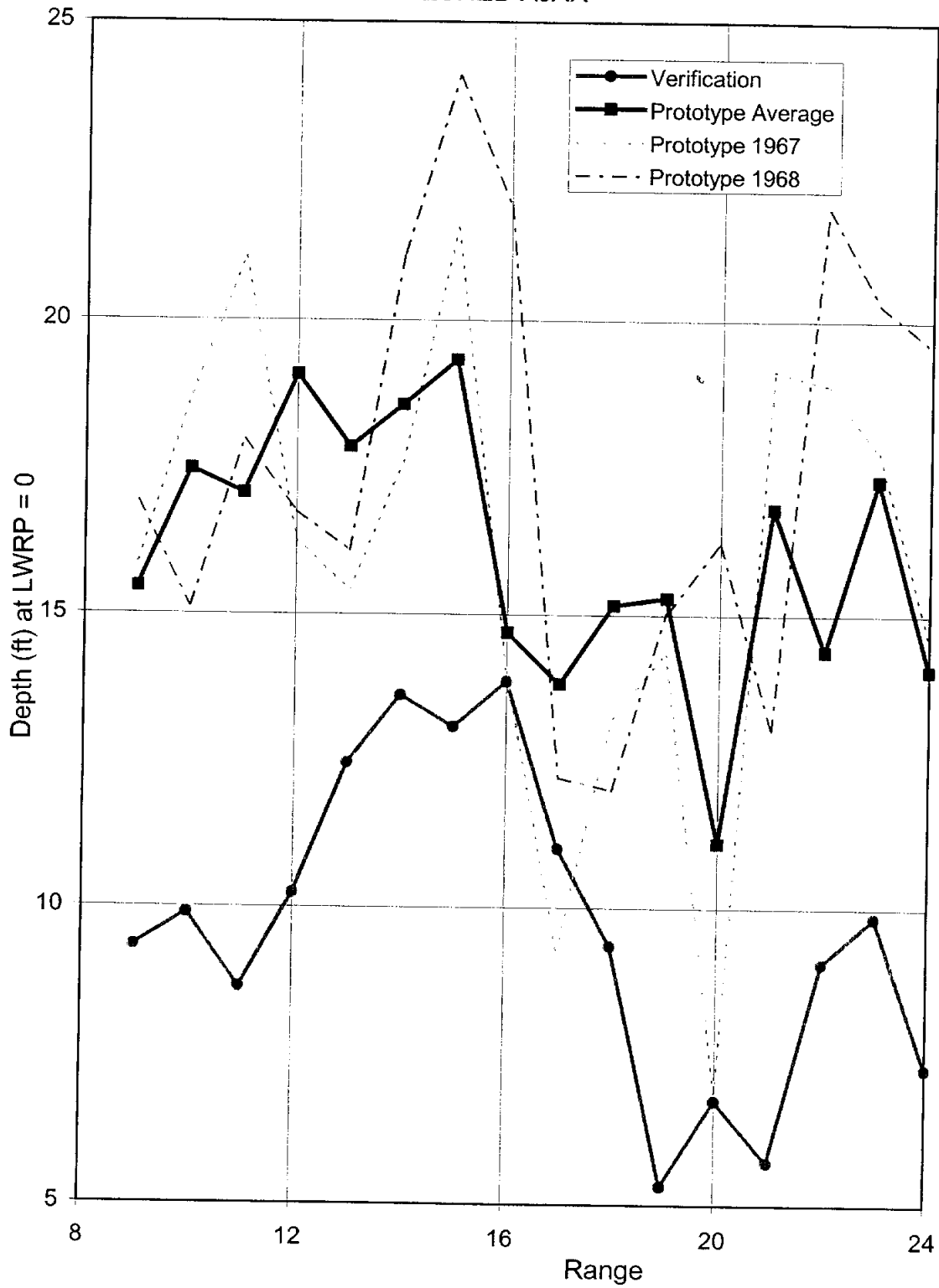


Figure B-1.2d Hydraulic Depth by Range, Baleshed Ajax

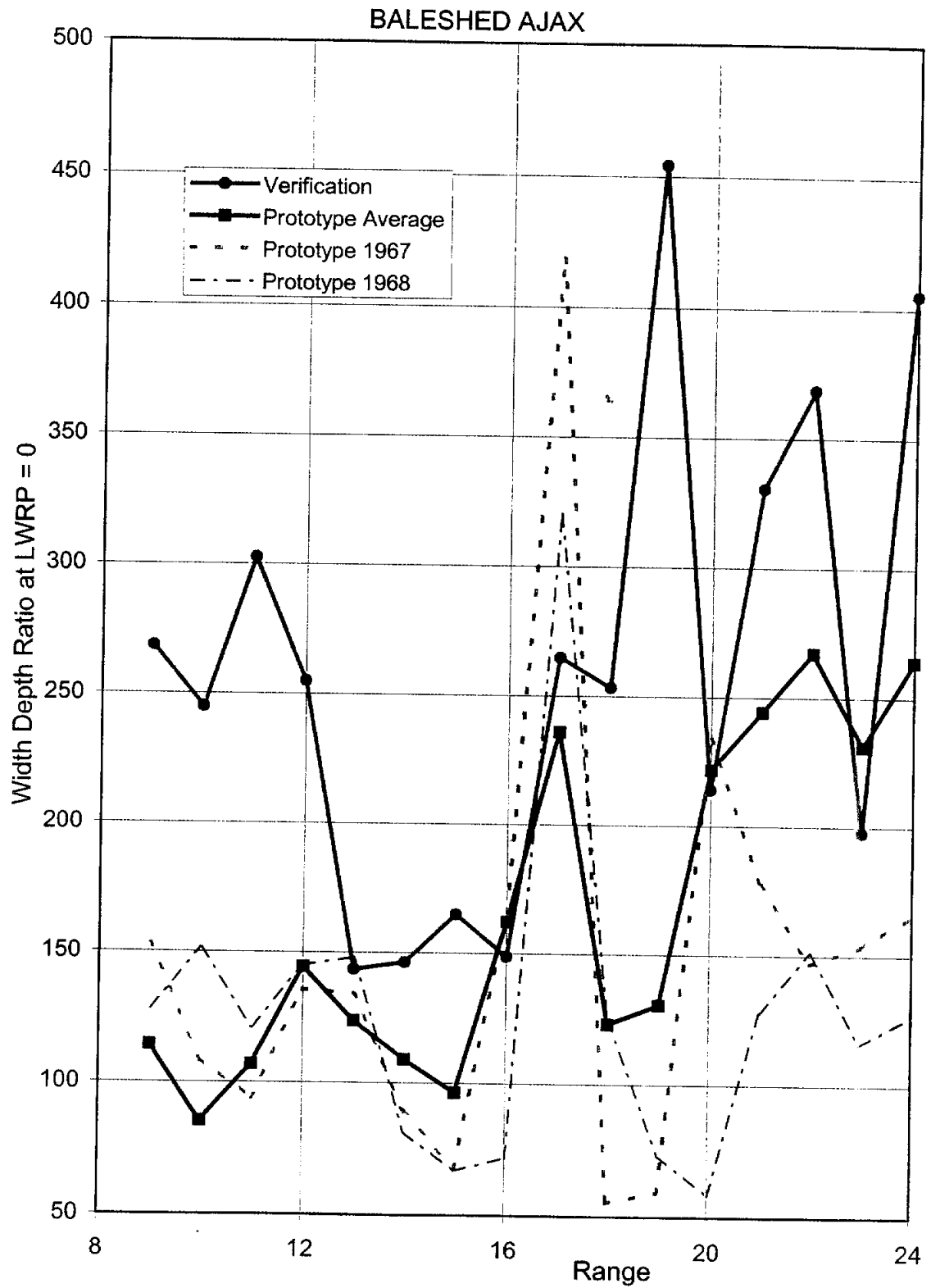


Figure B-1.2e Width/Depth Ratio by Range, Baleshed-Ajax

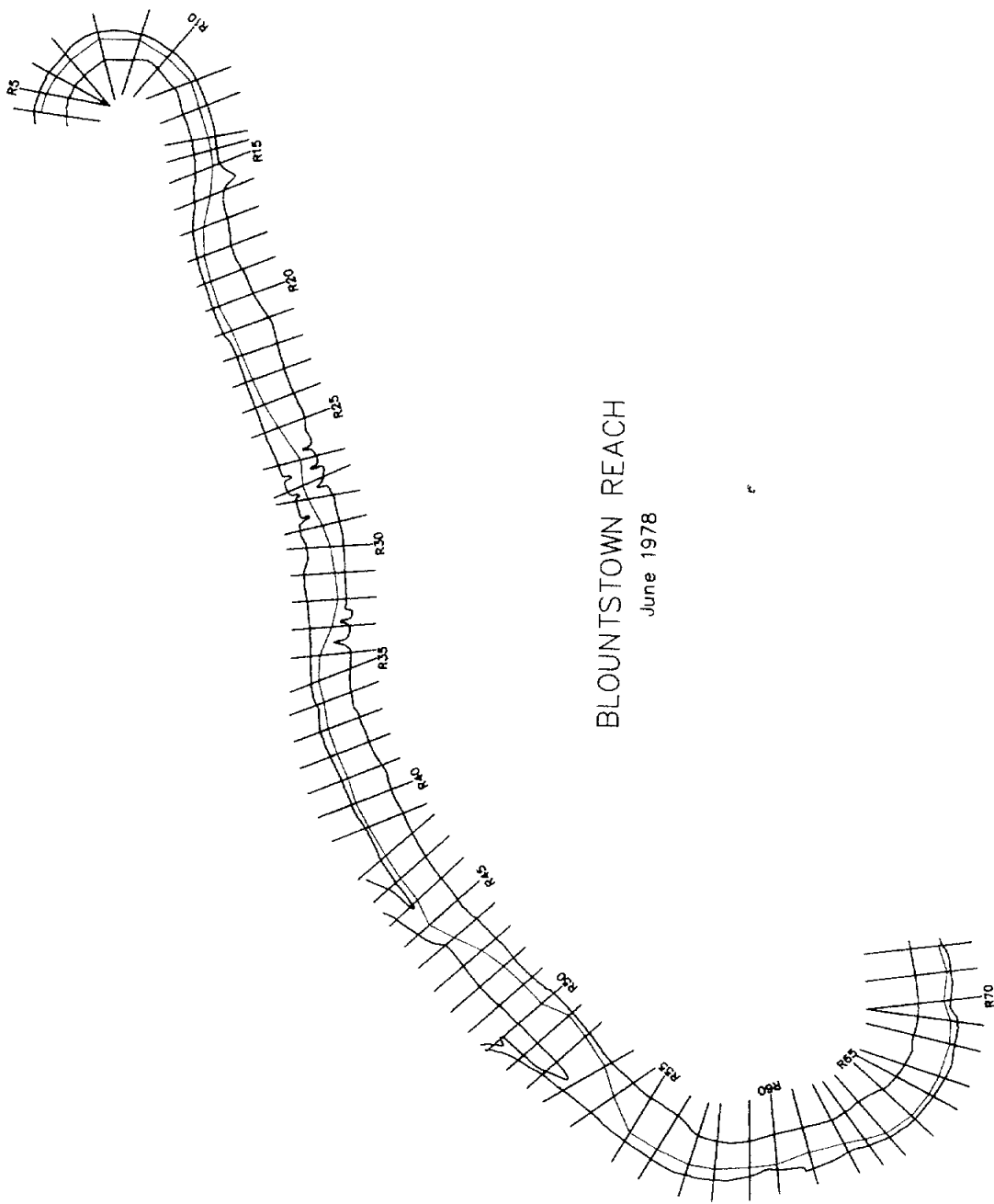


Figure B-2.1a Blountstown Model Plan View

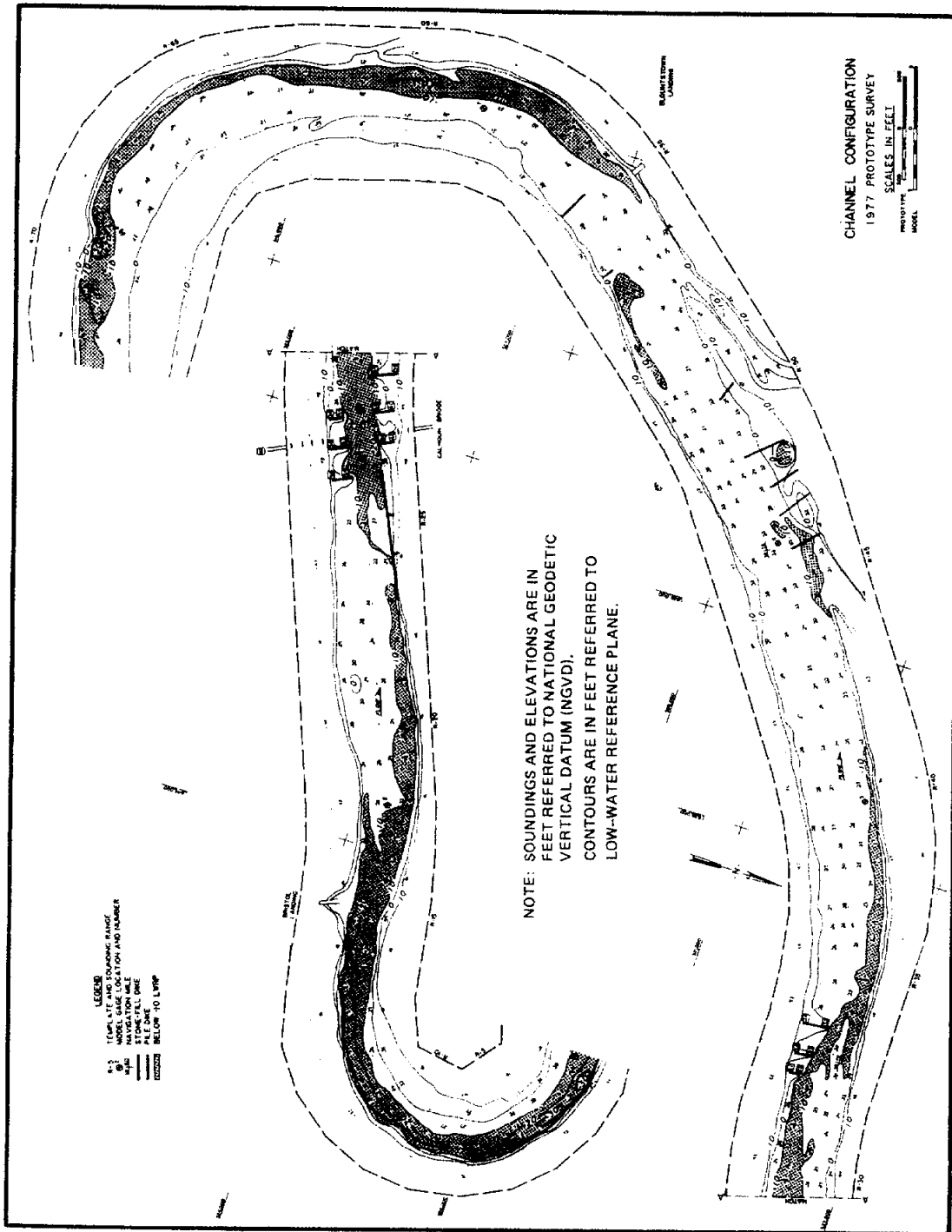


Figure B-2.1b Blountstown June 1977 Prototype Survey

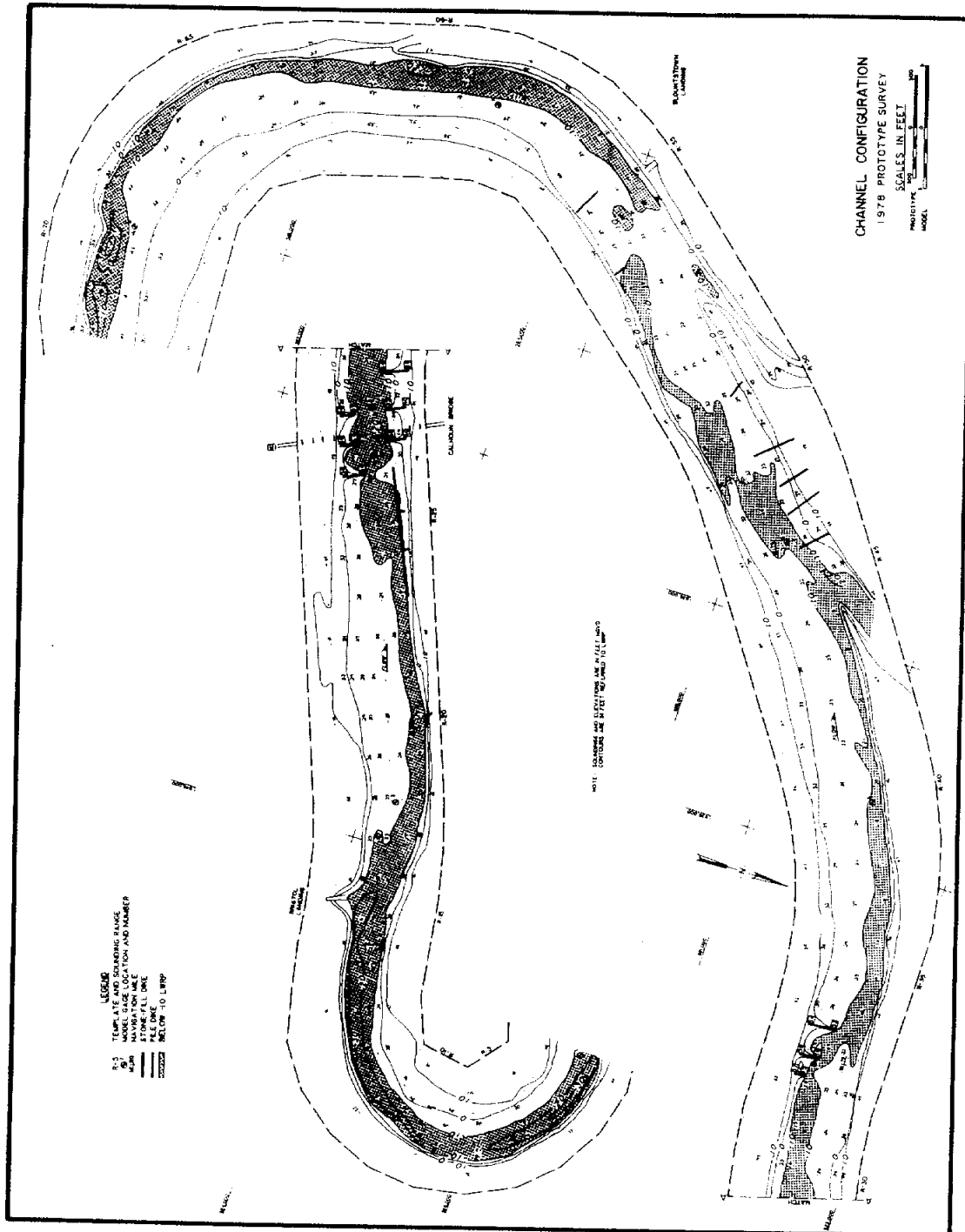
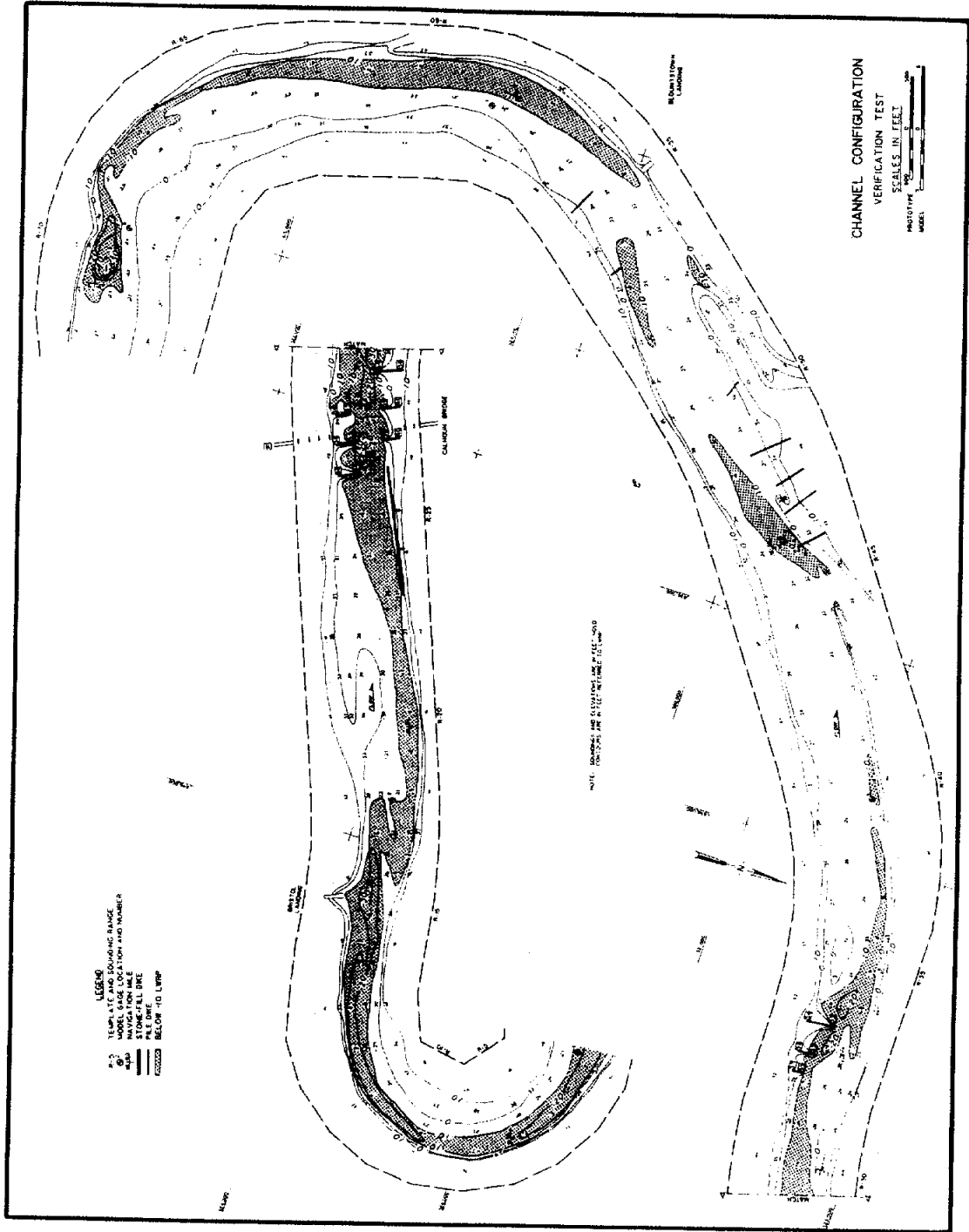


Figure B-2.1c Blountstown June 1978 Prototype Survey



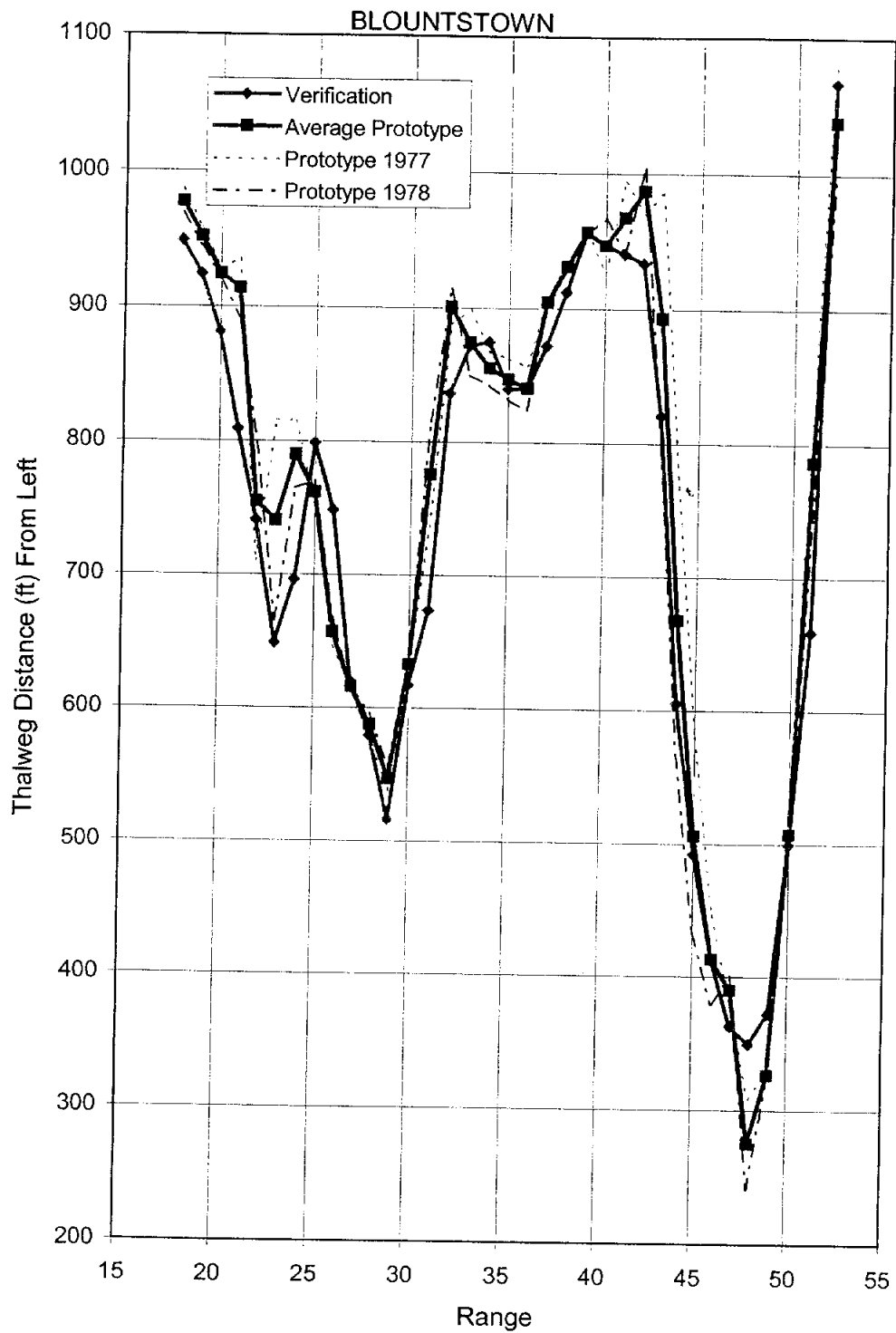


Figure B-2.2a Thalweg Position From Left by Range, Blountstown Reach

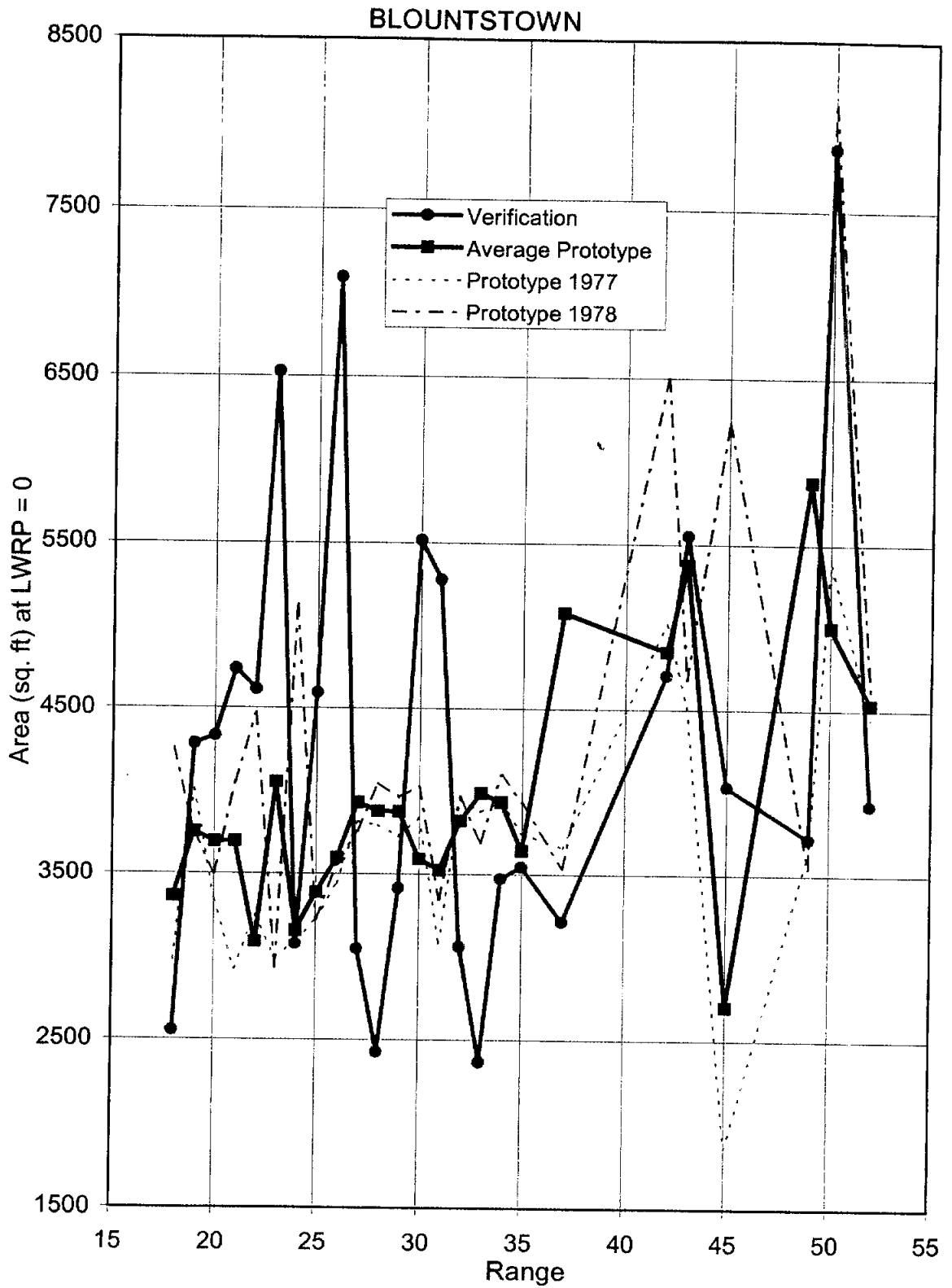


Figure B-2.2b Cross-Section Area by Range, Blountstown Reach

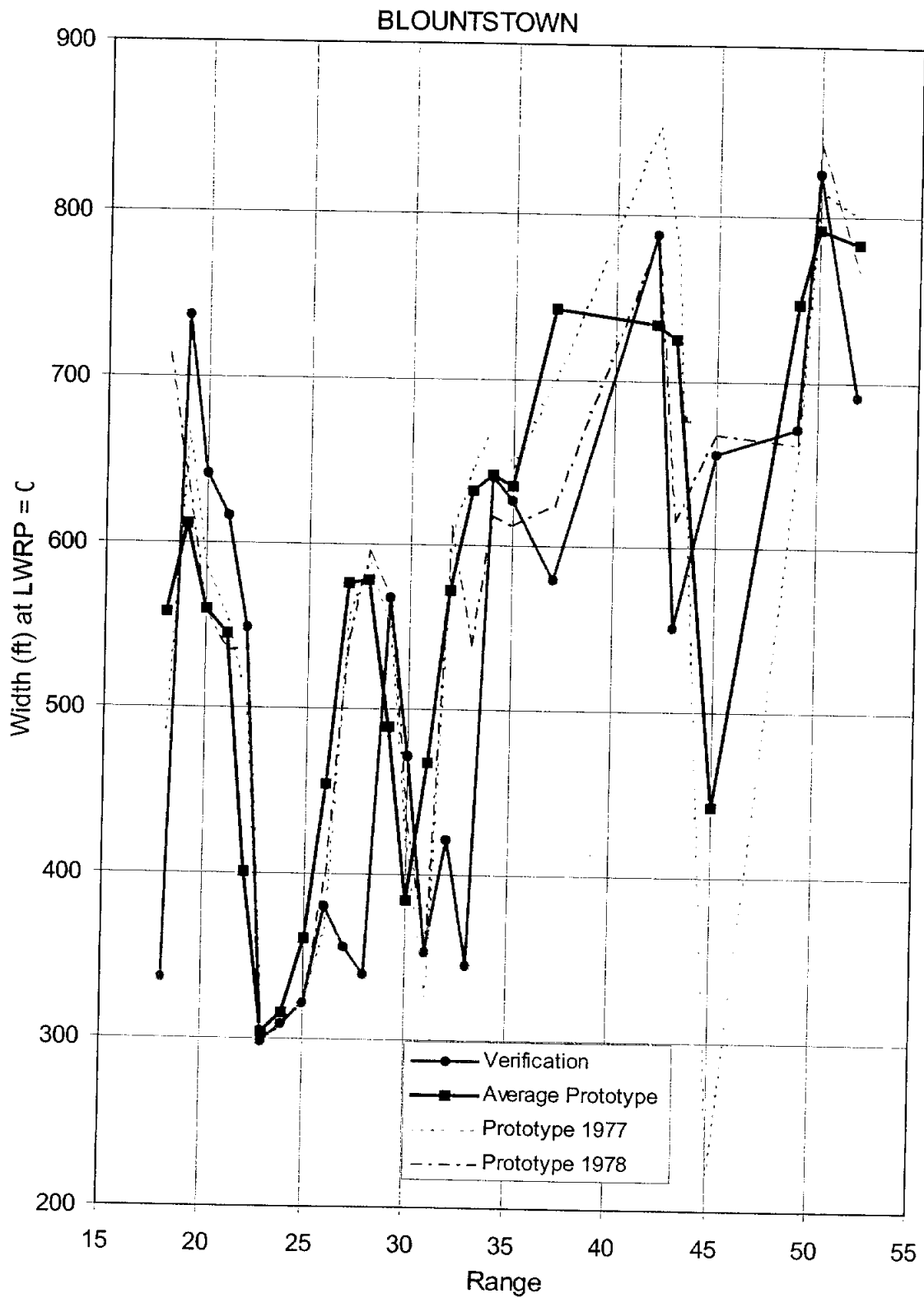


Figure B-2.2c Top Width by Range, Blountstown Reach

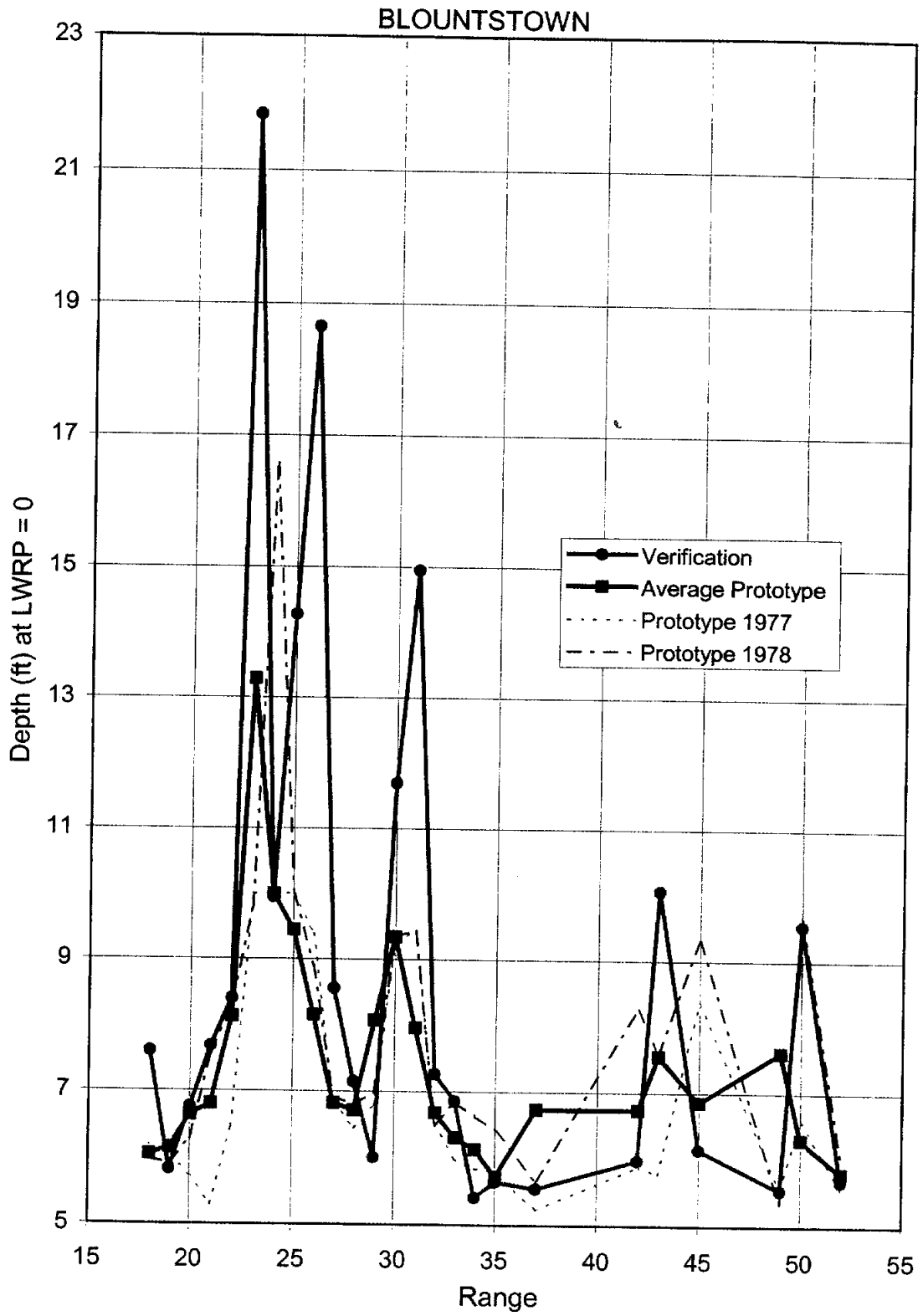


Figure B-2.2d Hydraulic Depth by Range, Blountstown Reach

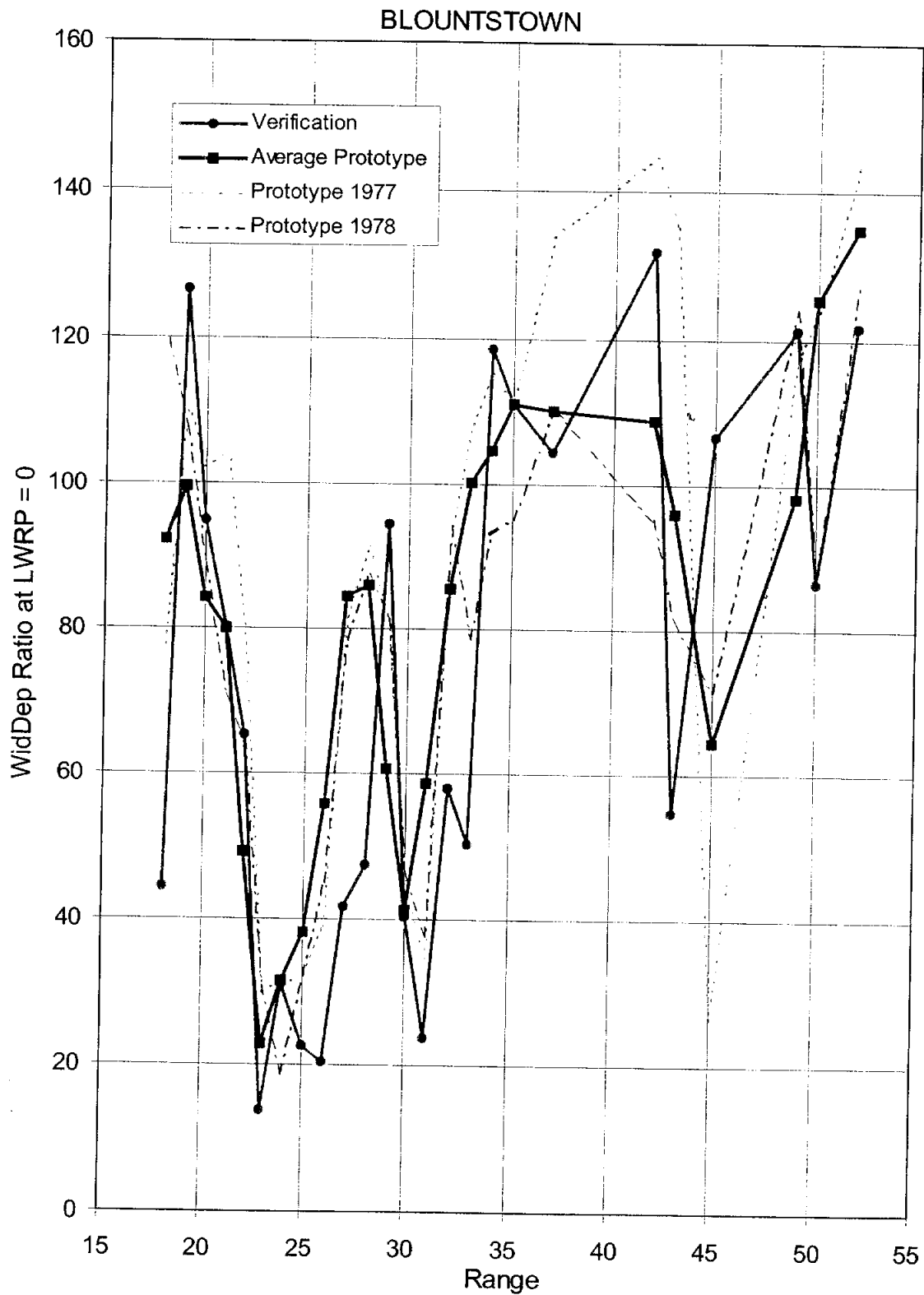


Figure B-2.2e Width/Depth Ratio by Range, Blountstown Reach

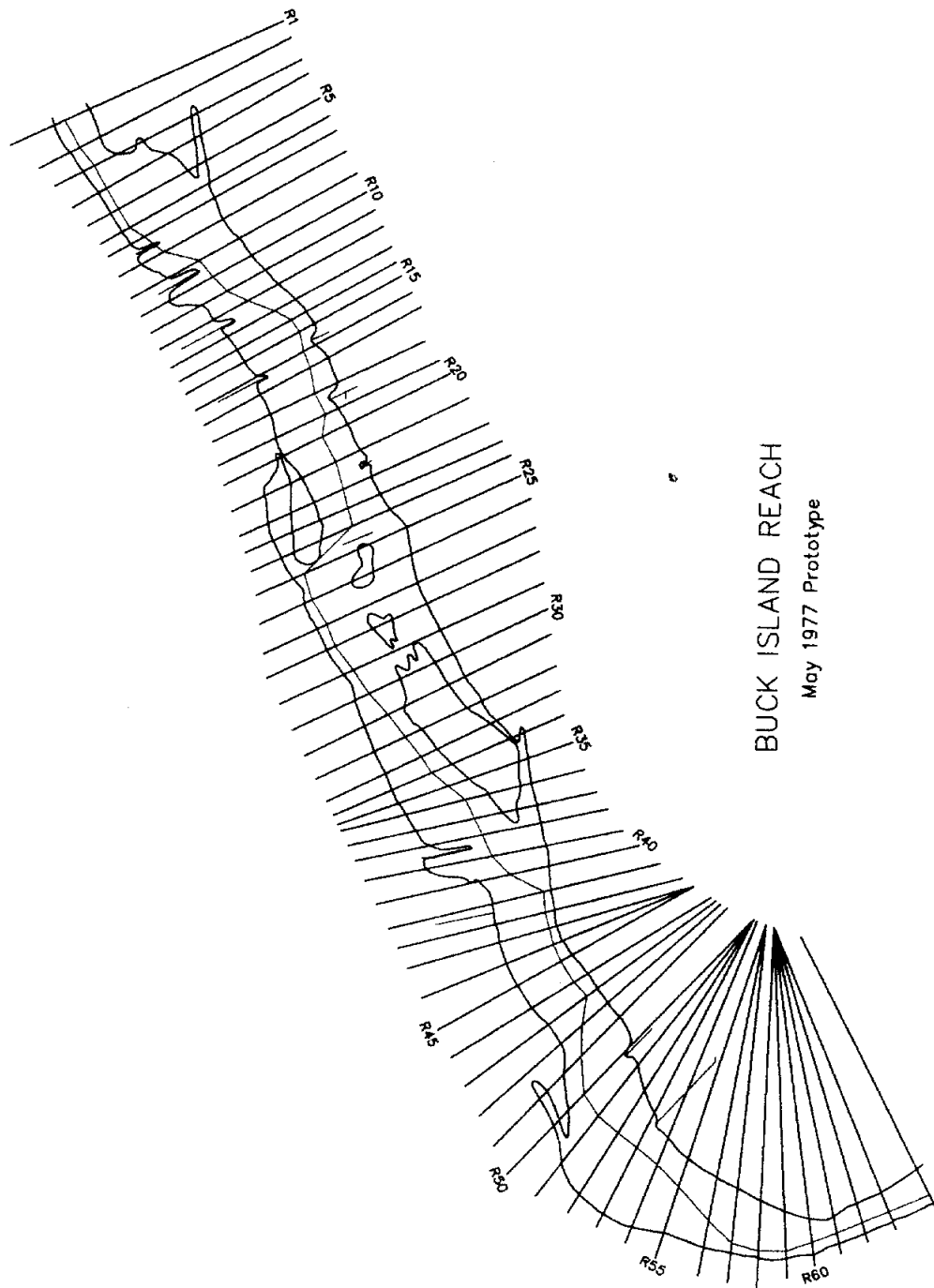


Figure B-3.1a Buck Island Model Plan View

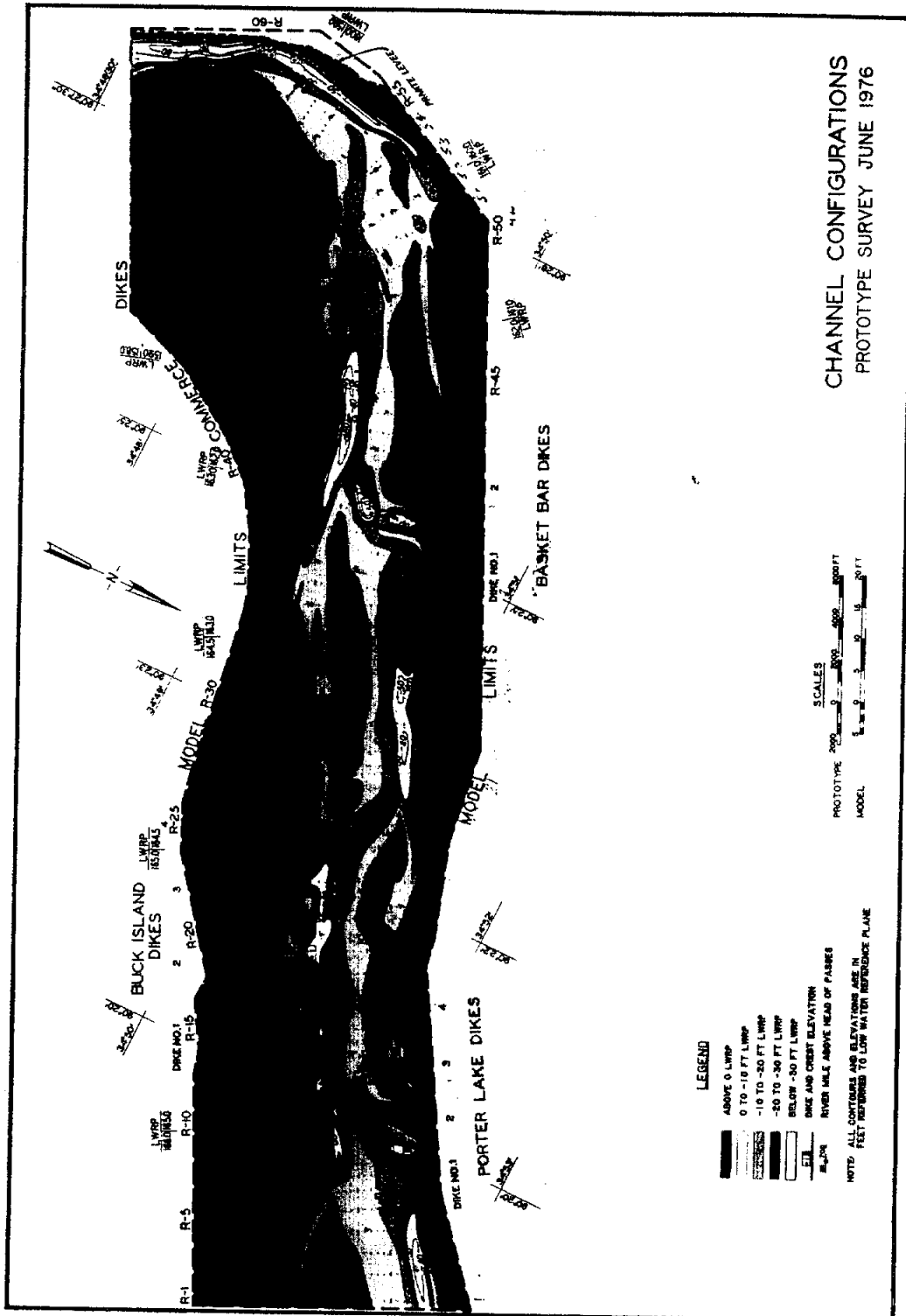


Figure B-3.1b Buck Island June 1976 Prototype Survey

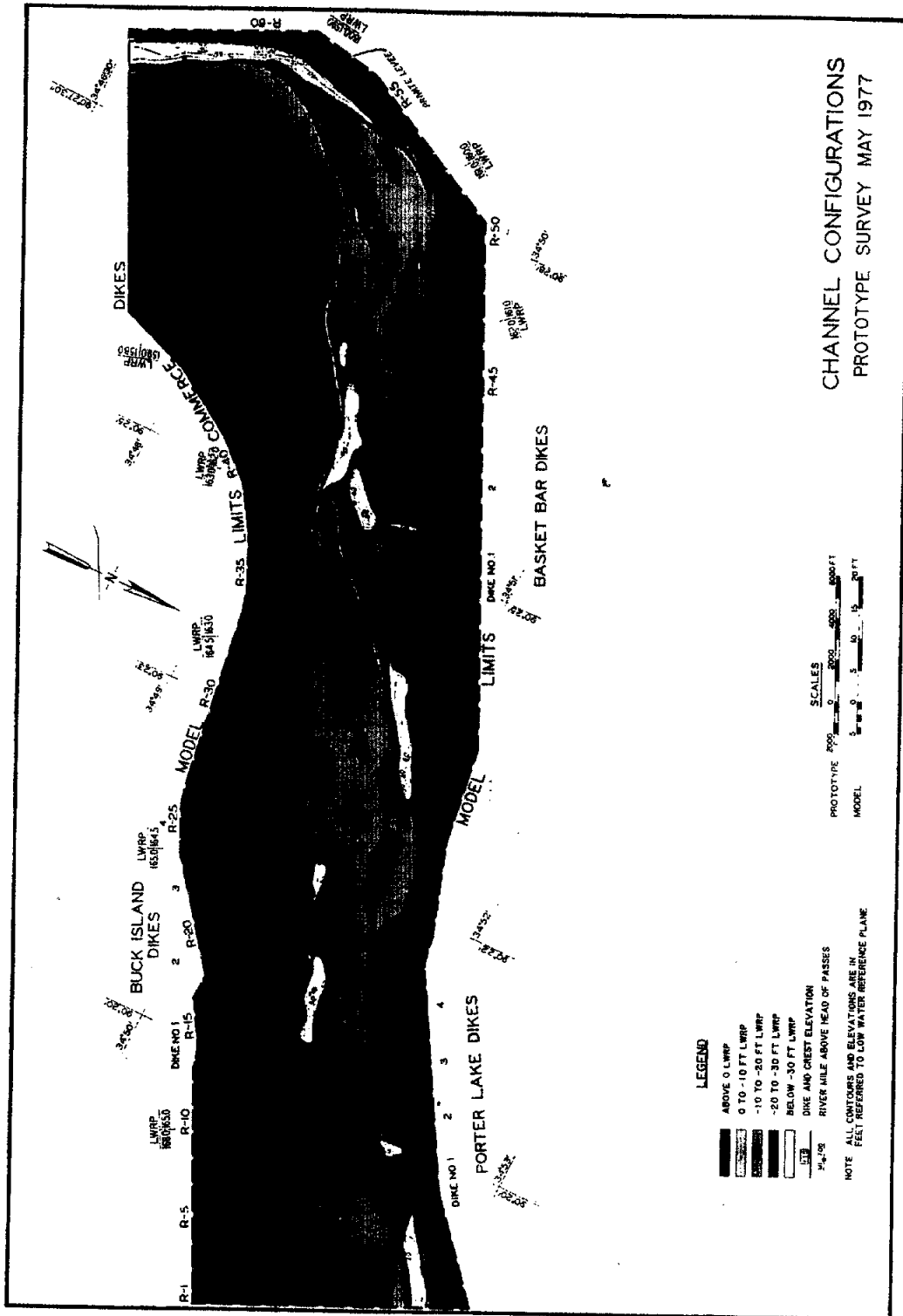


Figure B-3.1c Buck Island May 1977 Prototype Survey

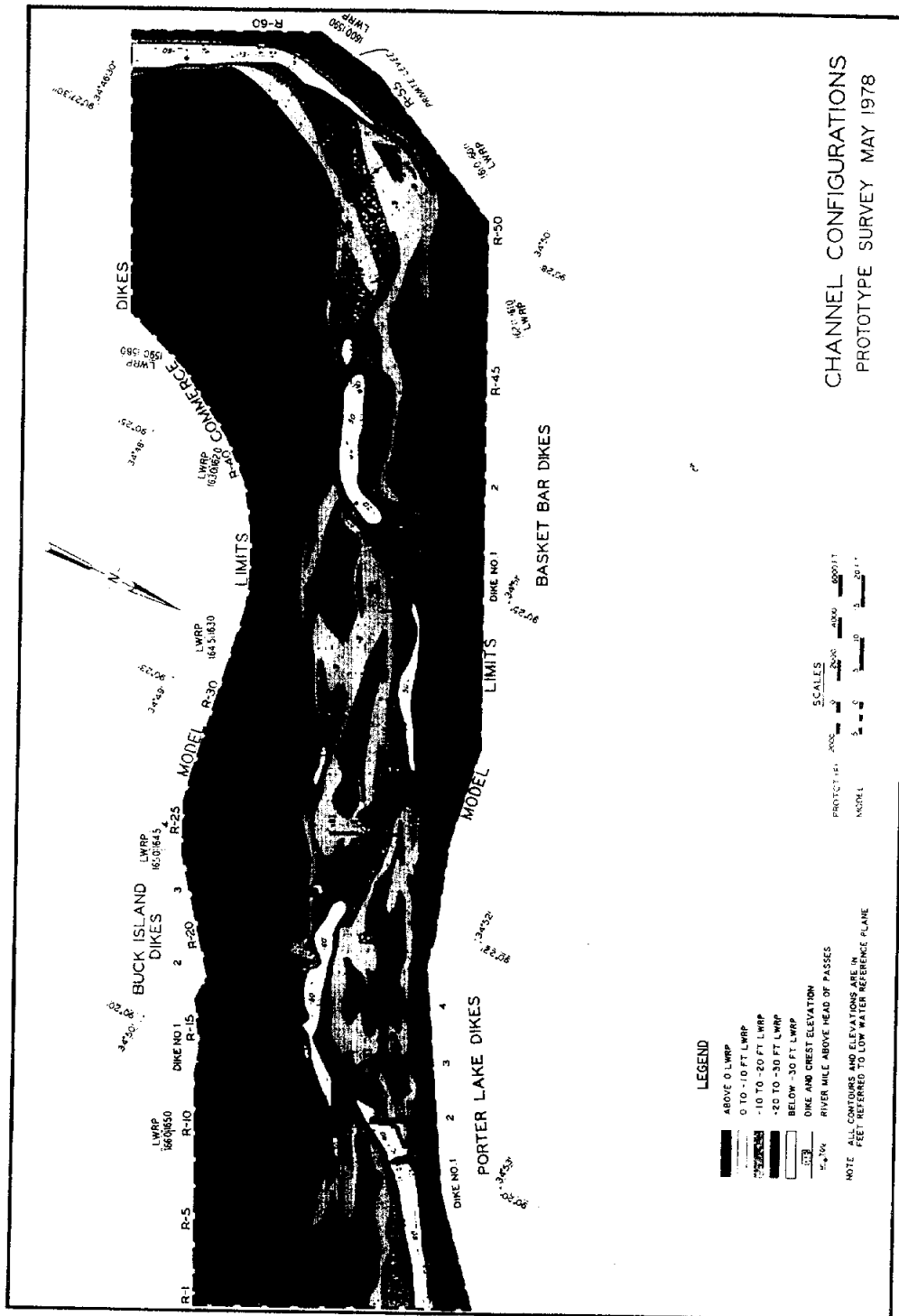


Figure B-3.1d Buck Island May 1978 Prototype Survey

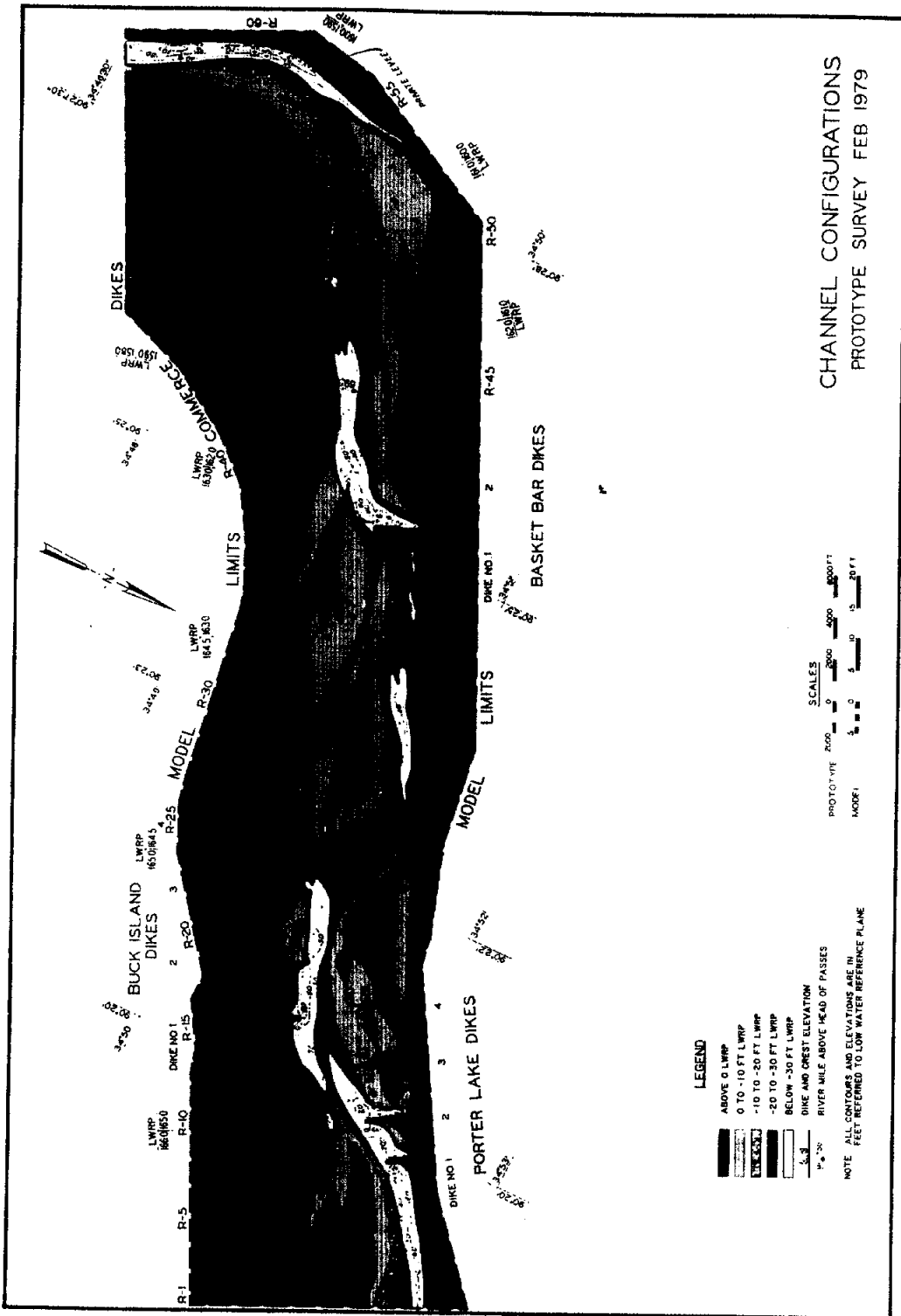


Figure B-3.1e Buck Island February 1979 Prototype Survey

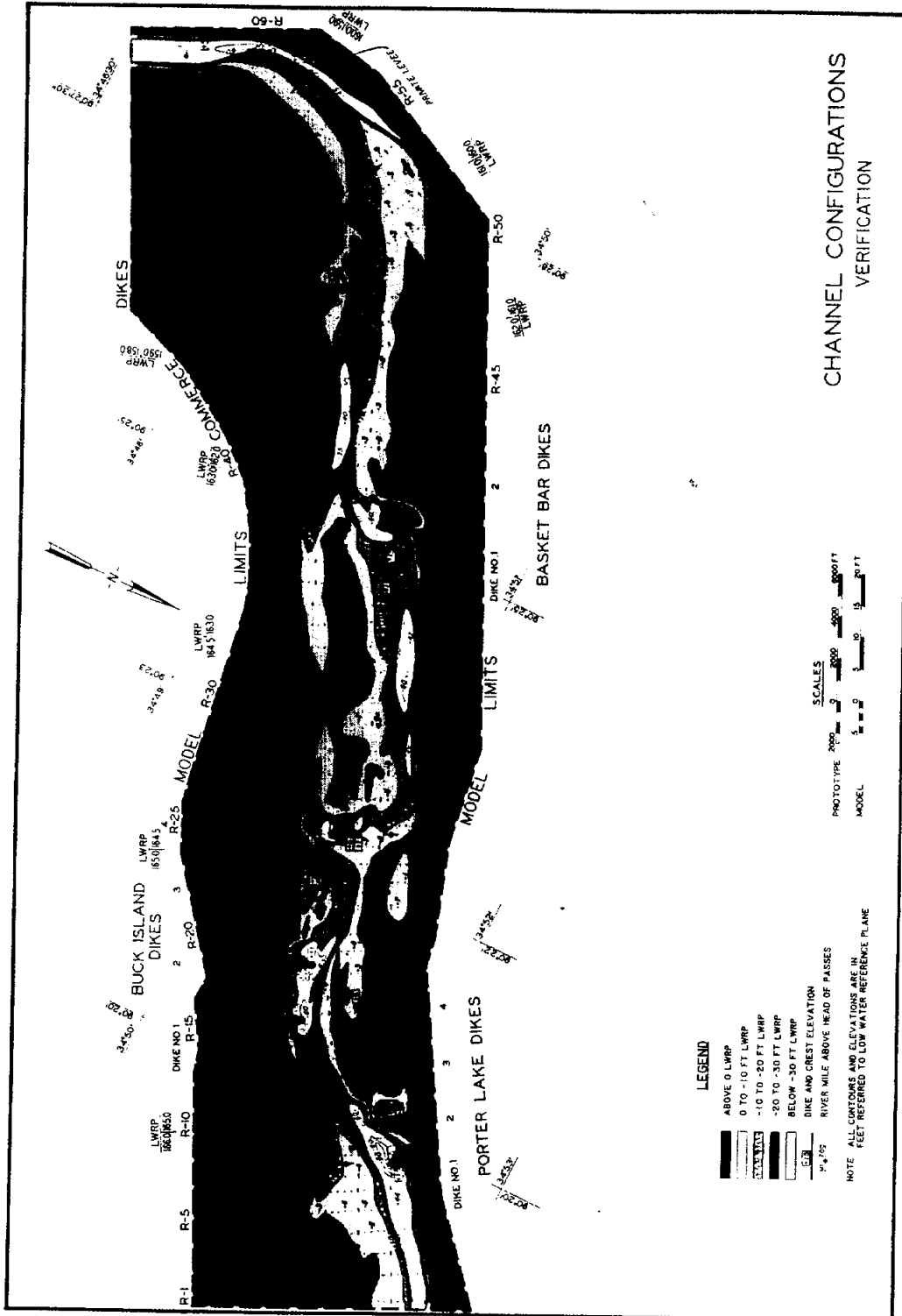


Figure B-3.1f Buck Island Verification Test Survey

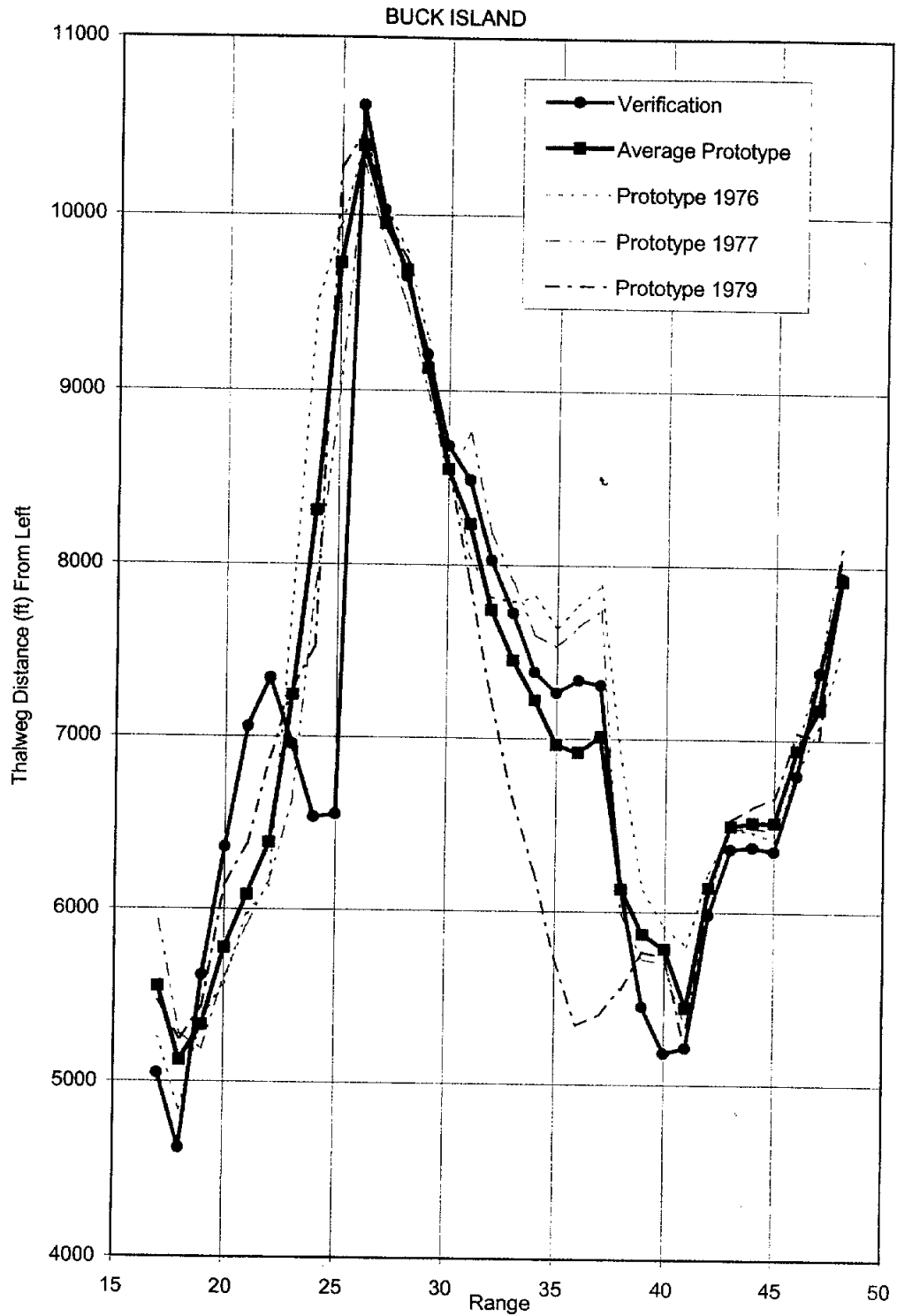


Figure B-3.2a Thalweg Position From Left by Range, Buck Island

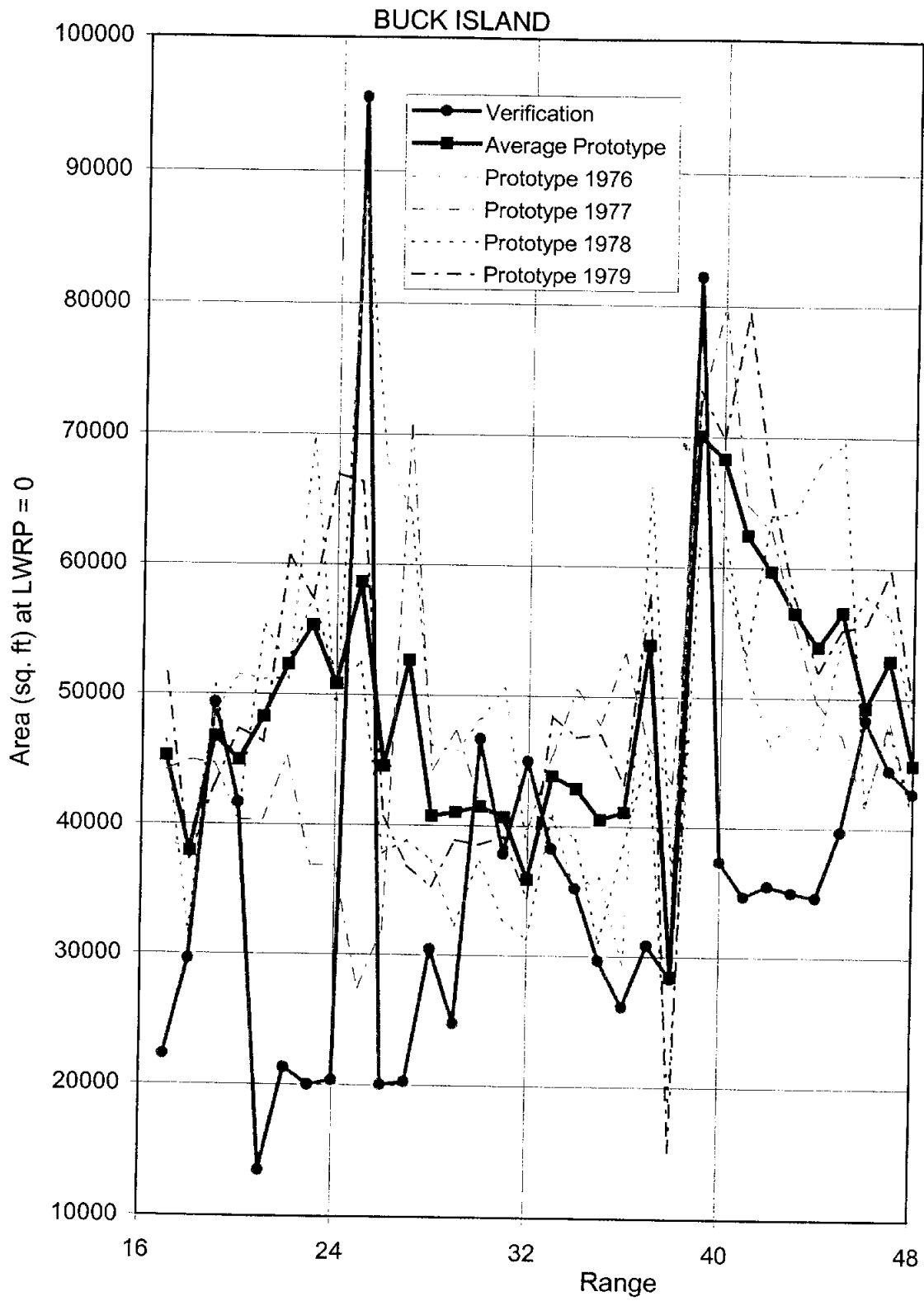


Figure B-3.2b Cross-Section Area by Range, Buck Island

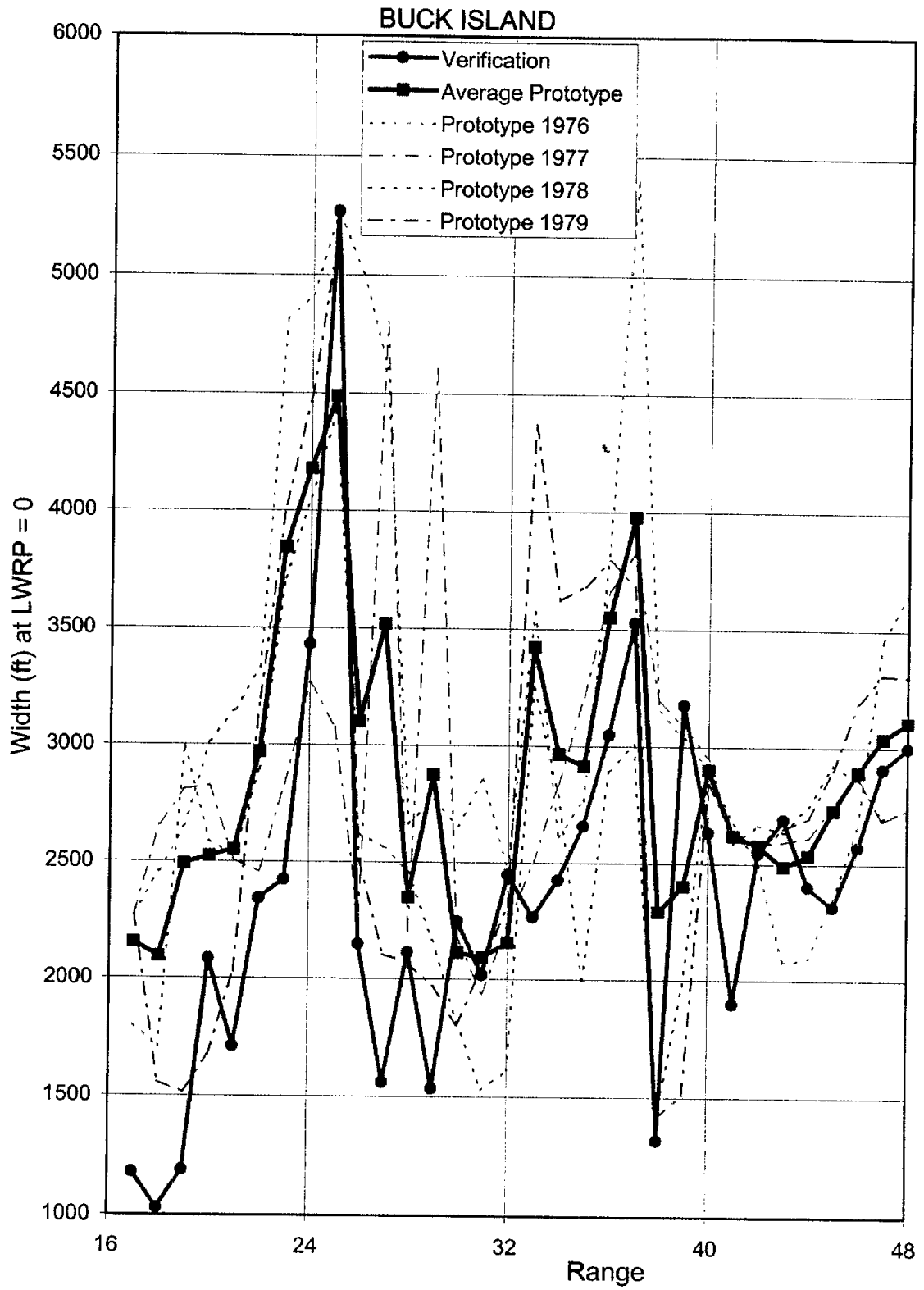


Figure B-3.2c Top Width by Range, Buck Island

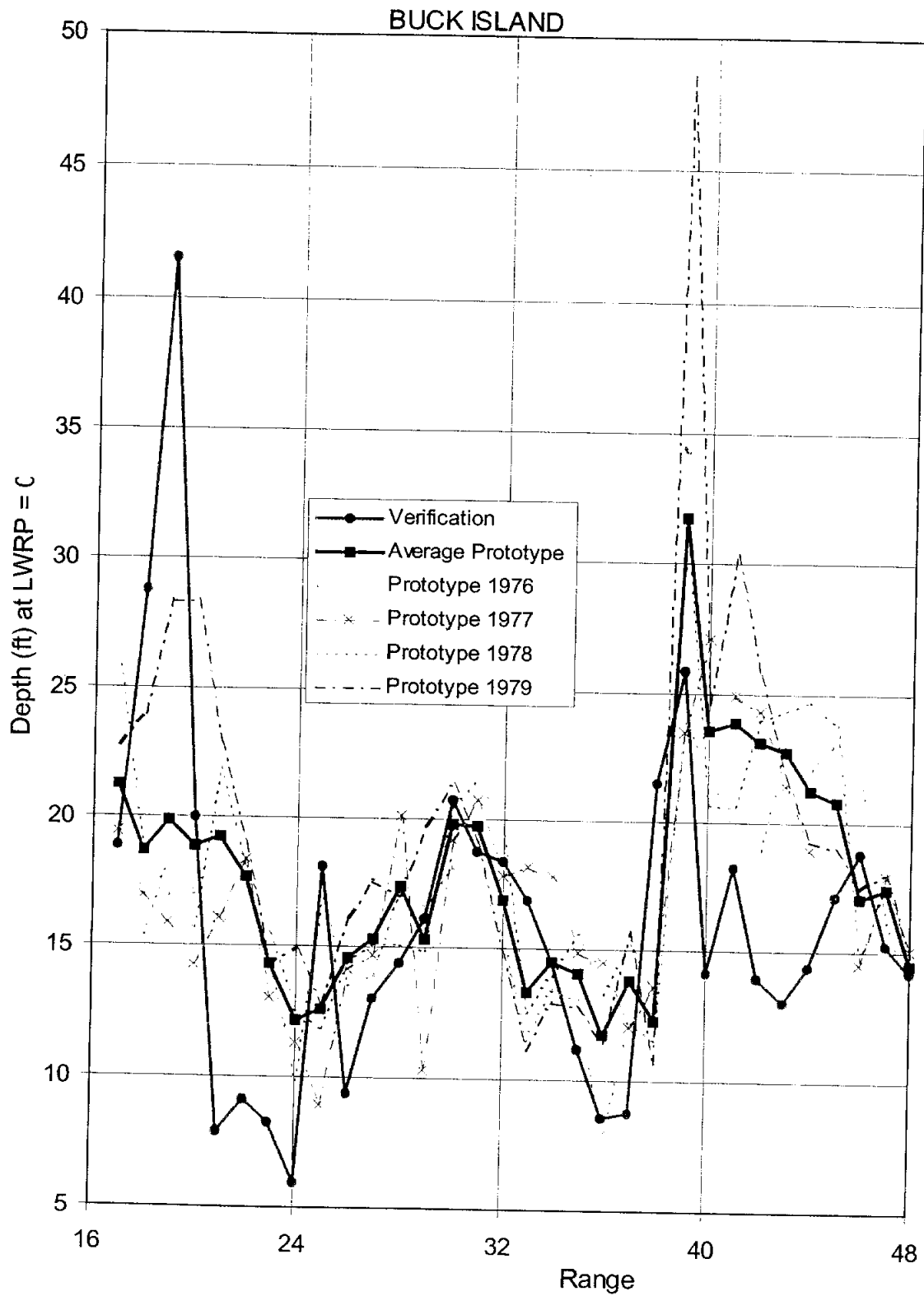


Figure B-3.2d Hydraulic Depth by Range, Buck Island

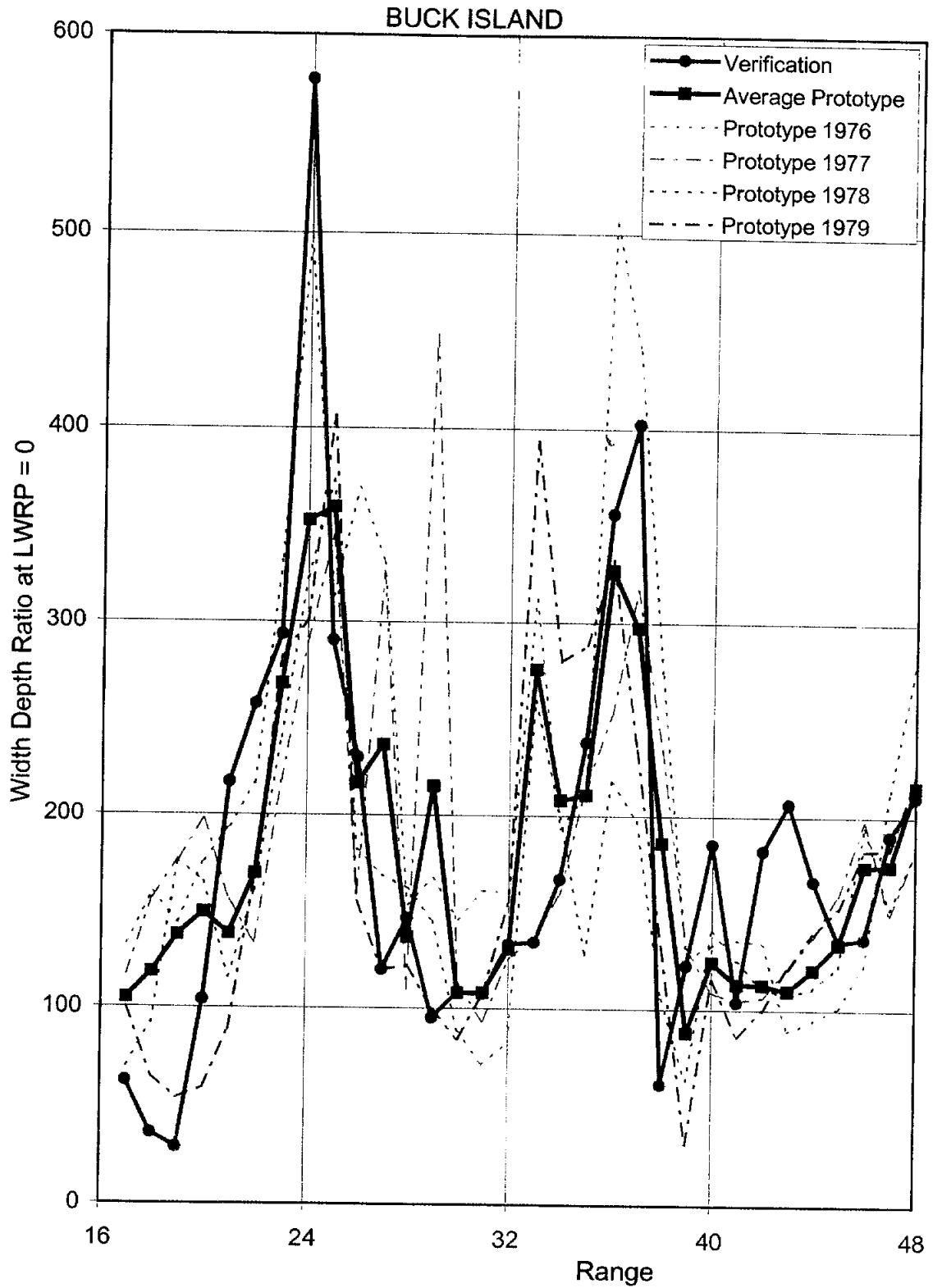


Figure B-3.2e Width/Depth Ratio by Range, Buck Island

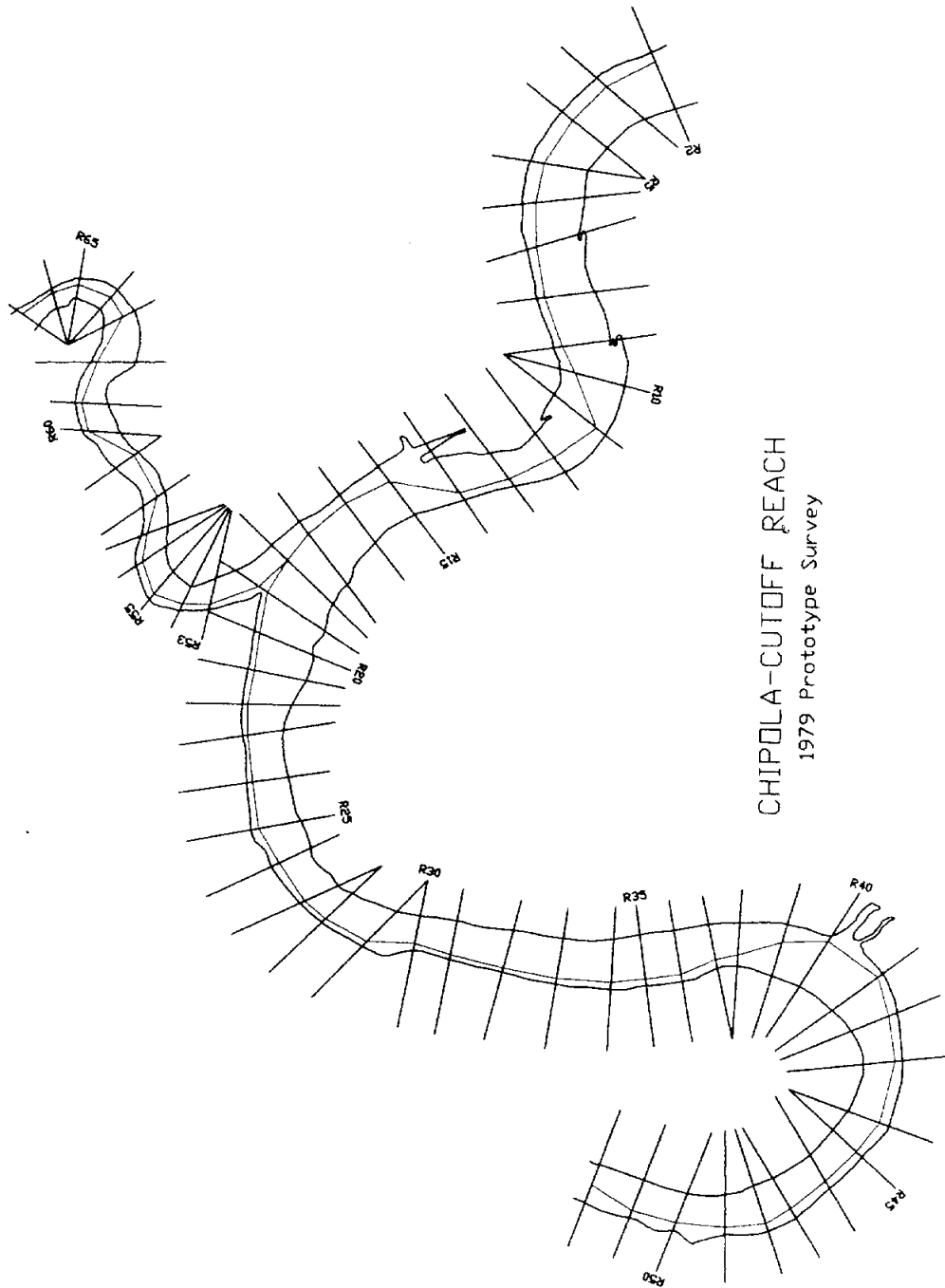


Figure B-4.1a Chipola-Cutoff Model Plan View

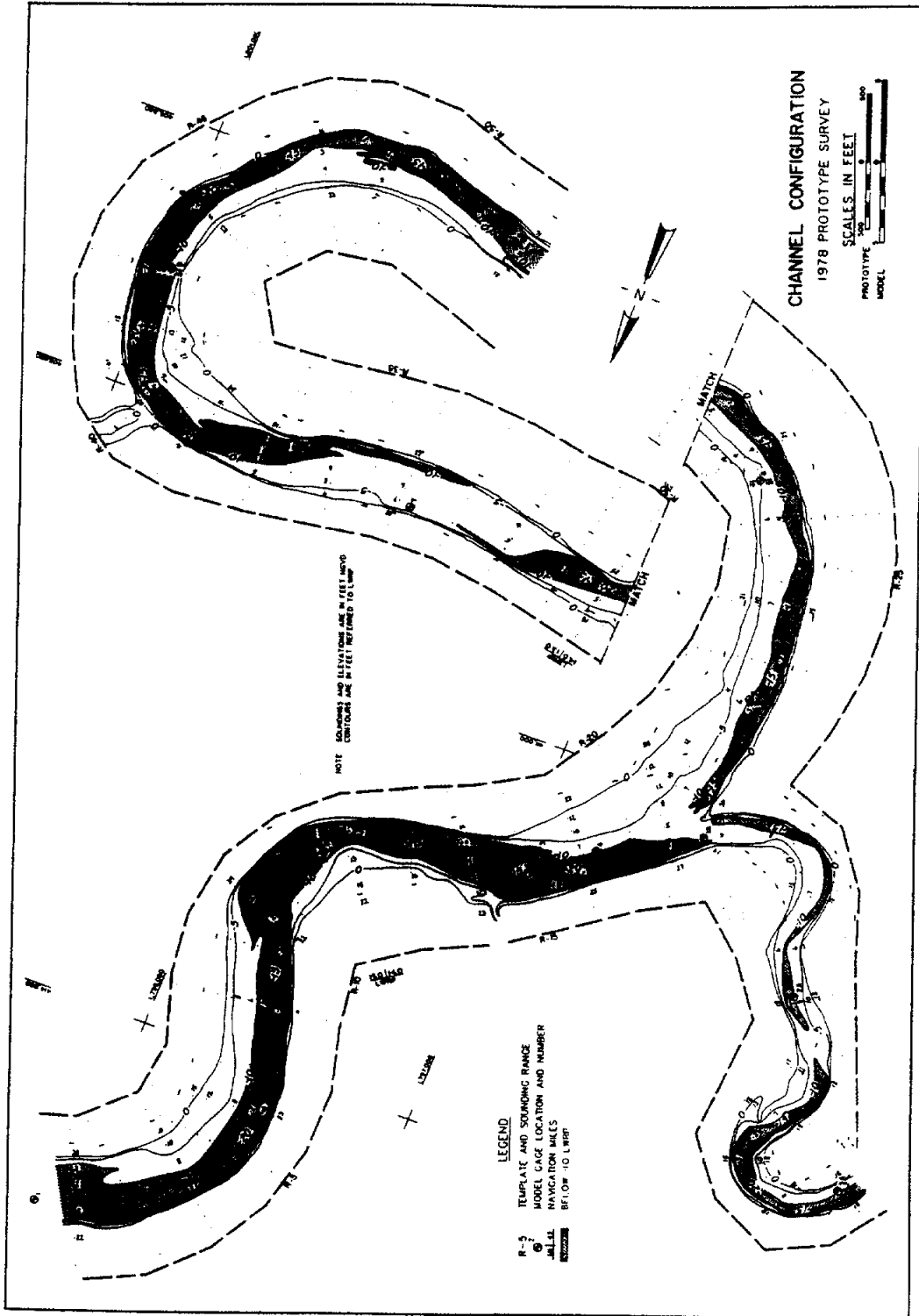


Figure B-4.1b Chipola-Cutoff January 1978 Prototype Survey

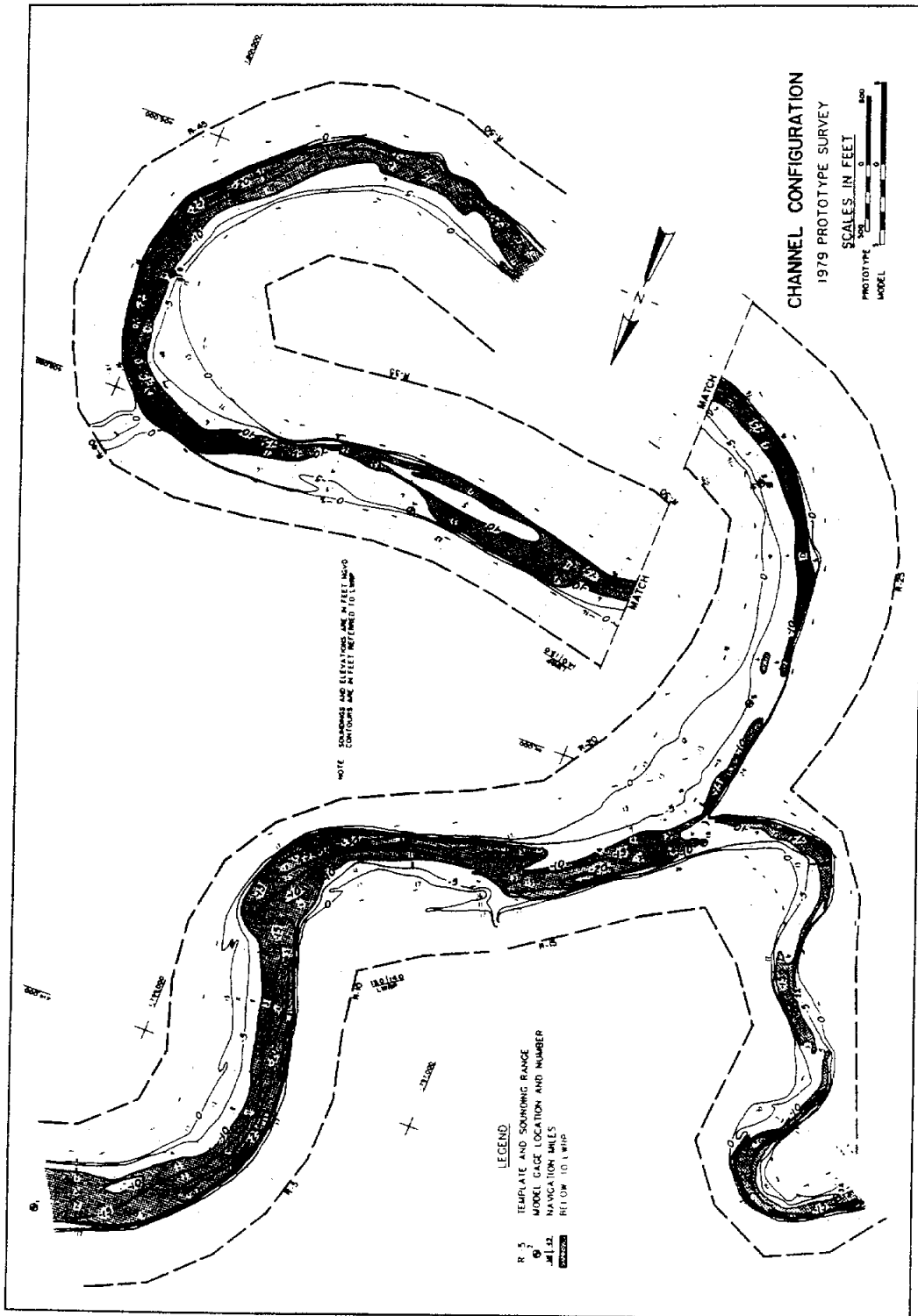


Figure B-4.1c Chipola-Cutoff June 1979 Prototype Survey

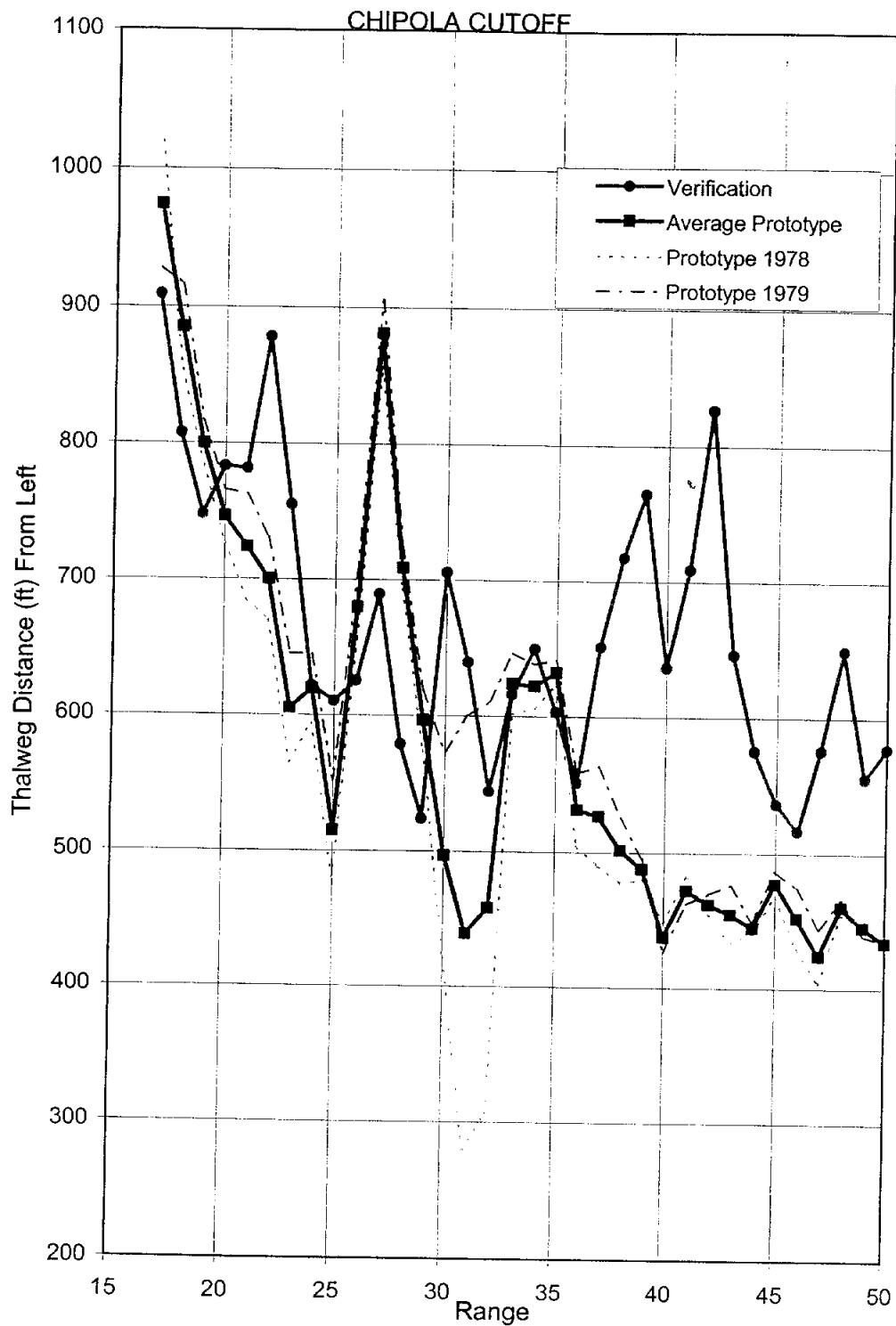


Figure B-4.2a Thalweg Position From Left by Range, Chipola Cutoff

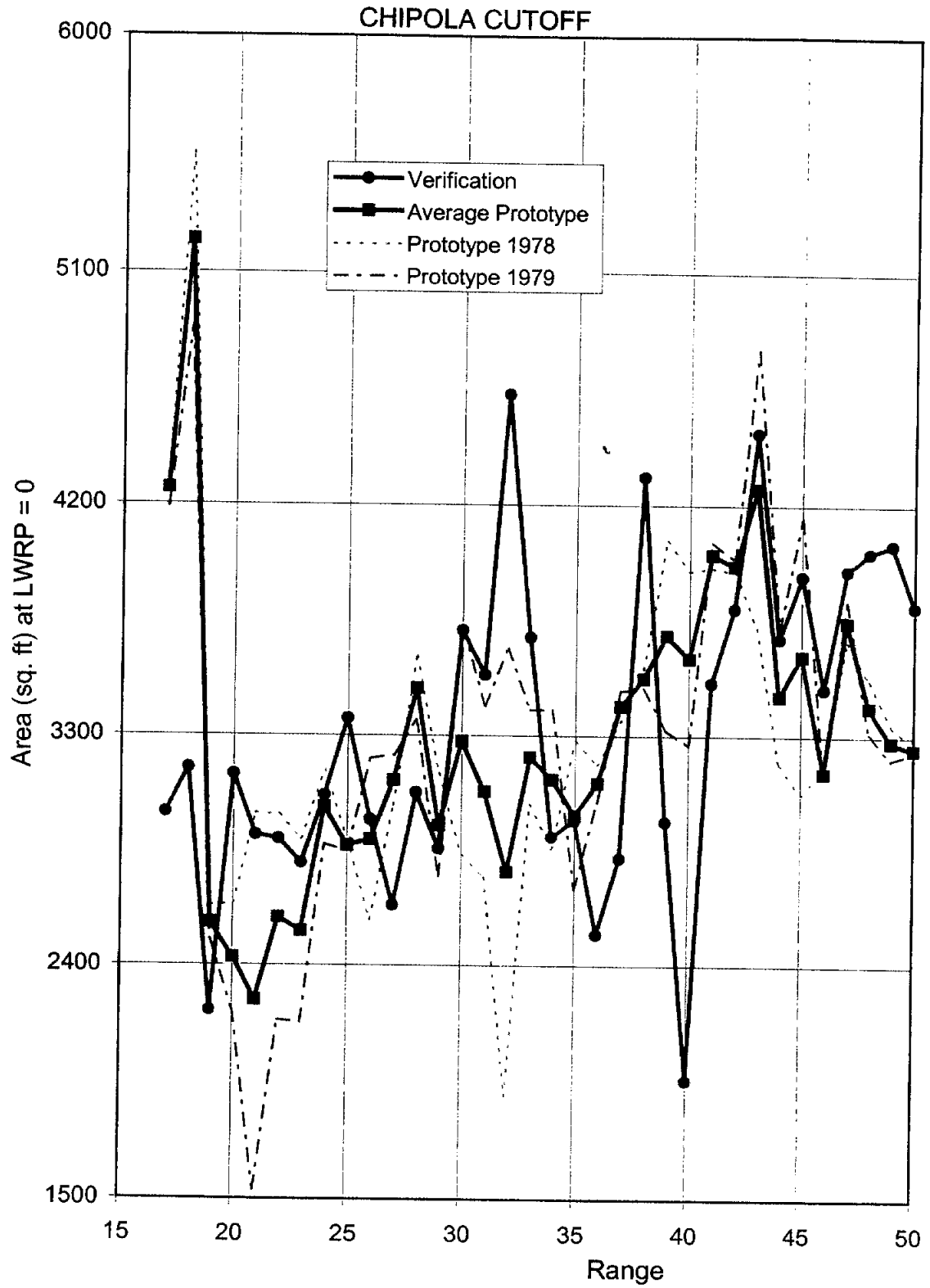


Figure B-4.2b Cross-Section Area by Range, Chipola Cutoff

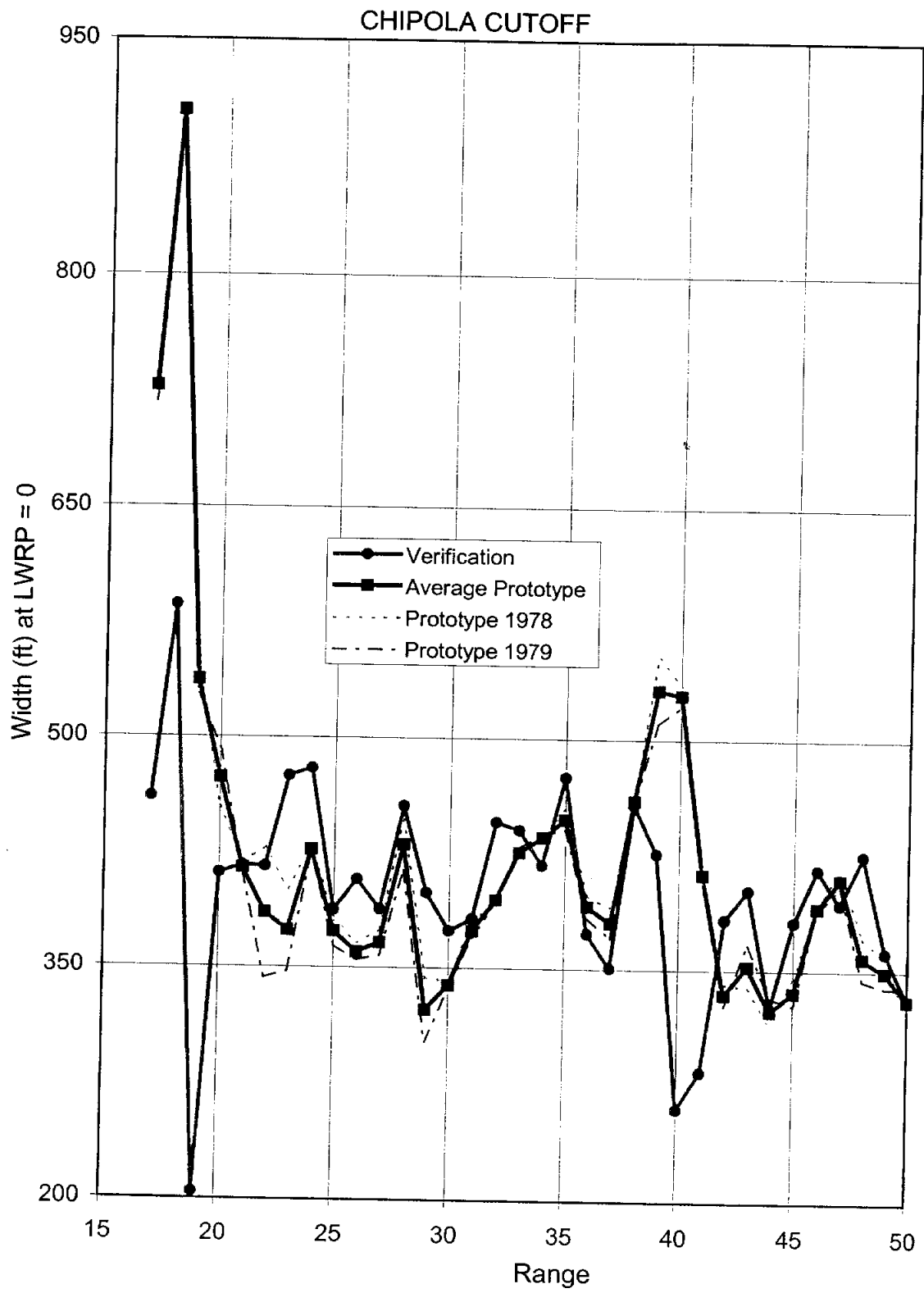


Figure B-4.2c Top Width by Range, Chipola Cutoff

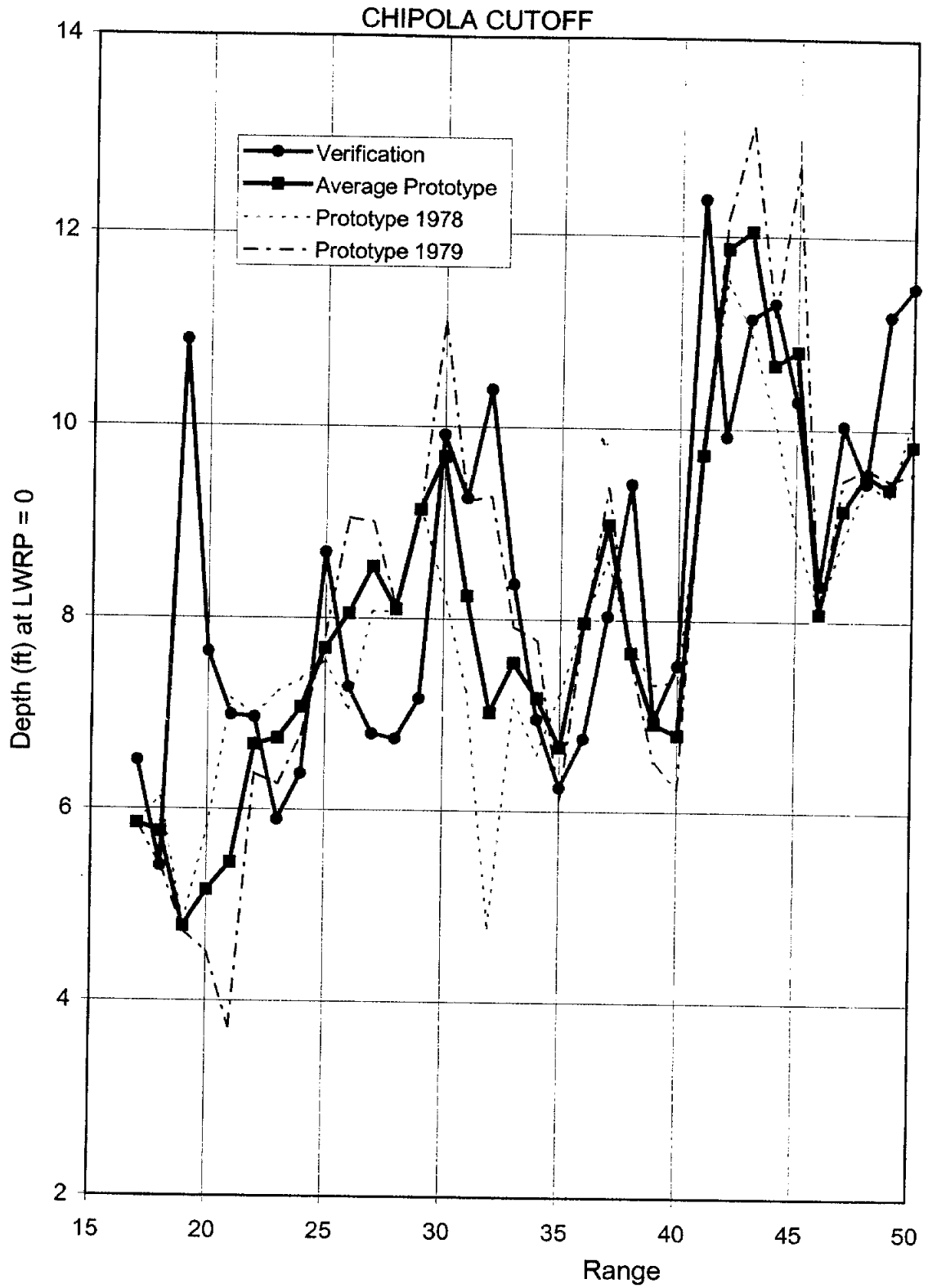


Figure B-4.2d Hydraulic Depth by Range, Chipola Cutoff

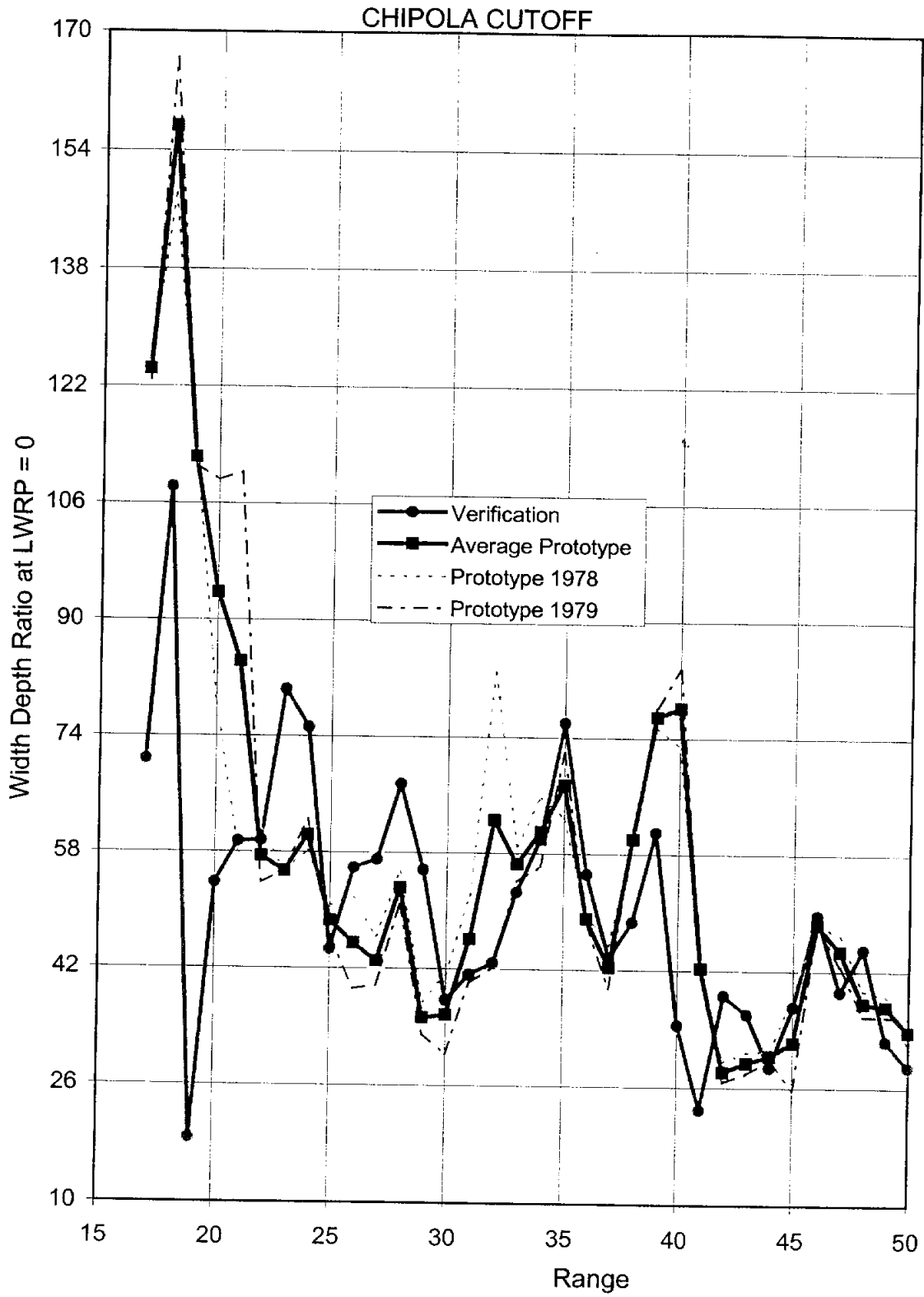
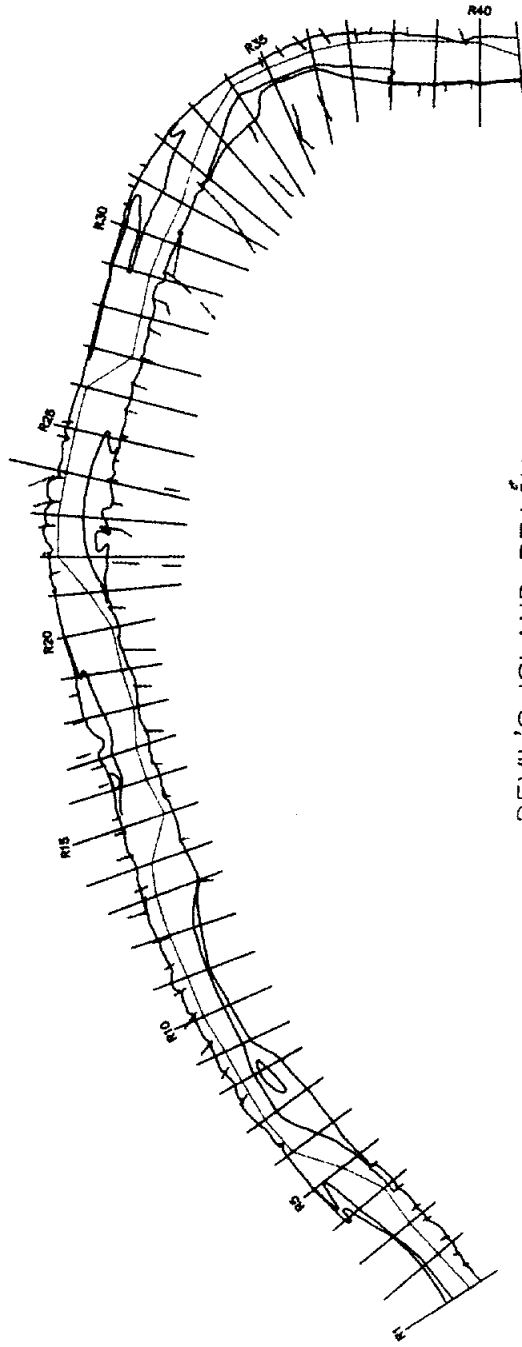


Figure B-4.2e Width/Depth Ratio by Range, Chipola Cutoff



DEVIL'S ISLAND REACH
November 1969 Prototype

Figure B-5.1a Devil's Island Model Plan View

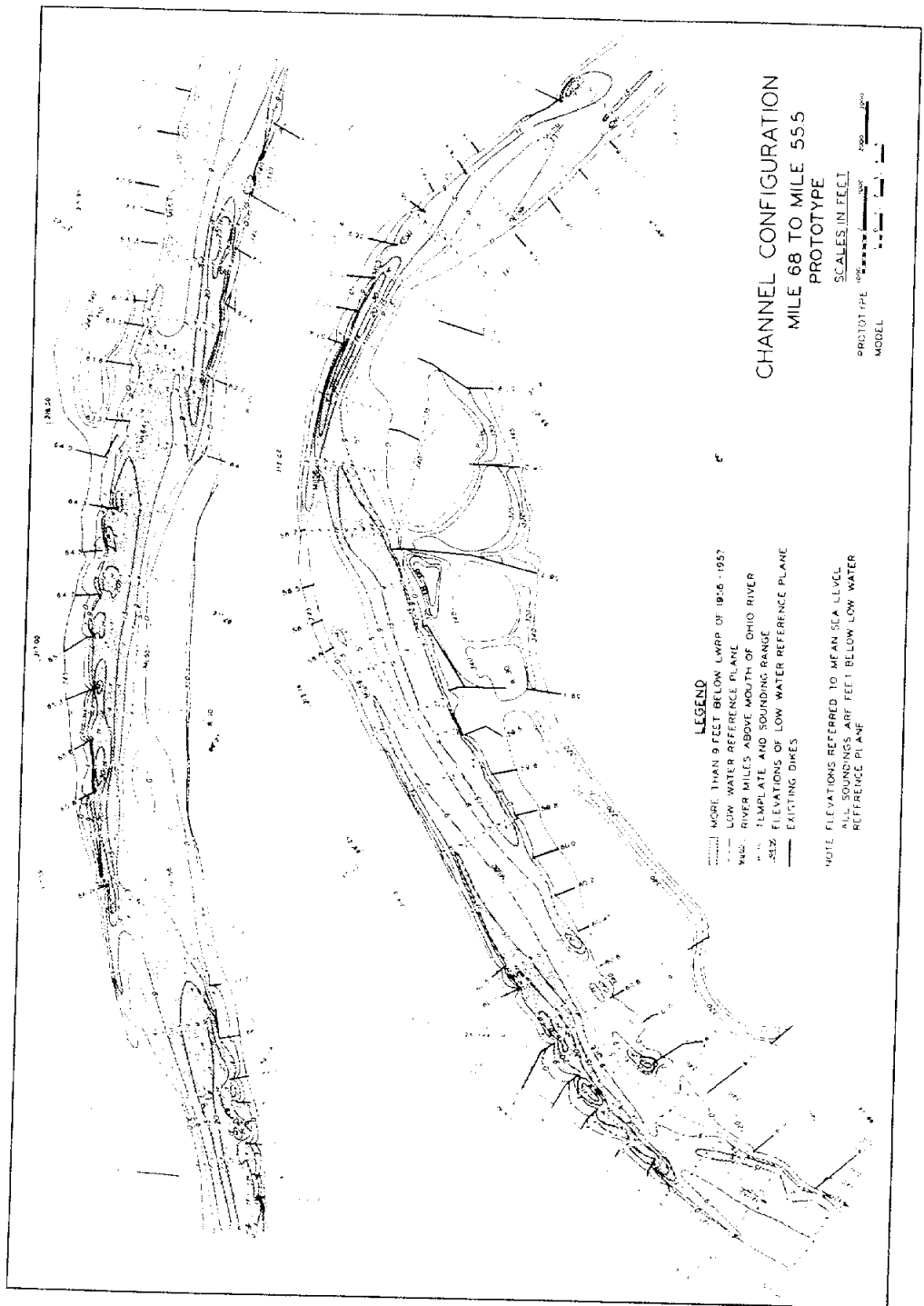


Figure B-5.1b Devil's Island November 1969 Prototype Survey

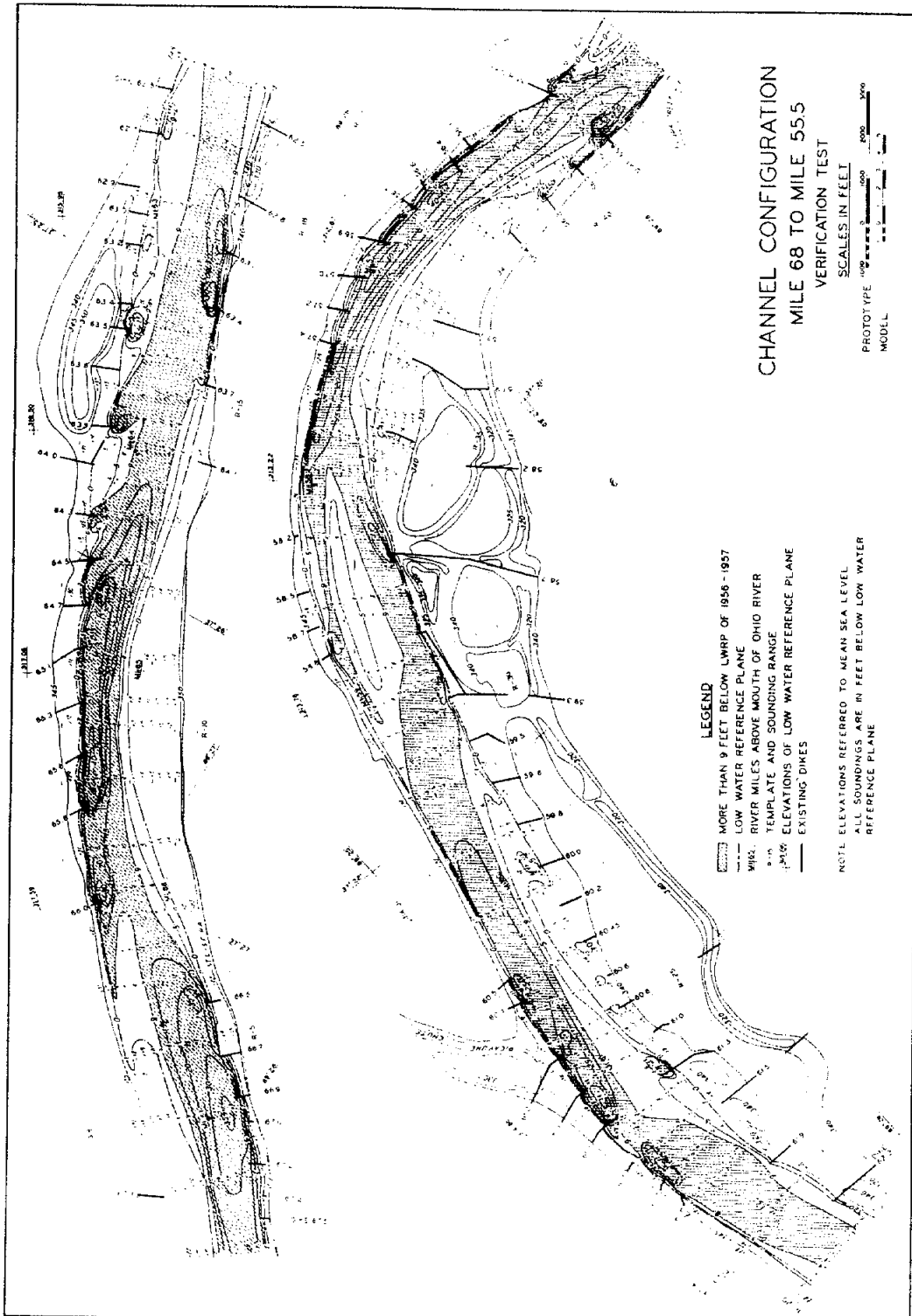


Figure B-5.1c Devil's Island Verification Test Survey

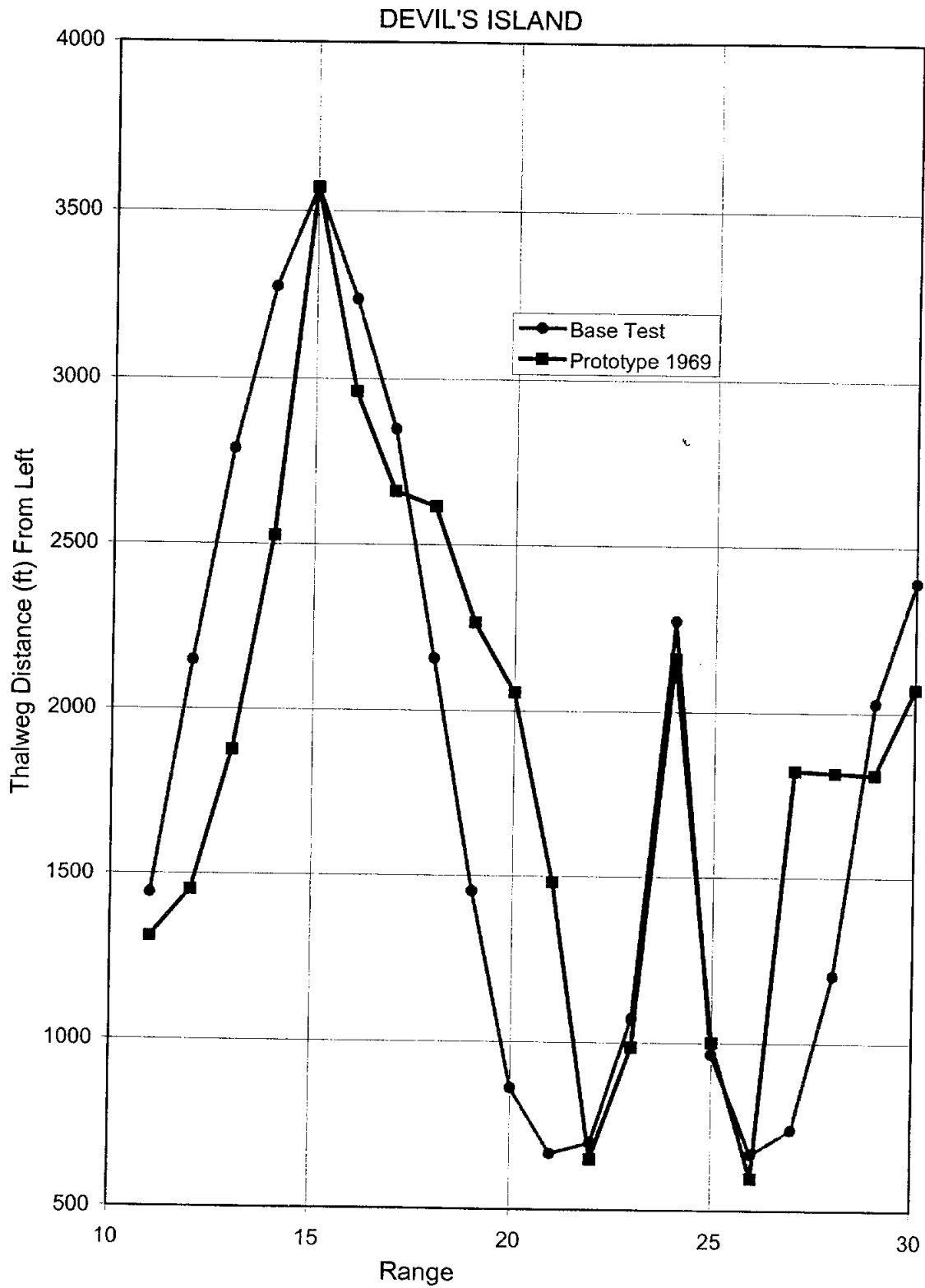


Figure B-5.2a Thalweg Position From Left by Range, Devil's Island

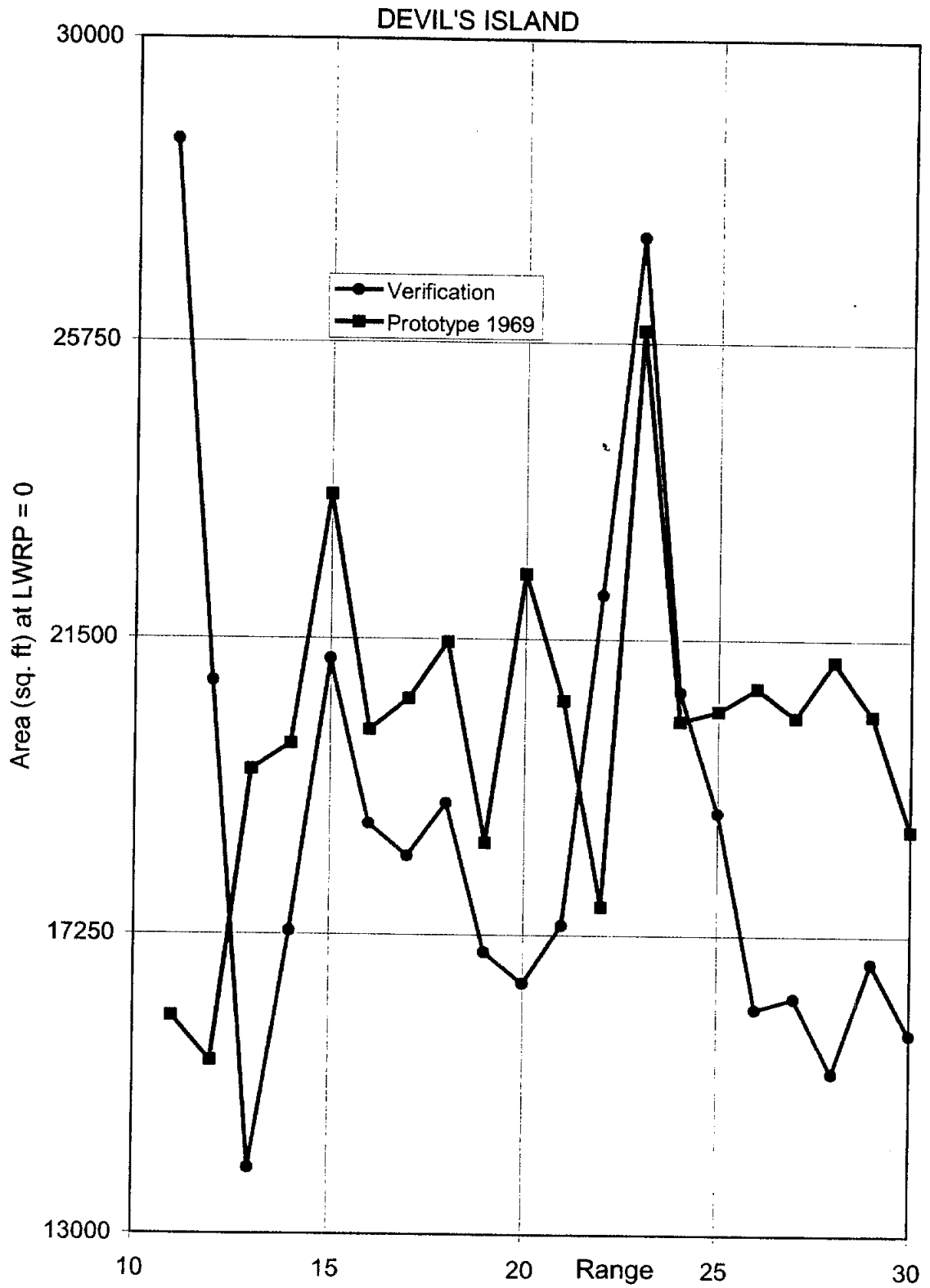


Figure B-5.2b Cross-Section Area by Range, Devil's Island

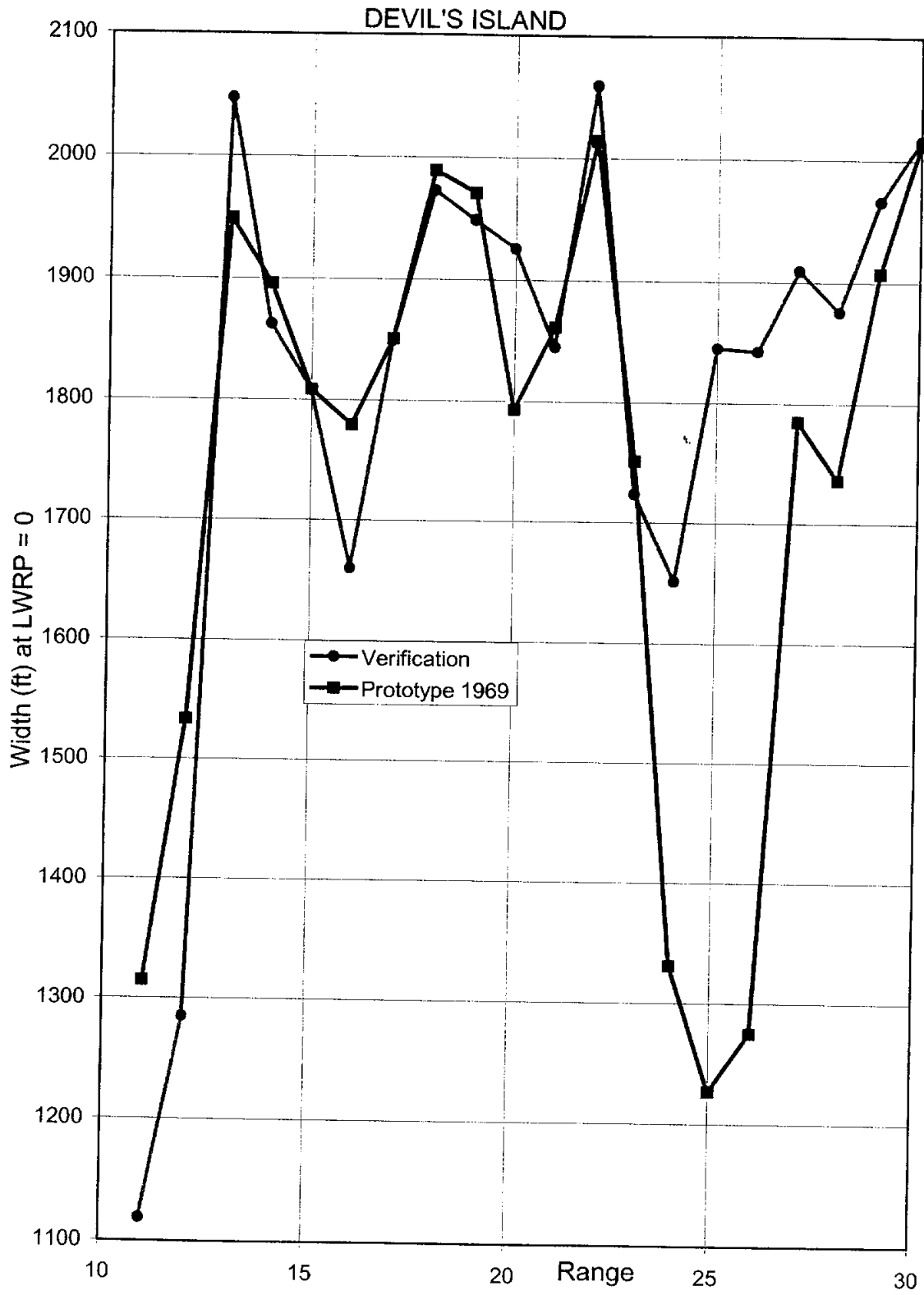


Figure B-5.2c Top Width by Range, Devil's Island

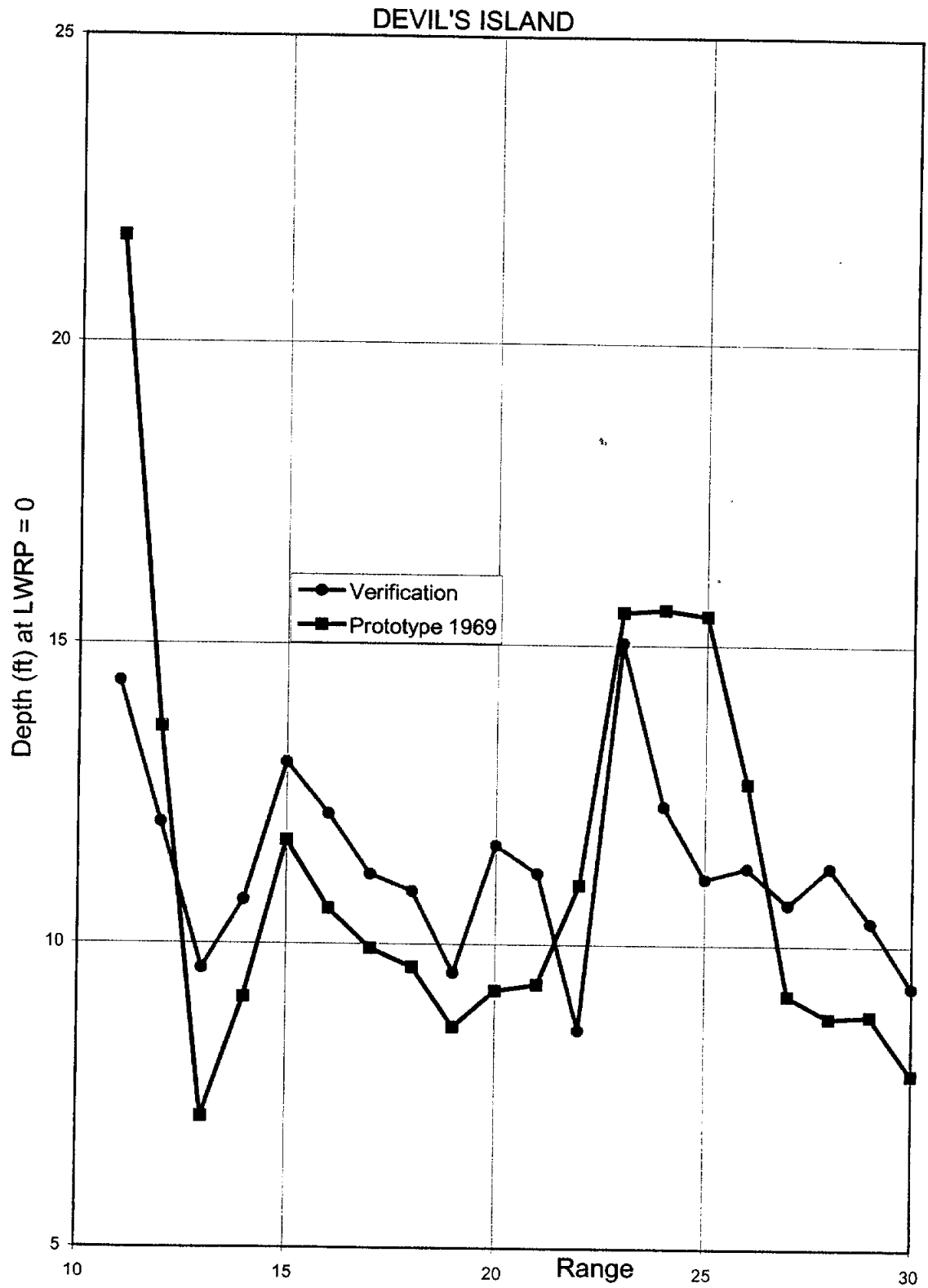


Figure B-5.2d Hydraulic Depth by Range, Devil's Island

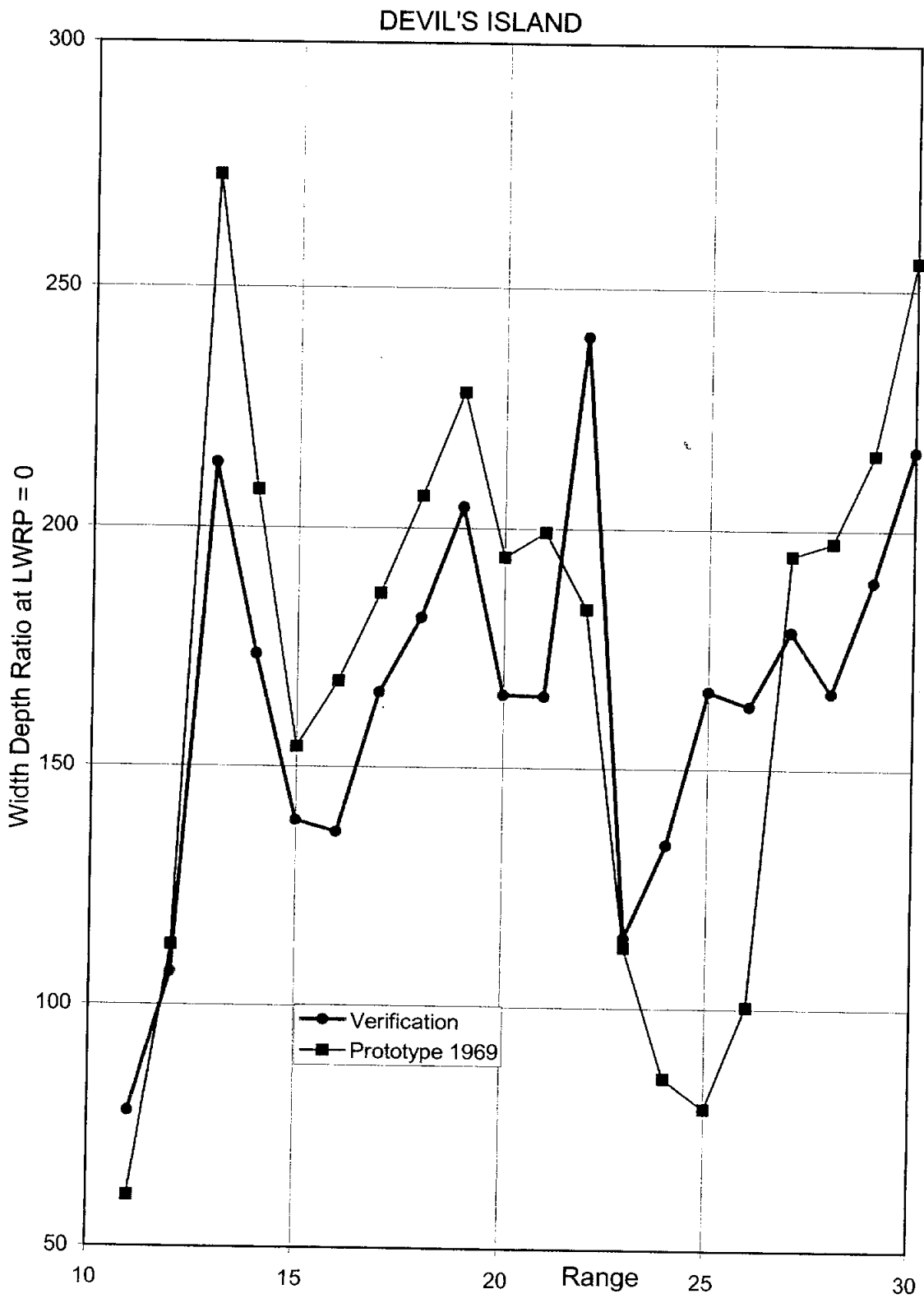


Figure B-5.2e Width/Depth Ratio by Range, Devil's Island

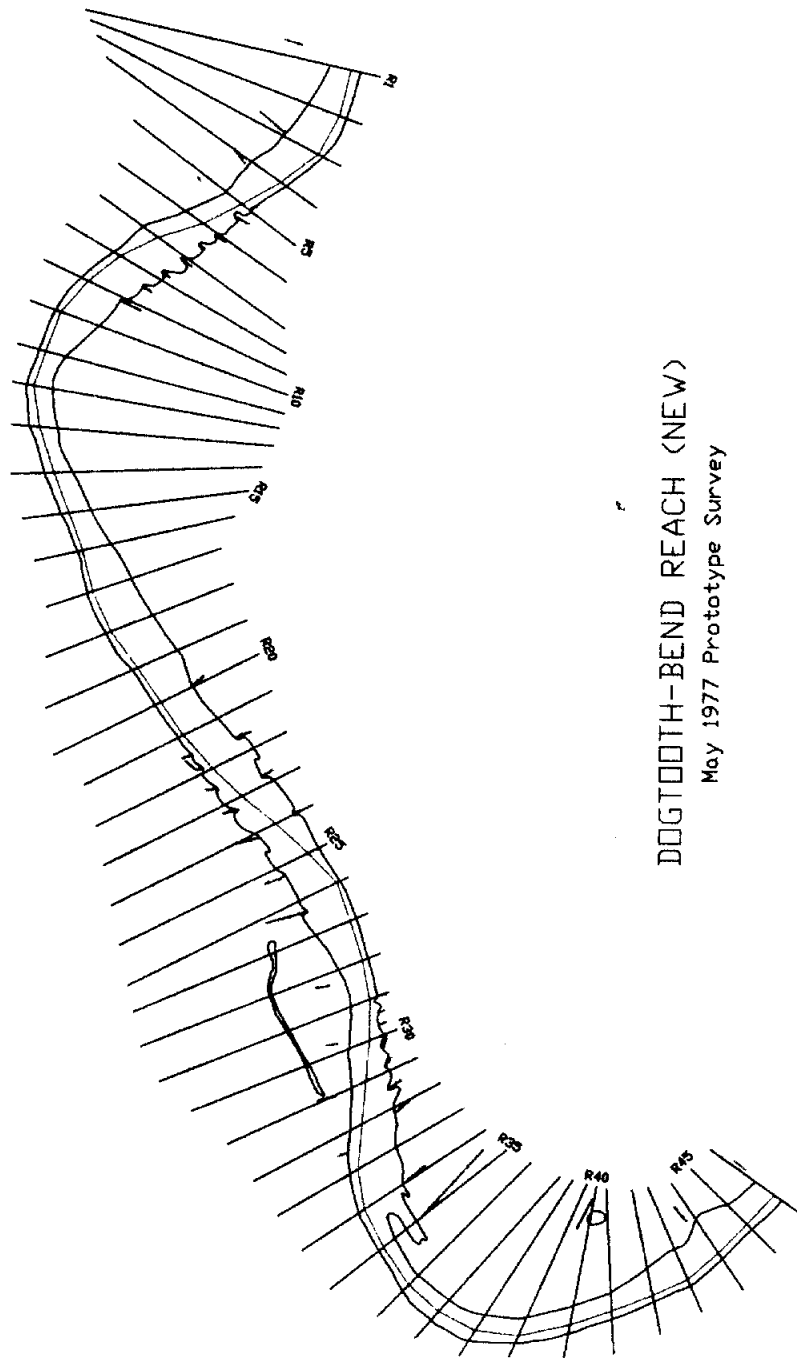


Figure B-6.1a Dogtooth Bend Model Plan View

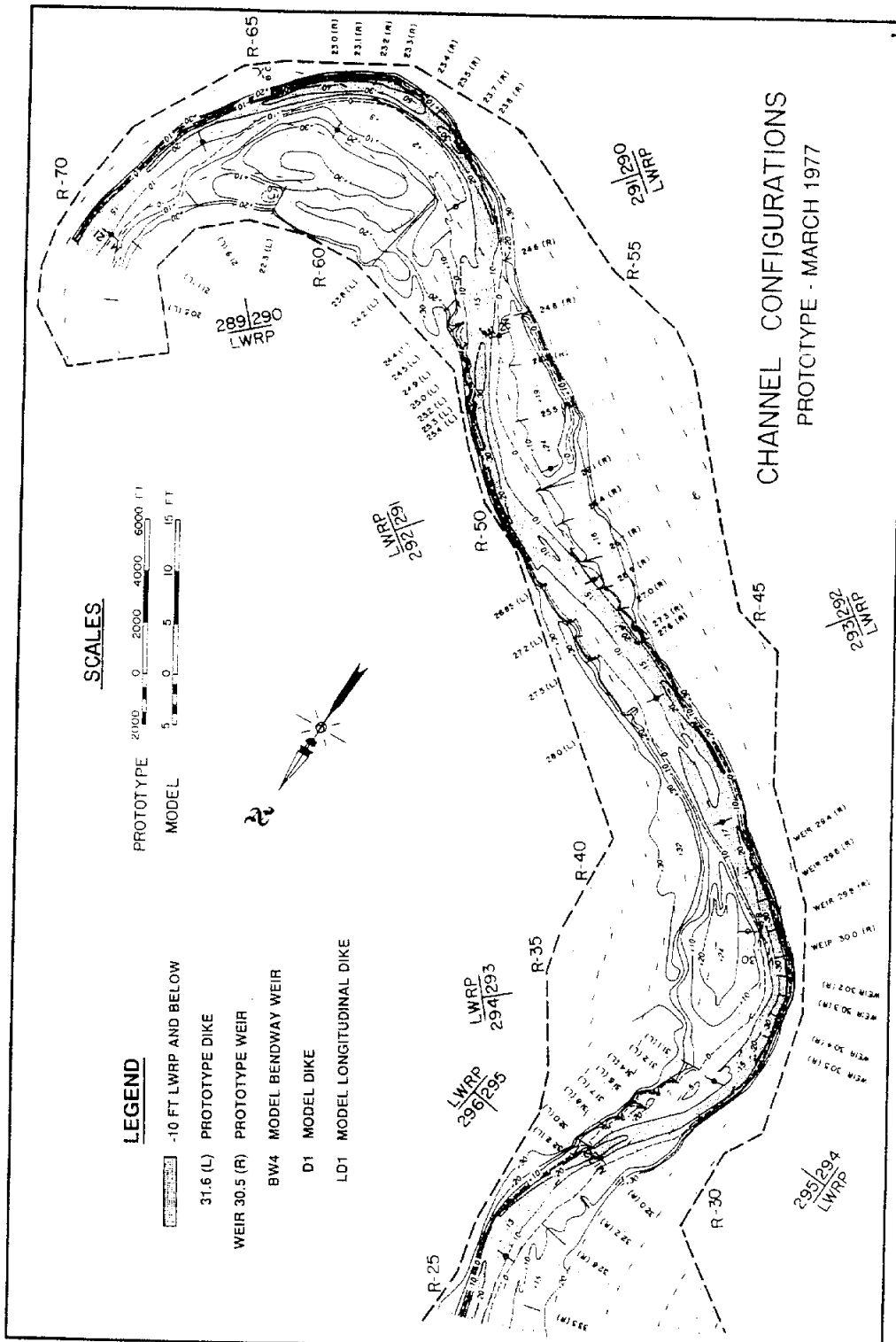


Figure B-6.1b Dogtooth Bend March 1977 Prototype Survey

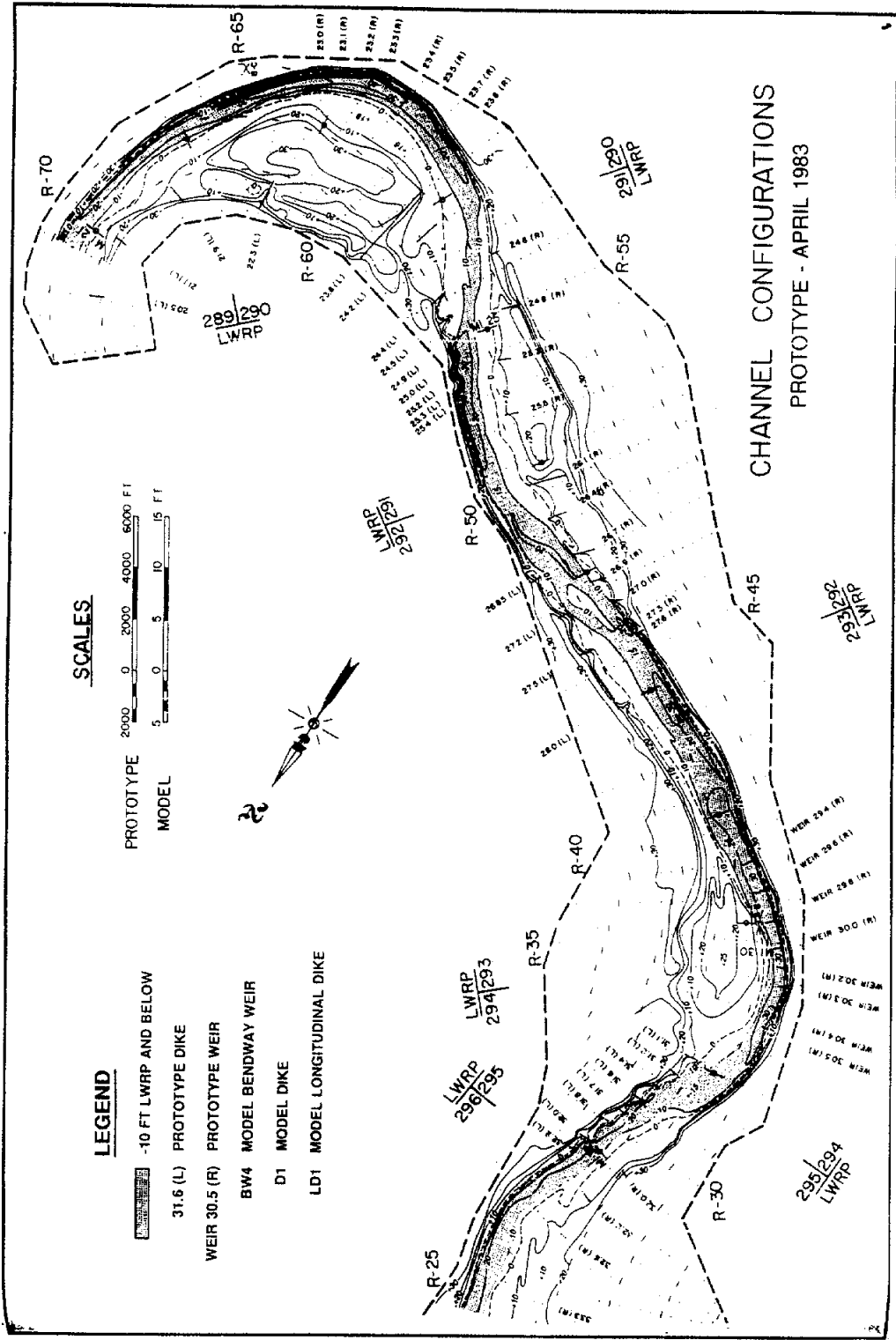


Figure B-6.1c Dogtooth Bend April 1983 Prototype Survey

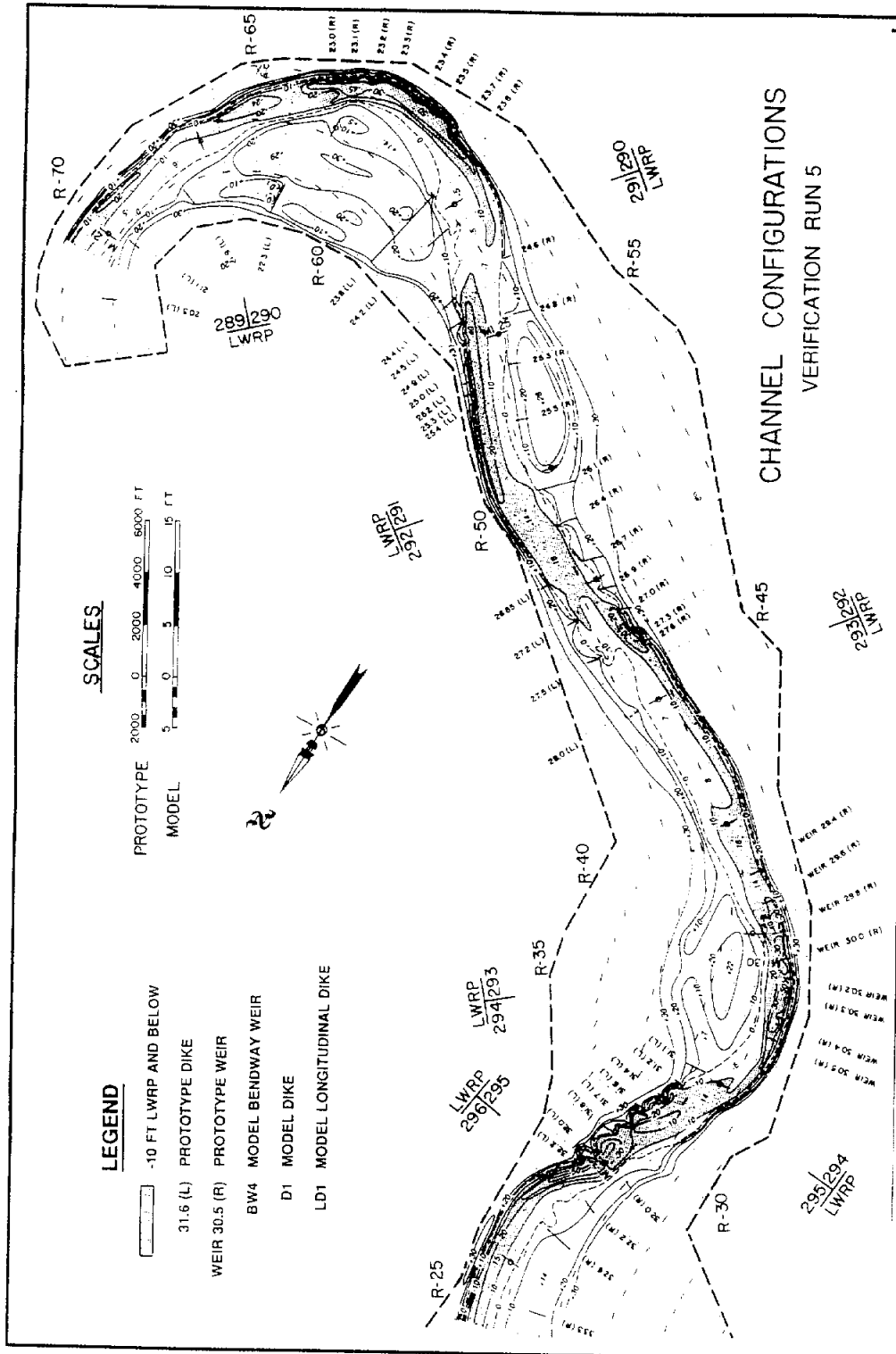


Figure B-6.1d Dogtooth Bend Verification Test Survey

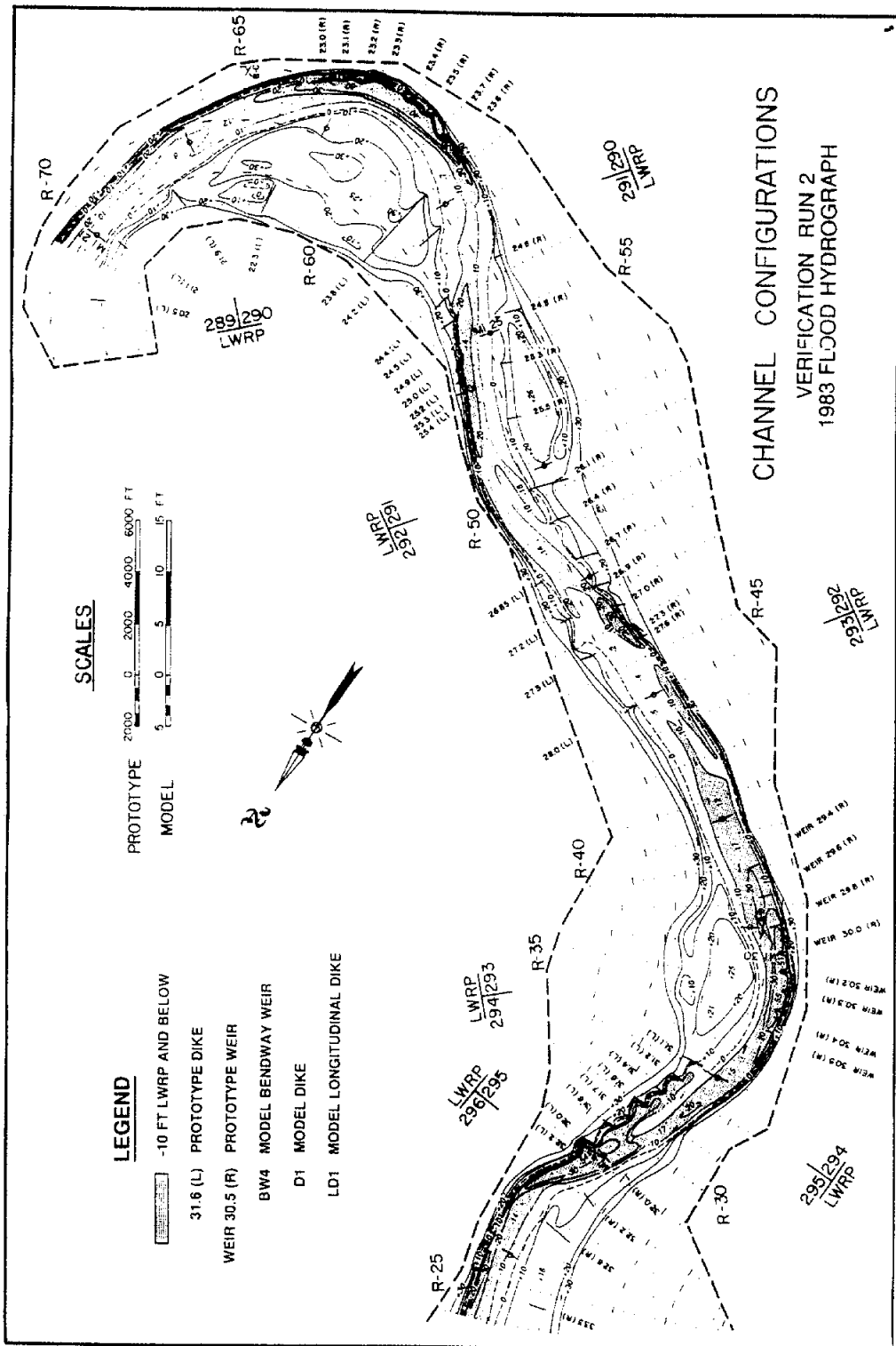


Figure B-6.1e Dogtooth Bend Verification Test Survey (with 1983 flood hydrograph)

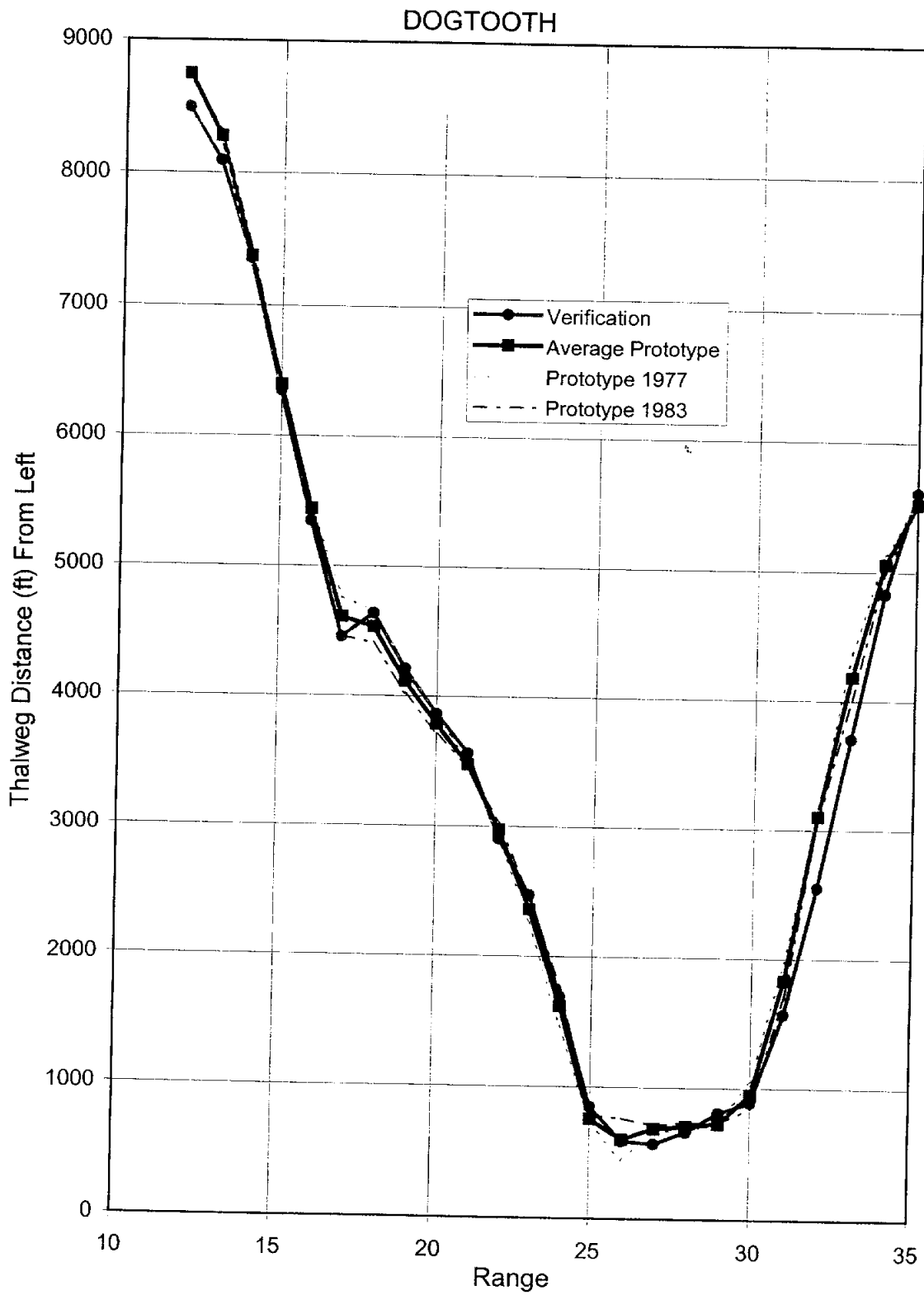


Figure B-6.2a Thalweg Position From Left by Range, Dogtooth

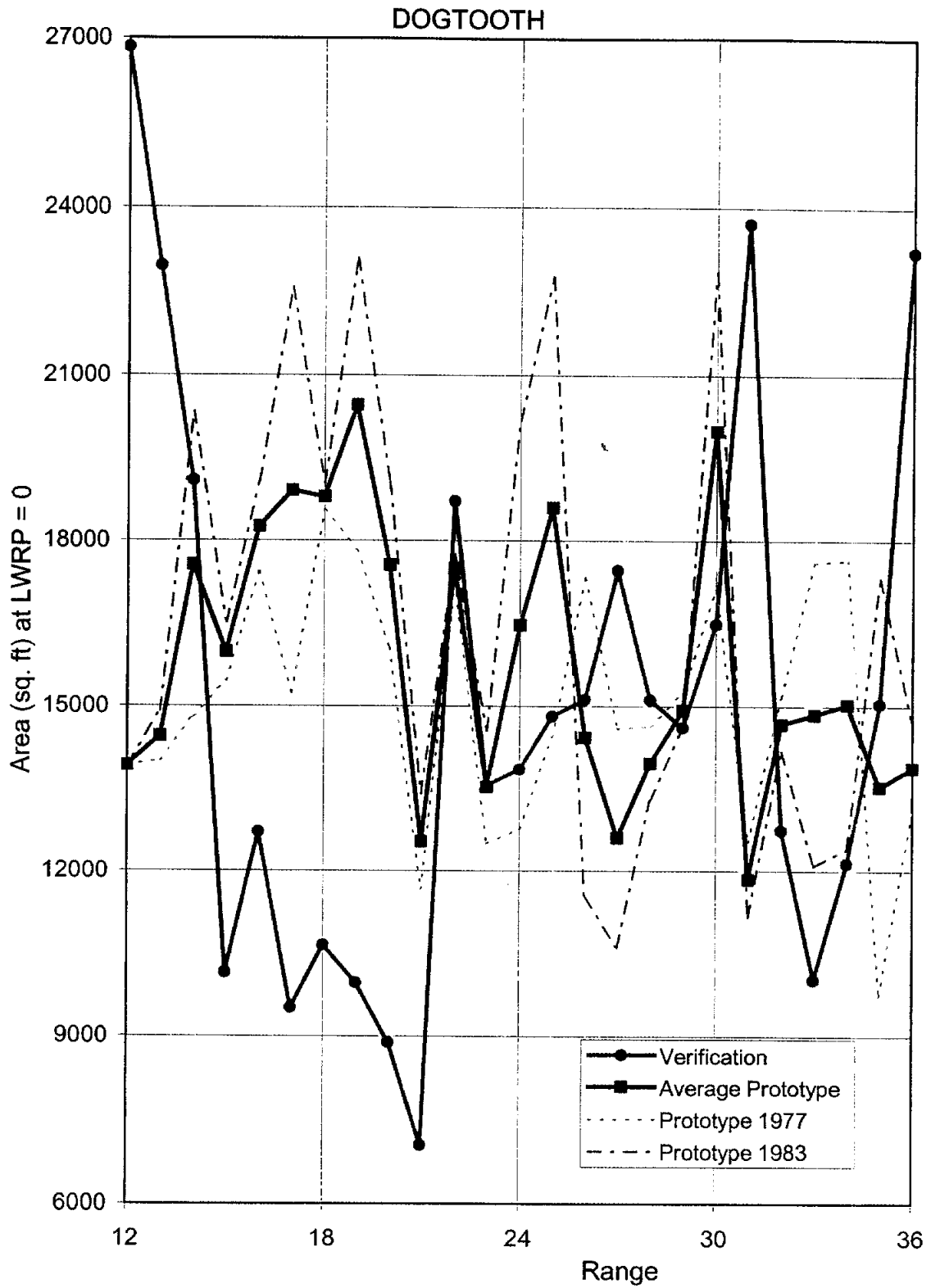


Figure B-6.2b Cross-Section Area by Range, Dogtooth

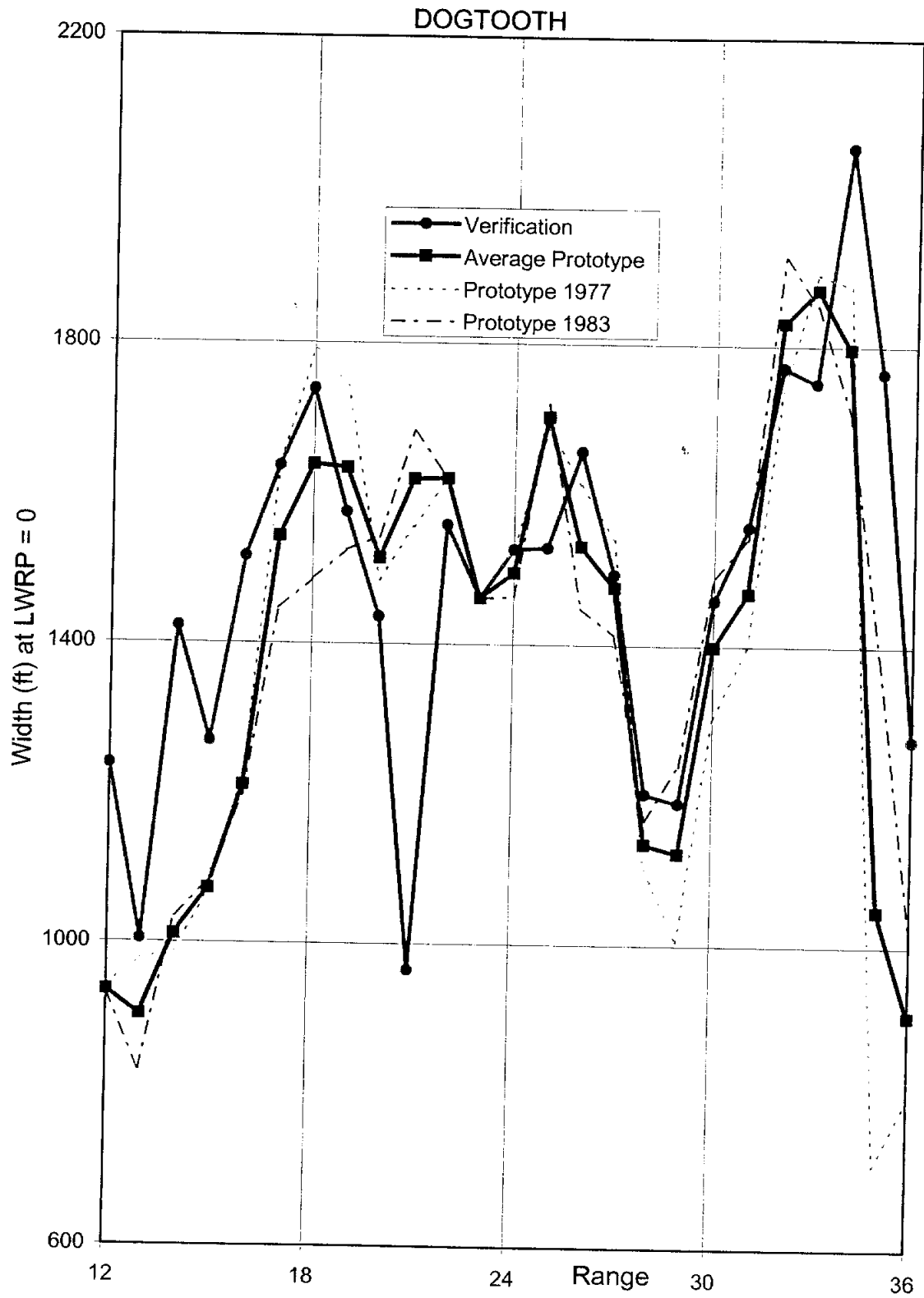


Figure B-6.2c Top Width Area by Range, Dogtooth

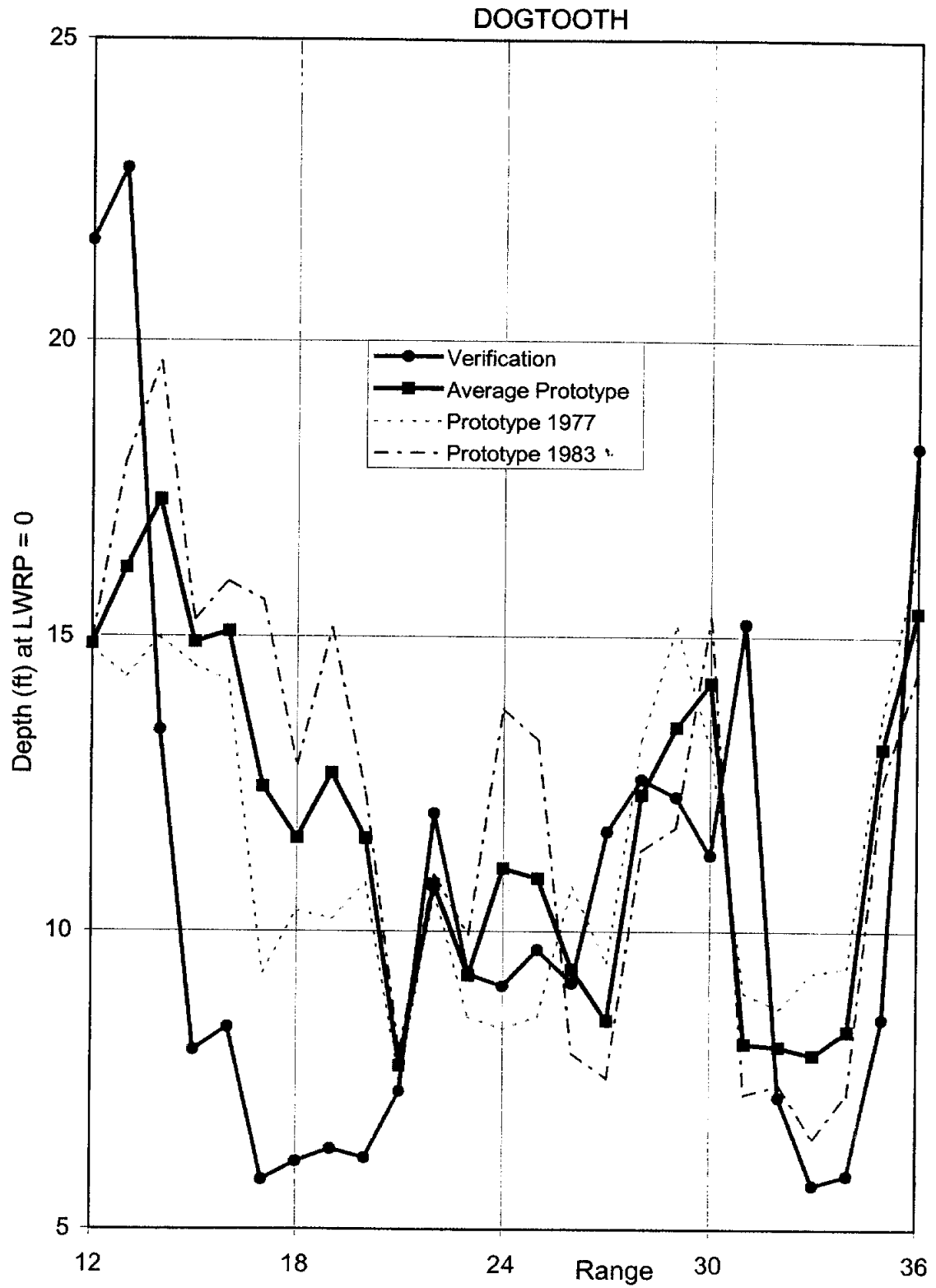


Figure B-6.2d Hydraulic Depth by Range, Dogtooth

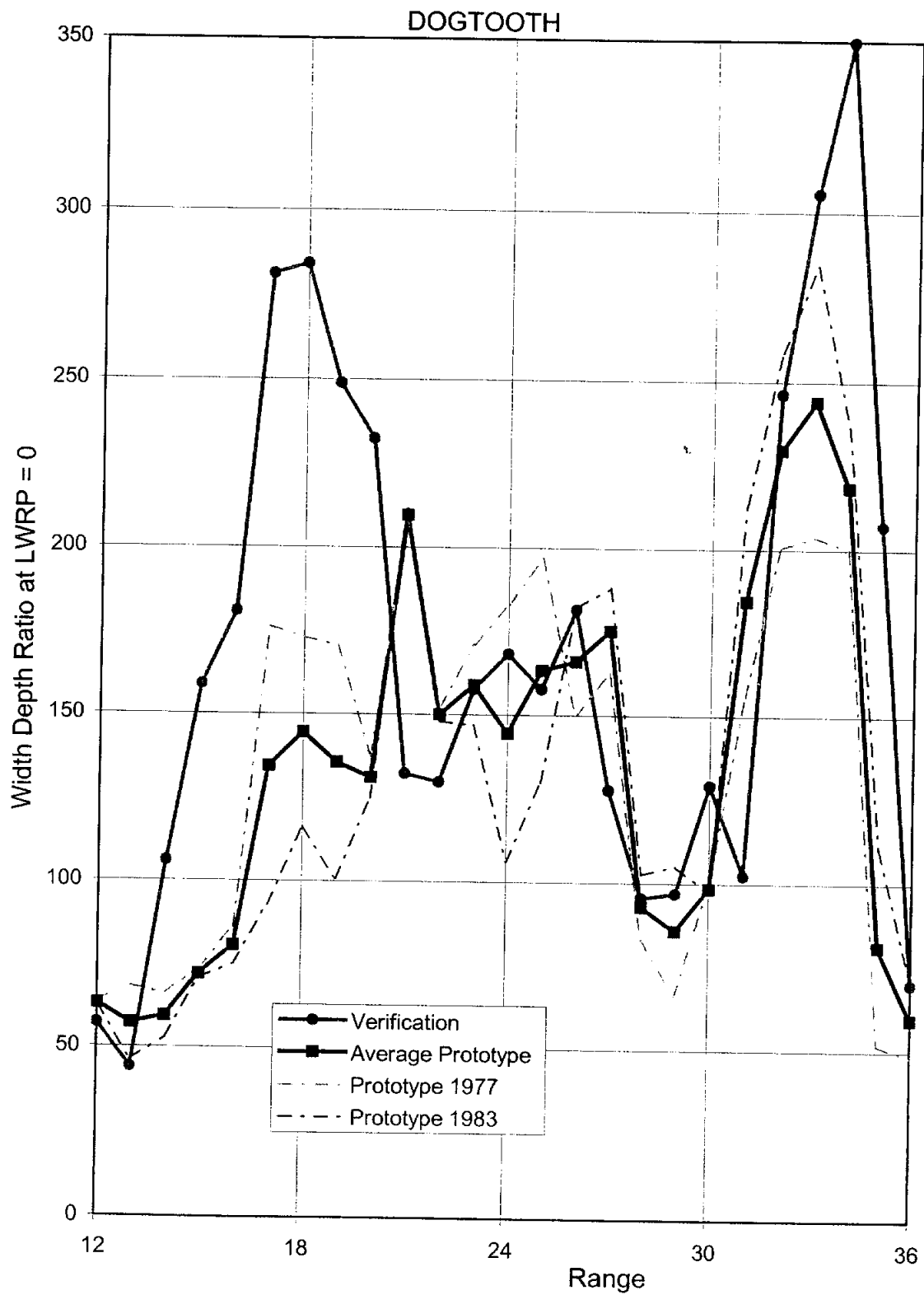
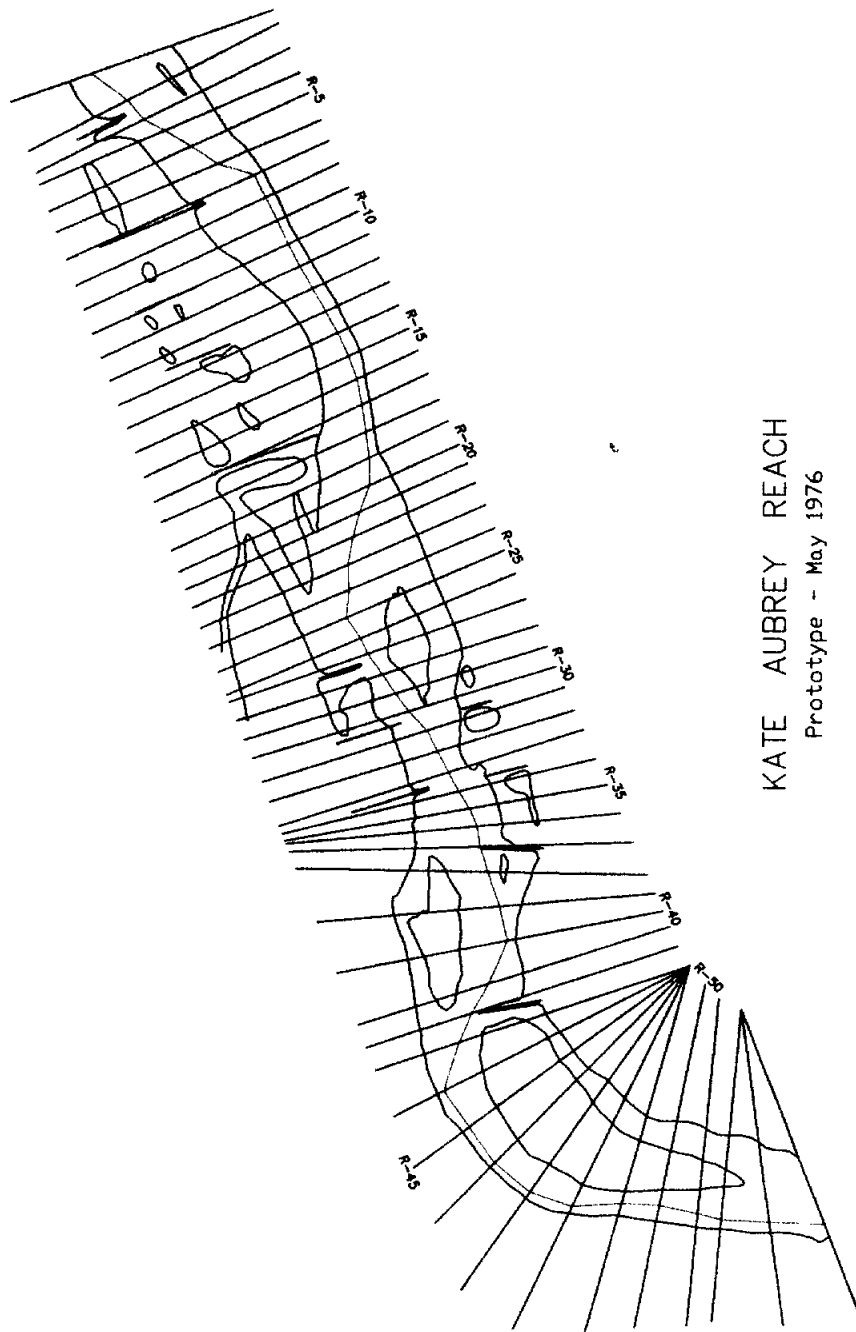


Figure B-6.2e Width/Depth Ratio by Range, Dogtooth



KATE AUBREY REACH
 Prototype - May 1976

Figure B-7.1a Kate Aubrey Model Plan View

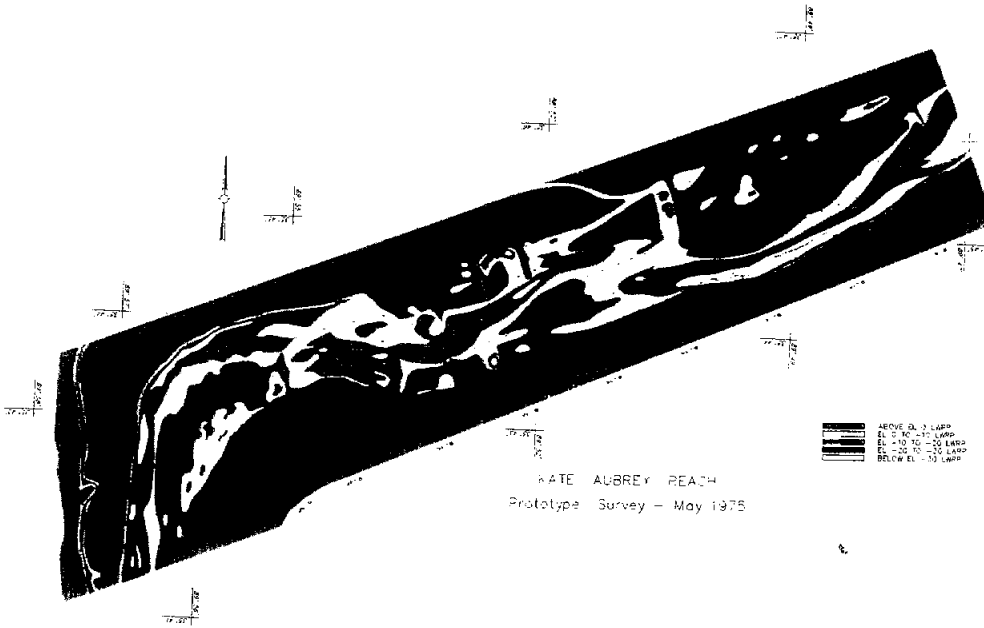


Figure B-7.1b Kate Aubrey May 1975 Prototype Survey

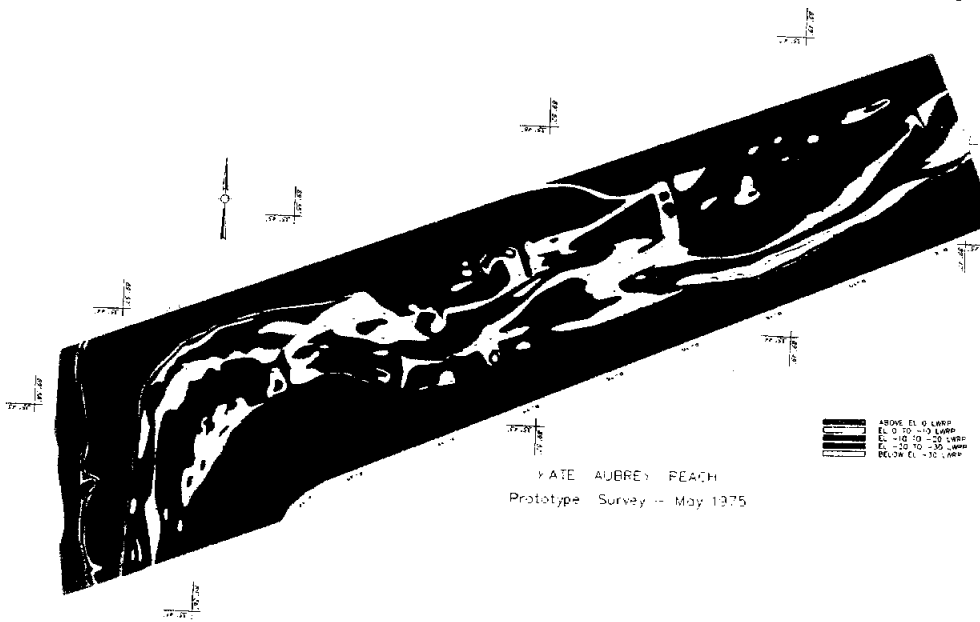


Figure B-7.1c Kate Aubrey May 1976 Prototype Survey

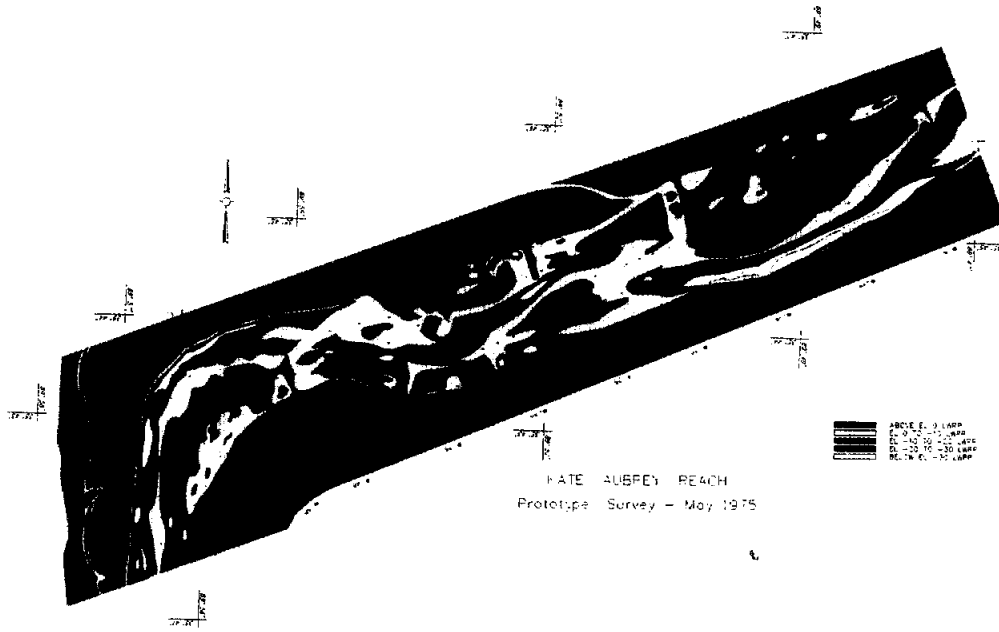


Figure B-7.1d Kate Aubrey Verification Test Survey

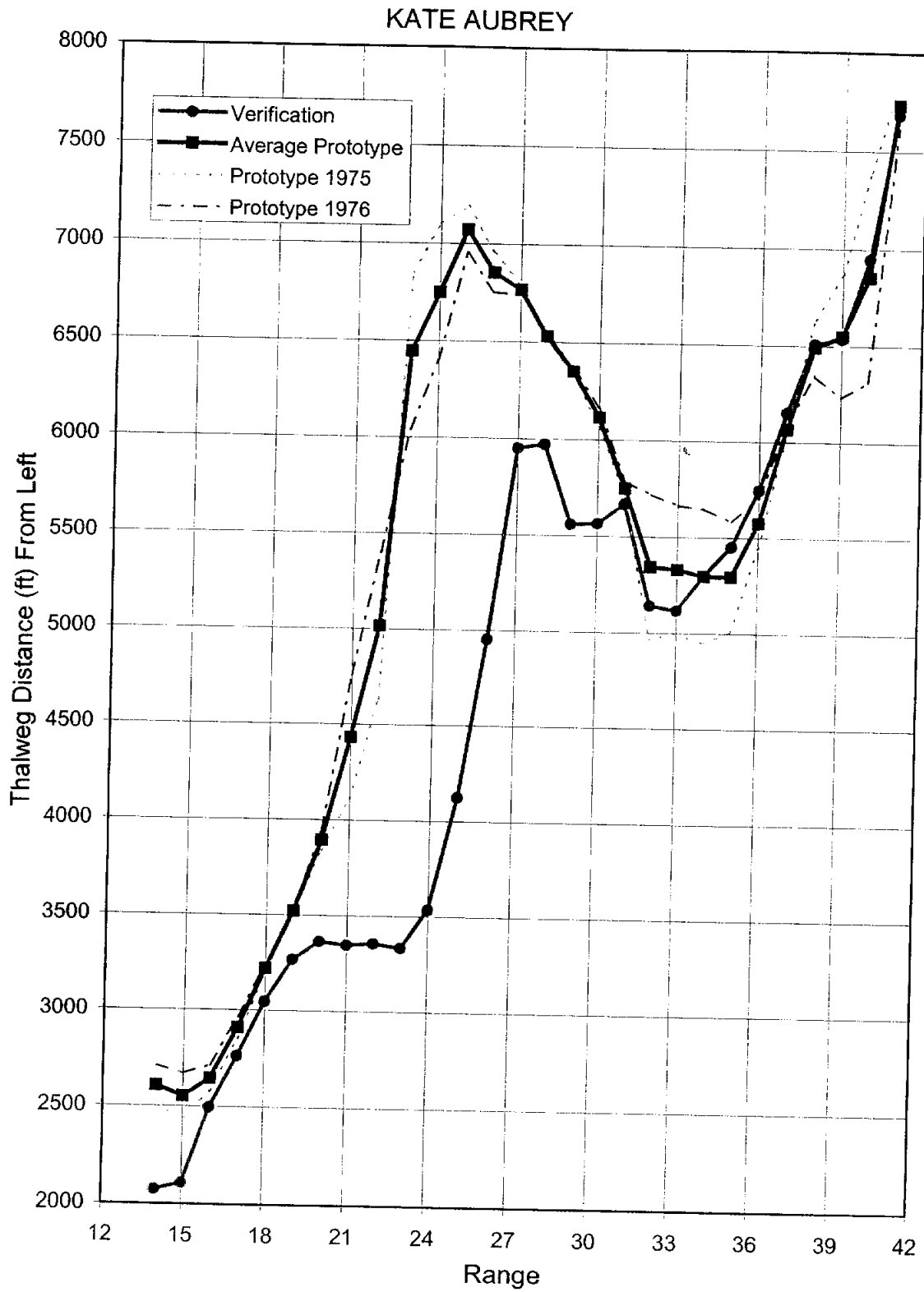


Figure B-7.2a Thalweg Position From Left by Range, Kate Aubrey

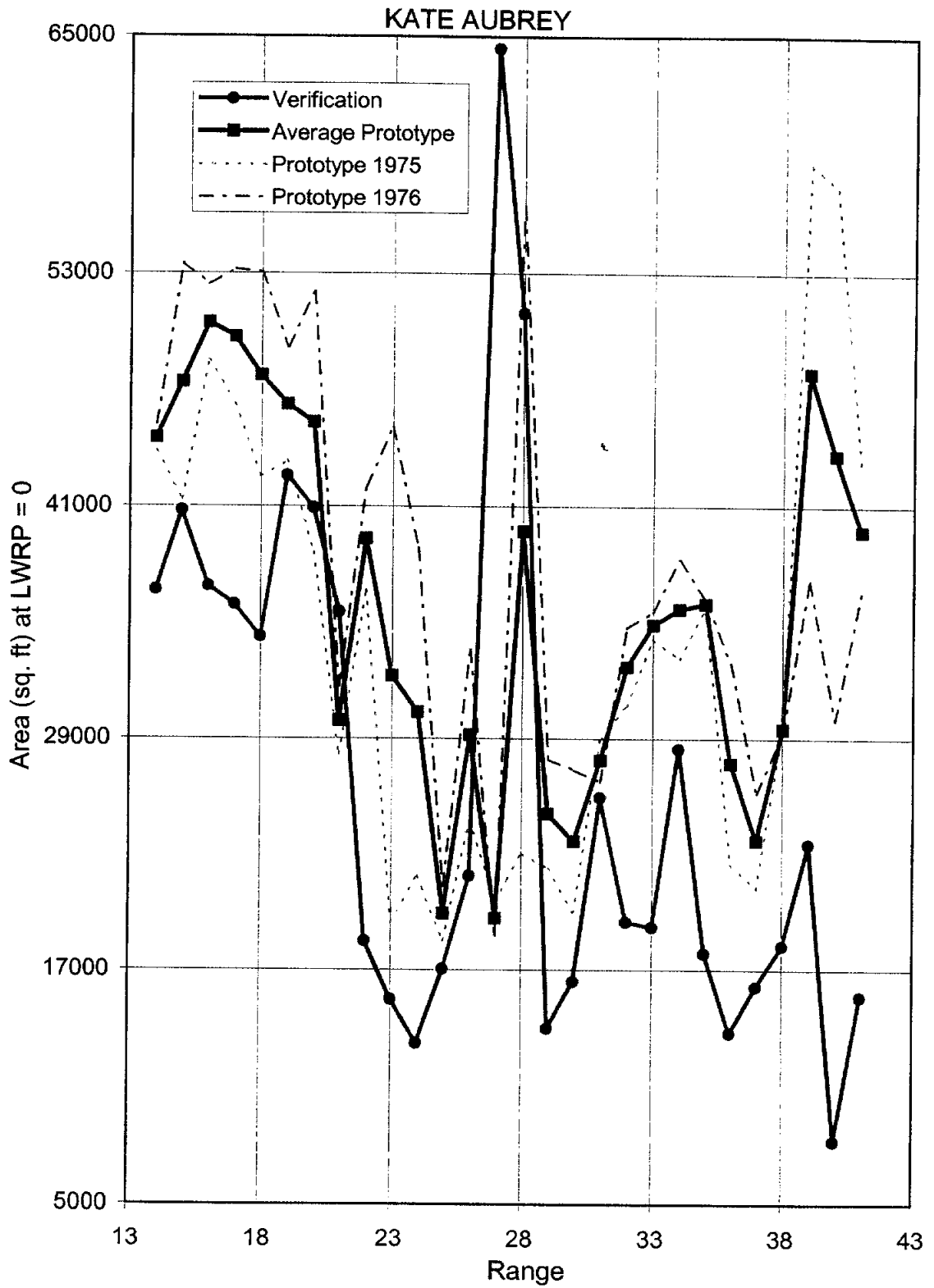


Figure B-7.2b Cross-Section Area by Range, Kate Aubrey

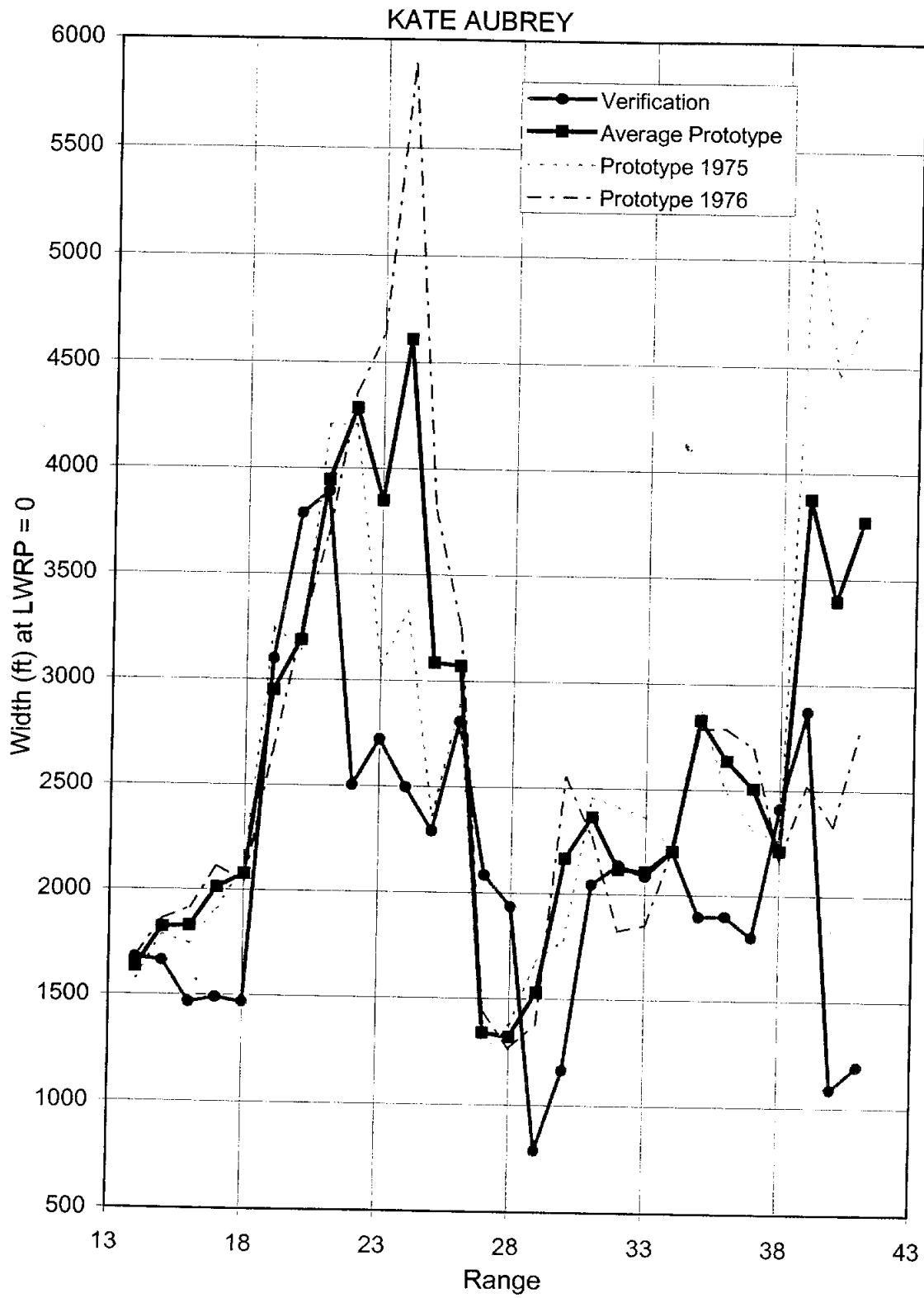


Figure B-7.2c Top Width by Range, Kate Aubrey

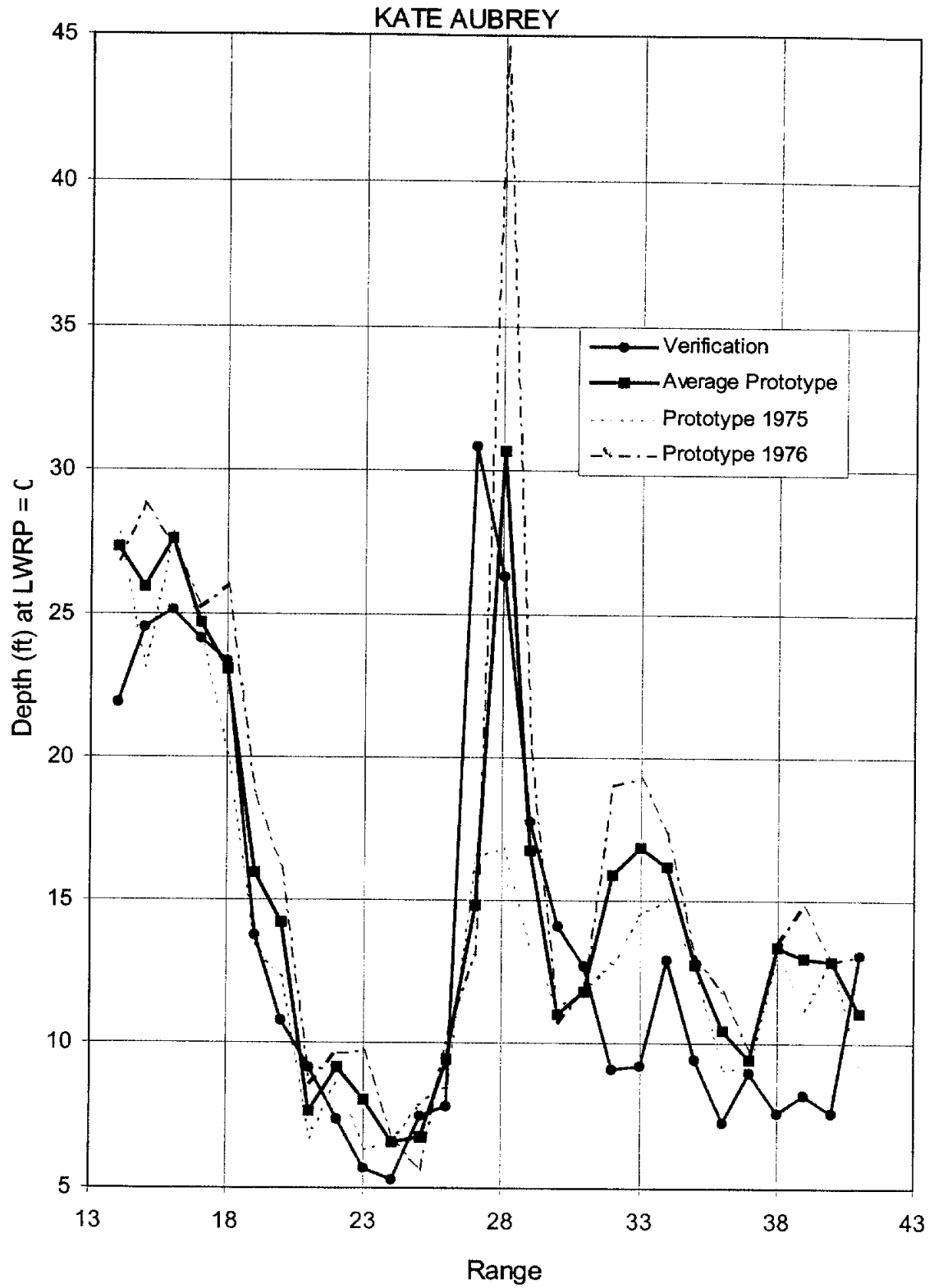


Figure B-7.2d Hydraulic Depth by Range, Kate Aubrey

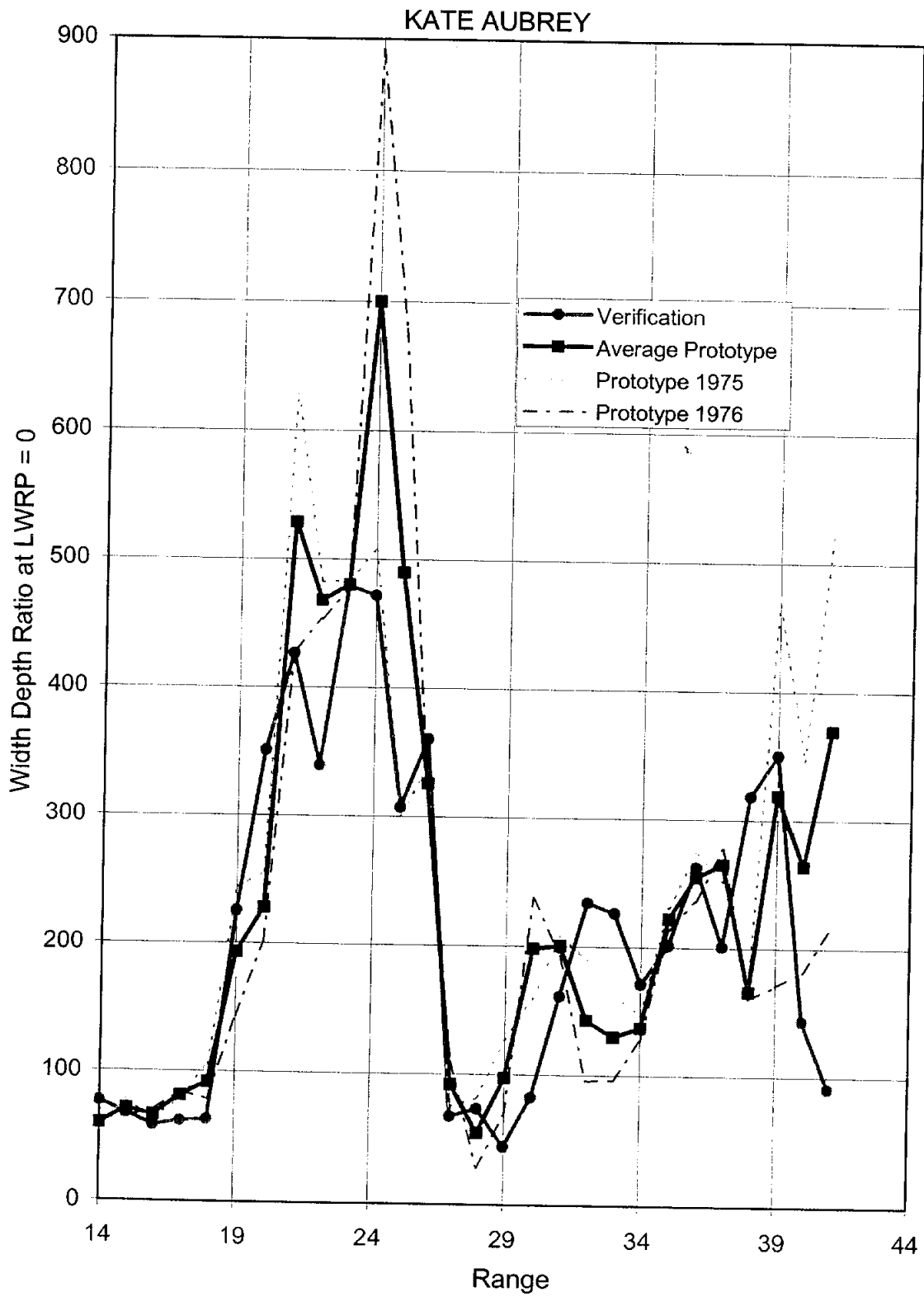
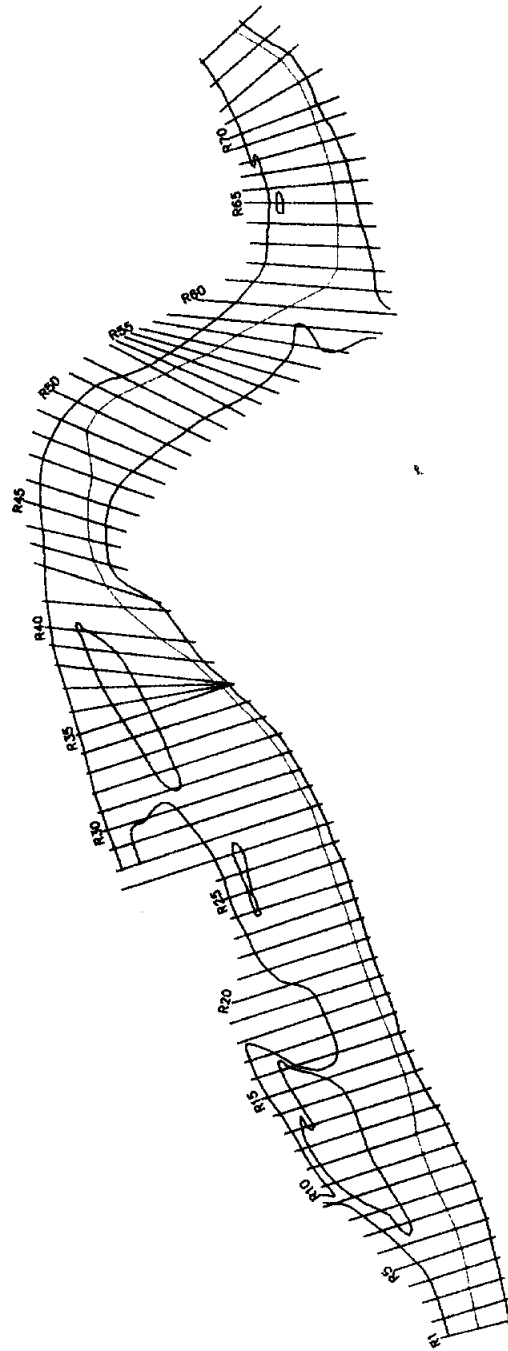


Figure B-7.2e Width/Depth Ratio by Range, Kate Aubrey



LAKE DARDANELLE
October 1973 Prototype

Figure B-8.1a Lake Dardanelle Model Plan View

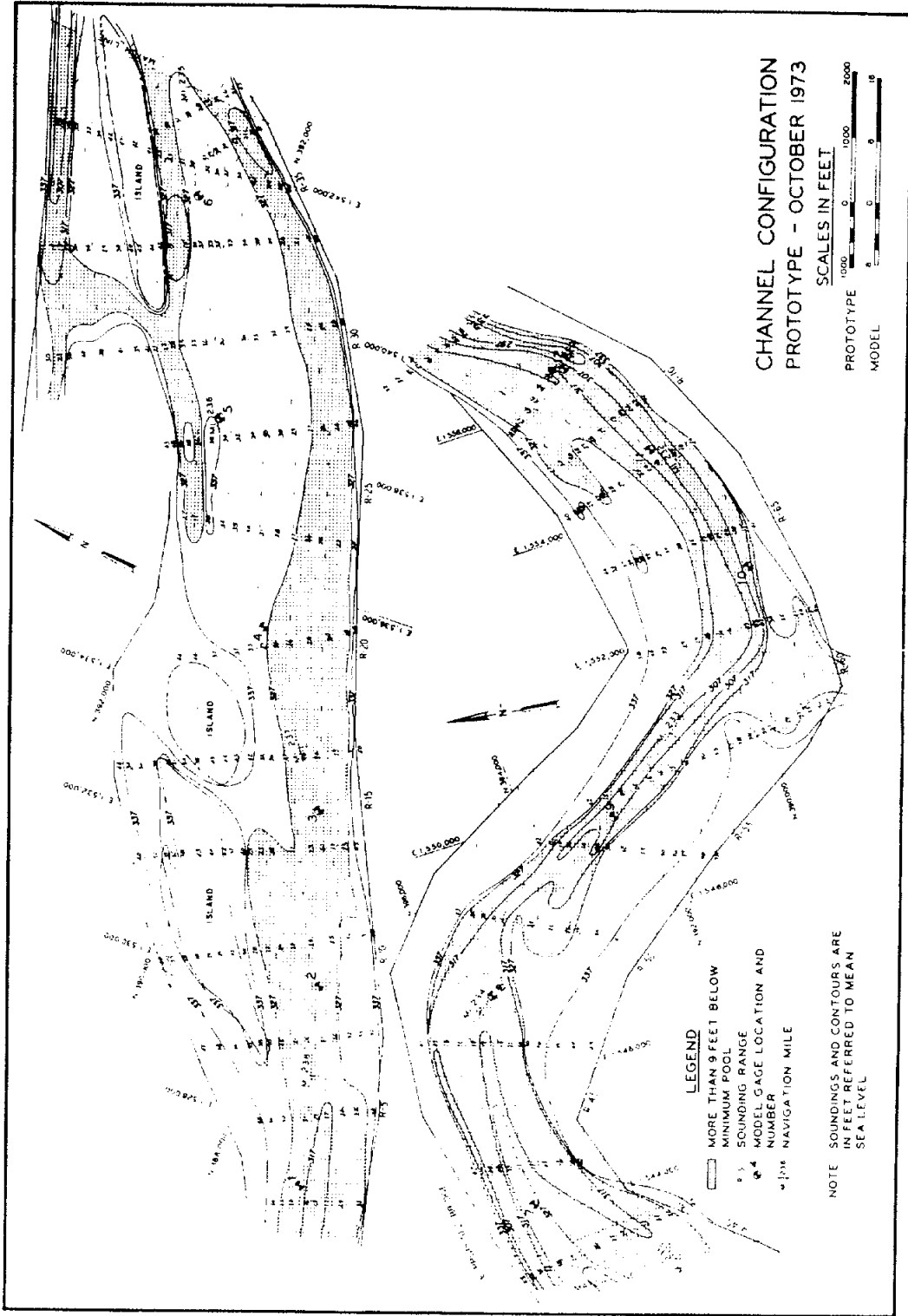


Figure B-8.1c Lake Dardanelle October 1973 Prototype Survey

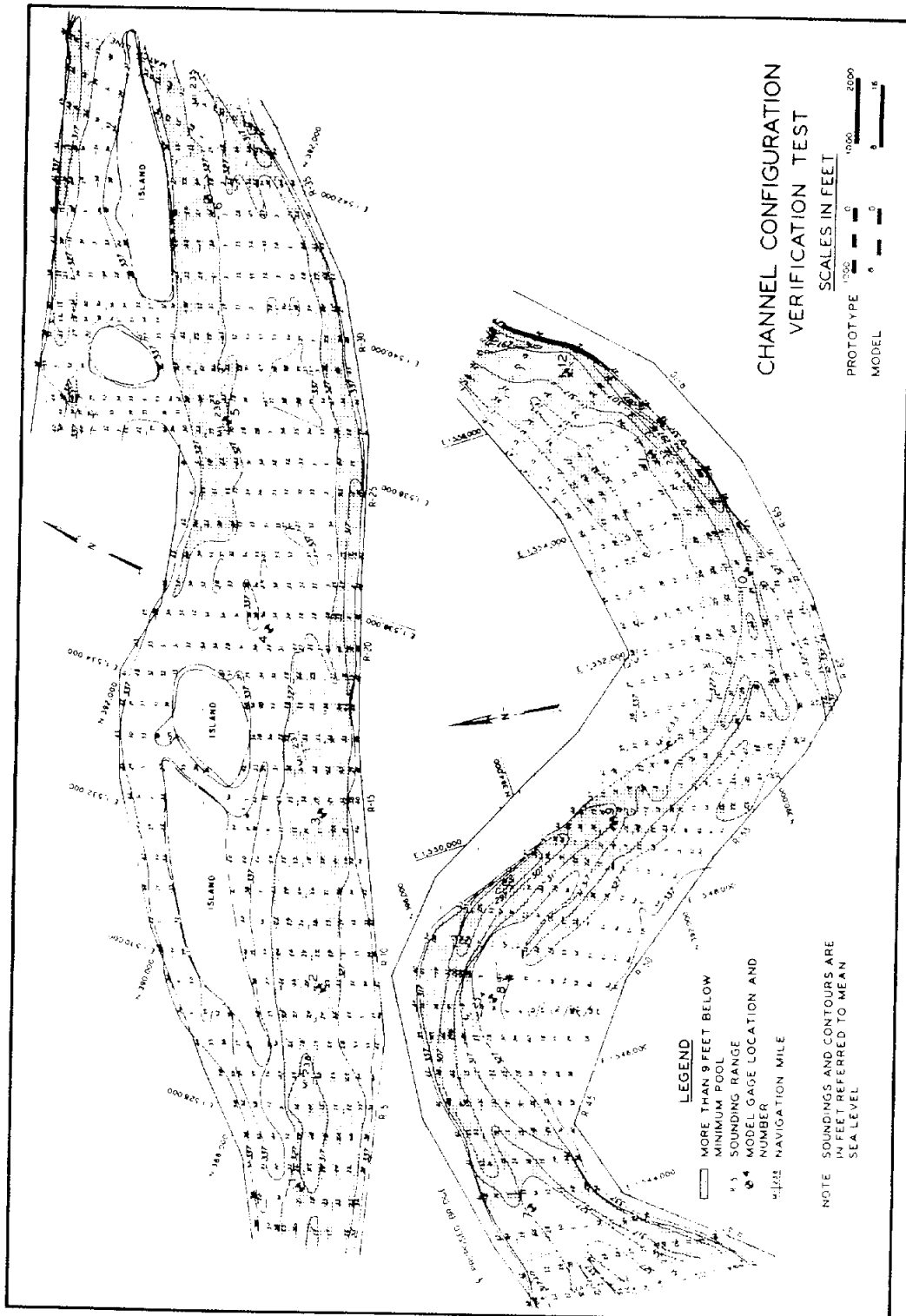


Figure B-8.1d Lake Dardanelle Verification Test Survey

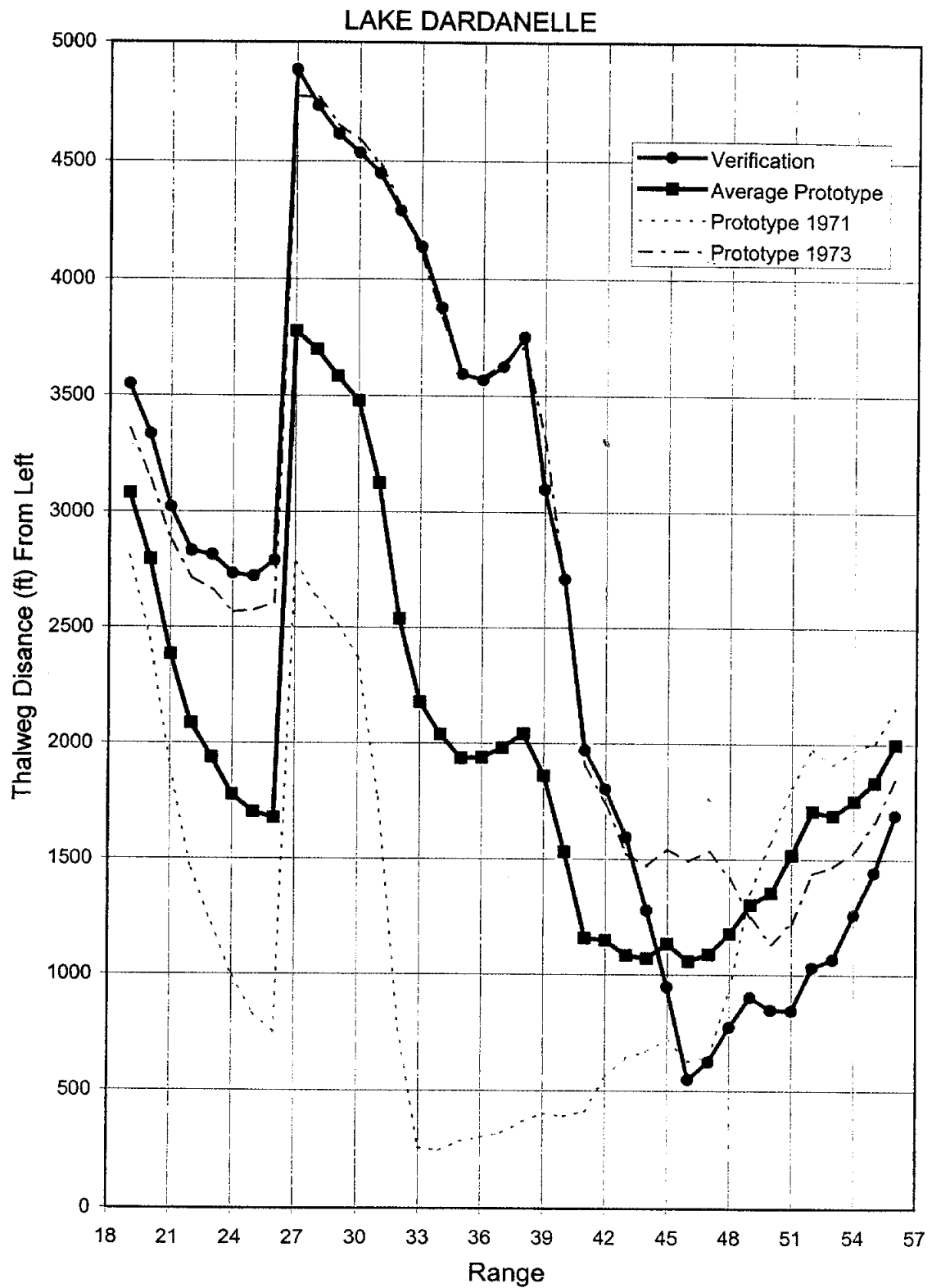


Figure B-8.2a Thalweg Position From Left by Range, Lake Dardanelle

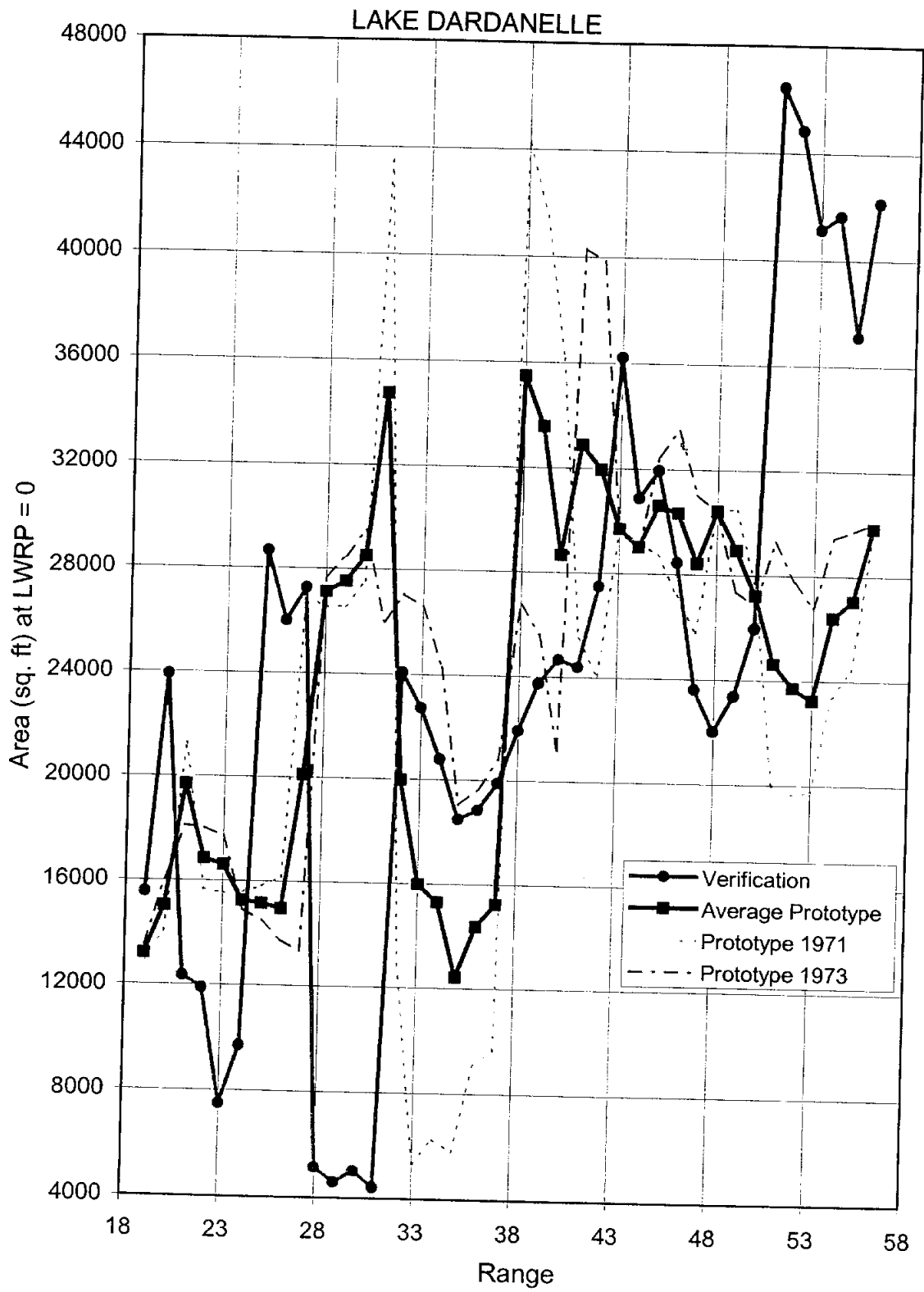


Figure B-8.2b Cross-Section Area by Range, Lake Dardanelle

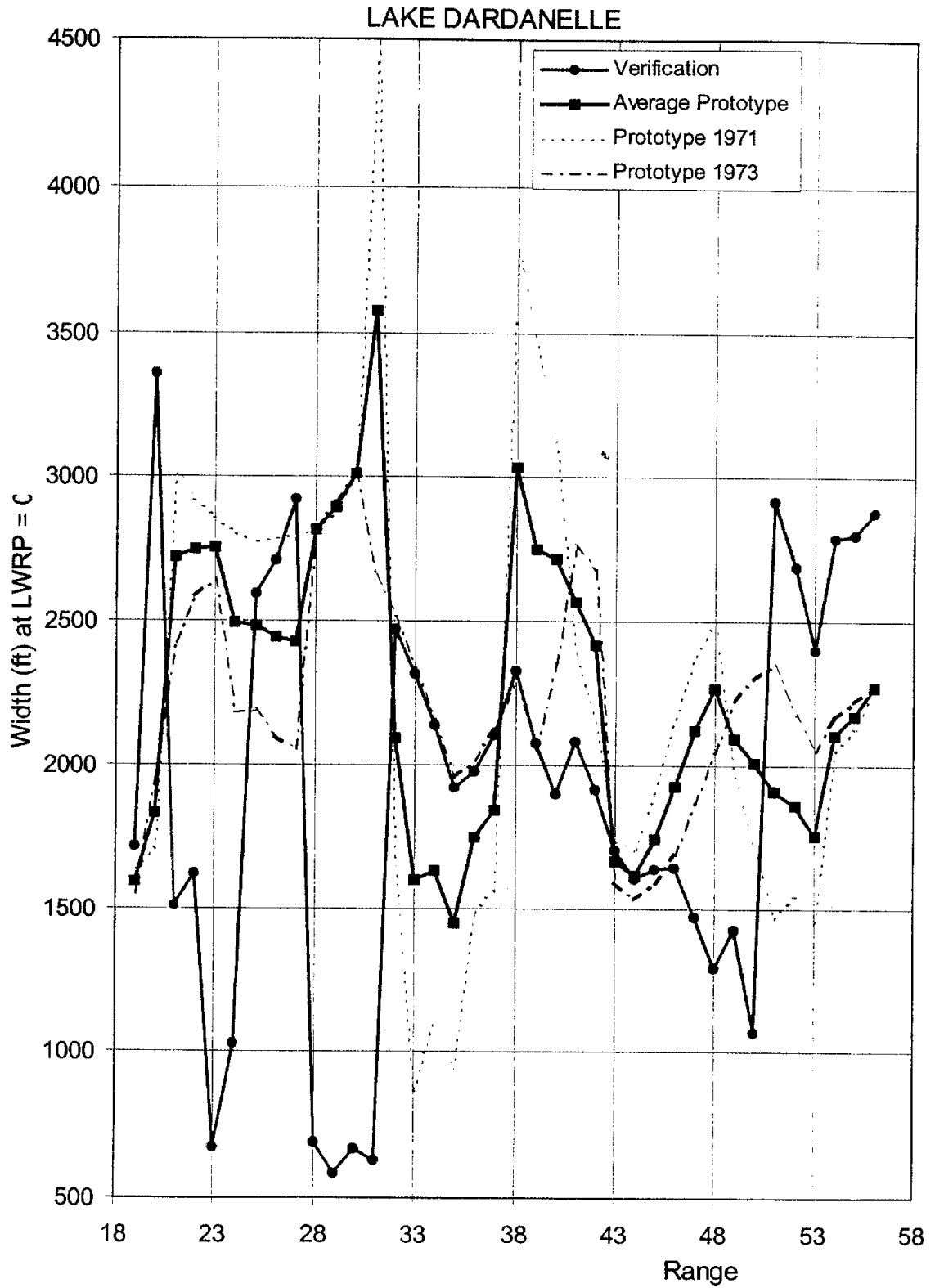


Figure B-8.2c Top Width by Range, Lake Dardanelle

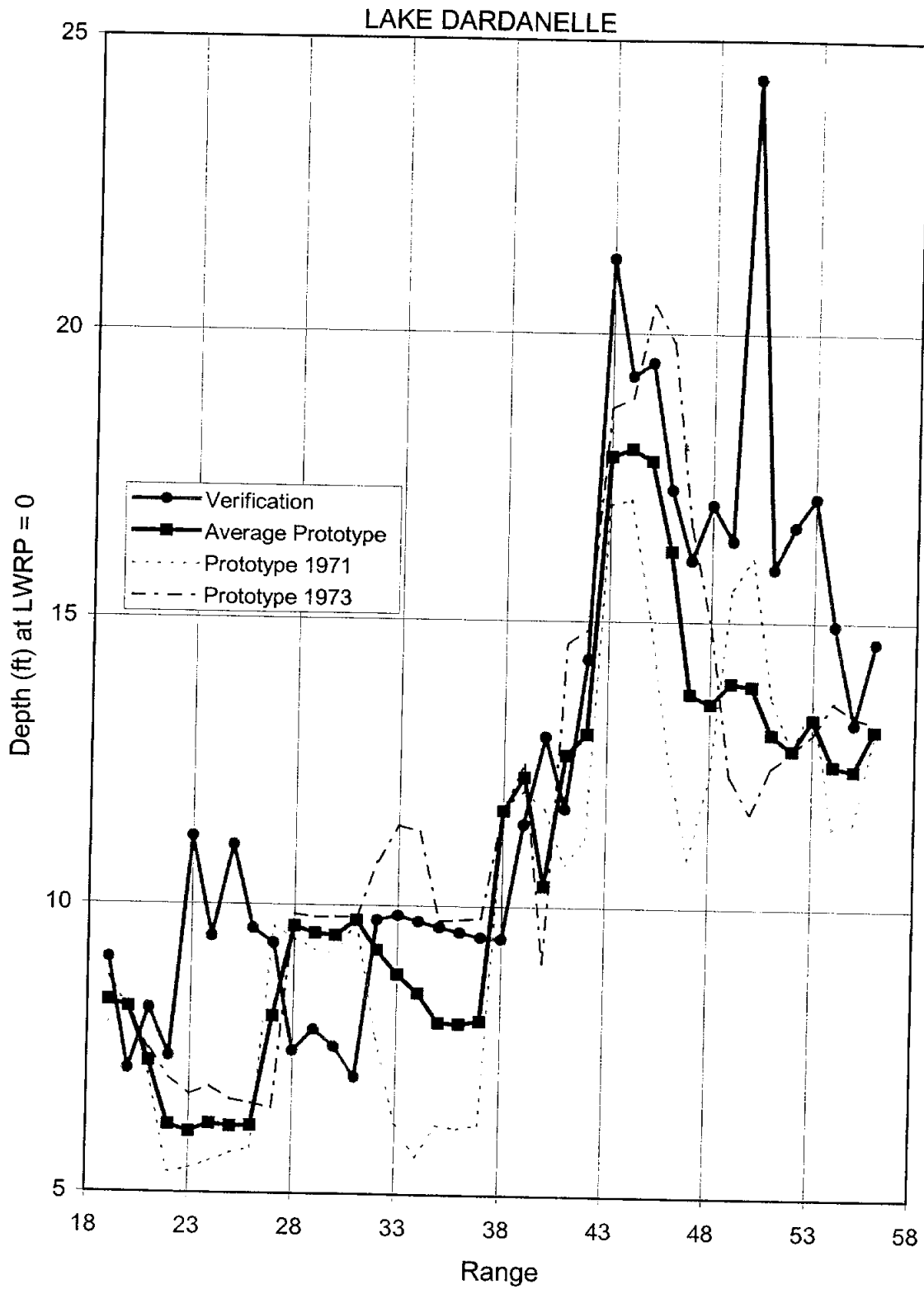


Figure B-8.2d Hydraulic Depth by Range, Lake Dardanelle

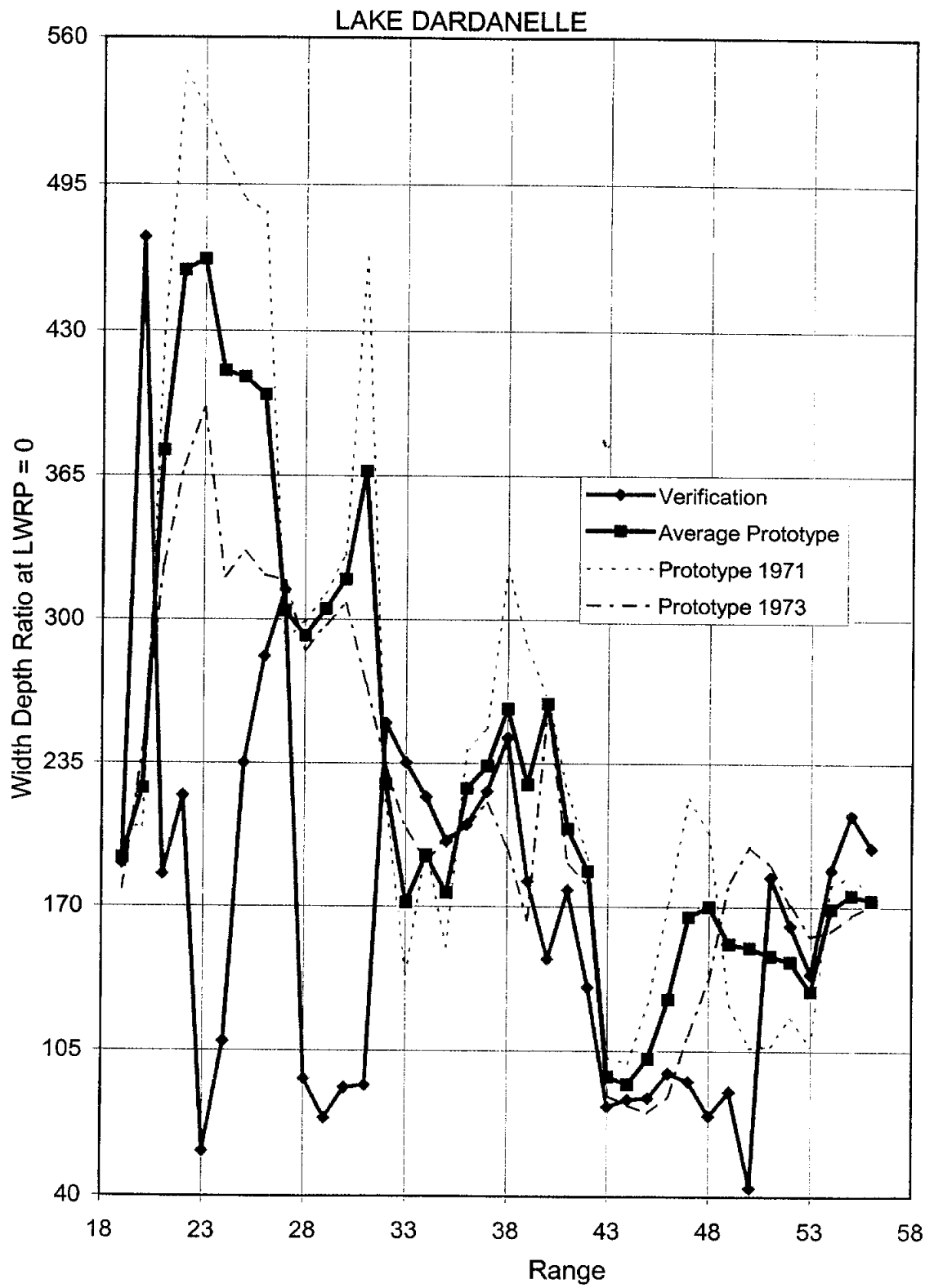
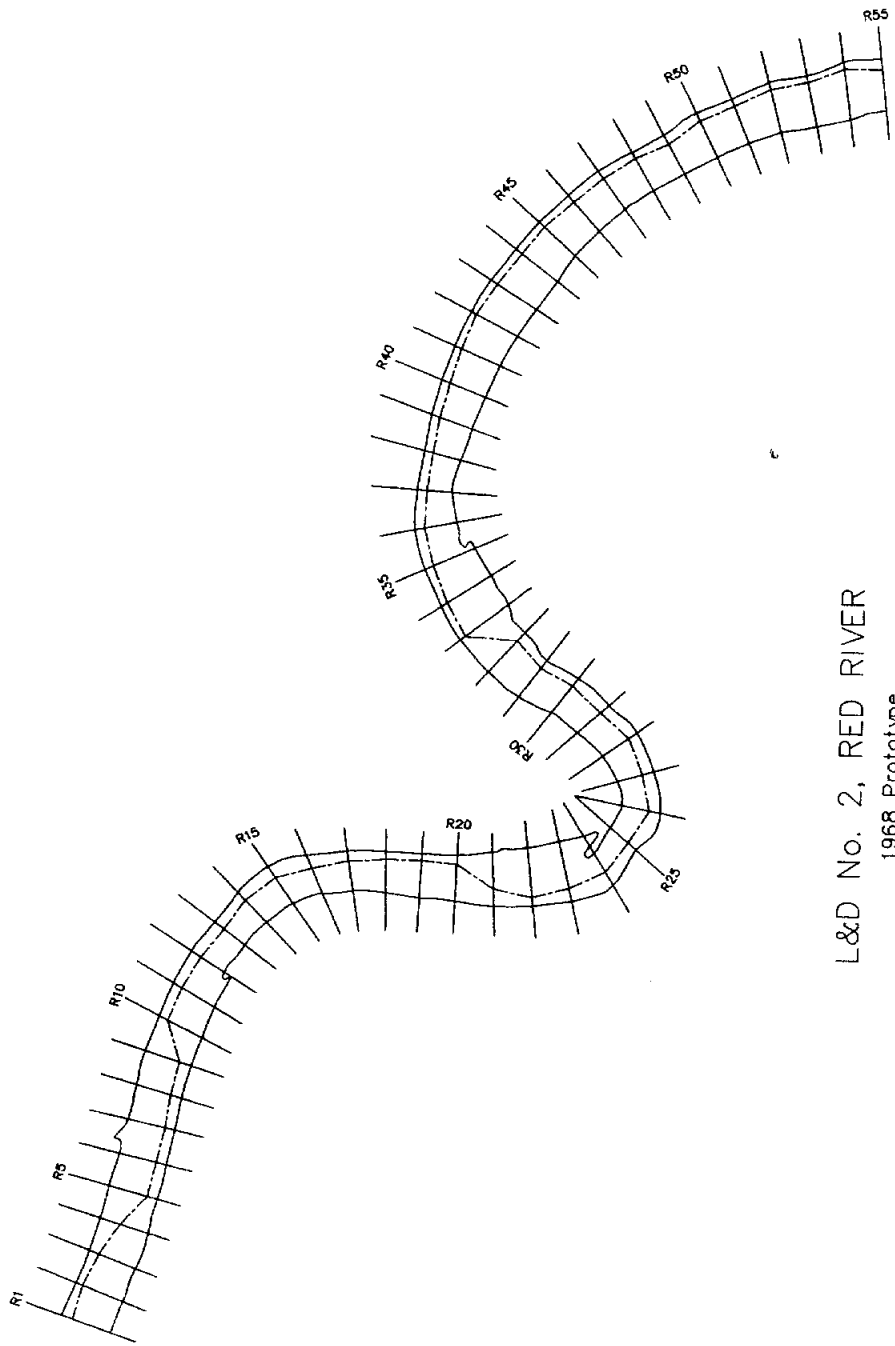


Figure B-8.2e Width/Depth Ratio by Range, Lake Dardanelle



L&D No. 2, RED RIVER
1968 Prototype

Figure B-9.1a Lock and Dam No. 2, Red River Model Plan View

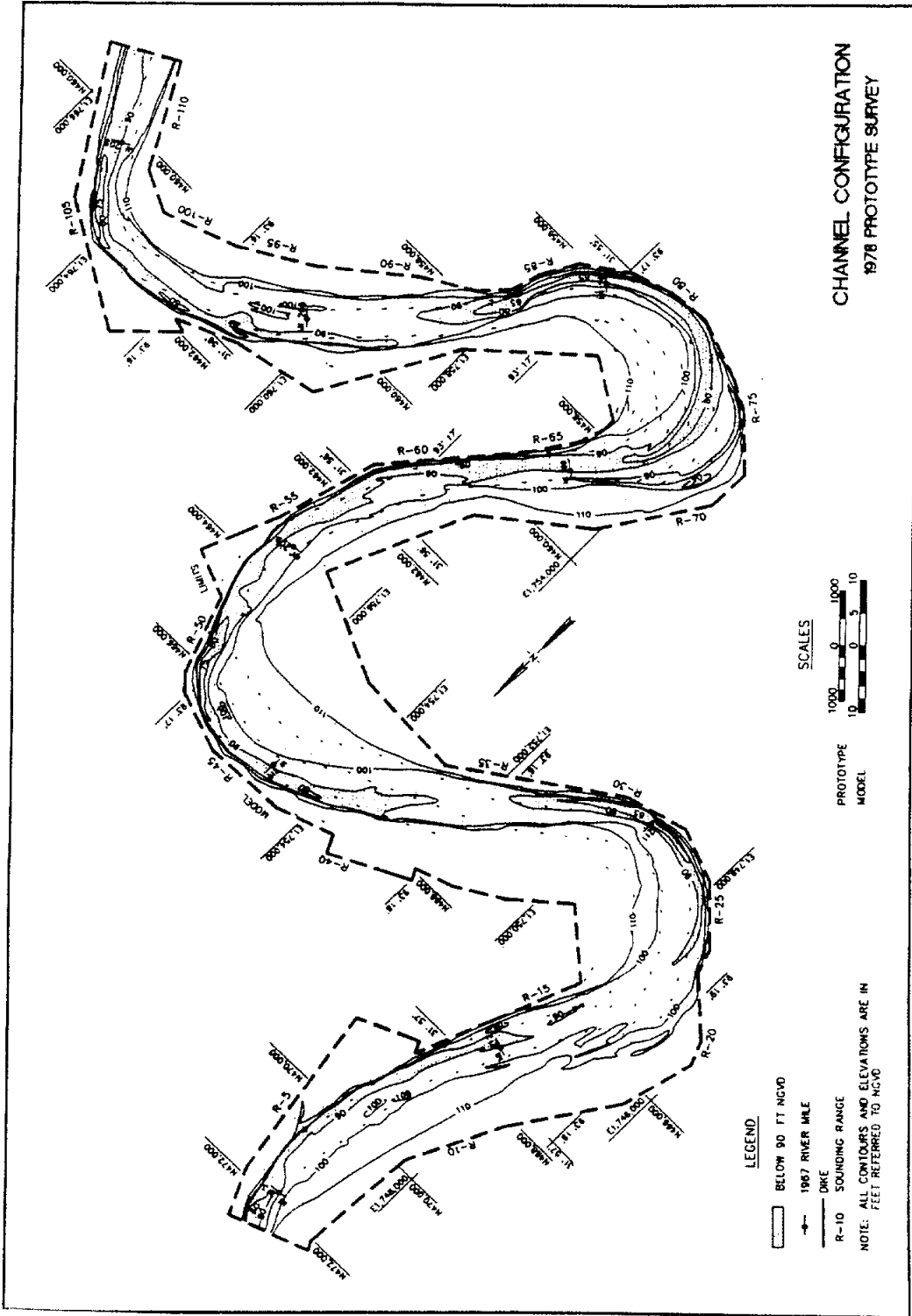


Figure B-9.1b L & D No. 2 1968 Prototype Survey

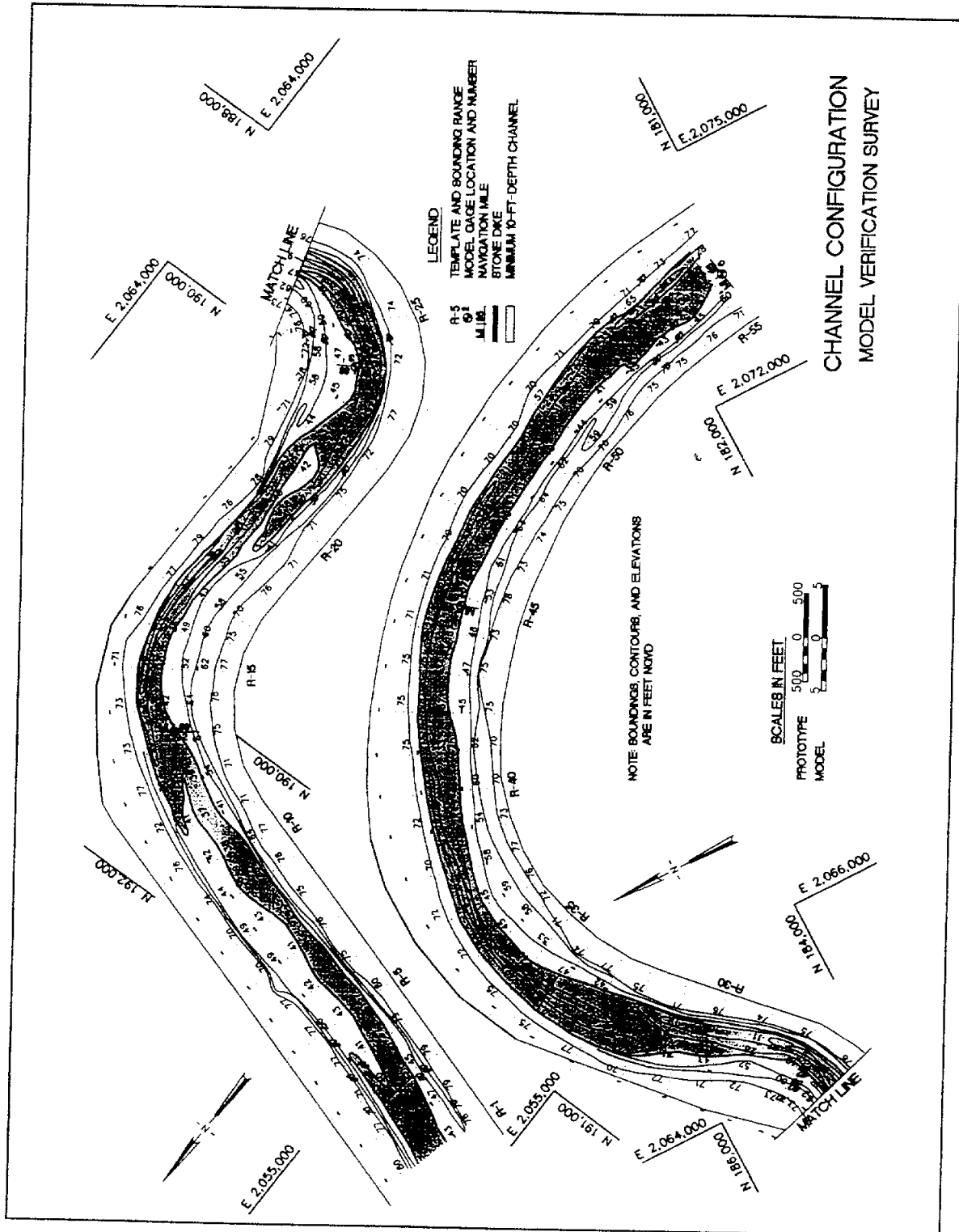


Figure B-9.1c L & D No. 2 Verification Test Survey

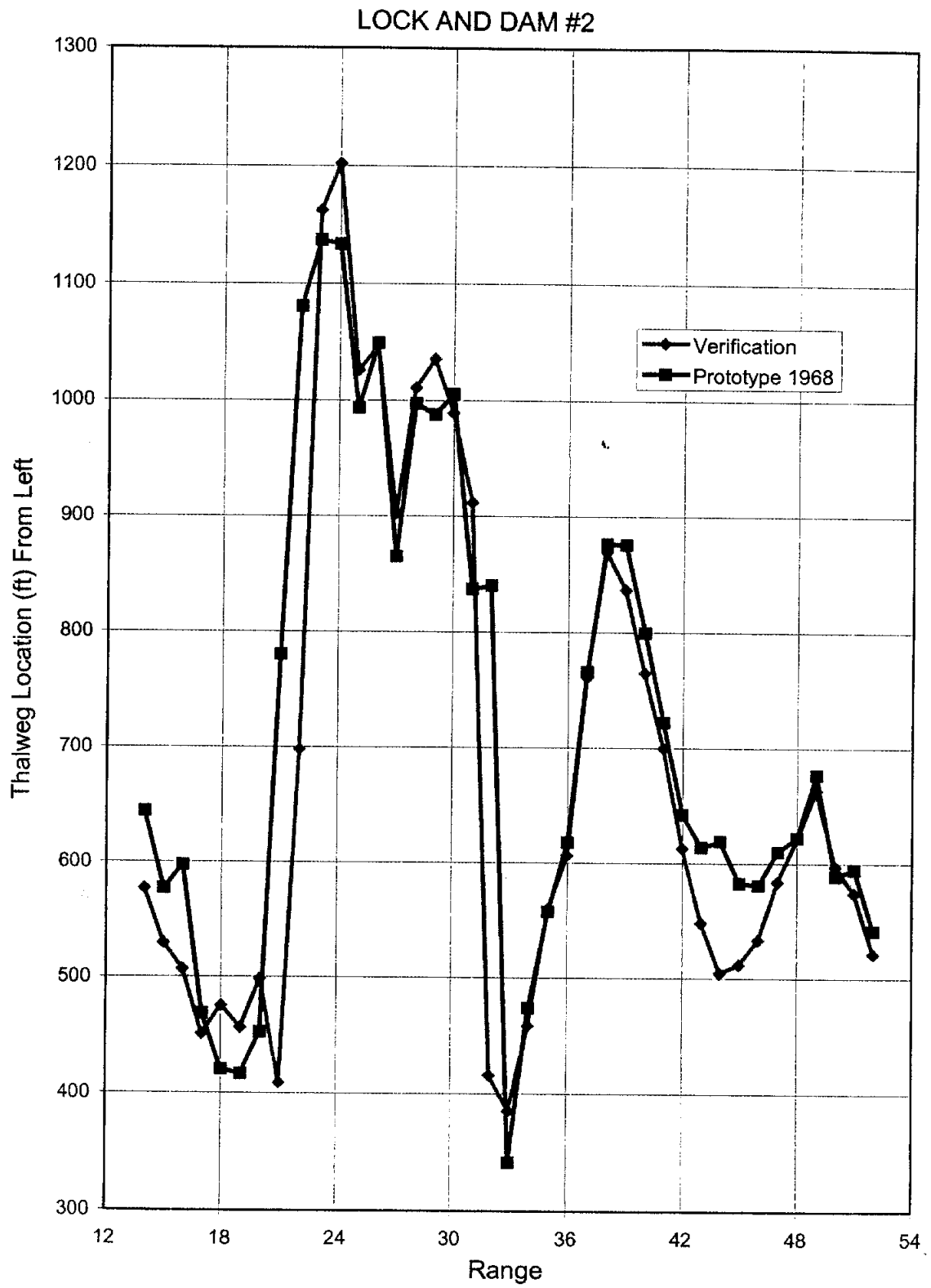


Figure B-9.2a Thalweg Location From Left by Range, Lock and Dam 2

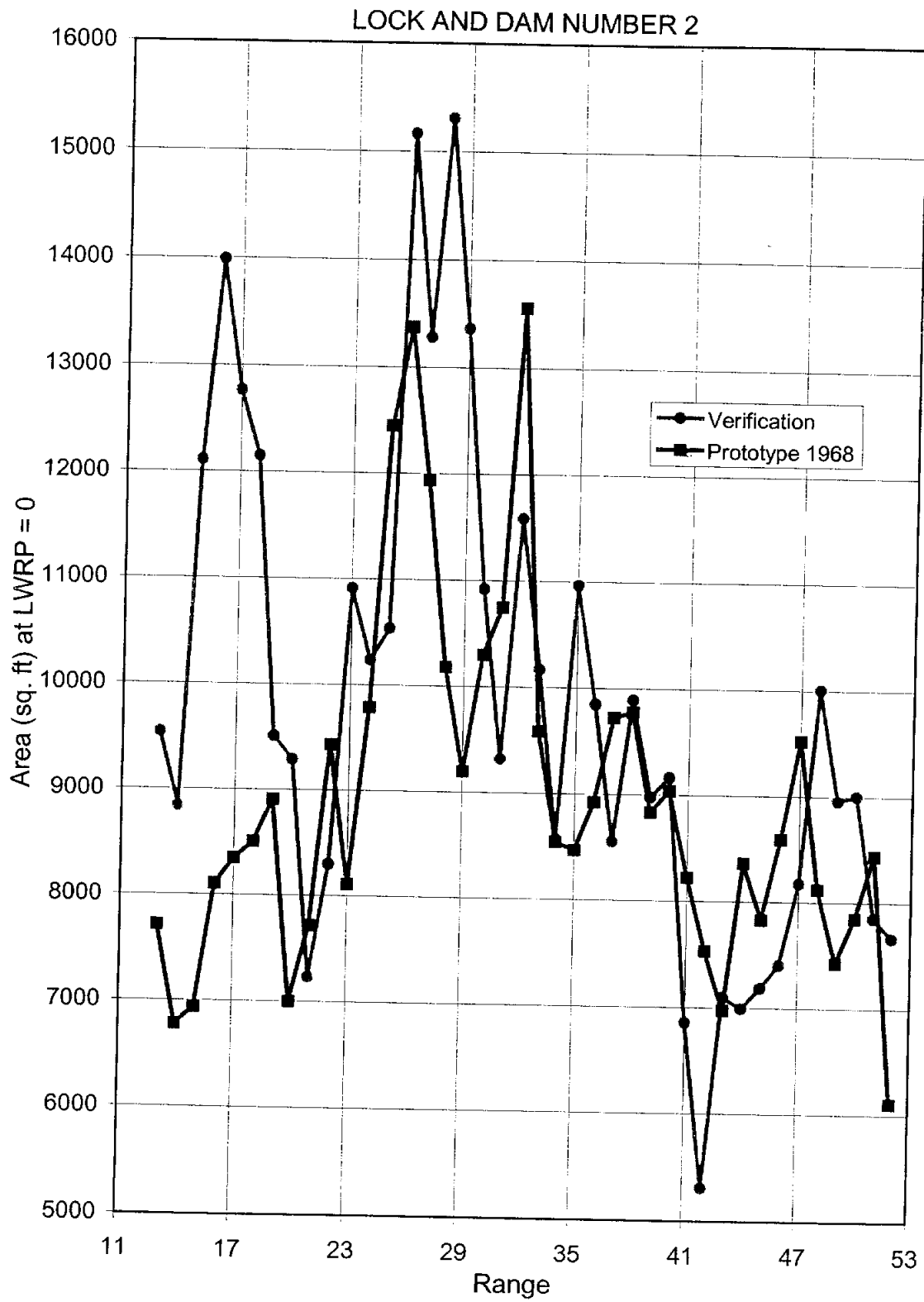


Figure B-9.2b Cross-Section Area by Range, Lock and Dam 2

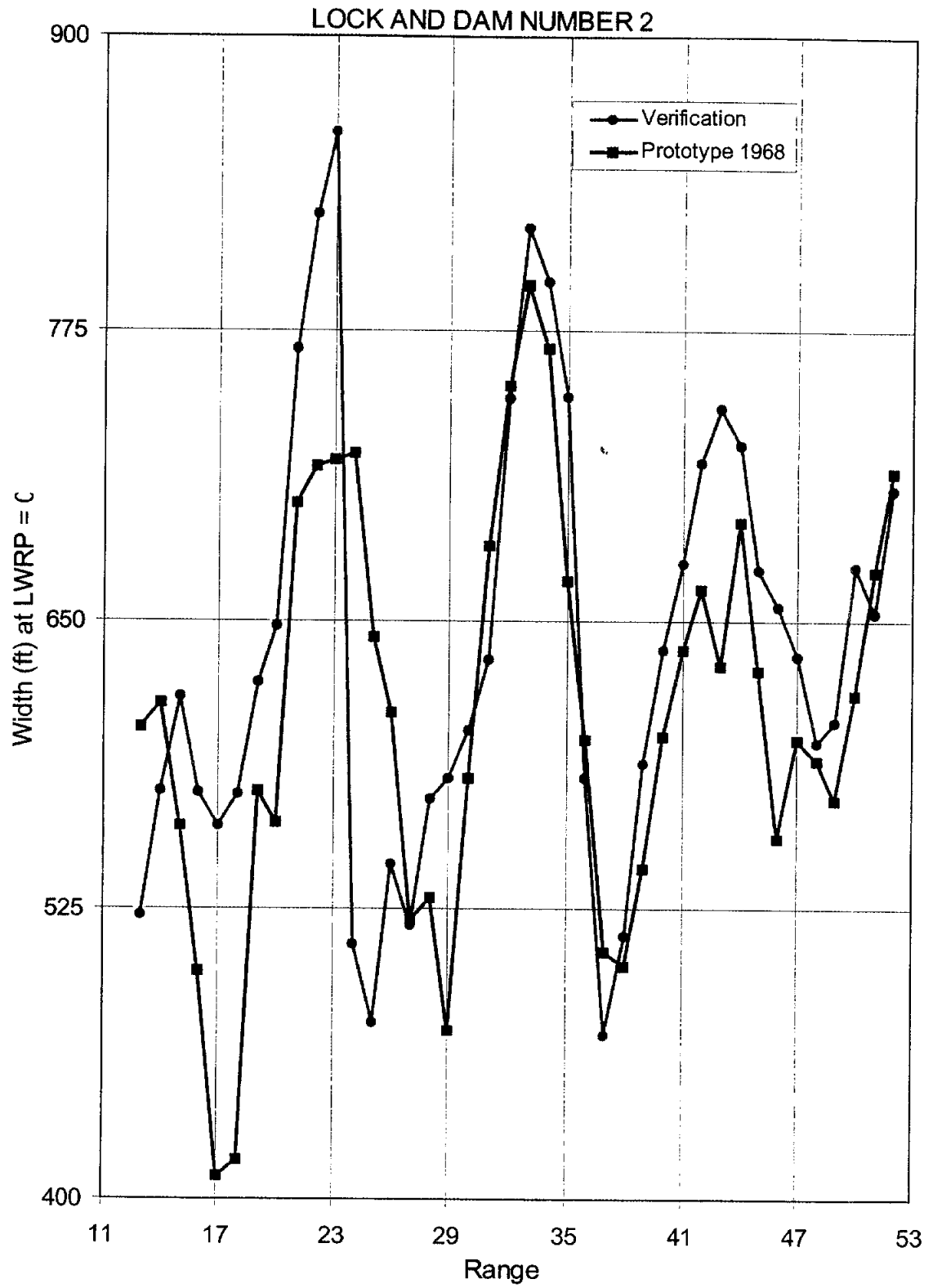


Figure B-9.2c Top Width by Range, Lock and Dam 2

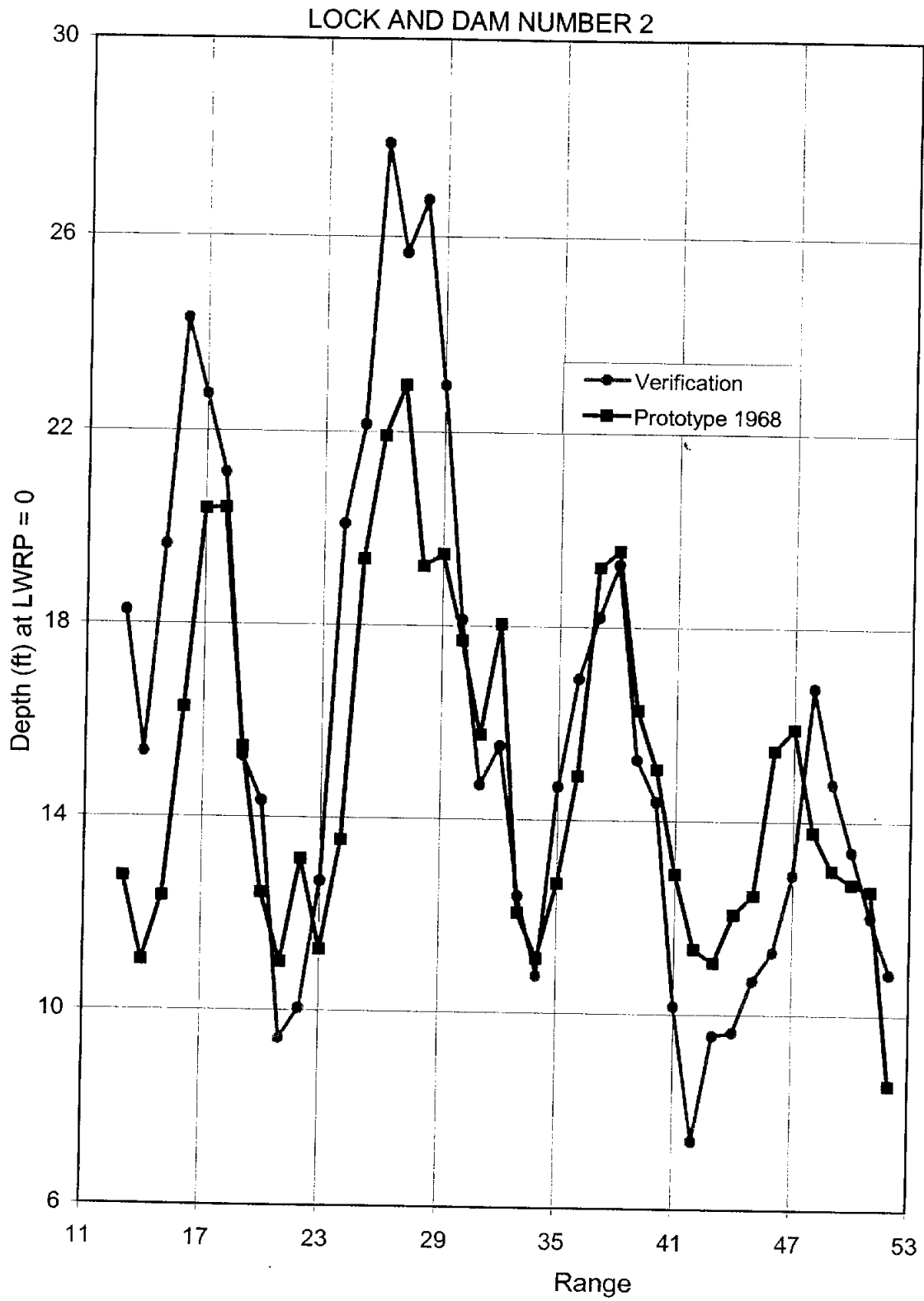


Figure B-9.2d Hydraulic Depth by Range, Lock and Dam 2

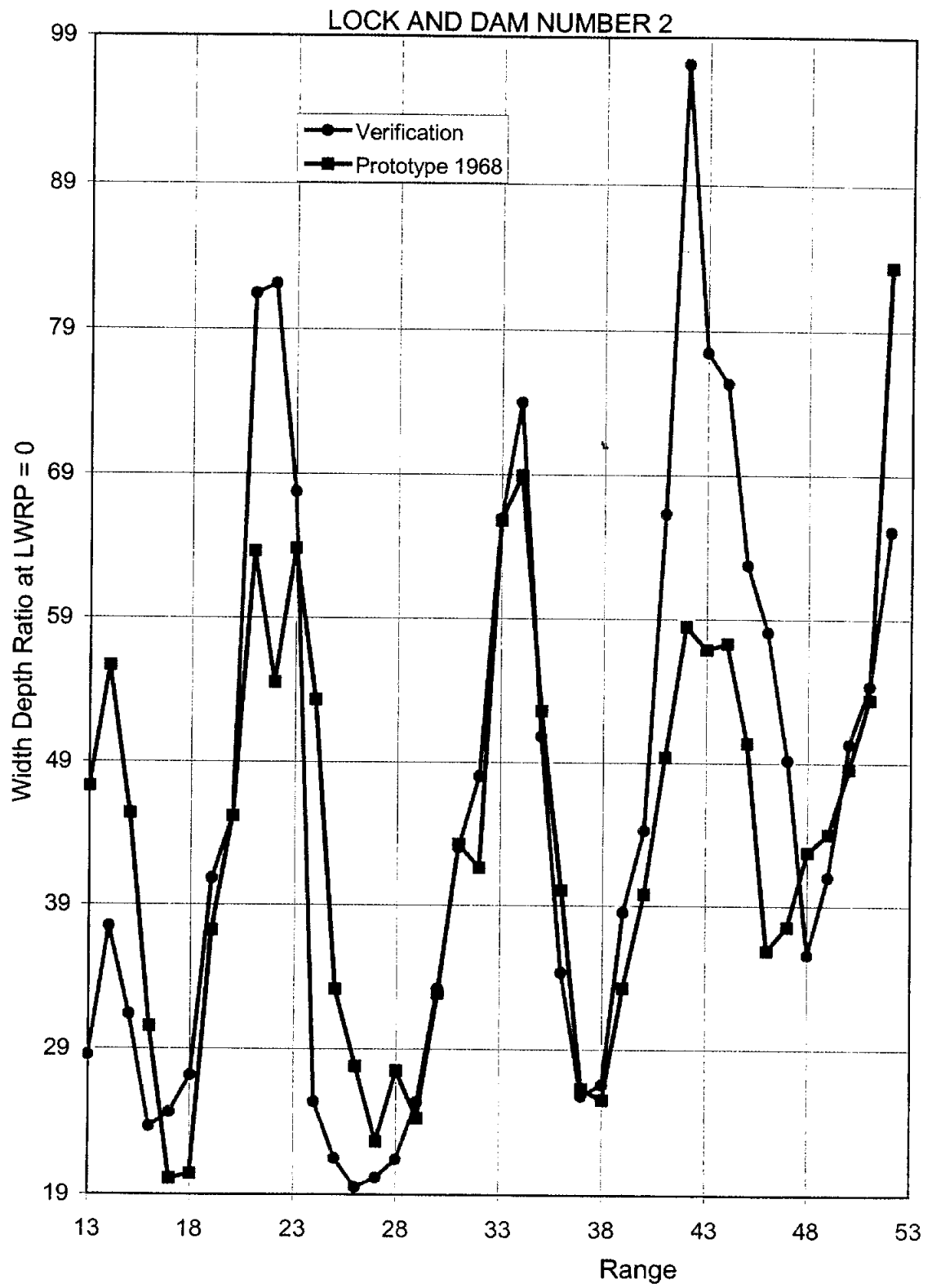
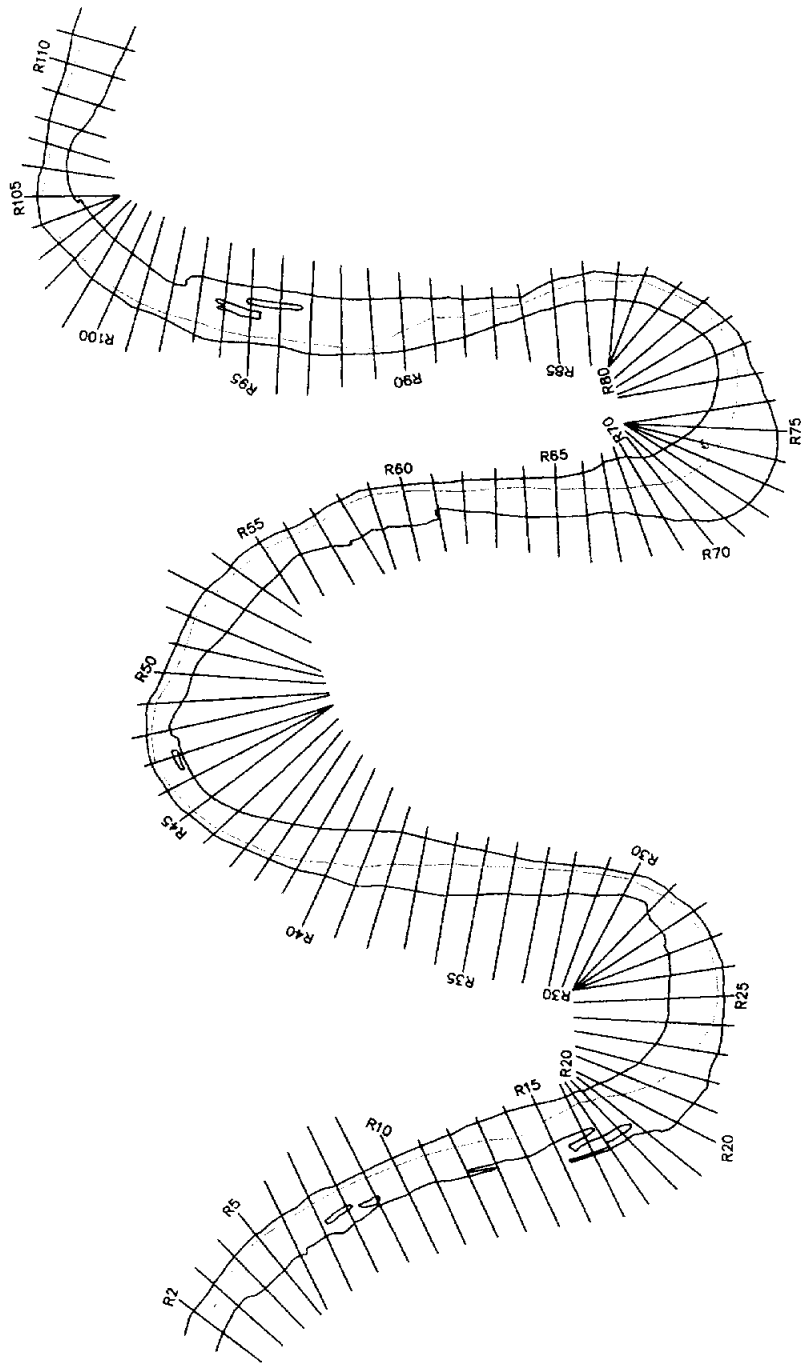


Figure B-9.2e Width/Depth Ratio by Range, Lock and Dam 2



L&D No. 4, RED RIVER
1978 Prototype Survey

Figure B-10.1a Lock and Dam No. 4 Model Plan View

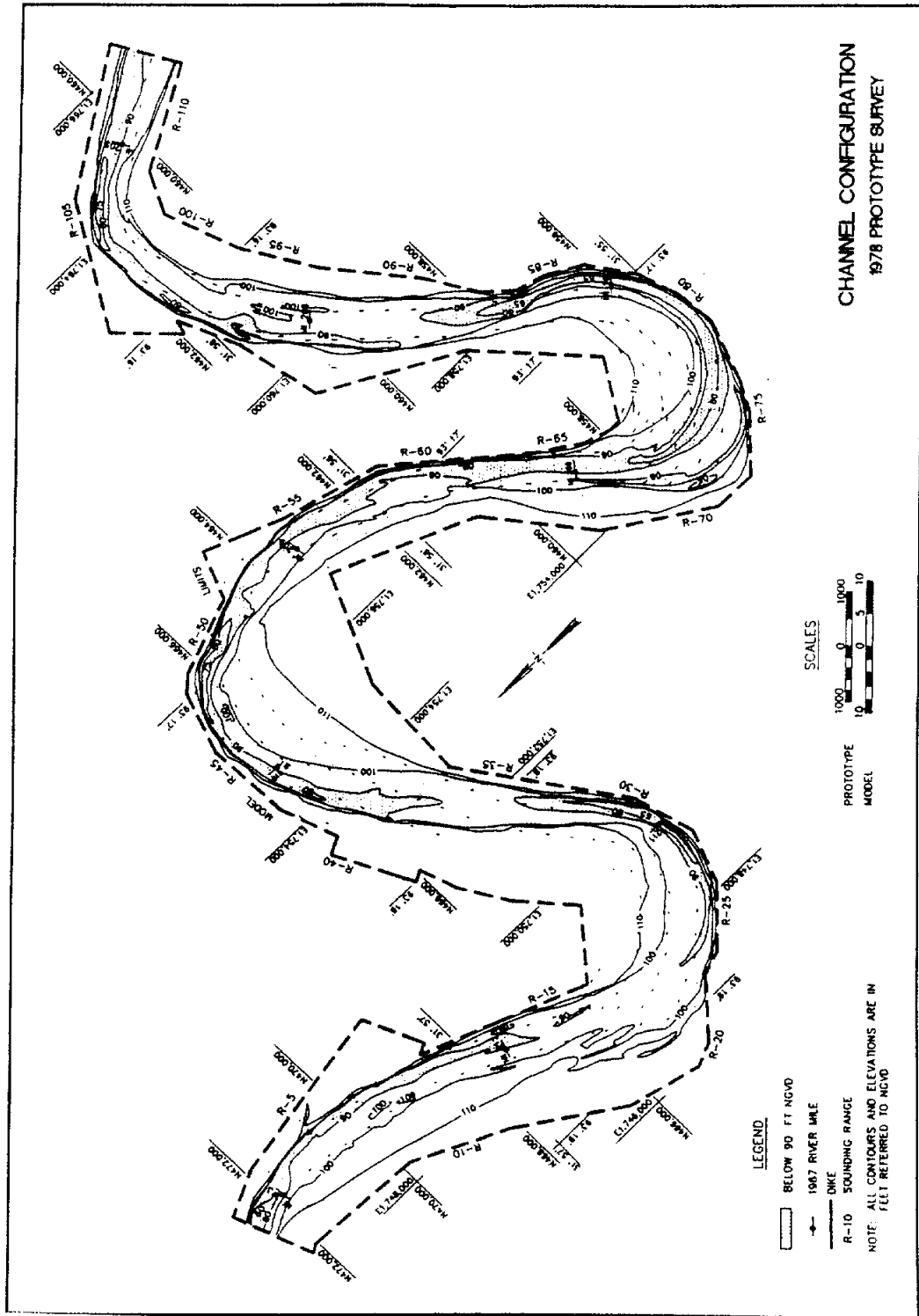


Figure B-10.1b L & D No. 4 1978 Prototype Survey

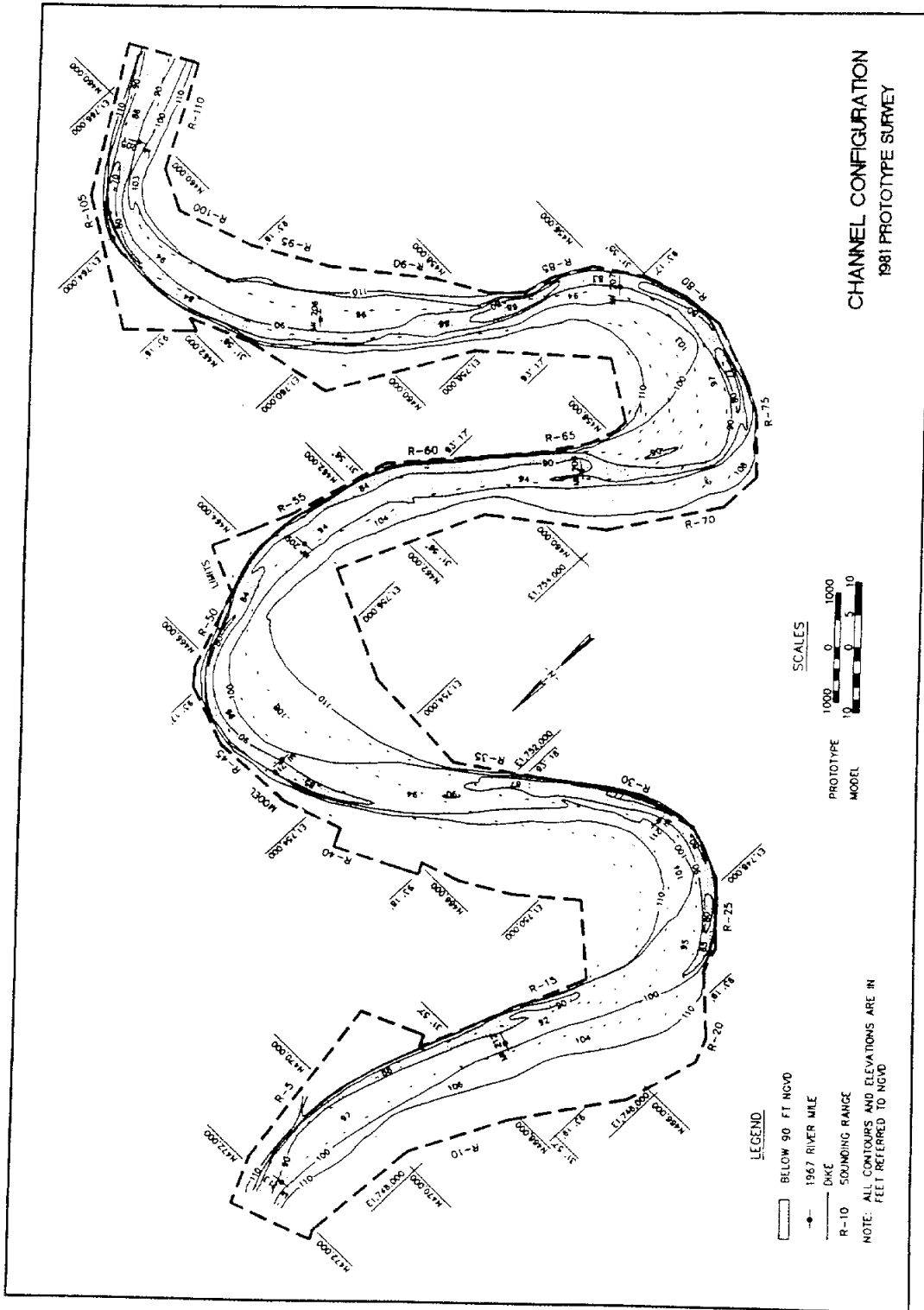


Figure B-10.1c L & D No. 4 1981 Prototype Survey

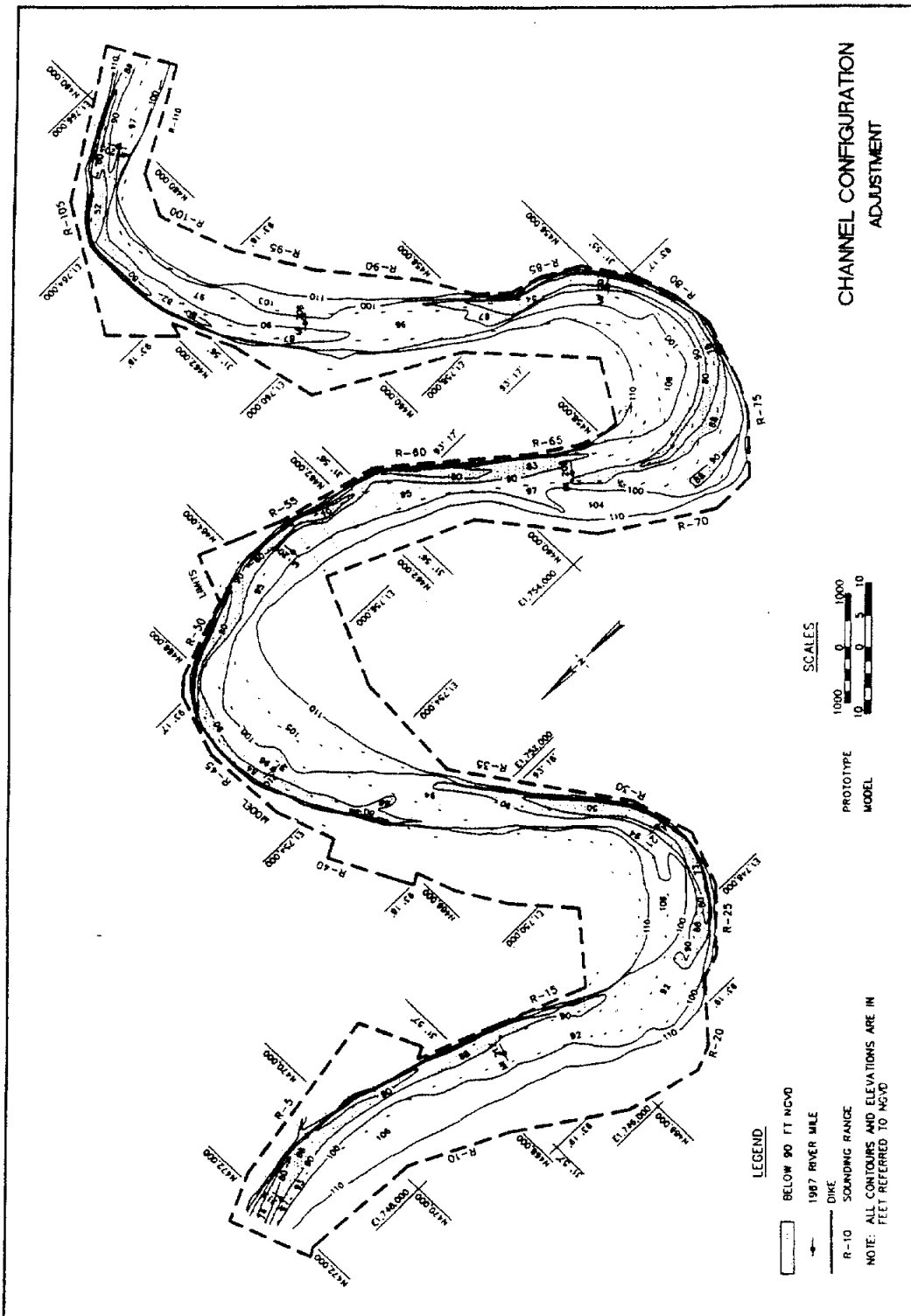


Figure B-10.1d L & D No. 4 Verification Test Survey

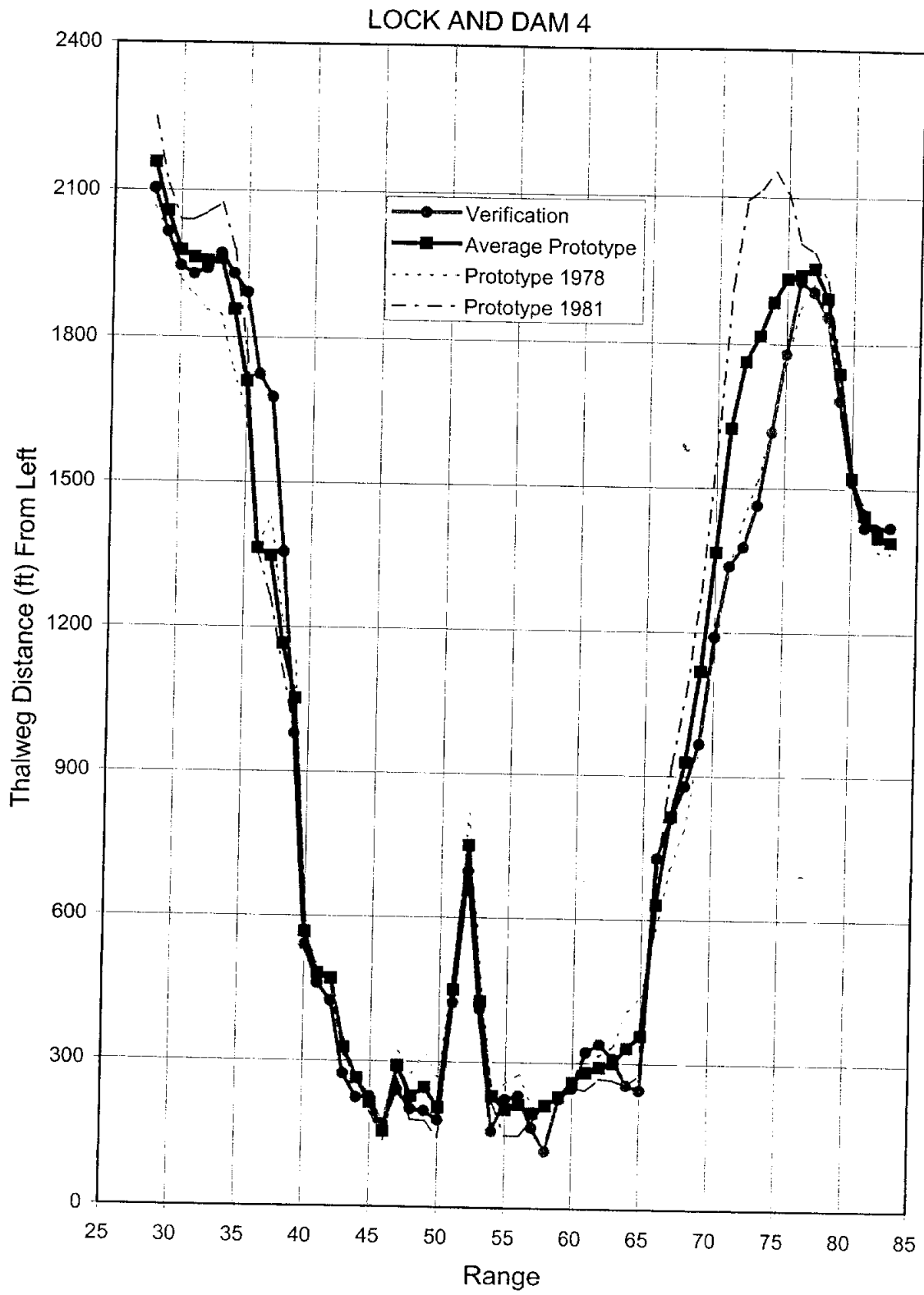


Figure B-10.2a Thalweg Location From Left by Range, Lock and Dam 4

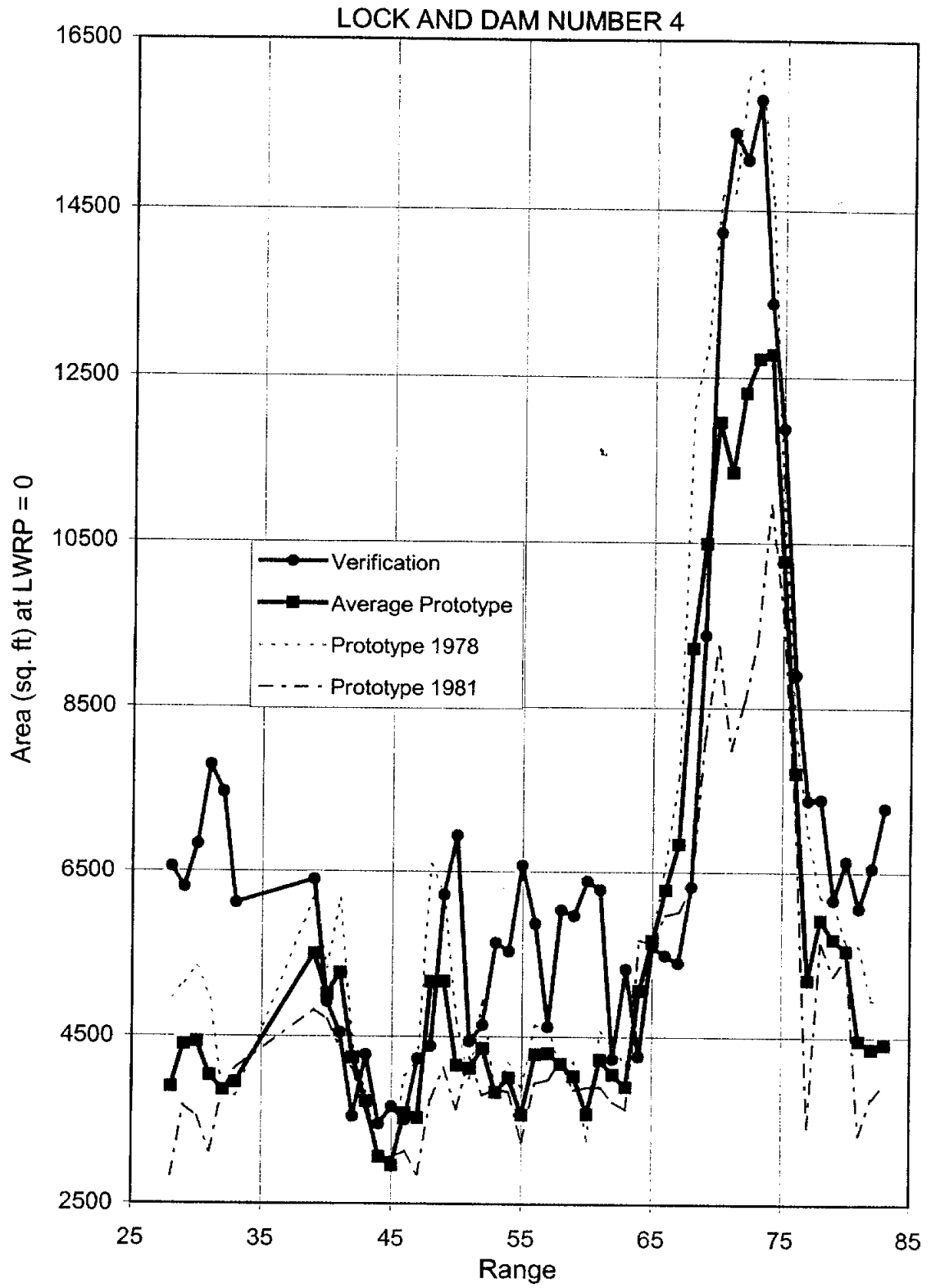


Figure B-10.2b Cross-Section Area by Range, Lock and Dam 4

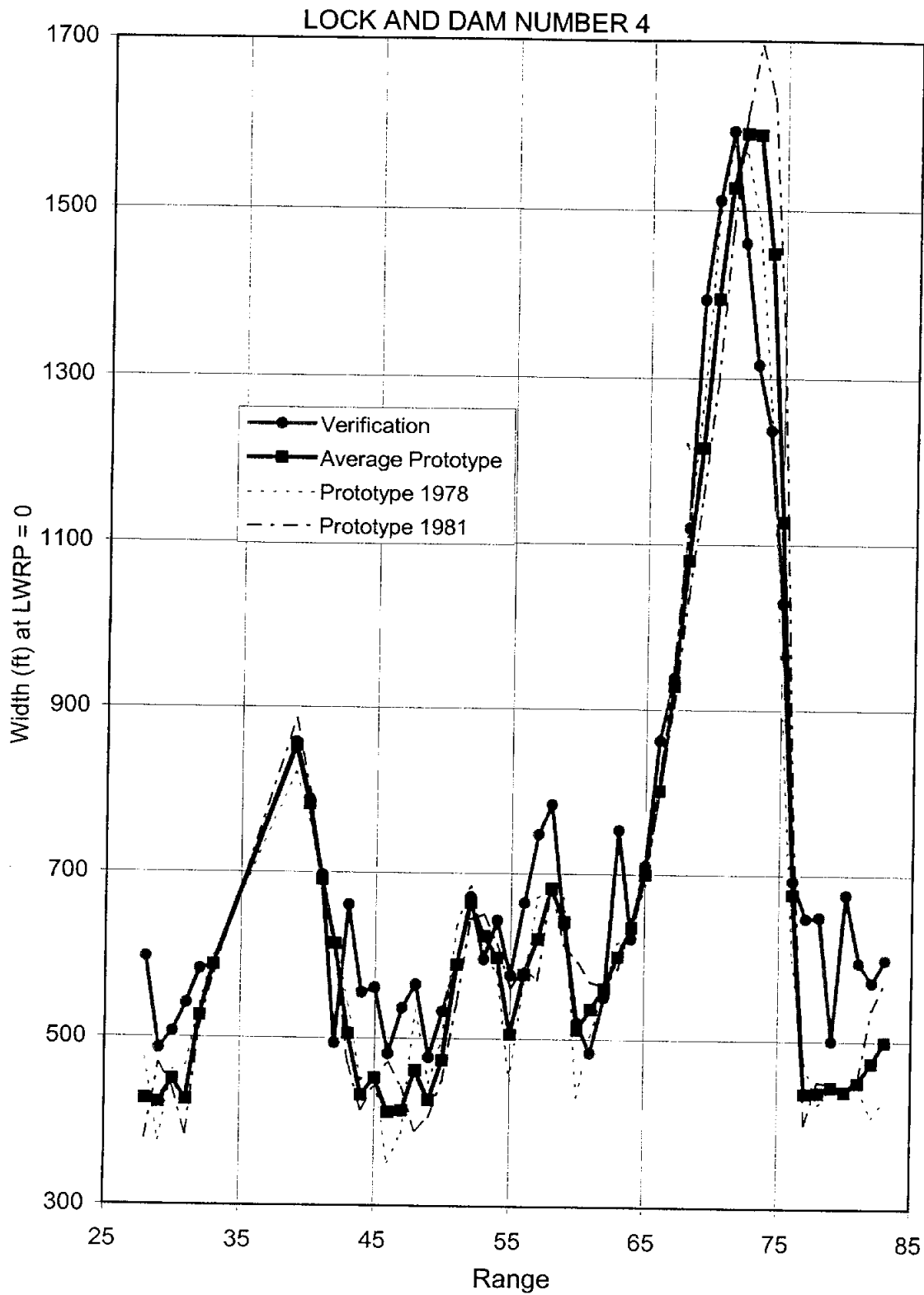


Figure B-10.2c Top Width by Range, Lock and Dam 4

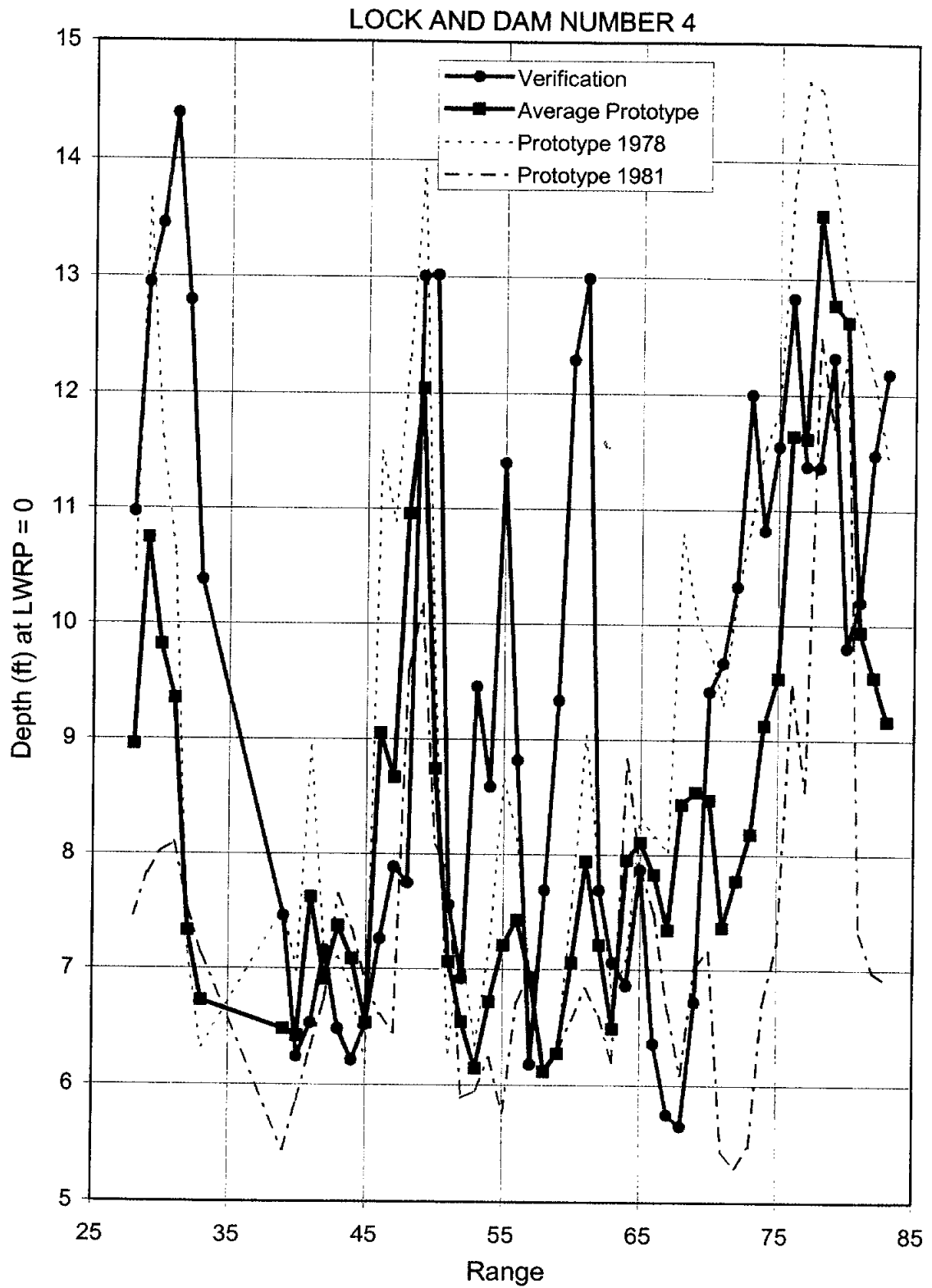


Figure B-10.2d Hydraulic Depth by Range, Lock and Dam 4

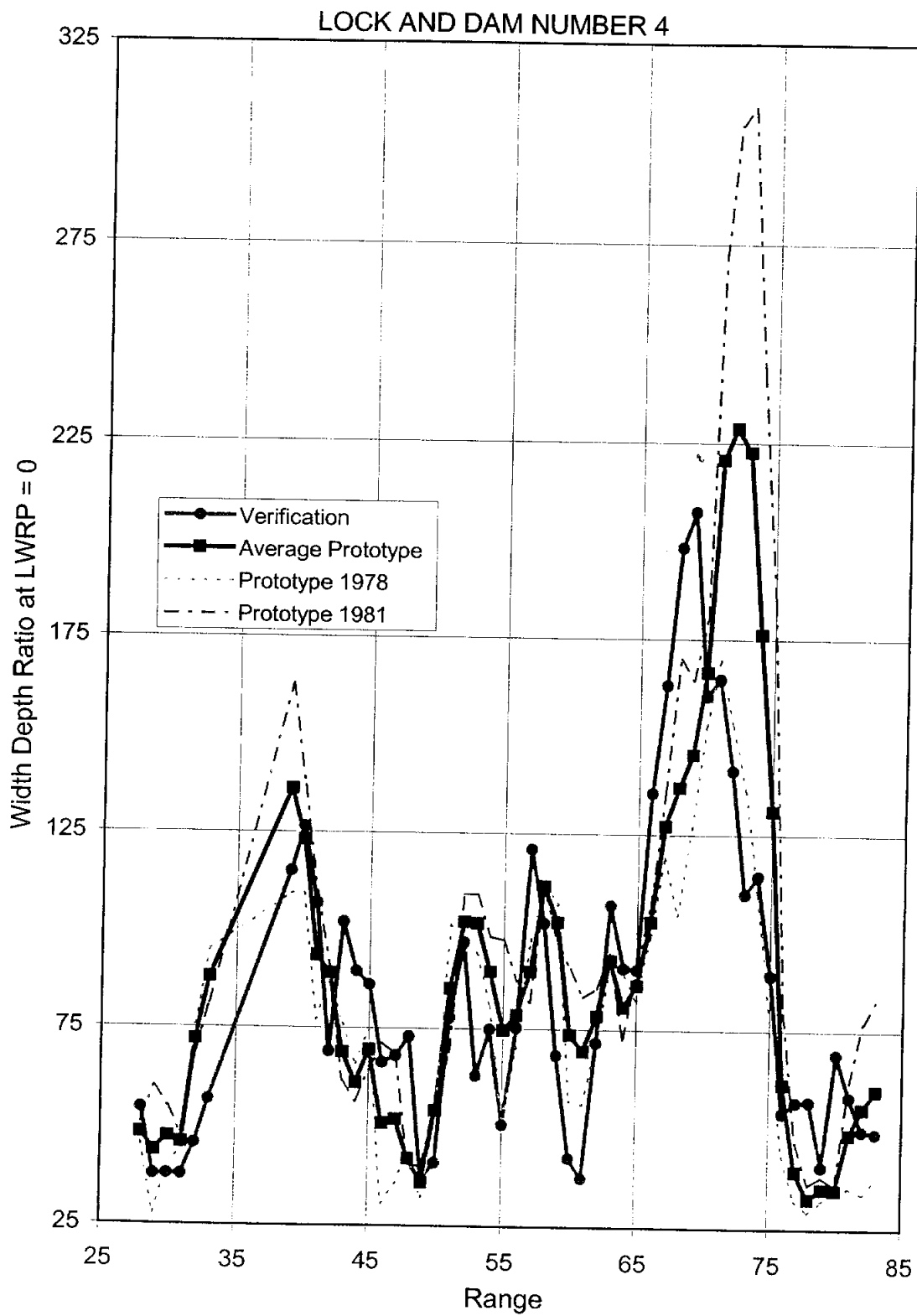
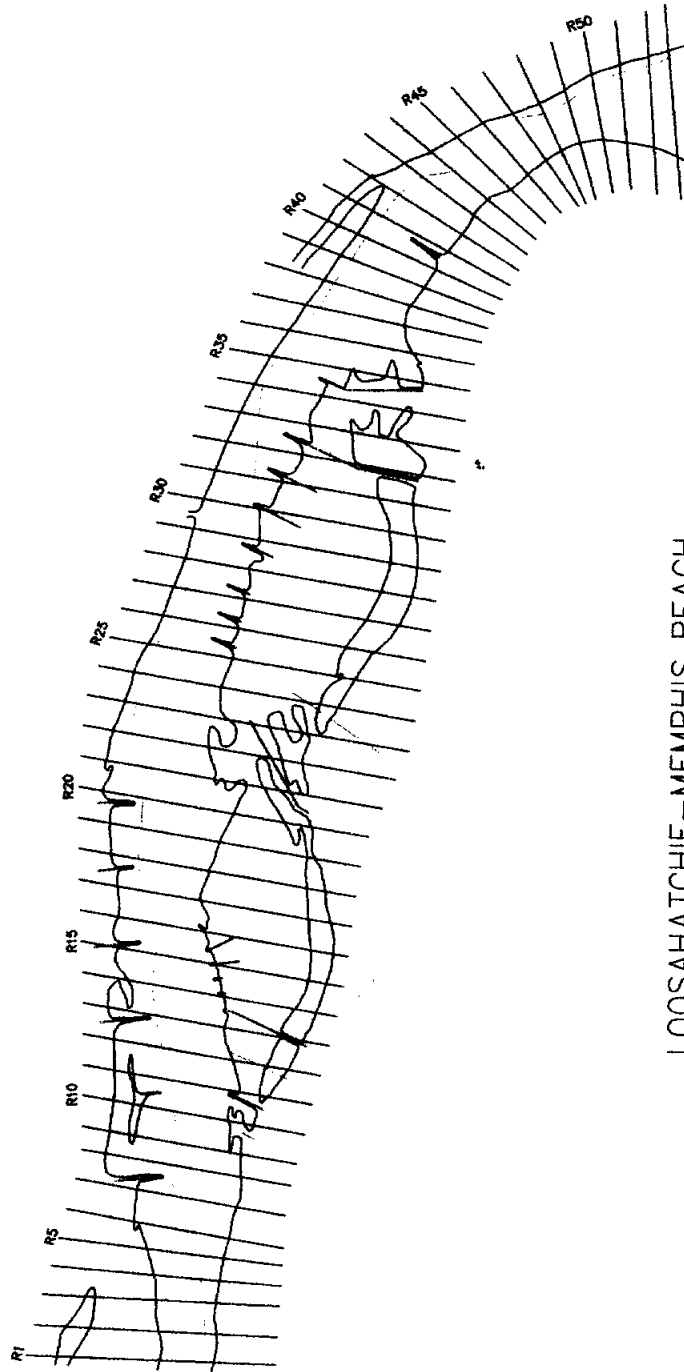


Figure B-10.2e Width/Depth Ratio by Range, Lock and Dam 4



LOOSAHATCHIE-MEMPHIS REACH

November 1986 Prototype

Figure B-11.1a Loosahatchie-Memphis Model Plan View

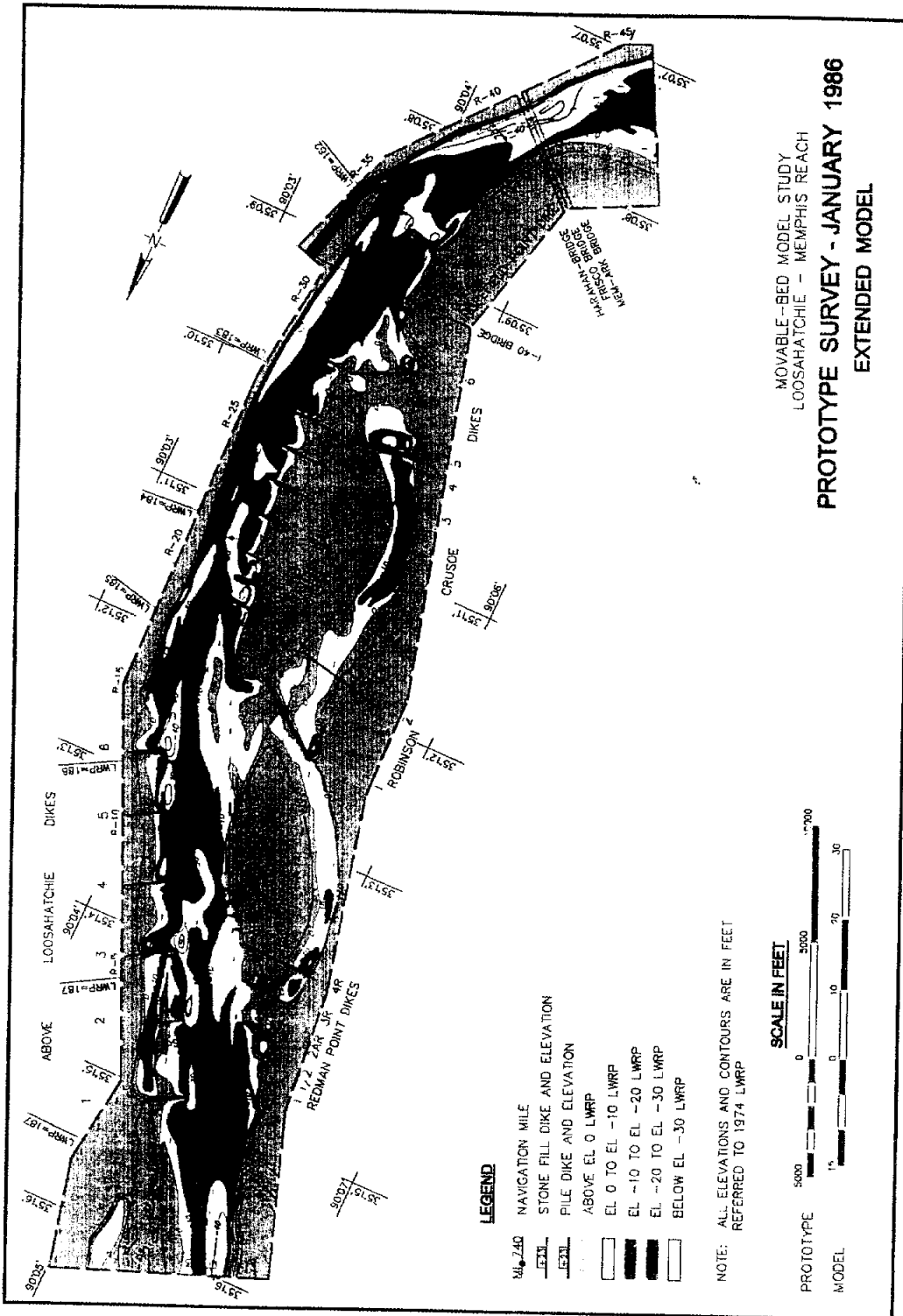


Figure B-11.1b January 1986 Prototype Survey, Loosahatchie-Memphis

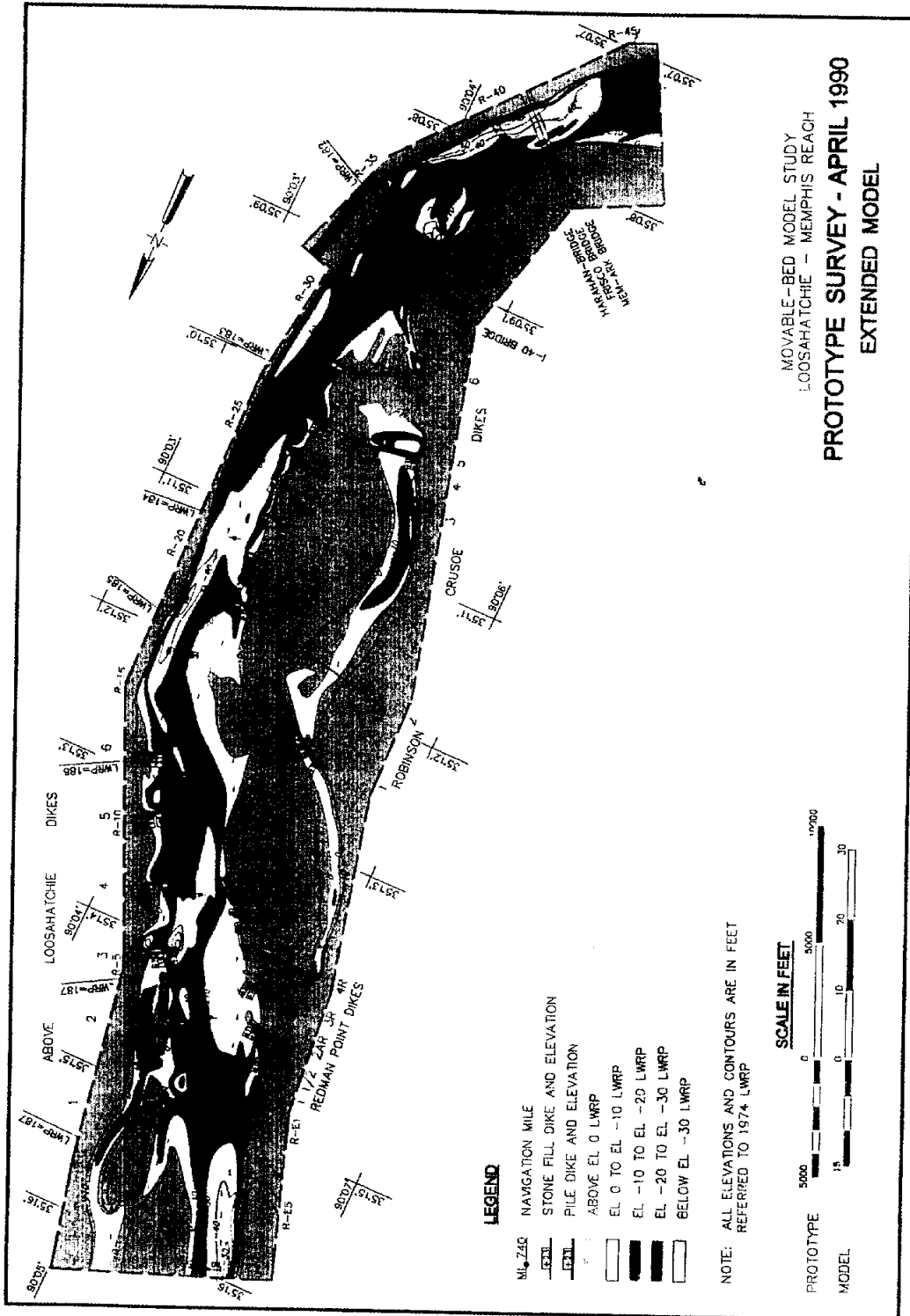


Figure B-11.1d April 1990 Prototype Survey, Loosahatchie-Memphis

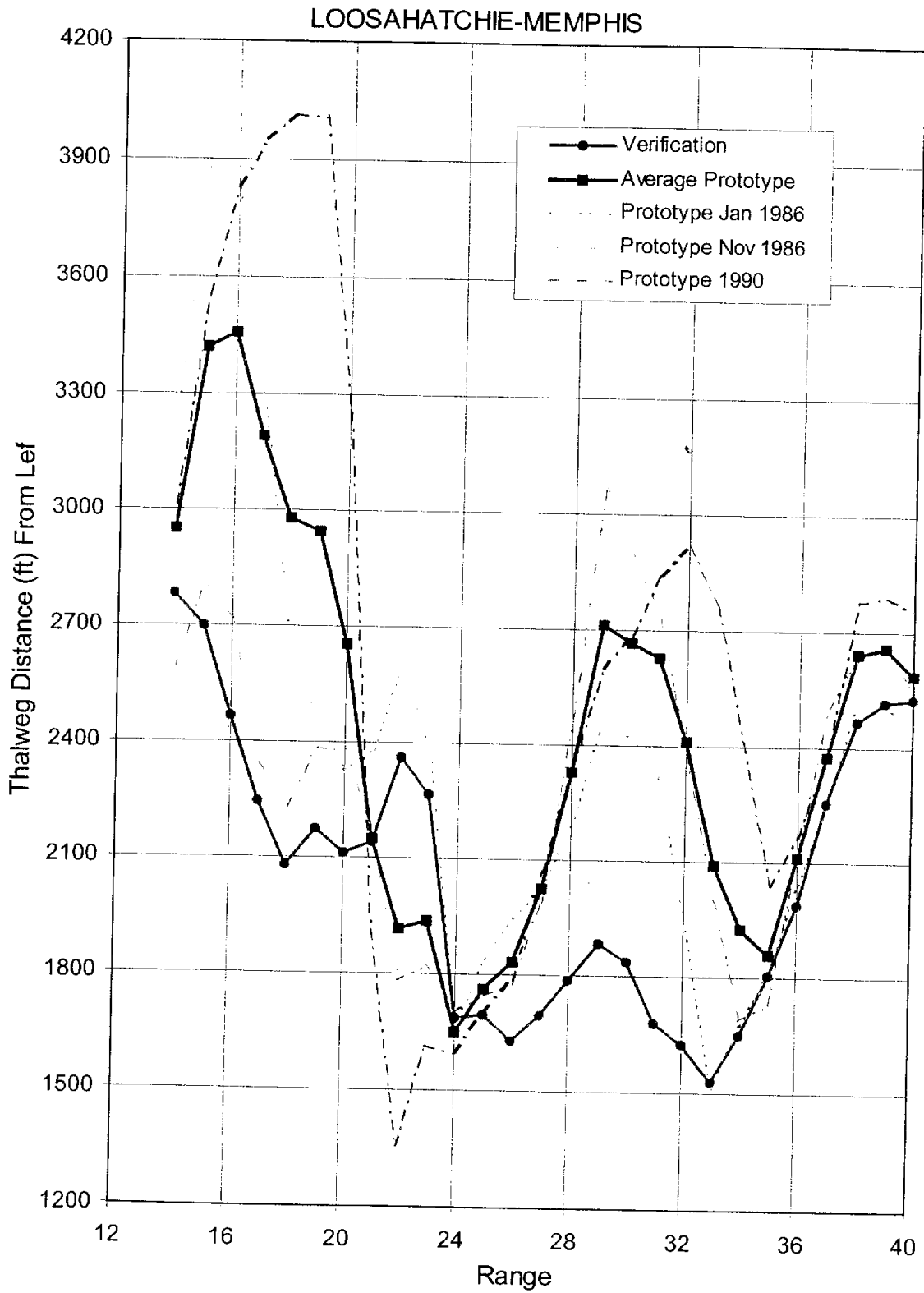


Figure B-11.2a Thalweg Location From Left by Range, Loosahatchie Memphis

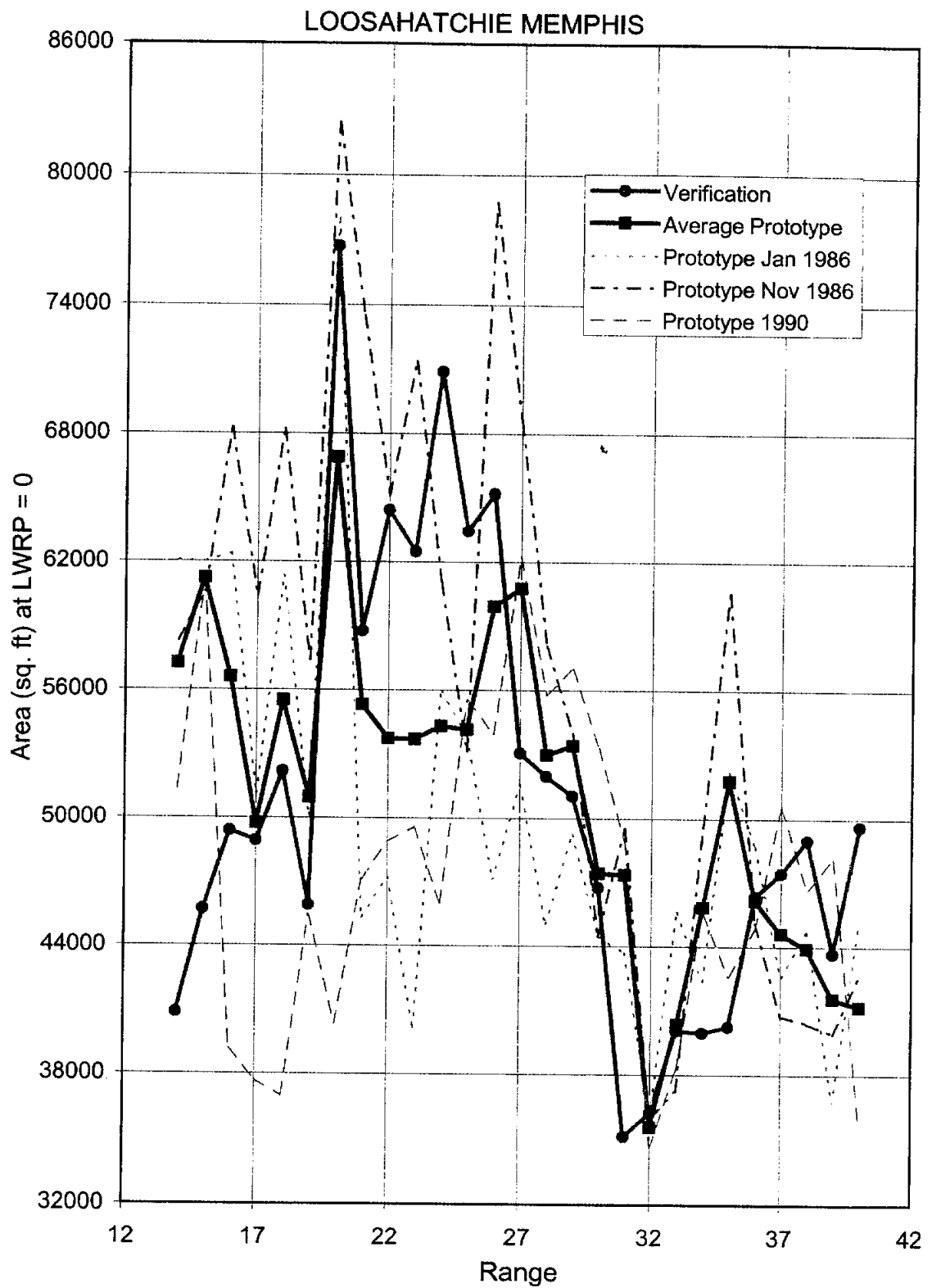


Figure B-11.2b Cross-Section Area by Range, Loosahatchie Memphis

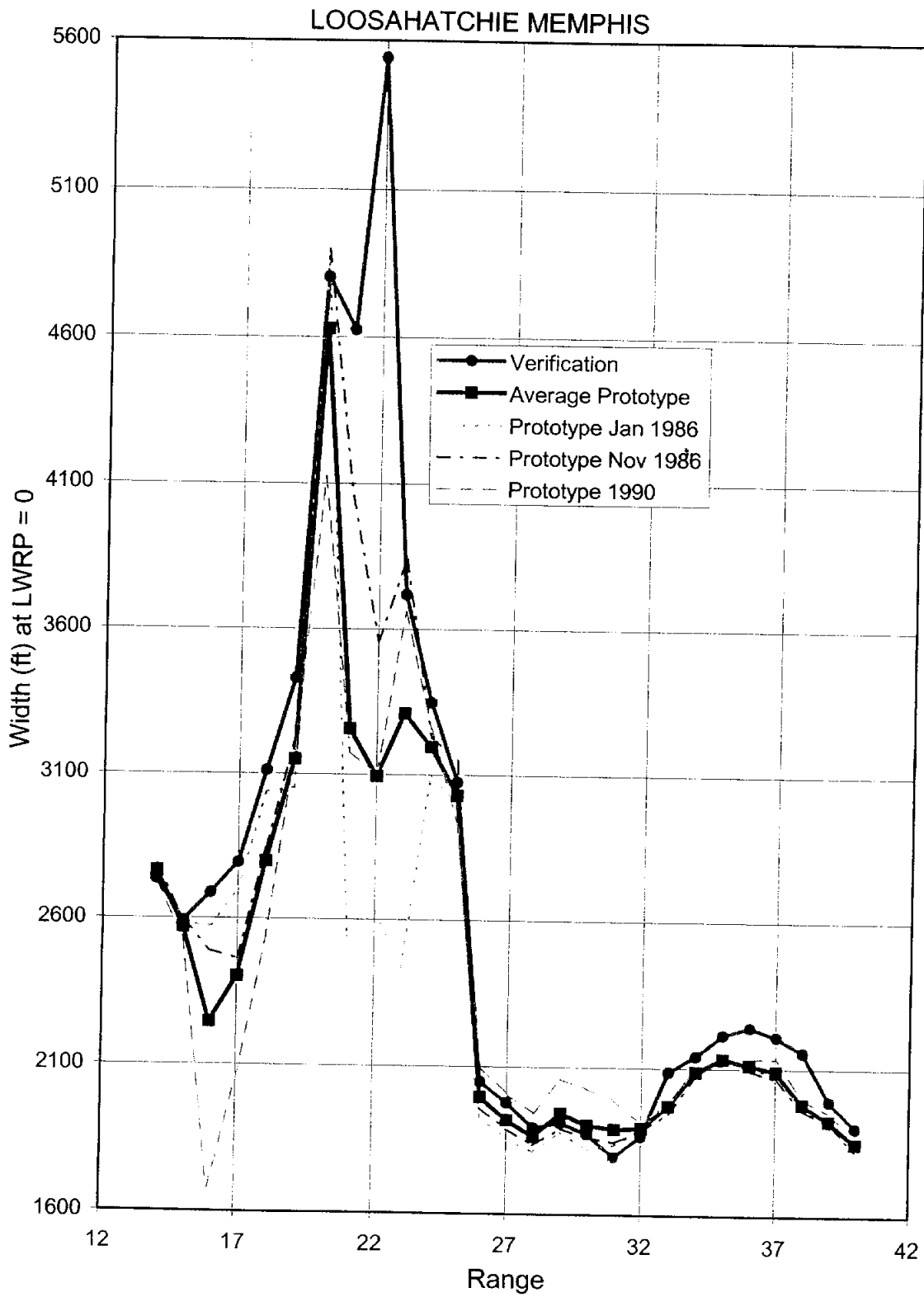


Figure B-11.2c Top Width by Range, Loosahatchie Memphis

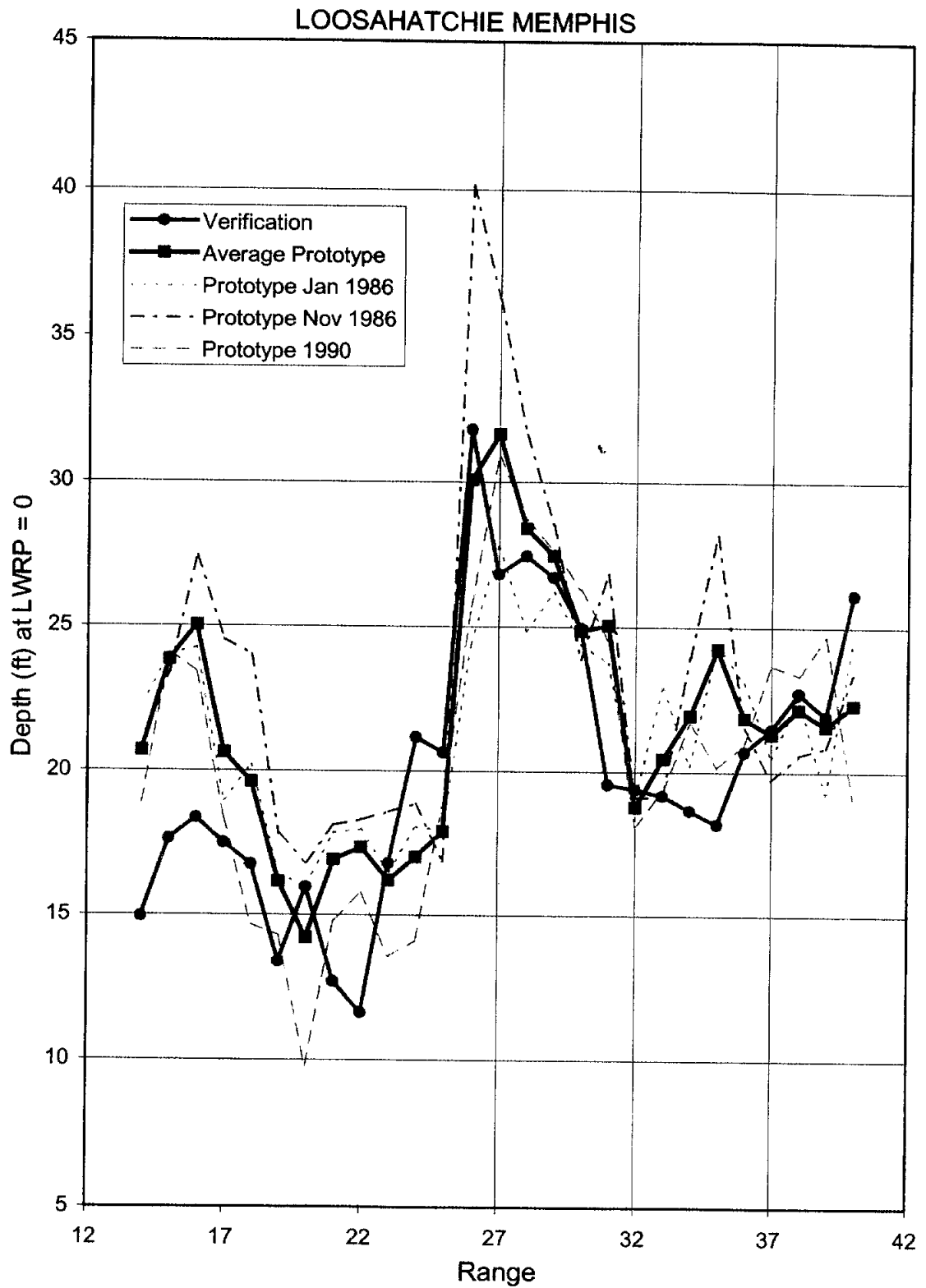


Figure B-11.2d Hydraulic Depth by Range, Loosahatchie Memphis

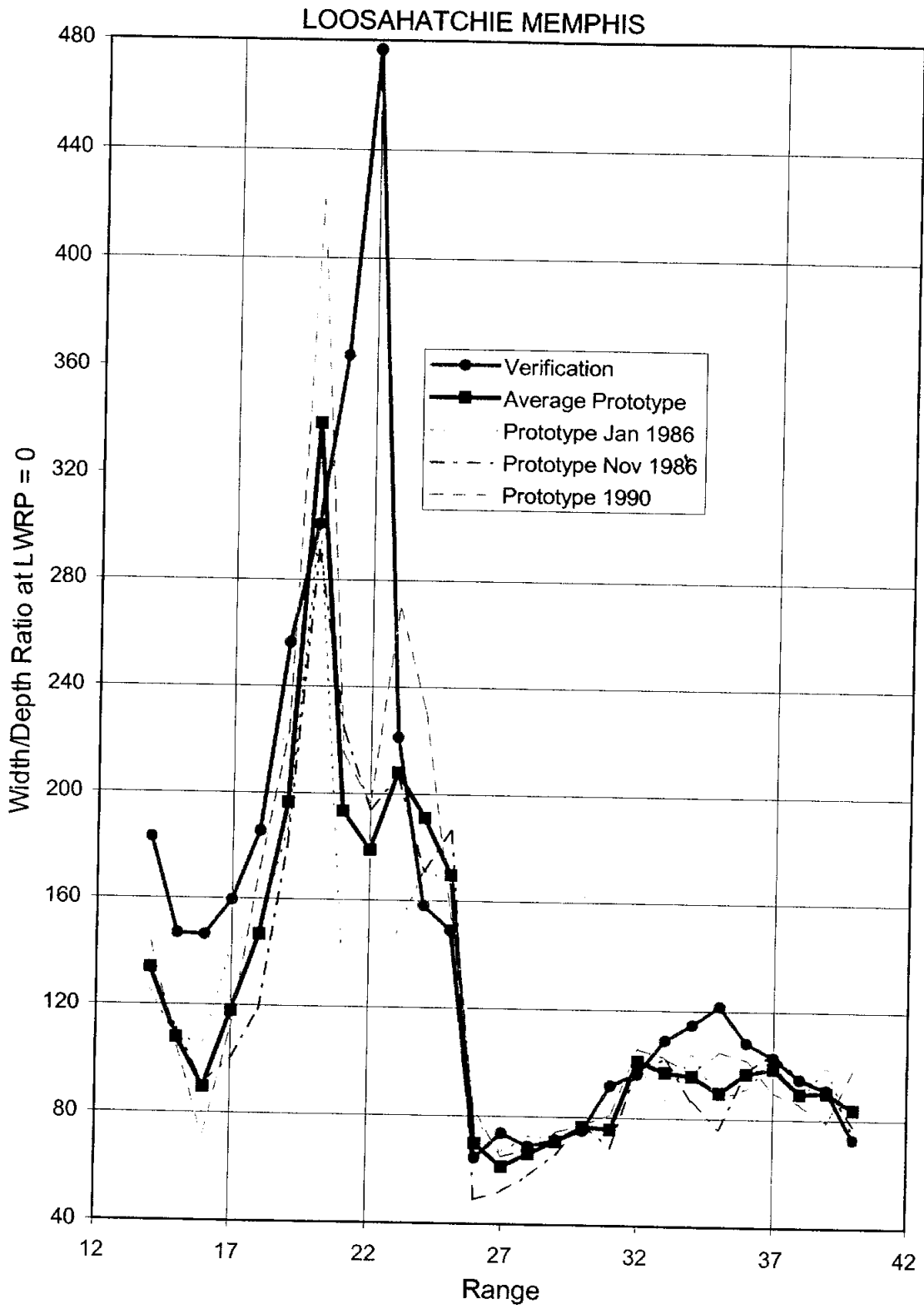


Figure B-11.2e Width/Depth Ratio by Range, Loosahatchie Memphis

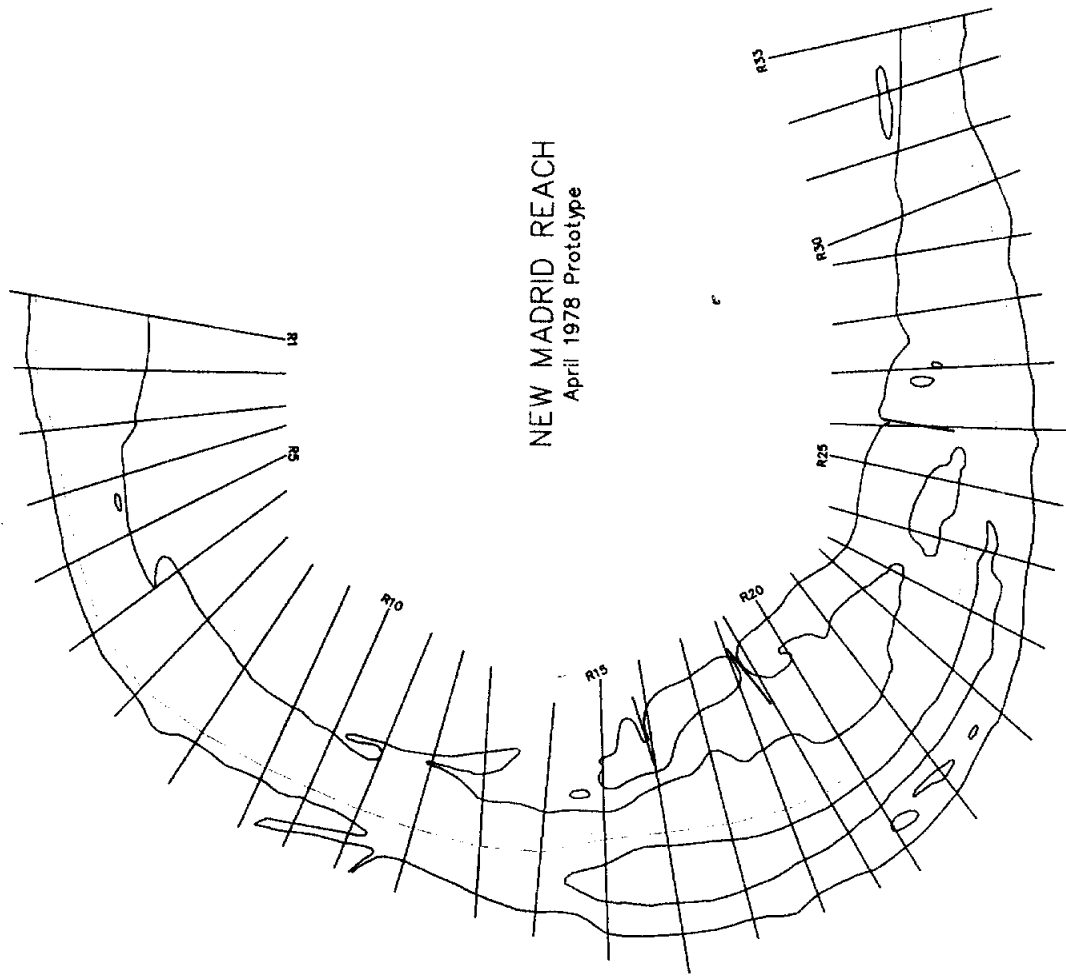


Figure B-12.1a New Madrid Model Plan View

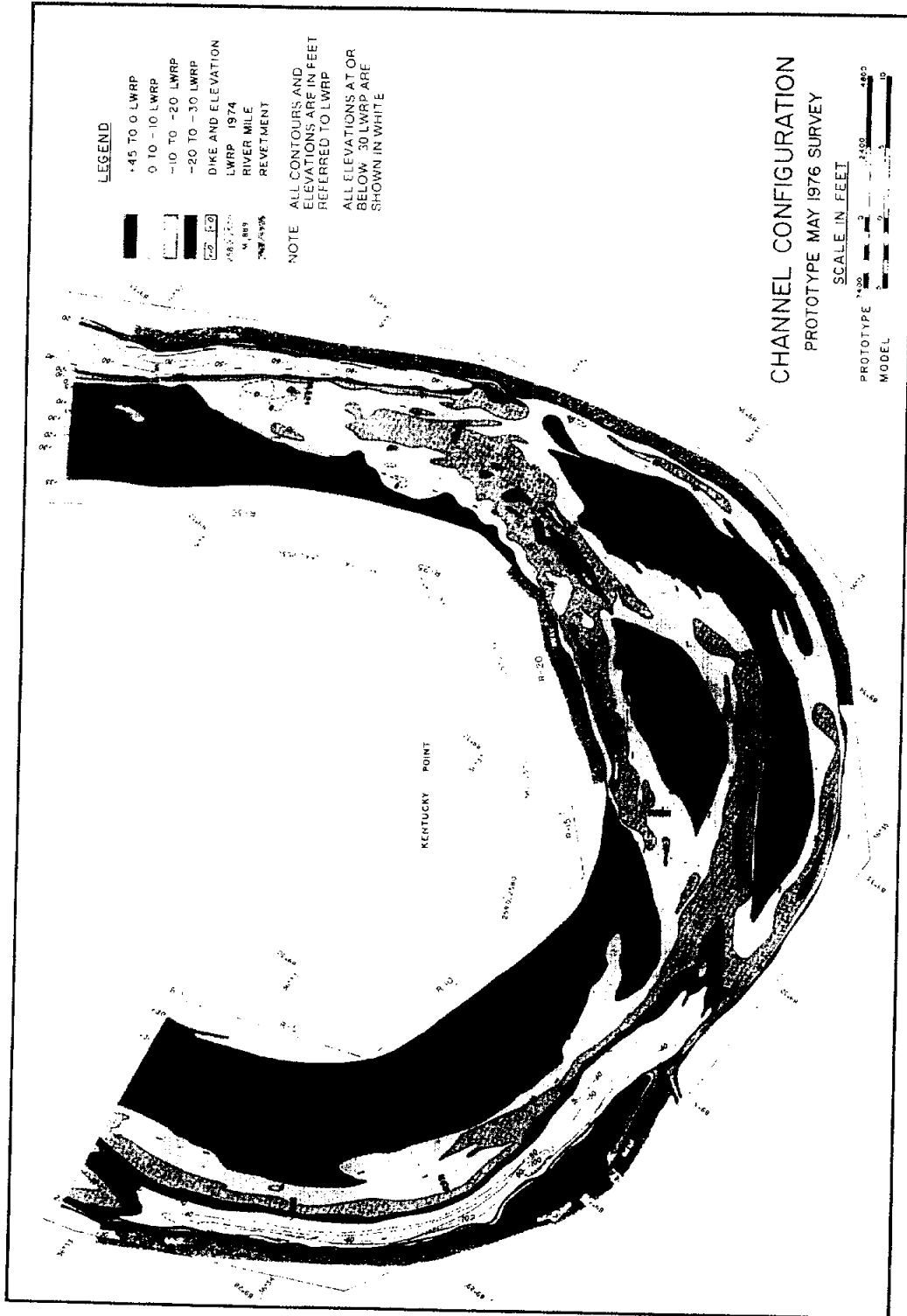


Figure B-12.1b New Madrid May 1976 Prototype Survey

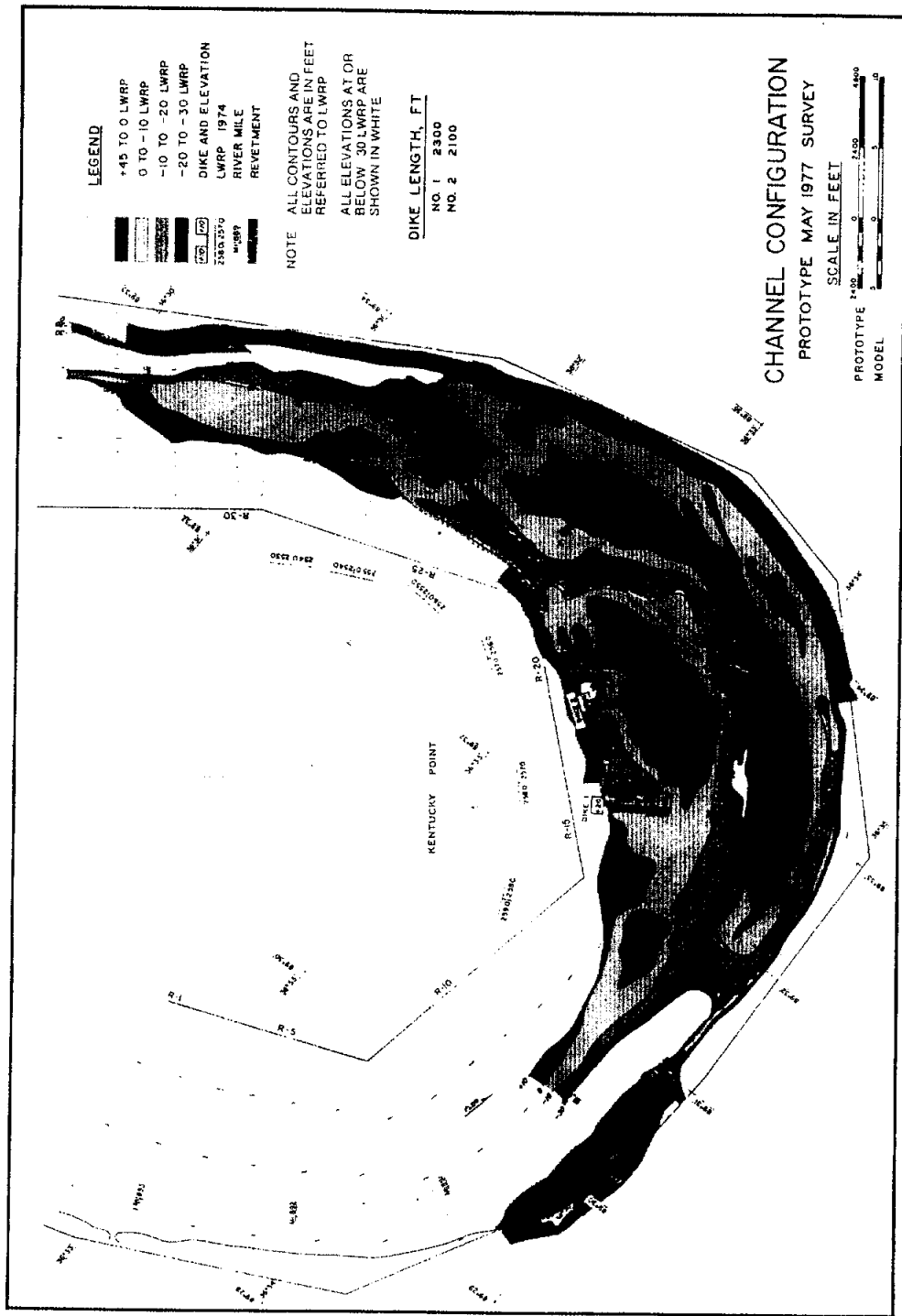


Figure B-12.1c New Madrid May 1977 Prototype Survey

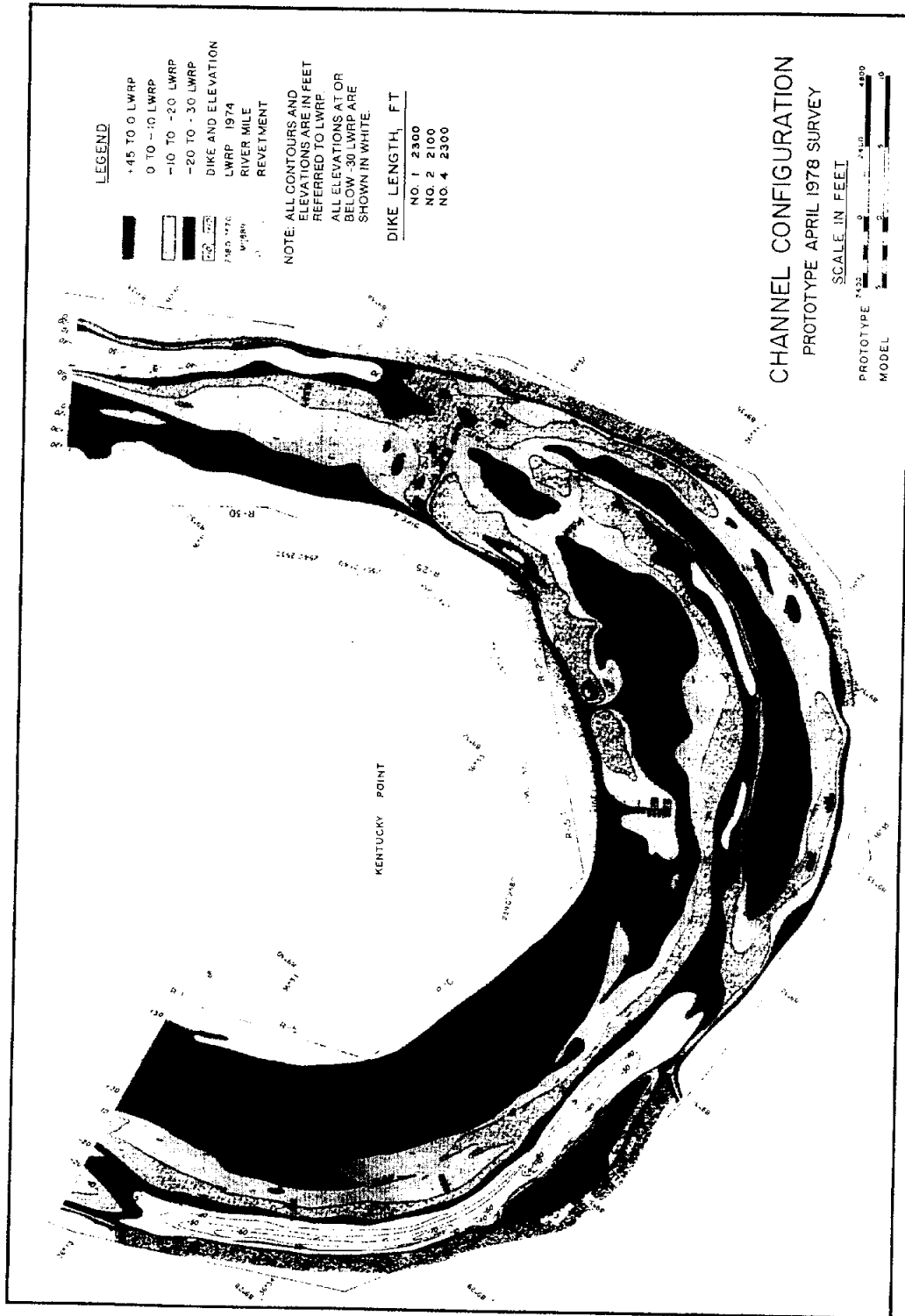


Figure B-12.1d New Madrid April 1978 Prototype Survey

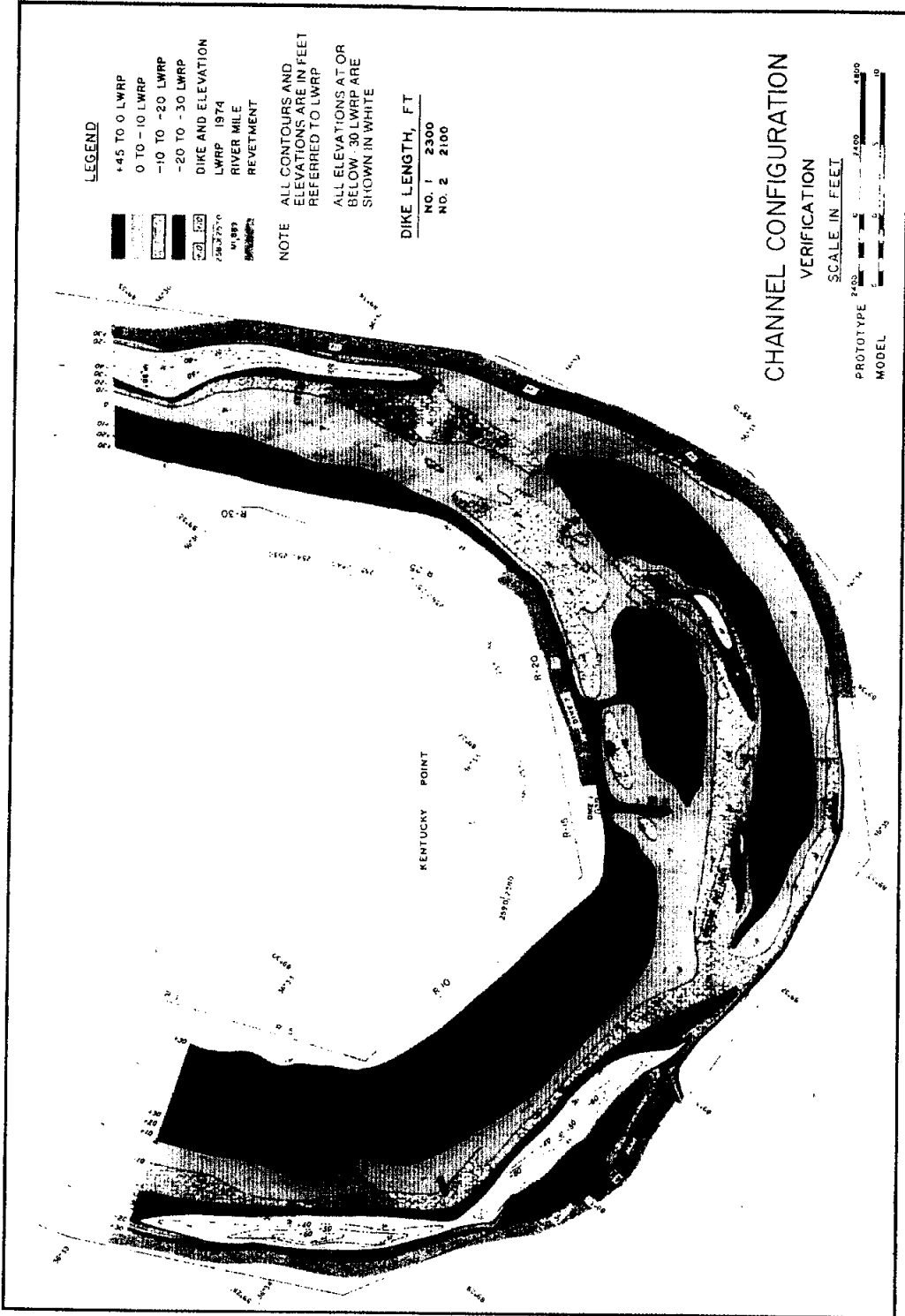


Figure B-12.1e New Madrid Verification Test Survey

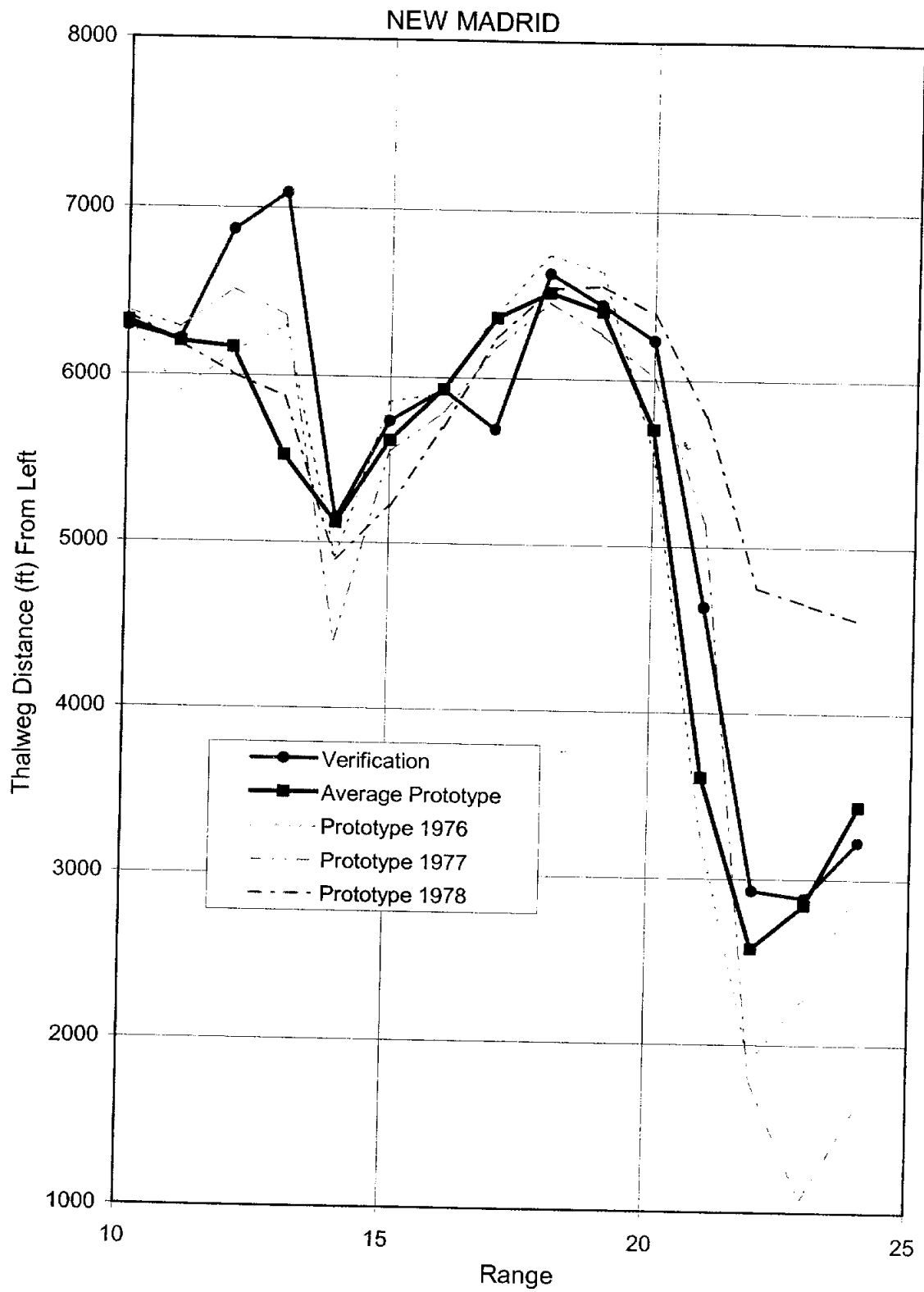


Figure B-12.2a Thalweg Position From Left by Range, New Madrid

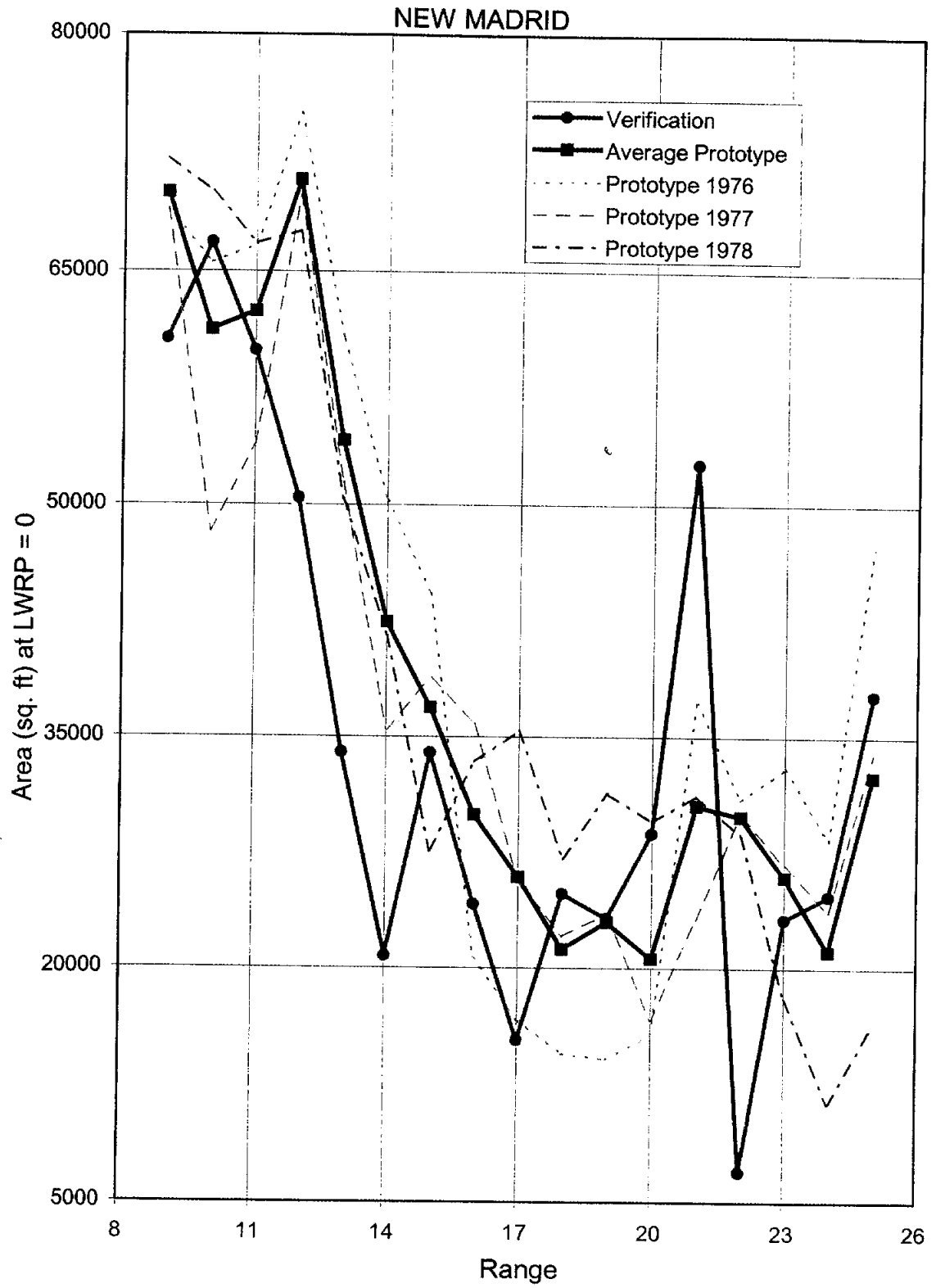


Figure B-12.2b Cross-Section Area by Range, New Madrid

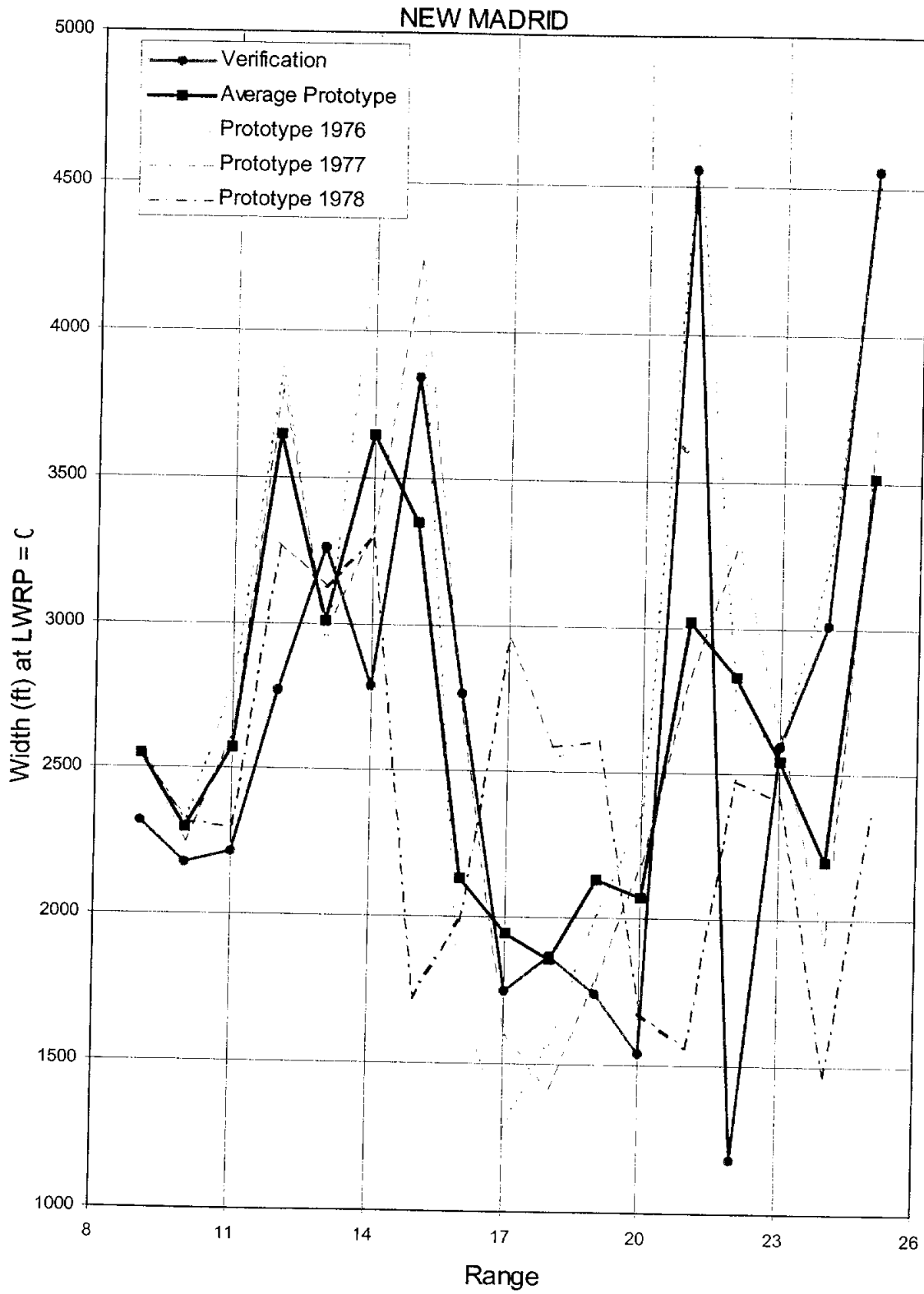


Figure B-12.2c Top Width by Range, New Madrid

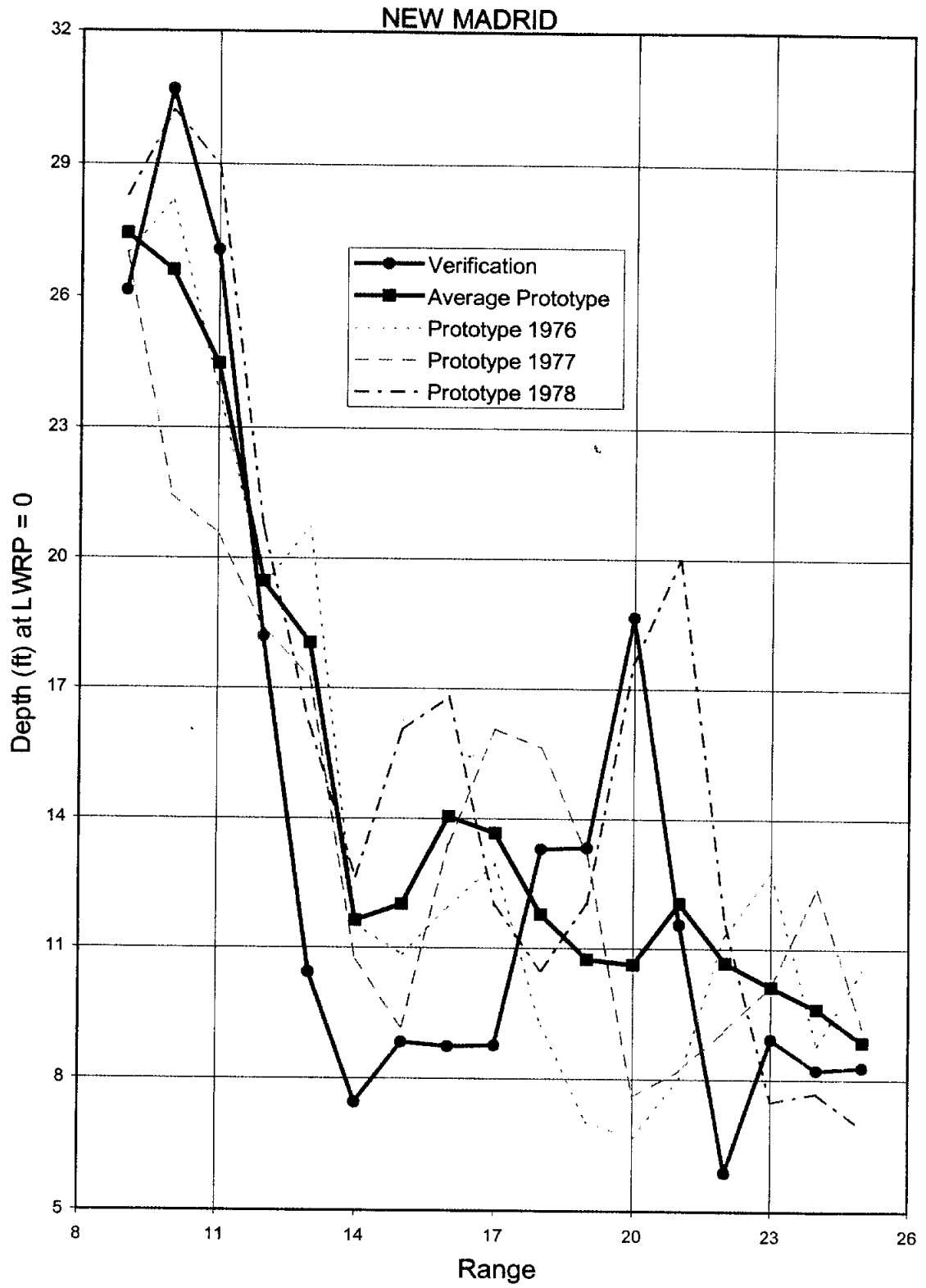


Figure B-12.2d Hydraulic Depth by Range, New Madrid

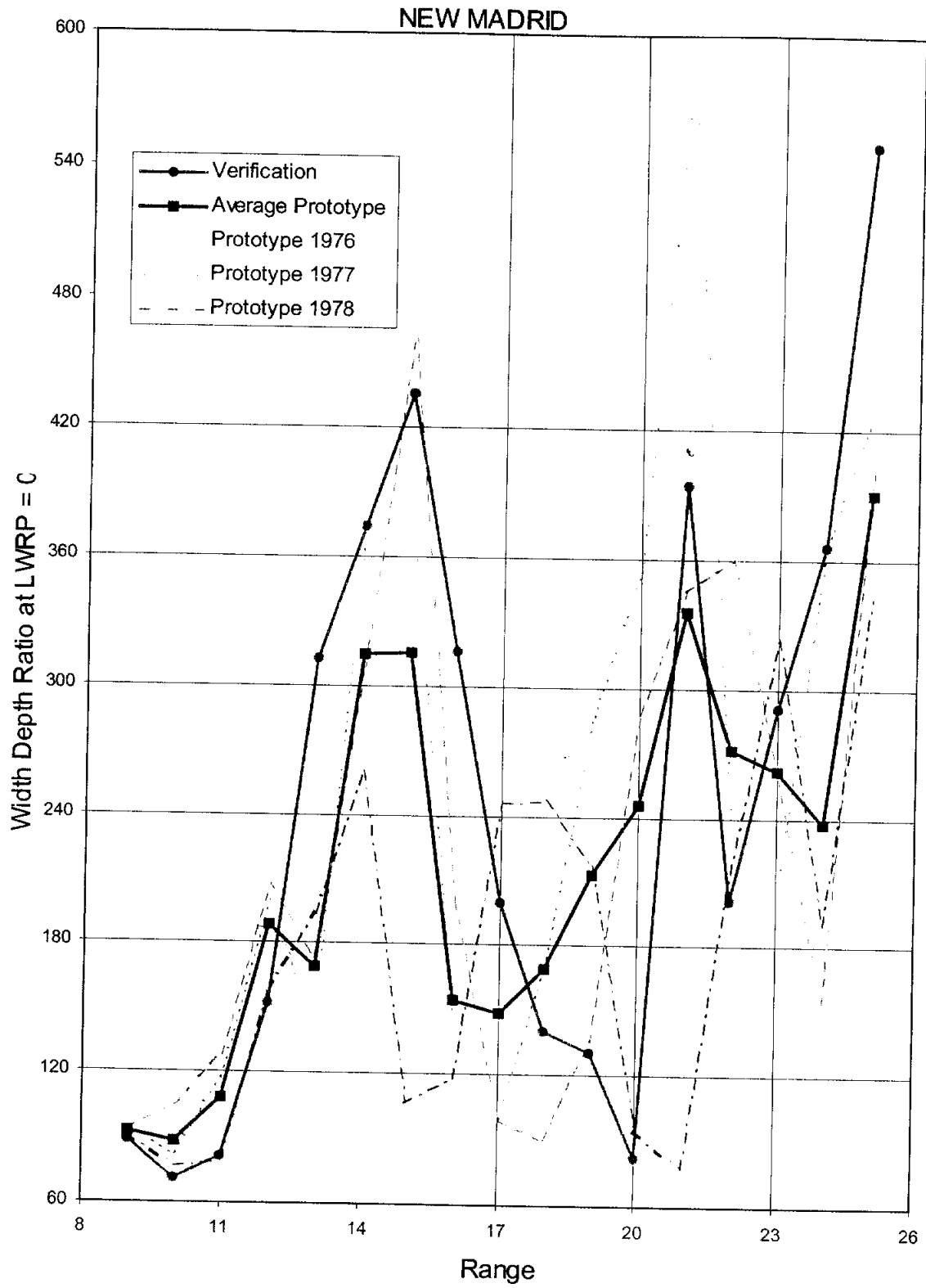
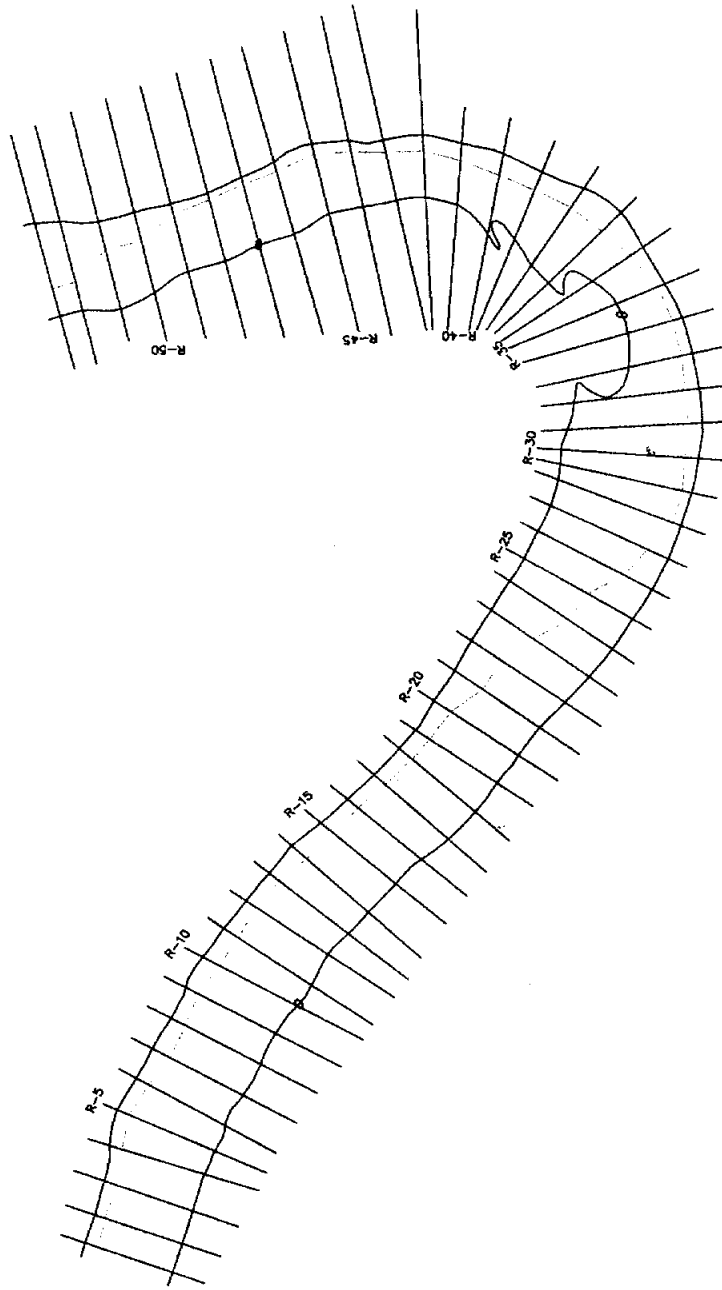


Figure B-12.2e Width/Depth Ratio by Range, New Madrid



REDEYE CROSSING REACH
 August 1983 Prototype

Figure B-13.1a Redeye Crossing Model Plan View

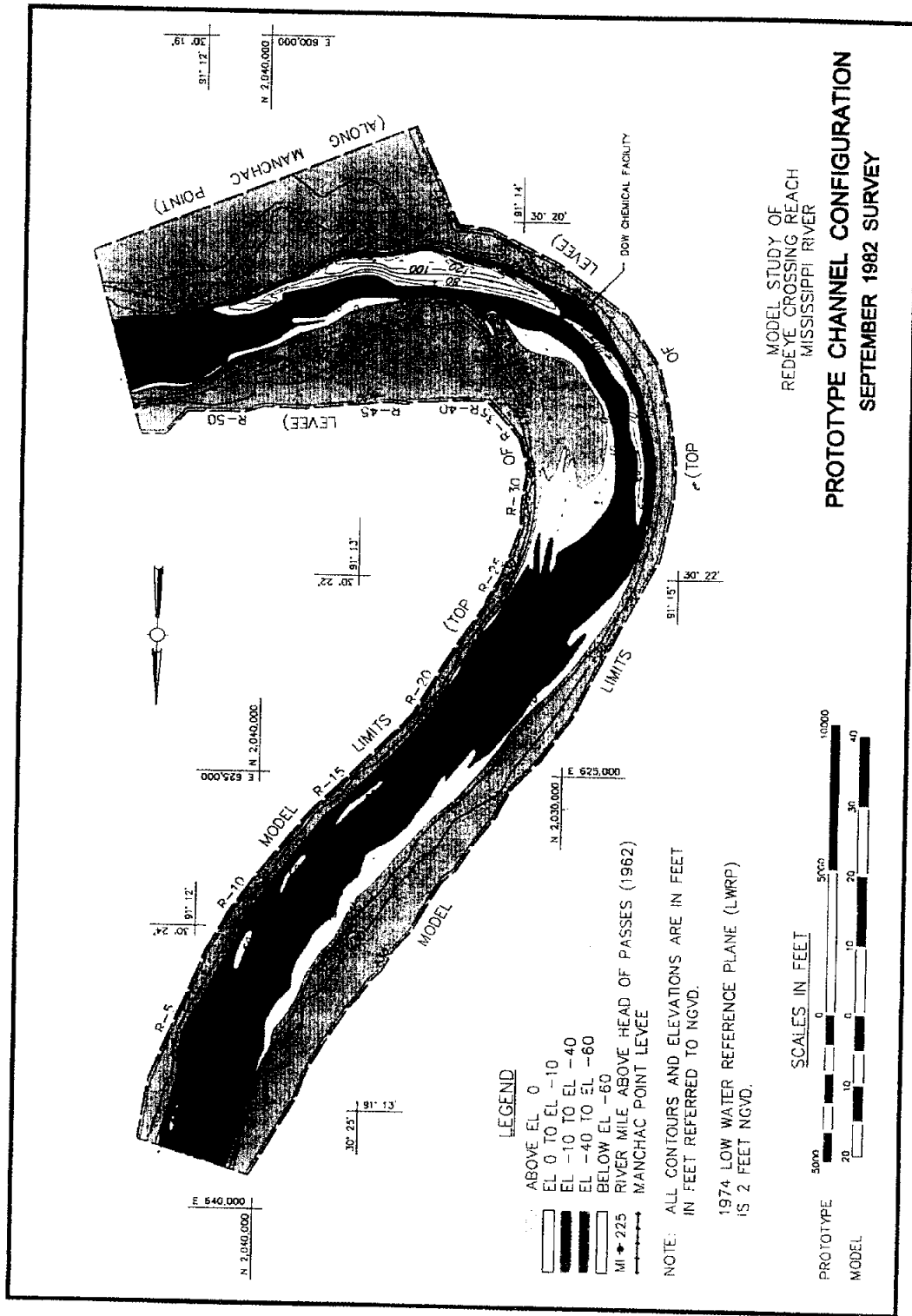


Figure B-13.1b 1982 Prototype Survey, Redeye Crossing

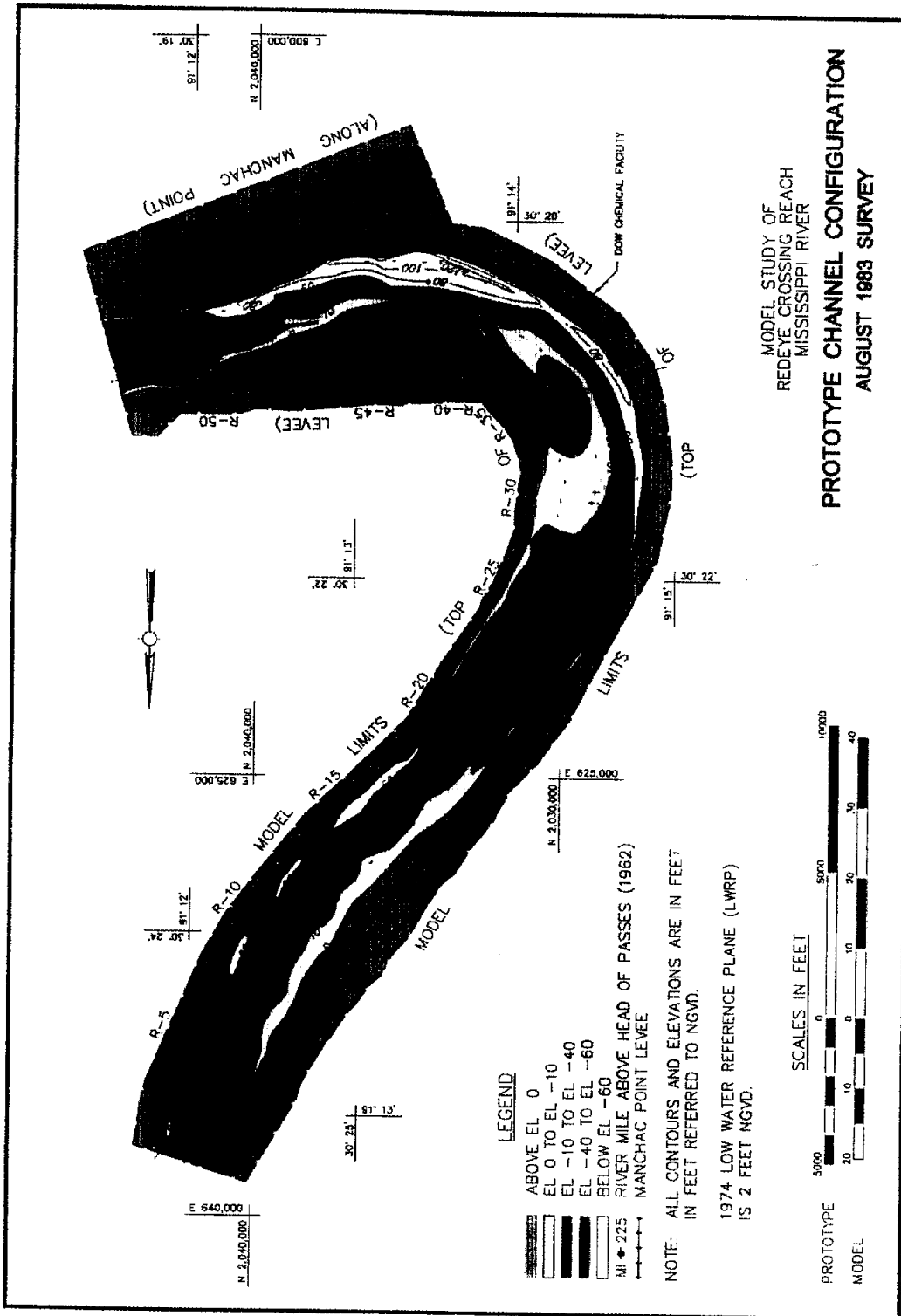


Figure B-13.1c 1983 Prototype Survey, Redeye Crossing

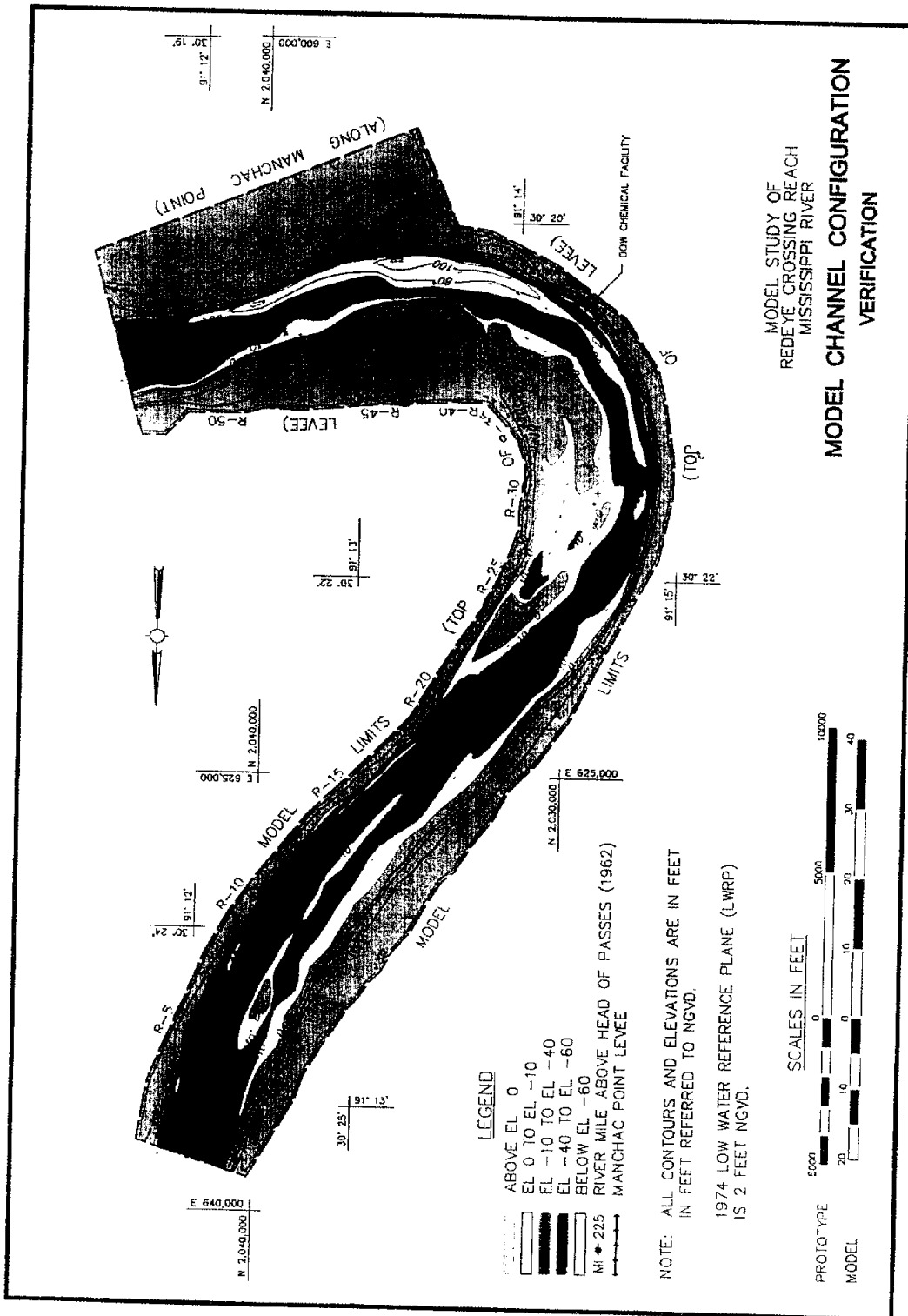


Figure B-13.1d Verification Survey, Redeye Crossing

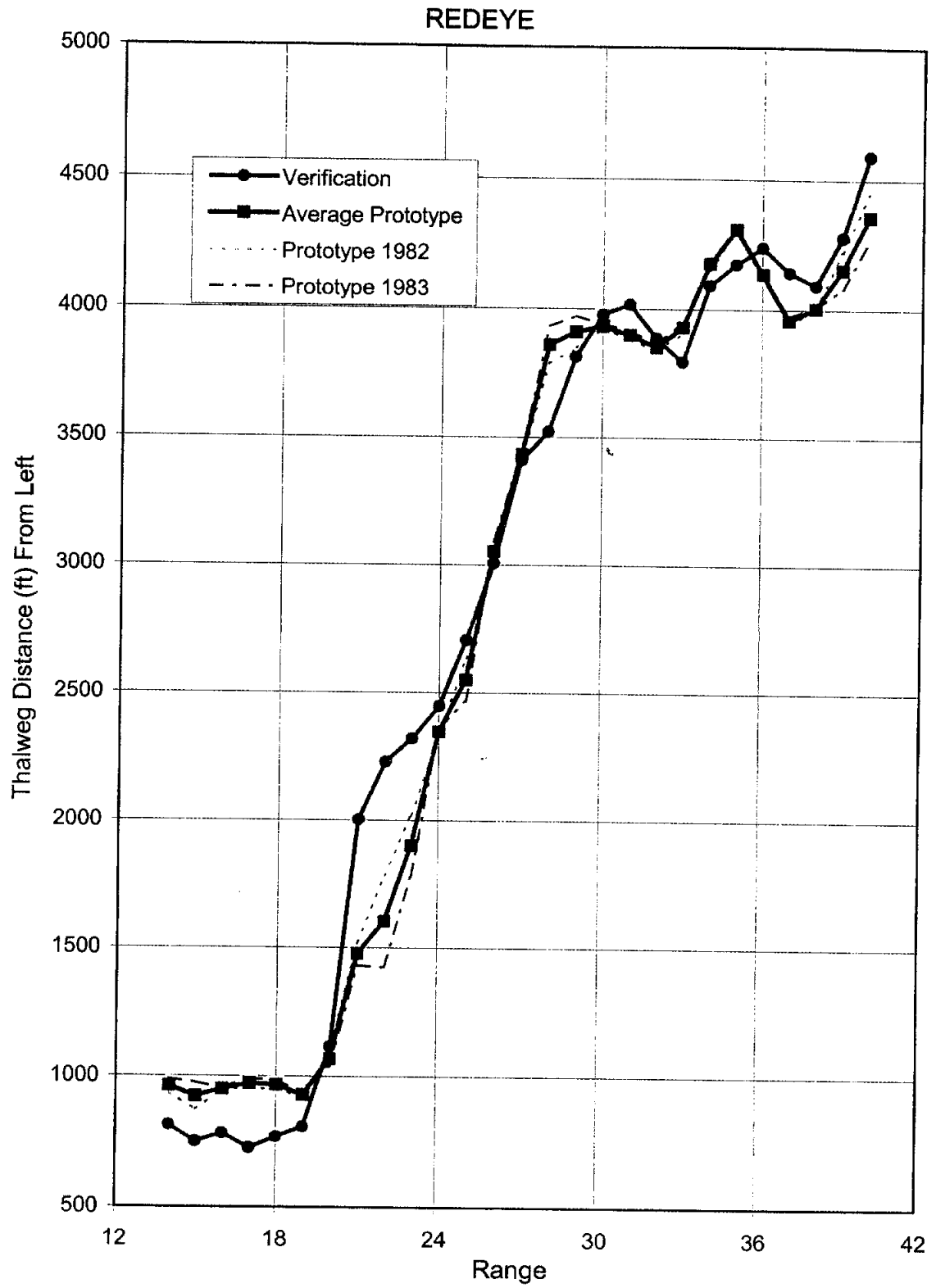


Figure B-13.2a Thalweg Location From Left by Range, Redeye Crossing

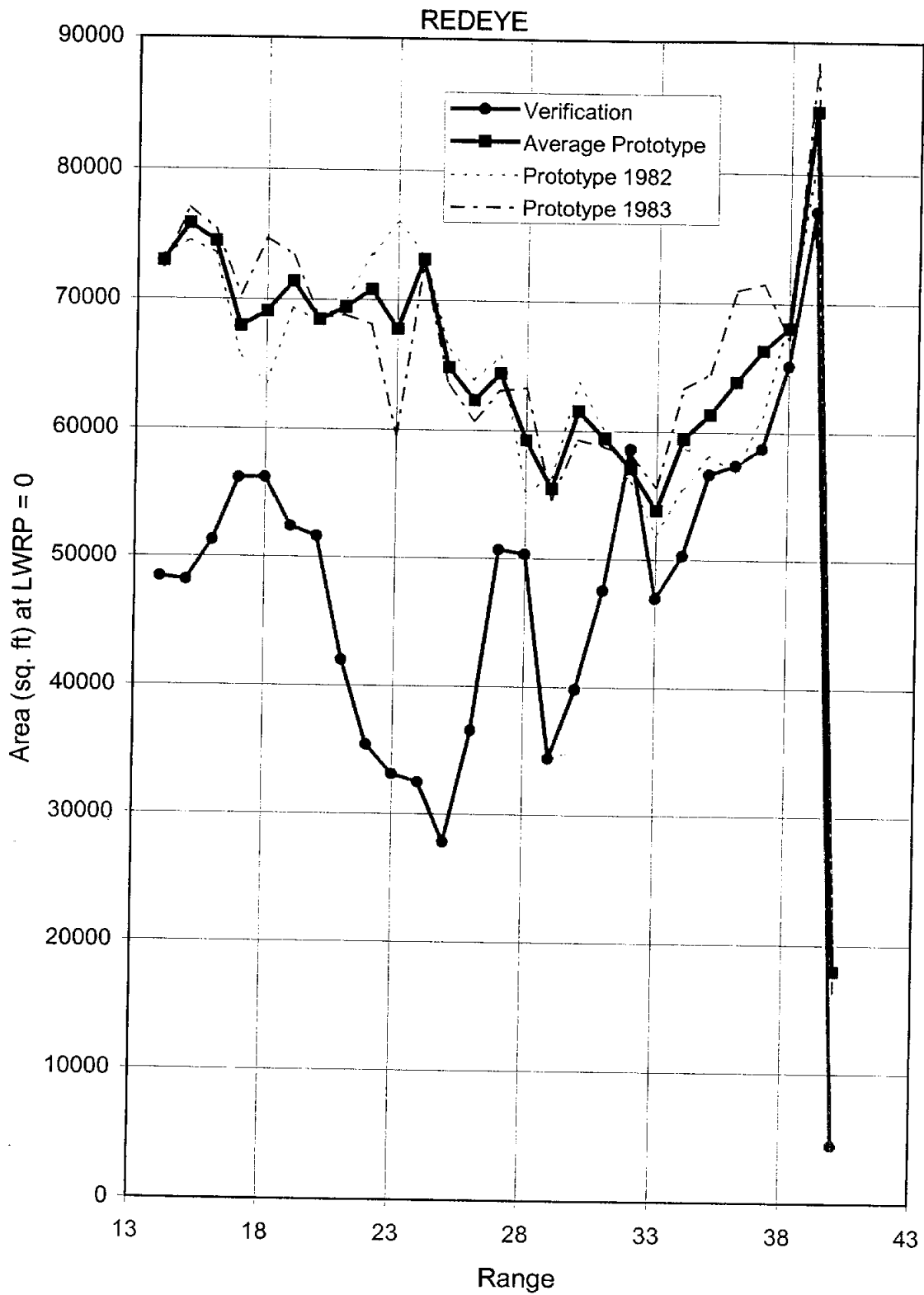


Figure B-13.2b Cross-Section Area by Range, Redeye Crossing

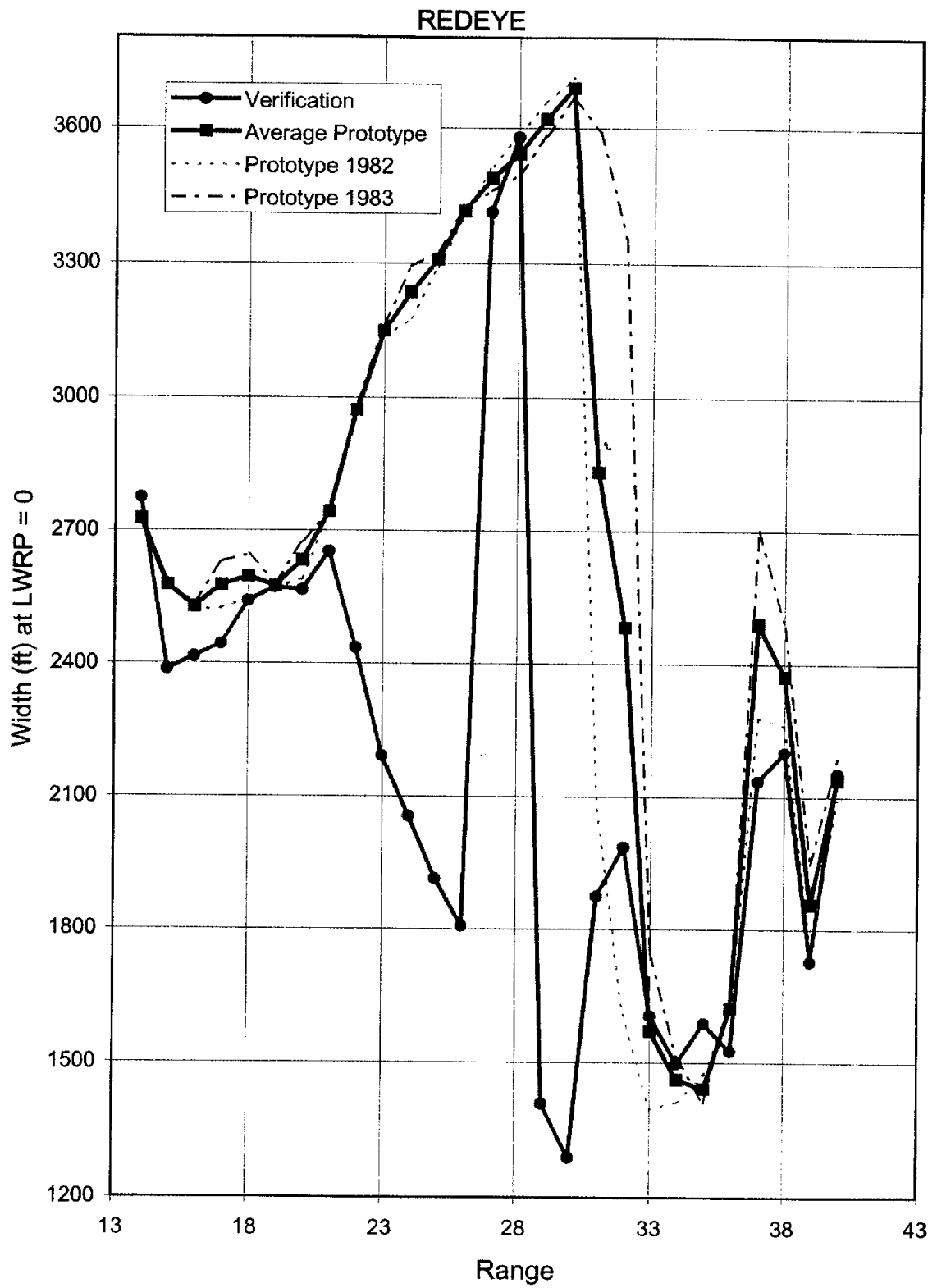


Figure B-13.2c Top Width by Range, Redeye Crossing

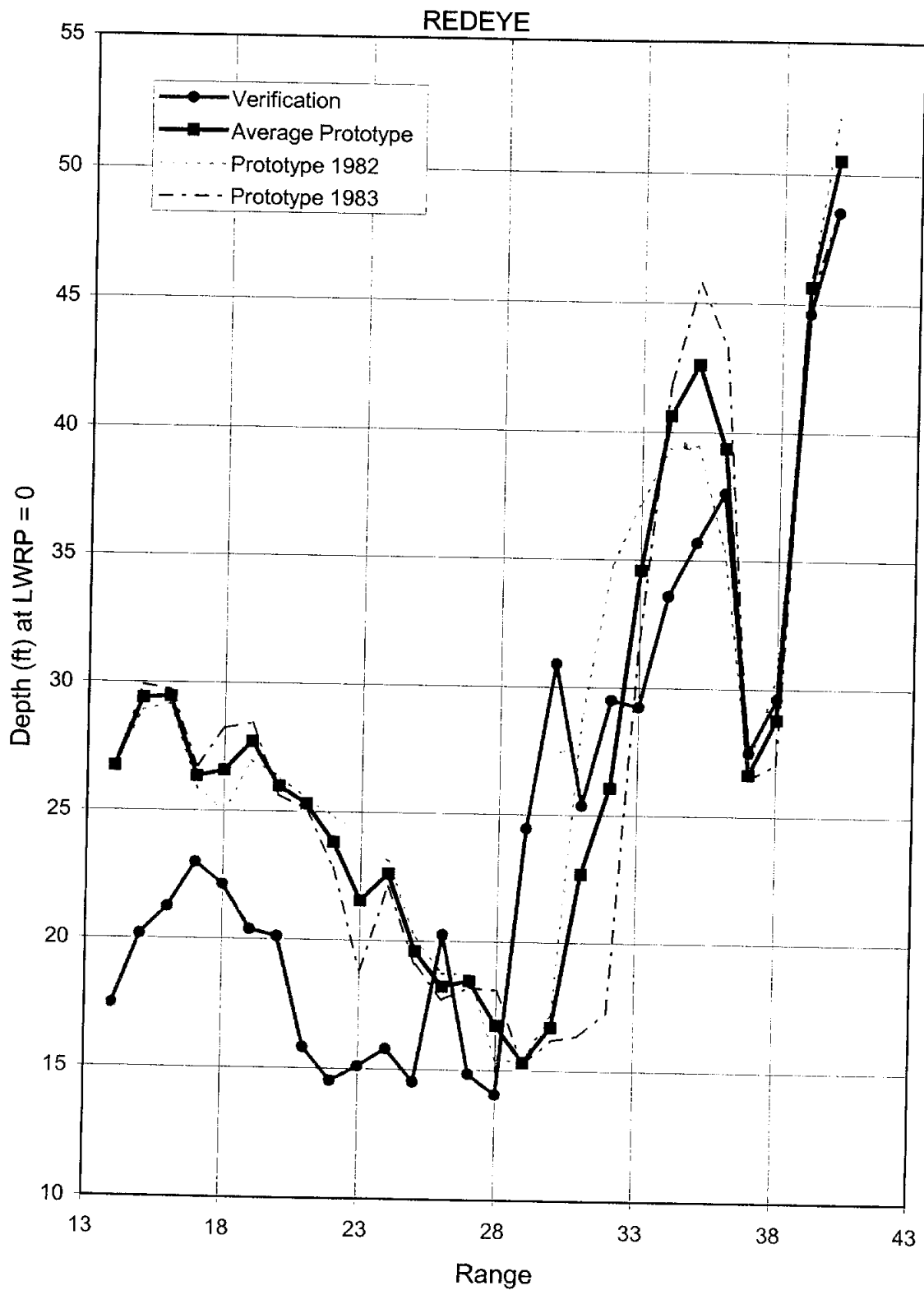


Figure B-13.2d Hydraulic Depth by Range, Redeye Crossing

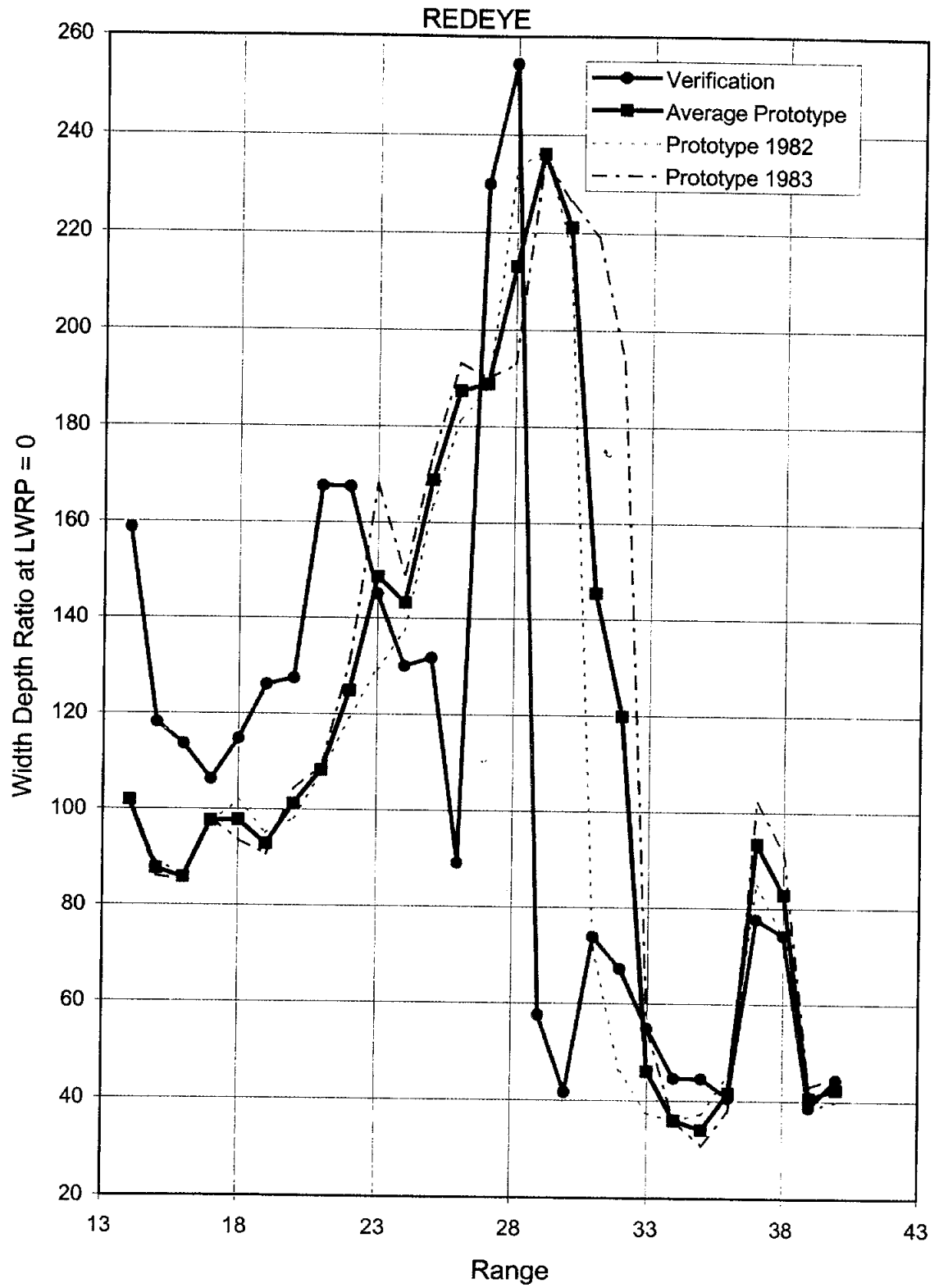
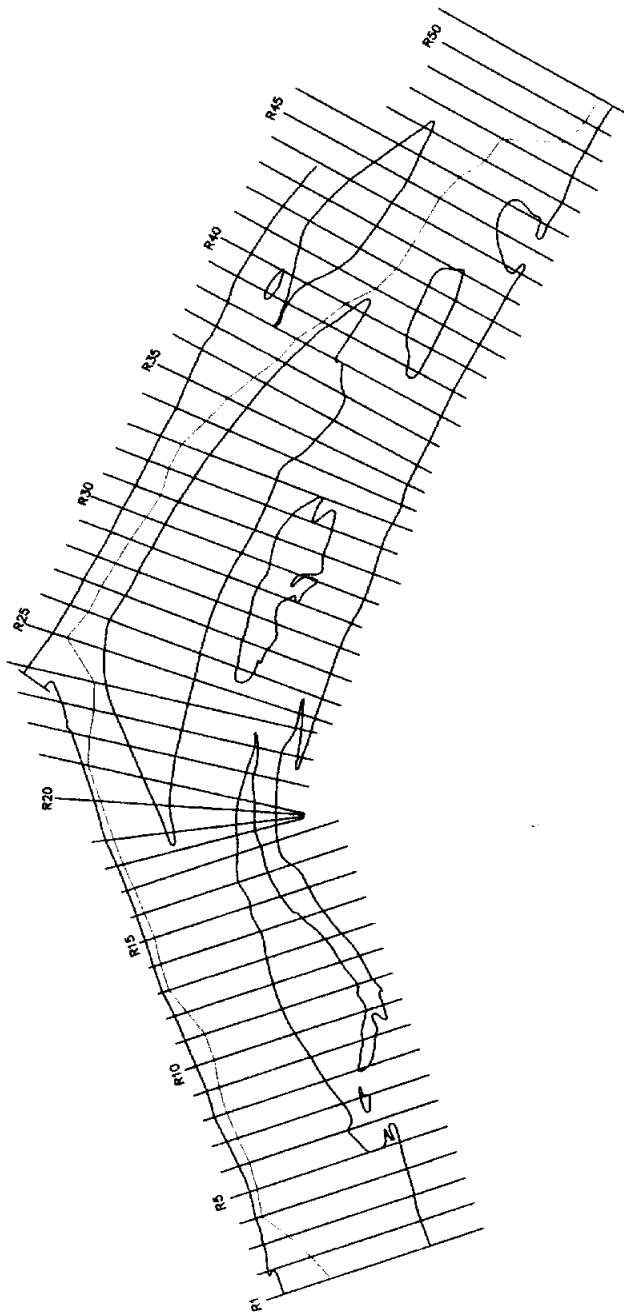


Figure B-13.2e Width/Depth Ratio by Range, Redeye Crossing



SMITHLAND LOCK and DAM
October 1965 Prototype

Figure B-14.1a Smithland Lock Model Plan View

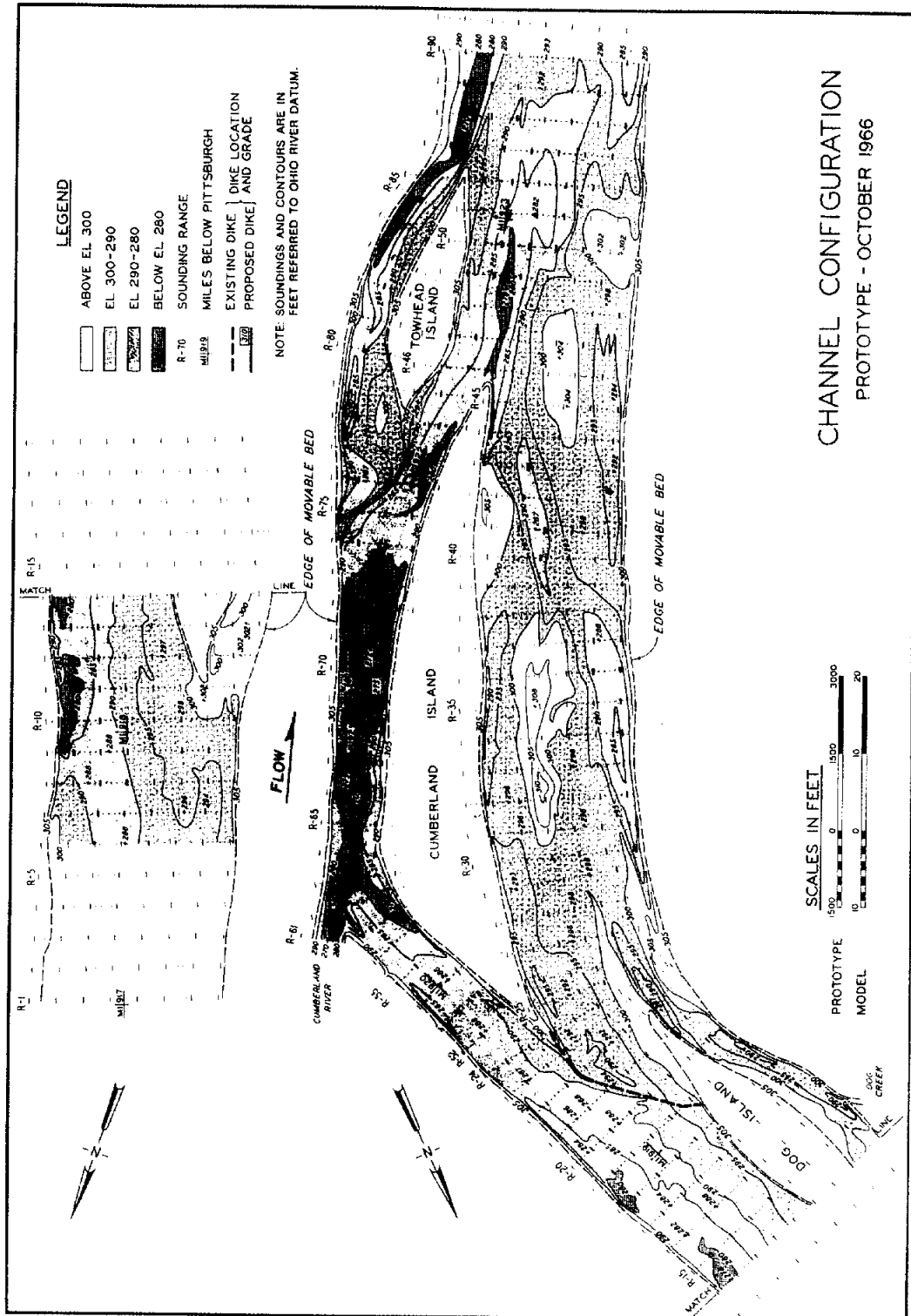


Figure B-14.1b Smithland Lock October 1966 Prototype Survey

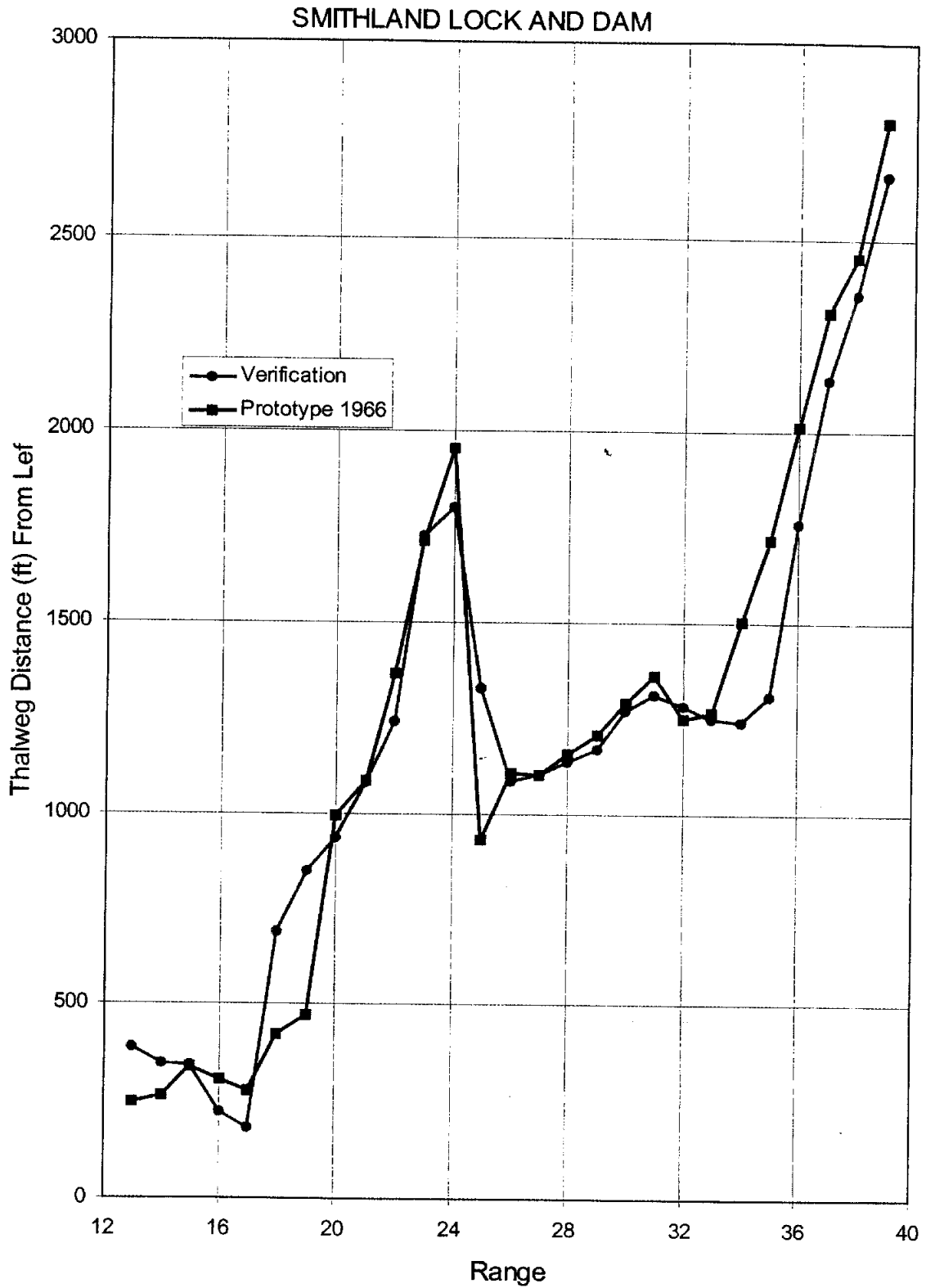


Figure B-14.2a Thalweg Location From Left by Range, Smithland Lock and Dam

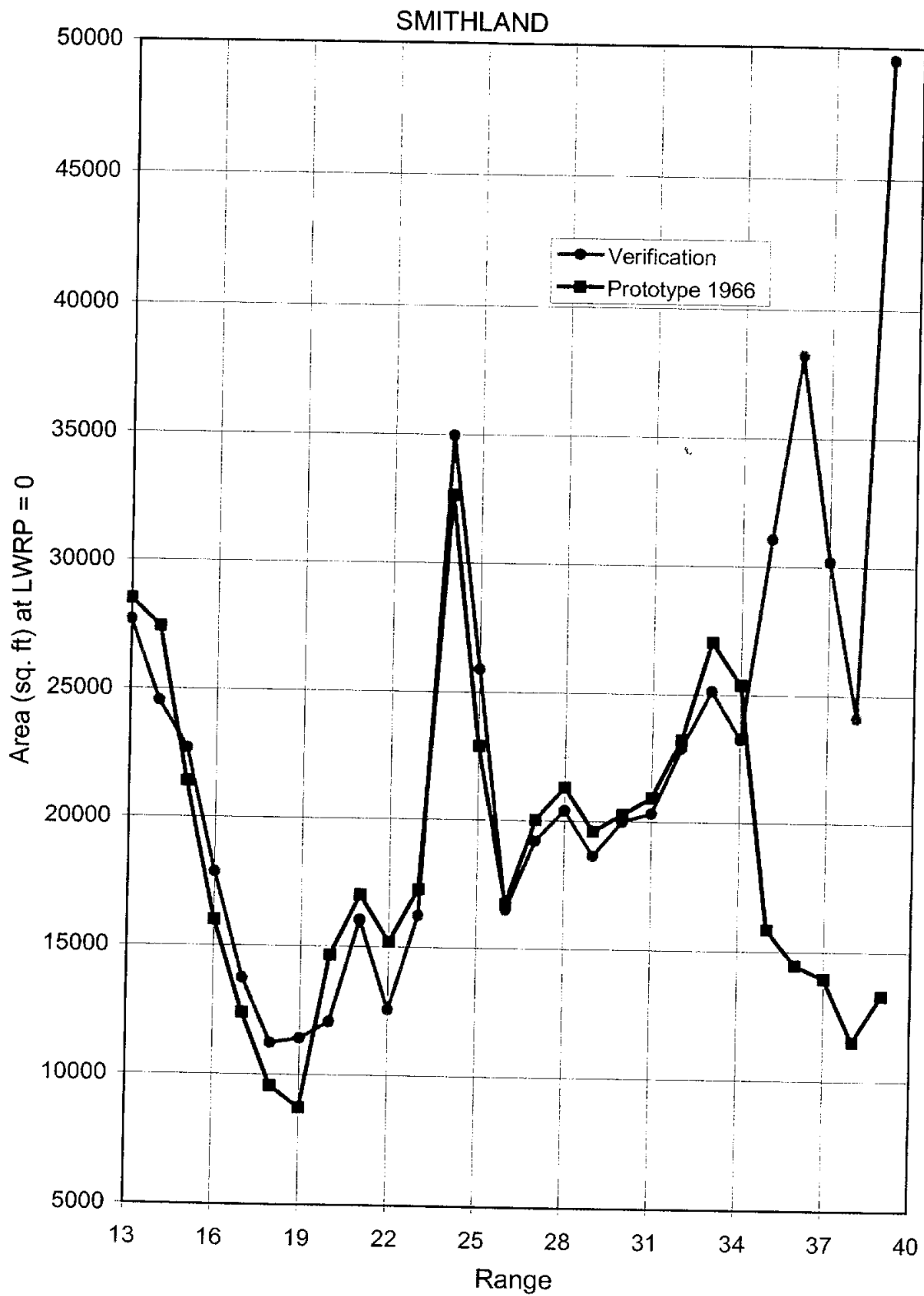


Figure B-14.2b Cross-Section Area by Range, Smithland Lock and Dam

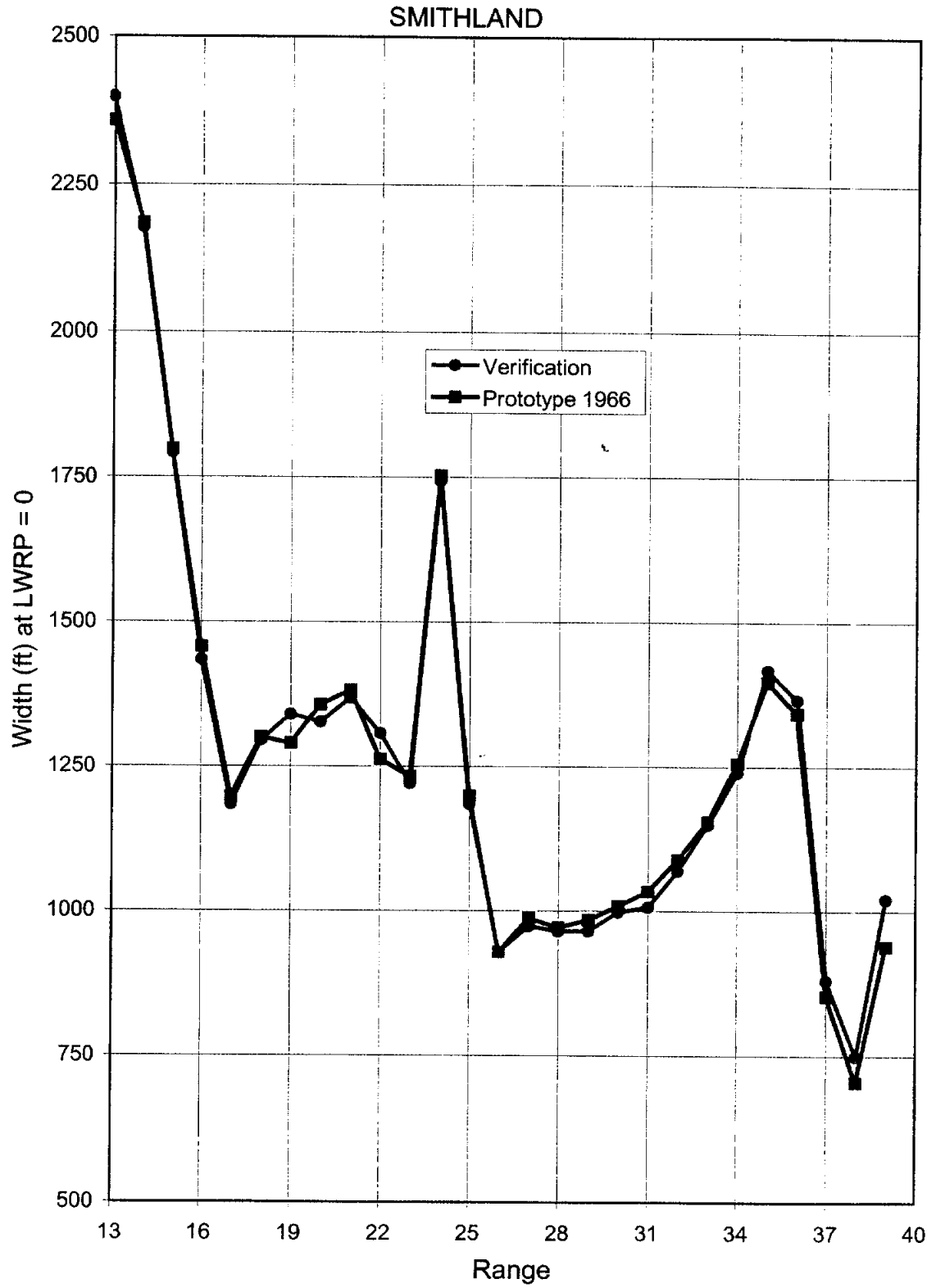


Figure B-14.2c Top Width by Range, Smithland Lock and Dam

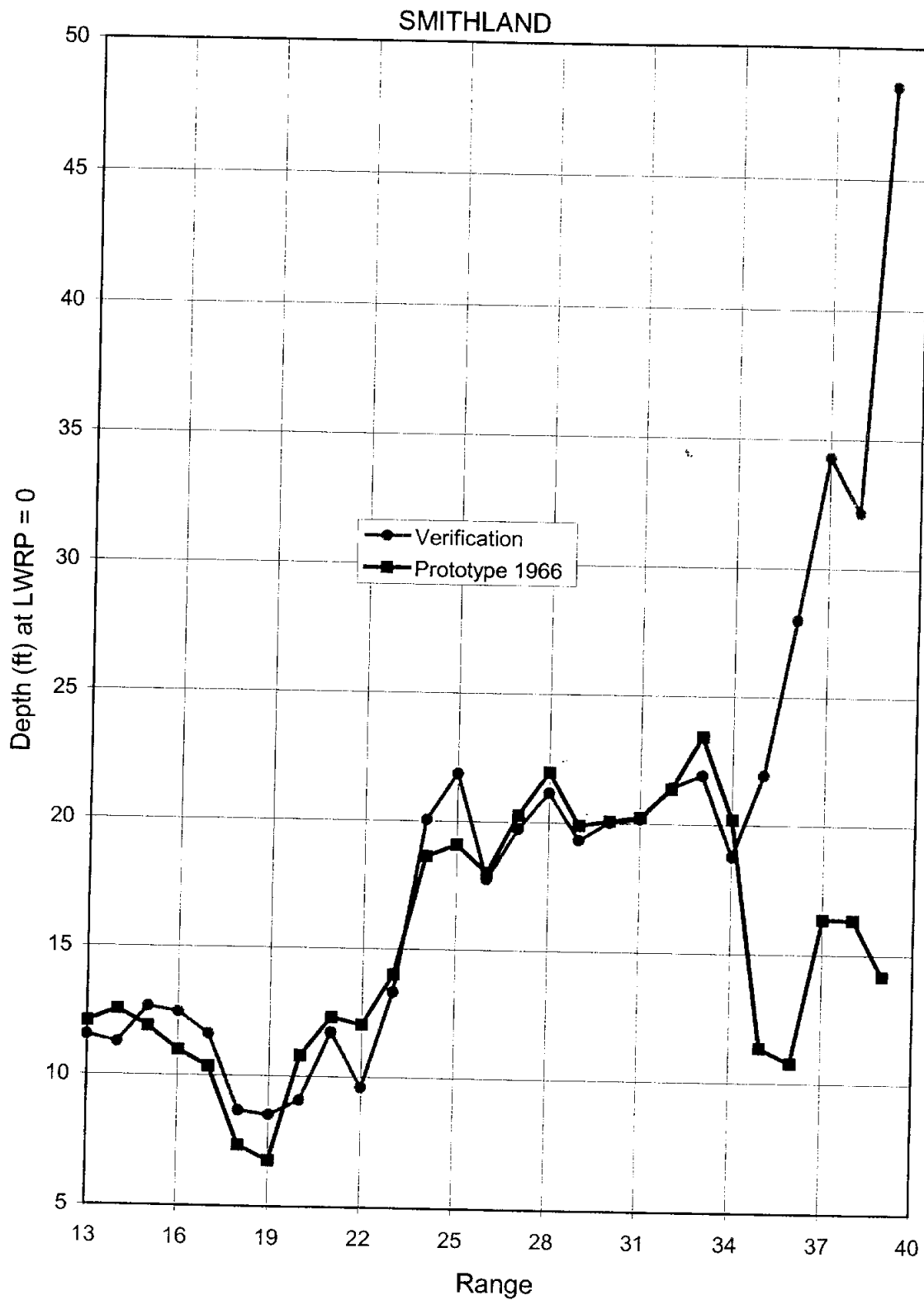


Figure B-14.2d Hydraulic Depth by Range, Smithland Lock and Dam

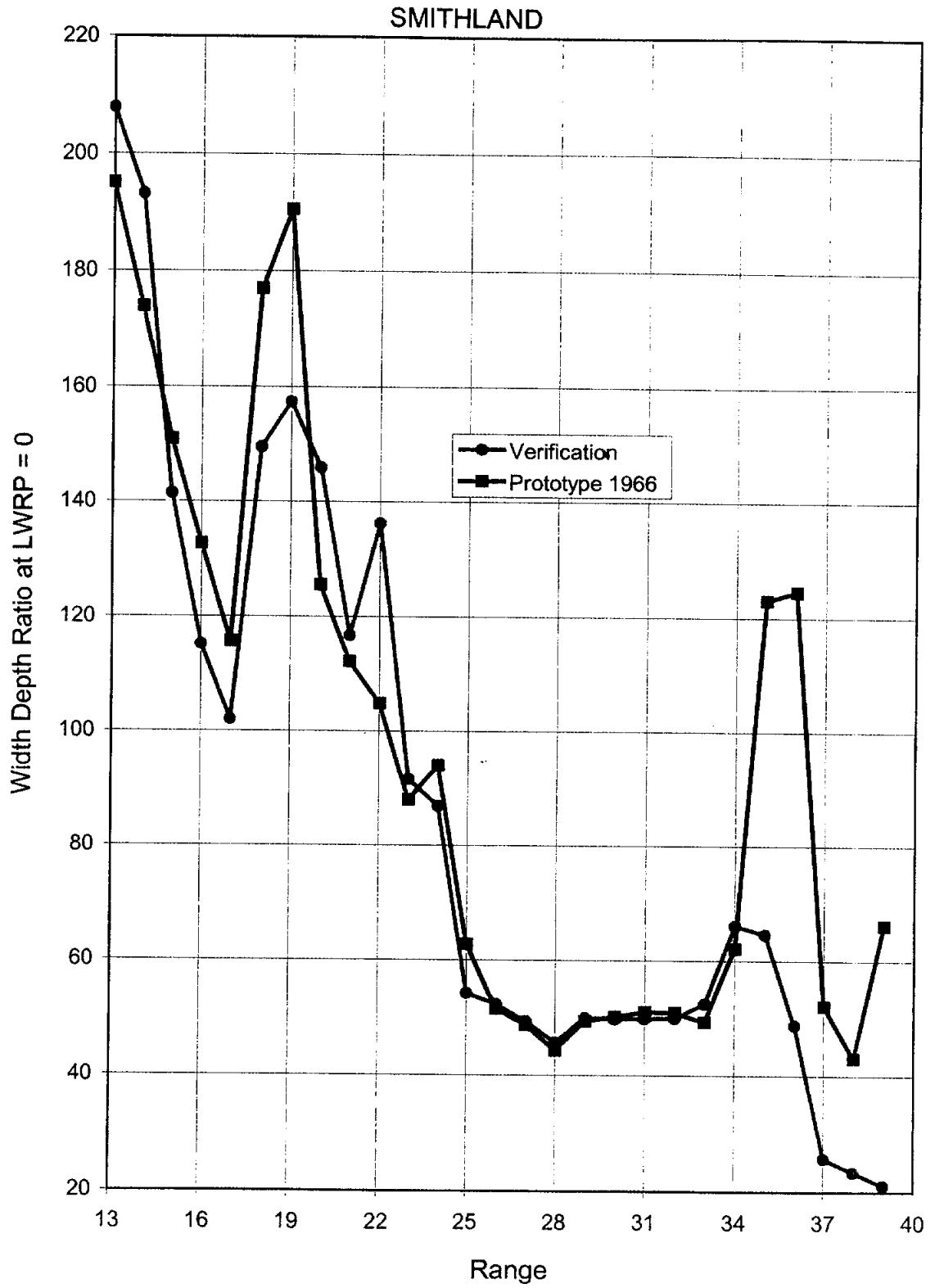
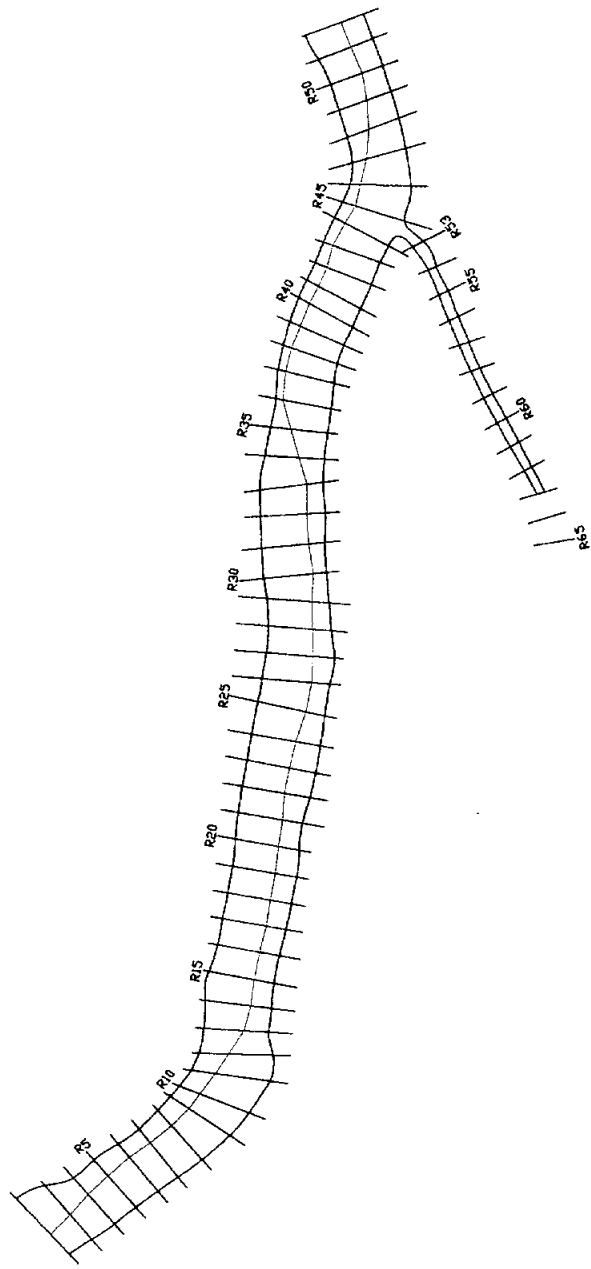


Figure B-14.2e Width/Depth Ratio by Range, Smithland Lock and Dam



WEST ACCESS CHANNEL REALIGNMENT
 June 1975 Prototype

Figure B-15.1a West Access Channel Model Plan View

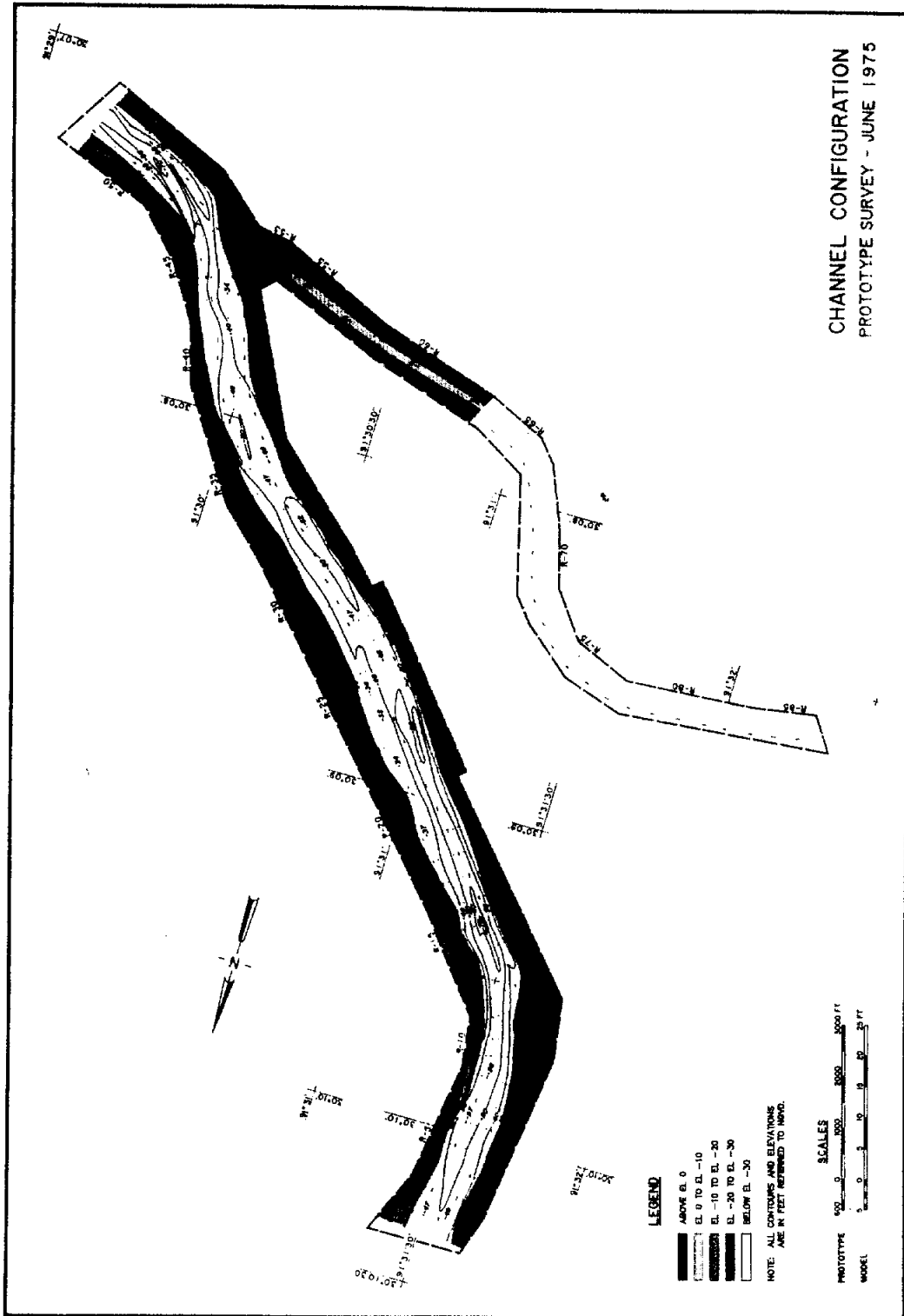


Figure B-15.1b West Access Channel 1975 Prototype Survey

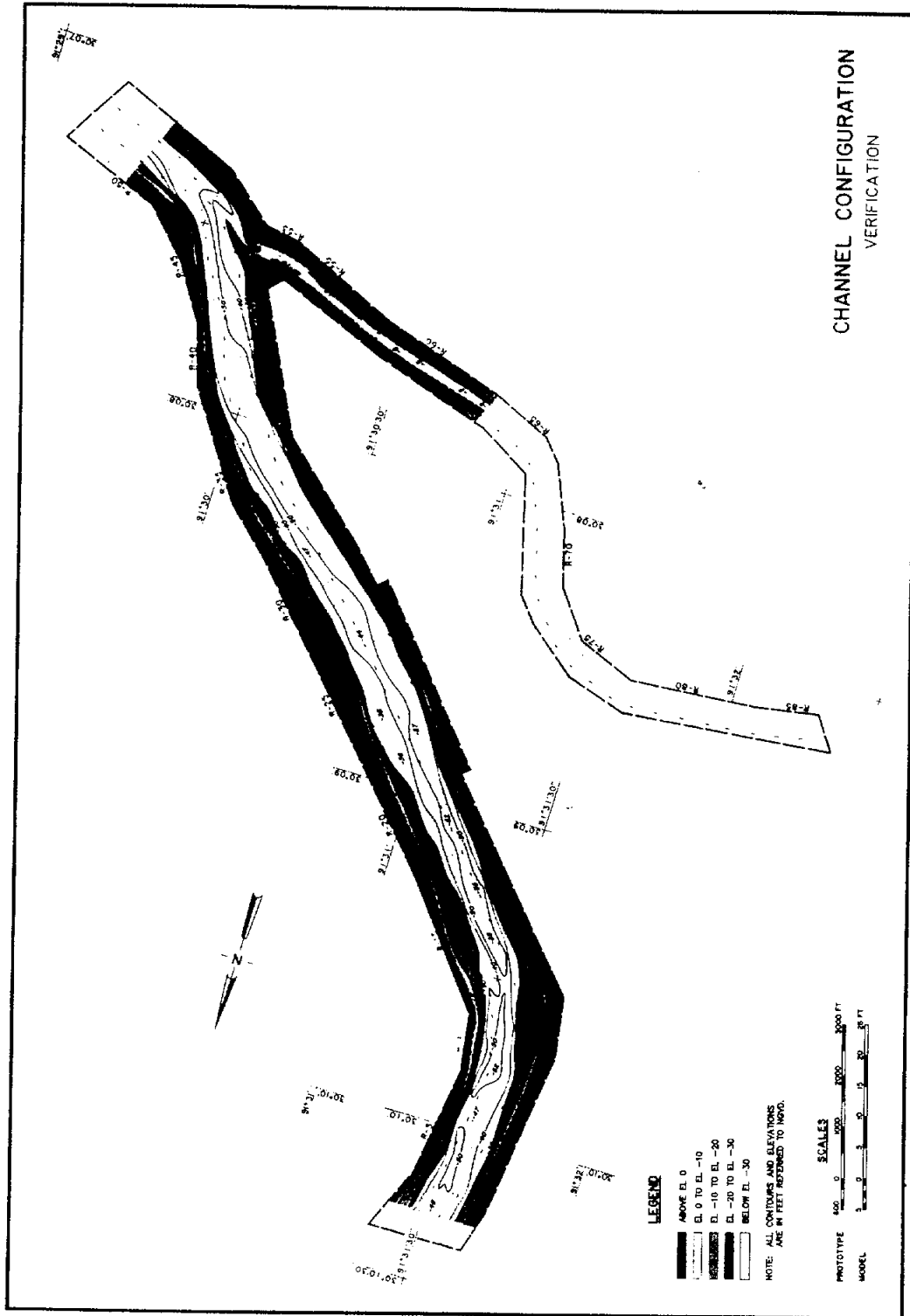


Figure B-15.1c West Access Channel Verification Test Survey

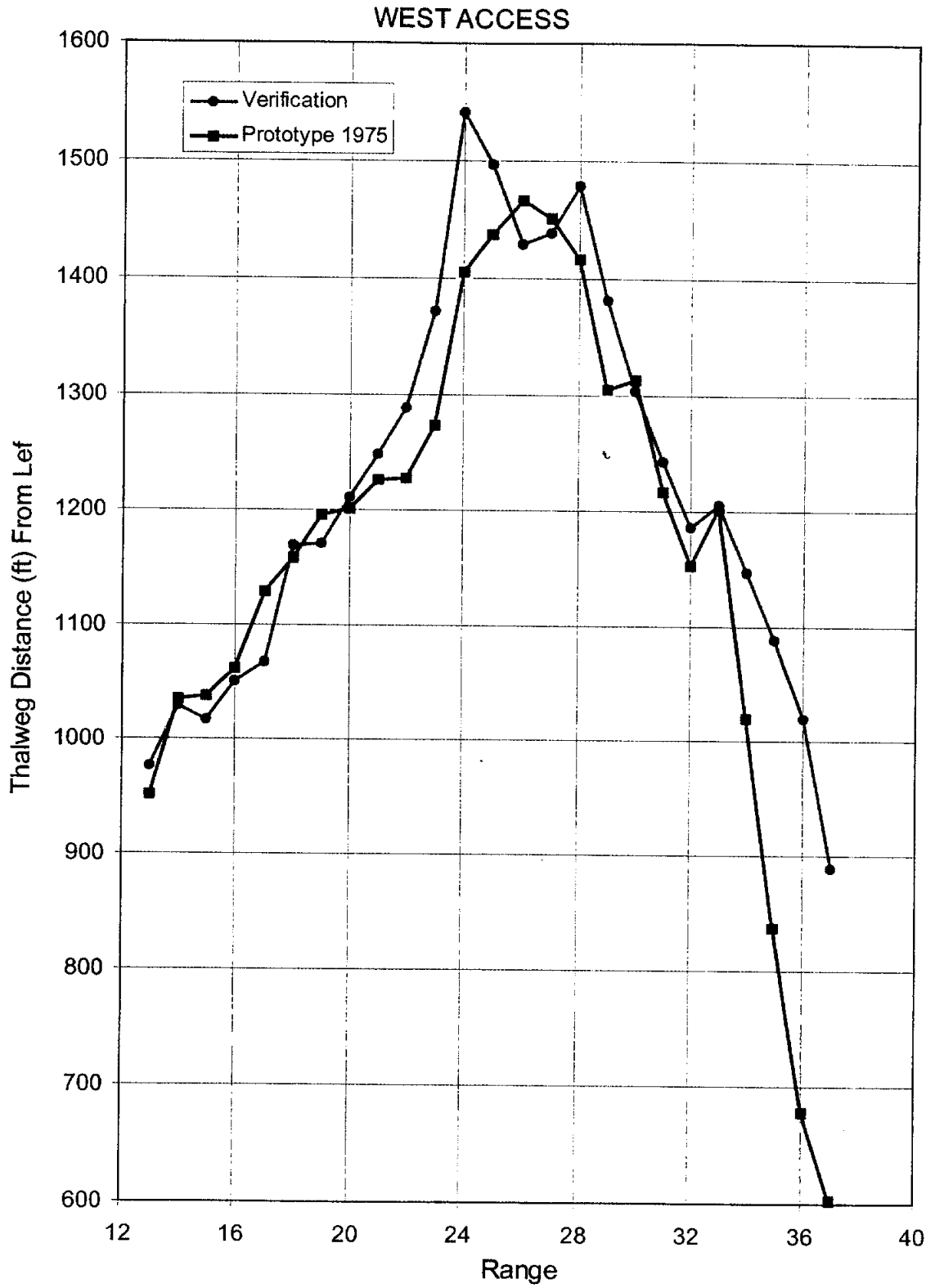


Figure B-15.2a Thalweg Location From Left by Range, West Access

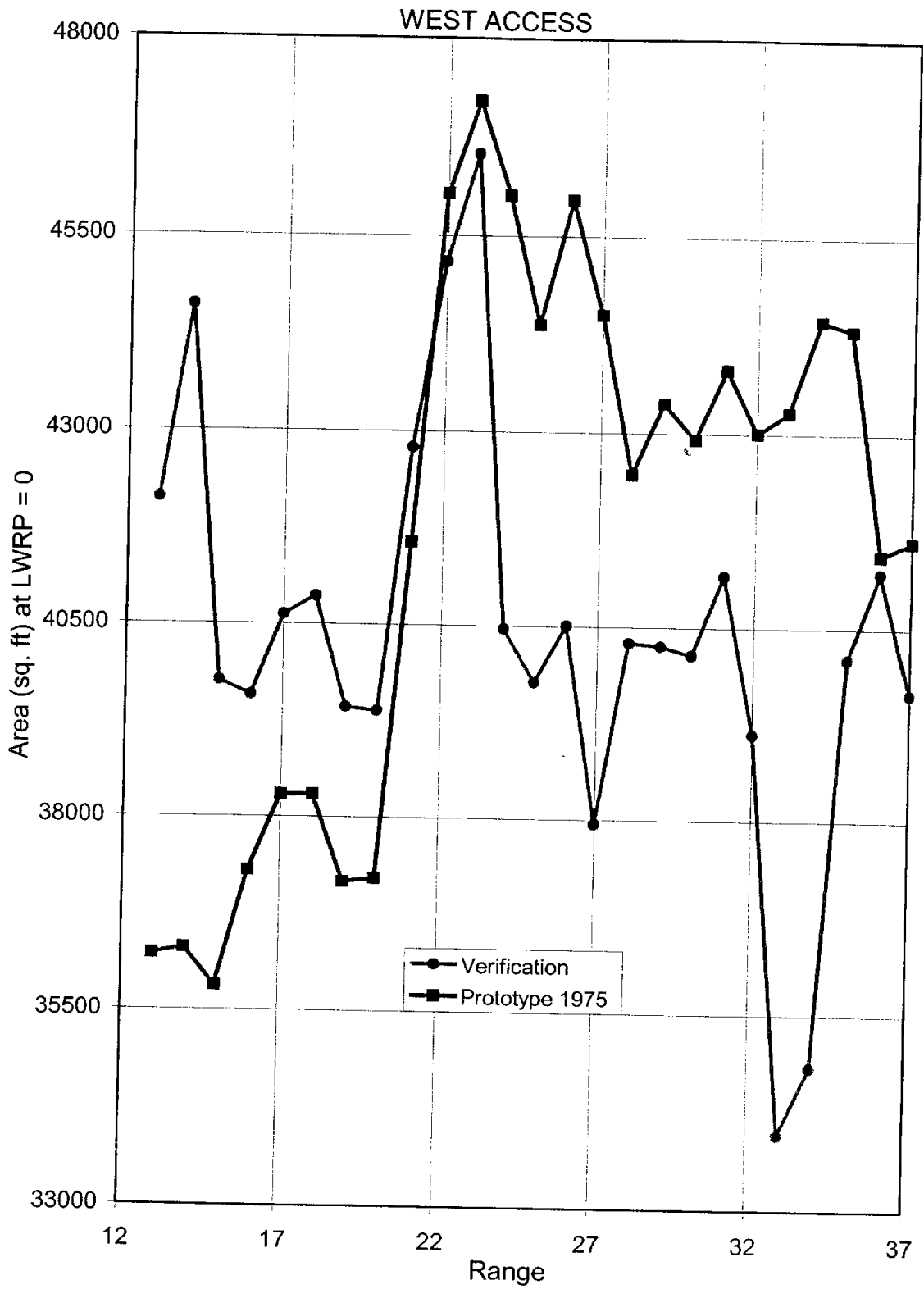


Figure B-15.2b Cross-Section Area by Range, West Access Channel

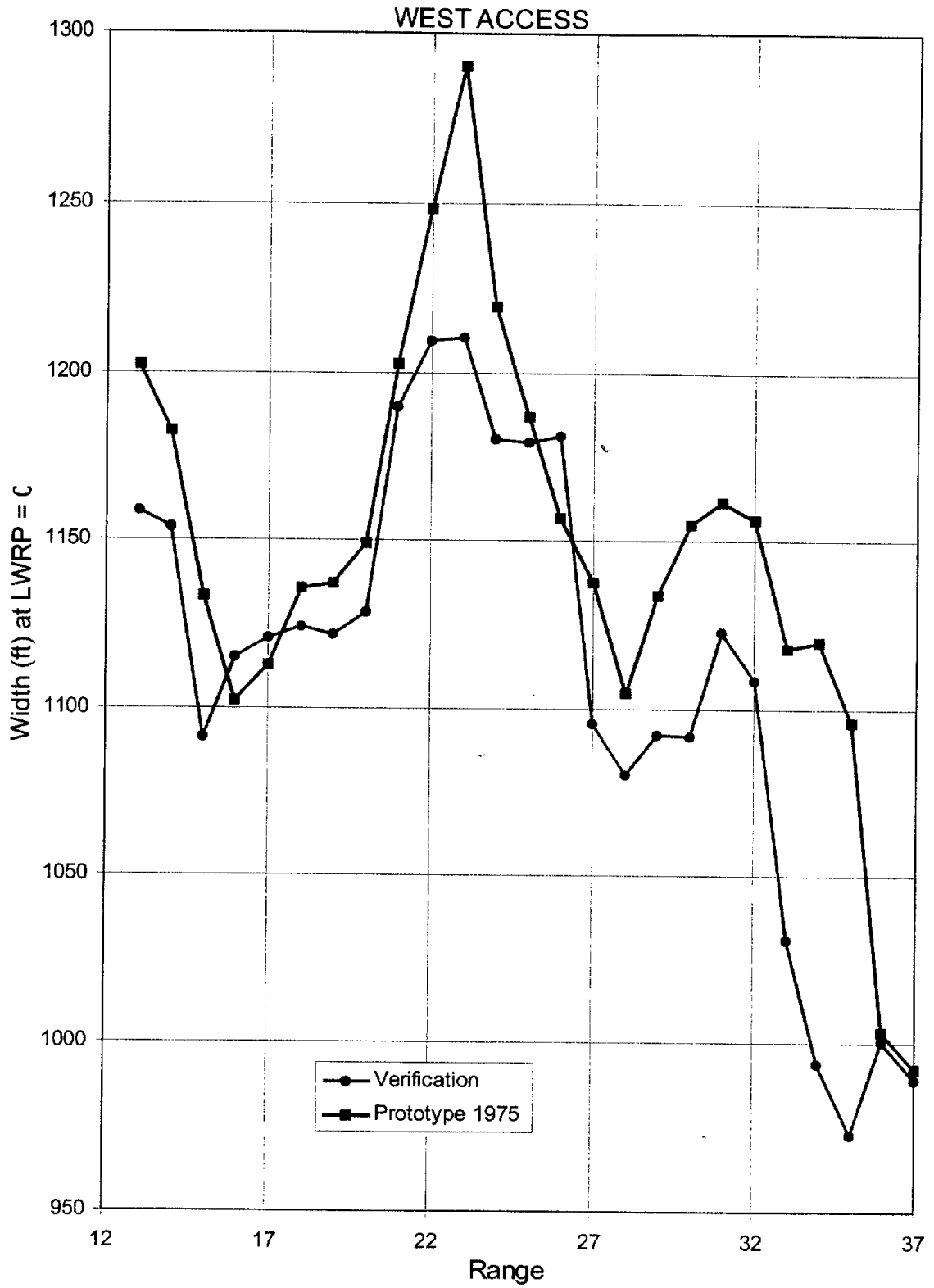


Figure B-15.2c Top Width by Range, West Access Channel

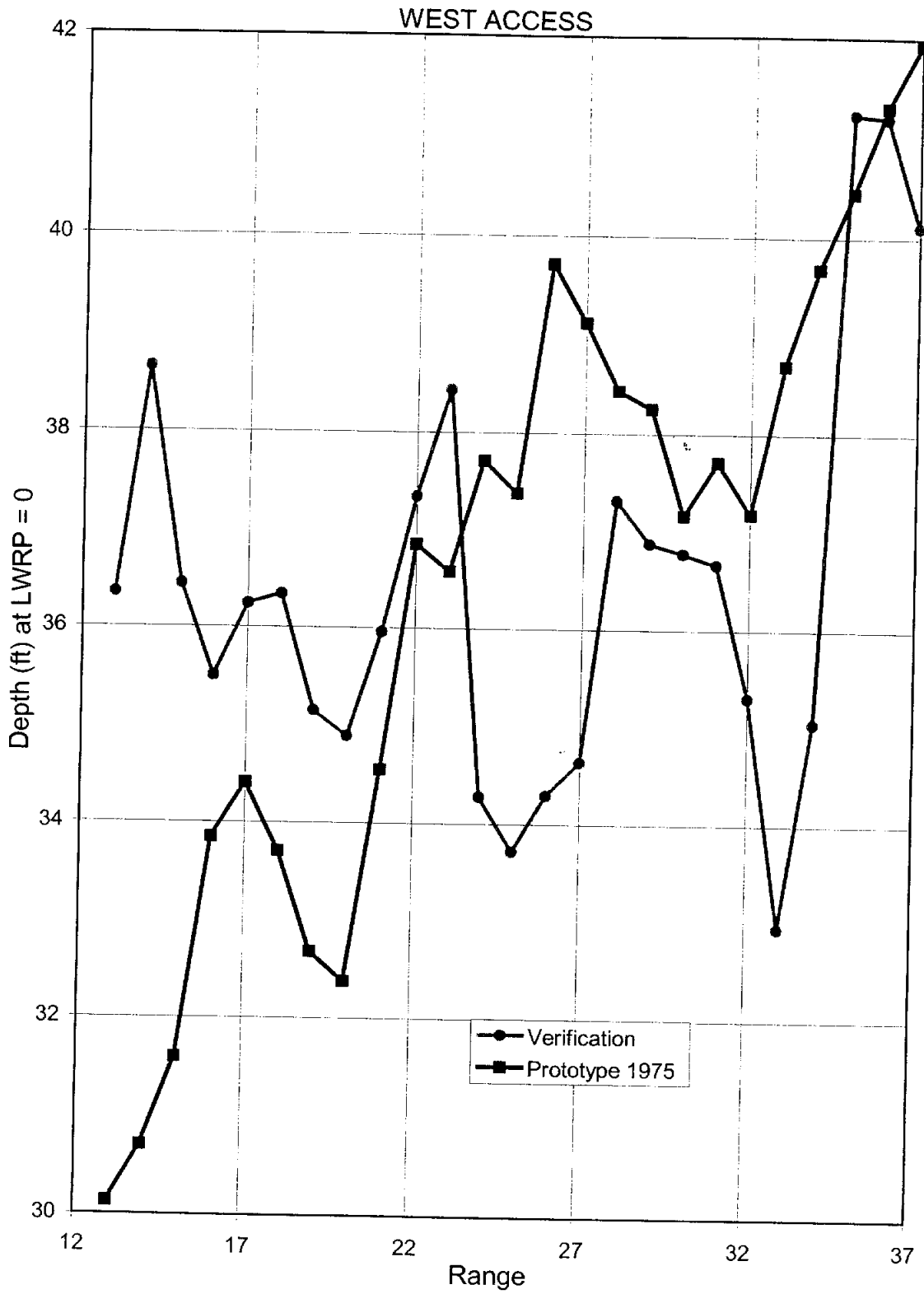


Figure B-15.2d Hydraulic Depth by Range, West Access Channel

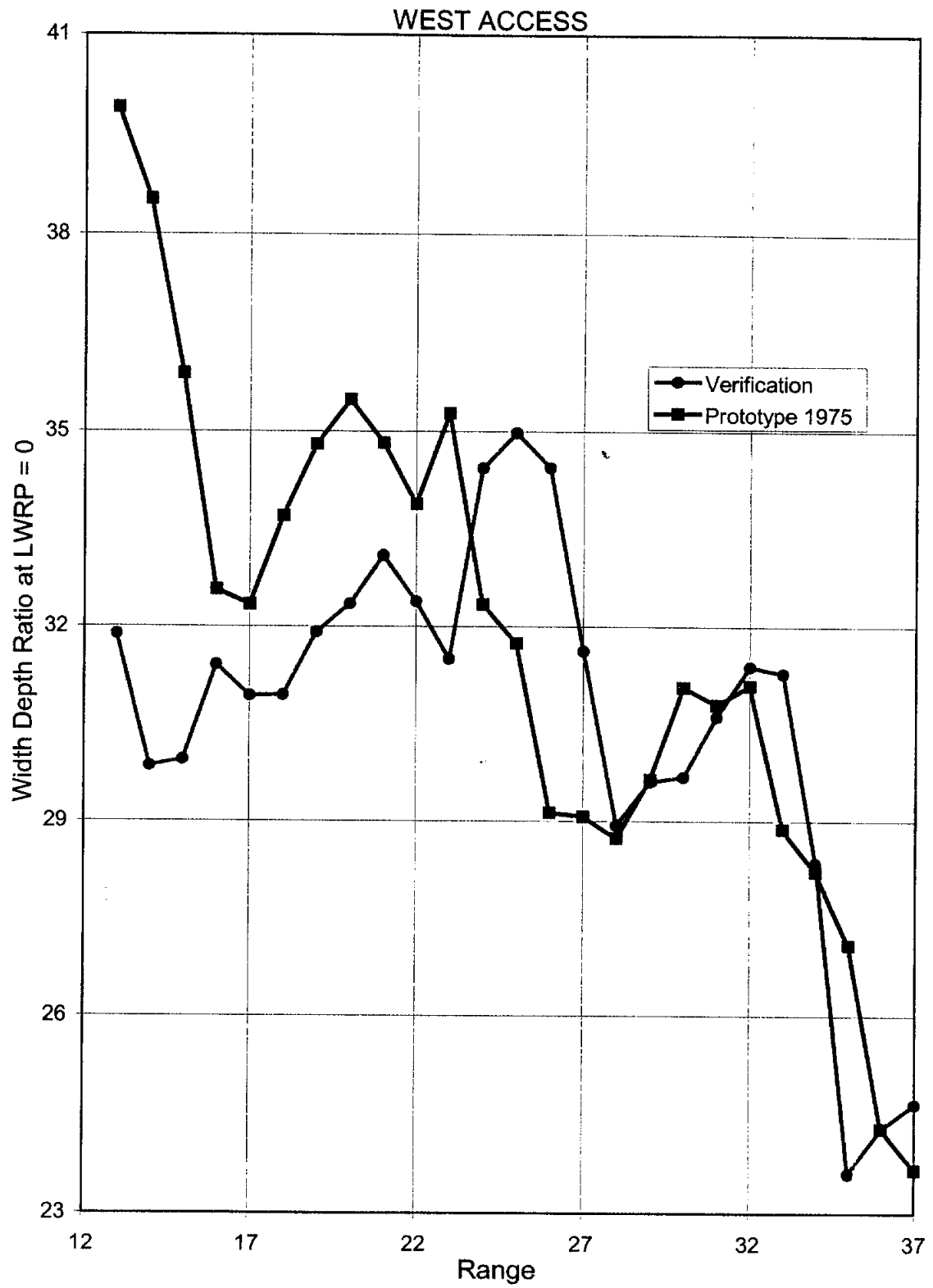


Figure B-15.2e Width/Depth Ratio by Range, West Access Channel

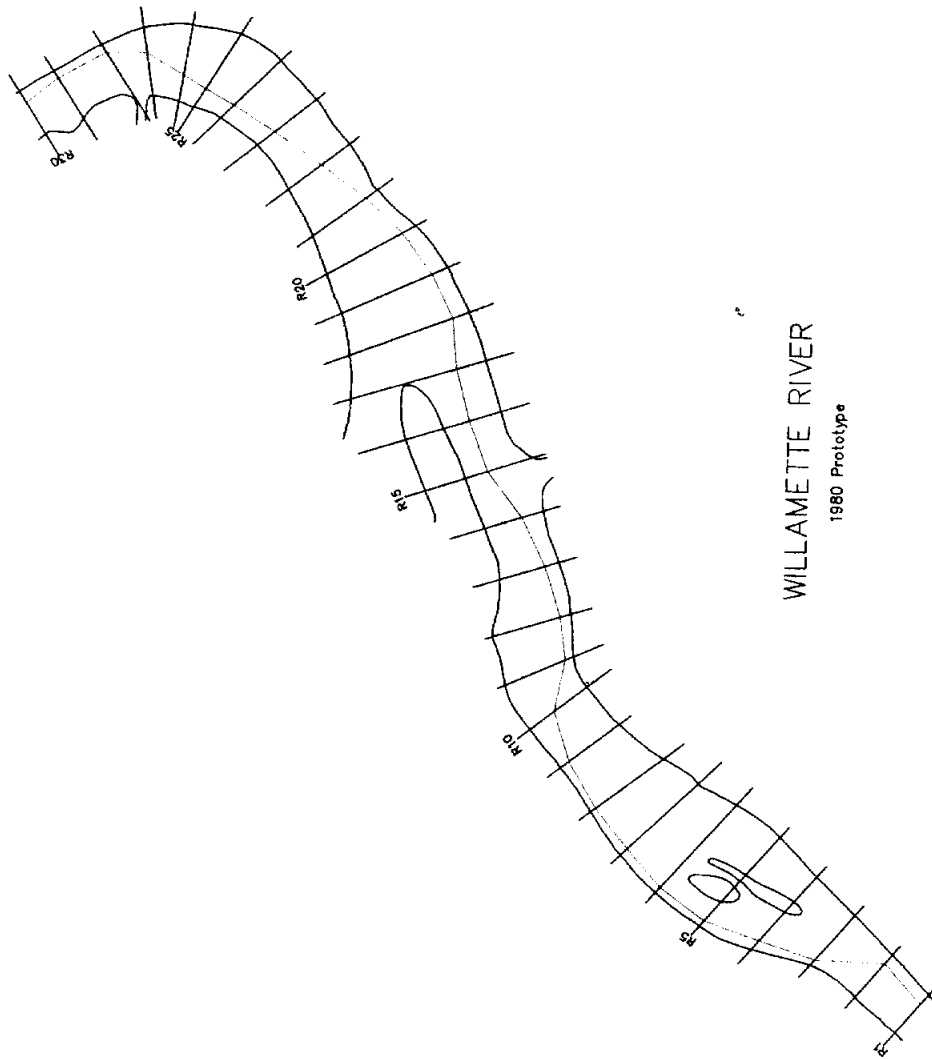


Figure B-16.1a Willamette River Model Plan View

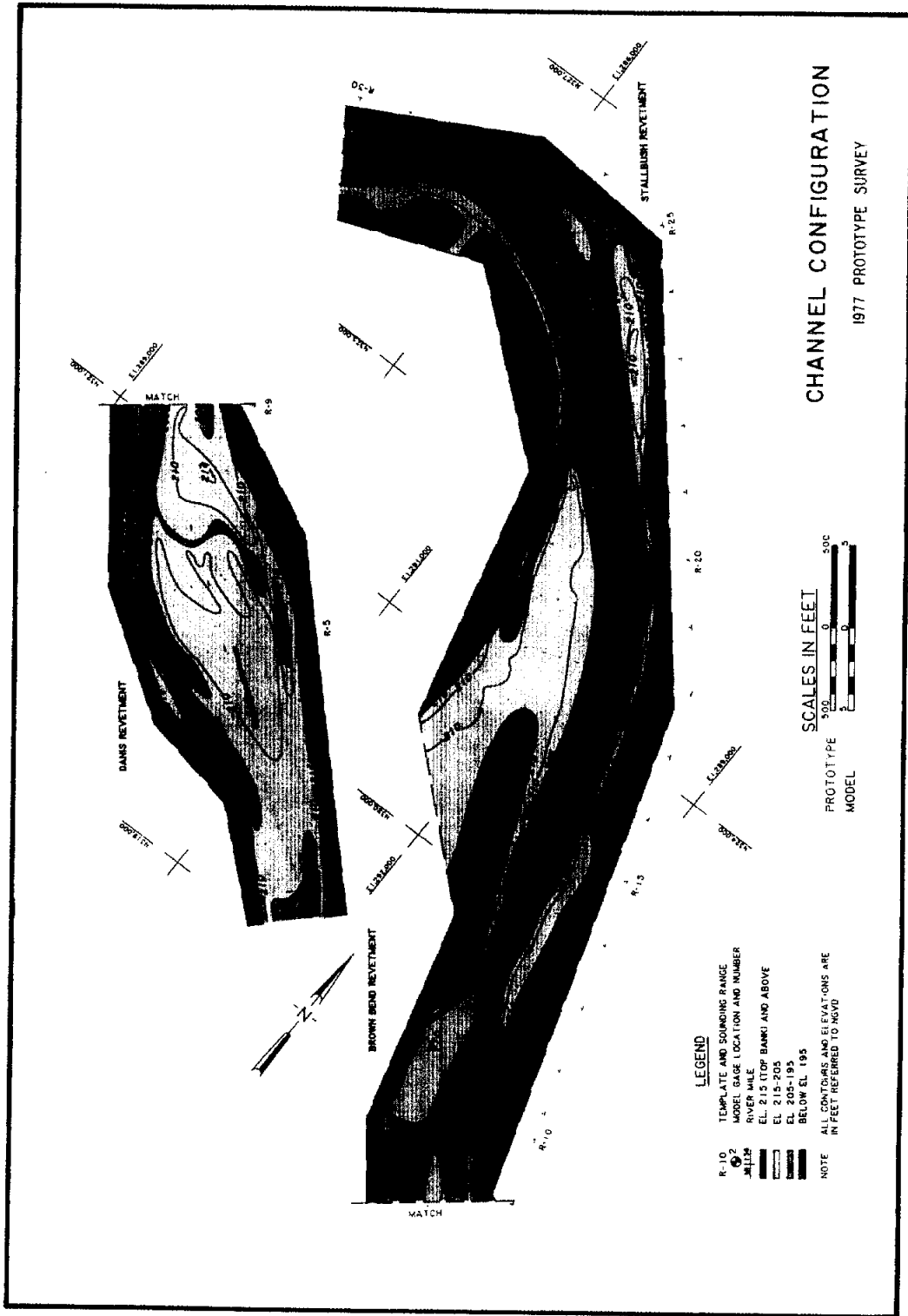


Figure B-16.1b 1977 Willamette River Prototype Survey

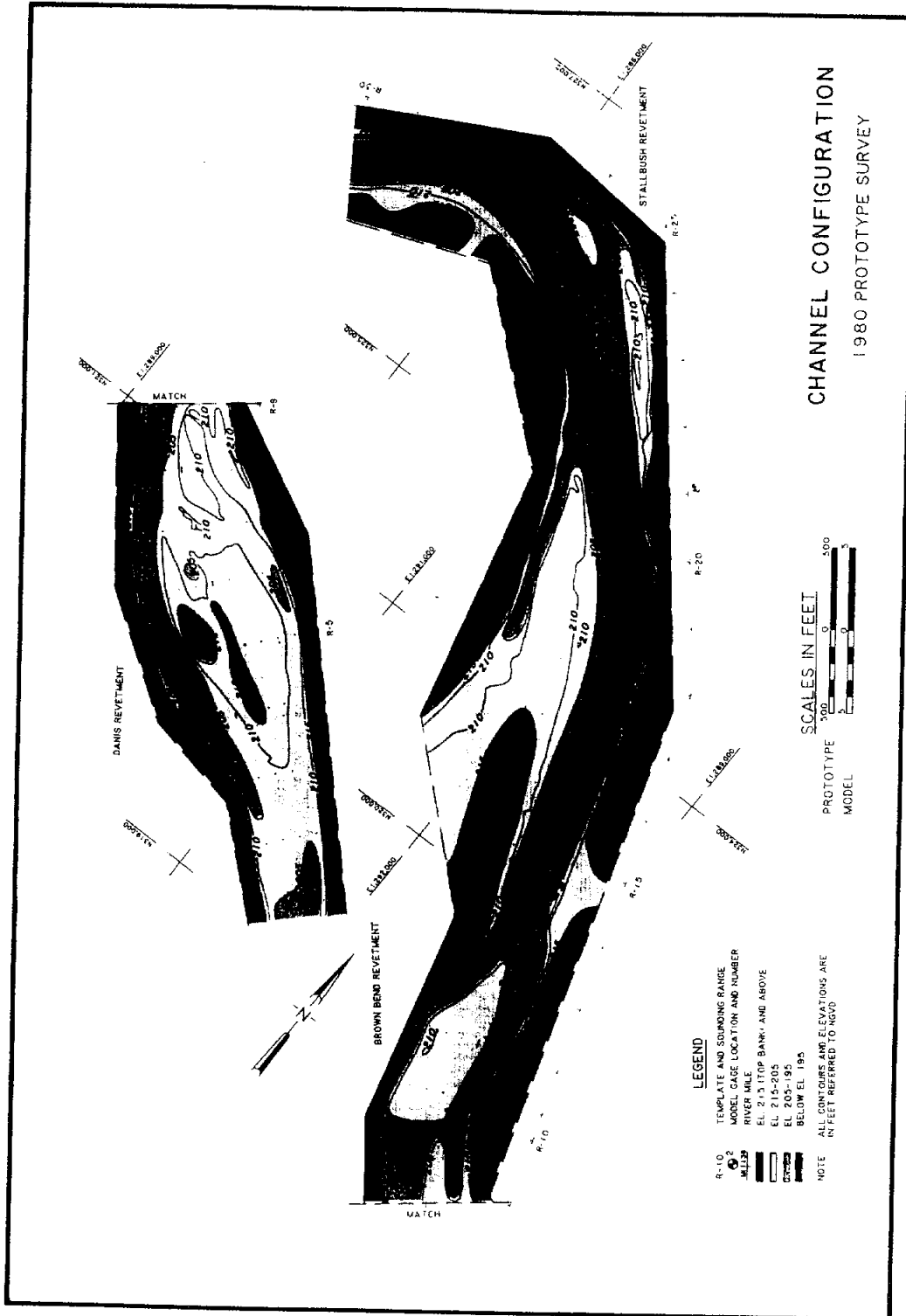


Figure B-16.1c 1980 Willamette River Prototype Survey

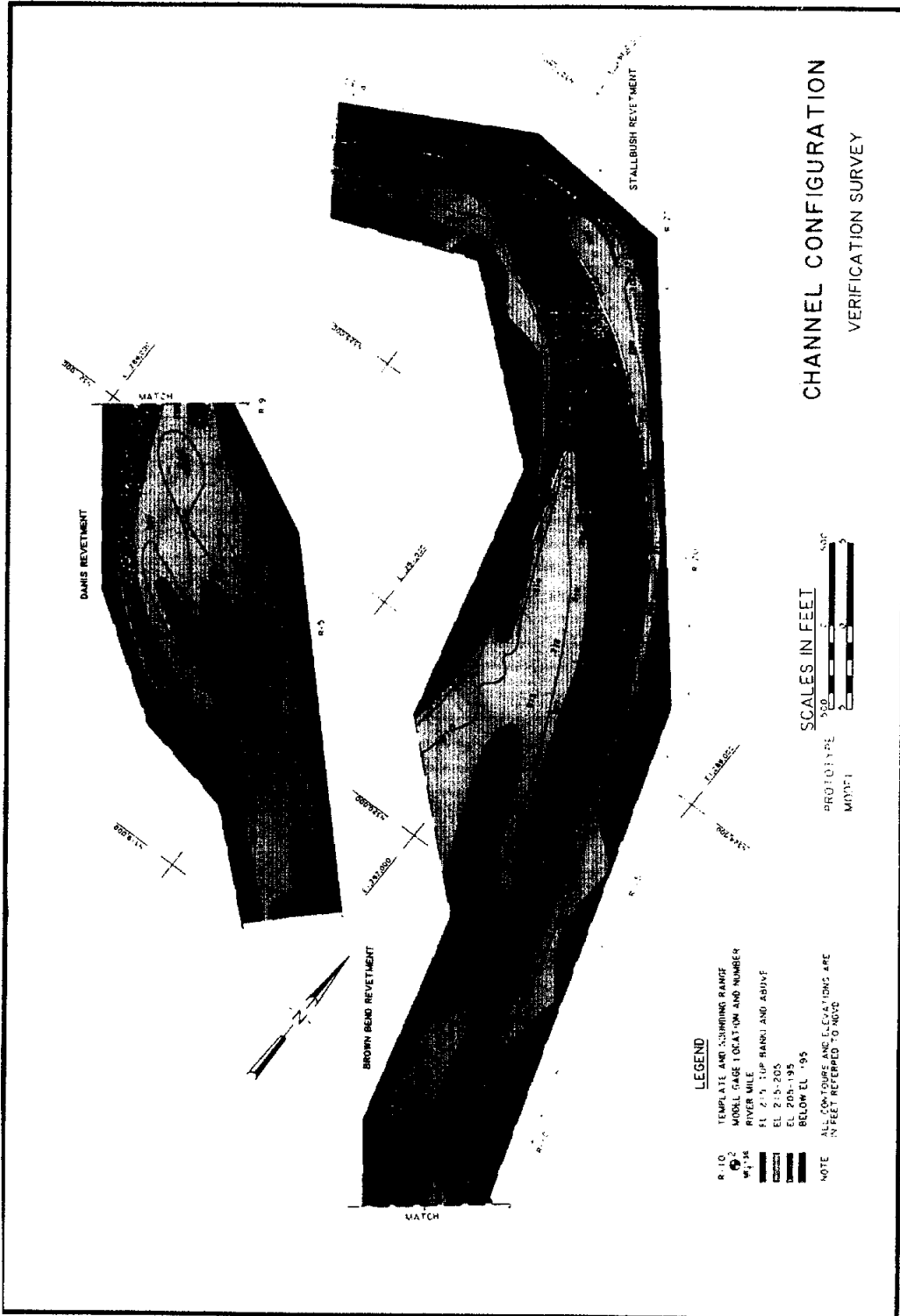


Figure B-16.1d Willamette River Verification Test Survey

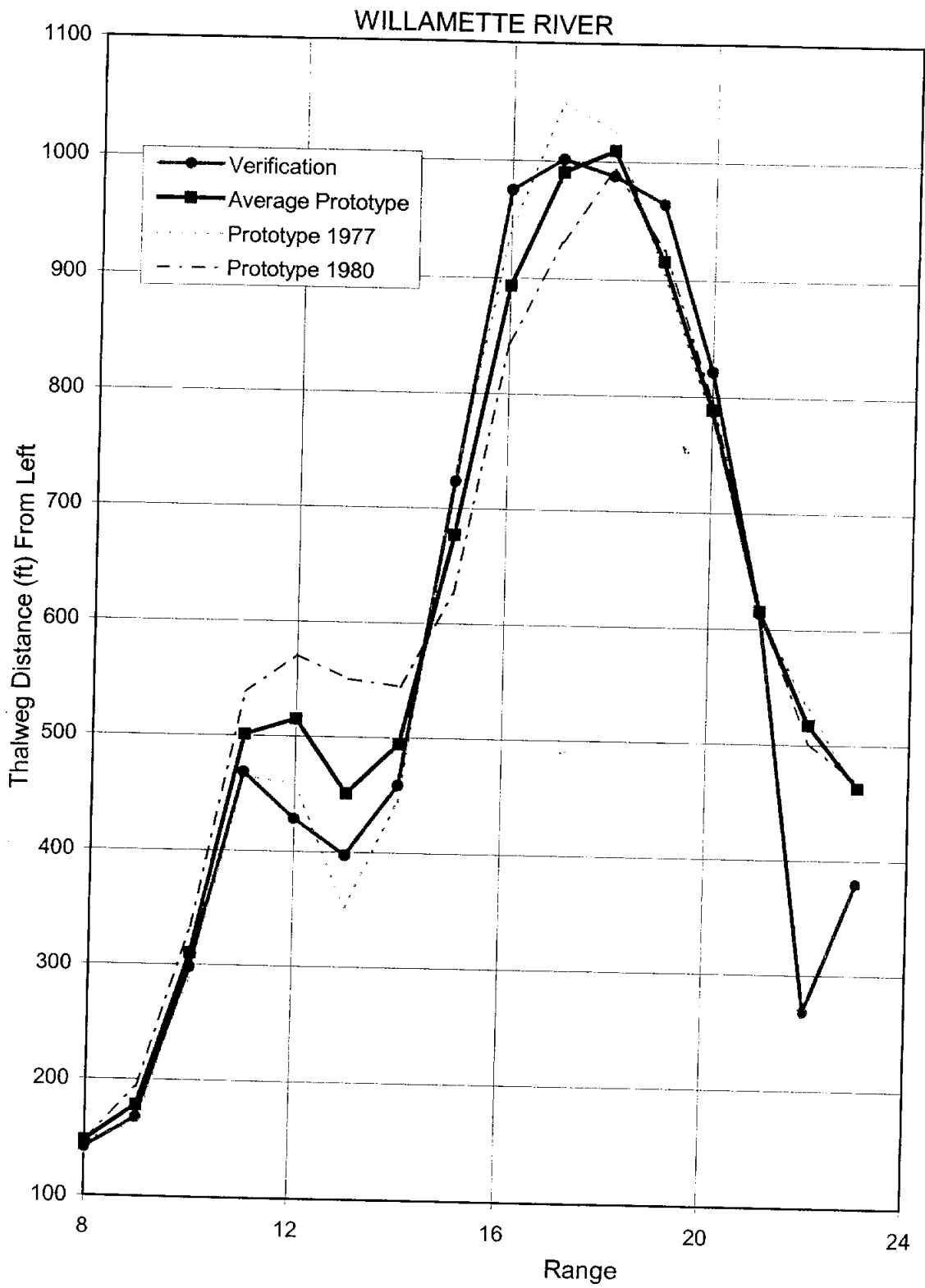


Figure B-16.2a Thalweg Location From Left by Range, Willamette River

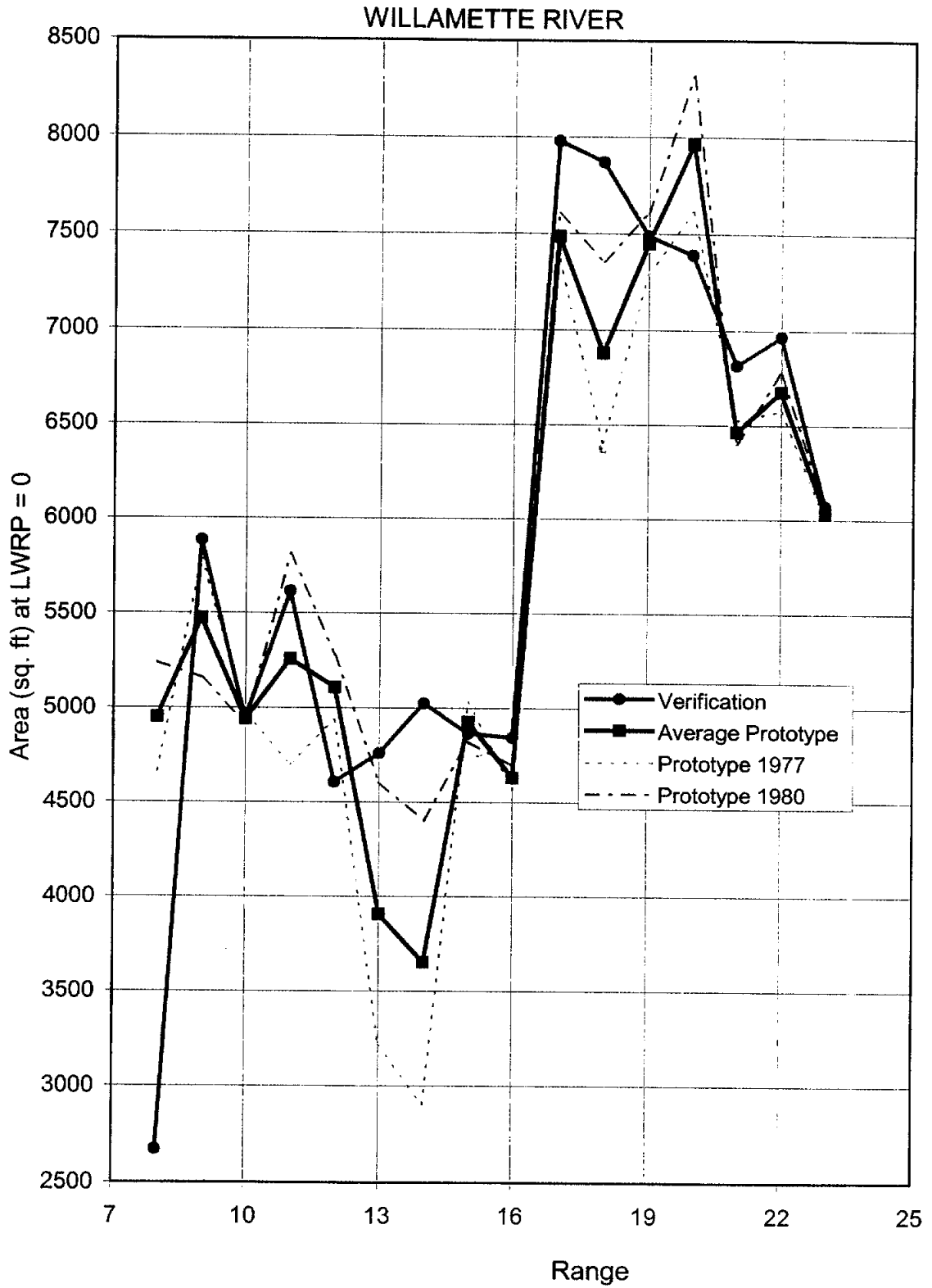


Figure B-16.2b Cross-Section Area by Range, Willamette River

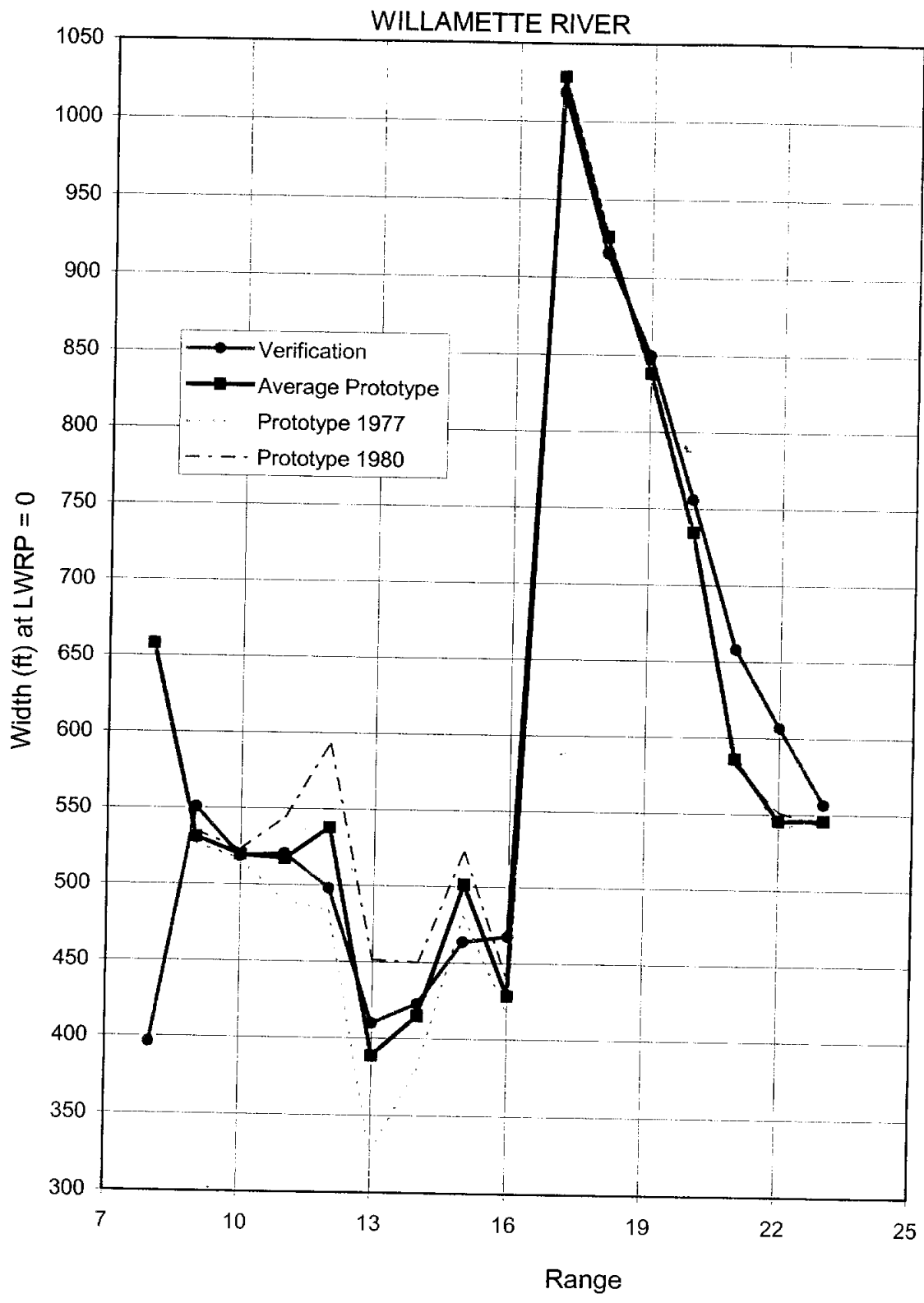


Figure B-16.2c Top Width by Range, Willamette River

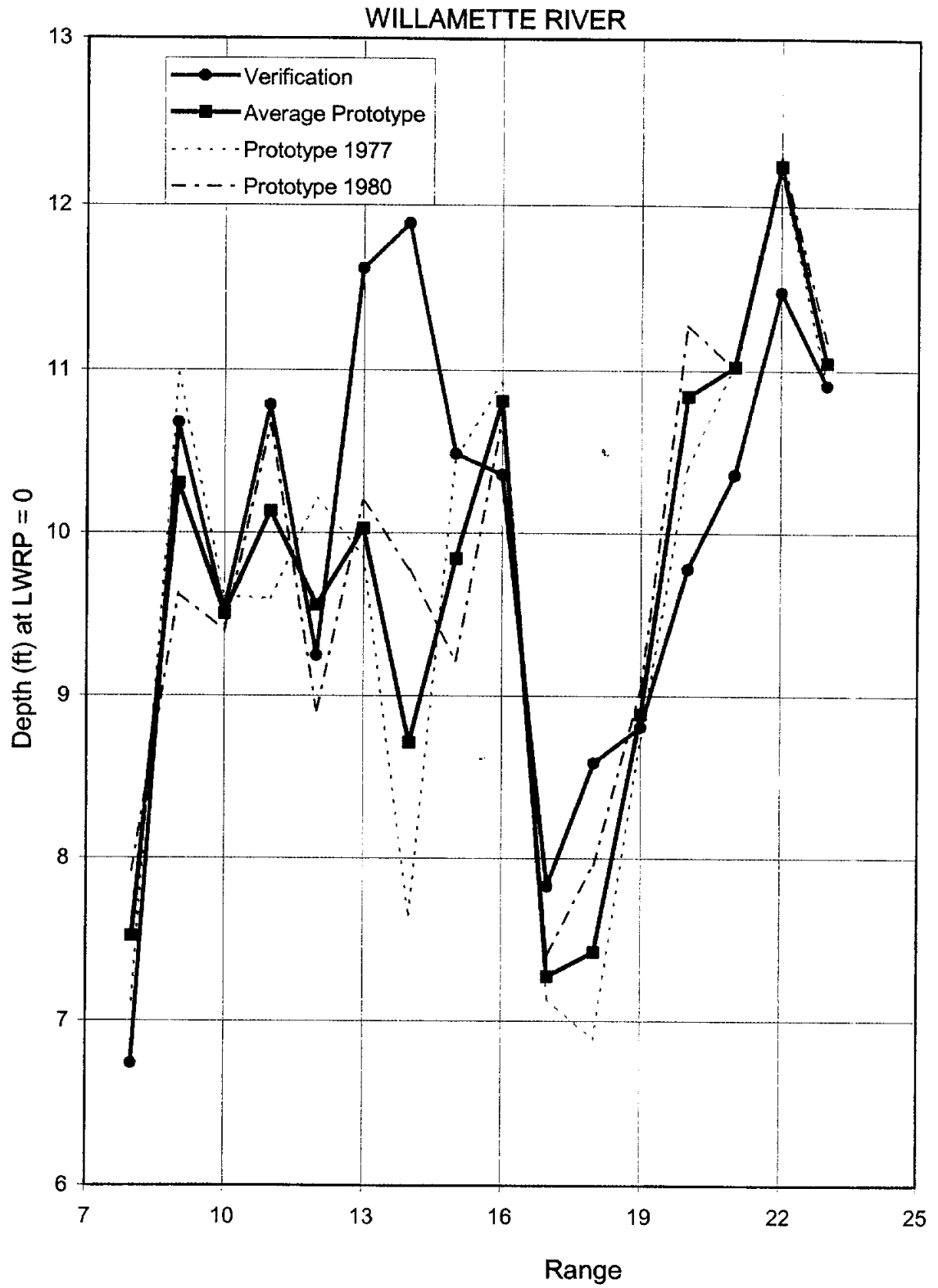


Figure B-16.2d Hydraulic Depth by Range, Willamette River

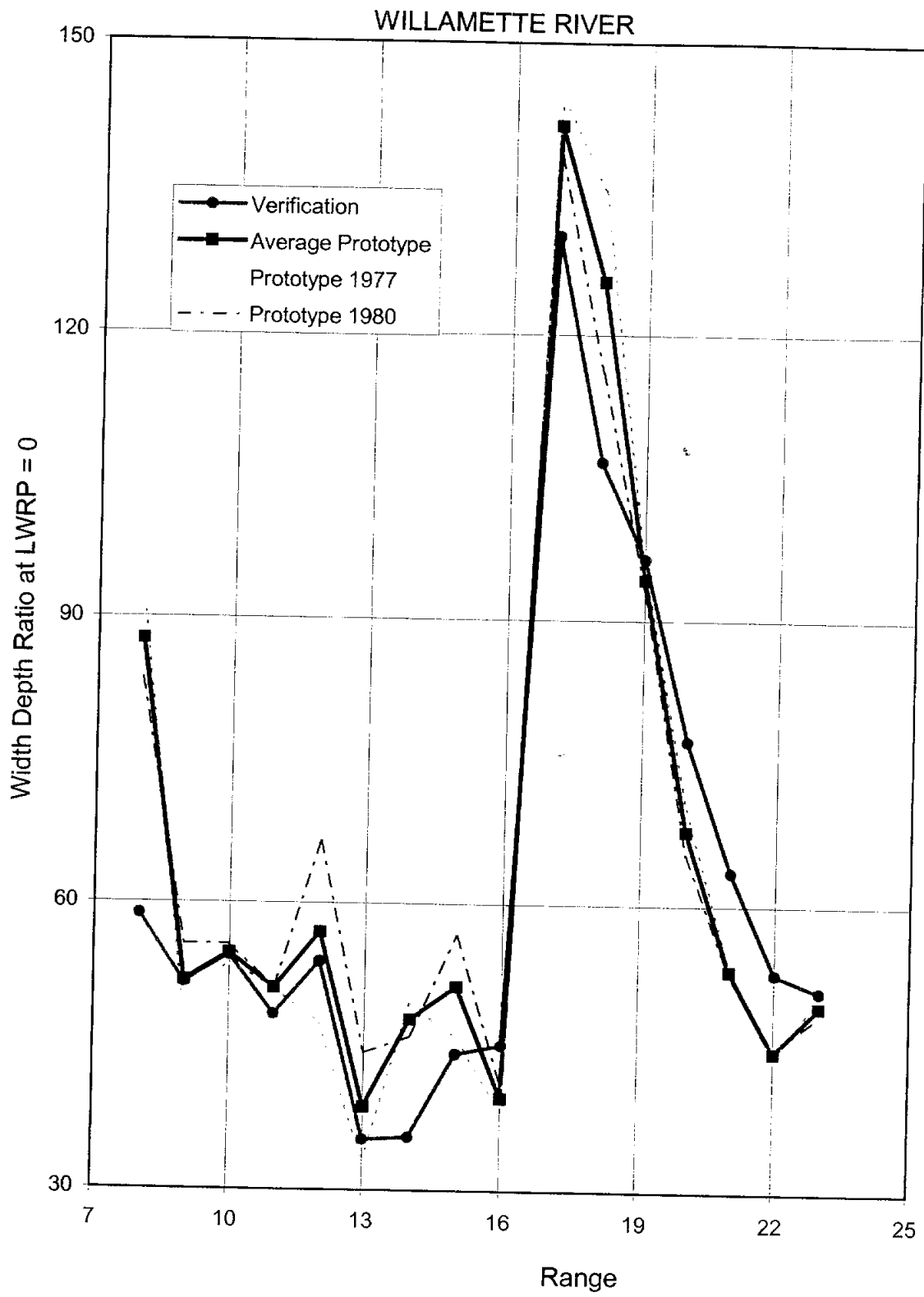


Figure B-16.2e Width/Depth Ratio by Range, Willamette River

APPENDIX C
PREVIOUS MICROMODEL STUDIES

Appendix C: Previous Small-Scale Model Investigations

Name (River)	Prototype Data Used in Model Calibration	Horizontal Scale ^a	Distortion (Horz.: Vert.)
Augusta, AR (White)	1999	3600:1	20:1
Clarendon, AR (White)	1999	4200:1	14:1
Copeland Bend (Missouri)	1991, 1996	3600:1	15:1
Kate Aubrey (Mississippi) ¹	1973, 1975, 1976	8000:1	13.3:1
Kate Aubrey (Mississippi) ¹	1973, 1975, 1976	16000:1	17.8:1
Lock & Dam 24 (Mississippi)	1993, 1995	9600:1	16:1
Memphis Harbor (Mississippi)	1996, 1997	4800:1	8:1
Morgan City/Berwick Bay (Atchafalaya)	1999	7200:1	6:1
New Madrid (Mississippi)	1994	20000:1	16.7:1
Salt Lake (Mississippi)	1993, 1995, 1996, 1998	9600:1	16:1
Savanna Bay (Mississippi)	1996	4800:1	8:1
Vicksburg Front (Mississippi)	1994, 1997	14400:1	12:1
Wolf Island (Mississippi)	1997, 1998	7200:1	12:1
^a Scale is prototype/model ratio. ¹ Models conducted as part of present research for studying scale effects.			

TABLE OF CONTENTS

1.1 Augusta Reach, White River, Arkansas	1
1.2 Copeland Bend Reach, Missouri River	1
1.3 Clarendon Reach, White River, Arkansas	2
1.4 Kate Aubrey Reach, Mississippi River	2
1.5 Lock and Dam 24 Reach, Upper Mississippi River	2
1.6 Memphis Harbor Reach, Lower Mississippi River	3
1.7 Morgan City/Berwick Bay Reach, Atchafalaya River, Louisiana.....	4
1.8 New Madrid Reach, Lower Mississippi River.....	4
1.9 Salt Lake Chute Reach, Middle Mississippi River	5
1.10 Vicksburg Front, Lower Mississippi River	5
1.11 White River Confluence Reach, Lower Mississippi River	6
1.12 Wolf Island Reach, Lower Mississippi River	6

TABLE OF CONTENTS

LIST OF FIGURES

Figure	Page
C-1.1a Augusta Model Plan View.....	8
C-1.1b 1999 Augusta Prototype Survey.....	9
C-1.1c Augusta Micromodel Base Test	10
C-1.2a Thalweg Distance From Left by Range, Augusta Reach (White River).....	11
C-1.2b Cross-Section Area by Range, Augusta (White River).....	12
C-1.2c Top Width by Range, Augusta (White River).....	13
C-1.2d Hydraulic Depth by Range, Augusta (White River)	14
C-1.2e Width/Depth Ratio by Range, Augusta (White River).....	15
C-2.1a Copeland Bend Model Plan View.....	16
C-2.1b 1991 Copeland Bend Prototype Survey	17
C-2.1c 1996 Copeland Bend Prototype Survey	18
C-2.1d Copeland Bend Micromodel Base Test	19
C-2.2a Thalweg Distance From Left by Range, Copeland Bend (Mississippi River).....	20
C-2.2b Cross-Section Area by Range, Copeland Bend (Mississippi River).....	21
C-2.2c Top Width by Range, Copeland Bend (Mississippi River)	22
C-2.2d Hydraulic Depth by Range, Copeland Bend (Mississippi River)	23
C-2.2e Width/Depth Ratio by Range, Copeland Bend (Mississippi River)	24
C-3.1a Clarendon Model Plan View.....	25
C-3.1b 1999 Clarendon Prototype Survey	26
C-3.1c Clarendon Micromodel Base Test.....	27
C-3.2a Thalweg From Left by Range, Clarendon Reach (White River)	28
C-3.2b Cross-Section Area by Range, Clarendon Reach (White River)	29
C-3.2c Top Width by Range, Clarendon Reach (White River)	30
C-3.2d Hydraulic Depth by Range, Clarendon Reach (White River).....	31

LIST OF FIGURES

C-3.2e Width/Depth Ratio by Range, Clarendon Reach (White River).....	32
C-4.1a Lock and Dam No. 24 Model Plan View.....	33
C-4.1b Lock and Dam No. 24 1993 Prototype Survey.....	34
C-4.1c Lock and Dam No. 24 1995 Prototype Survey.....	35
C-4.1d Lock and Dam No. 24 Micromodel Base Test.....	36
C-4.2a Lock and Dam No. 24 Thalweg Position From Left, L and D 24 (Mississippi River)	37
C-4.2b Cross-Section Area by Range, Lock and Dam No. 24 (Mississippi River).....	38
C-4.2c Top Width by Range, Lock and Dam No. 24 (Mississippi River).....	39
C-4.2d Hydraulic Depth by Range, Lock and Dam No. 24 (Mississippi River).....	40
C-4.2e Width/Depth Ratio by Range, Lock and Dam No. 24 (Mississippi River).....	41
C-5.1a Memphis Harbor Micromodel Plan View.....	42
C-5.1b Memphis Harbor Prototype Survey 1996.....	43
C-5.1c Memphis Harbor Prototype Survey 1997.....	44
C-5.1d Memphis Harbor Micromodel Base Test.....	45
C-5.2a Thalweg Distance From Left by Range, Memphis Harbor (Mississippi River).....	46
C-5.2b Cross-Section Area by Range, Memphis Harbor (Mississippi River).....	47
C-5.2c Top Width by Range, Memphis Harbor (Mississippi River).....	48
C-5.2d Hydraulic Depth by Range, Memphis Harbor (Mississippi River).....	49
C-5.2e Width/Depth Ratio by Range, Memphis Harbor (Mississippi River).....	50
C-6.1a Morgan City/Berwick Bay Micromodel Plan View.....	51
C-6.1b Morgan City/Berwick Bay Prototype Survey 1999.....	52
C-6.1c Morgan City/Berwick Bay Micromodel Base Test.....	53
C-6.2a Thalweg Position From Left by Range, Morgan City (Atchafalaya River).....	54
C-6.2b Cross-Section Area, Morgan City (Atchafalaya River).....	55

LIST OF FIGURES

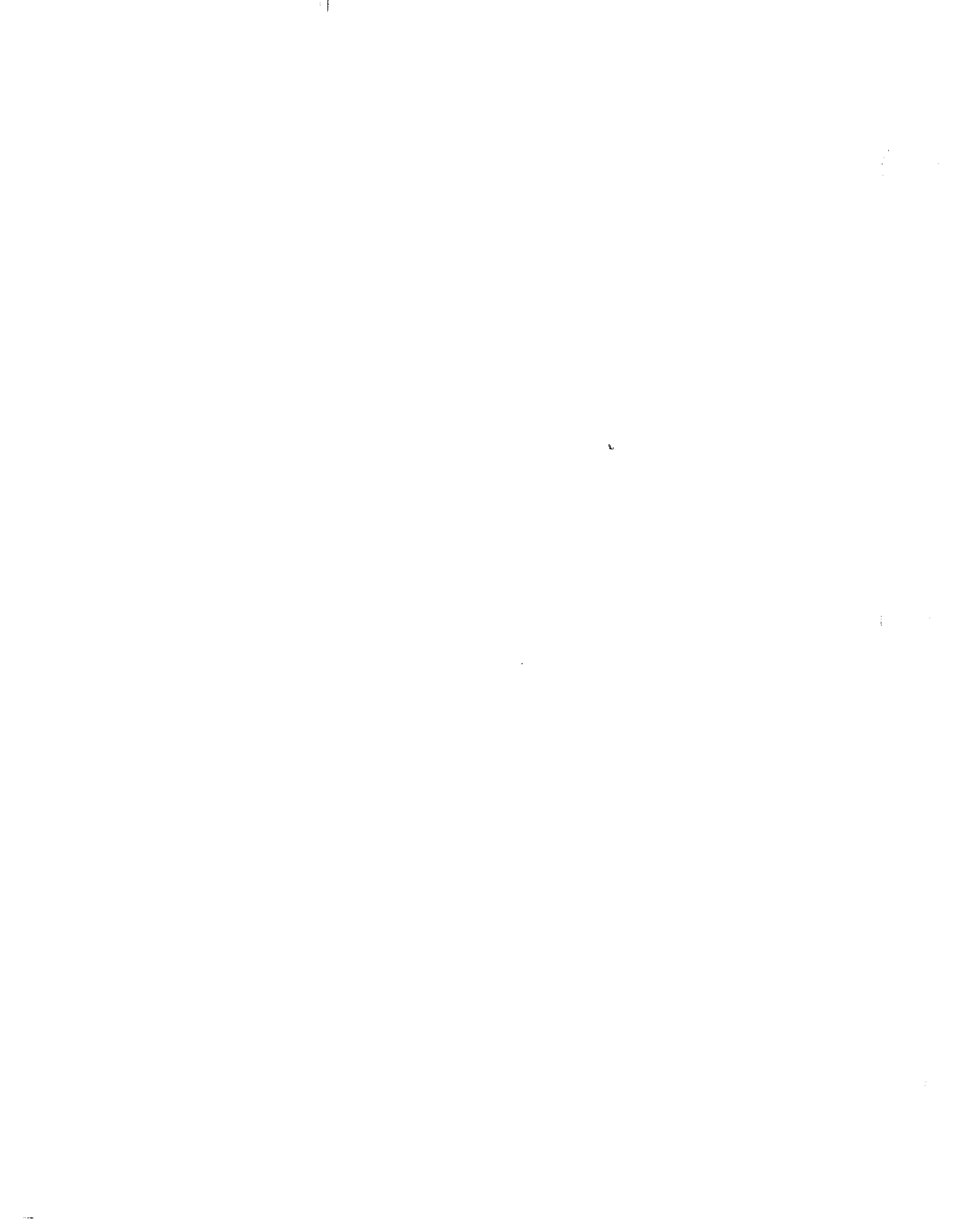
C-6.2c Top Width by Section, Morgan City (Atchafalaya River).....	56
C-6.2d Hydraulic Depth by Section, Morgan City (Atchafalaya River)	57
C-6.2e Width/Depth Ratio by Range, Morgan City (Atchafalaya River).....	58
C-7.1a New Madrid Micromodel Plan View	59
C-7.1b New Madrid Prototype Survey 1994	60
C-7.1c New Madrid Micromodel Base Test	61
C-7.2a Thalweg Position From Left by Range, New Madrid Reach..... (Mississippi River).....	62
C-7.2b Cross-Section Area by Range, New Madrid Reach (Mississippi River).....	63
C-7.2c Top Width by Range, New Madrid Reach (Mississippi River).....	64
C-7.2d Hydraulic Depth by Range, New Madrid Reach (Mississippi River)	65
C-7.2e Width/Depth Ratio by Range, New Madrid Reach (Mississippi River).....	66
C-8.1a Salt Lake Chute Micromodel Plan View	67
C-8.1b Salt Lake Chute Prototype Survey 1989	68
C-8.1c Salt Lake Chute Prototype Survey 1993	69
C-8.1d Salt Lake Chute Prototype Survey 1995	70
C-8.1e Salt Lake Chute Prototype Survey 1996	71
C-8.1f Salt Lake Chute Prototype Survey 1998.....	72
C-8.1g Salt Lake Chute Micromodel Base Test	73
C-8.2a Thalweg Position From Left by Range,	74
Salt Lake Chute (Mississippi River).....	74
C-8.2b Cross-Section Area by Range, Salt Lake Chute (Mississippi River).....	75
C-8.2c Top Width by Range, Salt Lake Chute (Mississippi River)	76
C-8.2d Hydraulic Depth by Range, Salt Lake Chute (Mississippi River).....	77
C-8.2e Width/Depth Ratio by Range, Salt Lake Chute (Mississippi River)	78

LIST OF FIGURES

C-9.1a Vicksburg Front Micromodel Plan View	79
C-9.1b Vicksburg Front Prototype Survey 1994	80
C-9.1c Vicksburg Front Prototype Survey 1997.....	81
C-9.1d Vicksburg Front Micromodel Base Test.....	82
C-9.2a Thalweg Position From Left by Range, Vicksburg Front (Mississippi River).....	83
C-9.2b Cross-Section Area by Range, Vicksburg Front (Mississippi River).....	84
C-9.2c Top Width by Range, Vicksburg Front (Mississippi River).....	85
C-9.2d Hydraulic Depth by Range, Vicksburg Front (Mississippi River)	86
C-9.2e Width/Depth Ratio by Range, Vicksburg Front (Mississippi River).....	87
C-10.1a White River Confluence with Mississippi River Micromodel Plan View	88
C-10.1b White River Confluence with Mississippi River Prototype Survey 1994	89
C-10.1c White River Confluence with Mississippi River Prototype Survey 1997.....	90
C-10.1d White River Confluence with Mississippi River Micromodel Base Test.....	91
C-10.2a Thalweg Distance From Left by Range, White River Confluence with Mississippi River.....	92
C-10.2b Cross-Section Area by Range, White River Confluence with Mississippi River... 93	
C-10.2c Top Width by Range, White River Confluence with Mississippi River.....	94
C-10.2d Hydraulic Depth by Range, White River Confluence with Mississippi River	95
C-10.2e Width/Depth Ratio by Range, White River Confluence with Mississippi River....	96
C-11.1a Wolf Island Micromodel Plan View	97
C-11.1b Wolf Island Prototype Survey 1997.....	98
C-11.1c Wolf Island Prototype Survey 1998.....	99
C-11.1d Wolf Island Micromodel Base Test.....	100
C-11.2a Thalweg Position From Left by Range, Wolf Island (Mississippi River)	101
C-11.2b Cross-Section Area by Range, Wolf Island (Mississippi River)	102

LIST OF FIGURES

C-11.2c Top Width by Range, Wolf Island (Mississippi River)	103
C-11.2d Hydraulic Depth by Range, Wolf Island (Mississippi River).....	104
C-11.2e Width/Depth Ratio by Range, Wolf Island (Mississippi River)	105



1.1 Augusta Reach, White River, Arkansas

Location: The Augusta reach is located on the White River about 193 river miles above its confluence with the Mississippi River.

Purpose of Study: The purpose of the study was to investigate structural methods to improve navigation depths and reduce dredging.

Data: Data used in this movable bed micro model included (1) 1999 Prototype Survey (2) Micro Model base test.

Scale: The micro model used in this study had a horizontal scale of 1 inch = 300 feet and a vertical scale of 1 inch = 15 feet, and reproduced approximately 7 miles of the White River between Miles 197 and 190.

Actual Model Limits: RM 201.5 to 189.5

Study Limits: RM 196.2 to 190.0

Reference: John D. Boeckmann, Robert D. Davinroy, David C. Gordon, Aron M. Rhoads (2000) "Sedimentation and Navigation Study of the Lower White River, Near Augusta and Clarendon, Arkansas" Technical Report M12. U.S. Army Engineer District, St. Louis, MO.

1.2 Copeland Bend Reach, Missouri River

Location: The Copeland Bend reach is located on the Missouri River about 567 river miles above its confluence with the Mississippi River.

Purpose of Study: The purpose of this study was to evaluate design alternatives focused on environmental enhancement for the creation of shallow water habitat within Copeland Bend.

Data: Data used in this movable bed analysis included (1) 1991 Prototype Survey (2) 1996 Prototype Survey (3) Micro Model base test.

Scale: The micro model used in this study had a horizontal scale of 1 inch = 300 feet and a vertical scale of 1 inch = 20 feet, and reproduced approximately 5 miles of the Missouri River between Miles 569 and 564.5.

Actual Model Limits: RM 570.0 to 564.0

Study Limits: RM 569.0 to 564.5

Reference: Robert D. Davinroy, David C. Gordon, Aron M. Rhoads, James R. Abbott (1999) "Sedimentation and Navigation Study of the Missouri River, Copeland Bend, Miles 569 to 564.5" Technical Report M10. U.S. Army Engineer District, St. Louis, MO.

1.3 Clarendon Reach, White River, Arkansas

Location: The Clarendon reach is located on the White River about 96 river miles above its confluence with the Mississippi River.

Purpose of Study: The purpose of the study was to investigate structural methods to improve navigation depths and reduce dredging.

Data: Data used in this movable bed micro model included (1) 1999 Prototype Survey (2) Micro Model base test.

Scale: The micro model used in this study had a horizontal scale of 1 inch = 350 feet and a vertical scale of 1 inch = 25 feet, and reproduced approximately 6 miles of the White River between Miles 100 and 94.

Actual Model Limits: RM 100.1 to 93.0

Study Limits: RM 99.8 to 93.5

Reference: John D. Boeckmann, Robert D. Davinroy, David C. Gordon, Aron M. Rhoads (2000) "Sedimentation and Navigation Study of the Lower White River, Near Augusta and Clarendon, Arkansas" Technical Report M12. U.S. Army Engineer District, St. Louis, MO.

1.4 Kate Aubrey Reach, Mississippi River

Please See Chapter 3 for complete information

1.5 Lock and Dam 24 Reach, Upper Mississippi River

Location: Lock and Dam 24 is located on the Upper Mississippi River about 273 river miles above its confluence with the Ohio River.

Purpose of Study: The purpose of the Lock and Dam 24 micro model study was to investigate possible solutions to the dangerous outdraft currents that existed at the downstream approach to the lock.

Data: Data used in the Movable bed analysis included: (1) 1993 Prototype survey, (2) 1995 Prototype survey and, (3) Micro Model base test.

Scale: The micro model used in this study had a horizontal scale of 1 inch = 800 feet and a vertical scale of 1 inch = 50 feet, and reproduced approximately 6 miles of the Upper Mississippi River between Miles 271 and 277.

Actual Model Limits: RM 281.0 to 270.0

Study Limits: RM 277.0 to 272.0

Reference: Robert D. Davinroy, David C. Gordon, Robert D. Hetrick (1998). "Navigation Study at the Approach to Lock and Dam 24, Upper Mississippi River" Technical Report M2, U.S. Army Engineer District, St. Louis, MO.

1.6 Memphis Harbor Reach, Lower Mississippi River

Location: Memphis Harbor is located on the Lower Mississippi River about 739 river miles above the Head of Passes.

Purpose of Study: The purpose of the Memphis Harbor study was to evaluate proposed design enhancements at the harbor.

Data: Data used in the movable bed analysis included (1) 1996 Prototype Survey (2) 1997 Prototype Survey (3) Micro Model base test.

Scale: The micro model used in this study had a horizontal scale of 1 inch = 500 feet and a vertical scale of 1 inch = 50 feet, and reproduced approximately 7 miles of the Lower Mississippi River between miles 742 and 735.

Actual Model Limits: RM 743.0 to 734.0

Study Limits: RM 741.5 to 735.0

Reference: Robert D. Davinroy, David C. Gordon, Edward H. Riiff, (2000) "Sedimentation Study at Memphis Harbor, Lower Mississippi River, River Miles 742 at 735" Technical Report M8. U.S. Army Engineer District, St. Louis, MO.

1.7 Morgan City/Berwick Bay Reach, Atchafalaya River, Louisiana

Location: Morgan City is located on the Atchafalaya River about 120 river miles below the Old River Control Structure and the Mississippi River.

Purpose of Study: The purpose of the study was to improve navigation depths, reduce dredging, and improve navigation alignment through several bridge spans.

Data: Data used in this movable bed study included (1) 1999 Prototype Survey (2) Micro Model base test.

Scale: The micro model used in this study had a horizontal scale of 1 inch = 600 feet and a vertical scale of 1 inch = 100 feet, and reproduced approximately 6 miles of the Atchafalaya River between Miles 124 and 118.5.

Actual Model Limits: RM 116.5 to 126.0

Study Limits: RM 119.0 to 124.0

Reference: Robert D. Davinroy, David C. Gordon, Edward H. Riiff, Aron M. Rhoads, (2001) "Sedimentation and Navigation Study of the Lower Atchafalaya River at Morgan City and Berwick, Louisiana, River Miles 124.0 to 118.5, Hydraulic Micro Model Study" Technical Report M14. U.S. Army Engineer District, St. Louis, Mo.

1.8 New Madrid Reach, Lower Mississippi River

Location: New Madrid is located on the Lower Mississippi River about 889 river miles above the Head of Passes.

Purpose of Study: The purpose of the New Madrid study was to improve navigation depths and alignment.

Data: Data used in the movable bed analysis included (1) 1994 Prototype Survey (2) Micro Model base test.

Scale: The micro model used in this study had a horizontal scale of 1 inch = 1667 feet and a vertical scale of 1 inch = 100 feet, and reproduced approximately 8 miles of the Lower Mississippi River between Miles 891 and 883.

Actual Model Limits: RM 899.0 to 881.0

Study Limits: RM 890.0 to 884.0

Reference: Robert D. Davinroy (1995) "Sedimentation Study of the Mississippi River, New Madrid Bar Reach, River Miles 891 at 883, Hydraulic Micro Model Investigation" U.S. Army Engineer District, St. Louis, MO.

1.9 Salt Lake Chute Reach, Middle Mississippi River

Location: Salt Lake Chute is located on the Middle Mississippi River about 138 river miles above its confluence with the Ohio River.

Purpose of Study: The purpose of the Salt Lake Chute Micro Model study was to investigate design alternatives that were intended to improve environmental health and enhance side channel habitat.

Data: Data used in this movable bed study included (1) 1989 Prototype Survey (2) 1993 Prototype Survey (3) 1995 Prototype Survey (4) 1996 Prototype Survey (5) 1998 Prototype Survey (6) Micro Model base test.

Scale: The micro model used in this study had a horizontal scale of 1 inch = 800 feet and a vertical scale of 1 inch = 50 feet, and reproduced approximately 8 miles of the Middle Mississippi River between river miles 141 and 133.

Actual Model Limits: RM 142.5 to 131.0

Study Limits: RM 140.5 to 136.0

Reference: David C. Gordon, Robert D. Davinroy, Peter M. Russell (2001) "Sedimentation Study of the Middle Mississippi River at Salt Lake Chute, River Miles 141 to 133" Technical Report M16, U.S. Army Engineer District, St. Louis, MO.

1.10 Vicksburg Front, Lower Mississippi River

Location: Vicksburg Front is located on the Lower Mississippi River about 437 river miles above the Head of Passes.

Purpose of Study: The purpose of the Vicksburg Front Micro Model study was to improve navigation alignment for tows traveling through the reach.

Data: Data used in this movable bed study included (1) 1994 Prototype Survey (2) 1997 Prototype Survey (2) Micro Model base test.

Scale: The micro model used in this study had a horizontal scale of 1 inch = 1200 feet and a vertical scale of 1 inch = 100 feet, and reproduced approximately 12 miles of the Lower Mississippi River between 441 and 429.

Actual Model Limits: RM 444.5 to 423

Study Limits: RM 440.0 to 432.5

Reference: Robert D. Davinroy, David C. Gordon, Aron M. Rhoads, James R. Abbott (2000) "Sedimentation and Navigation Study at Vicksburg Front, Lower Mississippi River Miles 441 to 429, Hydraulic Micro Model Study" Technical Report M15. U.S. Army Engineer District, St. Louis, Mo.

1.11 White River Confluence Reach, Lower Mississippi River

Location: The confluence of the Lower Mississippi River and the White River is located about 599 river miles above the Head of Passes.

Purpose of Study: The purpose of this study was to improve navigation alignment and currents at the confluence of the White and Mississippi Rivers.

Data: Data used in the movable bed analysis included (1) 1994 Prototype Survey (2) 1997 Prototype Survey (3) Micro model base test

Scale: The micro model used in this study had a horizontal scale of 1 inch = 1000 feet and a vertical scale of 1 inch = 100 feet, and reproduced approximately 7 miles of the Lower Mississippi River between Miles 596 and 603.

Actual Model Limits: RM 605.0 to 587.0

Study Limits: RM 600.0 to 597.5

Reference: David C. Gordon, Robert D. Davinroy, and Edward H. Riiff, (1998) "Sedimentation and Navigation Study of the Lower Mississippi River at the White River Confluence, Miles 603 to 596" Technical Report M7, U.S. Army Engineer District, St. Louis, MO.

1.12 Wolf Island Reach, Lower Mississippi River

Location: Wolf Island is located on the Lower Mississippi River about 934 river miles above the Head of Passes.

Purpose of Study: The purpose of this study was to improve navigation and enhance the side channel bathymetry and habitat.

Data: Data used in this movable bed analysis included (1) 1998 Prototype Survey (2) 1997 Prototype Survey (3) Micro Model base test

Scale: The micro model used in this study had a horizontal scale of 1 inch = 600 feet and a vertical scale of 1 inch = 50 feet, and reproduced approximately 8 miles of the Lower Mississippi River between Miles 937 and 929.

Actual Model Limits: RM 938.5 to 929.0

Study Limits: RM 937.0 to 930.5

Reference: Robert D. Davinroy, David C. Gordon, Aron M. Rhoads, Edward H Riiff (2000) "Environmental and Navigation Improvement Study of Wolf Island, Mississippi River Miles 936.5 to 929" Technical Report M9. U.S. Army Engineer District, St Louis, MO.

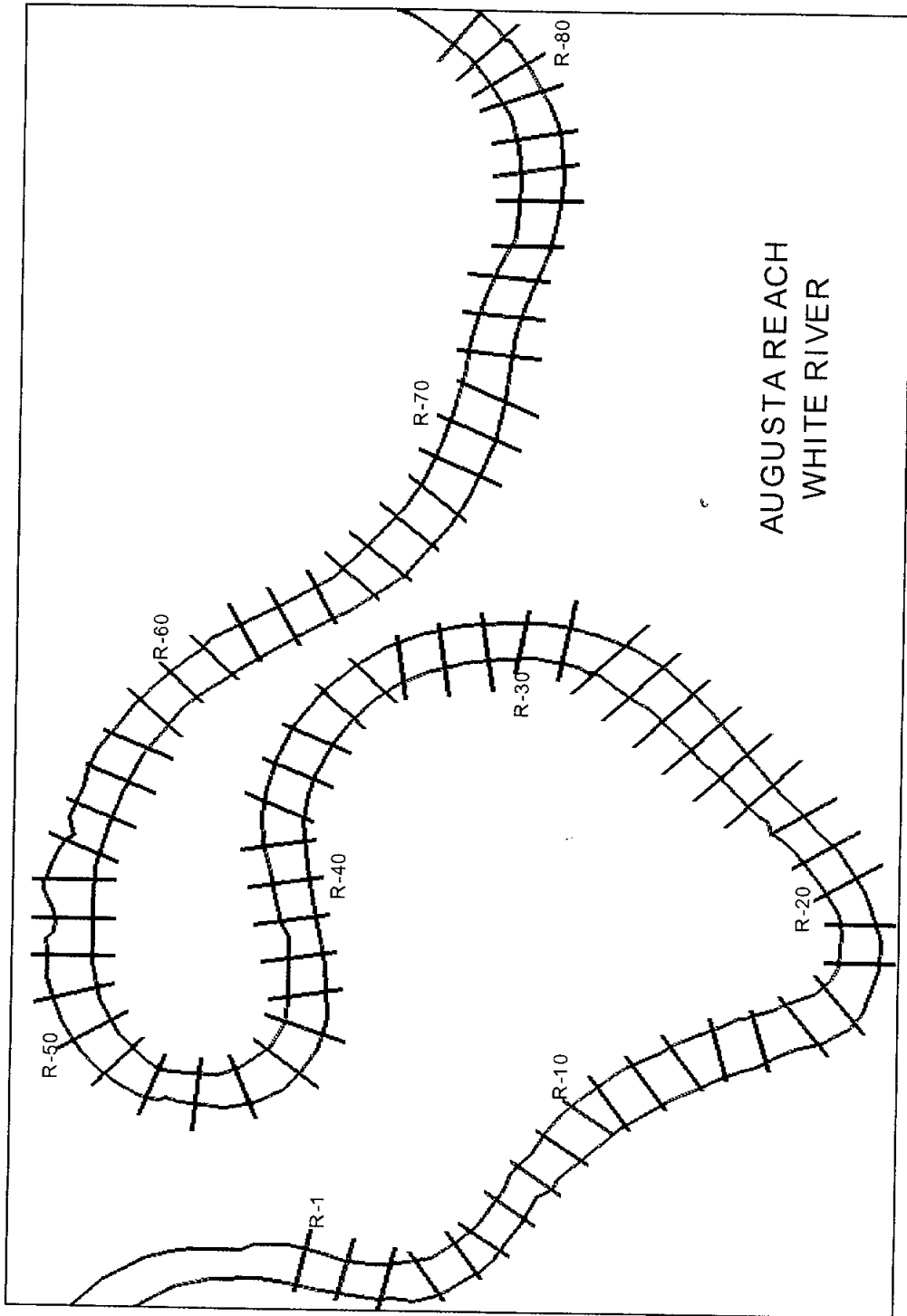


Figure C-1.1a Augusta Model Plan View

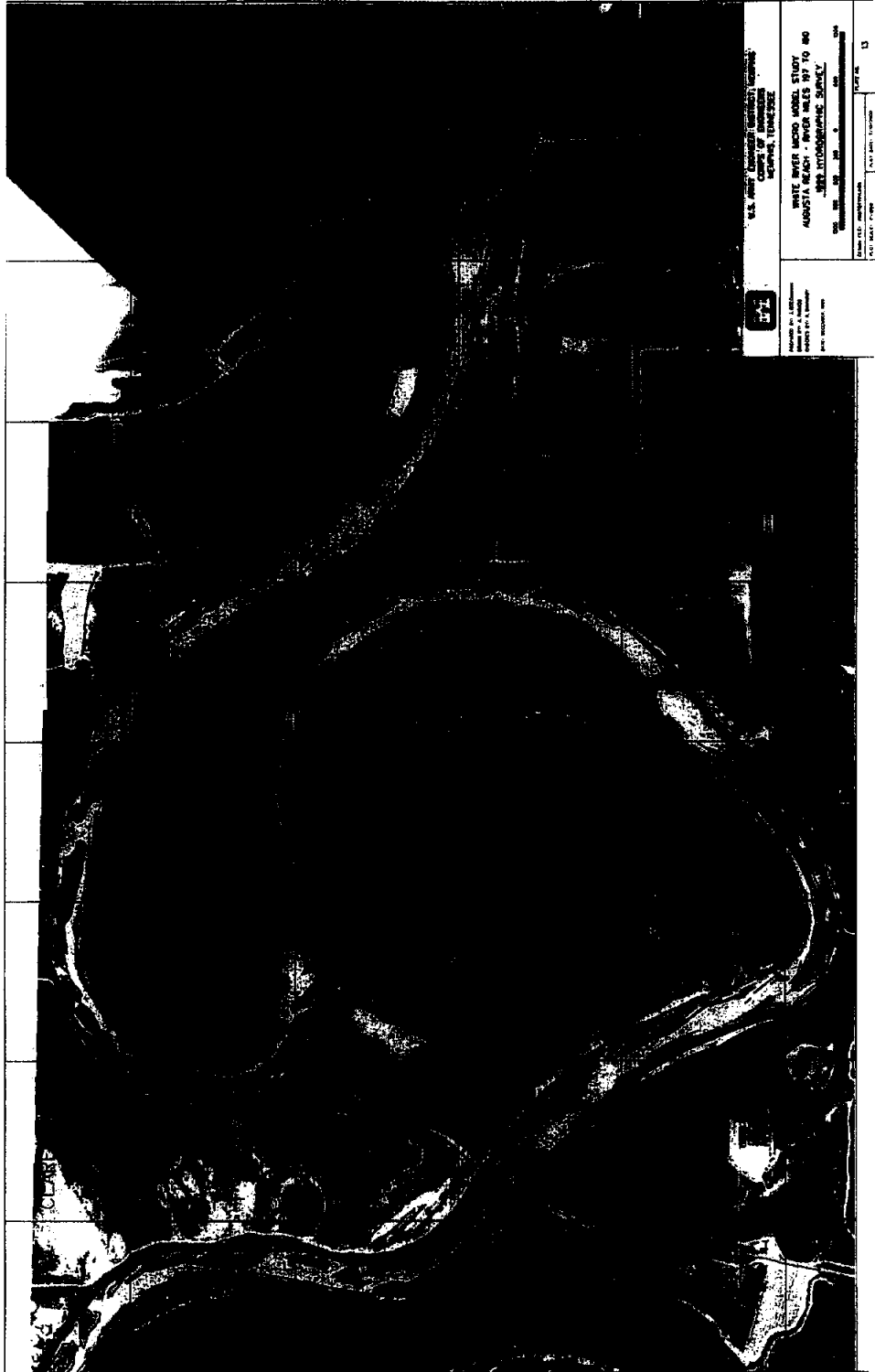


Figure C-1.1b 1999 Augusta Prototype Survey



Figure C-1.1c Augusta Micromodel Base Test

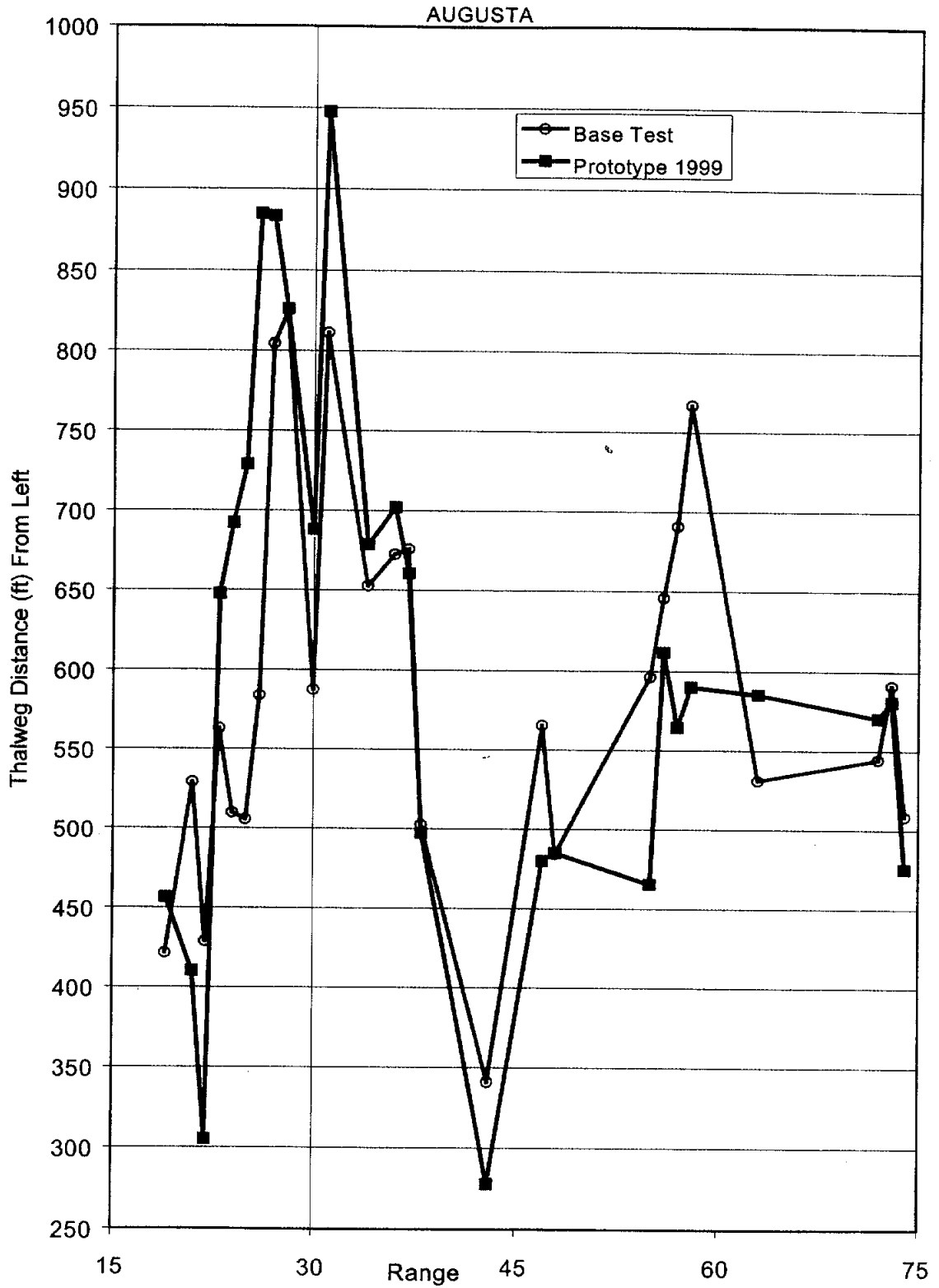


Figure C-1.2a Thalweg Distance From Left by Range, Augusta Reach (White River)

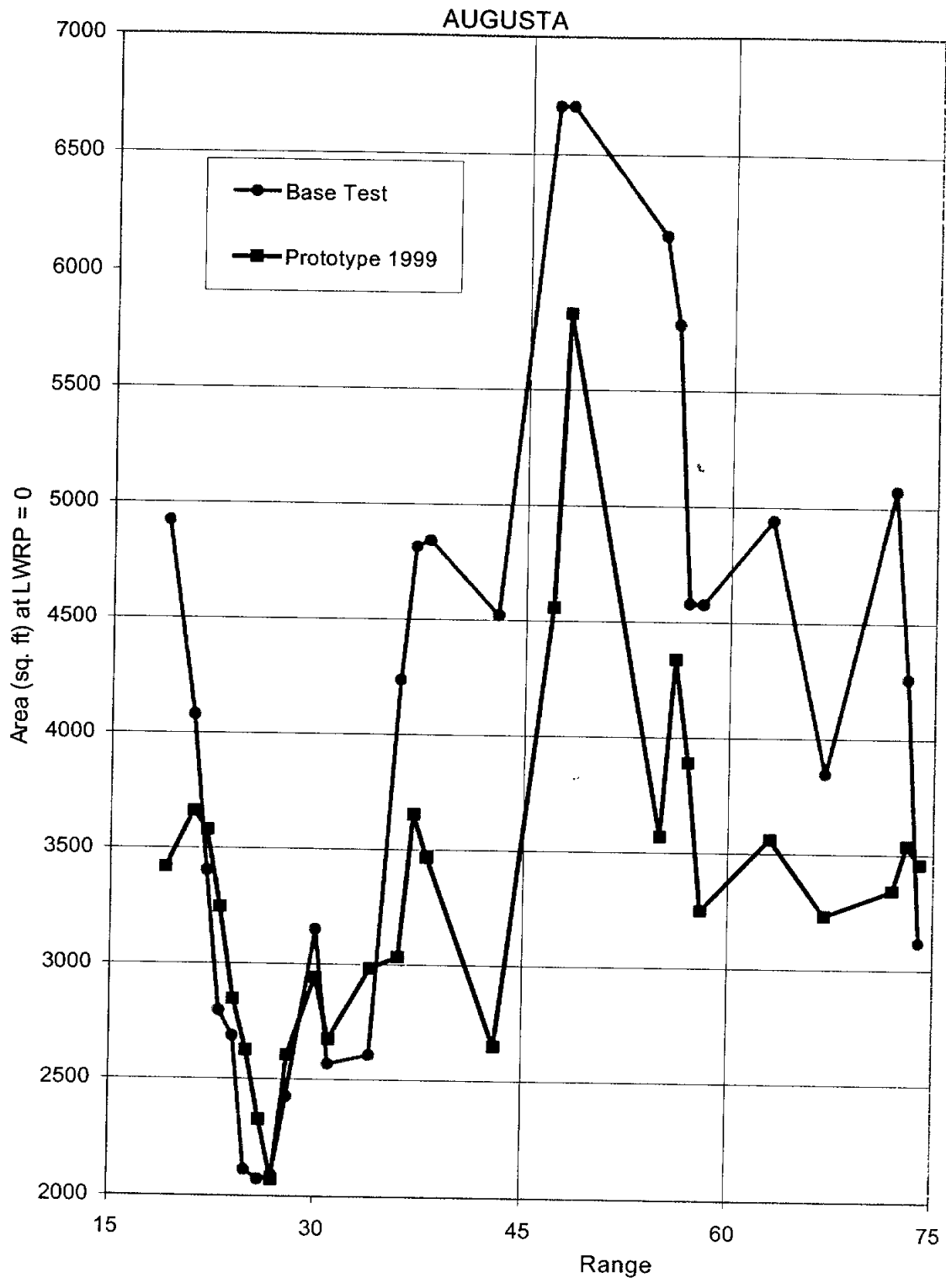


Figure C-1.2b Cross-Section Area by Range, Augusta (White River)

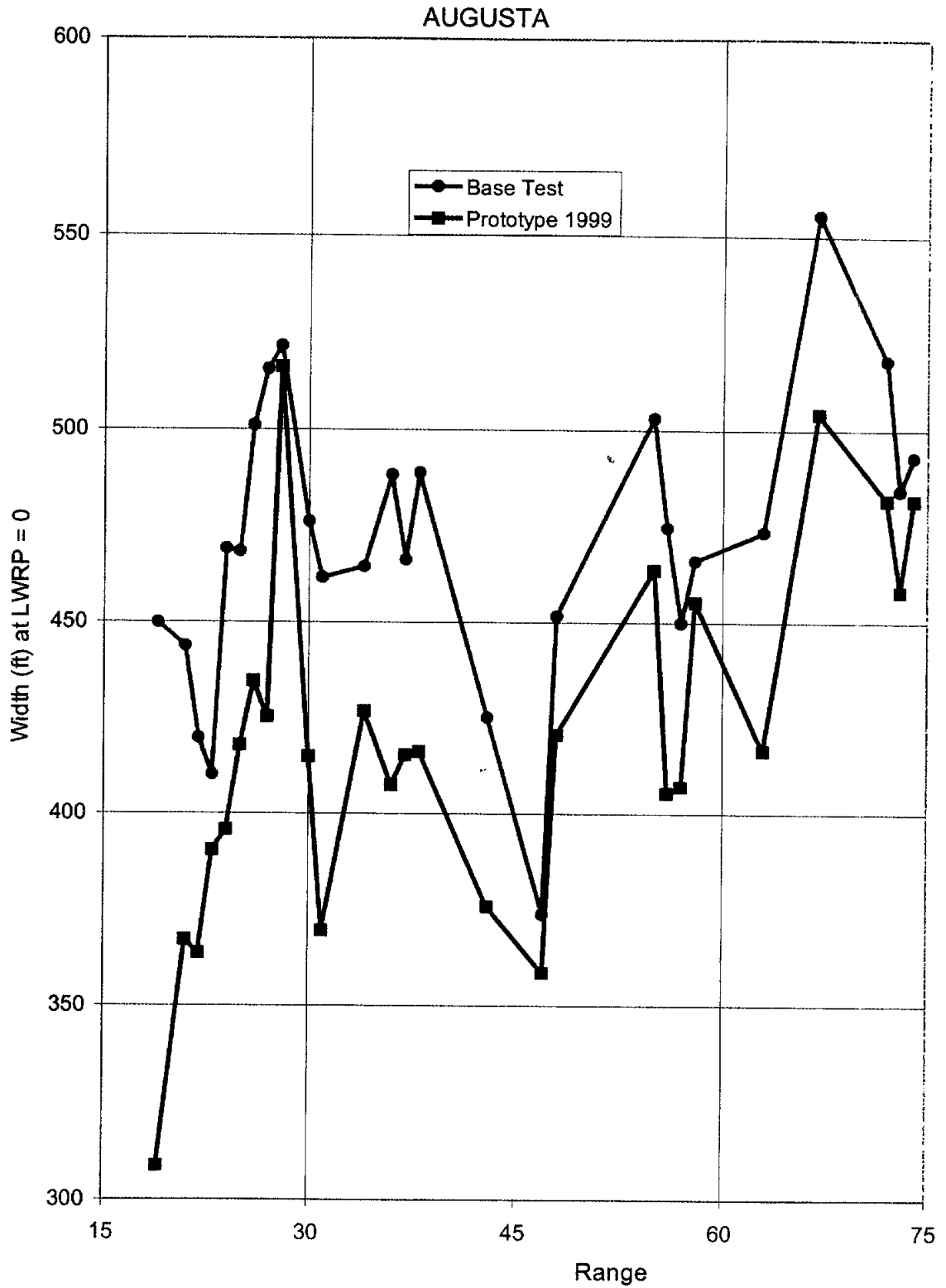


Figure C-1.2c Top Width by Range, Augusta (White River)

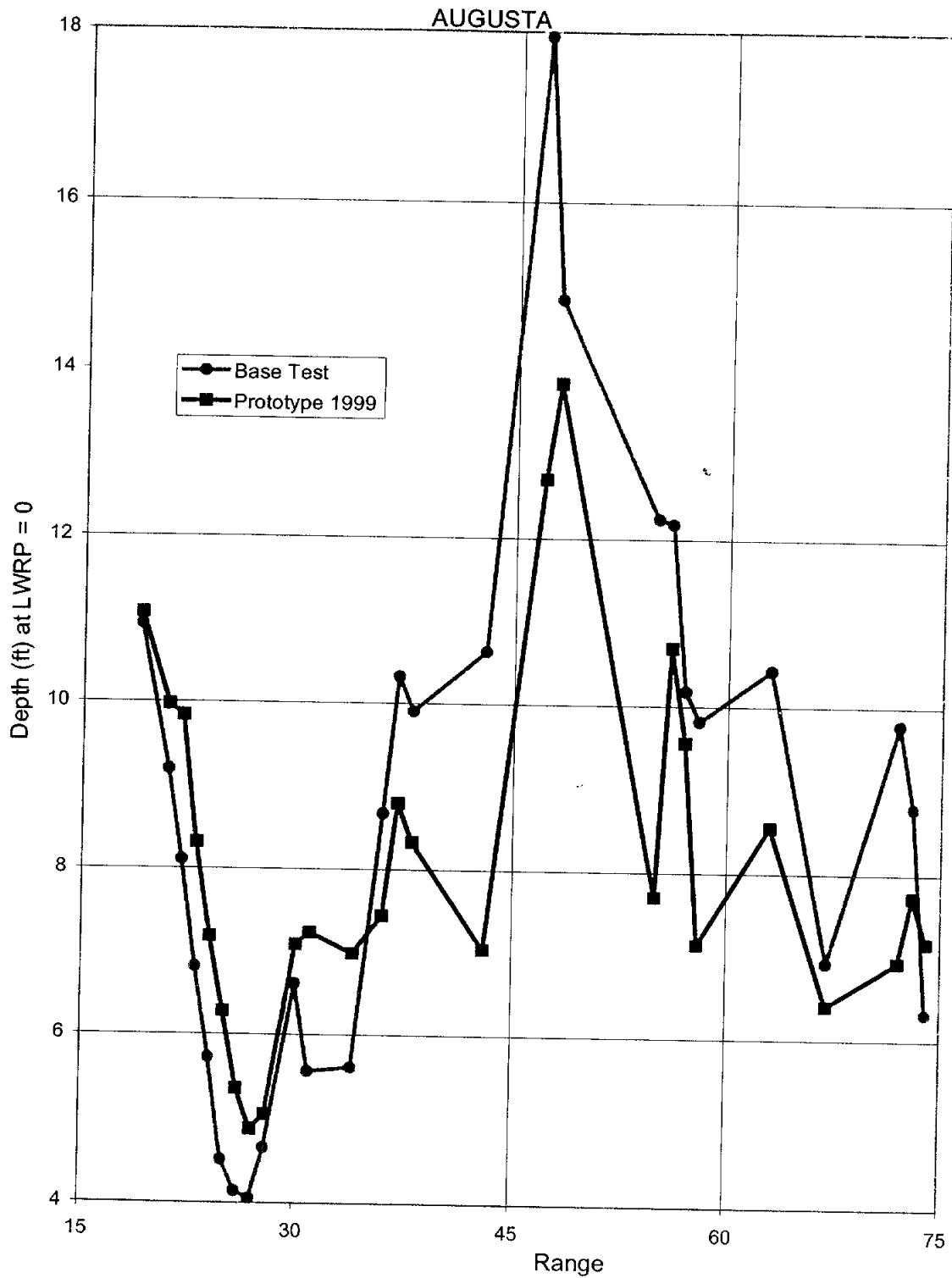


Figure C-1.2d Hydraulic Depth by Range, Augusta (White River)

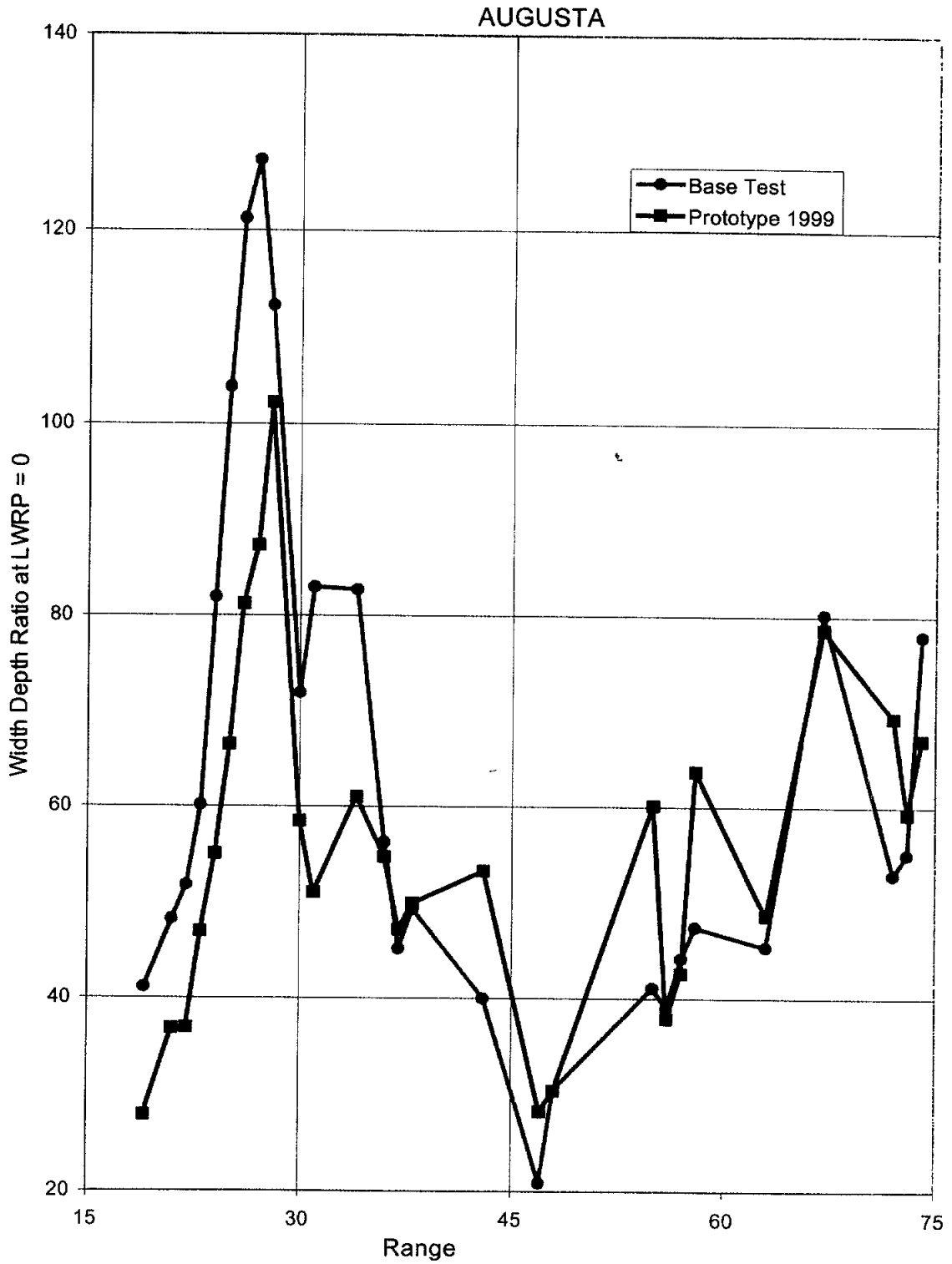


Figure C-1.2e Width/Depth Ratio by Range, Augusta (White River)

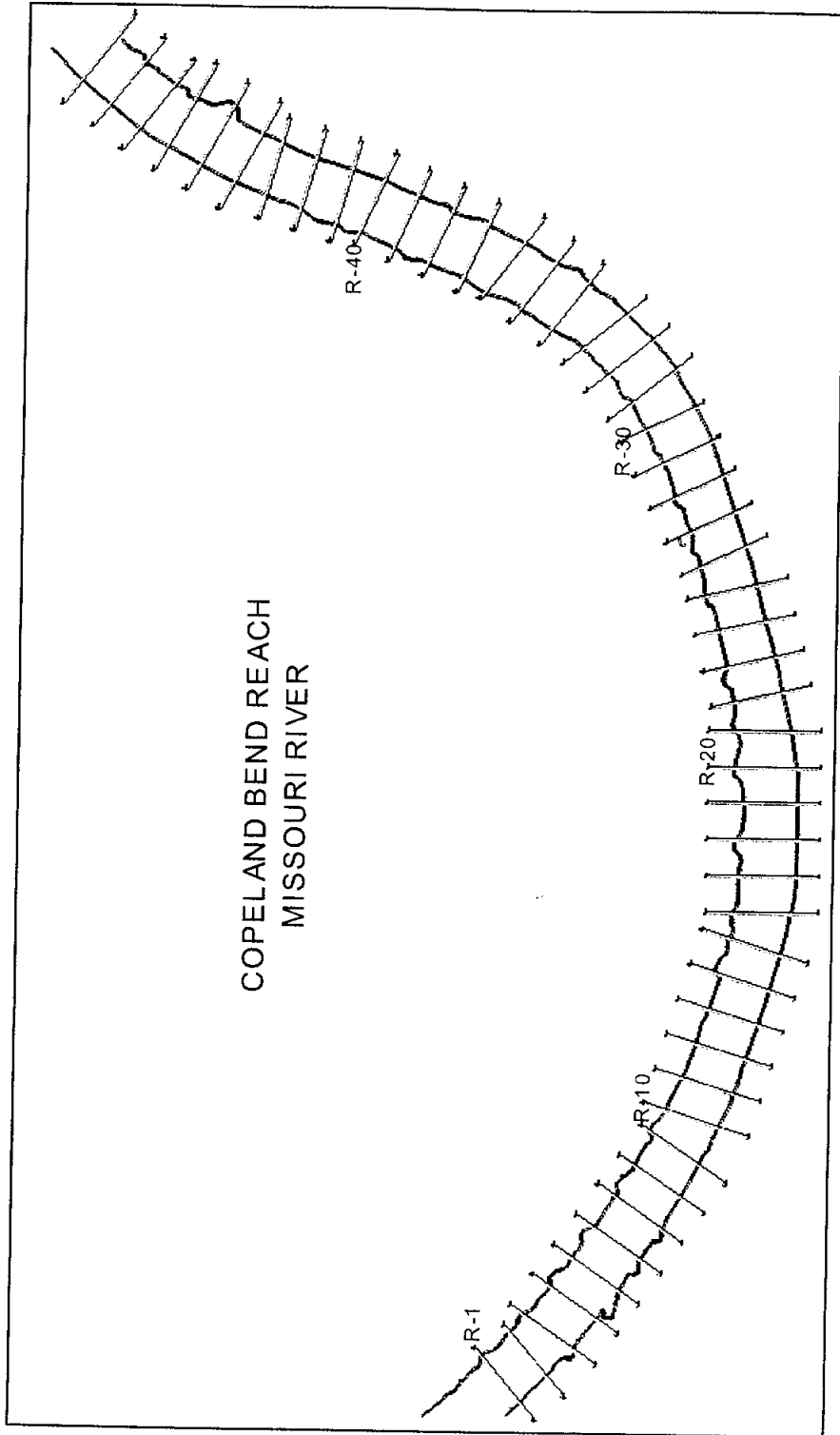


Figure C-2.1a Copeland Bend Model Plan View

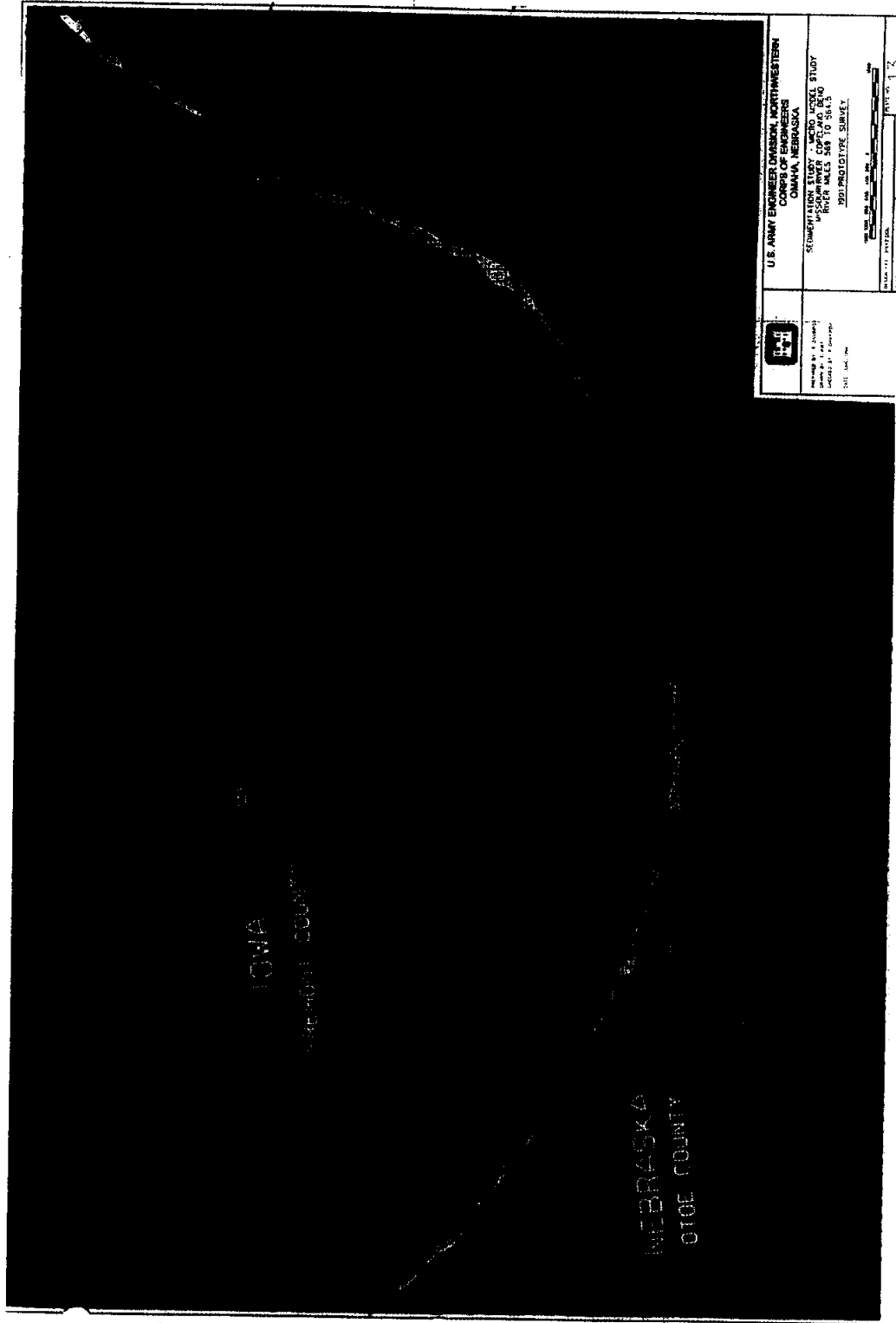


Figure C-2.1b 1991 Copeland Bend Prototype Survey

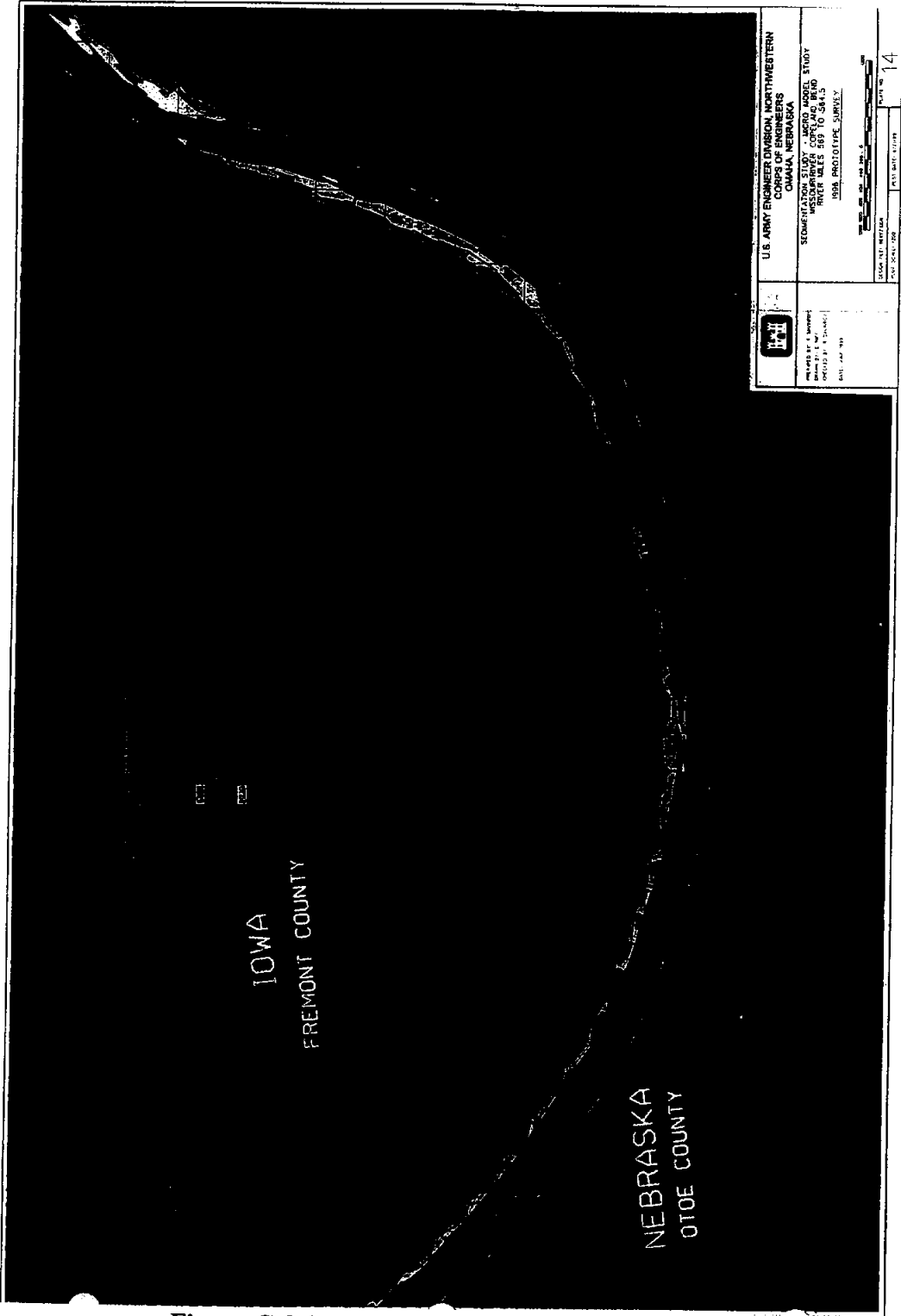


Figure C-2.1c 1996 Copeland Bend Prototype Survey

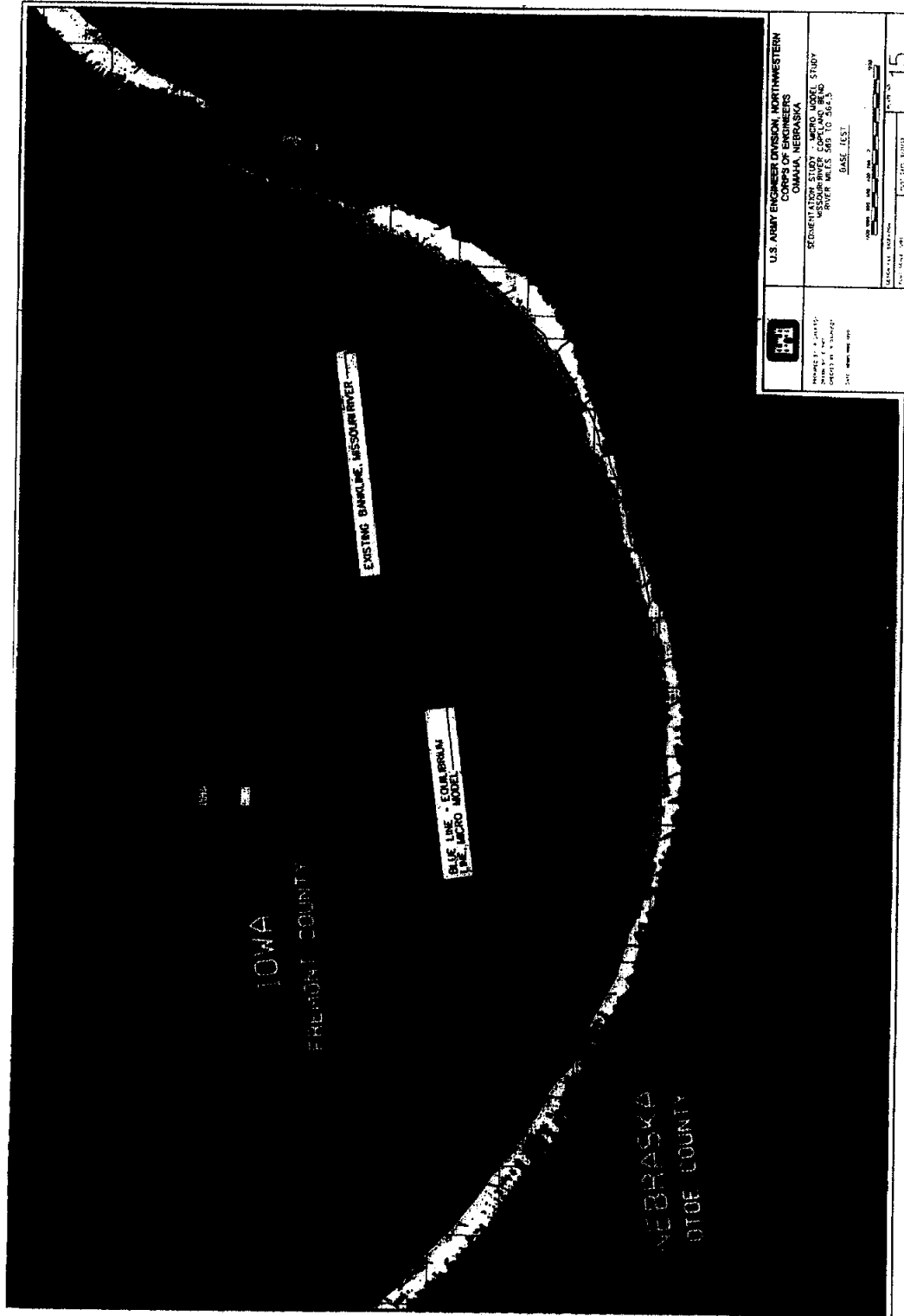


Figure C-2.1d Copeland Bend Micromodel Base Test

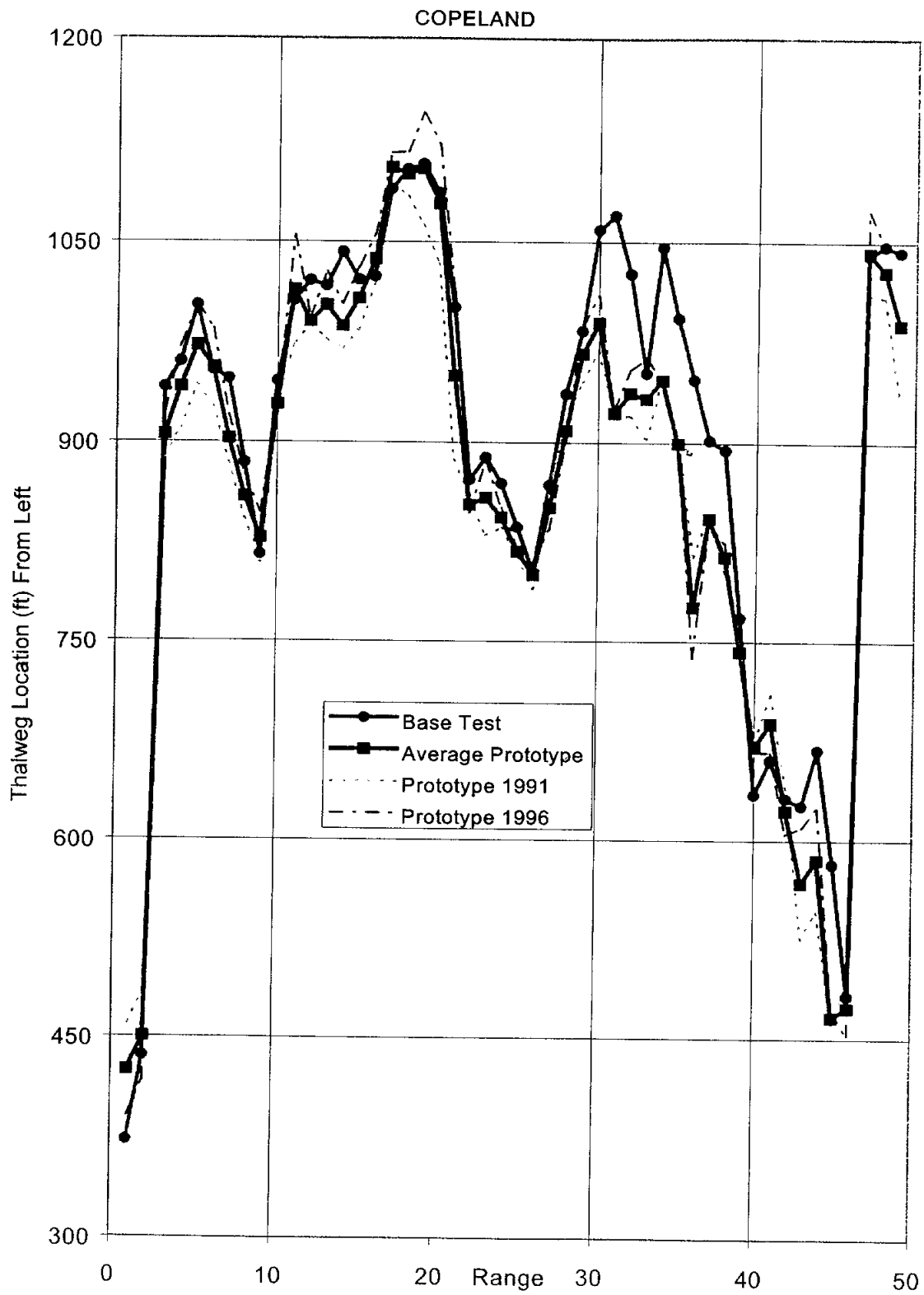


Figure C-2.2a Thalweg Distance From Left by Range, Copeland Bend (Mississippi River)

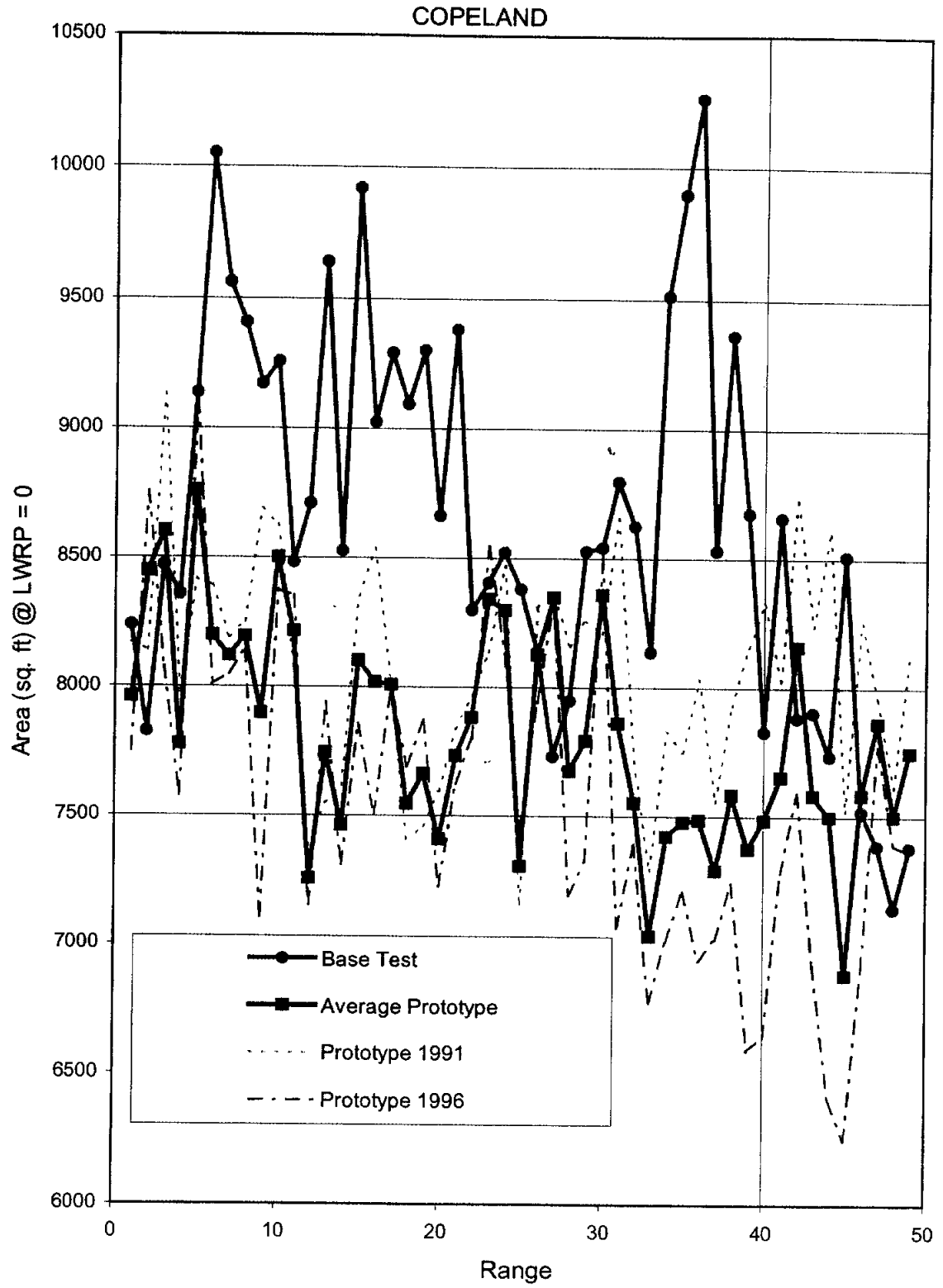


Figure C-2.2b Cross-Section Area by Range, Copeland Bend (Mississippi River)

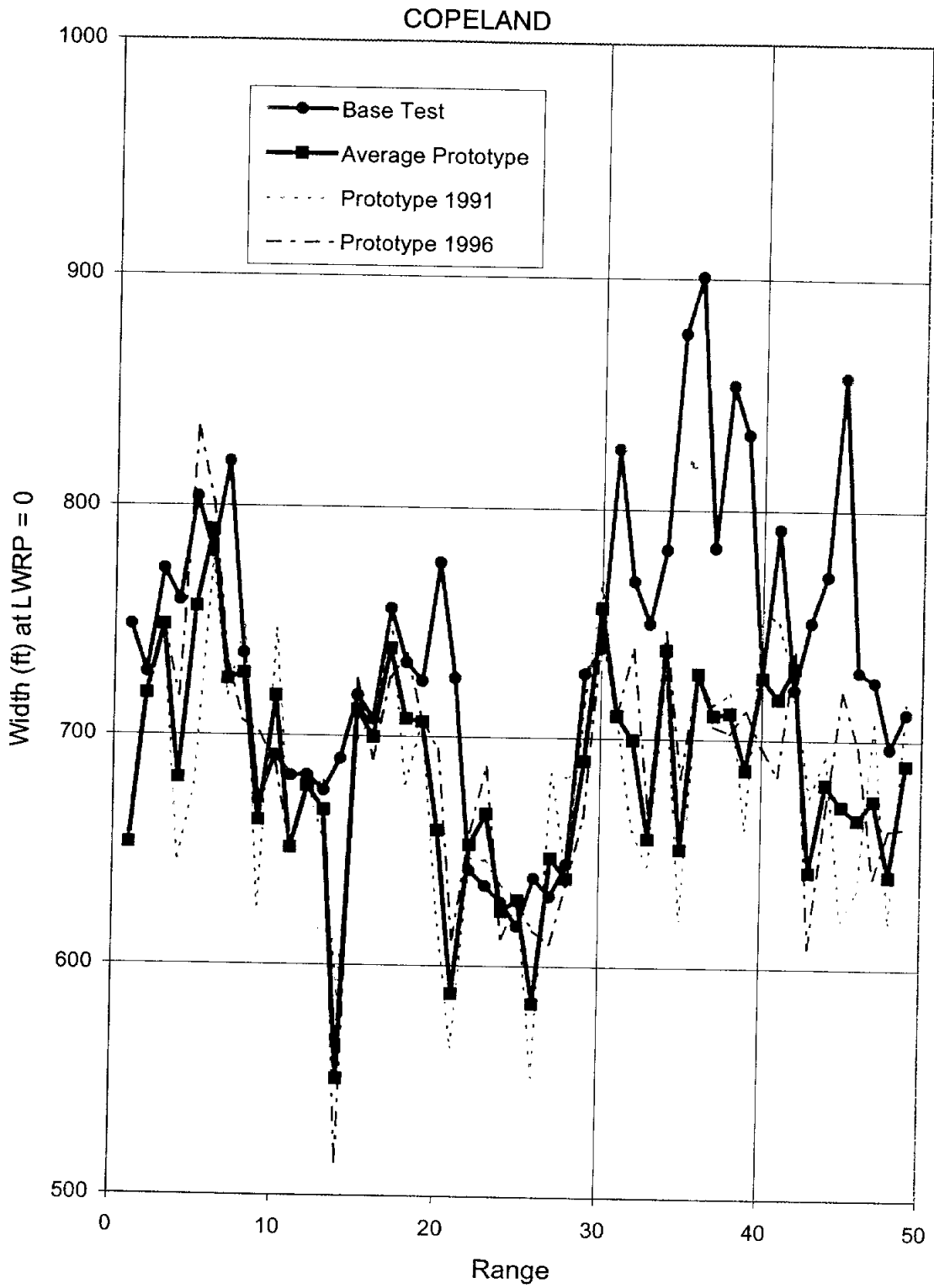


Figure C-2.2c Top Width by Range, Copeland Bend (Mississippi River)

COPELAND

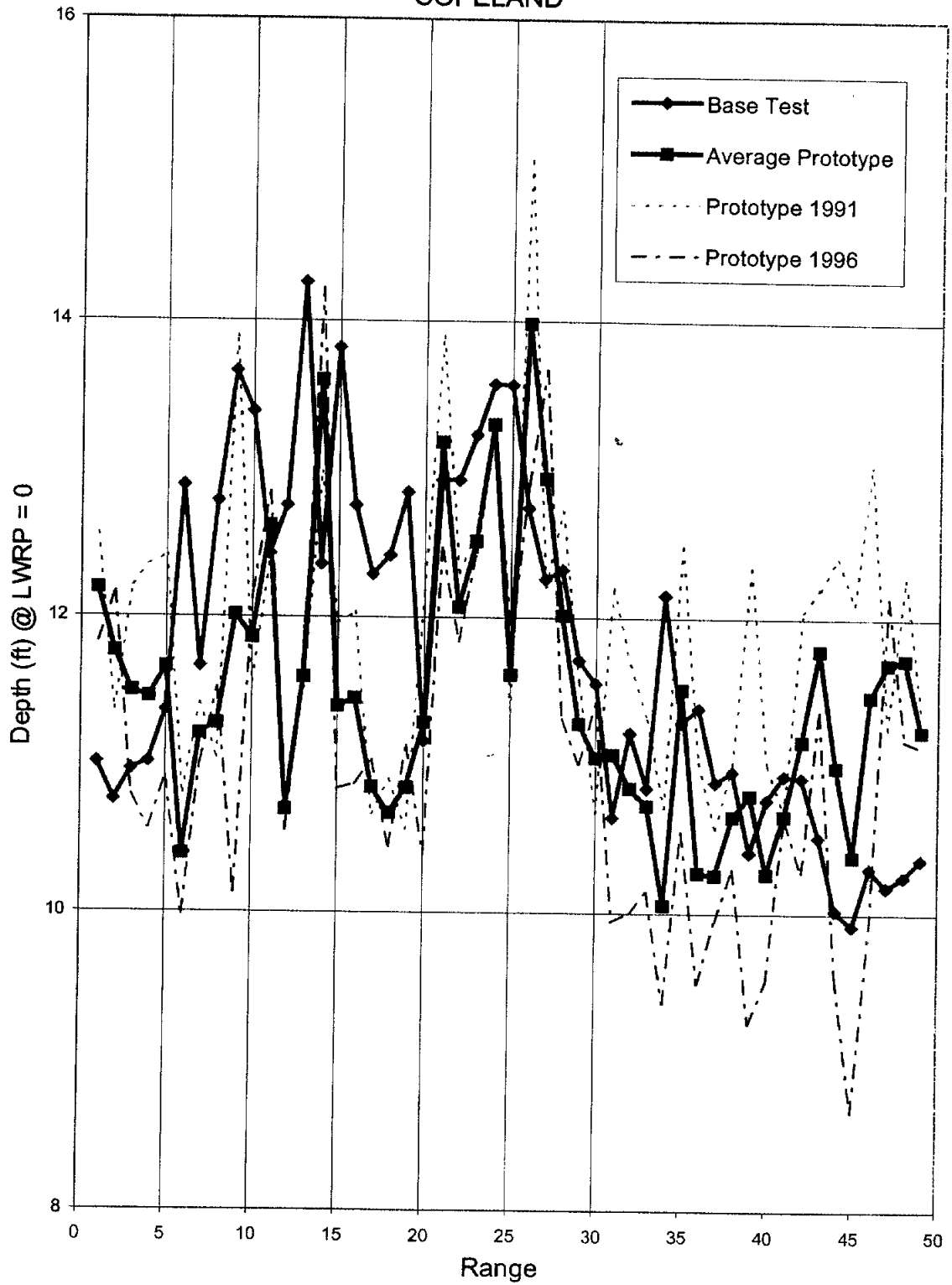


Figure C-2.2d Hydraulic Depth by Range, Copeland Bend (Mississippi River)

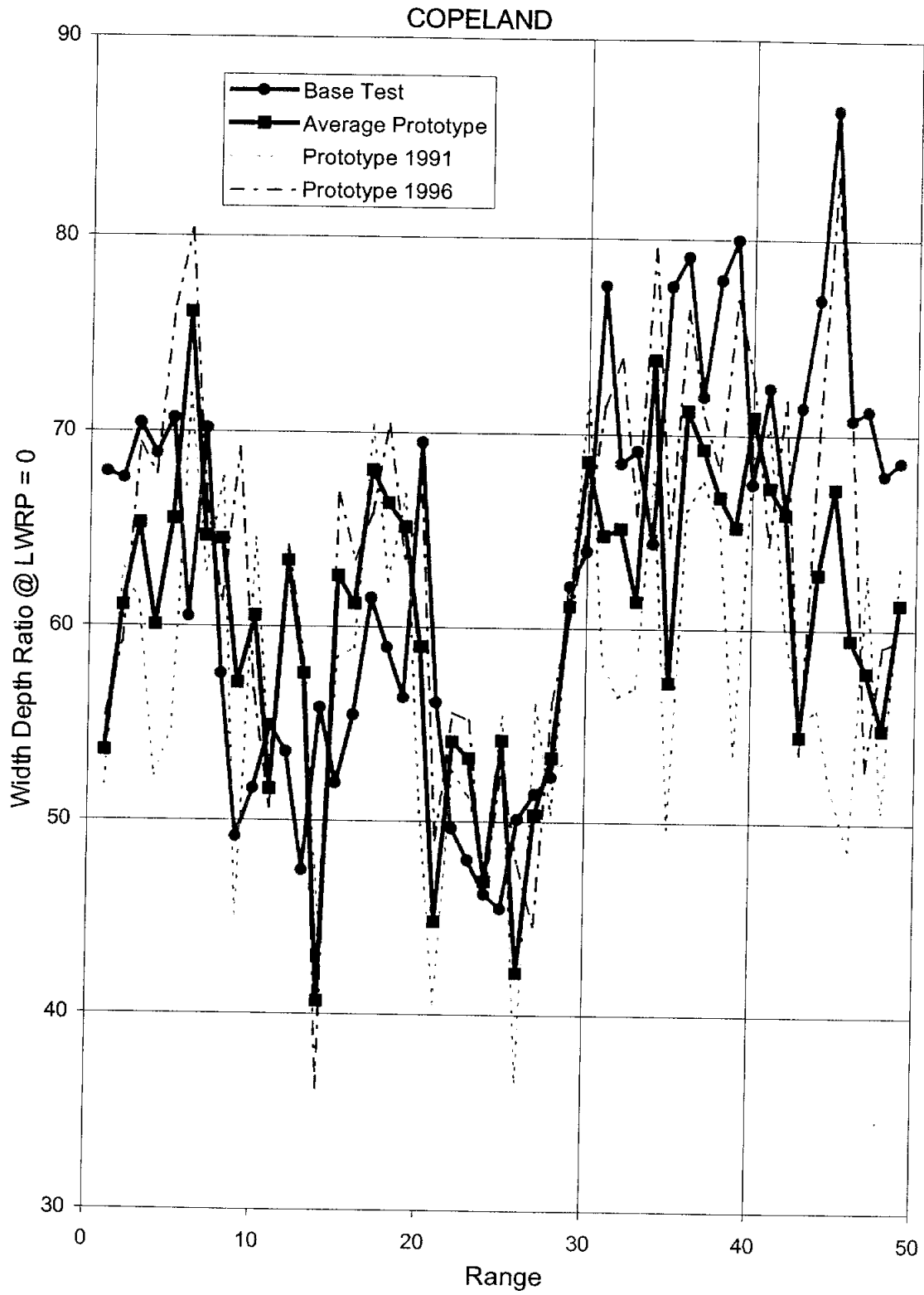


Figure C-2.2e Width/Depth Ratio by Range, Copeland Bend (Mississippi River)

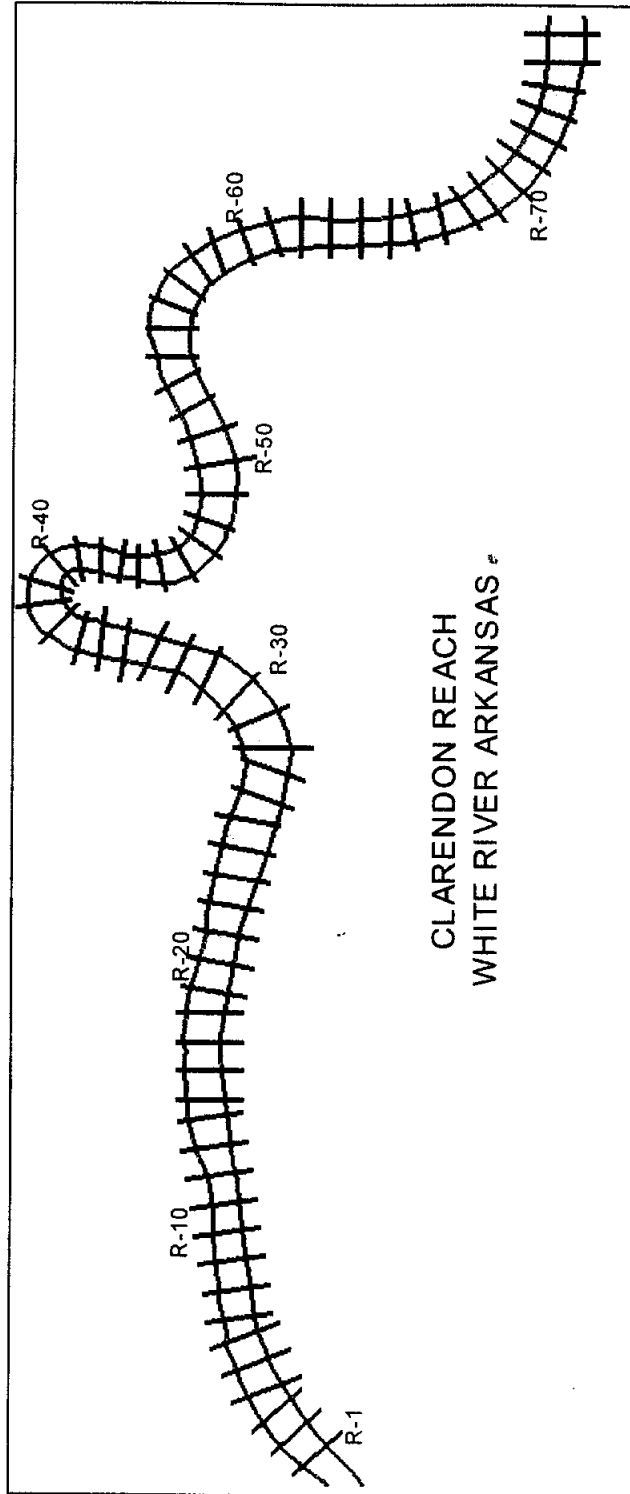


Figure C-3.1a Clarendon Model Plan View

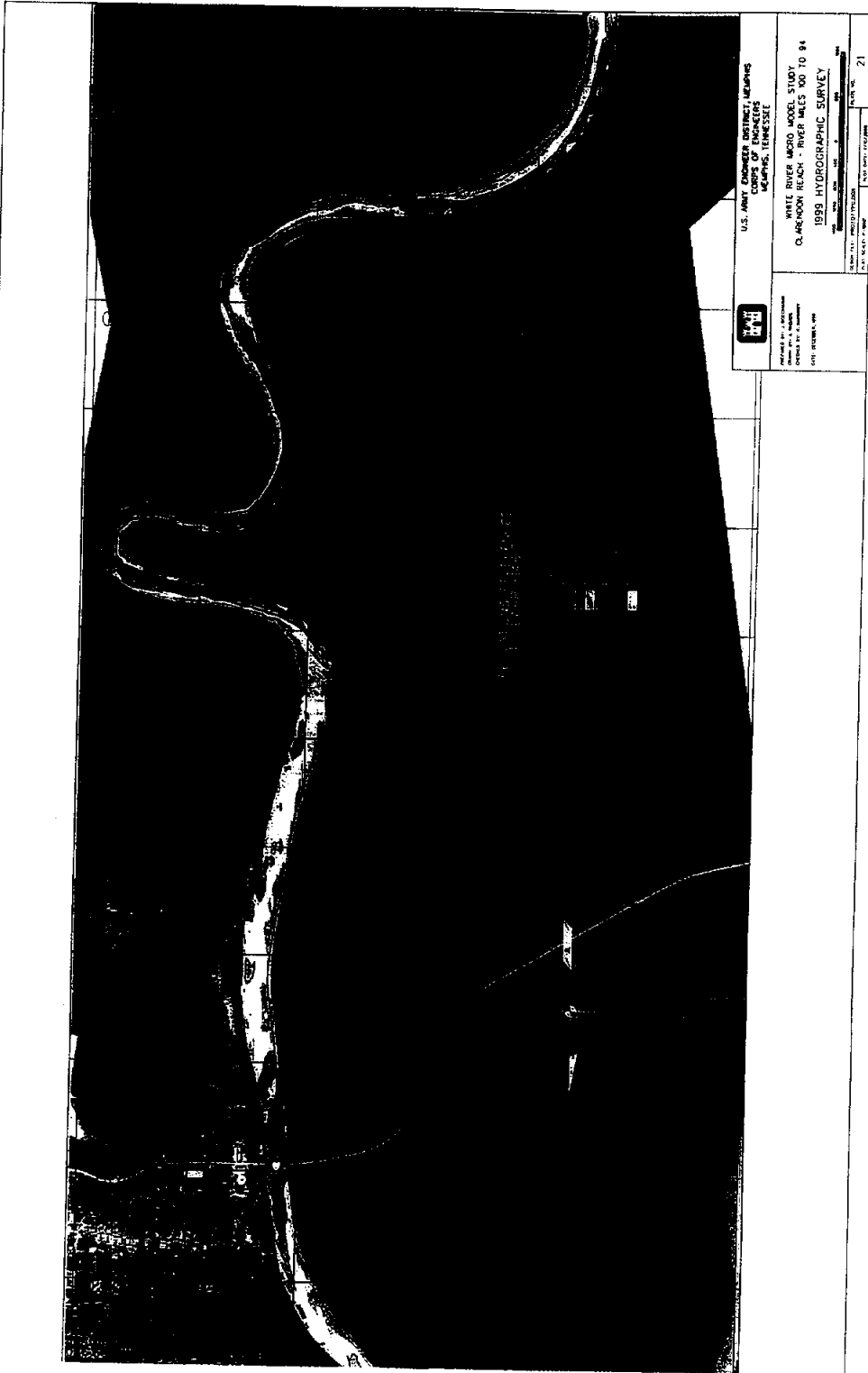


Figure C-3.1b 1999 Clarendon Prototype Survey

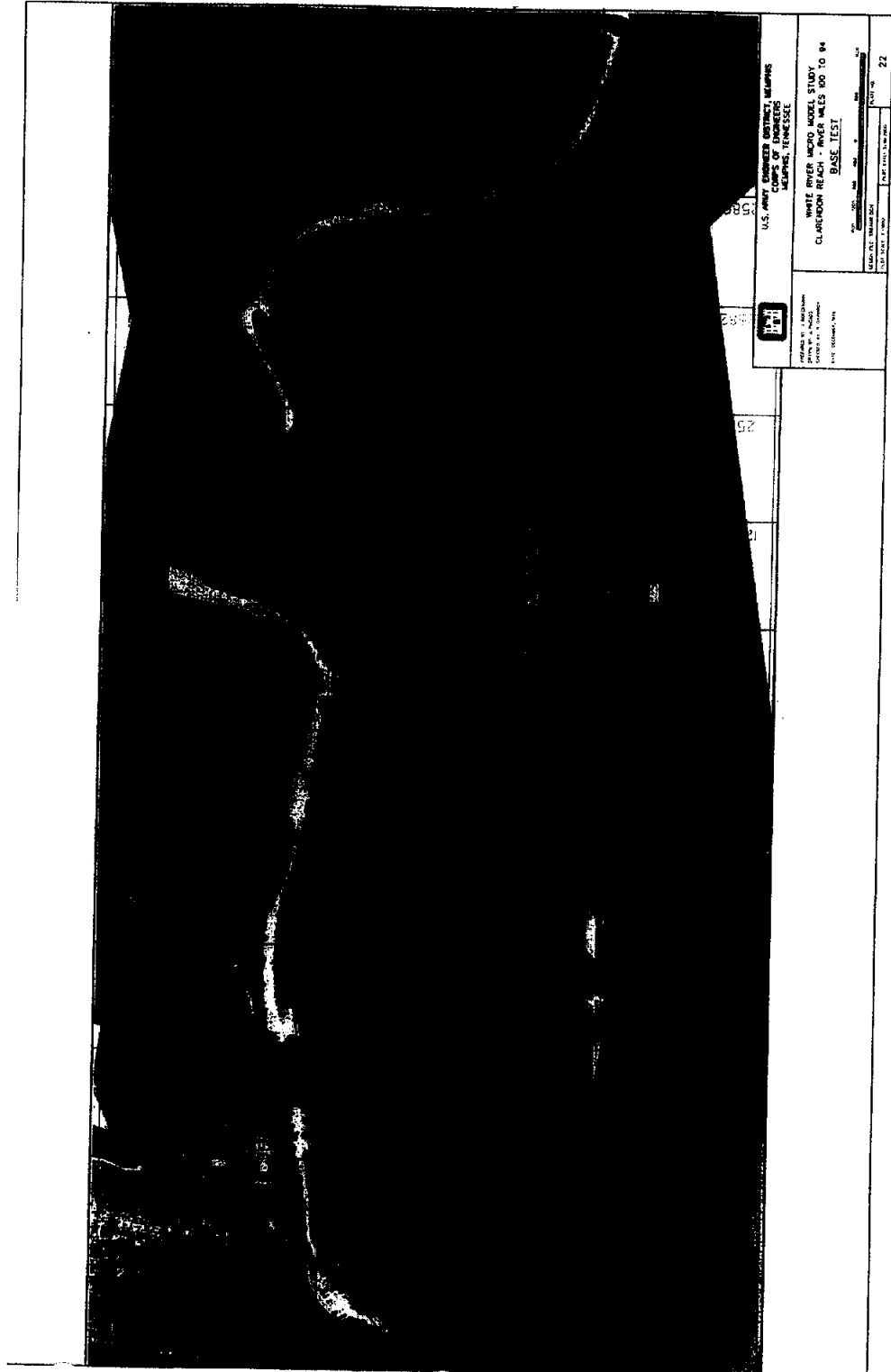


Figure C-3.1c Clarendon Micromodel Base Test

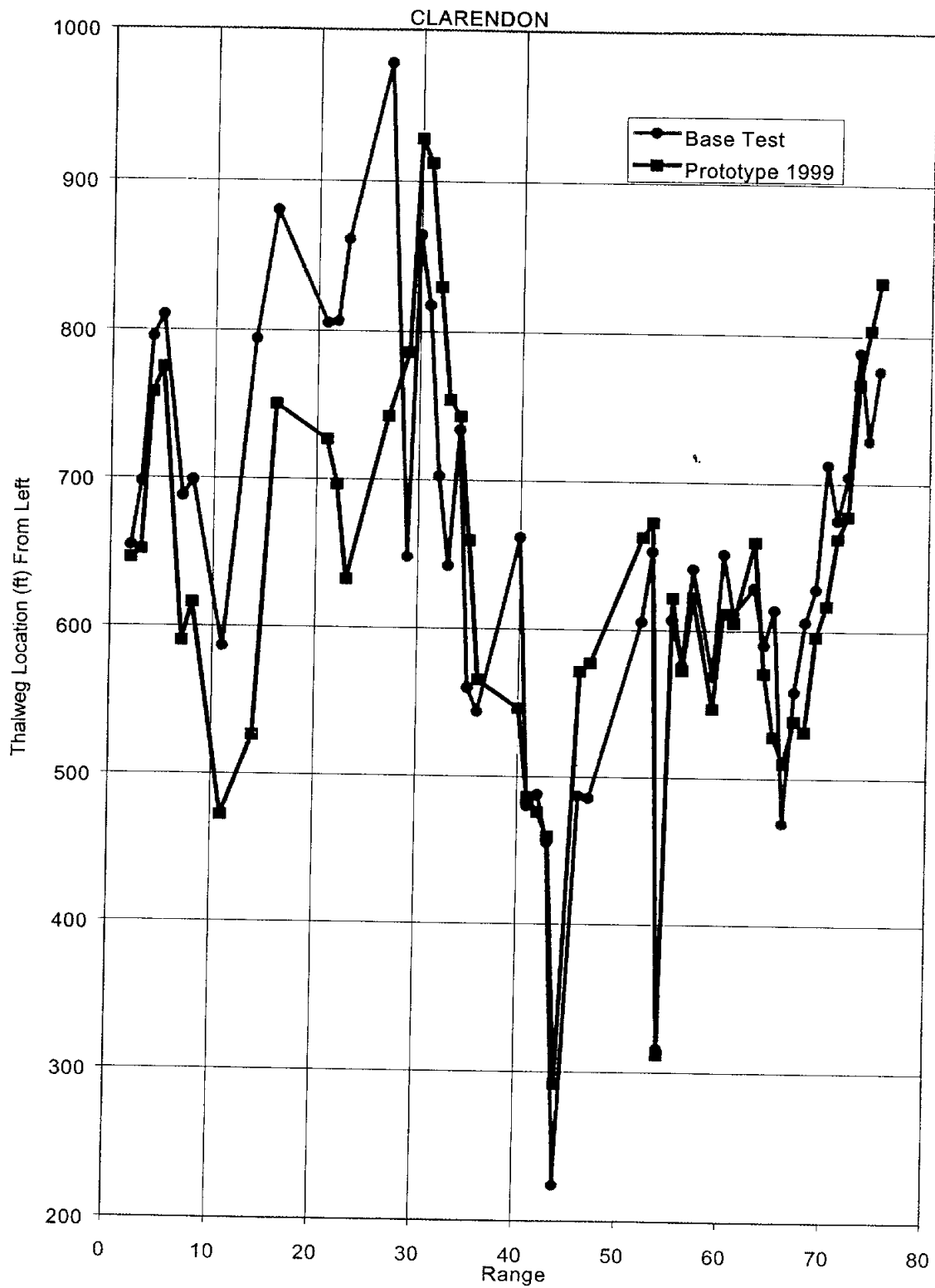


Figure C-3.2a Thalweg From Left by Range, Clarendon Reach (White River)

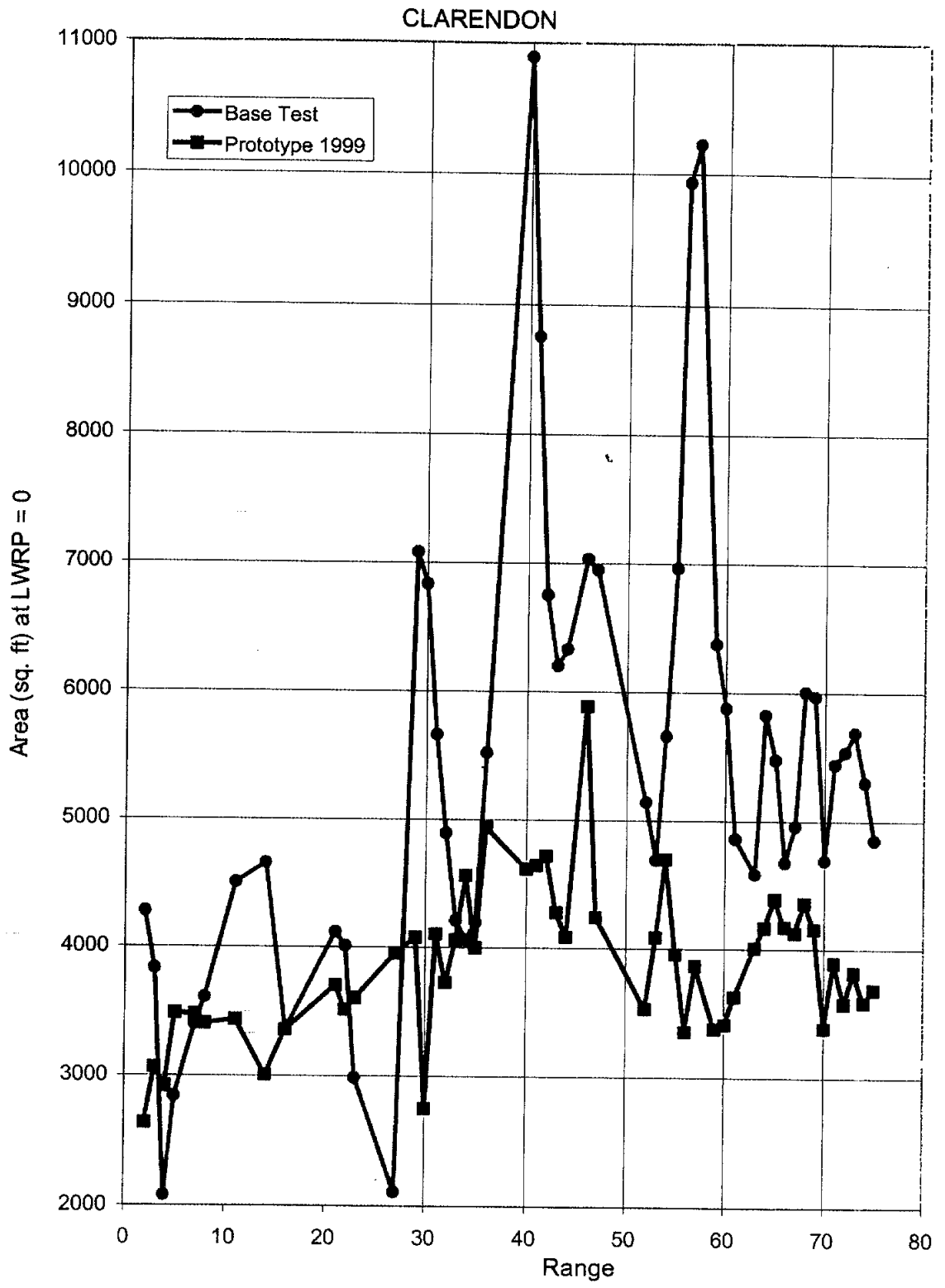


Figure C-3.2b Cross-Section Area by Range, Clarendon Reach (White River)

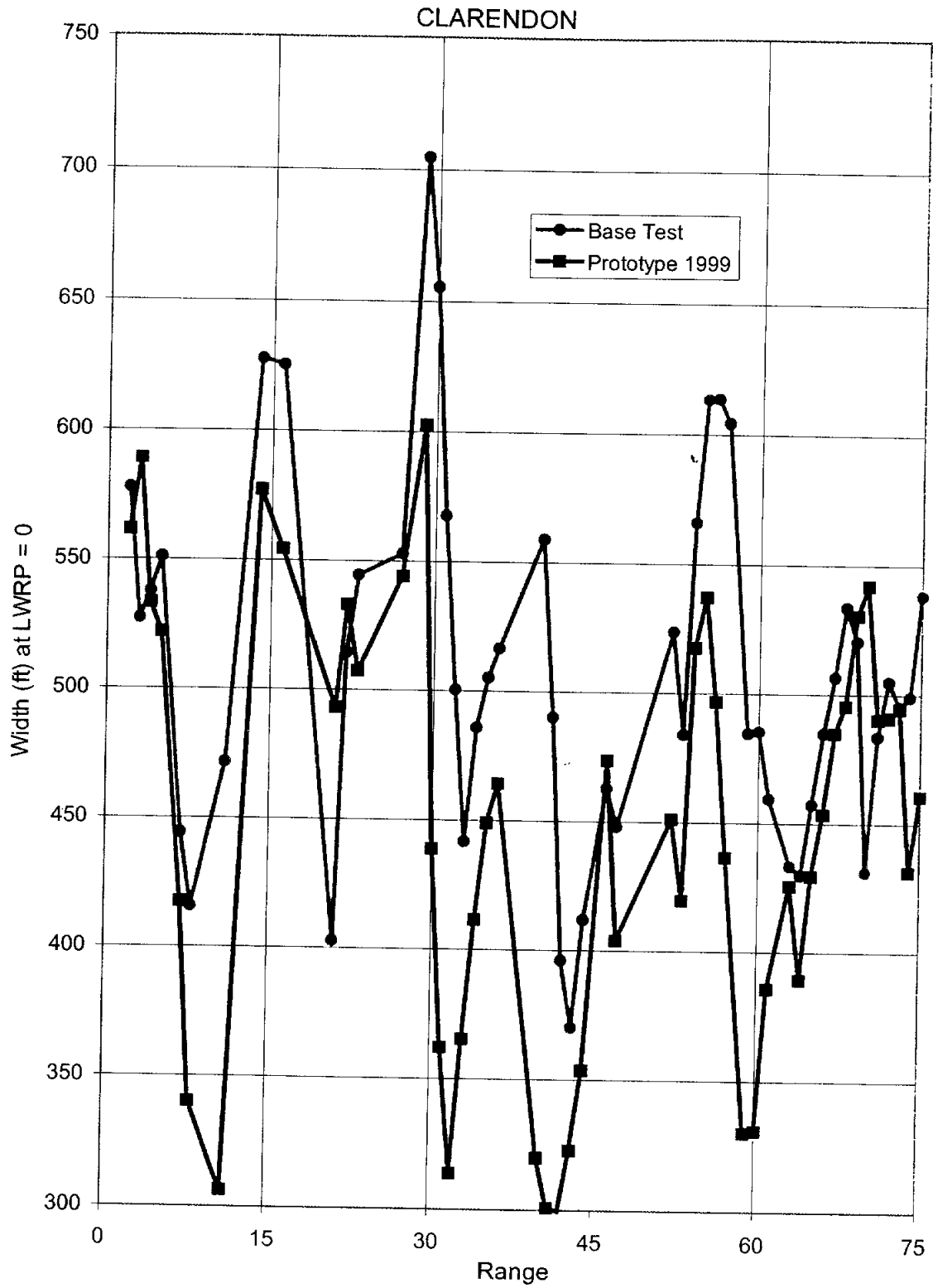


Figure C-3.2c Top Width by Range, Clarendon Reach (White River)

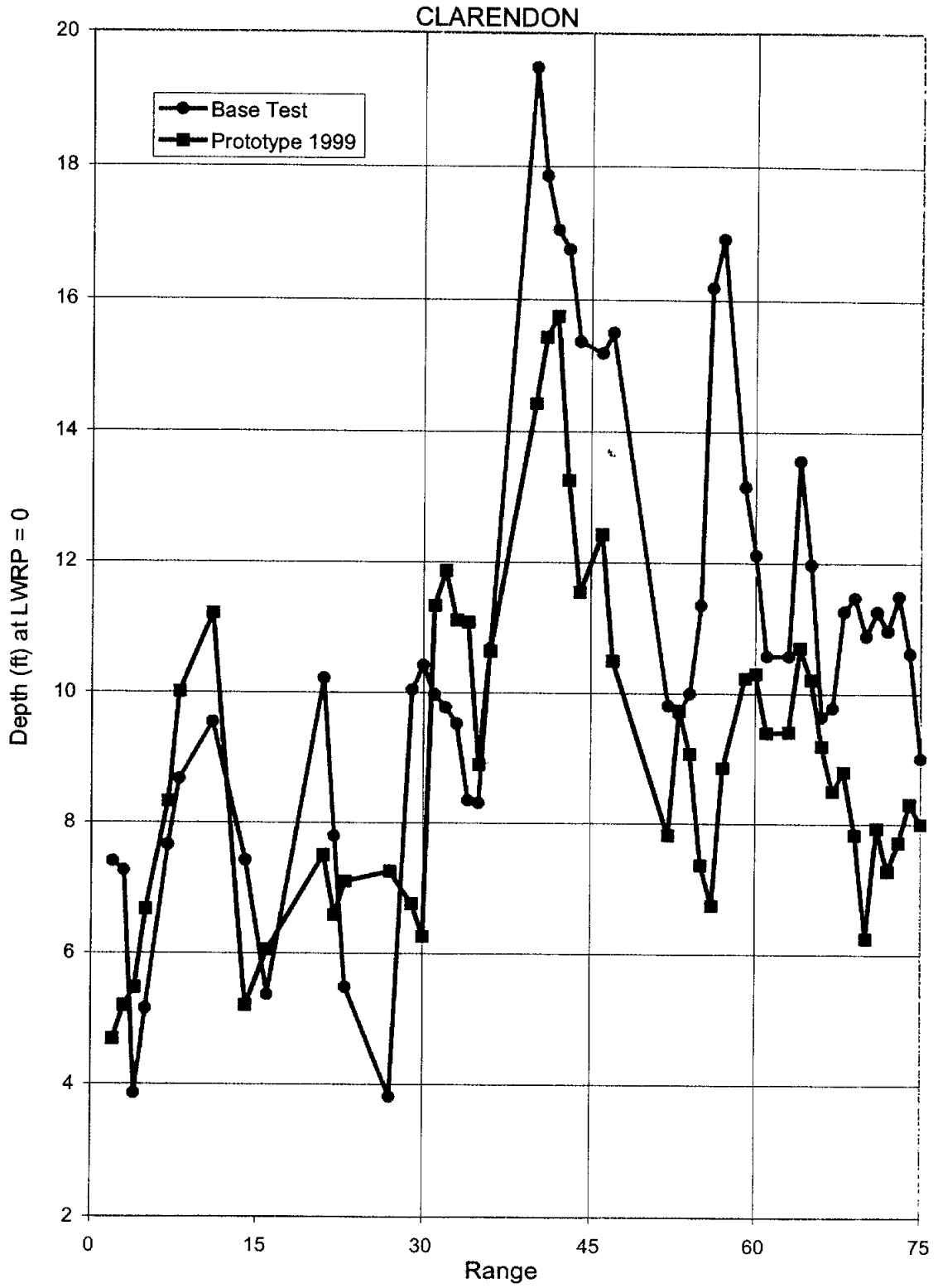


Figure C-3.2d Hydraulic Depth by Range, Clarendon Reach (White River)

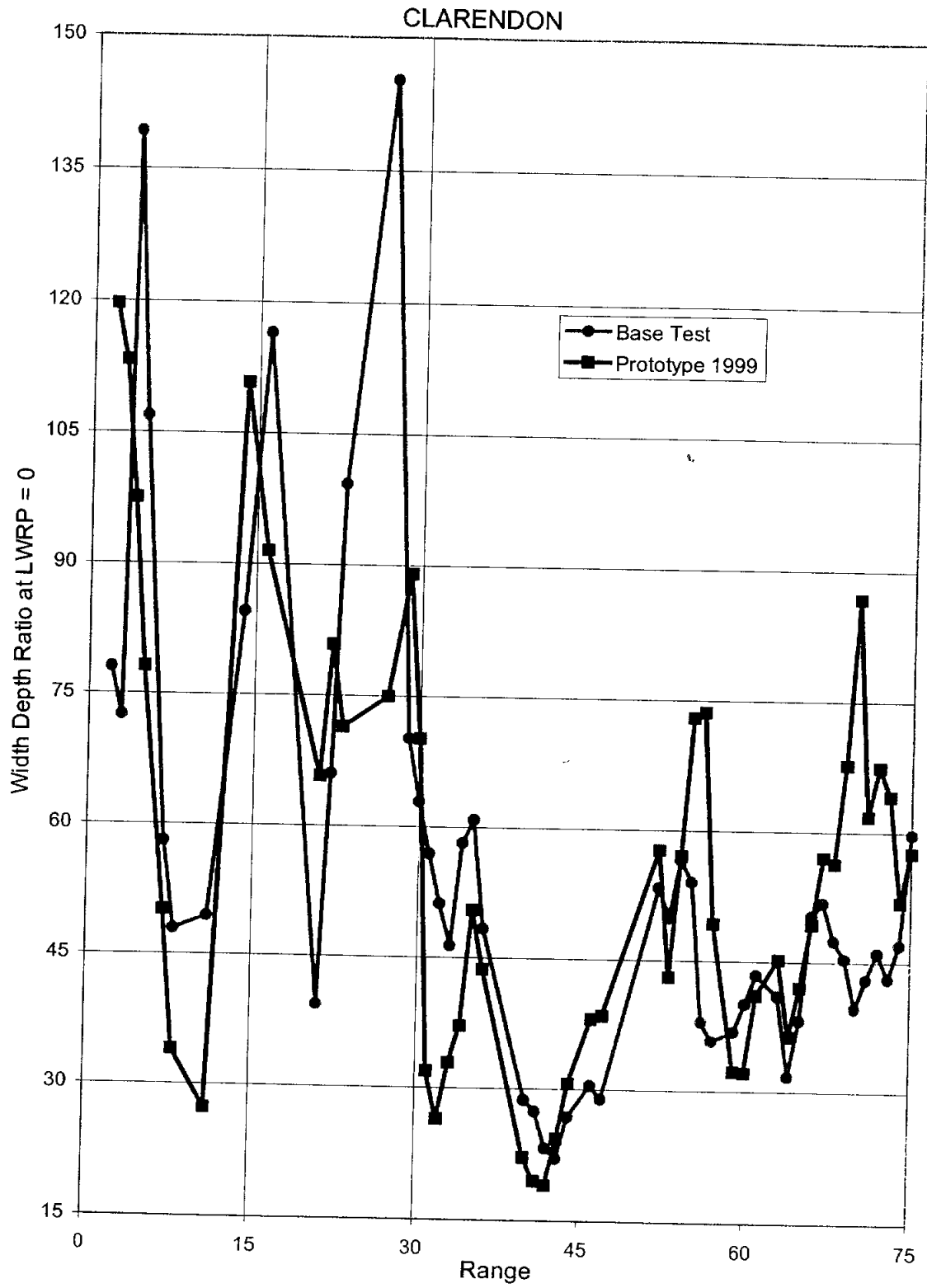


Figure C-3.2e Width/Depth Ratio by Range, Clarendon Reach (White River)

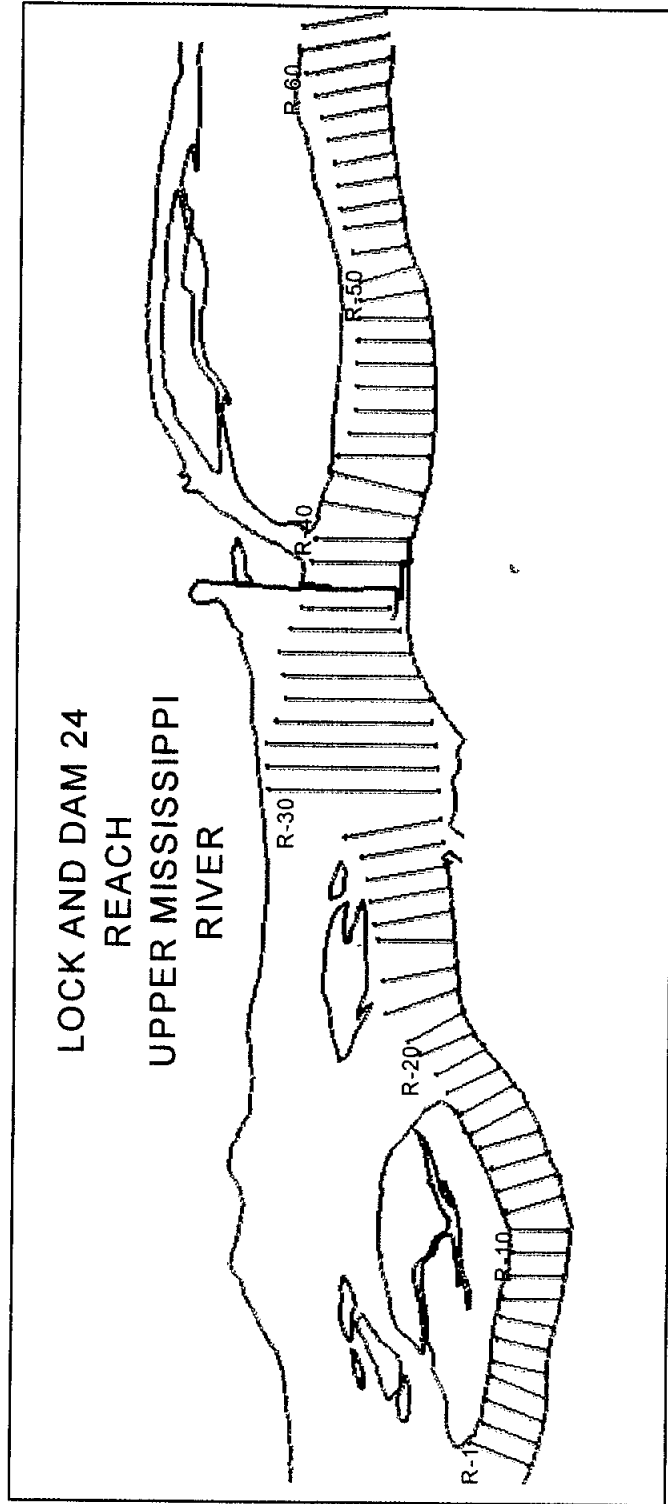


Figure C-4.1a Lock and Dam No. 24 Model Plan View

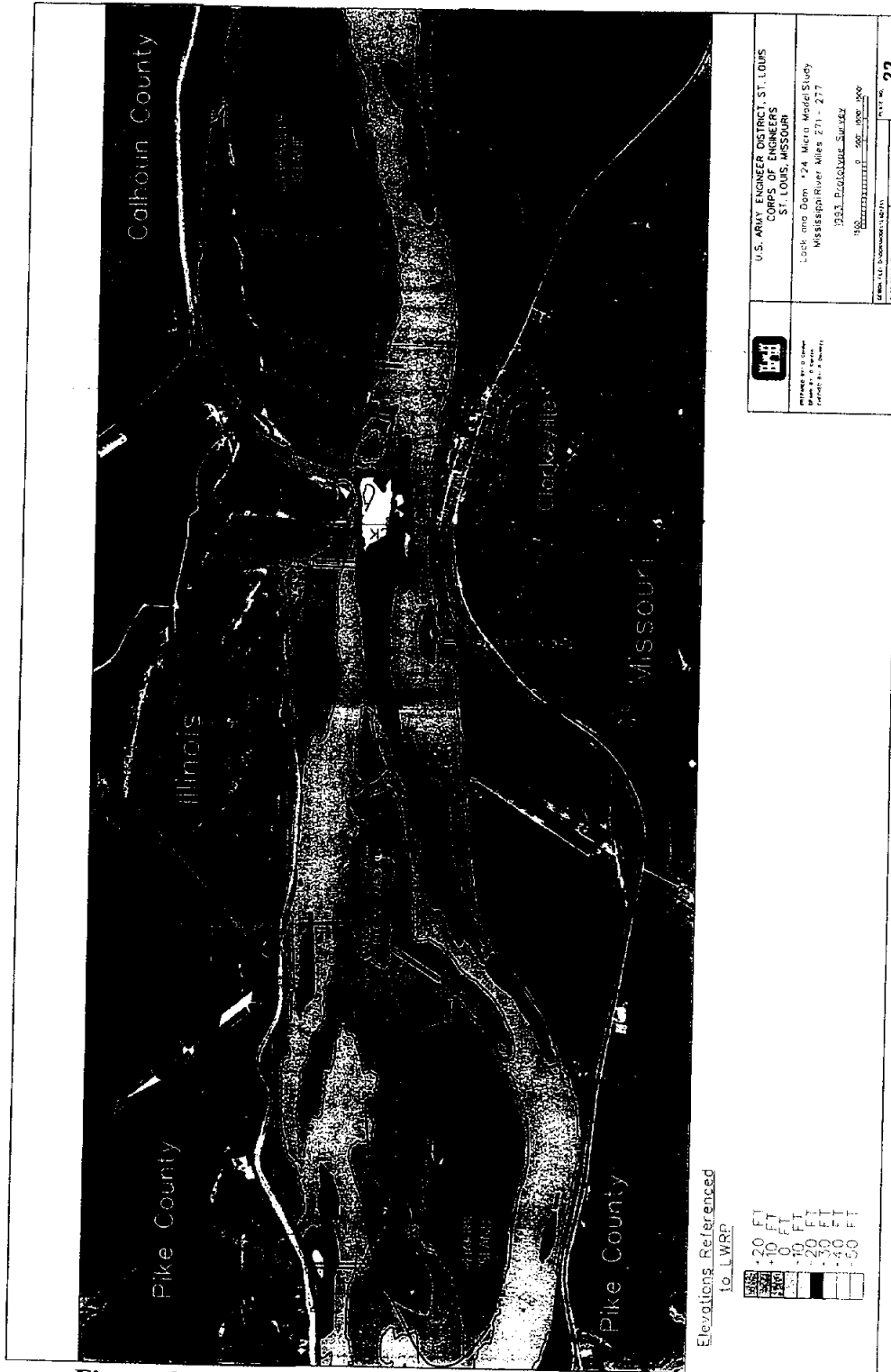
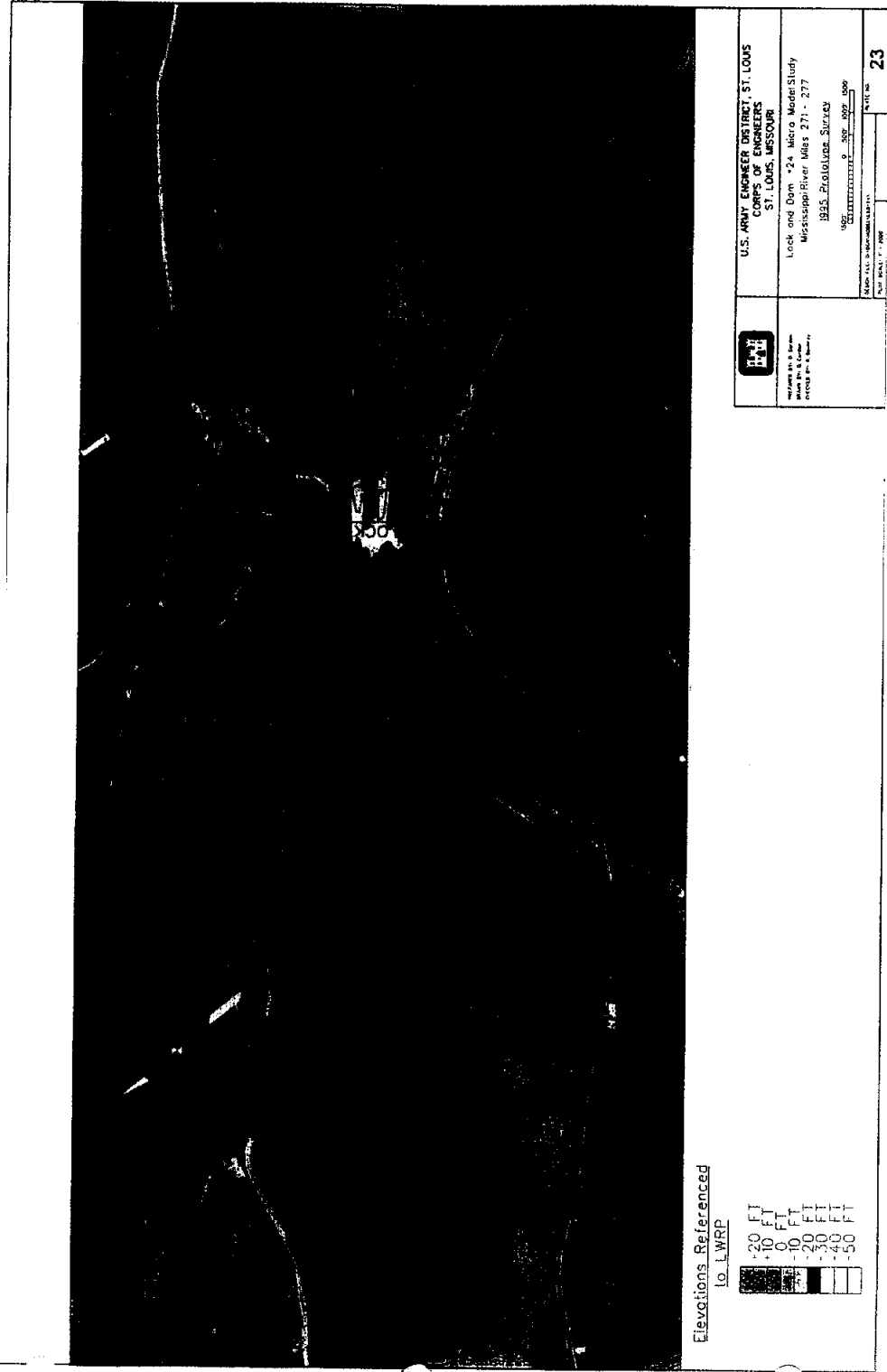
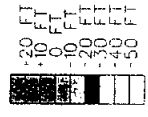


Figure C-4.1b Lock and Dam No. 24 1993 Prototype Survey



Elevations Referenced
to LWRP



	U.S. ARMY ENGINEER DISTRICT, ST. LOUIS CORPS OF ENGINEERS ST. LOUIS, MISSOURI
	Lock and Dam #24 Micro Model Study Mississippi River Miles 271 - 277 1995 Prototype Survey 9 300 000 000
APPROVED FOR PUBLICATION DATE: 11-1-1995	
SHEET NO. 23	

Figure C-4.1c Lock and Dam No. 24 1995 Prototype Survey

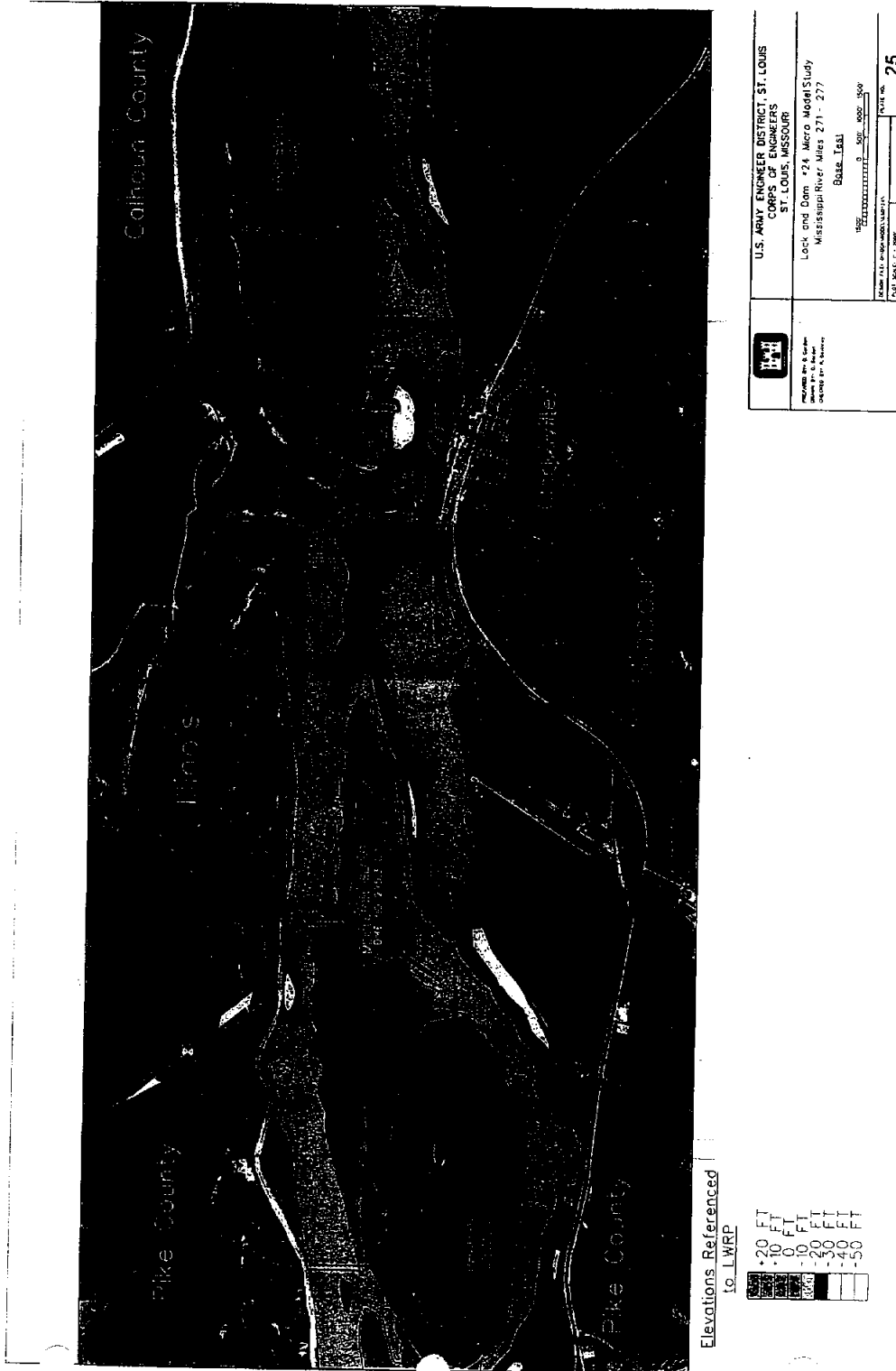


Figure C-4.1d Lock and Dam No. 24 Micromodel Base Test

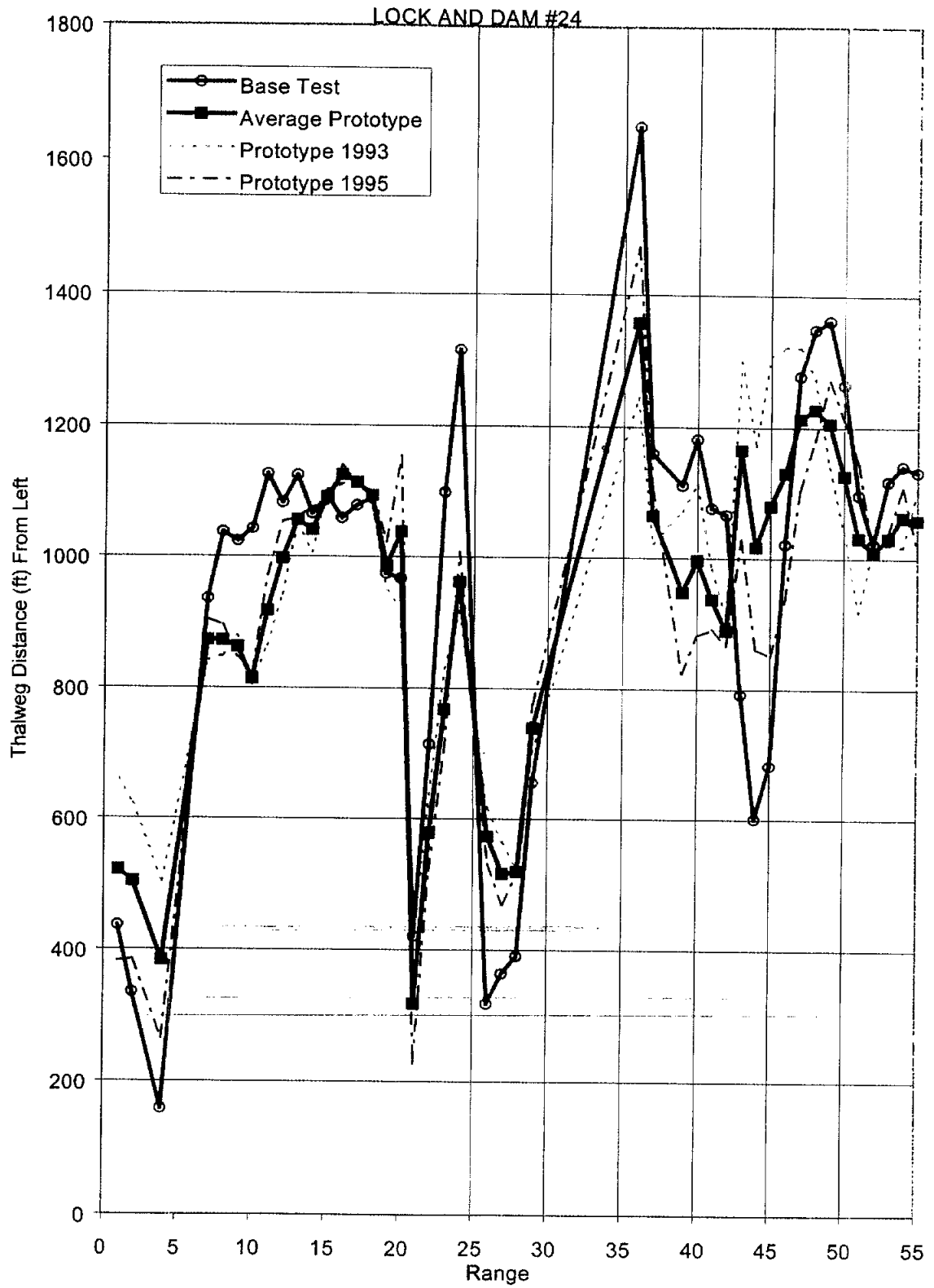


Figure C-4.2a Lock and Dam No. 24 Thalweg Position From Left, L and D 24 (Mississippi River)

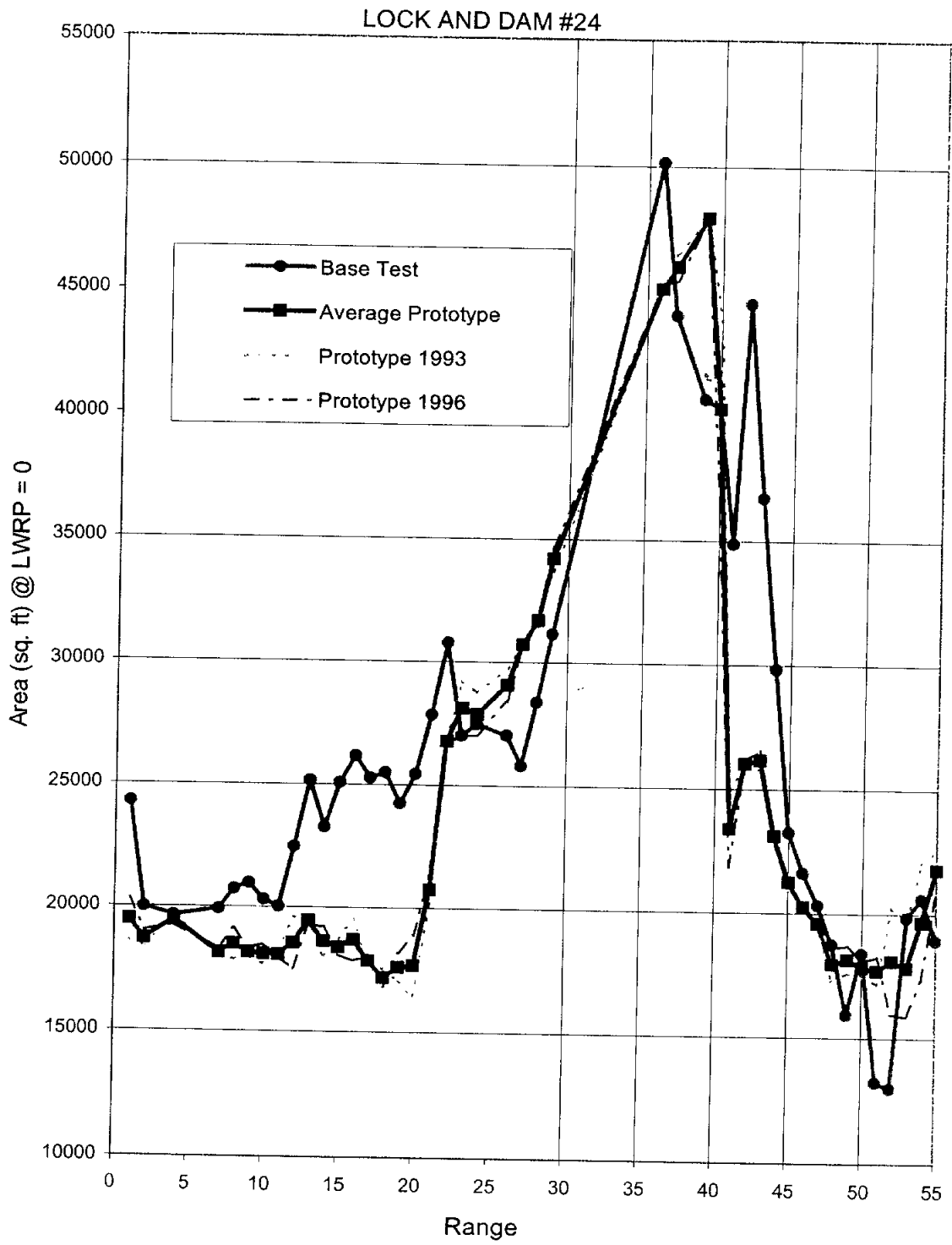


Figure C-4.2b Cross-Section Area by Range, Lock and Dam No. 24 (Mississippi River)

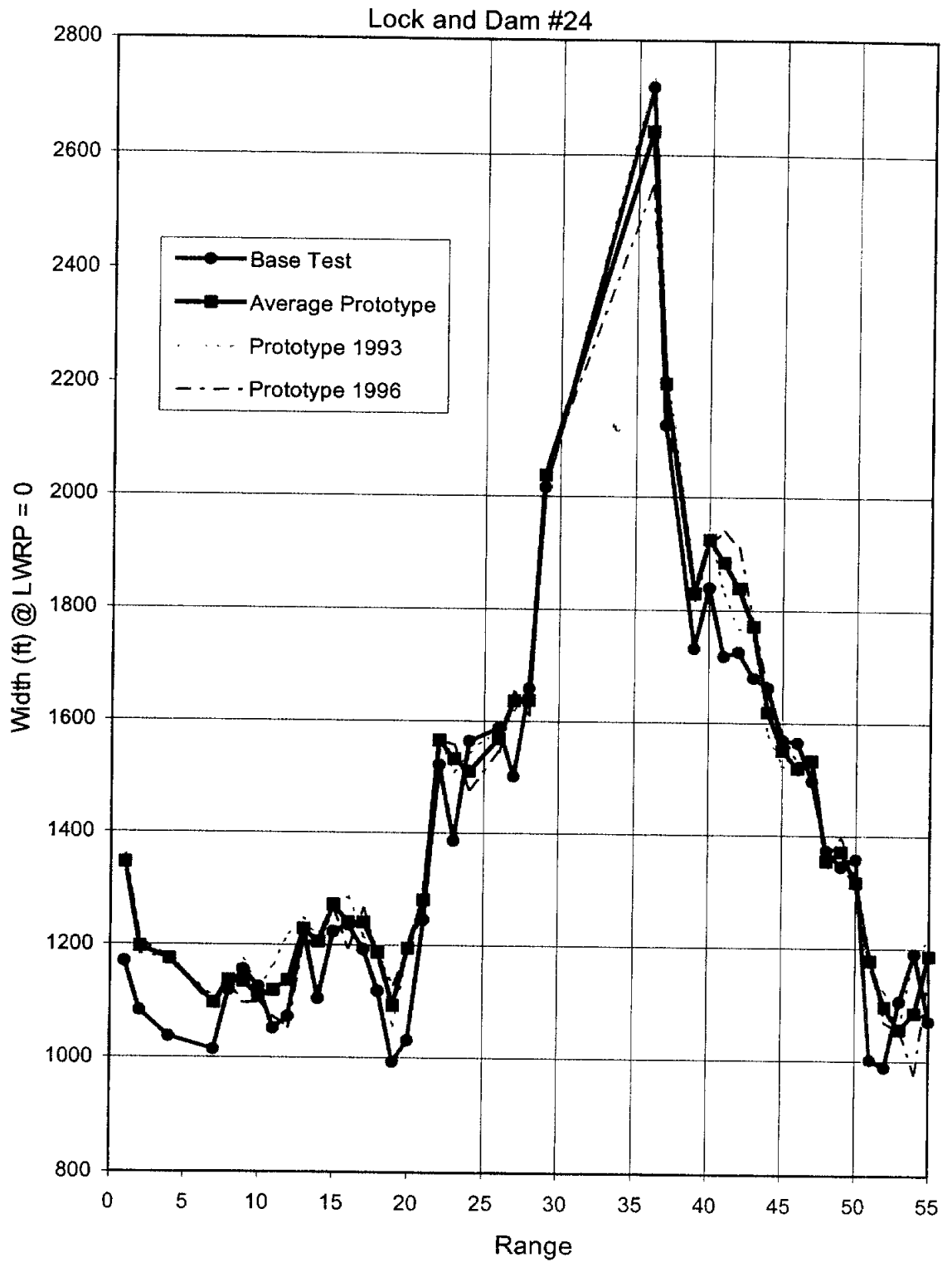


Figure C-4.2c Top Width by Range, Lock and Dam No. 24 (Mississippi River)

Lock and Dam #24

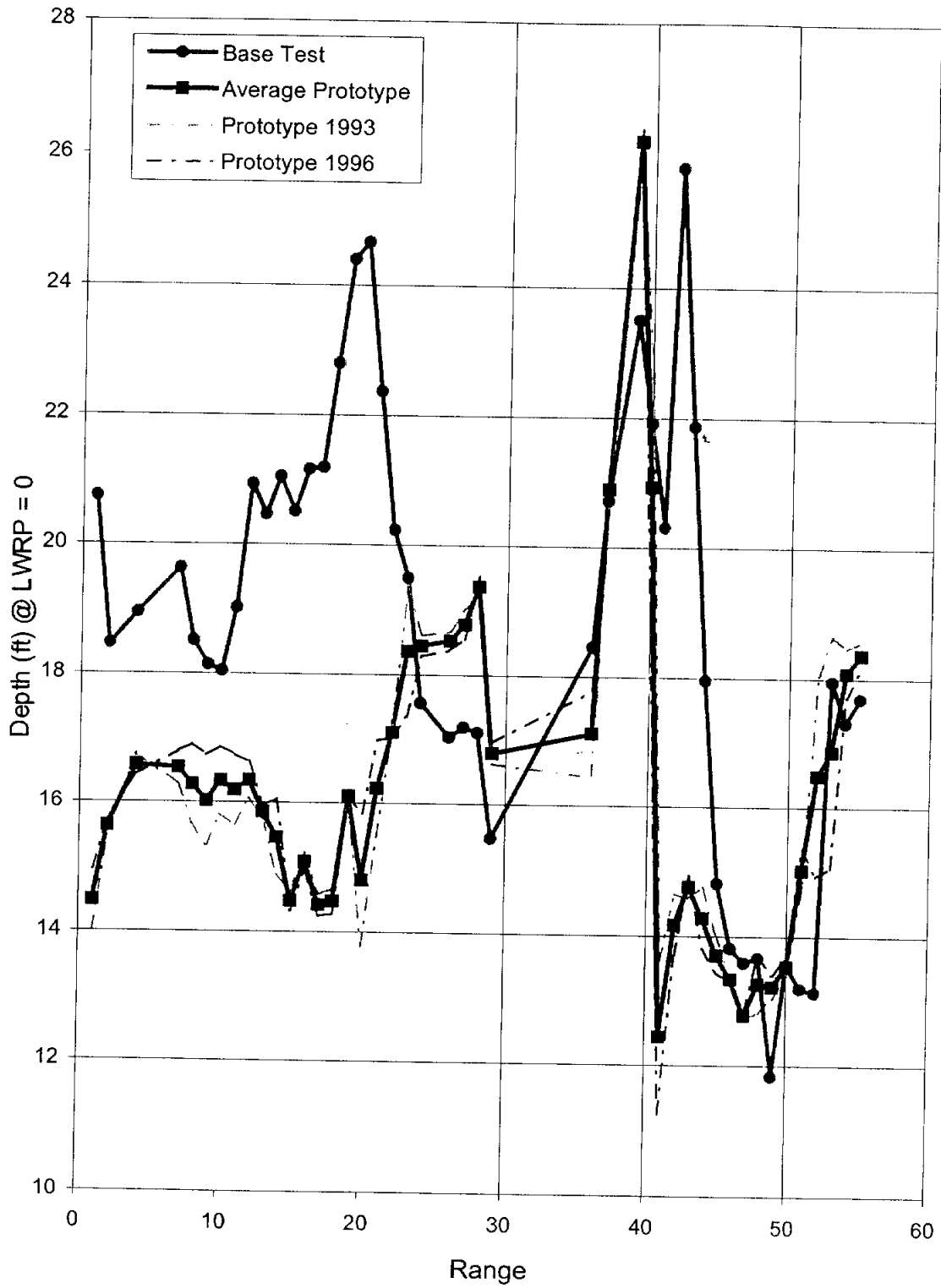


Figure C-4.2d Hydraulic Depth by Range, Lock and Dam No. 24 (Mississippi River)

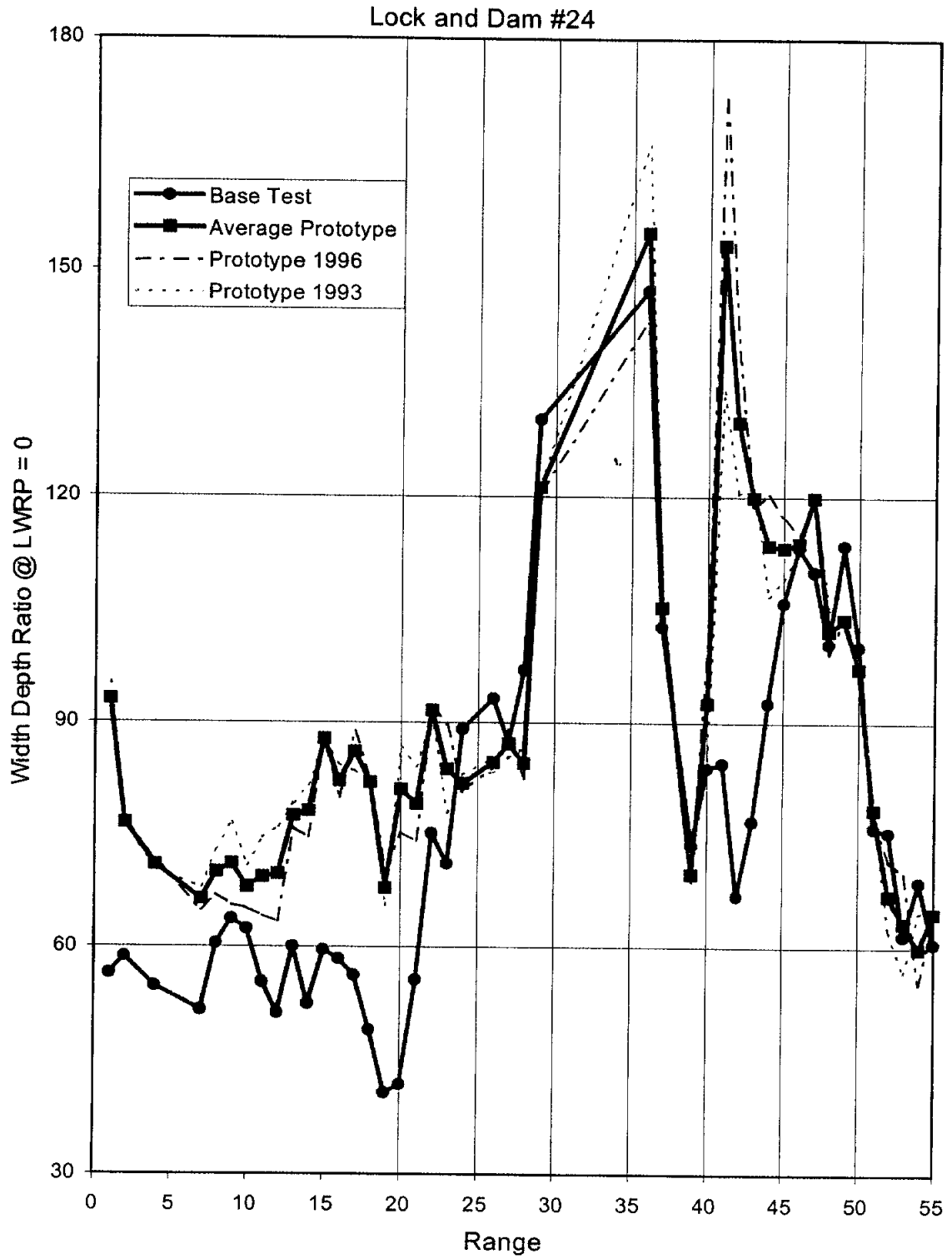


Figure C-4.2e Width/Depth Ratio by Range, Lock and Dam No. 24 (Mississippi River)

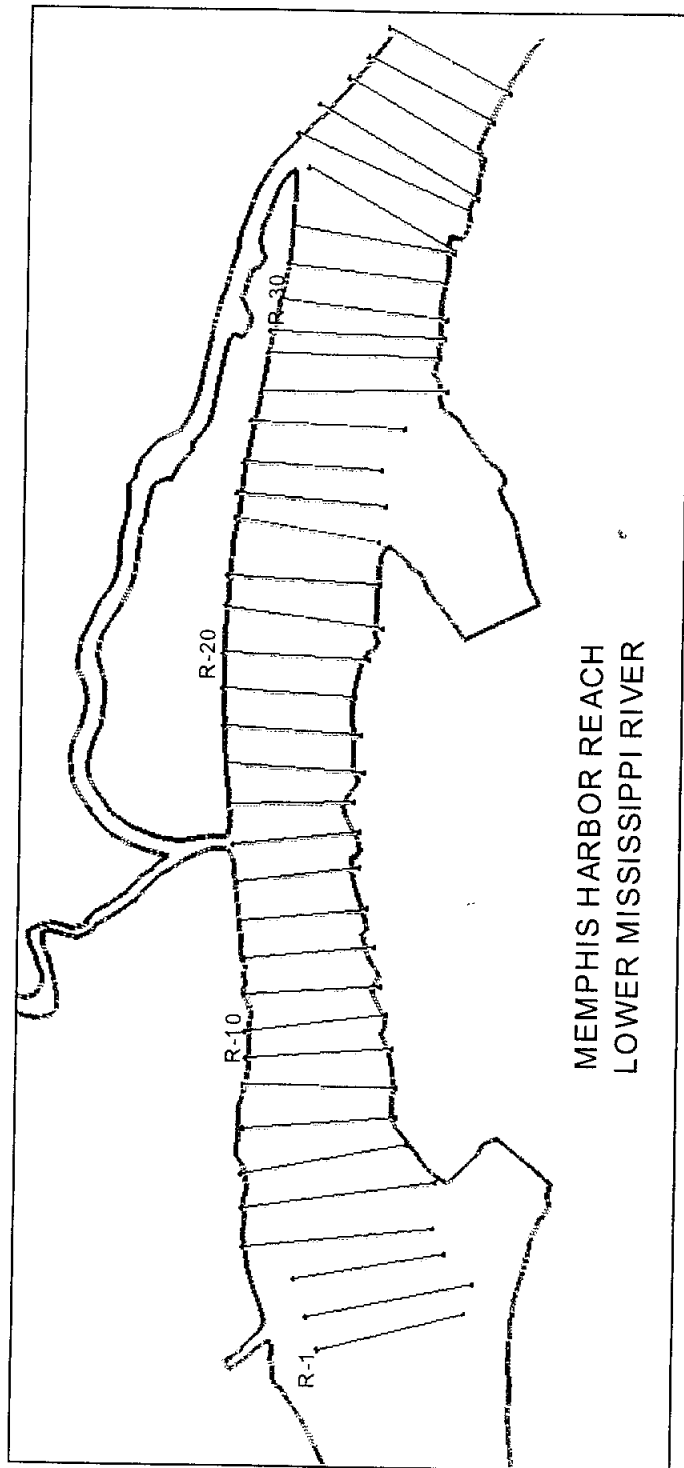


Figure C-5.1a Memphis Harbor Micromodel Plan View

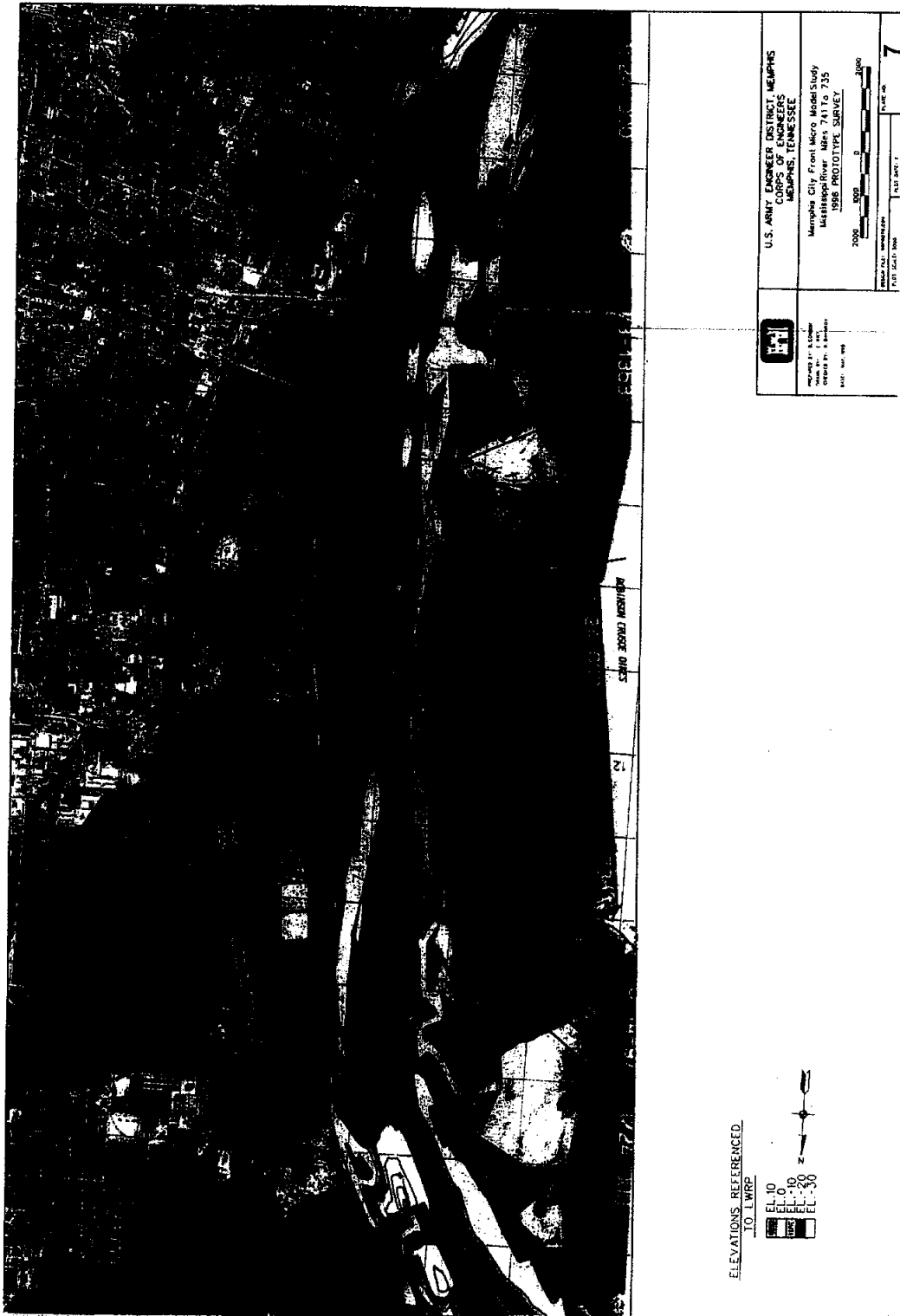


Figure C-5.1b Memphis Harbor Prototype Survey 1996

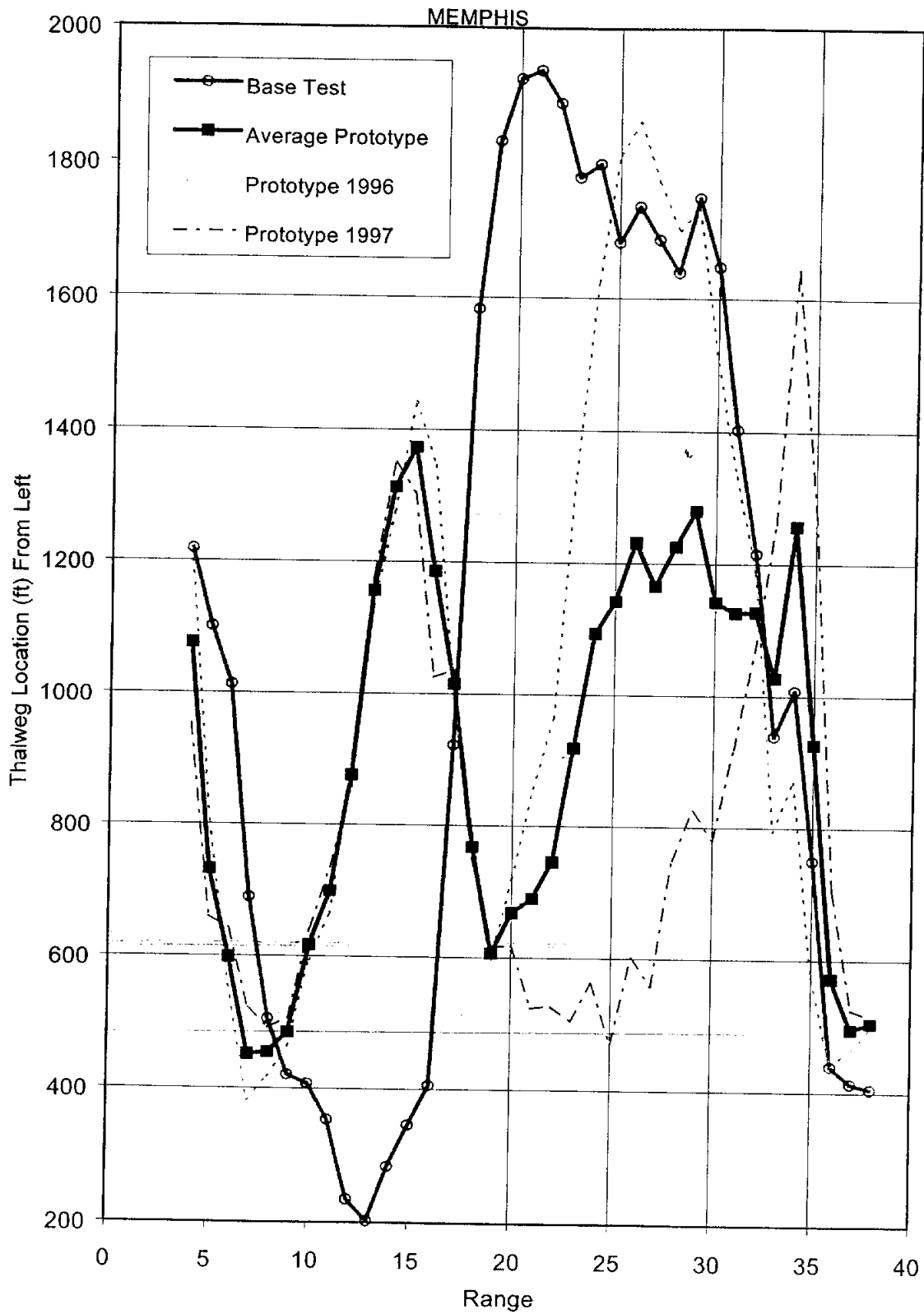


Figure C-5.2a Thalweg Distance From Left by Range, Memphis Harbor (Mississippi River)

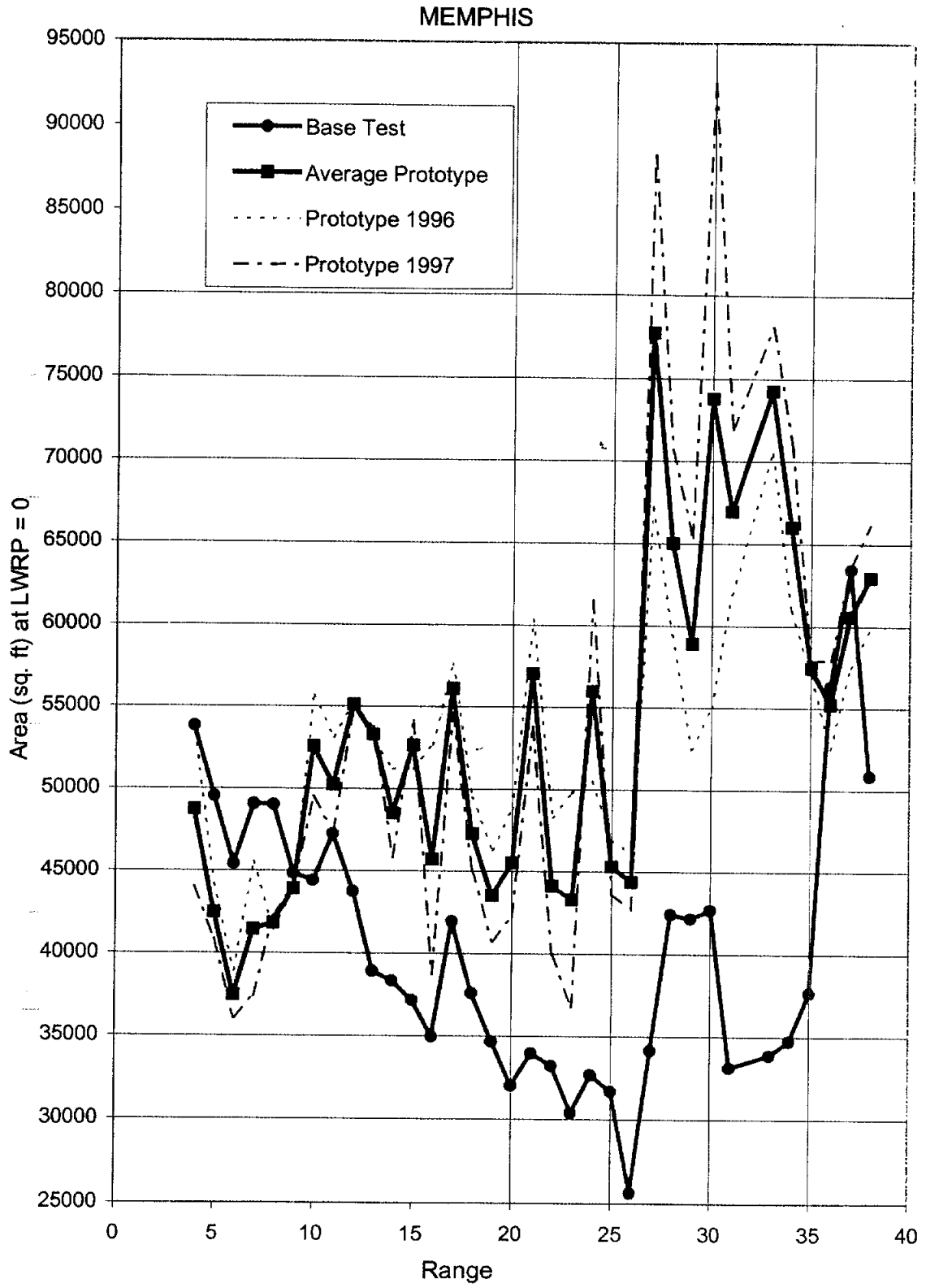


Figure C-5.2b Cross-Section Area by Range, Memphis Harbor (Mississippi River)

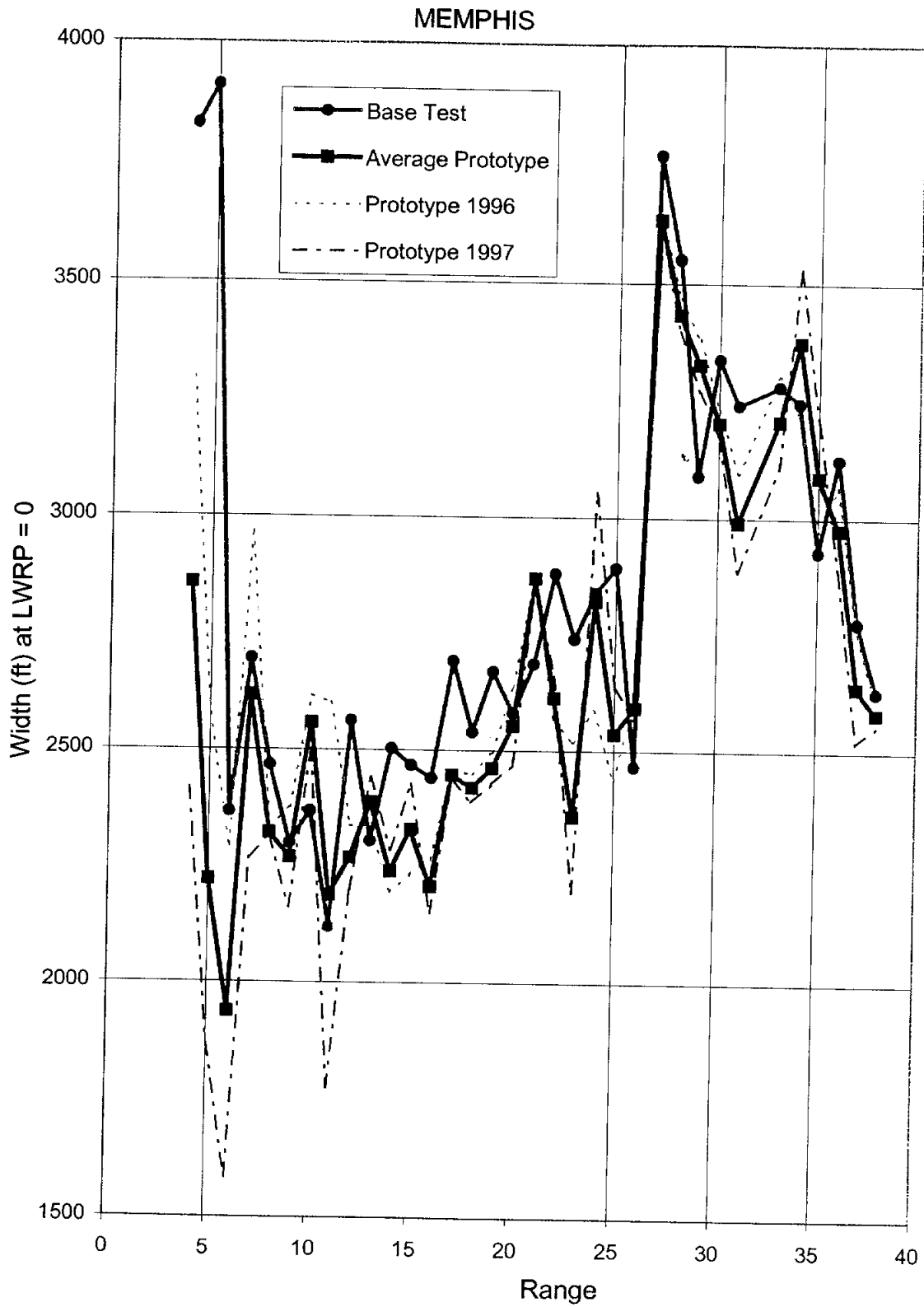


Figure C-5.2c Top Width by Range, Memphis Harbor (Mississippi River)

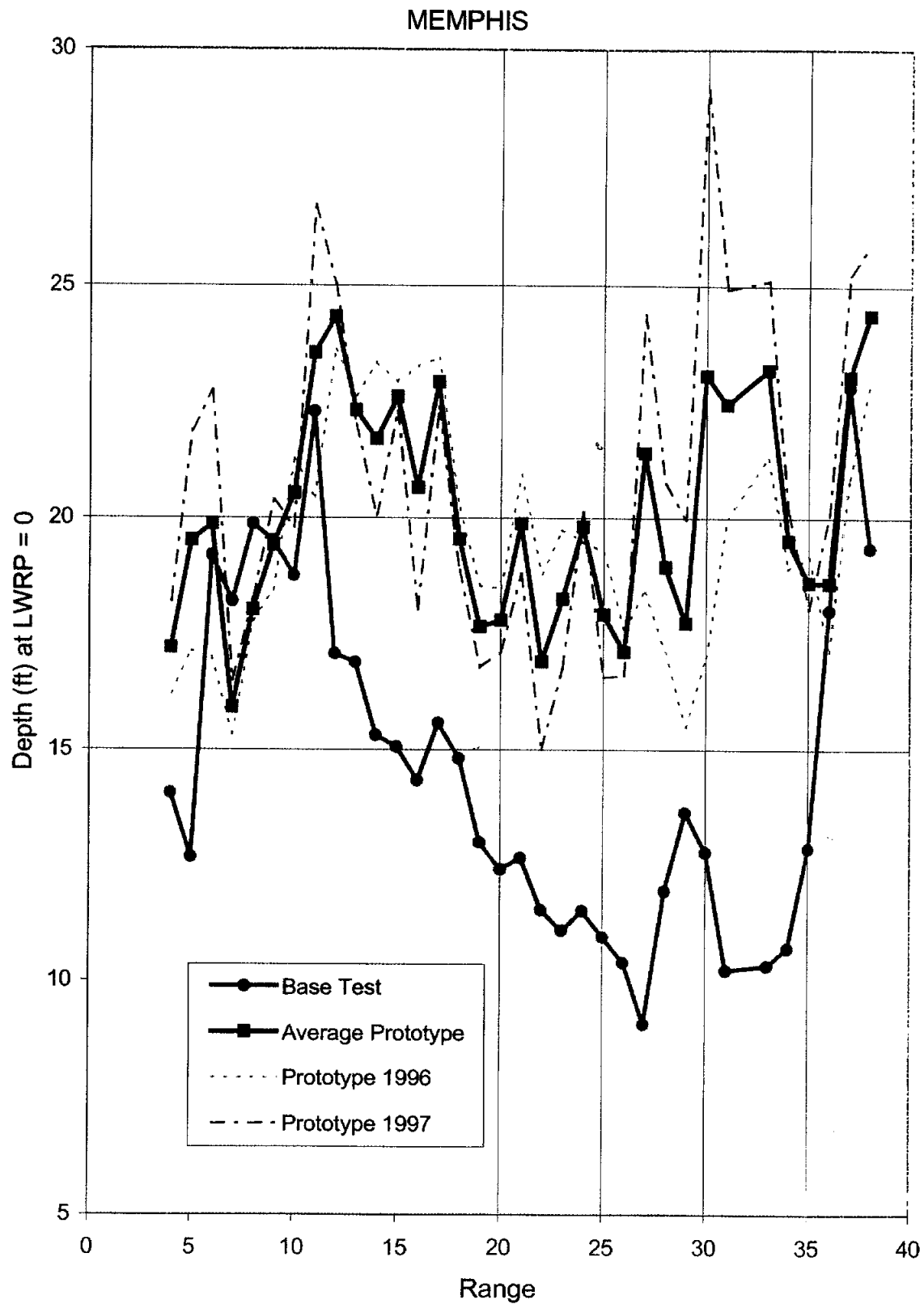


Figure C-5.2d Hydraulic Depth by Range, Memphis Harbor (Mississippi River)

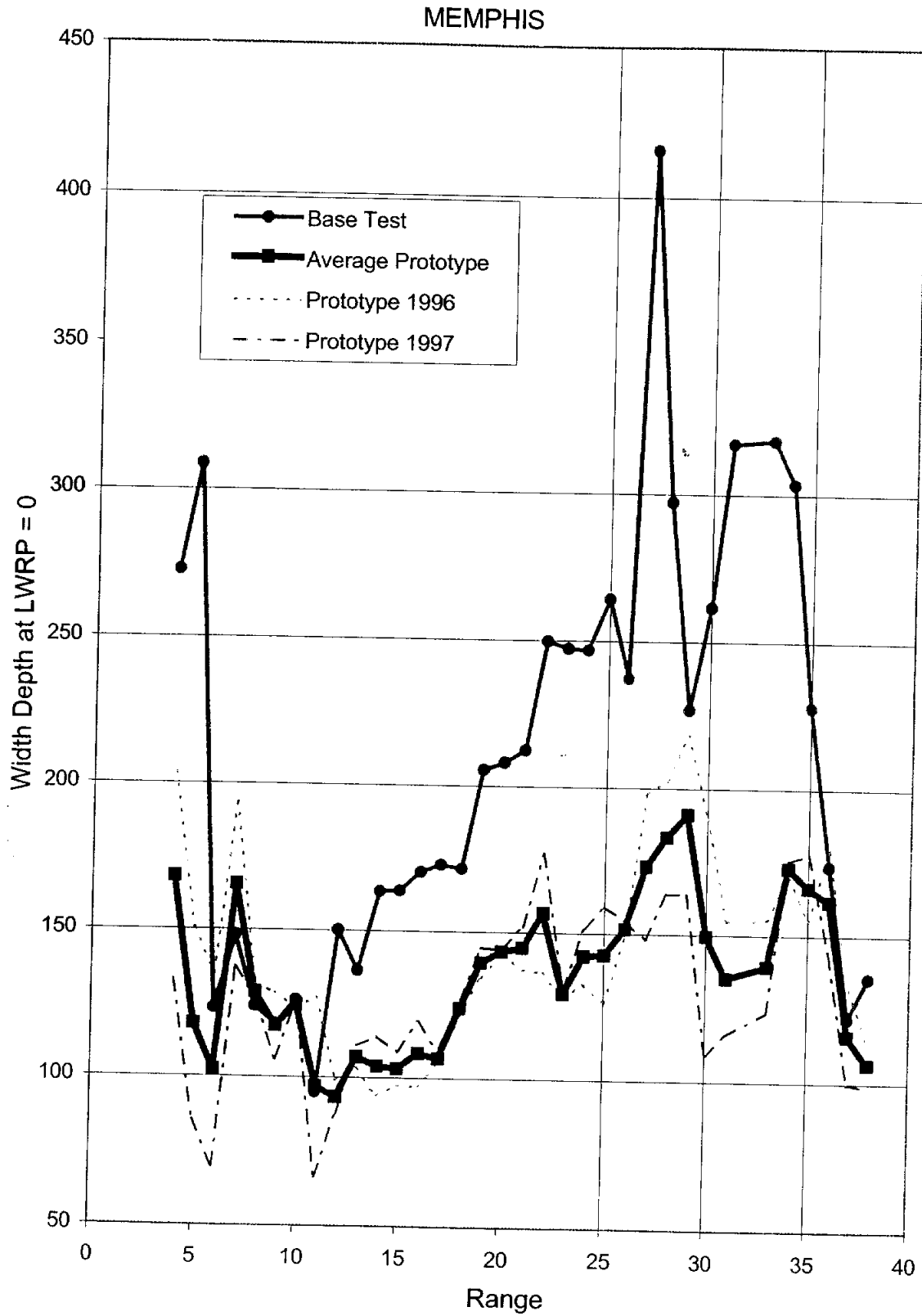


Figure C-5.2e Width/Depth Ratio by Range, Memphis Harbor (Mississippi River)

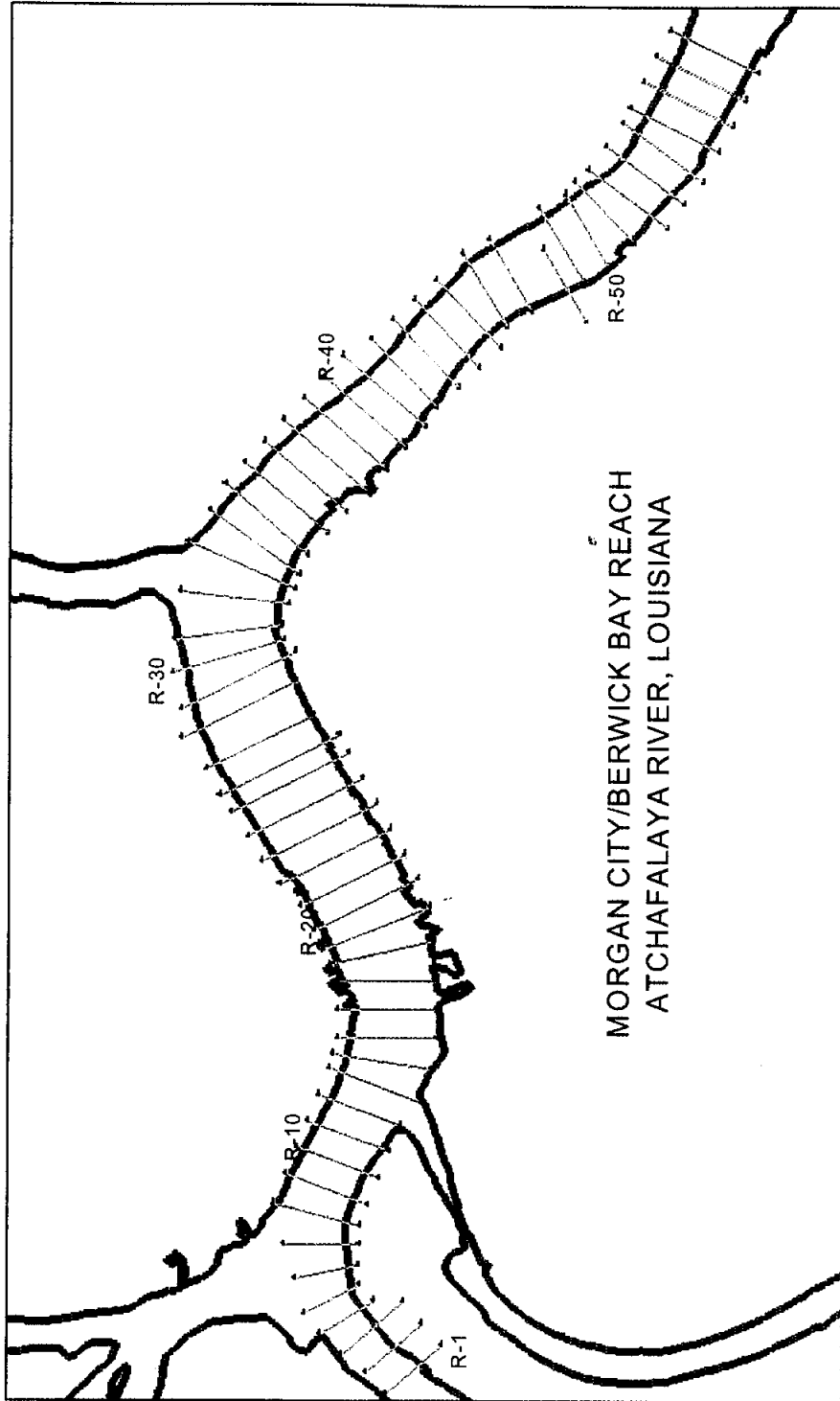


Figure C-6.1a Morgan City/Berwick Bay Micromodel Plan View

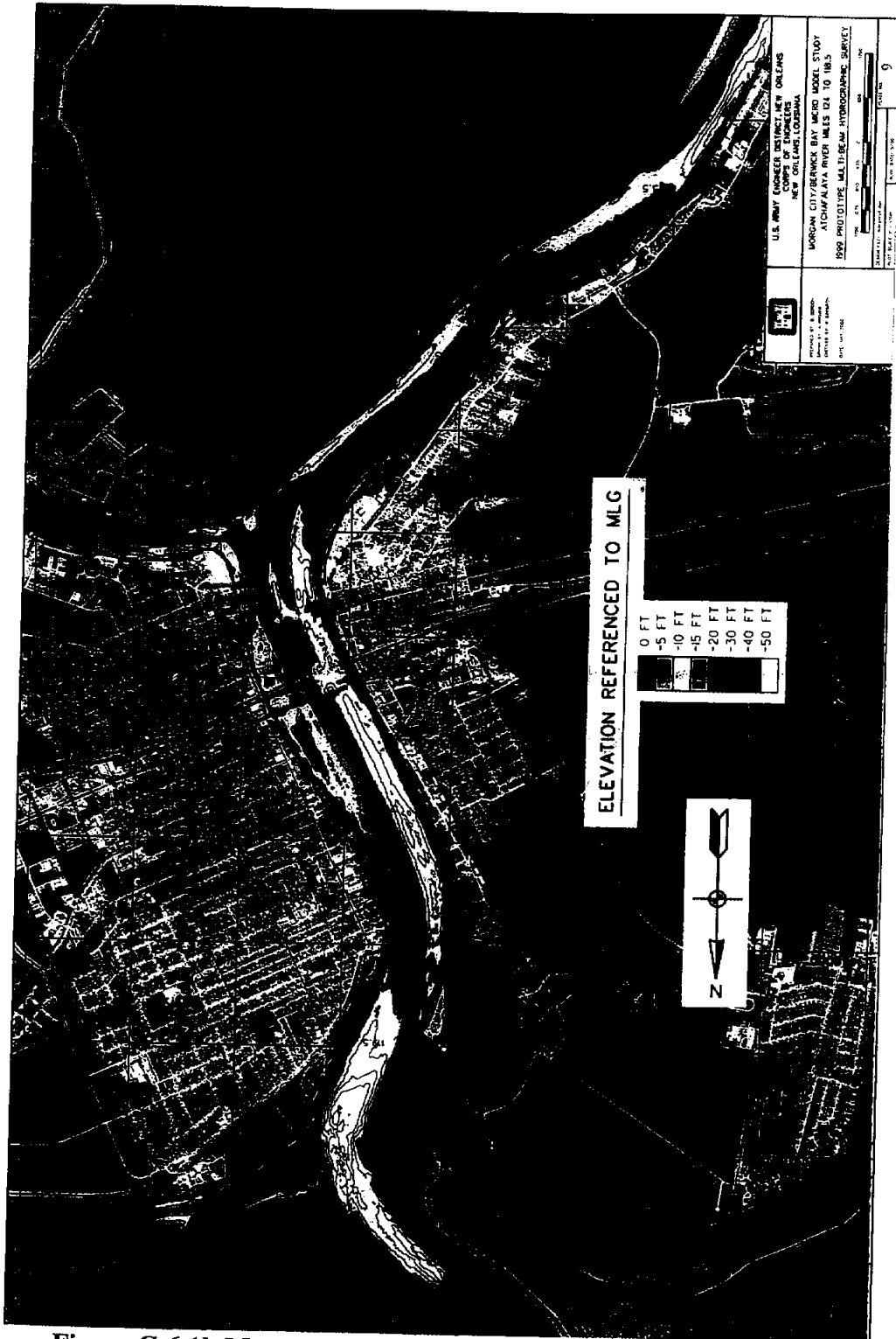


Figure C-6.1b Morgan City/Berwick Bay Prototype Survey 1999

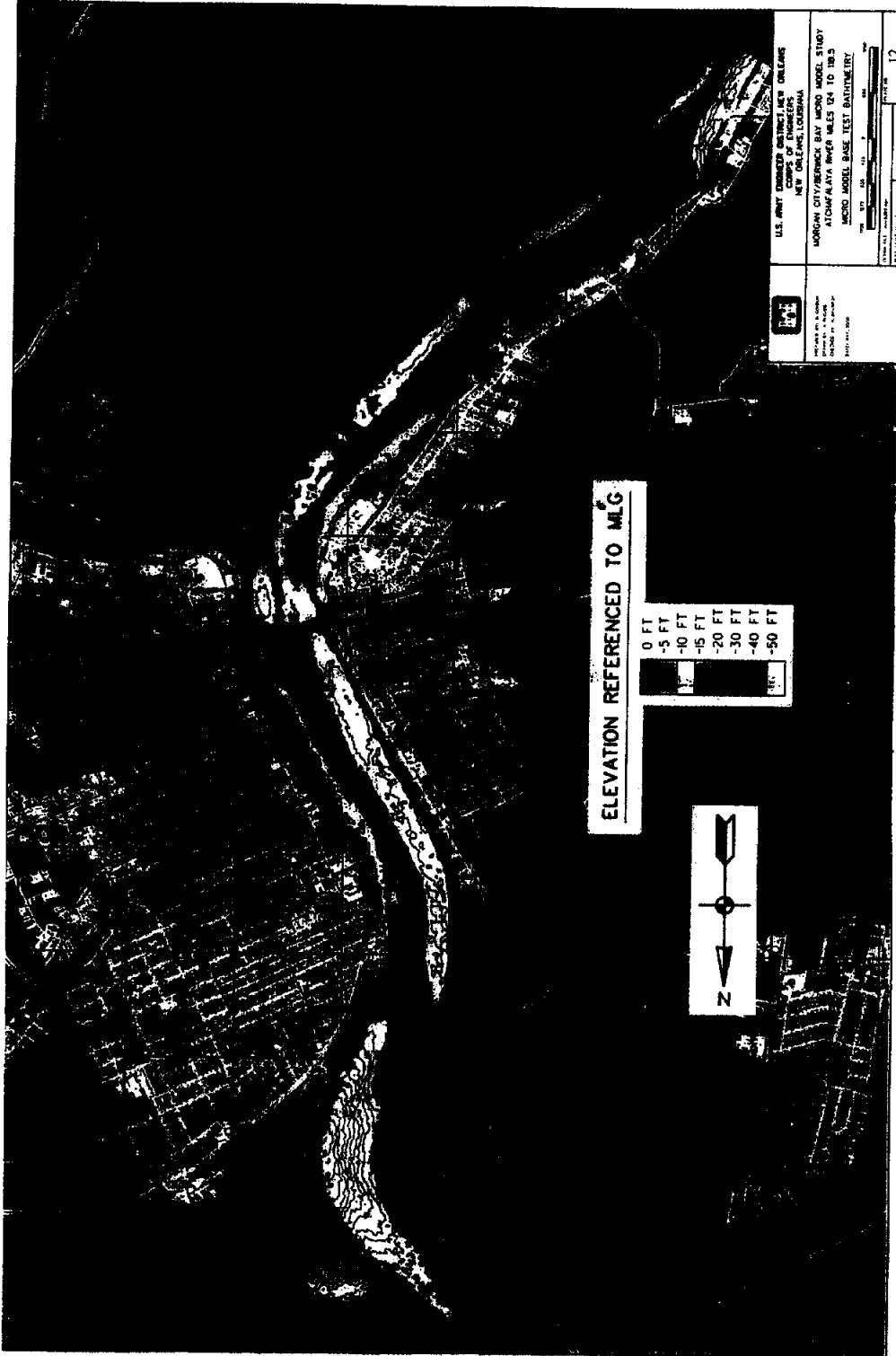
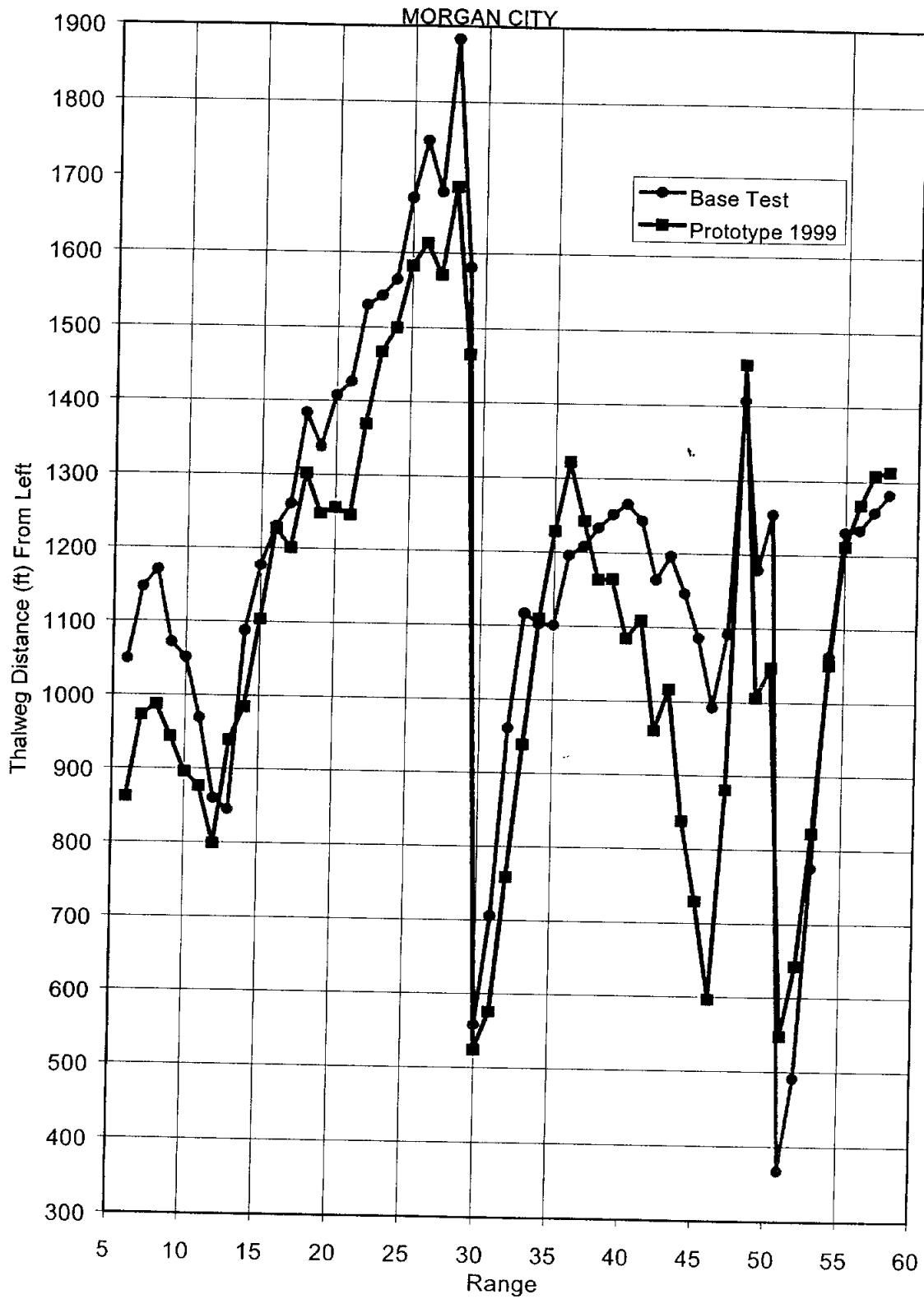


Figure C-6.1c Morgan City/Berwick Bay Micromodel Base Test



**Figure C-6.2a Thalweg Position From Left by Range,
Morgan City (Atchafalaya River)**

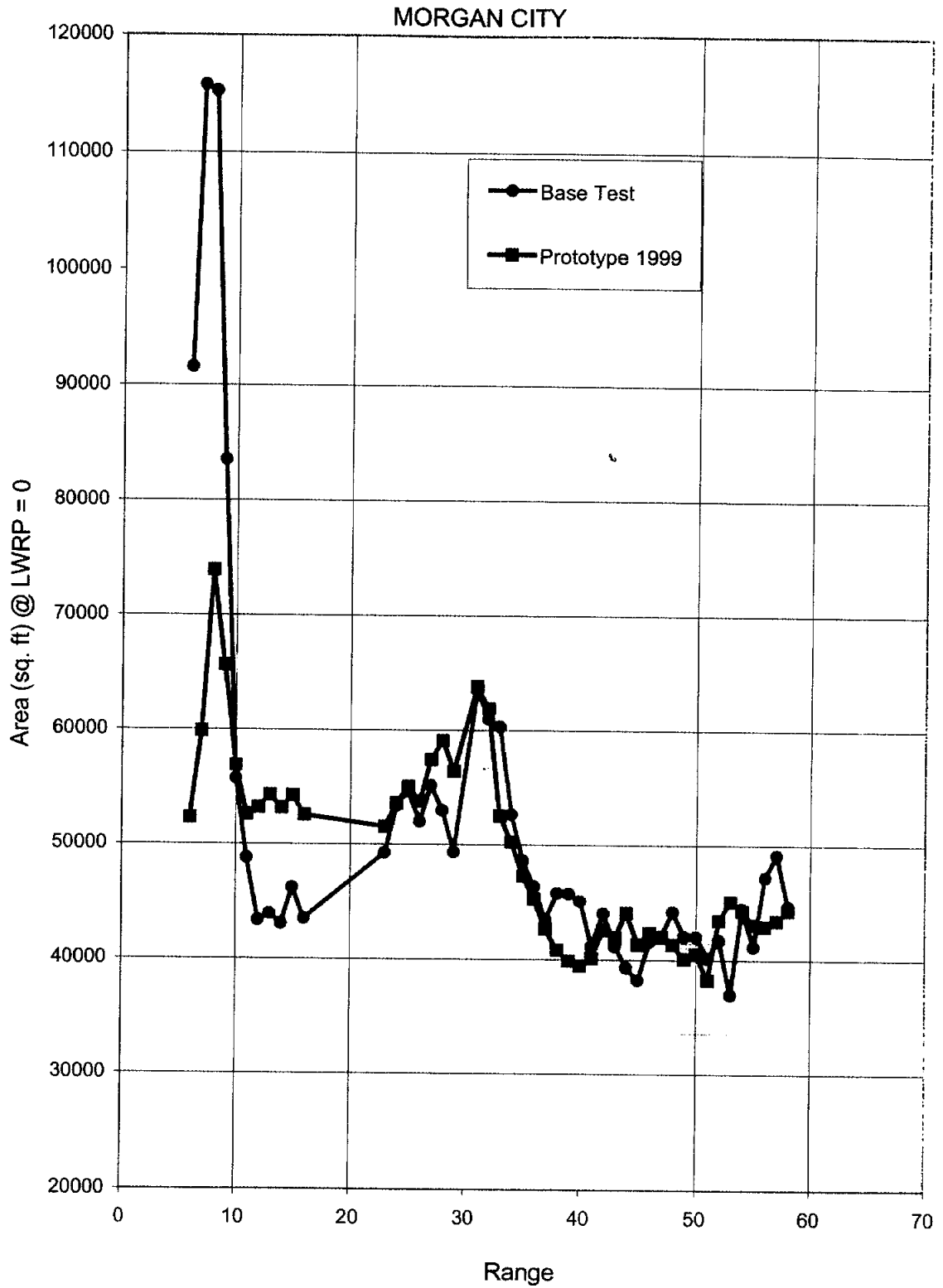


Figure C-6.2b Cross-Section Area, Morgan City (Atchafalaya River)

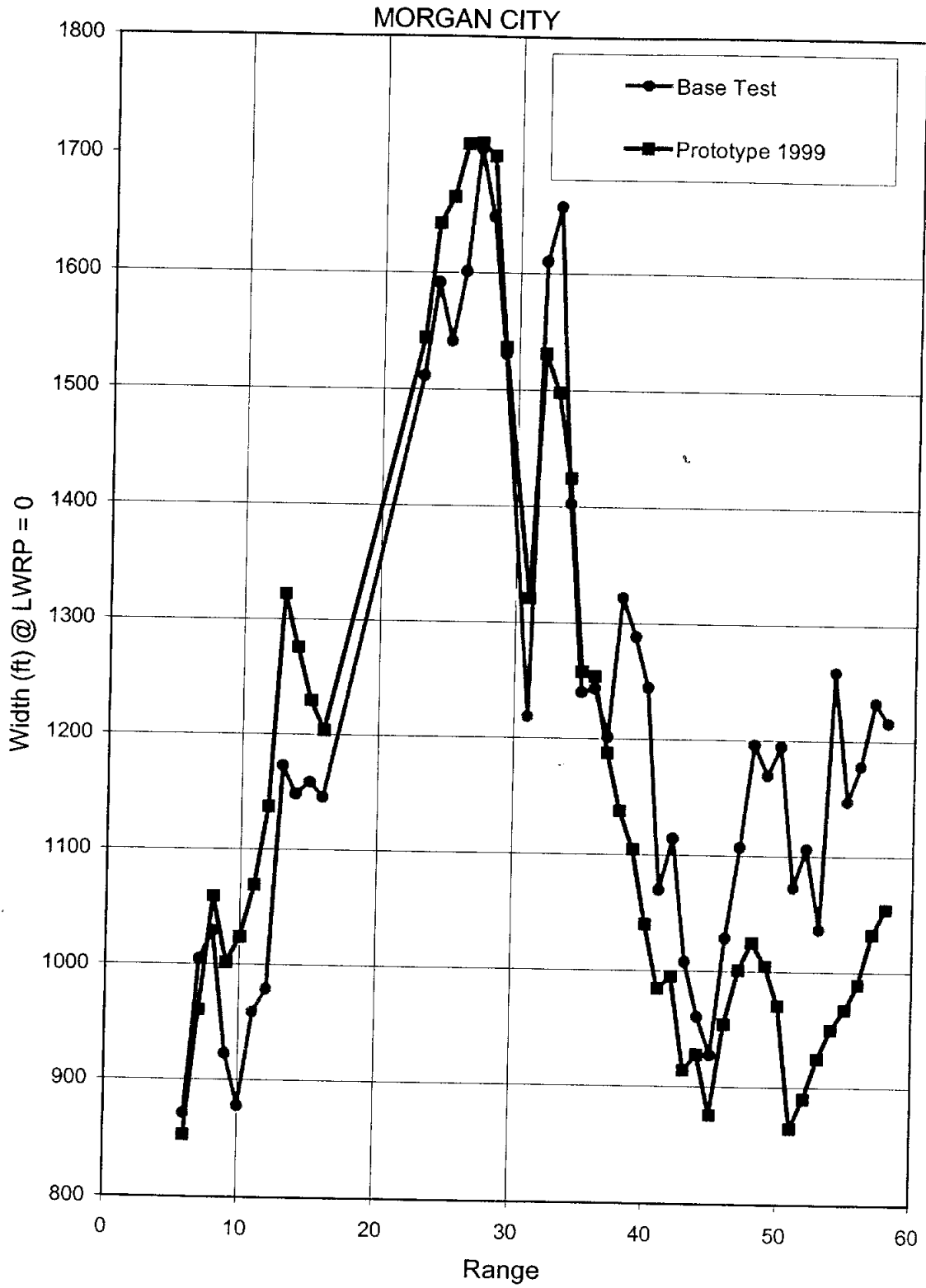


Figure C-6.2c Top Width by Section, Morgan City (Atchafalaya River)

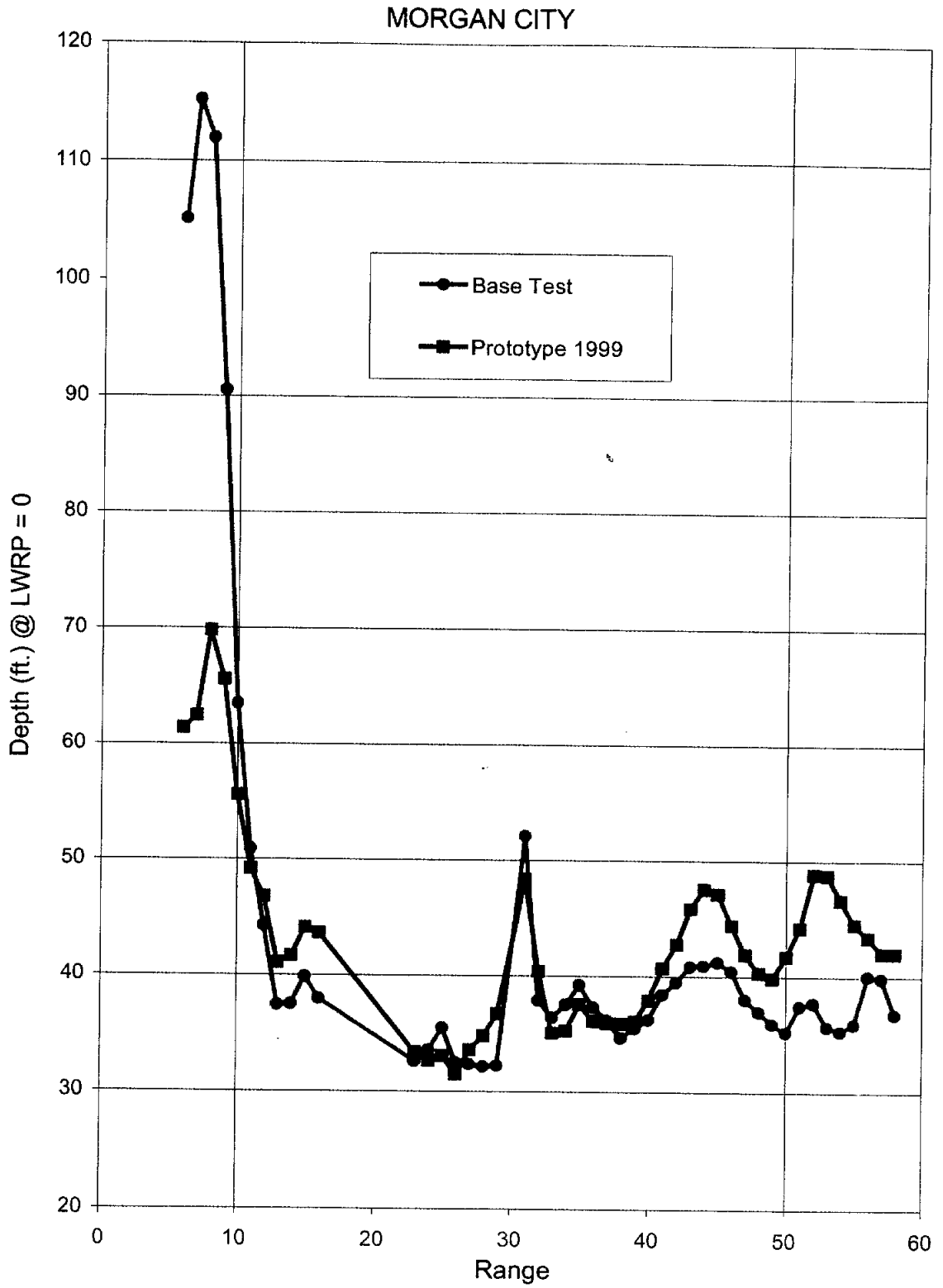


Figure C-6.2d Hydraulic Depth by Section, Morgan City (Atchafalaya River)

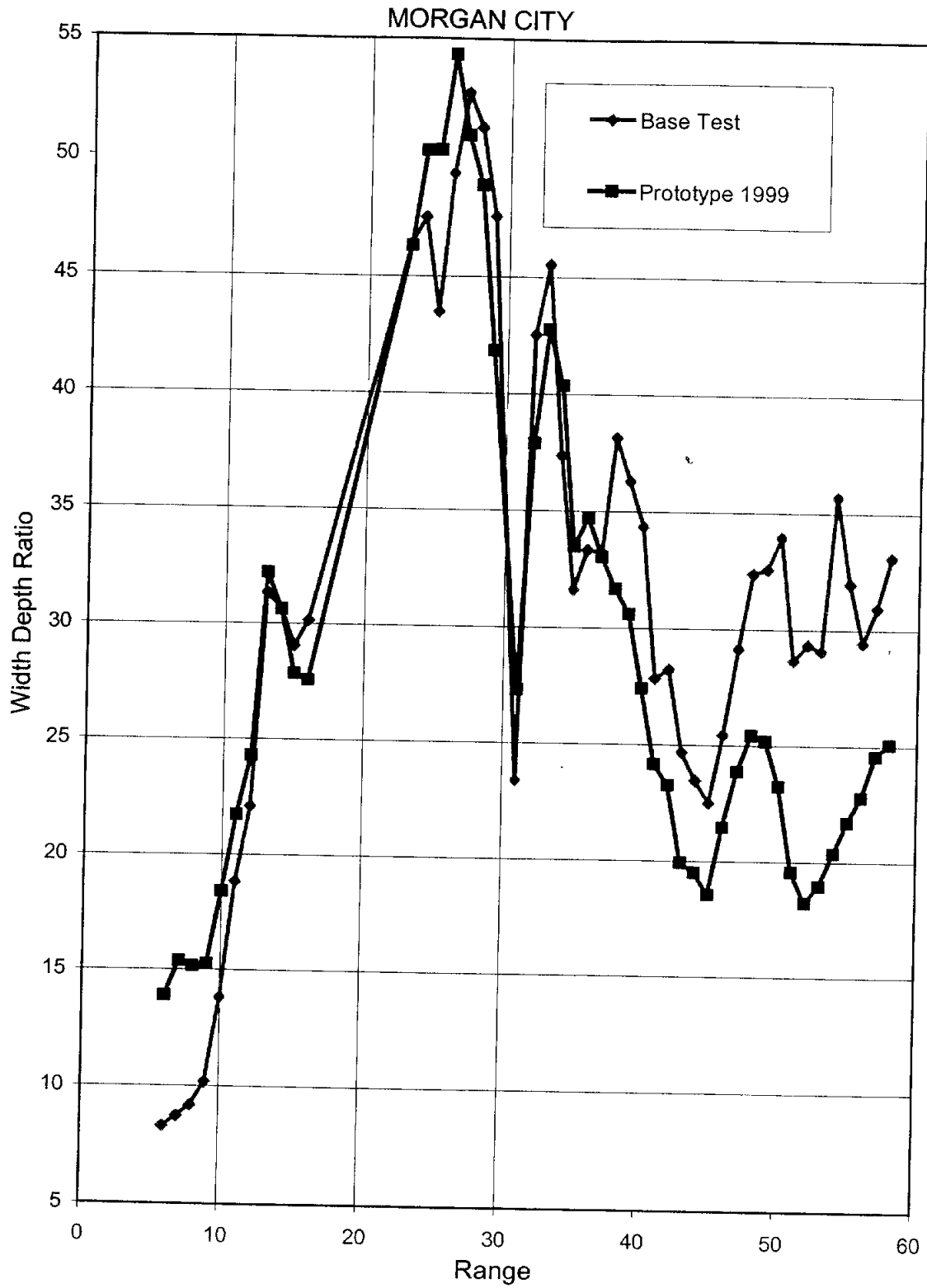


Figure C-6.2e Width/Depth Ratio by Range, Morgan City (Atchafalaya River)

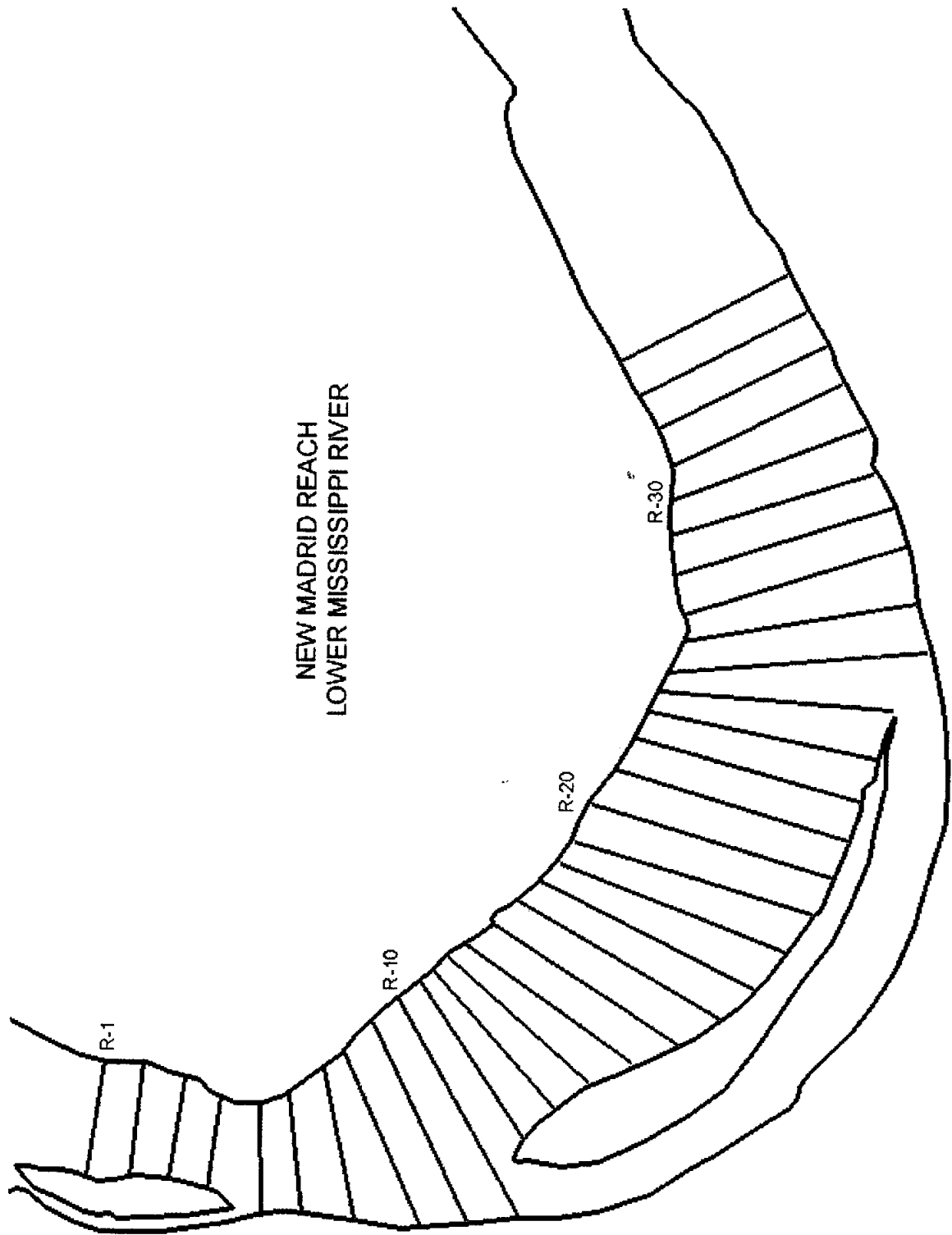


Figure C-7.1a New Madrid Micromodel Plan View

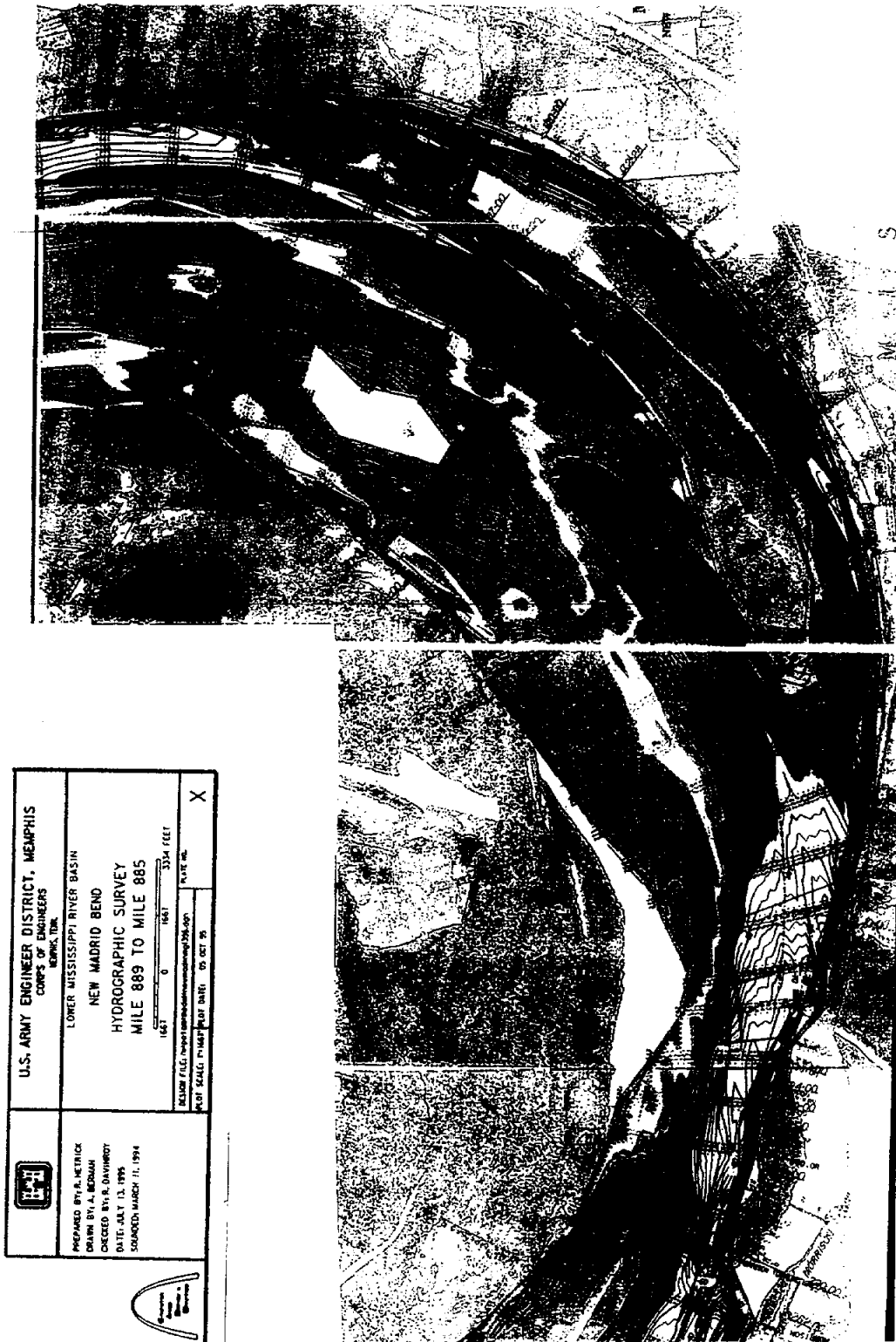


Figure C-7.1b New Madrid Prototype Survey 1994

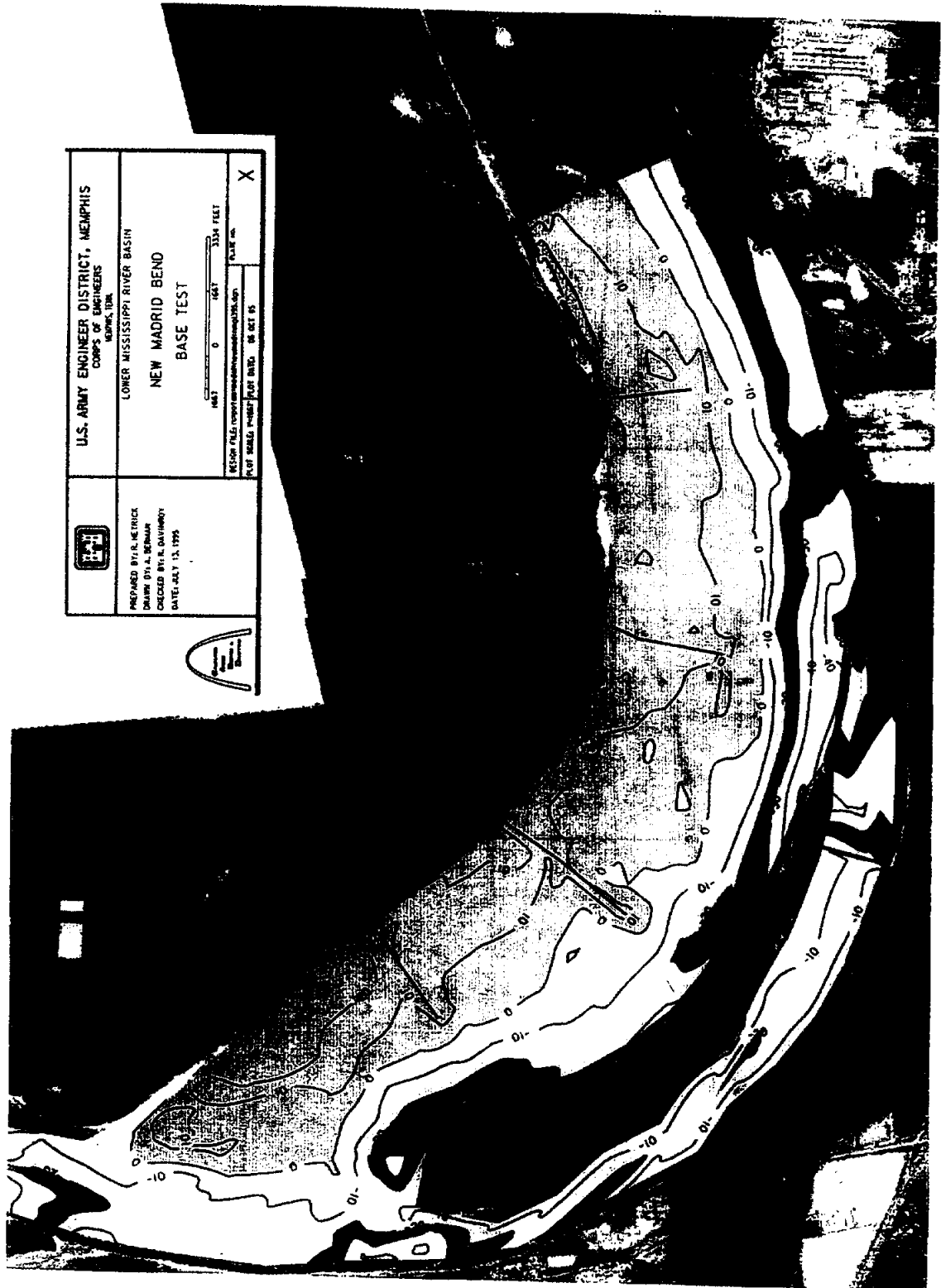


Figure C-7.1c New Madrid Micromodel Base Test

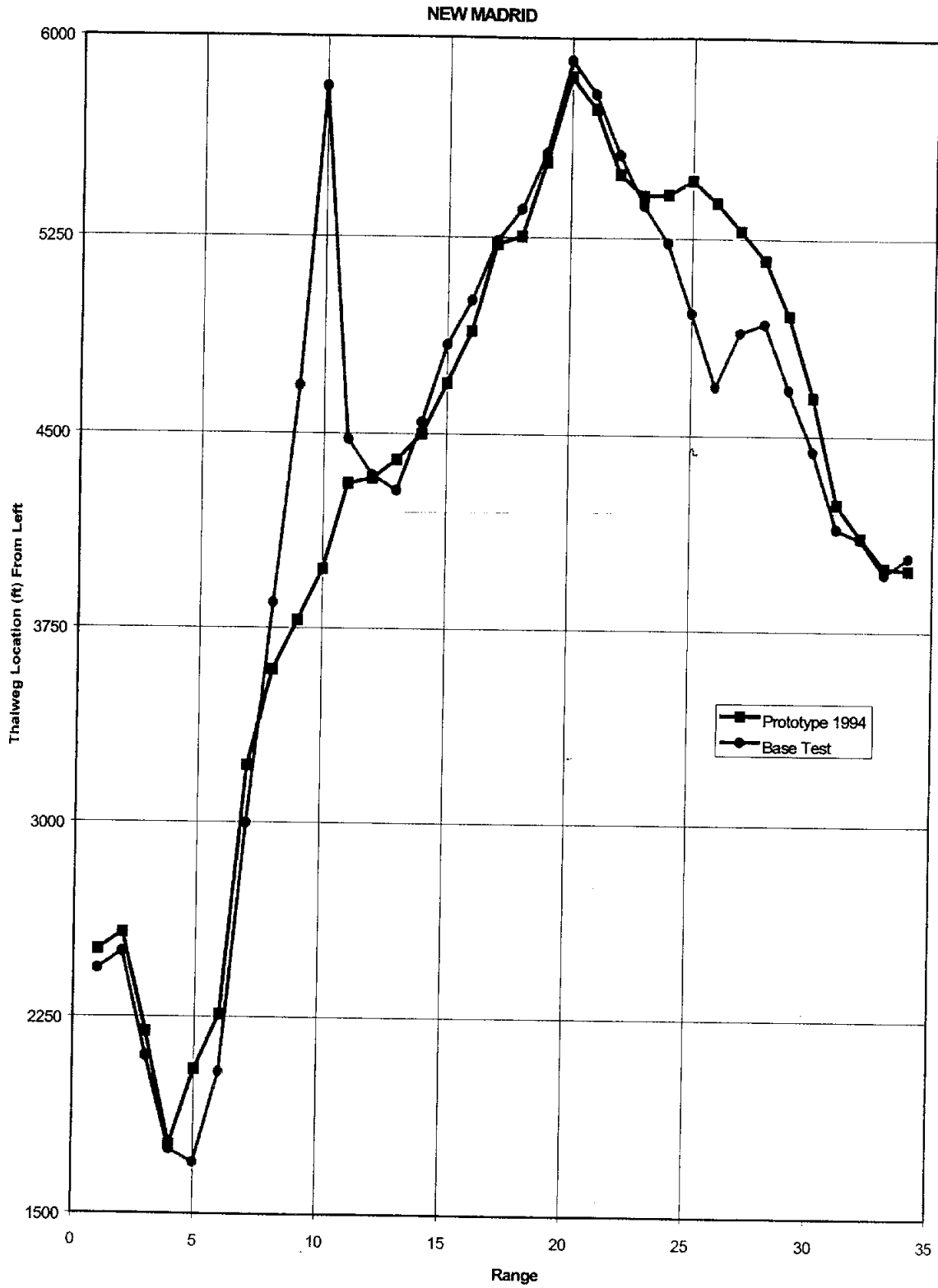


Figure C-7.2a Thalweg Position From Left by Range, New Madrid Reach (Mississippi River)

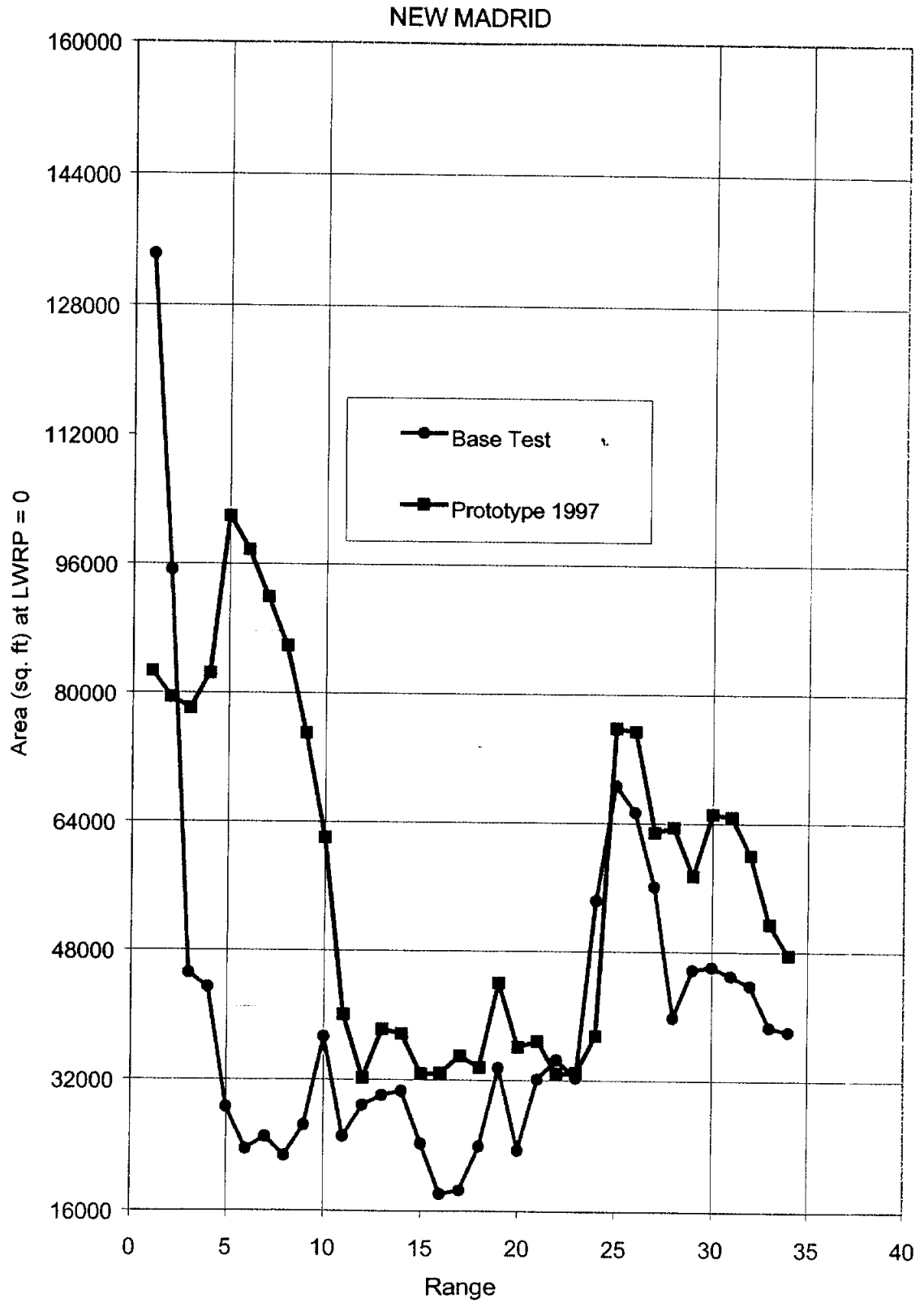


Figure C-7.2b Cross-Section Area by Range, New Madrid Reach (Mississippi River)

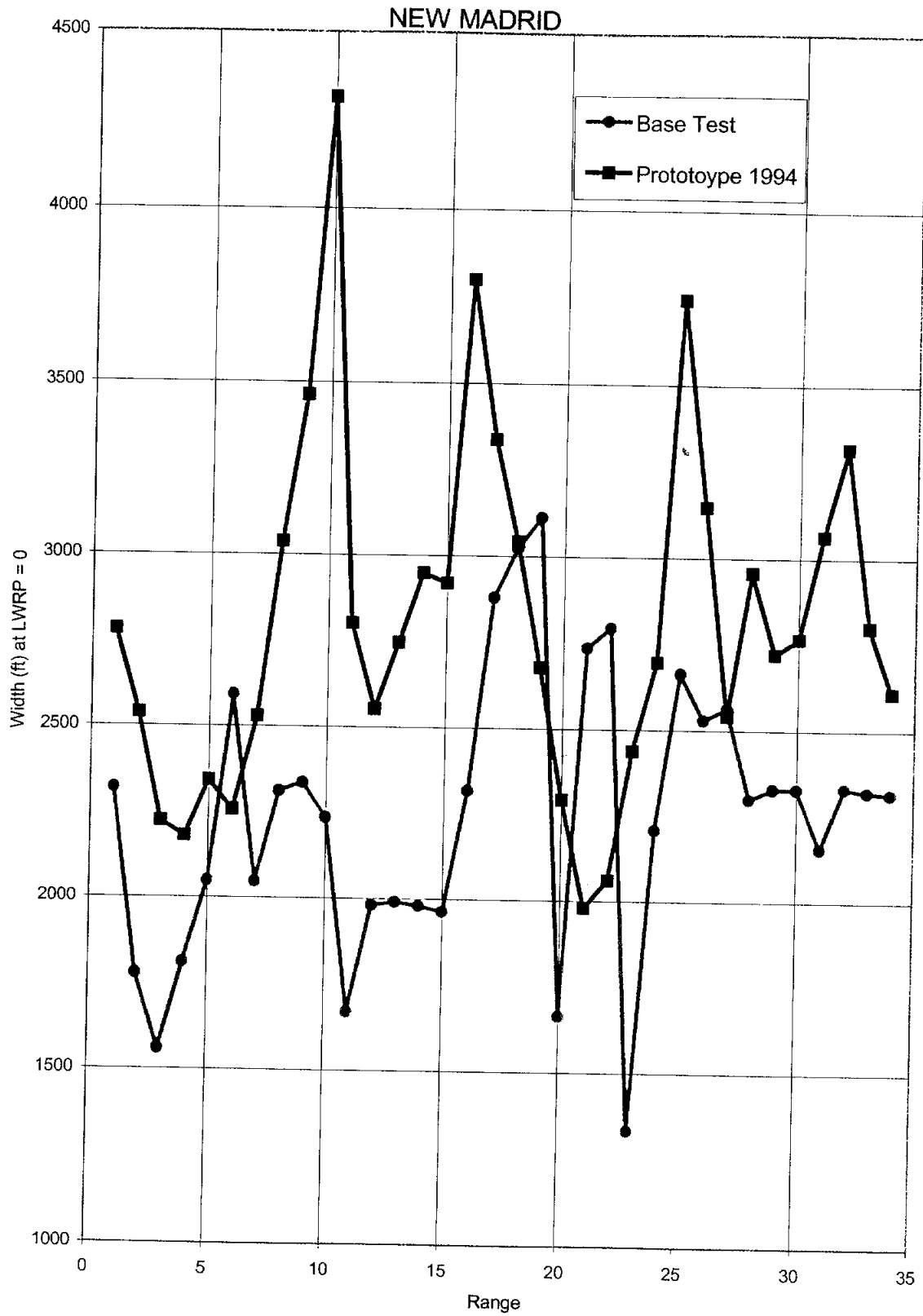


Figure C-7.2c Top Width by Range, New Madrid Reach (Mississippi River)

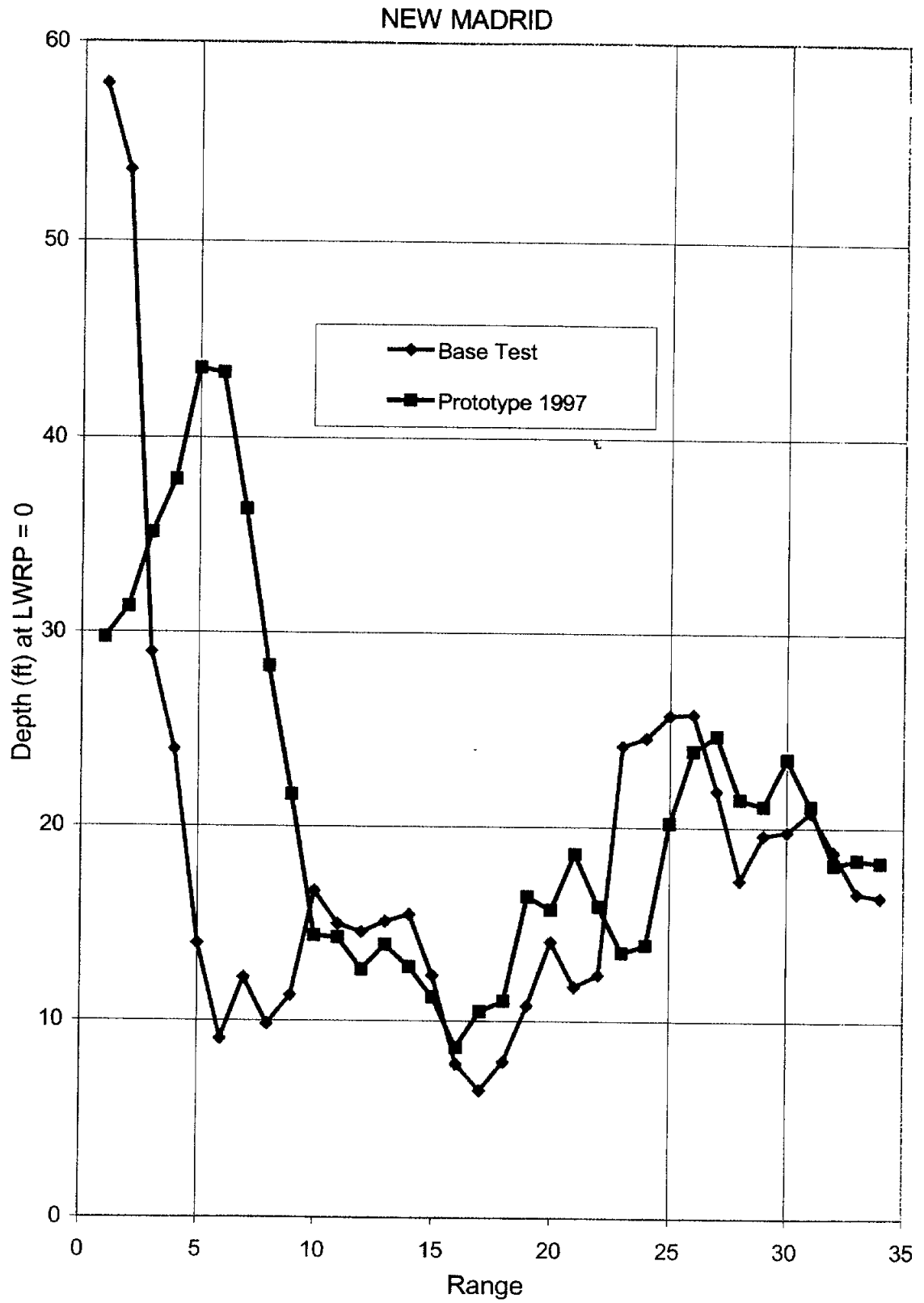


Figure C-7.2d Hydraulic Depth by Range, New Madrid Reach (Mississippi River)

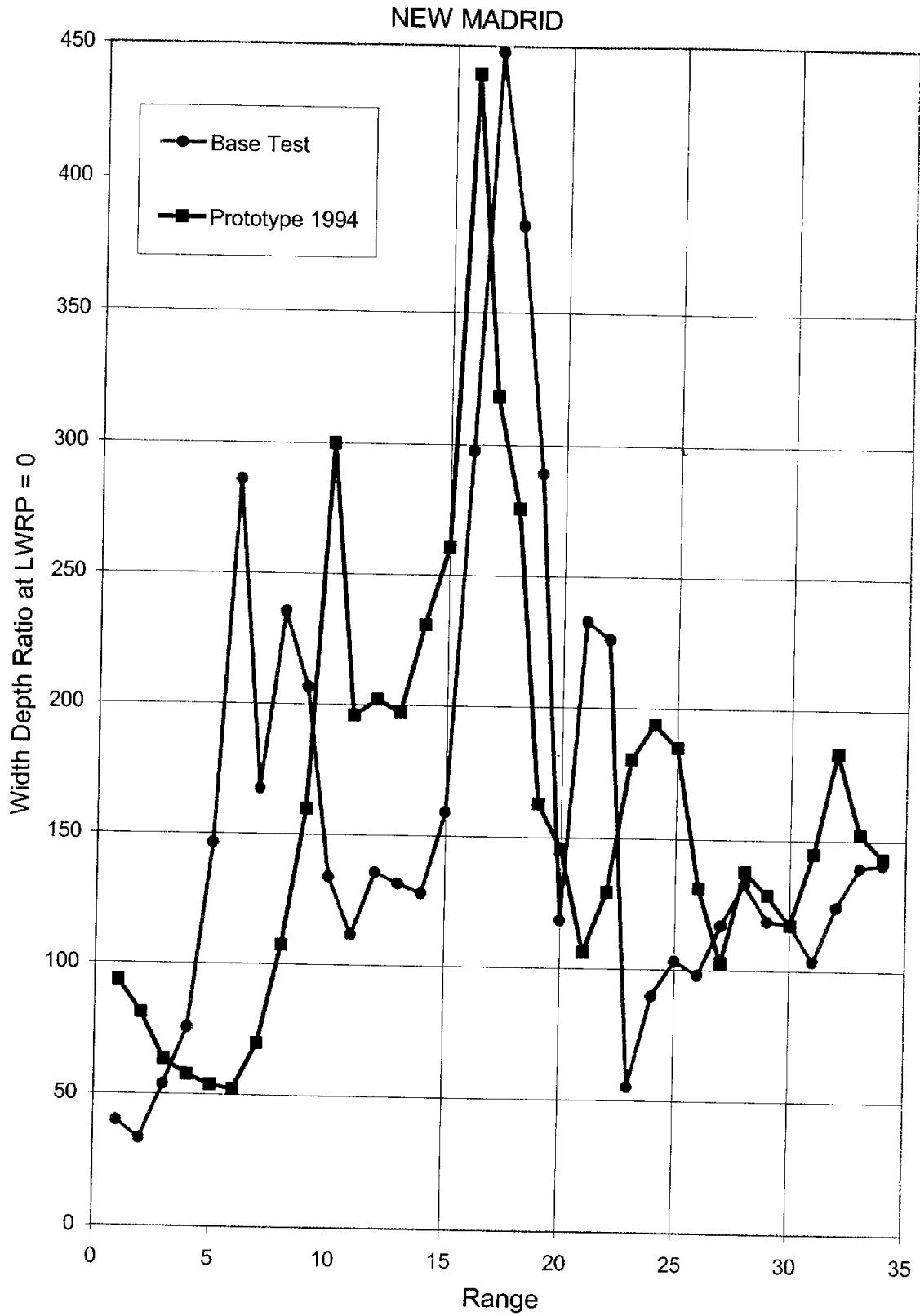


Figure C-7.2e Width/Depth Ratio by Range, New Madrid Reach (Mississippi River)

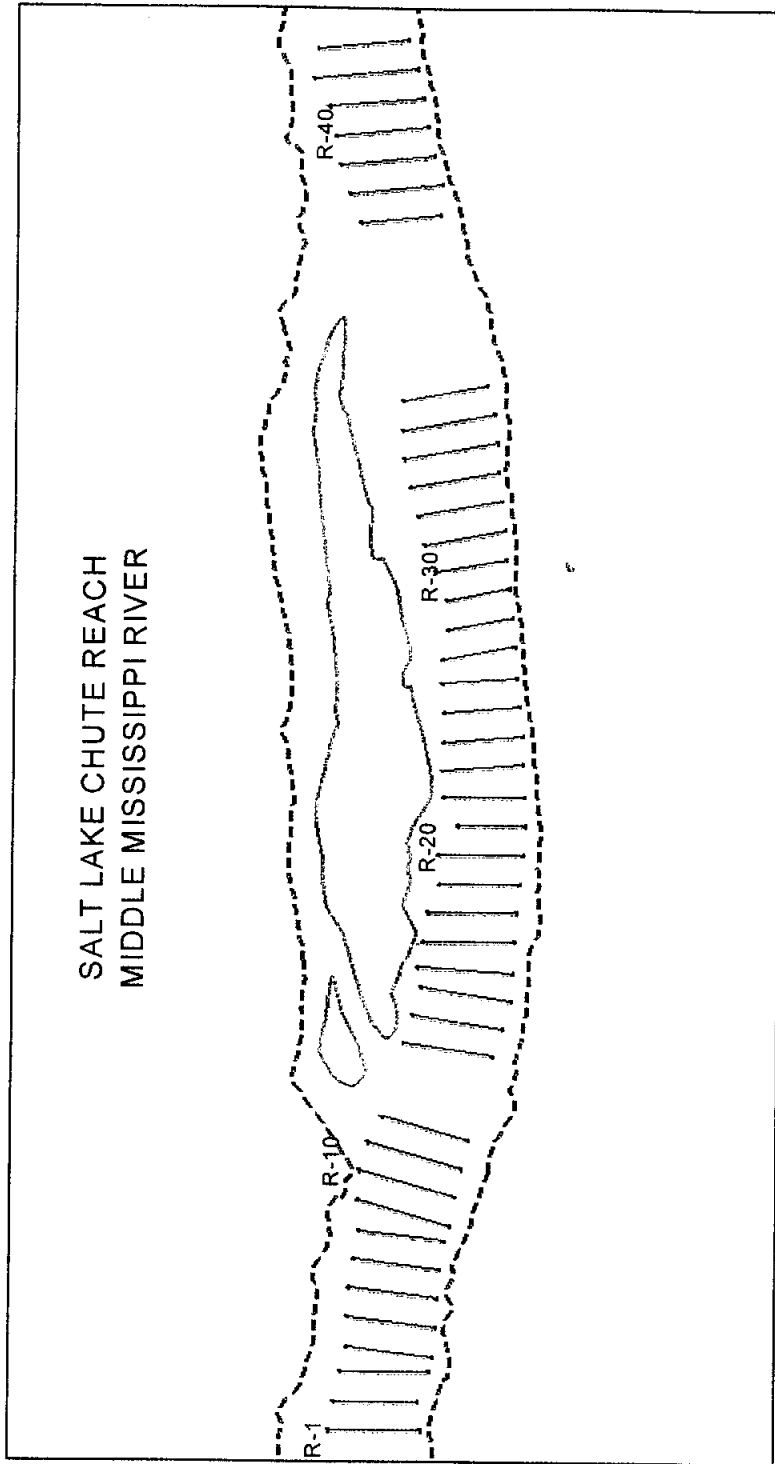


Figure C-8.1a Salt Lake Chute Micromodel Plan View

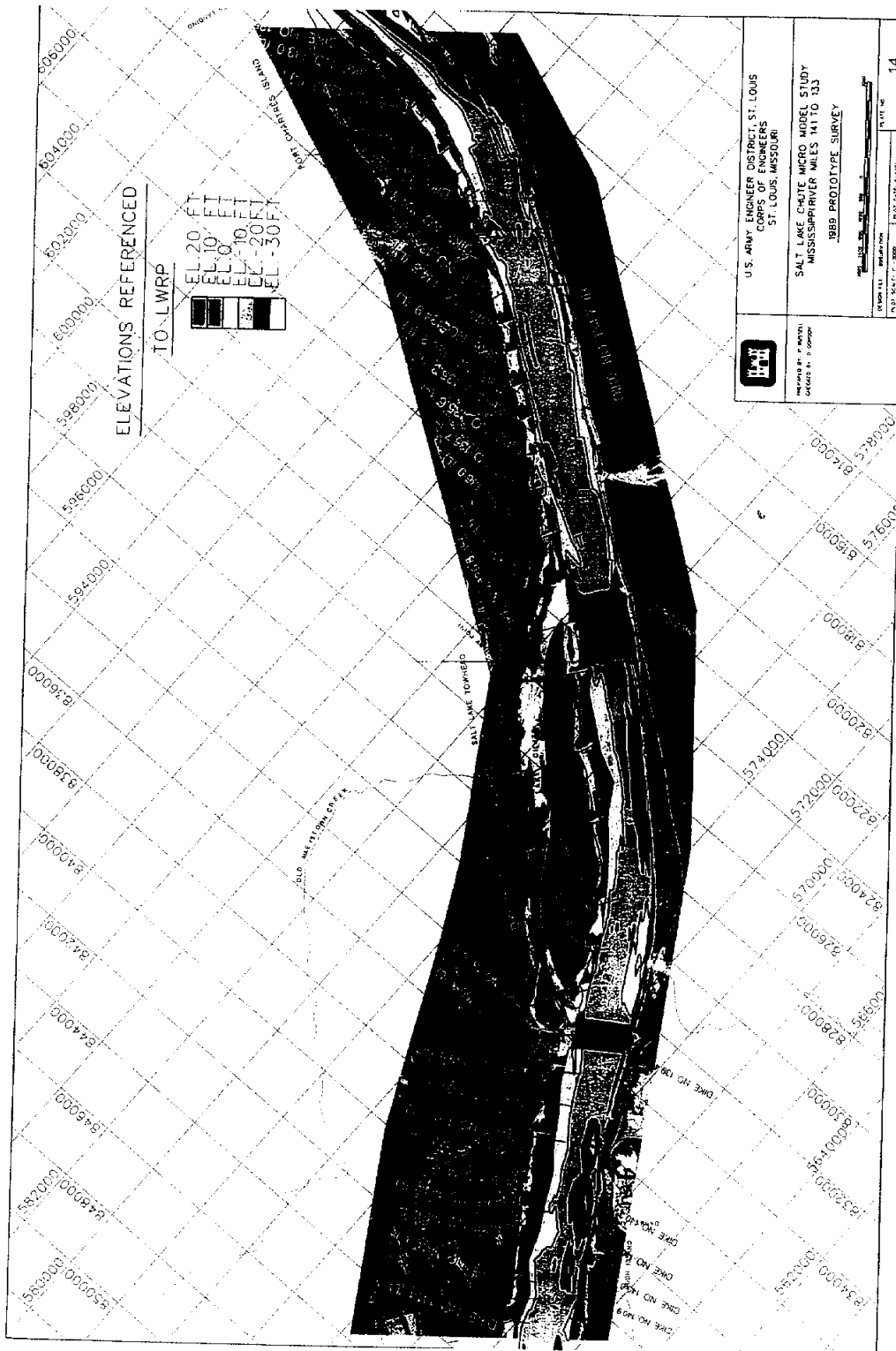


Figure C-8.1b Salt Lake Chute Prototype Survey 1989

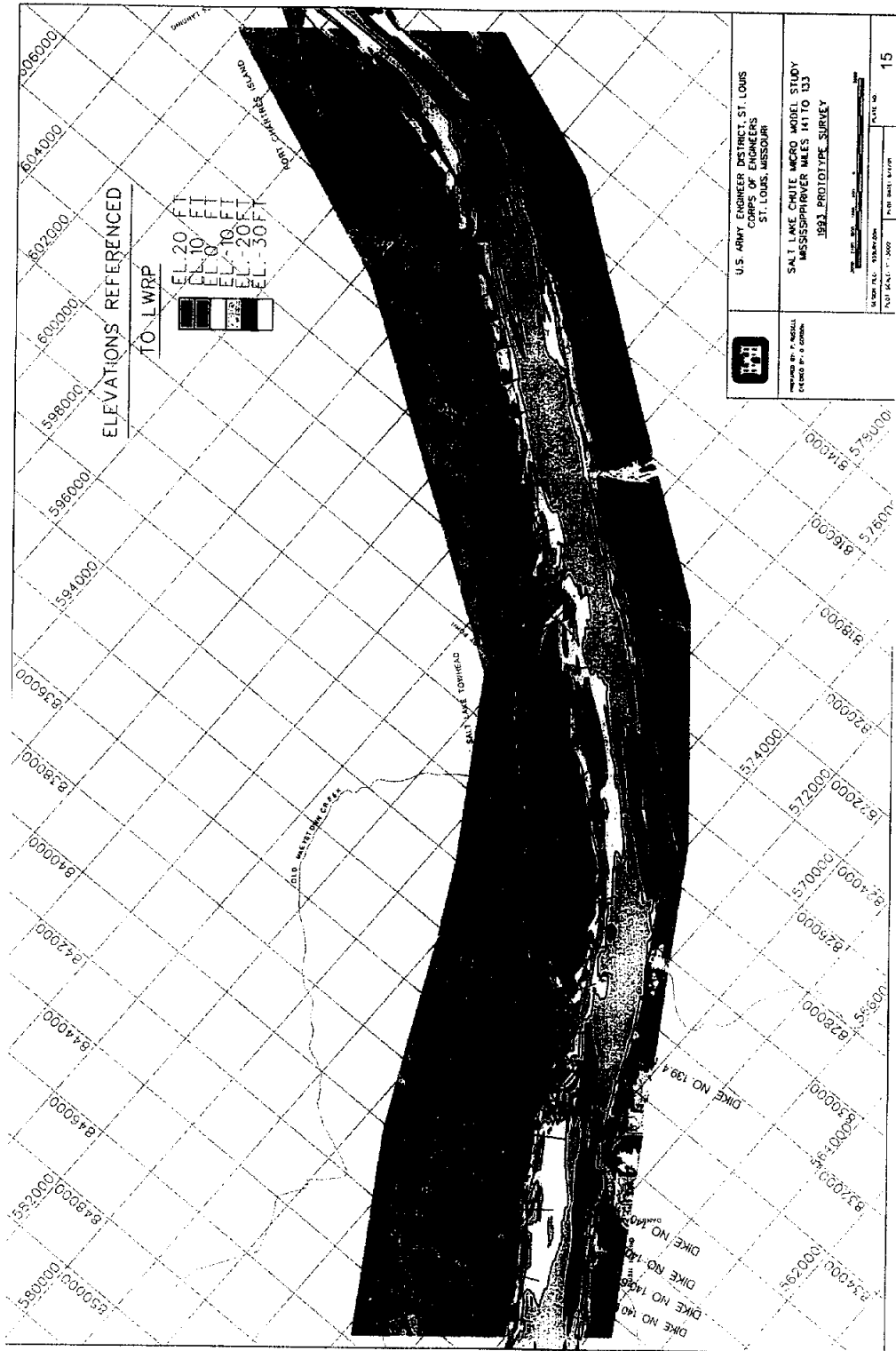


Figure C-8.1c Salt Lake Chute Prototype Survey 1993

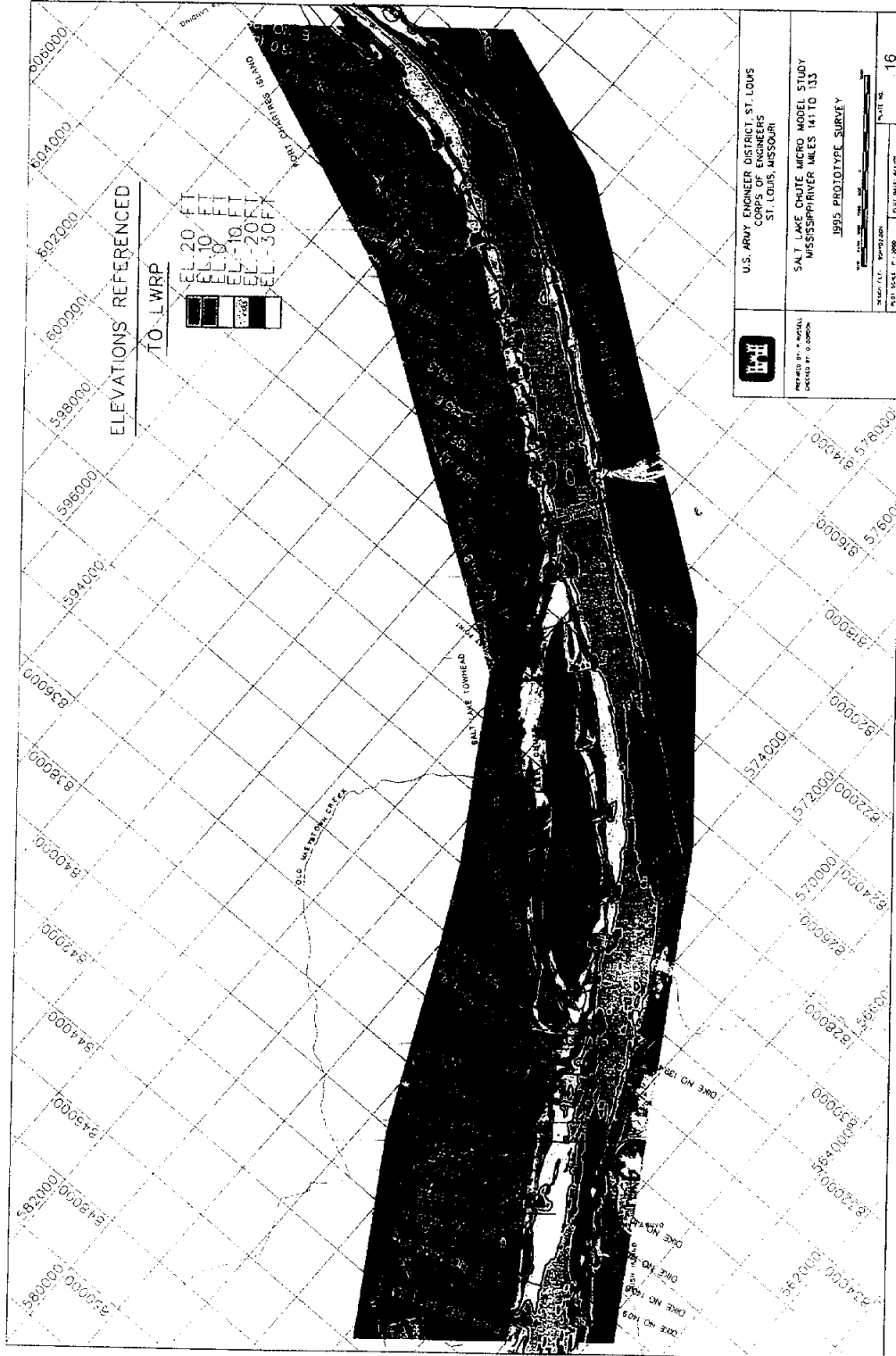


Figure C-8.1d Salt Lake Chute Prototype Survey 1995

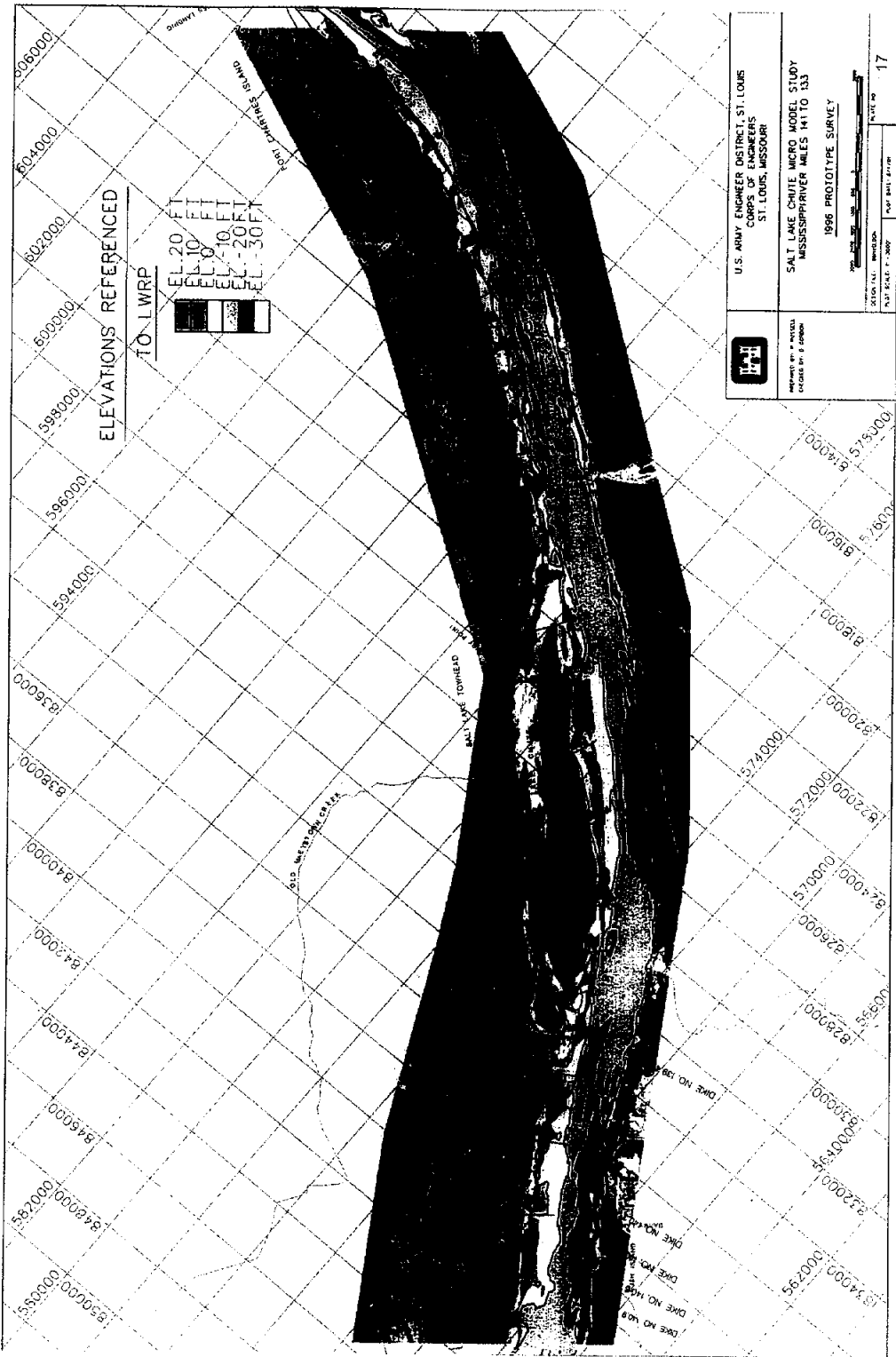


Figure C-8.1e Salt Lake Chute Prototype Survey 1996

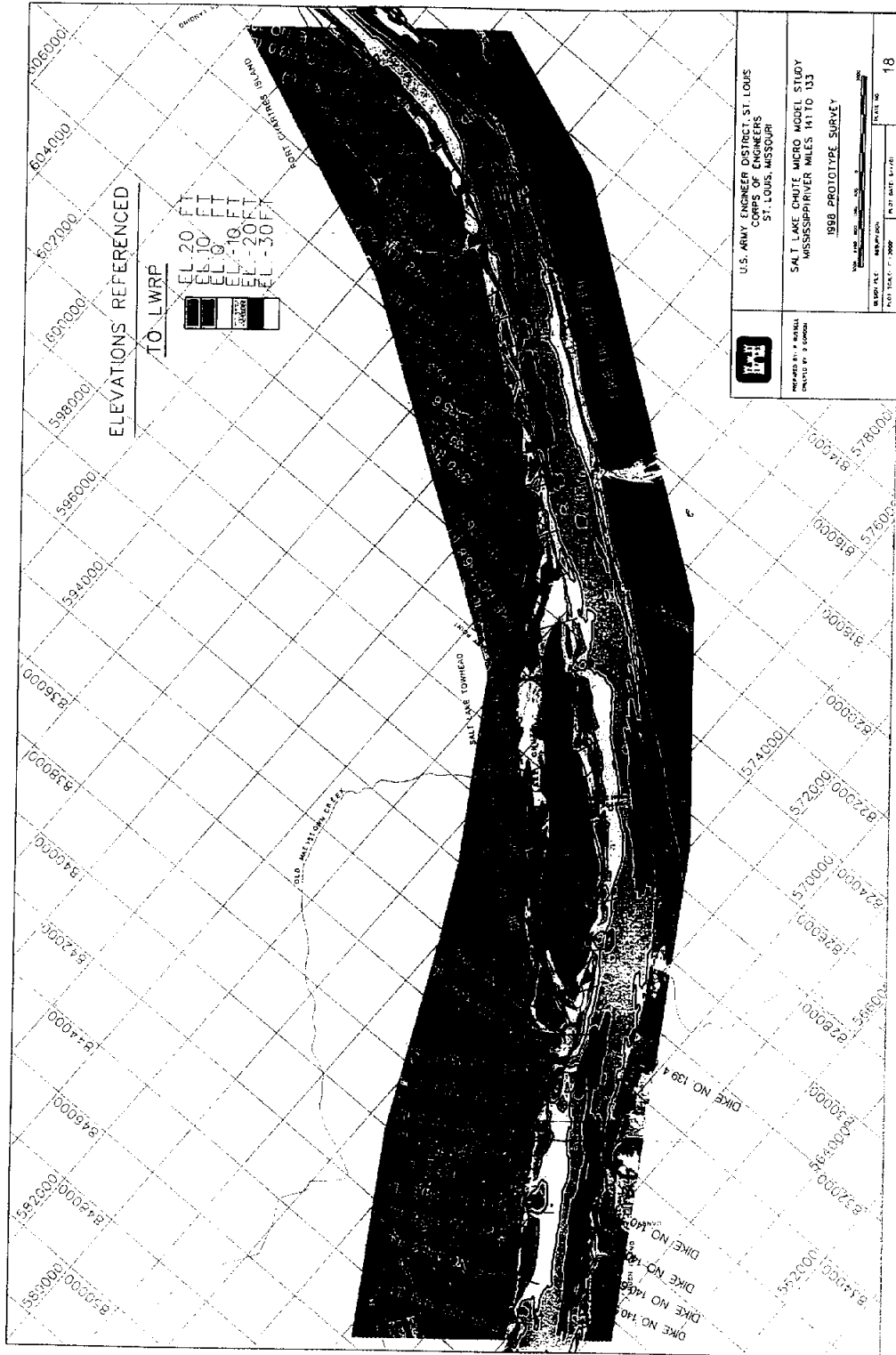


Figure C-8.1f Salt Lake Chute Prototype Survey 1998

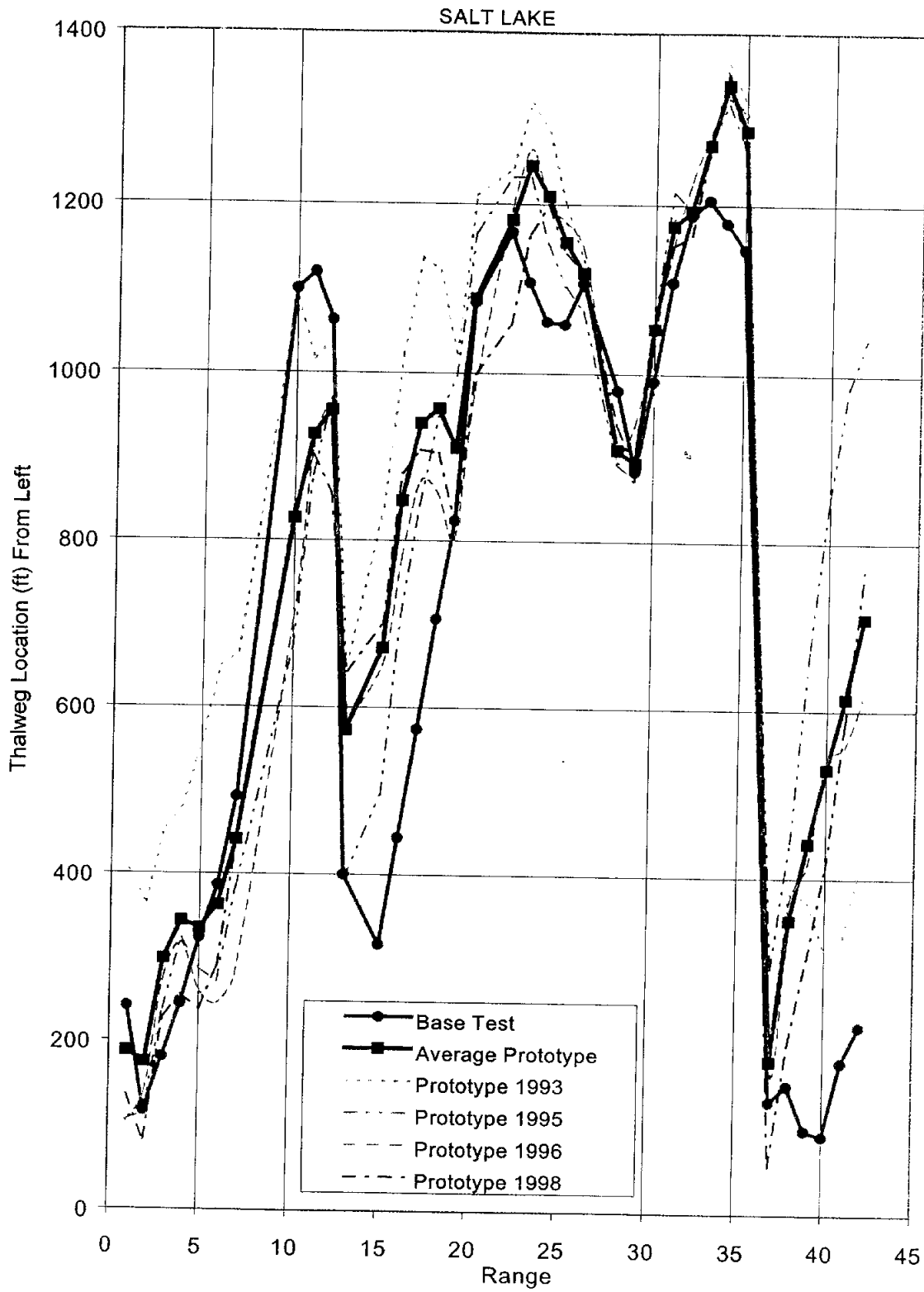


Figure C-8.2a Thalweg Position From Left by Range, Salt Lake Chute (Mississippi River)

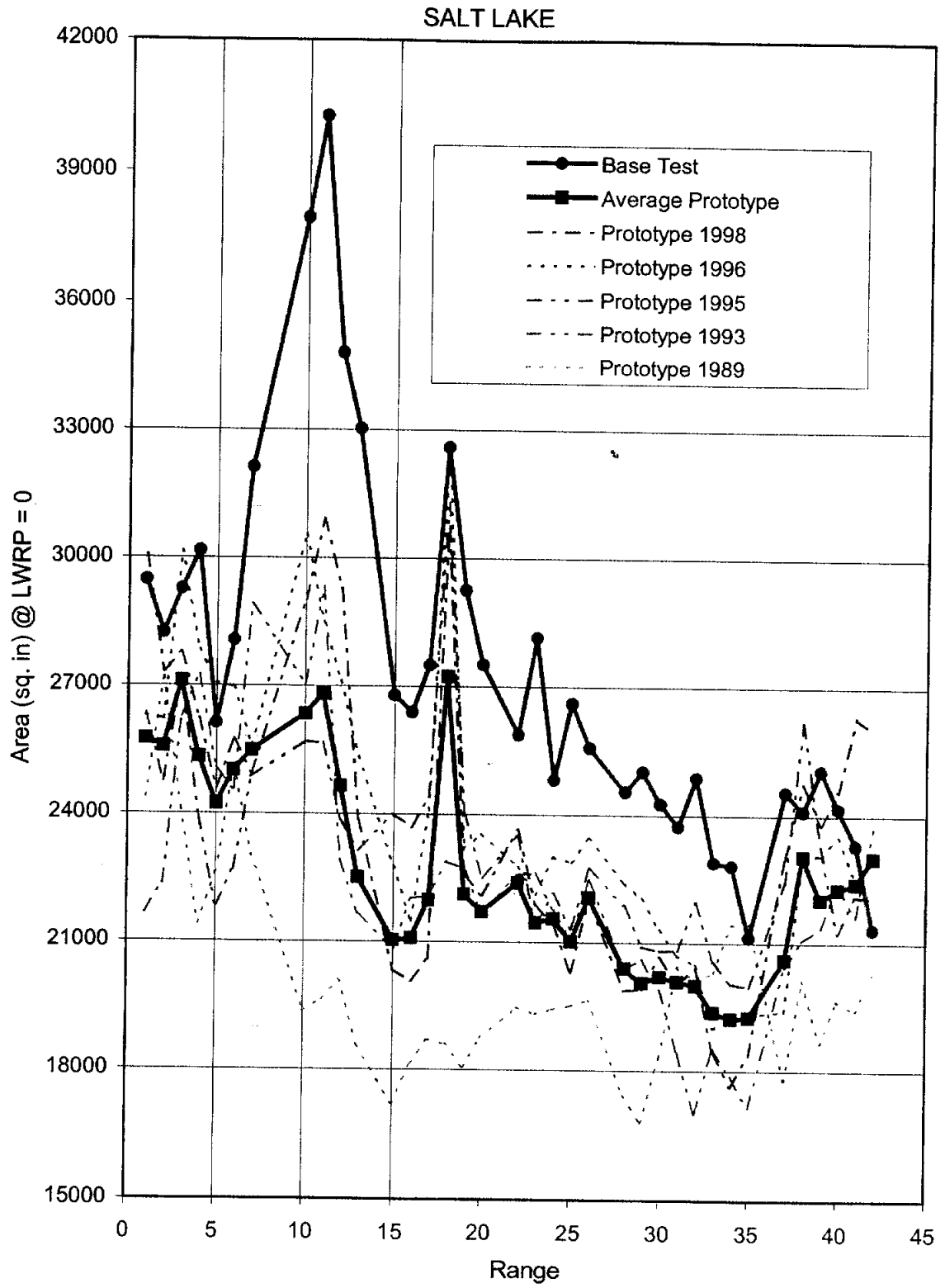


Figure C-8.2b Cross-Section Area by Range, Salt Lake Chute (Mississippi River)

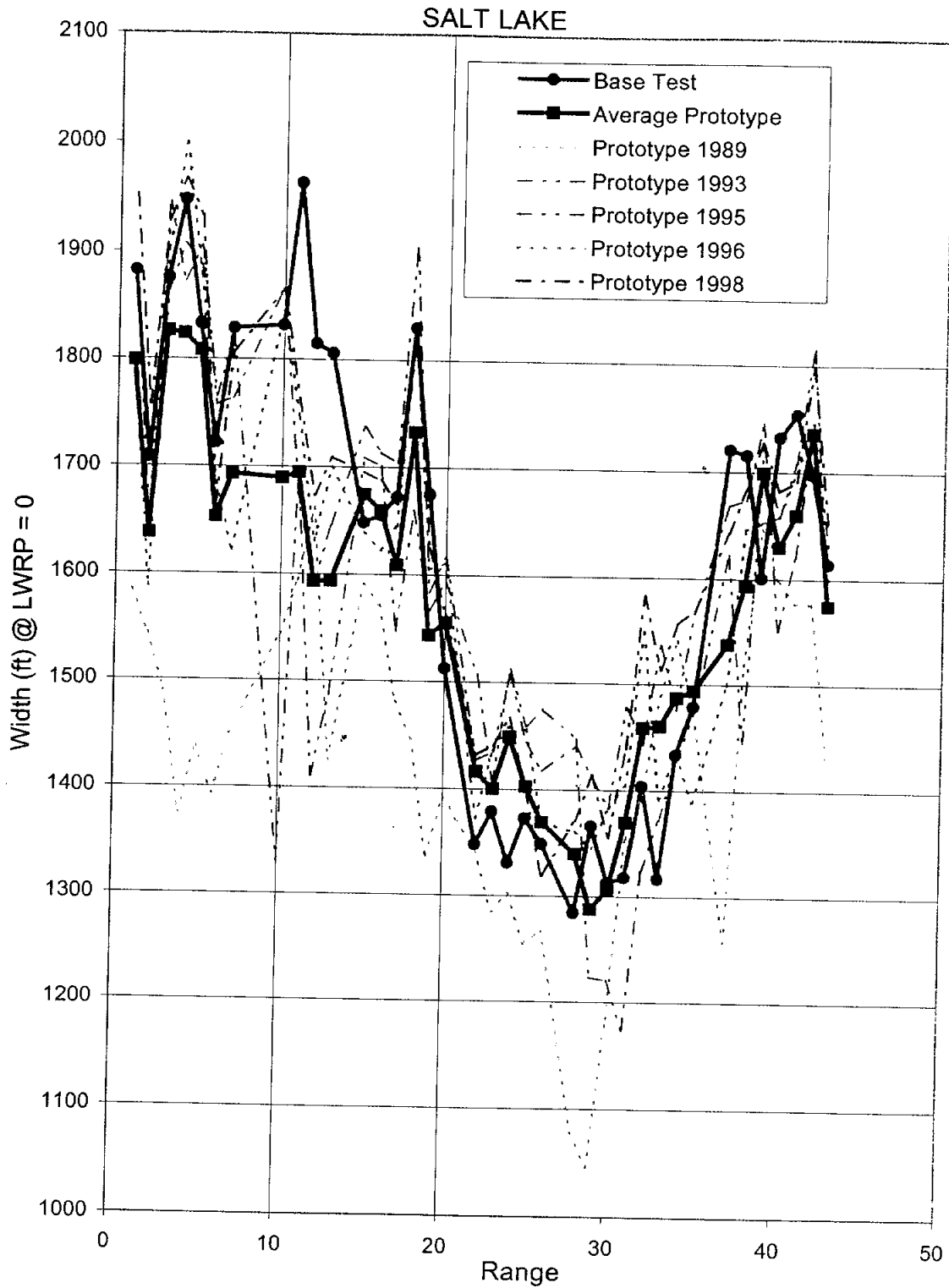


Figure C-8.2c Top Width by Range, Salt Lake Chute (Mississippi River)

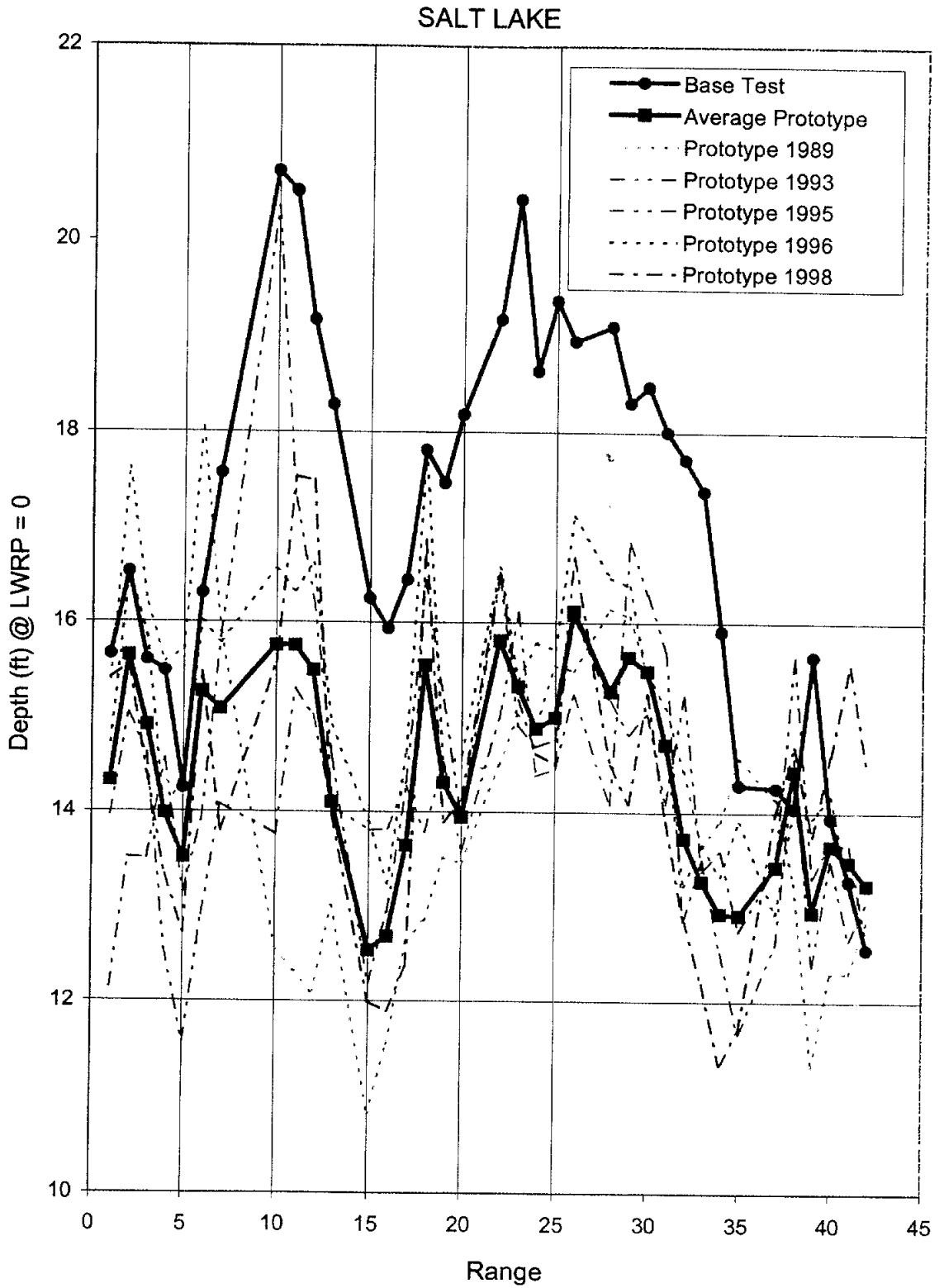


Figure C-8.2d Hydraulic Depth by Range, Salt Lake Chute (Mississippi River)

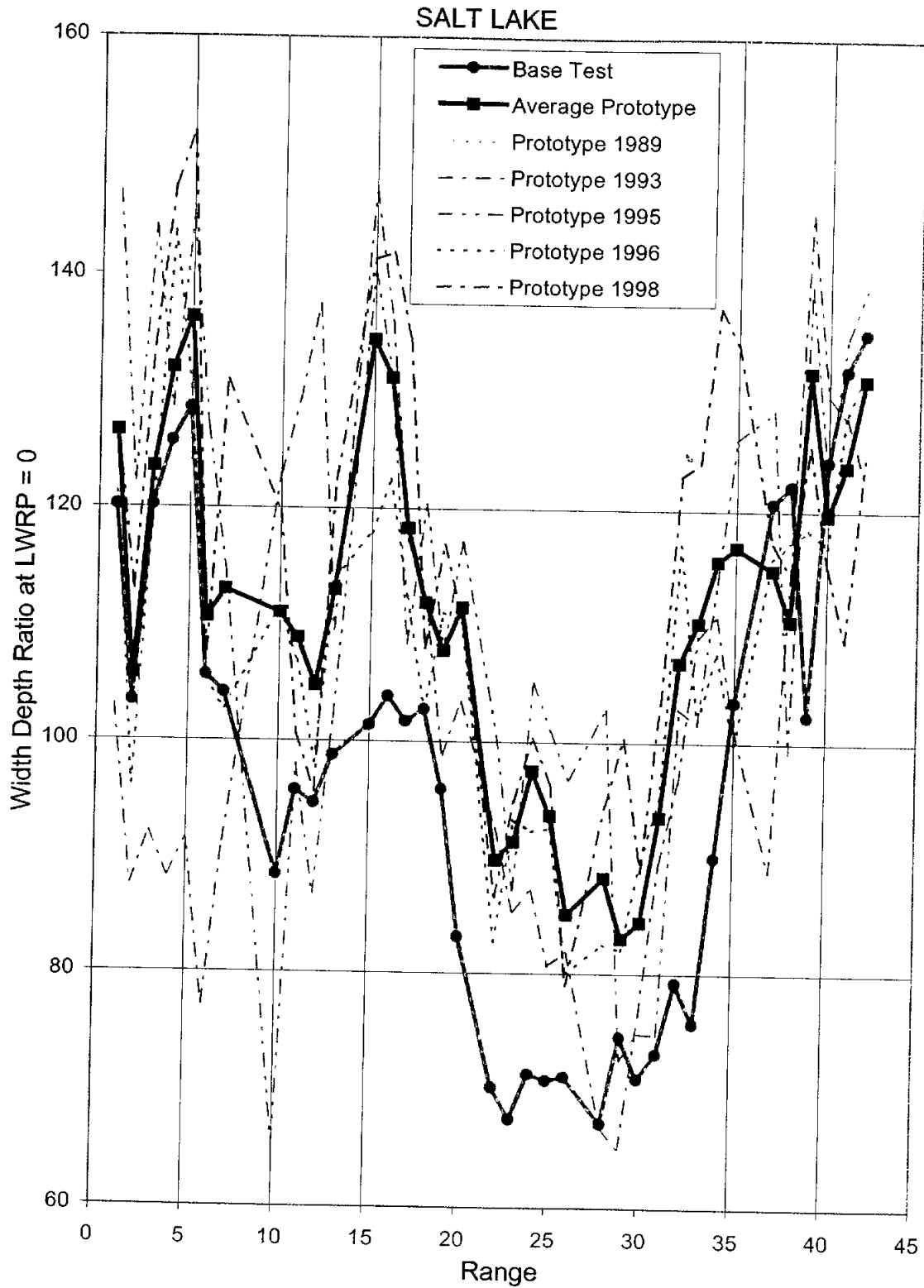


Figure C-8.2e Width/Depth Ratio by Range, Salt Lake Chute (Mississippi River)

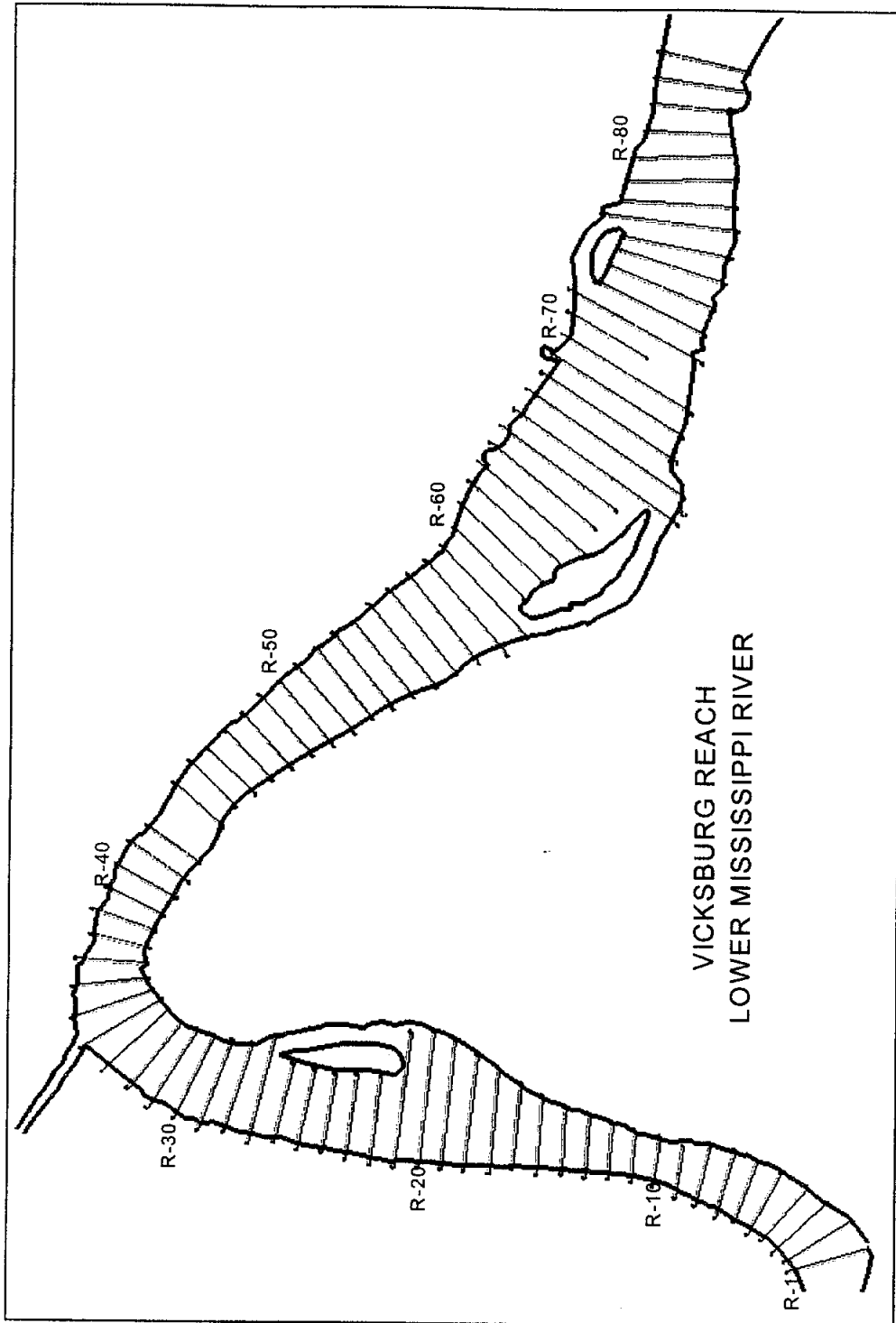


Figure C-9.1a Vicksburg Front Micromodel Plan View

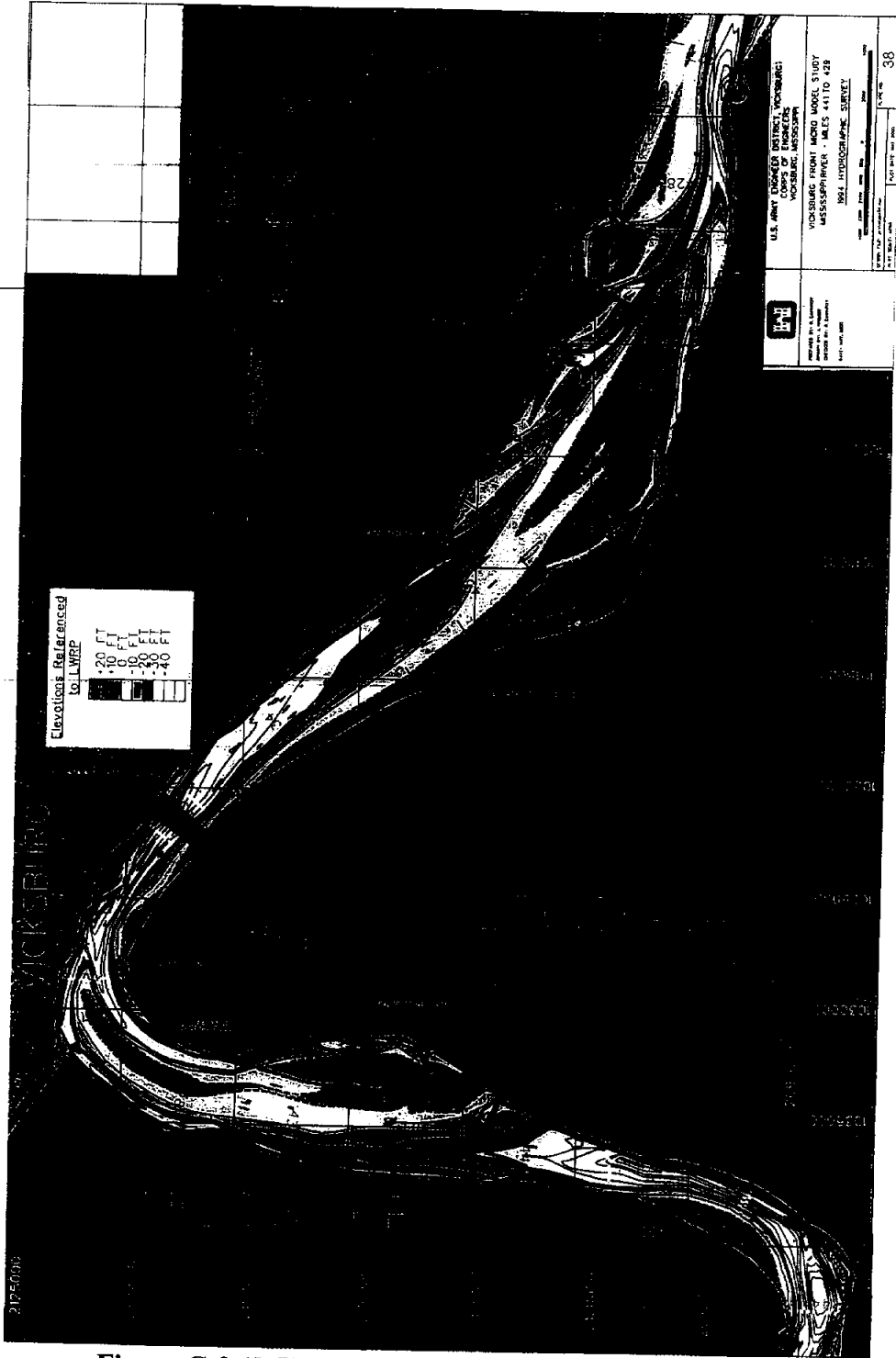


Figure C-9.1b Vicksburg Front Prototype Survey 1994

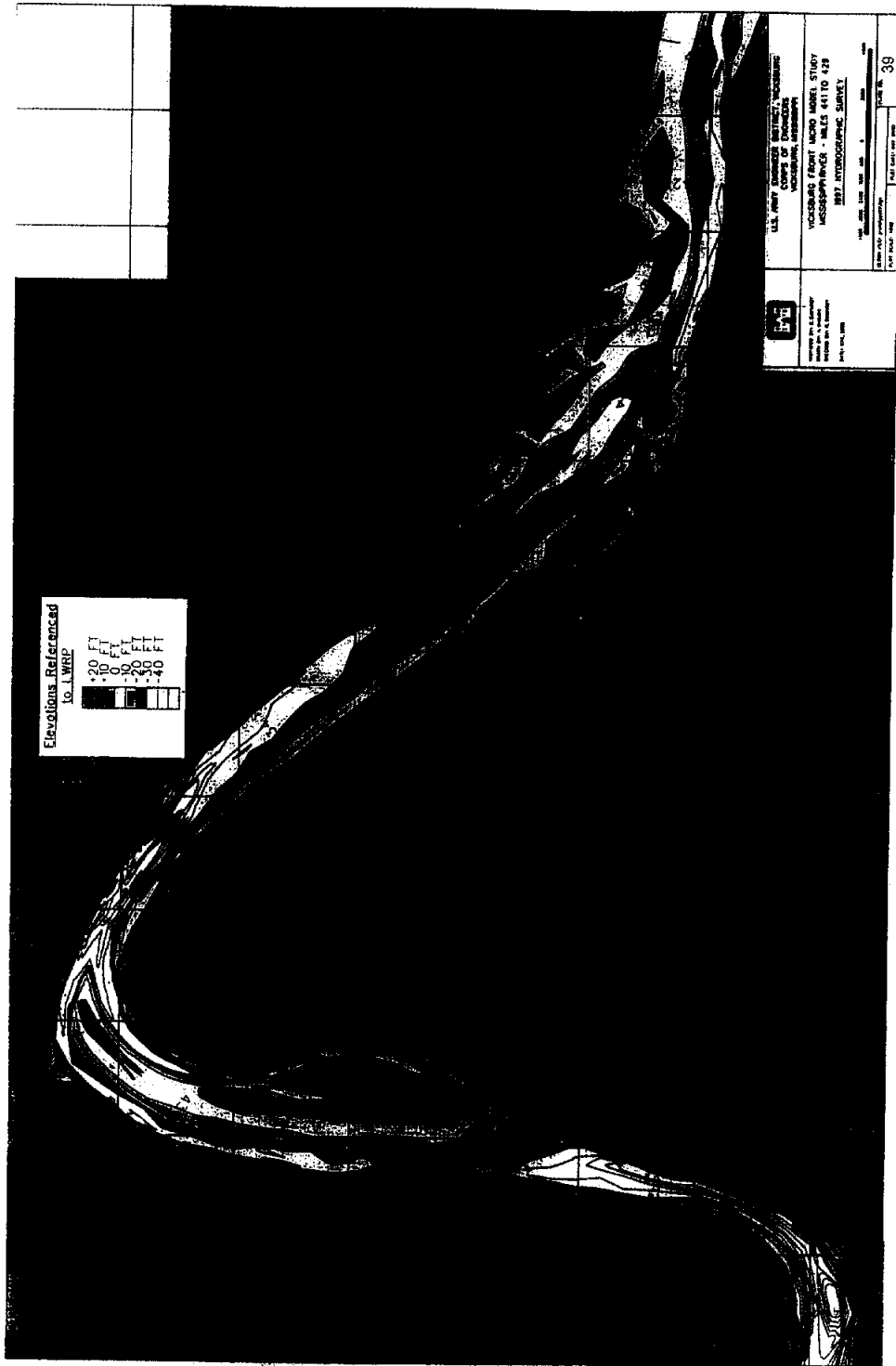


Figure C-9.1c Vicksburg Front Prototype Survey 1997

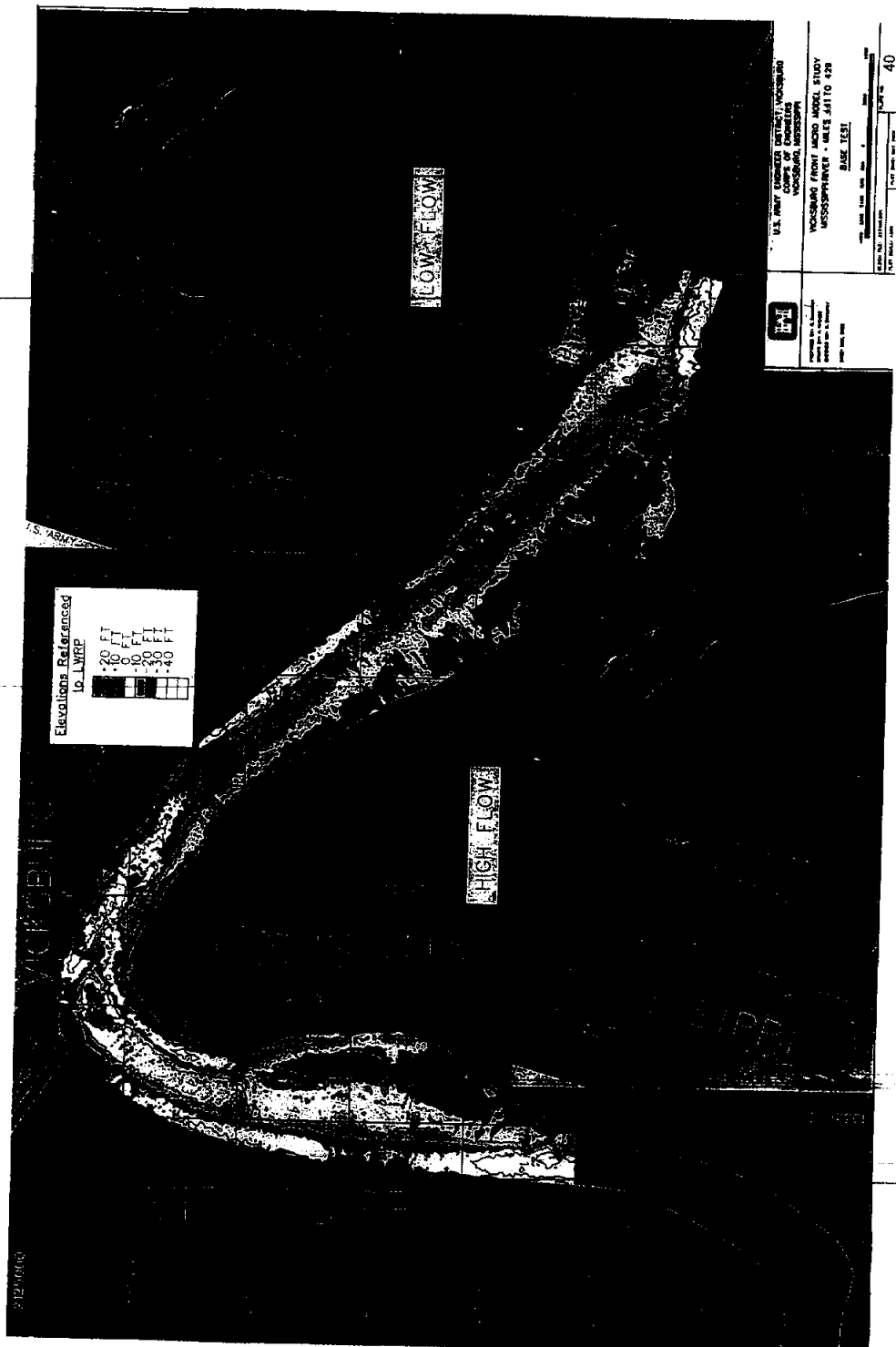
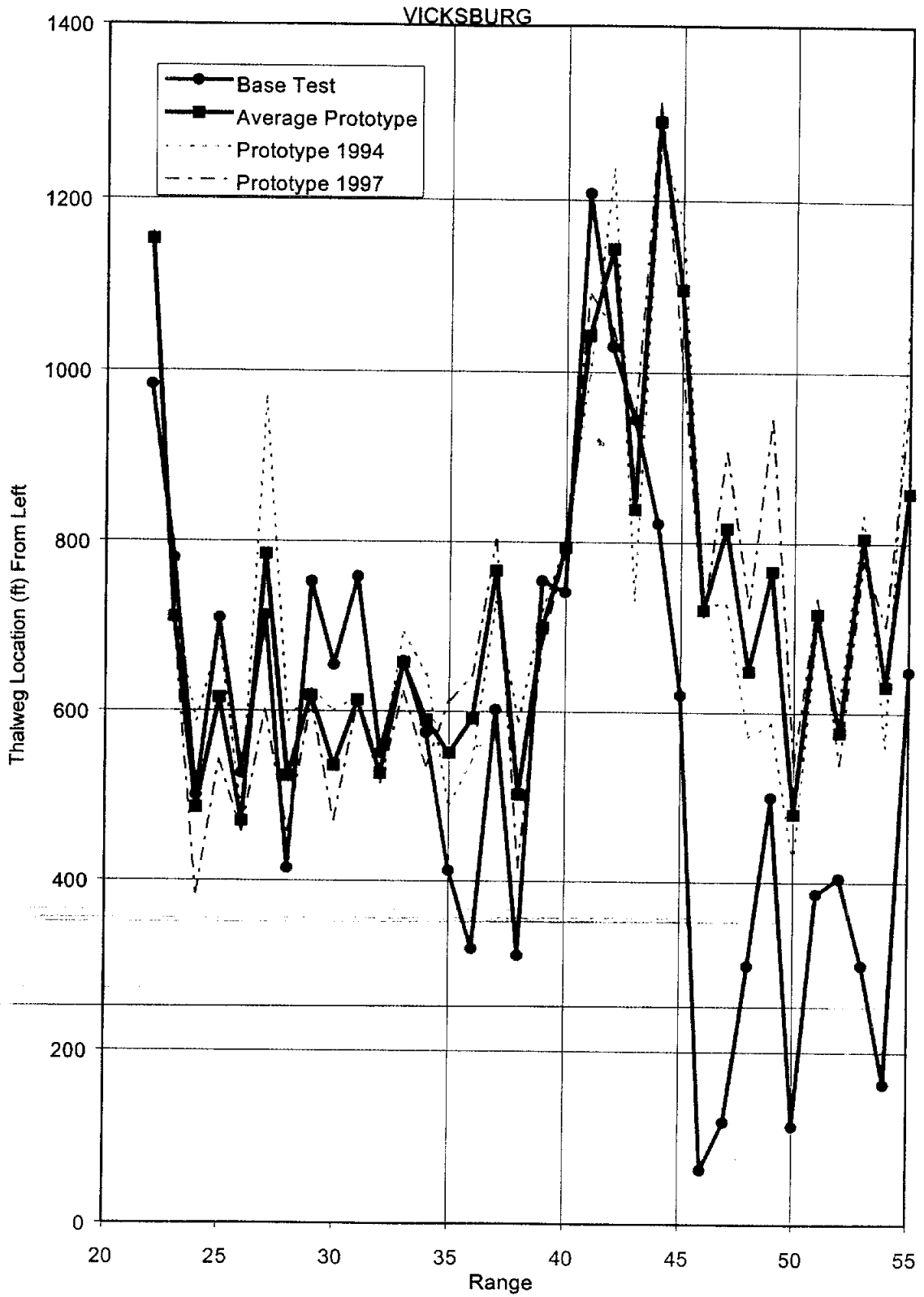


Figure C-9.1d Vicksburg Front Micromodel Base Test



**Figure C-9.2a Thalweg Position From Left by Range,
Vicksburg Front (Mississippi River)**

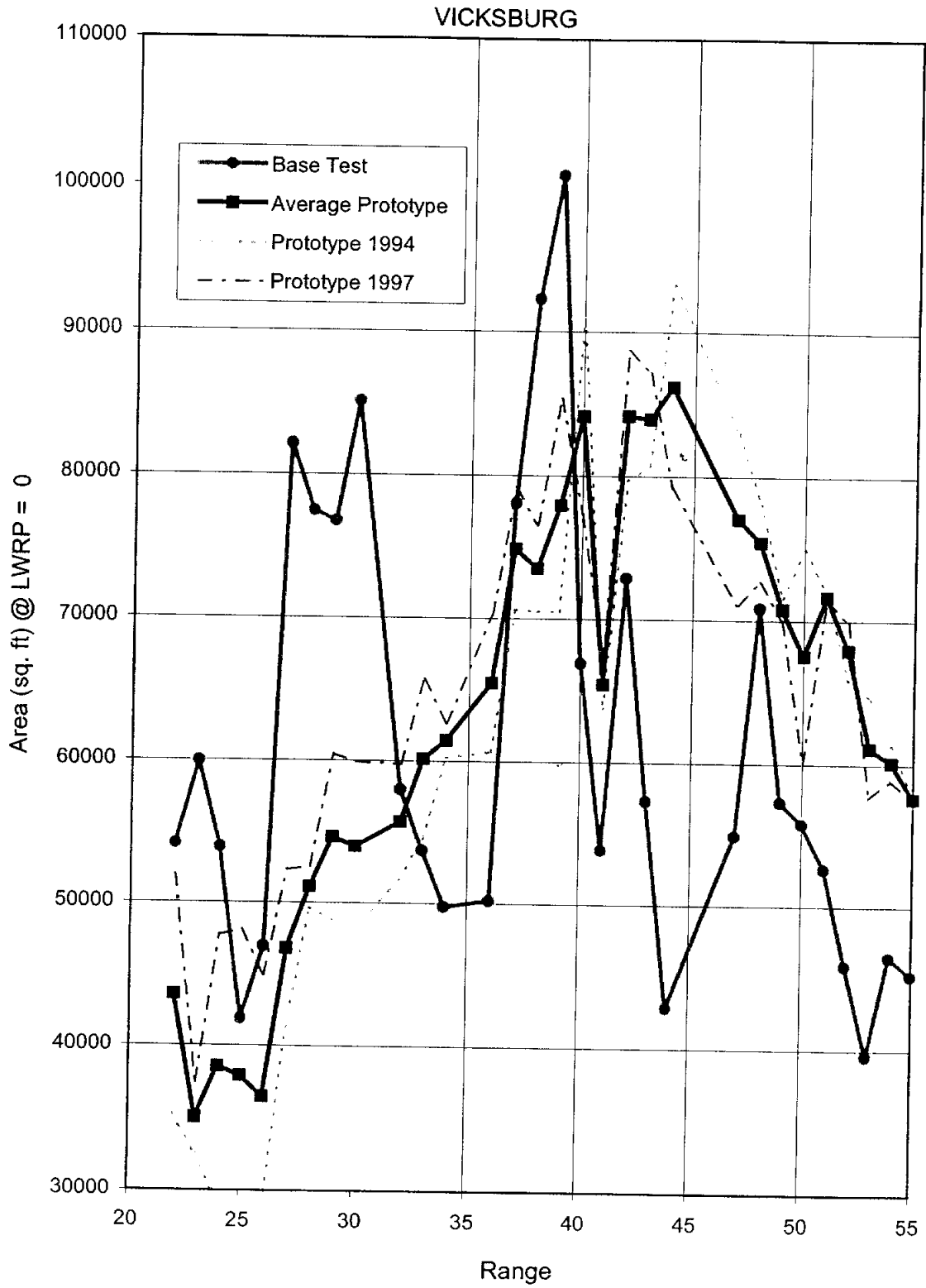


Figure C-9.2b Cross-Section Area by Range, Vicksburg Front (Mississippi River)

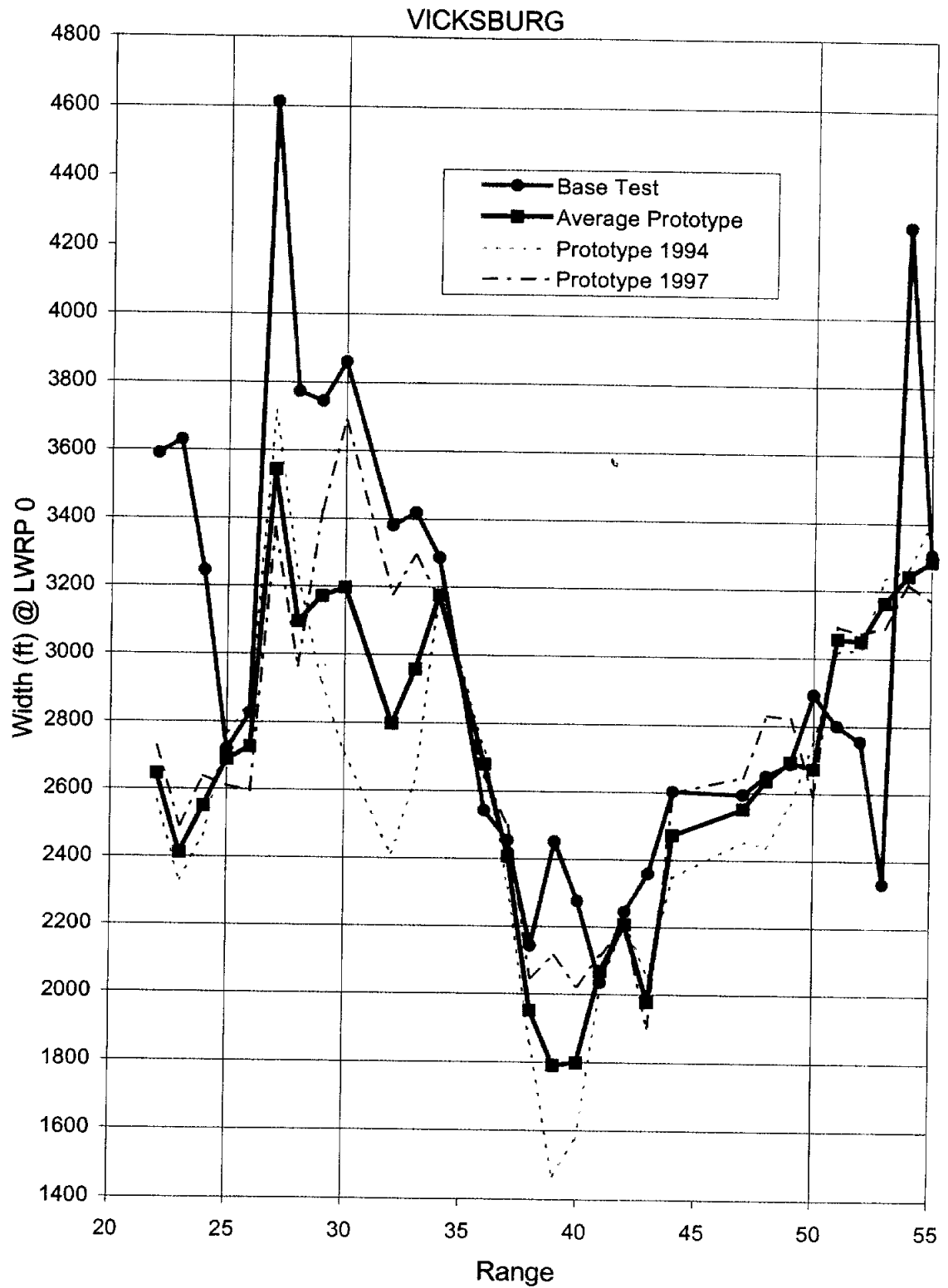


Figure C-9.2c Top Width by Range, Vicksburg Front (Mississippi River)

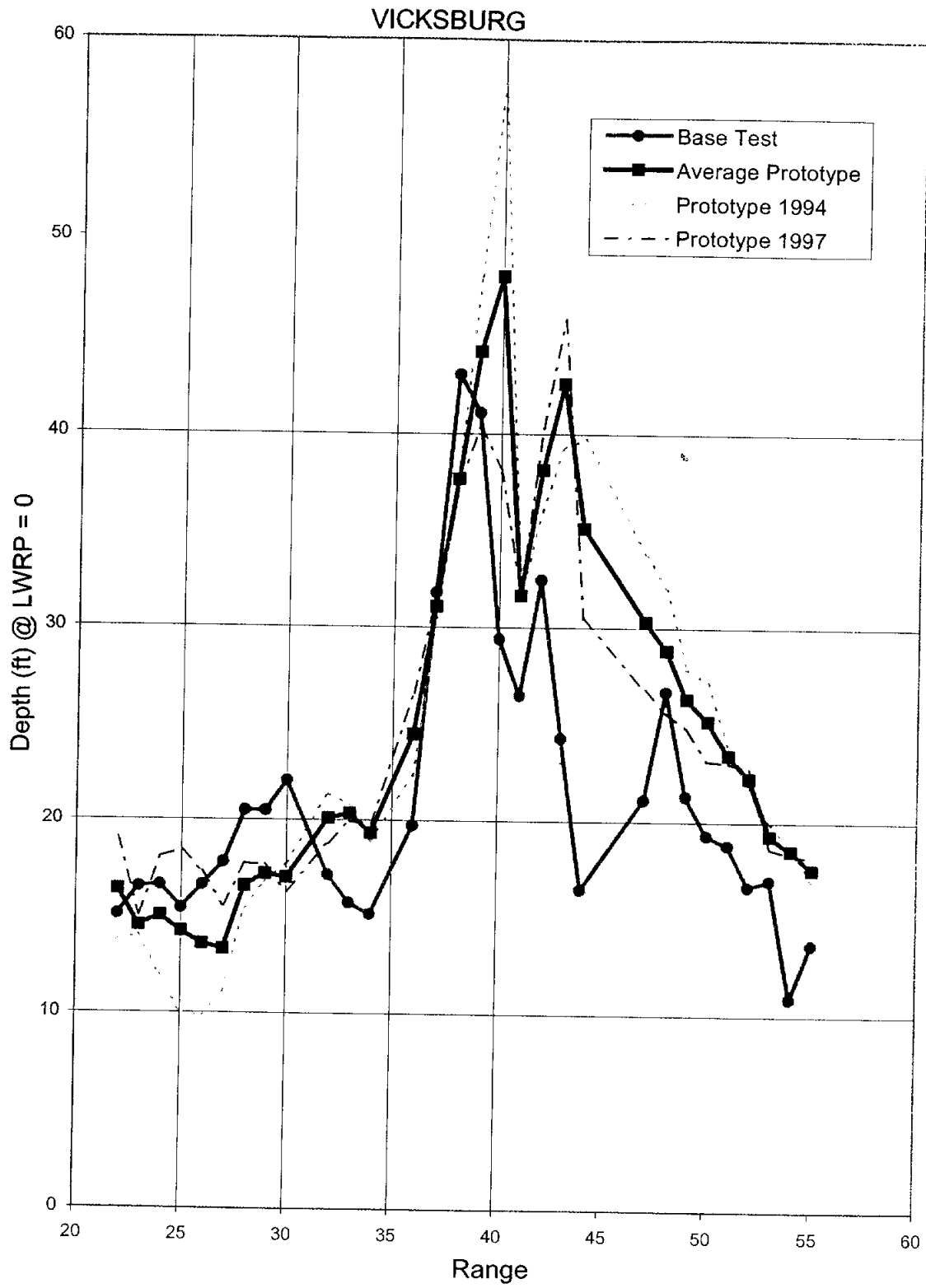


Figure C-9.2d Hydraulic Depth by Range, Vicksburg Front (Mississippi River)

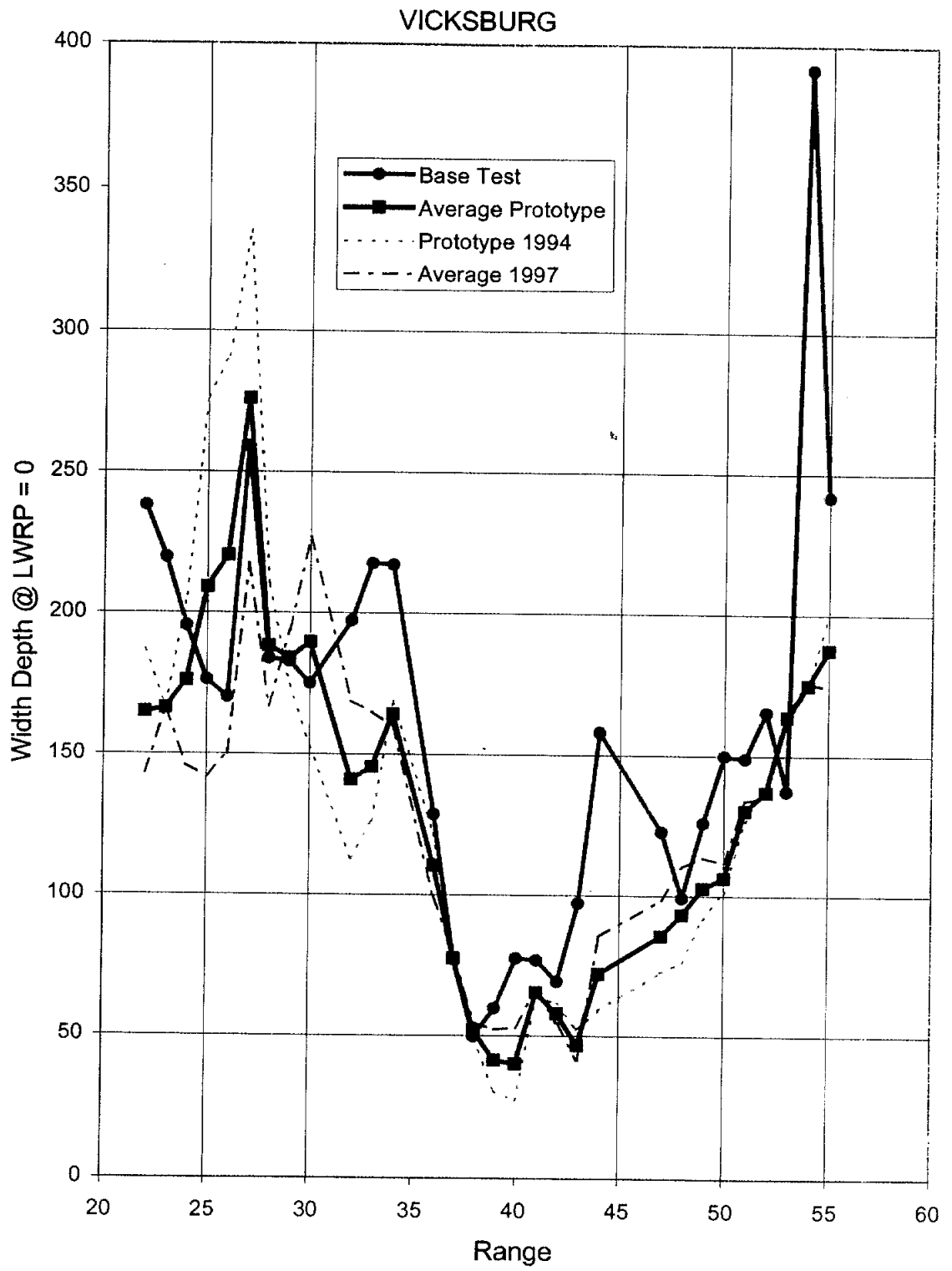


Figure C-9.2e Width/Depth Ratio by Range, Vicksburg Front (Mississippi River)

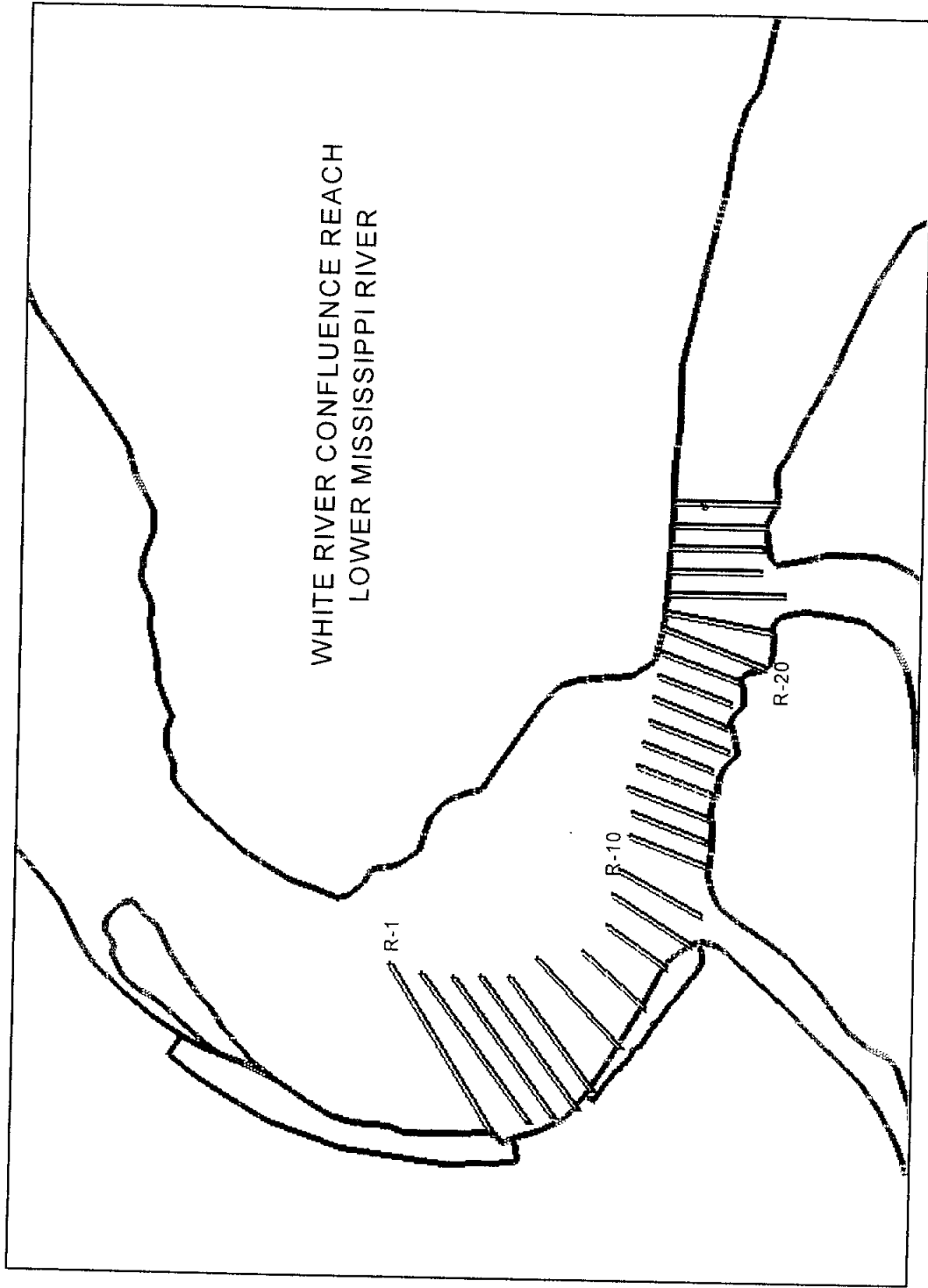
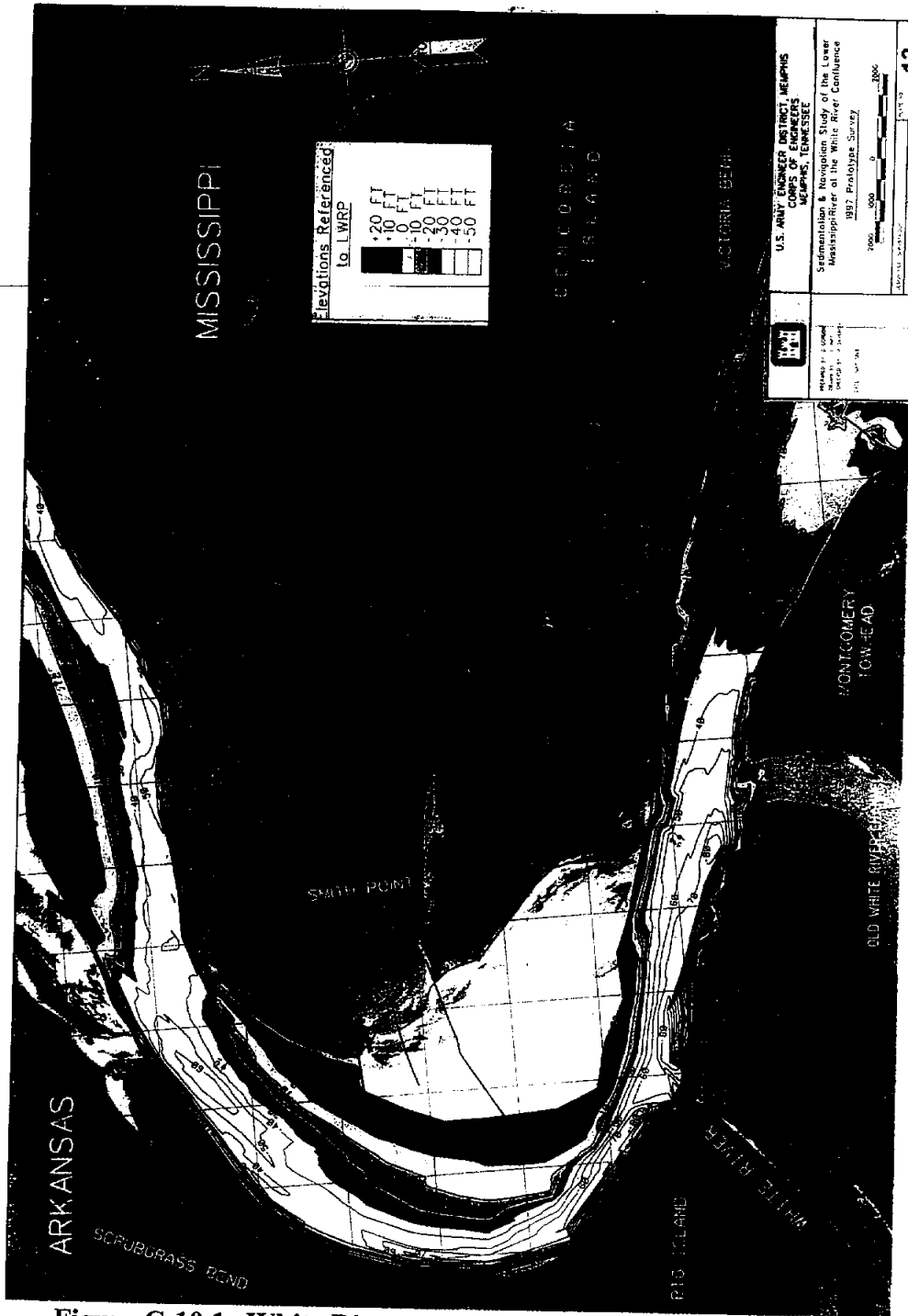


Figure C-10.1a White River Confluence with Mississippi River
Micromodel Plan View



**Figure C-10.1b White River Confluence with Mississippi River
 Prototype Survey 1994**



**Figure C-10.1c White River Confluence with Mississippi River
Prototype Survey 1997**



**Figure C-10.1d White River Confluence with Mississippi River
Micromodel Base Test**

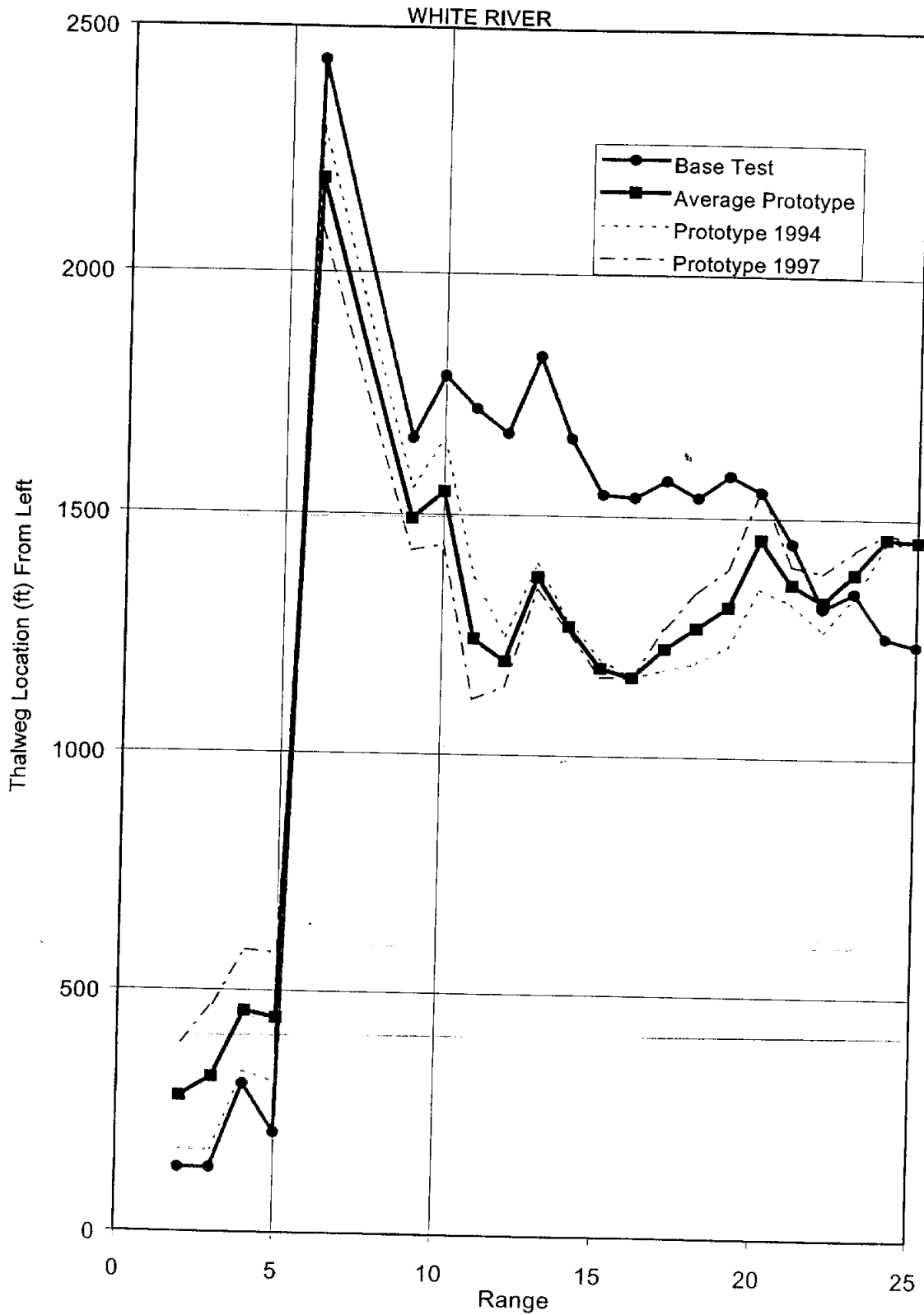


Figure C-10.2a Thalweg Distance From Left by Range, White River Confluence with Mississippi River

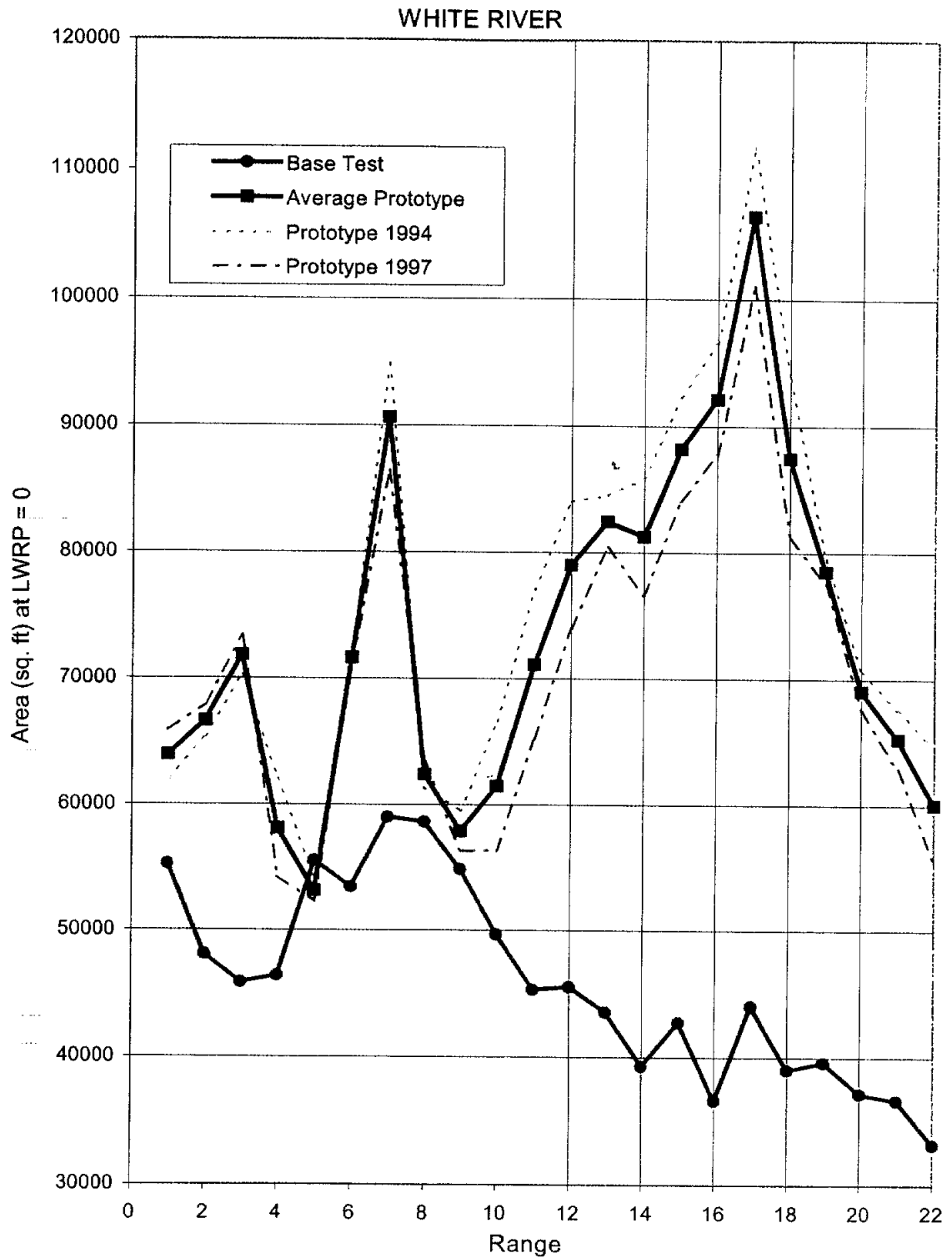


Figure C-10.2b Cross-Section Area by Range, White River Confluence with Mississippi River

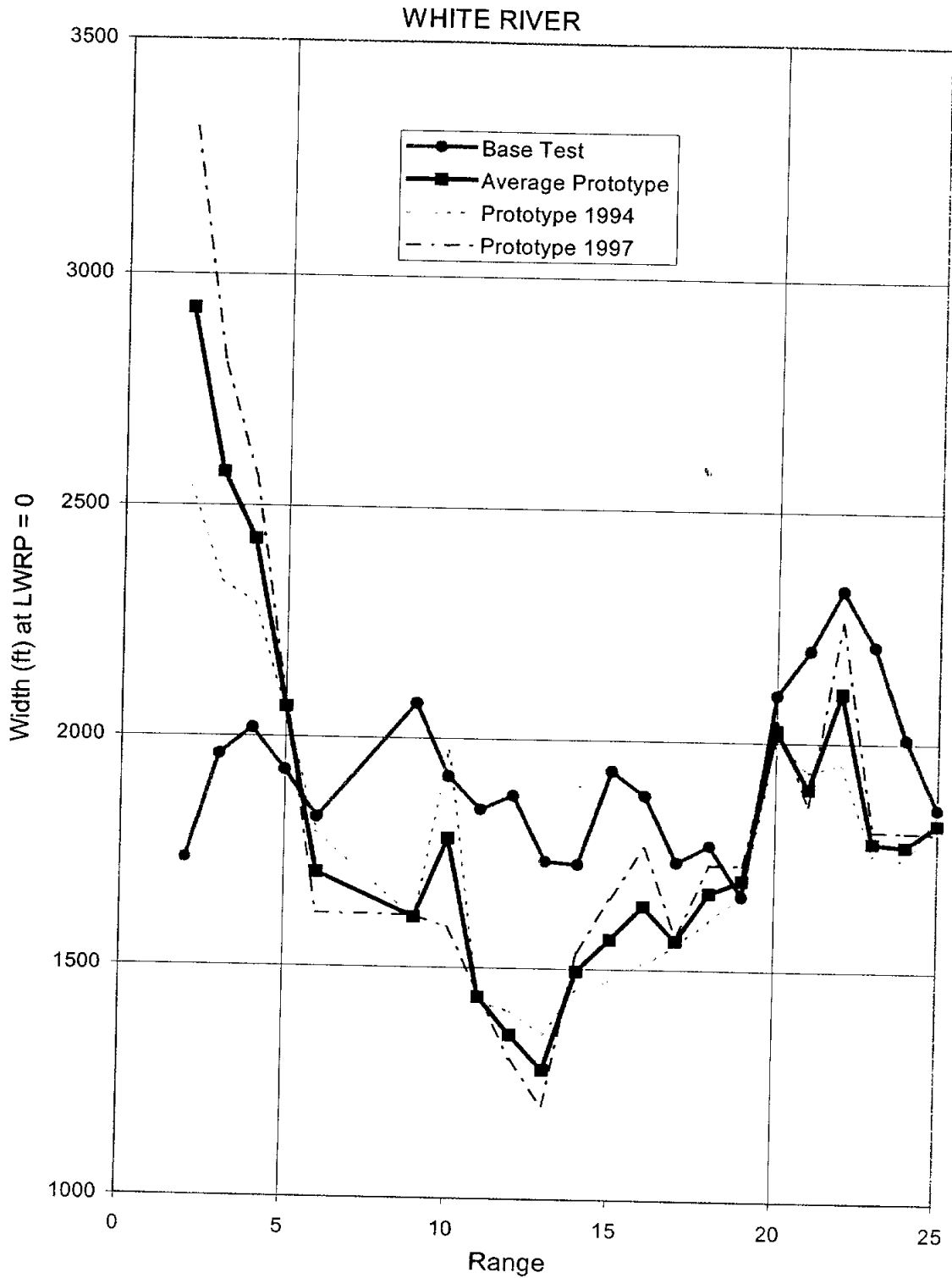


Figure C-10.2c Top Width by Range, White River Confluence with Mississippi River

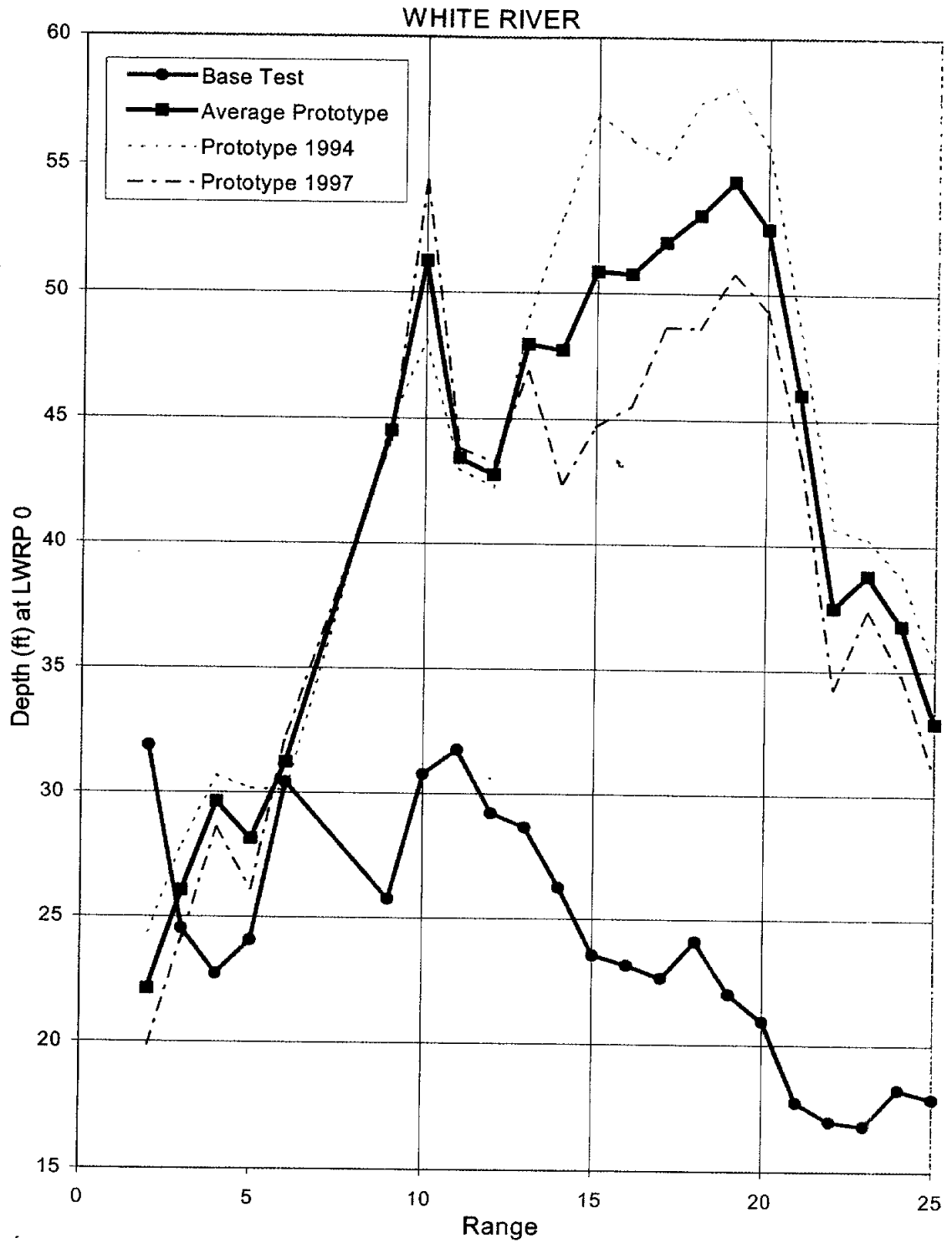


Figure C-10.2d Hydraulic Depth by Range, White River Confluence with Mississippi River

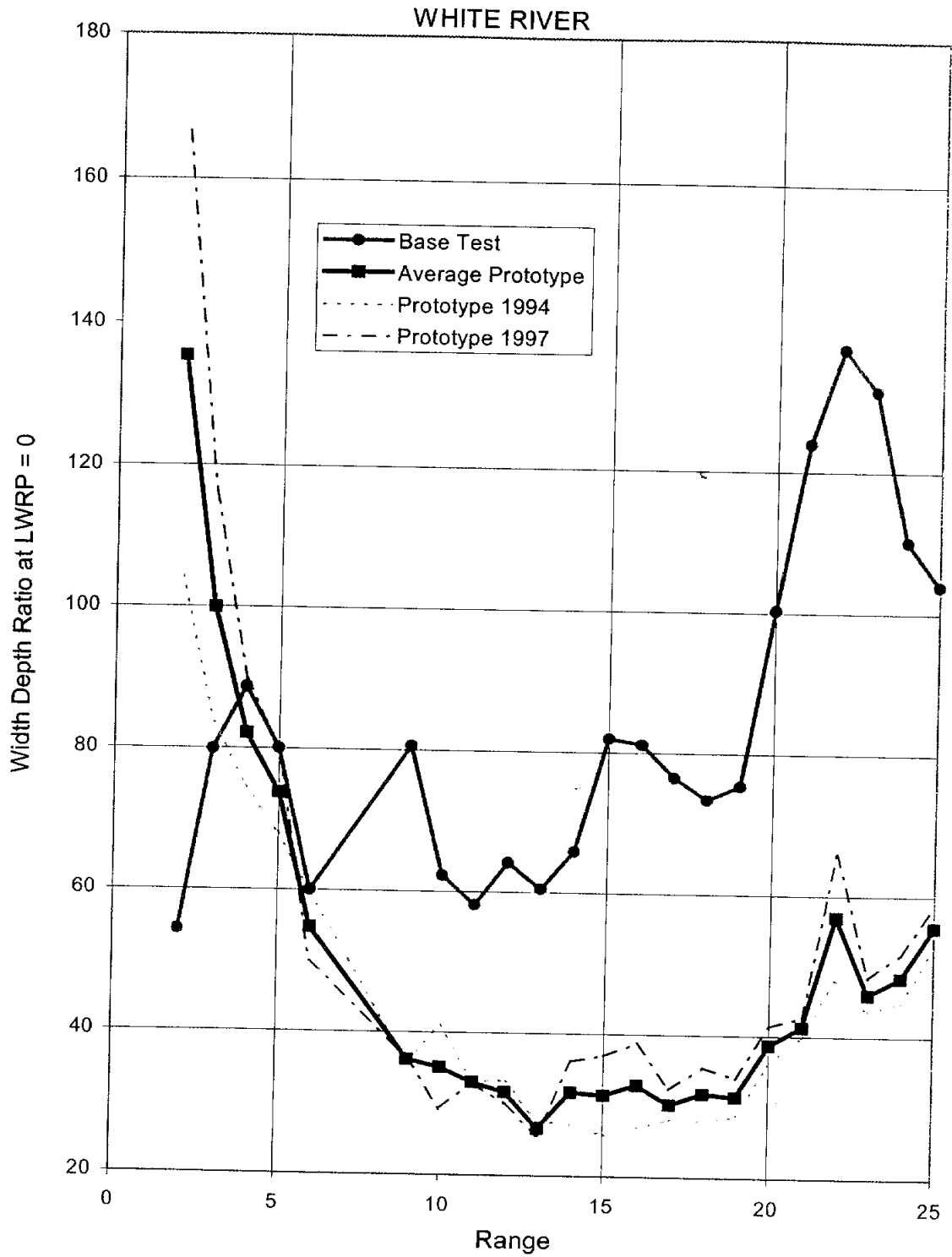


Figure C-10.2e Width/Depth Ratio by Range, White River Confluence with Mississippi River

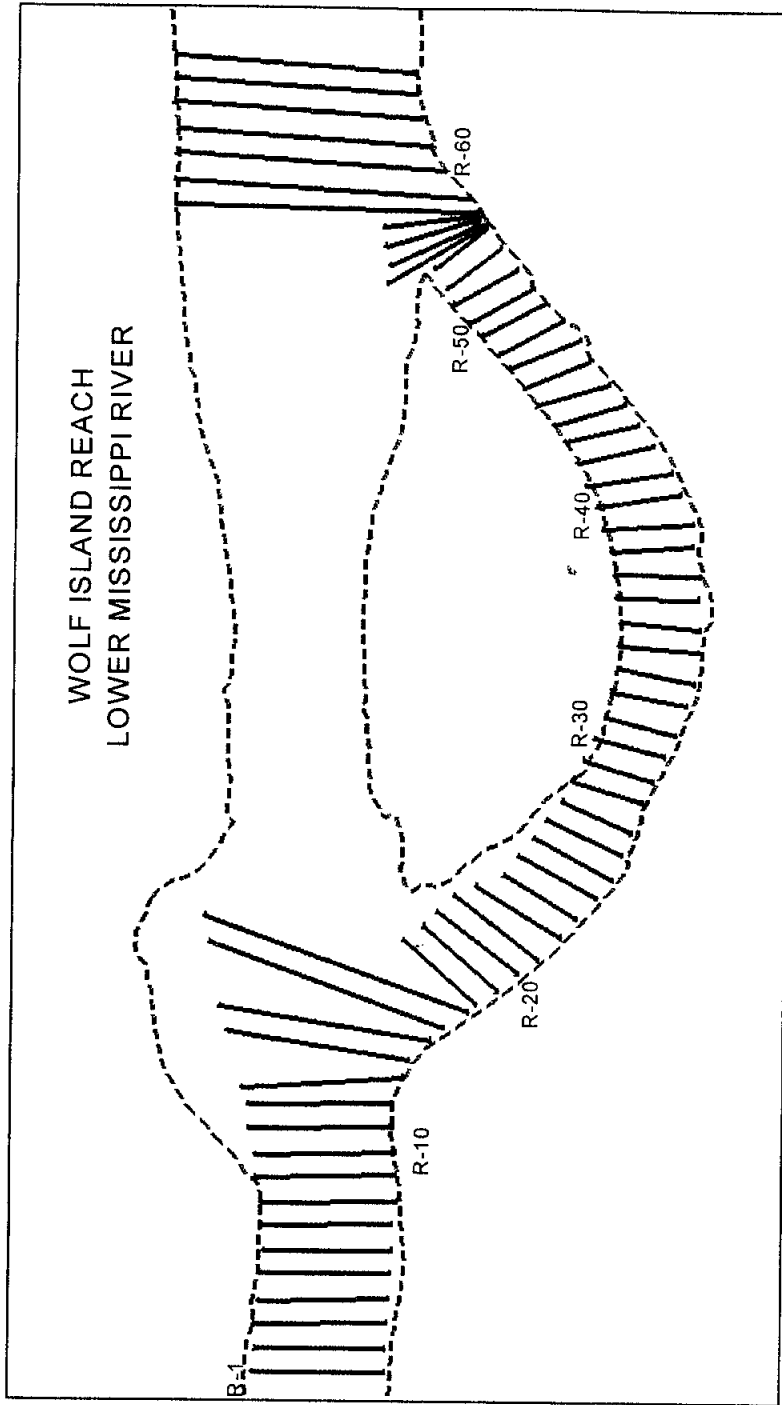


Figure C-11.1a Wolf Island Micromodel Plan View

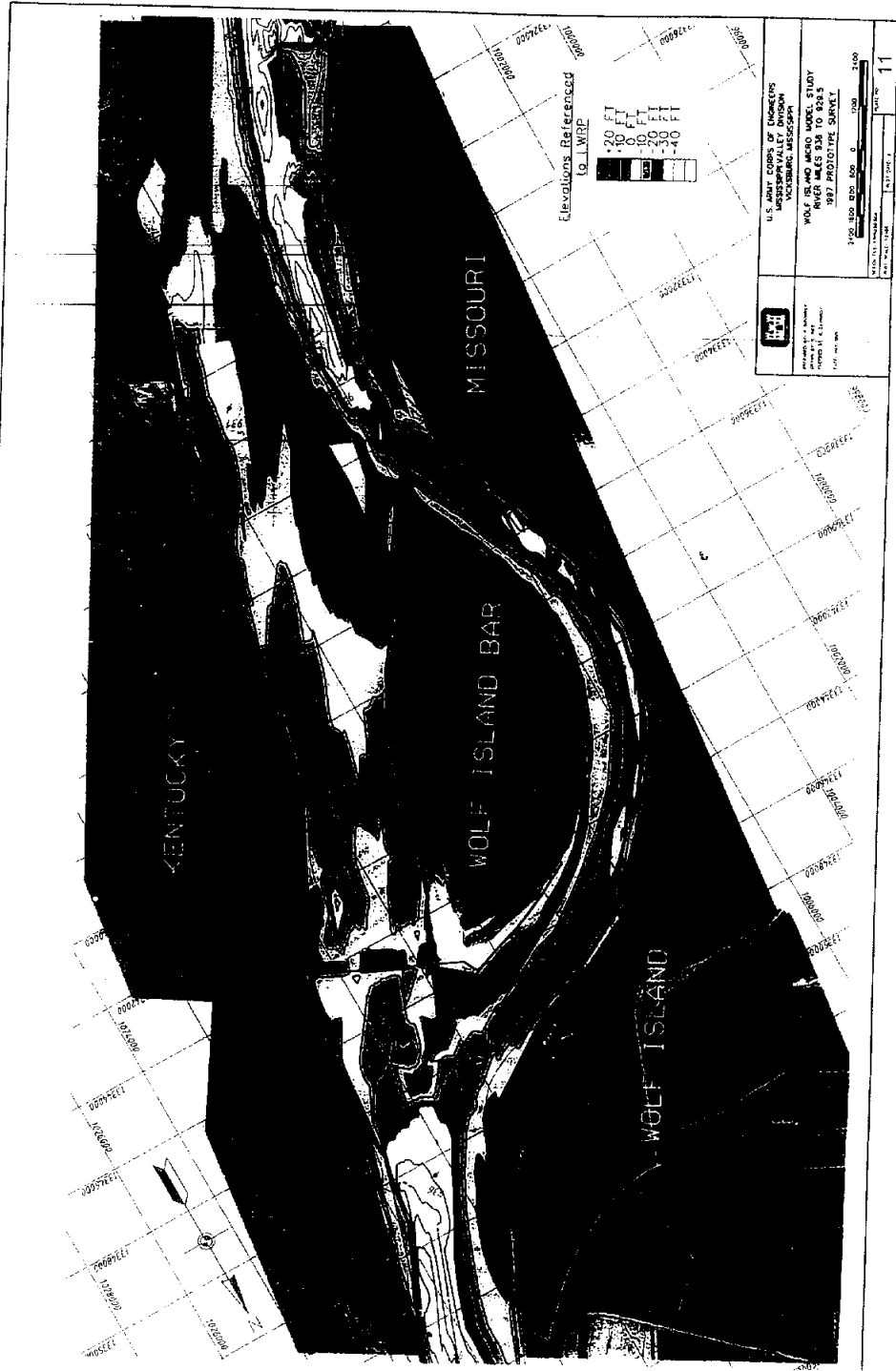


Figure C-11.1b Wolf Island Prototype Survey 1997

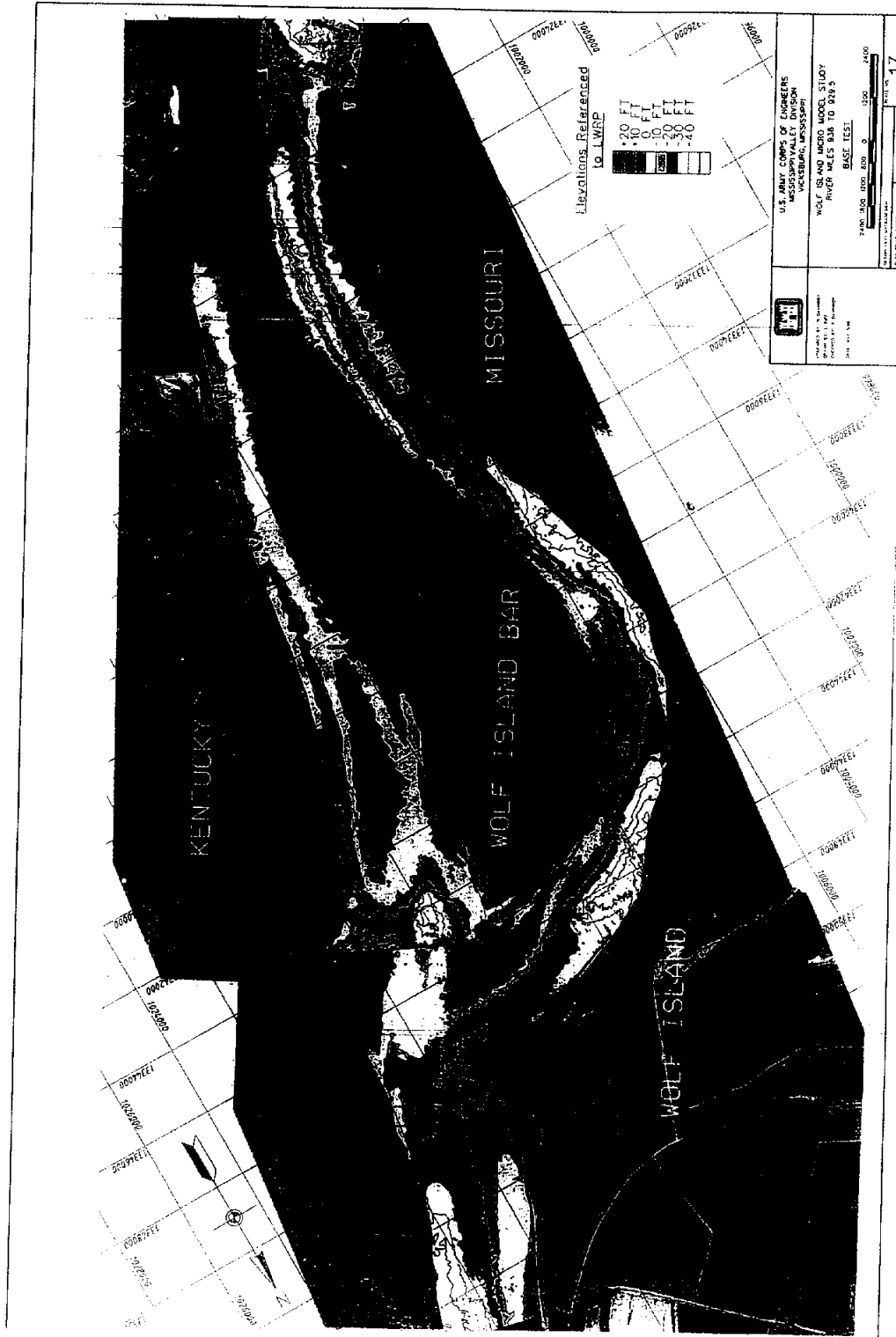


Figure C-11.1d Wolf Island Micromodel Base Test

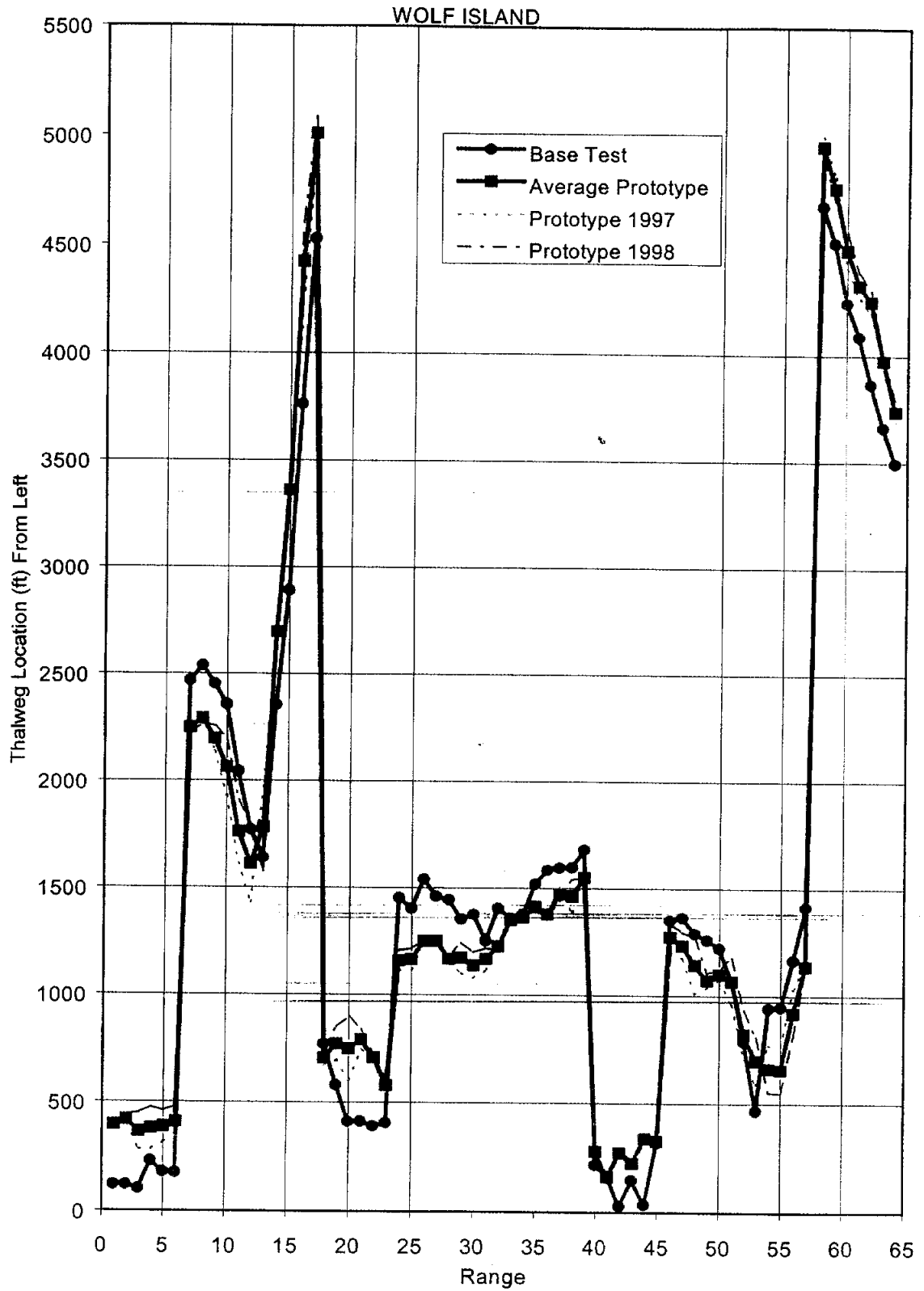


Figure C-11.2a Thalweg Position From Left by Range, Wolf Island (Mississippi River)

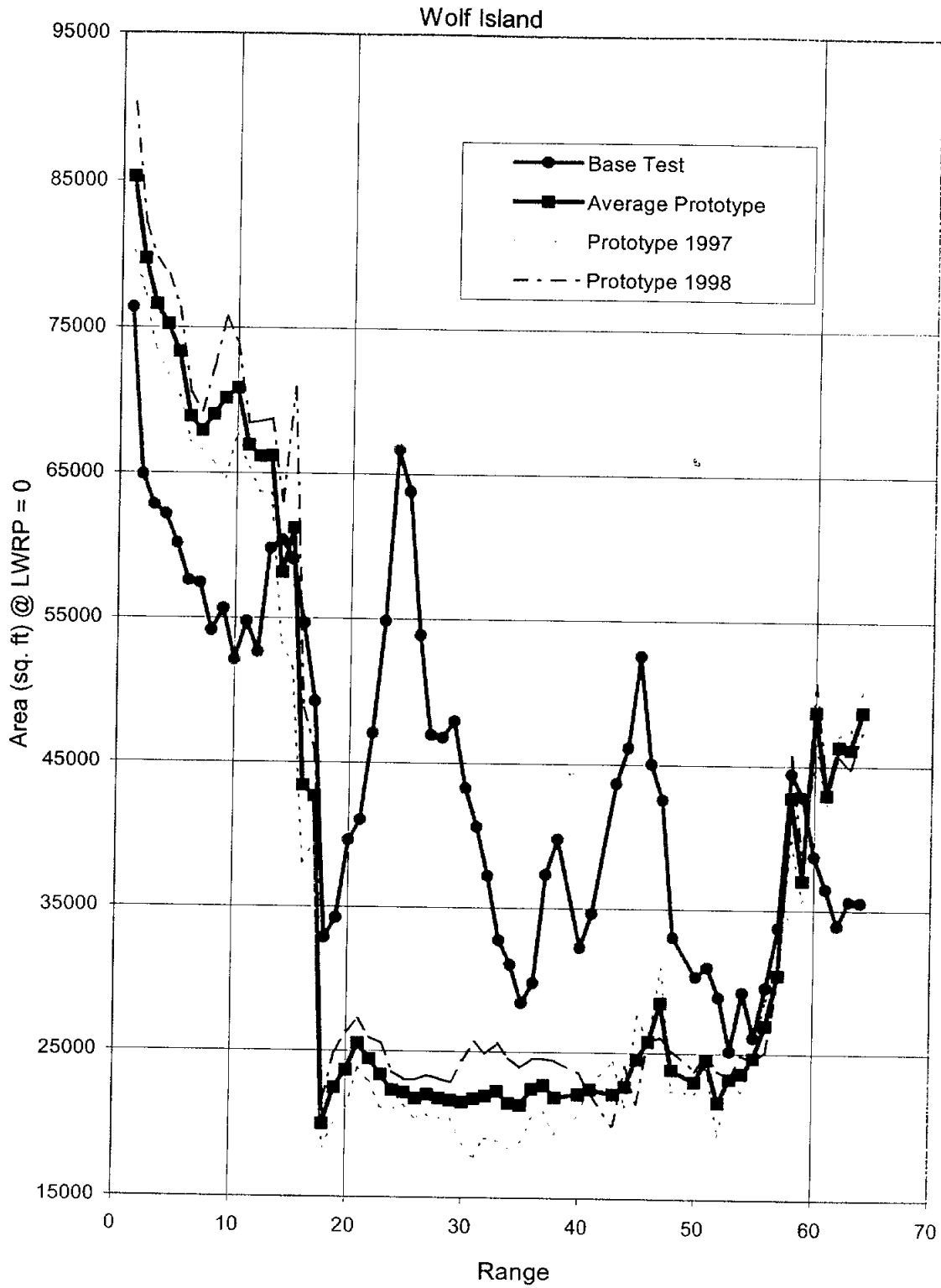


Figure C-11.2b Cross-Section Area by Range, Wolf Island (Mississippi River)

WOLF ISLAND

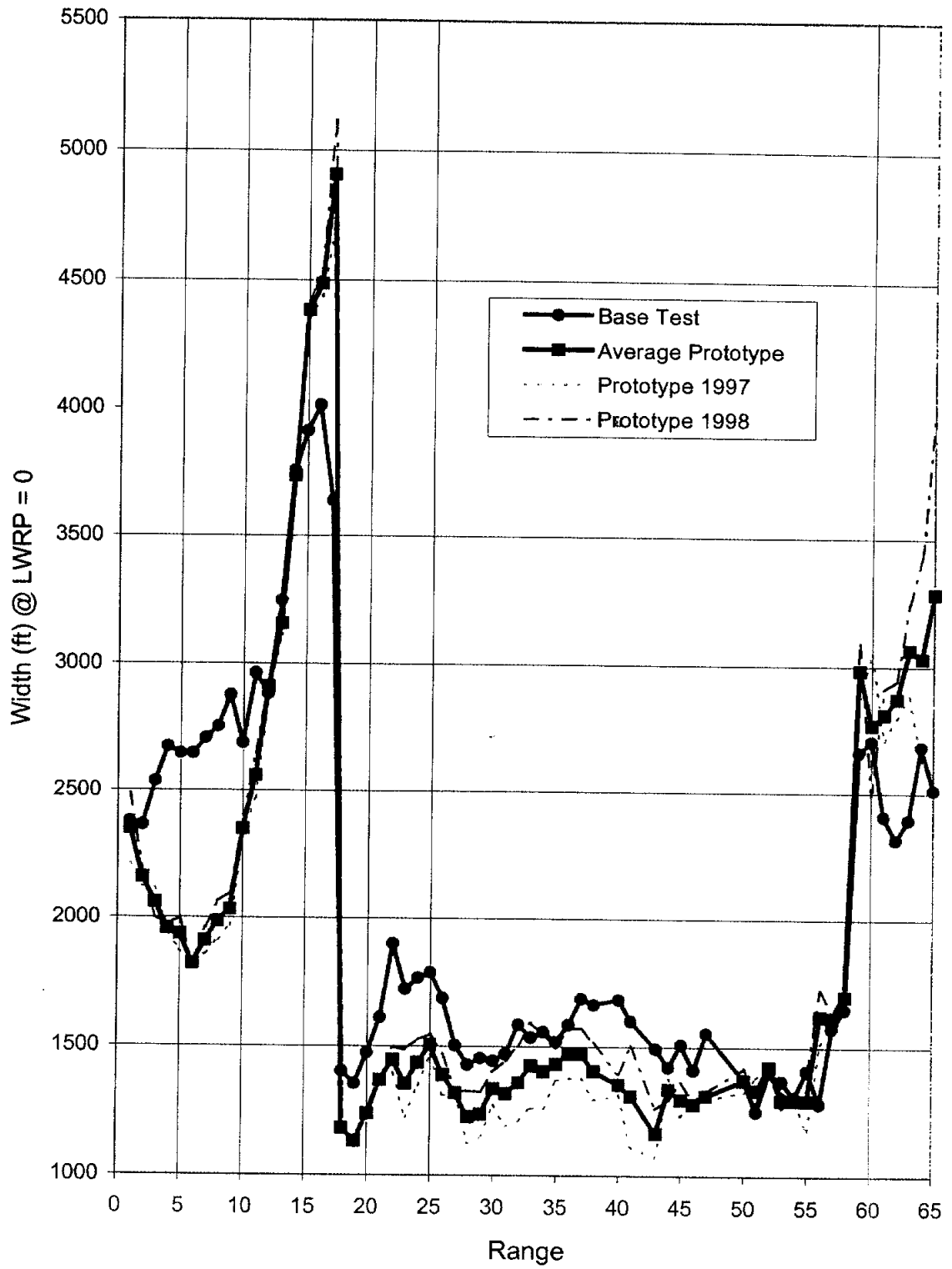


Figure C-11.2c Top Width by Range, Wolf Island (Mississippi River)

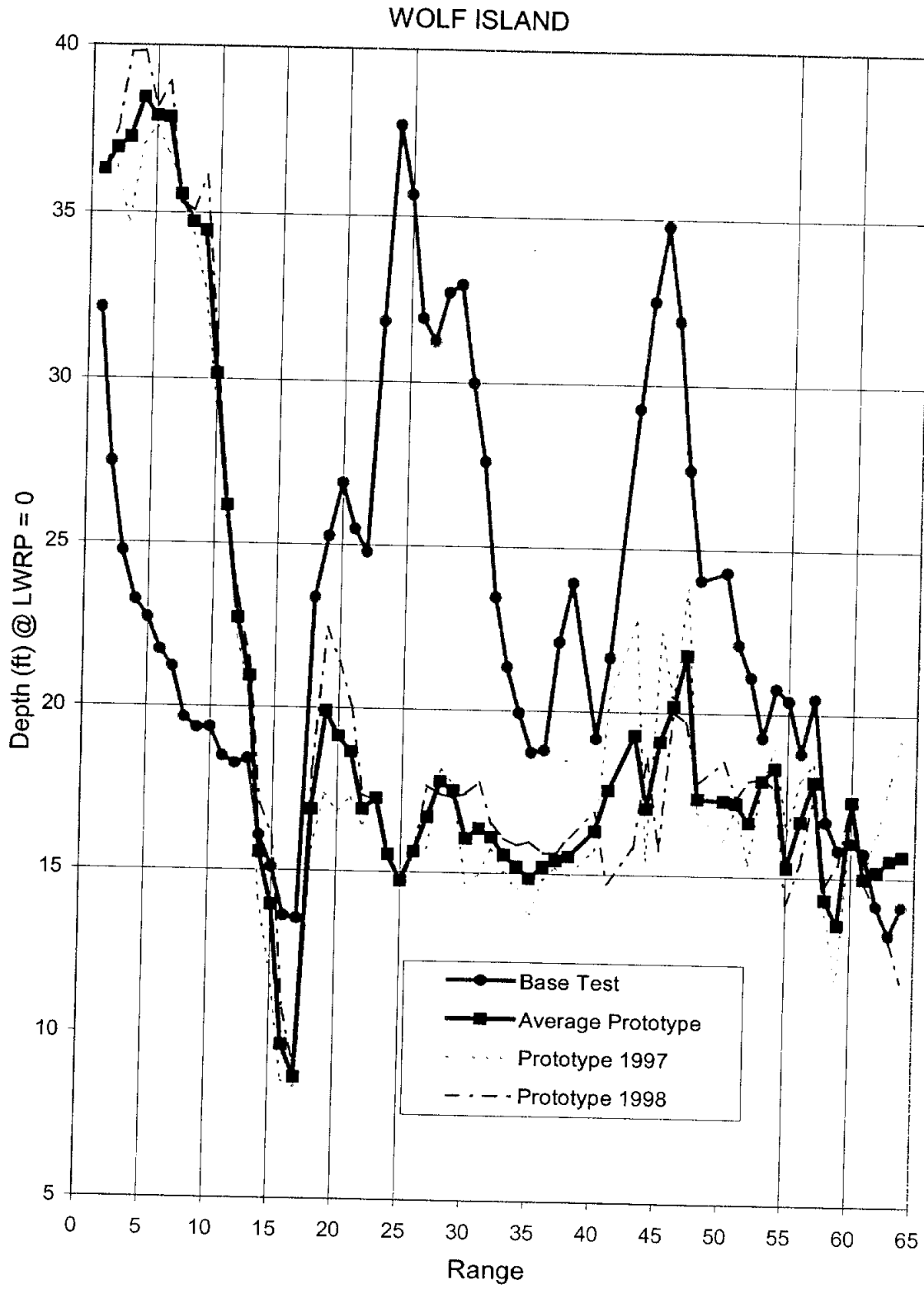


Figure C-11.2d Hydraulic Depth by Range, Wolf Island (Mississippi River)

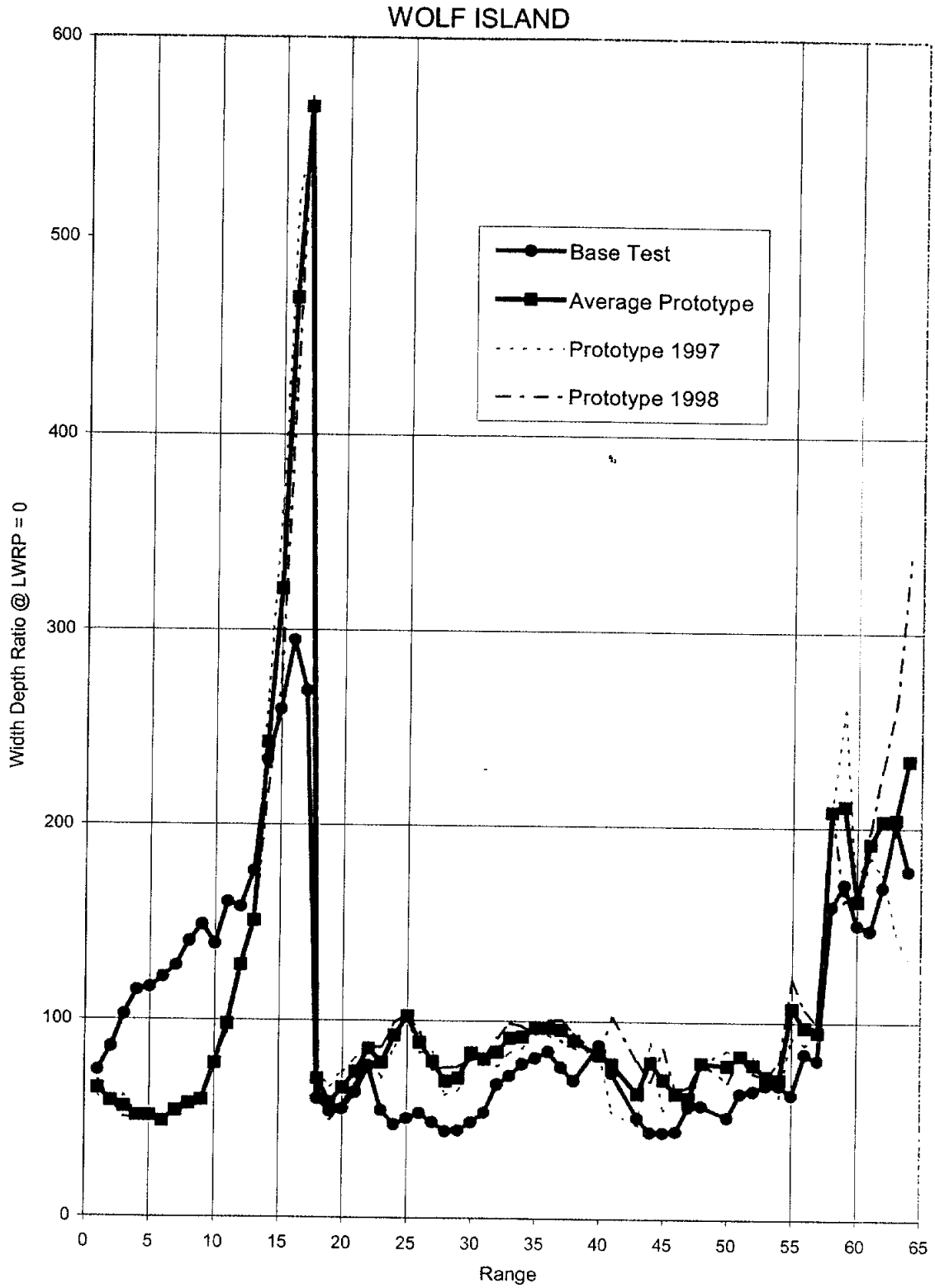


Figure C-11.2e Width/Depth Ratio by Range, Wolf Island (Mississippi River)

